FUNCTIONAL ANALYSIS OF THE *KEKKON* GENES IN THE *DROSOPHILA* NERVOUS SYSTEM

by

SIMON BISHOP

A thesis submitted to

The University of Birmingham

for the degree of

DOCTOR OF PHILOSOPHY

School of Biosciences

College of Life and Environmental Sciences

University of Birmingham

September 2013

The canonical vertebrate neurotrophin receptors — the Trk and $p75^{NTR}$ protein families — have not been found in *Drosophila*, thus it is unclear how neurotrophic signalling is implemented in fruit flies. The aim of my thesis was to investigate whether candidate receptors evolutionarily related to Trks or $p75^{NTR}$ may function as DNT receptors in fruit flies. The *Drosophila* neurotrophins DNT1 and DNT2 are known ligands for Toll6 and Toll7. Trk receptors comprise an extracellular ligand-binding module composed of Leucine-rich repeat domains and Immunoglobulin motifs (LIGs), and an intracellular tyrosine kynase (TyrK) signalling domain. Throughout evolution, domain shuffling resulted in different forms of Trk in vertebrates and invertebrates. The *Drosophila* genome encodes 9 members of the LIG superfamily of proteins, including the Kekkons (Keks), which are phylogenetically most similar to the Trks but lack the TyrK. Using *in situ* hybridisation, antibody labelling, genetic interactions and locomotion assays, I showed that of 12 candidate receptors the six Keks were the most promising to interact with DNTs. After generating overexpression constructs and loss of function mutants for the *keks*, I showed that: (1) overexpression of *kek2*, *kek3* and *kek6* could rescue the semi-lethality of *DNT1DNT2* double mutants; (2) Kek3, Kek4 and Kek6 interacted with DNT2 ligand eliciting a luciferase readout in S2 cells; (3) and that *kek3*, *kek4* and *kek6* interacted genetically with *DNT1* and *DNT2.* I subsequently focused on *kek6* and *kek4*. Kek6 was distributed in pioneer neurons and motor neurons. Both loss and gain of *kek6* function affected embryonic motor neuron targeting and larval locomotion behaviour. Using genetic rescues, I showed that Kek6 functions downstream of the DNTs and upstream of Ras and PI3K in axon targeting. Surprisingly, Kek4 was found to be distributed and function in the larval ring gland. Loss of *kek4* function delayed developmental timing, whereas overexpression of *kek4* advanced development. This was caused by *kek4* inhibiting juvenile hormone signalling, since *kek4* overexpression resulted in the upregulation of the ecdysone target Broad-Core in the fat body. Together, data reveal that the Keks have functions in CNS development and regulation of organism growth. They interact with the DNTs, strongly suggesting that they may function as DNT receptors. The work uncovers functional conservation of the LIG module in neurodevelopment despite domain shuffling throughout the animal kingdom.

For Rachel, Mum, Dad and Jo

Thank you for encouraging me to pursue this thesis,

for supporting me when things got tough,

and for celebrating with me when things went right

ACKNOWLEDGEMENTS

I would like to thank my PhD supervisor, Dr Alicia Hidalgo, for all of your support, enthusiasm and advice over the past 4 years. Without your guidance, ideas and insight, none of this would have been possible. I am grateful that you always had time for me, even — especially — when I had no idea what I was talking about.

I would like to thank the members of the Hidalgo laboratory, past and present. My thanks go to Kentaro, Ben, Graham, Jill, Samaher, István, Ann, Niki, Caitríona, Martin, Chris and Maria for discussions, advice, support and company over the course of the project. I am a richer person for getting to know you all. I am a better scientist for having had the pleasure of working with you.

Thank you to Prof Nick Gay and his lab, particularly Miranda, Jukka and Martin, for advice and discussions, and adventures in the Spanish mountains.

To Steve Publicover, Adam Gore and Jeremy Pritchard in the School of Biosciences, and Kenny Webster and Lynsey Fairweather at ThinkTank museum — thanks for supporting my pet projects.

Finally, my eternal gratitude belongs with Rachel, who lifted me every time I struggled. Ever since that evening in Harborne, as I tried to explain my project using wine glasses and cutlery, you have encouraged me unendingly. This project is as much yours as mine.

TABLE OF CONTENTS

	Page
Chapter 1 Introduction	1
1.1 Neurotrophin signalling	3
1.1.1 Neurotrophism, neurotrophins and neurotrophic factors	3
1.1.2 Neurotrophin signalling in neural development	5
1.1.3 Neurotrophins and neurotrophism in insects	7
1.1.4 Neurotrophins in the systemic control of growth	9
1.2 Domain Shuffling in the Evolution of Receptors	10
1.2.1 Principles of Domain Shuffling	10
1.2.2 Leucine-Rich Repeats	12
1.2.3 Immunoglobulin domains	14
1.2.4 Tyrosine Kinases	14
1.3 LIGs in vertebrates	15
1.3.1 Trk receptors	15
1.3.2 Non-Trk vertebrate LIGs	16
1.4 Evolution of the neurotrophin receptors	17
1.4.1 Domain shuffling in the Trk superfamily	17
1.4.2 Invertebrate Trks and Trk-like proteins	19
1.4.3 Truncated Trks	22
1.4.4 Evolution of the $p75^{NTR}$ superfamily	24
1.5 LIGs and candidate invertebrate neurotrophin receptors	24
1.5.1 Lambik	25
1.5.2 CG17839, Rickets and Wengen	25
1.5.3 The Kek protein family	26
1.5.4 Potential signalling downstream of Keks or dLIGs	27
1.6 *Drosophila* as a model organism	29
1.6.1 The *Drosophila* nervous system	30
1.6.2 The *Drosophila* ring gland and developmental timing	33
1.7 Aims	35
Chapter 2 Methods	37
2.1 Genetics	37
2.1.1 Genetic protocols	37
2.1.2 Null mutagenesis	37
2.1.3 Survival index	38
2.2 Molecular biology	39
2.2.1 Genomic DNA isolation	39
2.2.2 Cloning summary	40
2.2.3 PCR	40
2.2.4 Reverse Transcription-PCR	41
2.2.5 Gel electrophoresis and DNA purification	42
2.2.6 DNA ligation	42
2.2.7 Gateway cloning	42
2.2.8 Transformation of *E. coli* and DNA amplification	43
2.2.9 DNA sequencing	44
2.3 Cell culture	45
2.3.1 S2 cell culture	45
2.3.2 Luciferase reporter assay	45
2.4 Protein expression and purification	46

2.4.1 DNT purification 46
2.4.2 SDS-PAGE and Western blot 47
2.5 Immunochemistry 47
2.5.1 Fixation 47
2.5.2 Immunolabelling 48
2.5.3 Antisense RNA probe transcription 49
2.5.4 *In situ* hybridisation 50
2.5.5 Fluorescent *in situ* hybridisation 52
2.6 Microscopy 53
2.7 Phenotypic analysis 54
2.7.1 Axon guidance 54
2.7.2 Locomotion 54
2.7.3 Developmental timing 55
2.7.4 Body growth assays 55
2.8 Statistical analysis 56
Chapter 3 Characterisation of the *Drosophila* LIGs 57
3.1 Introduction 57
3.2 Results 58
3.2.1 Candidate receptor profiles 58
3.2.1.1 dLIG expression profiles 58
3.2.1.2 The *kek* genes are expressed in the CNS 59
3.2.1.3 Expression profiles of non-LIG candidates 63
3.2.2 The dLIGs interact with the DNTs 64
3.2.2.1 Genetic interactions of the dLIGs 65
3.2.2.2 *kek3* and *kek4* interact with *DNTs* to effect locomotion phenotypes 66
3.3 Discussion 69
Chapter 4 Gain of function analysis reveals Kek interactions with the DNTs 73
4.1 Introduction 73
4.2 Results 74
4.2.1 Molecular cloning of *kek* genes into *pAct5c* and *UAS* vectors 74
4.2.2 Phenotypic analysis of *kek* overexpression mutants 75
4.2.3 DNT2 can interact with Kek≡Toll6 chimaera receptors to induce NFκB signalling 76
4.3 Discussion 78
Chapter 5 Loss of function of analysis reveals Kek interactions with the DNTs 80
5.1 Introduction 80
5.2 Results 81
5.2.1 Generation of *kek3*, *kek4* and *kek6* null mutants by FRT mediated mutagenesis 81
5.2.2 *DNT–kek* genetic interactions 83
5.2.3 *kek3* and *kek4* null mutants affect locomotion 85
5.3 Discussion 85
Chapter 6 *kek6* function in the central nervous system 88
6.1 Introduction 88
6.2 Results 89
6.2.1 *kek6* is expressed in the embryonic nervous system 89
6.2.2 *kek6* is required for axon targeting 91
6.2.3 *kek6* is required for normal locomotion behaviour 94
6.3 Discussion 96

Chapter 7 *kek4* function in the ring gland 99
7.1 Introduction 99
7.2 Results 99
7.2.1 *kek4* is expressed in the ring gland 99
7.2.2 *kek4* controls larval developmental timing 100
7.2.3 kek4 inhibits juvenile hormone signalling 102
7.2.4 *kek4* does not influence larval or pupal body size 103
7.2.5 *kek4* is required for normal locomotion behaviour 104
7.3 Discussion 105
Chapter 8 Discussion and Conclusions 108
8.1 Main outcomes 108
8.2 The LIGs function in the *Drosophila* nervous system 109
8.3 dLIGs and the DNTs 110
8.4 Downstream signalling of Kek6 112
8.5 Evolution of domain shuffling 117
8.6 Implications: the evolution of receptors in the nervous system by domain shuffling 120
References 123
Appendix I: Statistical data, all Chapters
Appendix II: Cloning maps, supporting gels and sequencing data
Appendix III: Null mutagenesis lines summary

List of Figures

		Following page
1.1	Vertebrate neurotrophin structures	3
1.2	Vertebrate Trk signalling pathways	4
1.3	Vertebrate LIG proteins	15
1.4	Trk superfamily evolution by domain shuffling	17
1.5	Trk proteins in the metazoa	19
1.6	Truncated Trk signalling	23
1.7	Candidate neurotrophin receptors in *Drosophila*	25
1.8	The *Drosophila* nervous system	30
1.9	The *Drosophila* ring gland	33
2.1	Genetic protocol: double mutants, chromosomes II & III	37
2.2	Genetic protocol: double mutants, chromosomes X & III	37
2.3	Genetic protocol: recombination on chromosome III	37
2.4	Genetic protocol: mapping transgenic constructs	37
2.5	Genetic Protocol: Heat-shock Flippase-mediated mutagenesis, Chromosome II	37
2.6	Genetic protocol: Heat-shock Flippase-mediated mutagenesis - Chromosome III	37
2.7	Deletion of *kek3*, *kek4* and *kek6* by FRT transposon mutagenesis	37
2.8	Candidate gene models, P elements and probe hybridisation	39
2.9	Protein sequences of Kek3, Kek4, Kek5, Kek6 and Toll6	40
3.1	*CG15744* is expressed in the CNS	58
3.2	*CG16974* is exressed in the PNS	59
3.3	*lambik* is expressed in the PNS	59
3.4	*kek1* is expressed in the CNS	59
3.5	*kek1* is expressed in the CNS and PNS	60
3.6	*kek2* is expressed in the CNS	61
3.7	*kek3* is expressed in the larval CNS	62
3.8	*kek5* is expressed in the embryonic and larval CNS	62
3.9	*rickets* and *CG17839* expression profiles	63
3.10	*wengen* is expressed in trachea, the heart and glia	64
3.11	*dLIGs* interact genetically with the *DNTs*	65
3.12	*dLIGs* interact with *DNTs* to induce locomotion phenotypes	67
4.1	Overexpression constructs target the cell membrane in S2 cells	75
4.2	*kek1* overexpression induces a rough eye phenotype	75
4.3	*kek* overexpression rescues lethality in *DNT* mutants	75
4.4	Kek≡Toll6 chimaeras localize to the cell membrane	77
4.5	DNT2 can interact with Kek≡Toll6 chimaeras to induce NFκB signalling	77
5.1	*kek3* mutagenesis	81
5.2	*kek3* null verification primers	81
5.3	*kek4* mutagenesis	82
5.4	*kek4* and *kek6* null verification primers	82
5.5	*kek6* mutagenesis	82
5.6	*kek3* and *kek4* interact genetically with the *DNTs*	83
5.7	*kek6* genetically interacts with *DNT2*	84
5.8	*kek3* and *kek4* are required for adult locomotion	85
6.1	*kek6* is expressed in the CNS	89

6.2 Kek6 is distributed in motor neurons 90
6.3 *kek6* is required for motor axon targeting 92
6.4 *kek6* interacts with DNTs in motor axon targeting 93
6.5 *kek6* is upstream of Ras and PI3K in motor axon targeting 93
6.6 *kek6* is required for larval locomotion behaviour 94
6.7 Neuronal overexpression of *kek6* partially rescues *kek6* loss of function locomotion phenotypes 94
6.8 *kek6* interacts with *DNTs* in locomotion behaviour 95
6.9 *kek6* is upstream of Ras in locomotion behaviour 95
7.1 *kek4* is expressed in the ring gland 99
7.2 *kek4* is expressed in the corpus allatum and corpora cardiac 99
7.3 *kek4* controls developmental timing, by genotype 101
7.4 *kek4* controls developmental timing, by stage 101
7.5 *kek4* inhibits juvenile hormone signalling 102
7.6 *kek4* does not control body size 103
7.7 *kek4* controls cell number in the wing 104
7.8 *kek4* is required for larval locomotion 104
7.9 *kek3* is not required for larval locomotion 105
8.1 Evolution of the Trk family 121

Appendix II
Cloning of *kek1–6* into *pDONR^{221}*
Cloning of *kek1–6* into *pAct-attR-mCFP*
Cloning of *kek1–6* into *pAct-attR-FLAG*
Cloning of *kek1–6* into *pUASt-attR-mRFP*
Sequencing of *kek1–6+pAWC*
Chimaera cloning strategy
Cloning of *kek3–6≡toll6* chimaeras into *pDONR^{221}*
Cloning of *kek3–6≡toll6* chimaeras into *pAct5c-attR-3xHA*
Sequencing of *kek3–6≡toll6+pAWH* chimaeras

List of Tables

		Following page
2.1	Fly stocks	37
2.2	Summary of transposon alleles for survival index	39
2.3	Primers	39
2.4	Cloning constructs	39
2.5	Estimated protein domain spans for chimaera cloning	40
2.6	Antibodies	46
3.1	*DNT–dLIG* survival assays, Raw data, 18^0C experiments	65
4.1	*kek* null allele survival assays, Raw data, 25^0C experiments	75
5.1	*kek* null allele survival assays, Raw data, 18^0C experiments	83
5.2	*kek* null allele survival assays, Raw data, 25^0C experiments	83
8.1	Summary of thesis, by gene	108

Appendix I

Statistical tests, Chapter 3
Statistical tests, Chapter 4
Statistical tests, Chapter 5
Statistical tests, Chapter 6
Statistical tests, Chapter 7

Appendix III

Null mutagenesis lines summary

Abbreviations

20E	20-hydroxyecdysone
AKH	Adipokinetic hormone
BDNF	Brain-derived neurotrophic factor
BMP	Bone morphogenetic protein
CA	Corpora allata
CC	Corpora cardiaca
Cdc42	Cell division control protein 42
CNS	Central nervous system
CREB	cAMP response element-binding protein
CRNF	Cysteine-rich neurotrophic factor
DAG	Diacylglycerol
DmMANF	*Drosophila* melanogaster mesencephalic astrocyte-derived neurotrophic factor
DNT	*Drosophila* neurotrophin
ERK	Extracellular signal-regulated kinase
FN3	Fibronectin type III
FRT	Flippase recognition target
GAP	GTPase-activating protein
GEF	Guanine exchange factor
GPS	G protein-coupled receptor proteolytic site
Ig	Immunoglobulin domain
IP_3	Inositol trisphosphate
ISN	Intersegmental nerve
JH	Juvenile hormone
LIG	LRR and Ig-containing
(e)LRR	(Extracellular) Leucine-rich repeat
MAPK	Mitogen-activated protein kinase
MEK	MAPK/ERK
Musk	Muscle-specific kinase
NCAM	Neuronal cell adhesion molecule
NGF	Nerve growth factor
NGL1	Netrin G1 ligand
NLRR	Neuronal LRR protein
NMJ	Neuromuscular junction
NT-3	Neurotrophin-3
PtdIns	Phosphatidylinositol
PAK	p21-activated kinase
PG	Prothoracic gland
PI3K	Phosphatidylinositol 3-kinase
PLC	Phospholipase C
PNS	Peripheral nervous system
PKC	Protein kinase C
PTTH	Prothoracicotropic hormone

ROCK	Rho-associated protein kinase
RTK	Receptor TyrK
S.I.	Survival index
SN	Segmental nerve
TIR	Toll/Interleukin-1 receptor
TLR	Toll-like receptor
TN	Transverse nerve
TNF	Tumour necrosis factor
TyrK	Tyrosine kinase
UAS	Upstream activation sequence
UTR	Untranslated region
VNC	Ventral nerve cord
VUM	Ventral unpaired median neuron

CHAPTER 1

INTRODUCTION

The canonical vertebrate neurotrophin receptors — the Trk and $p75^{NTR}$ protein families — have not been found in *Drosophila*. Nonetheless, *Drosophila* has neurotrophins, thus posing a biological problem: how is neurotrophic signalling implemented in flies?

The Trk protein family is formed of transmembrane receptors with intracellular tyrosine kinase (TyrK) domains and with extracellular ligand-binding Leucine Rich Repeat (LRR) and Immunoglobulin (Ig) domains (i.e. LIG receptors; Huang and Reichardt (2001)). Studies to date searched for *Drosophila* Trks using hybridisation-based cDNA library screens for homology to the signalling TyrK, identifying dRor and dTrk (Oishi et al., 1997, Pulido et al., 1992). However, phylogenetic analysis of the full sequences of these candidates revealed them to be phylogenetically unrelated to the Trk family. Furthermore, dTrk was found to encode a catalytically dead kinase, and subsequently renamed Off-Track (Kroiher et al., 2001). Proteomic analyses have also detected no conserved TyrK of the Trk family in flies (Manning et al., 2002). Thus, no TyrK of the Trk family and no full length Trks have been identified in *Drosophila*.

Throughout evolution, the Trk superfamily has diversified through protein domain shuffling, yielding four protein families with distinct domain architectures — the Rors, muscle-specific kinases (Musks), Ddrs and the Trks (Sossin, 2006). Domain shuffling has also yielded different forms of Trks throughout the invertebrates, from TyrK-only Trk-like architectures in the mollusc *Aplysia* to a full length *Aplysia* Trk (Kassabov et al., 2013, Ormond et al., 2004, Wilson, 2009). Domain shuffling has also generated proteins unique to the insects which have retained some, but not all, of the Trk family protein domains. These are the *Drosophila* LIG (dLIG) proteins, which contain only the extracellular LIG module of Trks. They also resemble the naturally occurring truncated Trk isoforms, which lack an intracellular TyrK (Ohira and

Hayashi, 2009). Phylogenetic comparison of the *Drosophila* dLIGs to the vertebrate LIGs identifies the six member Kekkon (Kek) protein family as phylogenetically related to the Trks (Mandai et al., 2009). The Kek proteins form a single clade together with the Trks and are more similar to them than all other vertebrate and dLIGs are to each other. In my thesis I will ask: are the Keks functional Trks in *Drosophila*?

There is evidence that neurotrophic and gliatrophic signalling operates throughout the invertebrates. Some of the evidence is circumstantial: for example, in molluscs, L-EGF induces neurite outgrowth in culture and facilitates central nervous system (CNS) repair, and cysteine rich neurotrophic factor (CRNF) can interact with $p75^{NTR}$ *in vitro* (Fainzilber et al., 1996, Hermann et al., 2000). There is, however, functional *in vivo* evidence of neurotrophism in fruit flies. In *Drosophila*, the EGF ligands Spitz and Vein are required for midline and longitudinal glia survival, respectively (Bergmann et al., 2002, Hidalgo et al., 2001); the secreted ligand netrin is required for motor axon targeting (Mitchell et al., 1996, Newquist et al., 2013); and DmMANF regulates dopaminergic neuron survival (Palgi et al., 2009).

The *Drosophila* neurotrophins DNT1 and DNT2 were identified by homology to vertebrate brain-derived neurotrophic factor (BDNF; Zhu et al. (2008)). DNT1 and DNT2 regulate neuronal survival in the CNS, motor axon targeting and synaptogenesis (Sutcliffe et al., 2013, Zhu et al., 2008). It was recently shown that DNT1 and DNT2 are ligands for Toll7 and Toll6, which can signal via NFκB (McIlroy et al., 2013). Nonetheless, the role of Trk-like dLIG proteins remains unexplored.

Given their similarities to the Trks, the aim of my thesis was to investigate the roles of the dLIGs in the nervous system to determine whether they have Trk-like functions, and whether they can interact with the DNTs to function as DNT receptors.

1.1 Neurotrophin signalling

1.1.1 Neurotrophism, neurotrophins and neurotrophic factors

Neurotrophism is the process whereby neuronal innervation targets secrete finite concentrations of trophic factors to control axonal targeting and neuronal survival — neurons that receive neurotrophic support survive, whereas mistargeted neurons undergo apoptosis (Levi-Montalcini, 1987).

For clarity, a distinction must be made between the neurotrophins and neurotrophic factors. A neurotrophic factor is any trophic factor that regulates the survival of neurons (gliatrophic factors, conversely, regulate the survival of glia; Huang and Reichardt (2001)). Neurotrophins, meanwhile, are a family of neurotrophic factors defined by a specific structure — including a cleaved pro-domain and a characteristic cysteine knot (CysKnot) — that is absent from other neurotrophic factors (Figure 1.1; Bradshaw et al. (1993)).The first known neurotrophin, nerve growth factor (NGF), was identified as the secreted molecule that induced fibril growth of chick neurons in culture upon addition of mouse tumour tissue (Levi-Montalcini and Hamburger, 1951). NGF contains 6 key cysteine residues, all involved in intrachain disulphide bonds (Angeletti and Bradshaw, 1971, Bradshaw et al., 1993). This disulphide core is the founding member of a distinct family of CysKnot structure, since the separate TGFβ and PDGF CysKnot families both contain 8 key cysteine residues (Daopin et al., 1992, Oefner et al., 1992, Sun, 1995). Subsequent neurotrophins were identified by sequence homology with NGF, including the CysKnot (Jones and Reichardt, 1990, Rosenfeld et al., 1995).

In mammals, there are four neurotrophins — NGF, BDNF, NT-3 and NT-4/5 (Huang and Reichardt, 2001). The structures and sizes of vertebrate neurotrophins are shown in Figure 1.1. NT-4 was discovered in *Xenopus laevis* and NT-5 in rat, and both have since been shown to be structural orthologues (Berkemeier et al., 1991, Hallbook et al., 1991). The distributions

Figure 1.1 **Vertebrate neurotrophin structures**

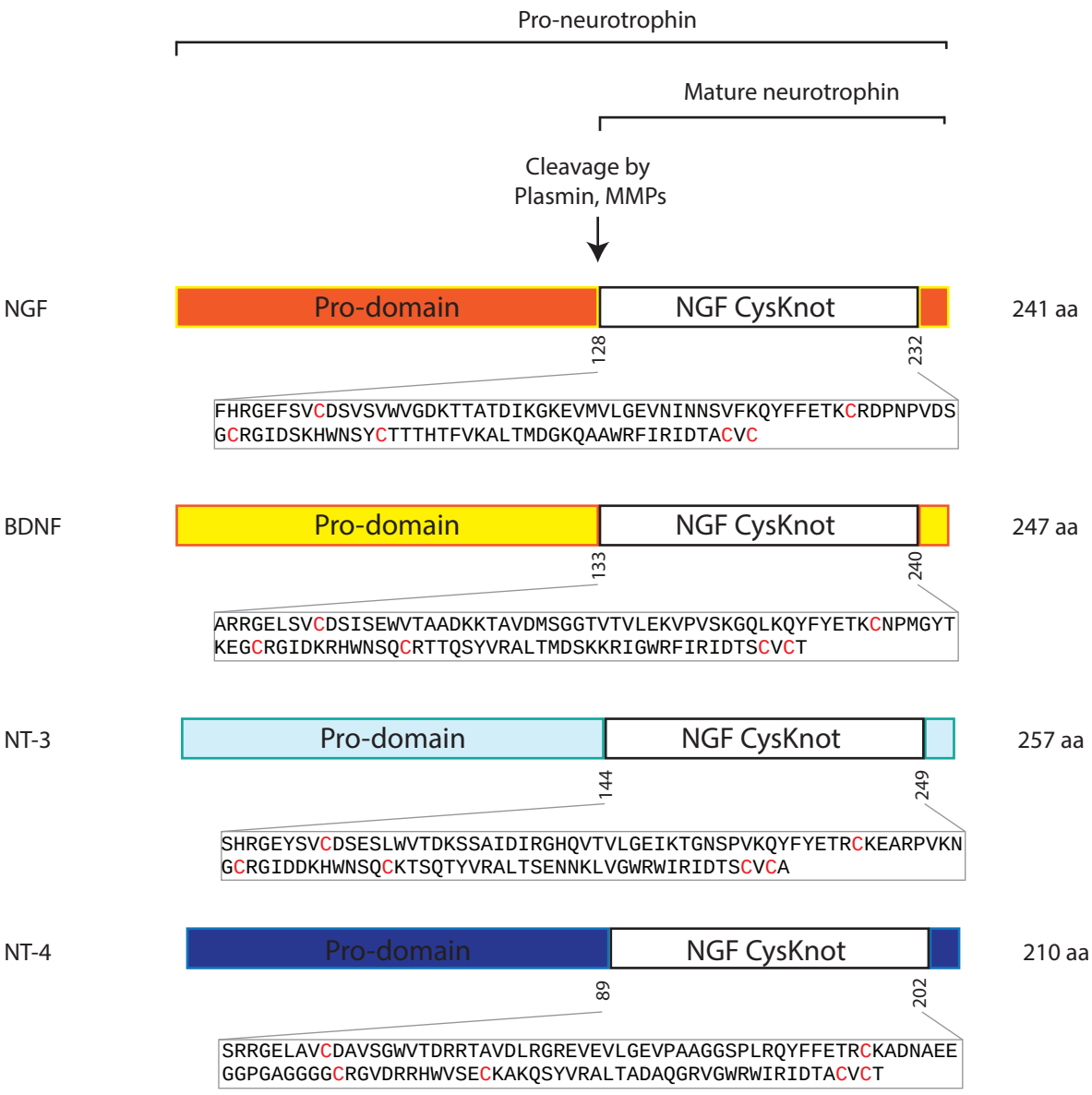

The structures of all four vertebrate neurotrophins are shown. NGF, BDNF, NT-3 and NT-4 are synthesised as pro-neurotrophins, including a pro-domain. The pro-domain is cleaved to produce a mature neurotrophin. Peptide lengths and cleavage positions are indicated. The peptide sequence of the neurotrophin family CysKnot is shown, with the six key Cysteine residues highlighted in red.

of neurotrophins throughout the chordates suggests that the neurotrophin family duplicated twice within the vertebrates: NGF, BDNF, NT-3 and NT-4/5 are present throughout the tetrapods (although NT-4/5 is absent in birds), NT-6 and NT-7 are found only in bony fish, and cartilaginous fish have only BDNF and NT-3 (Hallbook, 1999). Outside of the vertebrates, neurotrophins have been found in the lamprey (Lf-NT) and hagfish (Mg-NT), which diverged from the vertebrate lineage 460 million years ago (Hallböök et al., 1998, Kumar and Hedges, 1998). Thus, NGF and NT-3 formed from the duplication of one ancestral neurotrophin, and BDNF and NT-4/5 from a separate ancestral gene, both occurring between the branch of jawless fish (hagfish and lampreys) and the branch of the cartilaginous fish (Hallbook, 1999). NT-6/7 likely arose separately within the bony fish lineage, and the ancestral neurotrophins were subsequently lost (Hallbook, 1999).

Neurotrophins function as dimers and bind the Trk family of receptors, $p75^{NTR}$ and sortilin (Shen and Maruyama, 2011, Vilar et al., 2009). Neurotrophin–receptor interactions are unusual in that they are promiscuous (Figure 1.2). Furthermore, all four neurotrophins bind to $p75^{NTR}$, and signalling can be transduced by interaction between the Trks and $p75^{NTR}$, although evidence of TrkB and TrkC interactions with $p75^{NTR}$ is unclear (Wehrman et al., 2007). $p75^{NTR}$ can also interact with sortilin upon ligand binding (Skeldal et al., 2012).

Neurotrophins are secreted as precursor forms of 30–35kDa, called pro-neurotrophins, which are proteolytically cleaved to produce shorter, mature proteins of 12–13kDa (Lu et al., 2005, Seidah et al., 1996). Amino acid positions of proteolytic cleavage are shown in Figure 1.1. Pro-neurotrophins promote cell death through $p75^{NTR}$, whereas cleaved neurotrophins bind TrkA– $p75^{NTR}$ heterodimers, or $p75^{NTR}$ or Trk homodimers, to promote cell survival and manifest neurotrophic phenotypes (Chao, 2003). NGF–TrkA signalling, for example, is required for survival of nociceptive and sensory neurons in the skin (Smeyne et al., 1994). Targeting roles of neurotrophism are illustrated by, for example, the BDNF/TrkB-dependent navigation of retinal axon growth cones in chick embryos (Ernst et al., 2000). In addition to

Figure 1.2 **Vertebrate Trk signalling pathways**

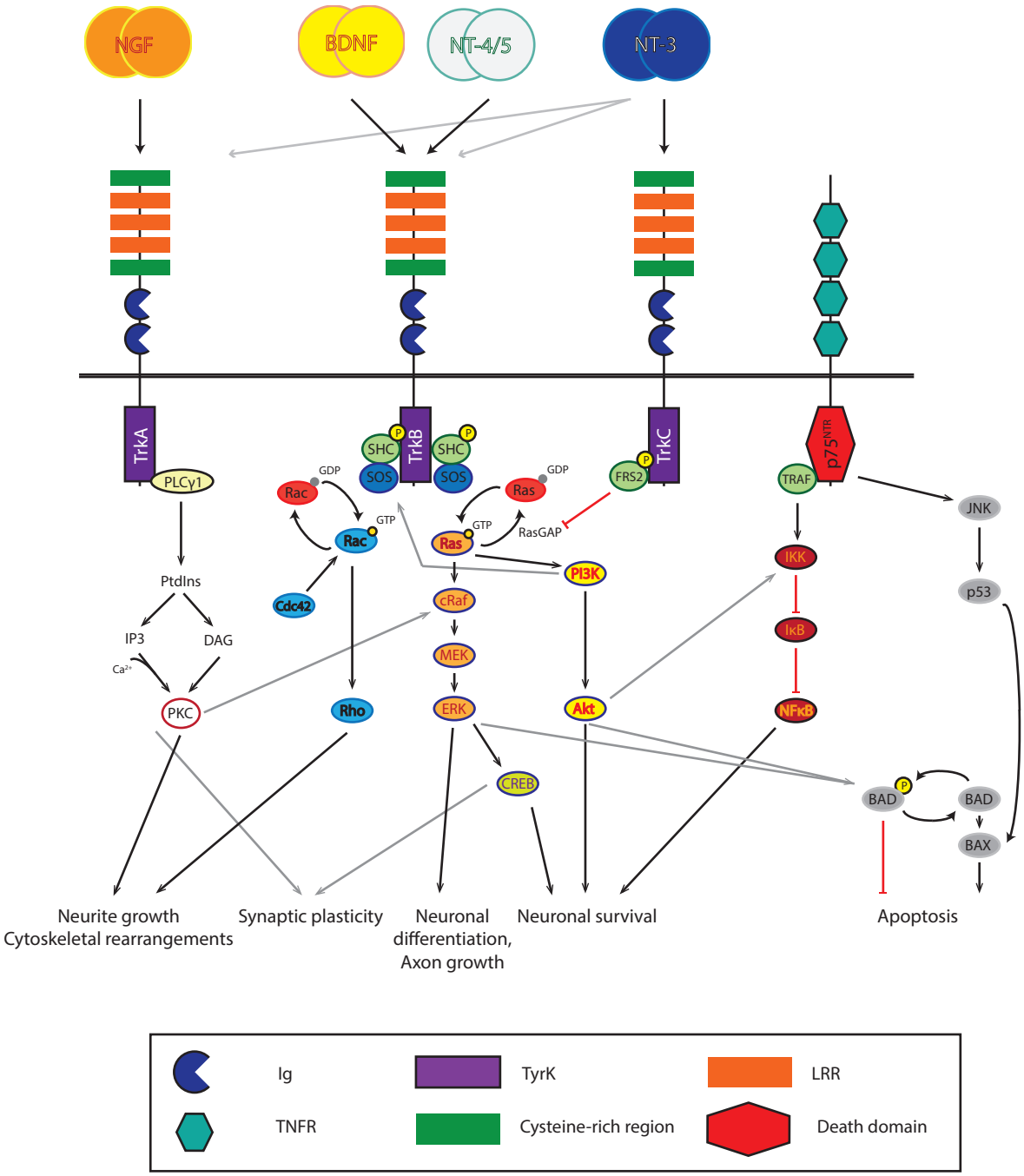

Neurotrophins bind in promiscuous combinations with the Trk and p75^{NTR} neurotrophin receptors. Ligand-receptor binding leads to downstream PLCγ1, ERK, PI3K and NFκB signalling, which promote neuronal development. Apoptosis is promoted by p75NTR via the JNK pathway. Pathway crosstalk is observed and indicated by grey arrows. See main text for references. Domains: Ig, immunoglobulin; LRR, leucine-rich repeat; TNFR, tumour necrosis factor receptor; TyrK, tyrosine kinase.

neuronal survival, neurotrophins are crucial for neuronal differentiation, axonal and dendritic growth, synaptogenesis and long term potentiation (Huang and Reichardt, 2001). The neurotrophins are also implicated in behaviour, memory and learning (Chao et al., 2006). Aberrant neurotrophin function is linked with a number of neurological pathologies, including neurodegenerative diseases and psychiatric disorders (Chao et al., 2006, Levi-Montalcini, 1976, Siggers et al., 1976).

Neurotrophins were recently found in insects (see Chapter 1.1.3). However, insect Trk receptors have been presumed to be absent (see Chapters 1.2.4 and 1.4.2; Manning et al. (2002)).

Nonetheless, a number of key points contribute to the complexity of neurotrophin signalling, and suggest that Trk or Trk-like proteins can be found in *Drosophila*: 1) Although the Drosophila neurotrophins can signal through Toll proteins (see Chapter 1.1.3), vertebrate neurotrophic ligand–receptor interactions are promiscuous. Alternative DNT receptors may yet be found. 2) The Trk superfamily predates the origin of vertebrates and Trk proteins are found in non-insect invertebrates (see Chapter 1.4). 3) Domain shuffling from ancestral Trk superfamily proteins has yielded modern Trks in vertebrates and novel proteins containing neurotrophin-binding modules in the *Drosophila* proteome (see Chapters 1.4 and 1.5). Some of these novel *Drosophila* proteins cluster phylogenetically with the vertebrate Trks (see Chapter 1.4.2; Mandai et al. (2009)). Because of these points, this thesis searched for functional Trk or Trk-like proteins in *Drosophila*, to solve this knowledge gap.

1.1.2 Neurotrophin signalling in neural development

Autophosphorylation of specific tyrosine residues following ligand binding allows the binding of adaptor proteins that link dimerized Trks to intracellular signalling pathways (Huang and Reichardt, 2001). Depending on signalling context, which is controlled by co-receptors and cell type, Trks may activate the mitogen-activated protein kinase (MAPK),

phosphatidylinositol 3-kinase (PI3K)/Akt and/or phospholipase Cγ (PLCγ) pathways (Figure 1.2):

- Trk activation by NGF leads to receptor phosphorylation and PLCγ1 recruitment (Vetter et al., 1991). Phosphorylated PLCγ1 subsequently catalyses the hydrolysis of phospholipids to inositol trisphosphate (IP_3) and diacylglycerol (DAG), both of which can activate protein kinase C, leading to downstream promotion of neurite growth and cytoskeletal rearrangements (Huang and Reichardt, 2001, Mellor and Parker, 1998). Protein kinase C (PKC) can promote the Extracellular signal-regulated kinase (ERK) pathway via Raf (Corbit et al., 1999).
- Ligand-dependent ERK signalling is more directly initiated upon recruitment of the TyrK adaptor SHC, which binds the Ras guanine exchange factor (GEF) SOS complex, leading to downstream activation of Ras, cRaf, MEK and ERK (Kaplan and Miller, 2000). ERK activation is required for neuronal differentiation and, via the cAMP response element-binding protein (CREB) pathway, neuronal survival (Dworkin and Mantamadiotis, 2010, Xing et al., 1998). The SOS complex also mediates the activation of Rac, and thereby downstream cytoskeletal rearrangements via Rho (Nimnual et al., 1998).
- Neuronal survival and differentiation can be mediated via PI3K, which requires activation by Ras (Diering et al., 2013). Motor neuron excitability and nerve terminal growth are both regulated by PI3K activity, although the former requires Ras activity, whereas the latter is activated via p85 (Johnson et al., 2012). Ras signalling via PI3K further promotes SOS-mediated activation of Rac and subsequent cytoskeletal rearrangement. Cleaved neurotrophins also bind $p75^{NTR}$ and TrkA to promote neuronal survival via NFkB (Maggirwar et al., 1998).

By contrast, pro-apoptotic signalling via neurotrophin-mediated $p75^{NTR}$ signalling occurs via the JNK pathway and BAD. Apoptosis is induced by the executioner proteins BAX and BAK,

which are functionally redundant (Oltvai et al., 1993, Wei et al., 2001). BAX undergoes conformational changes to bind the mitochondrial outer membrane (MOM), where it creates a pore, releasing lipids and proteins (such as cytochrome c) from the mitochondrial intermembrane space (Kuwana et al., 2002). MOM permeabilization is the final commitment step in apoptosis (Shamas-Din et al., 2013). JNK signalling via p53 activates the transcription of BAX (Miyashita and Reed, 1995).

BAX membrane localization and insertion is prevented by sequestration by the anti-apoptotic protein BCL-XL, thereby halting apoptosis (Billen et al., 2008). BCL-XL, in turn, can be sequestered by binding to GDP-bound BAD, thereby permitting apoptosis (Aloyz et al., 1998). BAD is deactivated downstream of mature neurotrophin signalling by both ERK and the PI3K target Akt (Datta et al., 1997, Huang and Reichardt, 2001).

1.1.3 Neurotrophins and neurotrophism in insects

Trophic interactions are required for nervous system development in *Drosophila* (Beck and Fainzilber, 2002, Hidalgo, 2002). For example, the EGFR ligand Vein is secreted by MP2 pioneer neurons and is required for longitudinal glia survival (Hidalgo et al., 2001). A second ligand of EGFR, Spitz, is derived from axons and required for midline glia survival (Bergmann et al., 2002). The growth cone guidance cue Netrin, a neurotrophic factor, is secreted from the *Drosophila* midline and required for commissure formation and motor axon targeting (Mitchell et al., 1996, Hiramoto et al., 2000). Furthermore, Netrin gradients are required for neuronal survival within the CNS, and correct axon guidance can be rescued in *Netrin* loss of function mutants by blocking apoptosis (Newquist et al., 2013). Last, flies lacking the secreted neurotrophic factor DmMANF exhibit embryonic dopaminergic neuron cell death (Palgi et al., 2009). However, neurotrophic factors were not found in flies until recently.

The Toll ligand Spz was found to contain an NGF domain as far back as 1998, but its similarity with the blood-clotting factor coagulogen in the horseshoe crab delayed investigation into its possible neurotrophic roles (Hu, 2004, Inamori et al., 2004, Parker et al., 2001, Weber et al., 2003). Coagulogen does not form a functional CysKnot dimer, a feature of the vertebrate neurotrophins, whereas Spz does (Mizuguchi et al., 1998). Nevertheless, it is interesting that both coagulogen and BDNF are cleaved by a common proteolytic cascade (Pang et al., 2004, Skrzypiec et al., 2008). A family of six *spz* paralogues was identified in *Drosophila* (Parker et al., 2001).

Subsequently, using sequence-based homology searches of the recently sequenced genomes, DNT1 (Spz2) and DNT2 (Spz5) were identified as homologues of vertebrate BDNF, the most conserved vertebrate neurotrophin (Götz et al., 1992, Zhu et al., 2008). Structural analysis confirmed that DNT1, DNT2 and Spz are closely related to the mammalian NTs, and of these, structure-based alignment revealed that the CysKnot sequences of DNT1 and DNT2 are more closely related to the vertebrate neurotrophins than that of Spz (Zhu et al., 2008). Structural alignment of the CysKnots further revealed that Spz3, Spz4 and Spz6 are too far diverged from the vertebrate neurotrophins. The DNTs also have functional conservation relative to the mammalian NTs. DNT1 and DNT2 are secreted from the embryonic midline and embryonic muscles, and DNT1 protein is detected in the larval lamina and adult central brain; they are target-derived functional neurotrophins required for motor axon targeting, synaptogenesis at the neuromuscular junction (NMJ) and regulation of naturally occurring cell death of neurons (Sutcliffe et al., 2013, Zhu et al., 2008). Phylogenetic comparison of the neurotrophins and Spz-related functional neurotrophins group the proteins into two separate clades, together forming the neurotrophin superfamily (Wilson, 2009).

Tolls do not signal via an intracellular TyrK (Dolan et al., 2007). Instead, Toll signals to the NFkB pathway through a Toll/Interleukin-1 receptor (TIR) domain. As such, they functionally resemble $p75^{NTR}$. Compared with related mammalian receptors, mammalian

$p75^{NTR}$ has increased affinity for the *Drosophila* TIR adaptor protein dTRAF2, suggesting that Toll family and $p75^{NTR}$ signalling may be evolutionarily linked (Zapata et al., 2000). Spz binding to Toll stimulates the expression of *drosomycin*, which is involved in the immune response to fungal infection, via the NFκB homologue Dif (Hu, 2004, Manfruelli et al., 1999, Meng et al., 1999). Alongside their immune role, *dif* and the second NFκB homologue *dorsal* are also expressed in the nervous system, and Spz–Toll binding-induced Dorsal nuclear translocation has a role in dorsoventral patterning (Ayyar et al., 2007, Beramendi et al., 2005, Cantera et al., 1999, DeLotto and DeLotto, 1998, Mindorff et al., 2007). The inhibitor of Dorsal and Dif, Cactus, is enriched at the NMJ, and is necessary for normal locomotion (Beramendi et al., 2005).

It was recently revealed that the DNTs can interact with Toll6 and Toll7 to activate Dif and Dorsal signalling (McIlroy et al., 2013). *toll6* and *toll7* are expressed in the ventral cord (VNC) and brain of embryos and larvae, and in the adult brain. In embryos and larvae, Toll6 and Toll7 are distributed in motor neurons and interneurons. Like $DNT2^{e0344}DNT1^{41}$ double mutants, *toll6*;*toll7* double mutants are also semi-lethal when bred at 18°C in combination with the *TM6B* balancer, and this semi-lethality can be rescued by the neuronal overexpression of activated *toll6* or *toll7* alleles (McIlroy et al., 2013). *toll6* and *toll7* loss of function mutations lead to an increase in neuronal cell death in the embryonic VNC and axon targeting phenotypes in motor axons, and *toll6*;*toll7* double mutant larvae display locomotion phenotypes (McIlroy et al., 2013). Co-immunoprecipitation of co-transfected Toll receptors and DNT ligands in S2 cell culture confirmed that Toll7 and Toll6 can bind DNT1 and DNT2, respectively (McIlroy et al., 2013).

1.1.4 Neurotrophins in the systemic control of growth

An often overlooked aspect of the neurotrophins is that their roles are not restricted to the CNS or peripheral nervous system (PNS) (Calza et al., 2003, Levi-Montalcini et al., 1990).

NGF could link the nervous, endocrine and immune systems (Tometten et al., 2005). Concordantly, Trks have been shown to have neurotrophin-independent roles, and the molluscan LTrk is enriched in endocrine cells (Schecterson and Bothwell, 2010, Schecterson et al., 2010, van Kesteren et al., 1998). Furthermore, $p75^{NTR}$ and the Trks are distributed in tissues derived from all three germ layers (Thomson et al., 1988).

NGF has roles in autonomic nervous system regulation (Levi-Montalcini, 1976, Siggers et al., 1976). Aberrant NGF function also contributes to autoimmune diseases, such as lupus (Aloe et al., 1994, Bracci-Laudiero et al., 1993, Levi-Montalcini et al., 1990). During pregnancy, environmental stress triggers progesterone-dependent NGF production, leading to cytokine production and apoptosis (Tometten et al., 2005). Reciprocally, NGF is upregulated in arthritic joint synovial fluid by cytokines during inflammation (Aloe et al., 1992, Aloe et al., 1993, Triaca and Tirassa, 2003). NGF levels are also increased in the cerebrospinal fluid of multiple sclerosis patients (Laudiero et al., 1992), and NGF can itself function in the immune system as a cytokine-like molecule, whereupon it induces mast cell proliferation (Aloe and Levi-Montalcini, 1977). Last, the mammalian Toll-like receptors (TLRs) have roles in both the neuroendocrine and immune systems as well as the microglia and neurons of the hippocampus: TLRs are detected in neurons and endocrine cells of the hypothalamus, as well as adipocytes and the islets of Langerhans, and autoimmune thyroid disease is linked to TLR misregulation (Kanczkowski et al., 2008).

1.2 Domain Shuffling in the Evolution of Receptors

1.2.1 Principles of Domain Shuffling

Natural selection reassigns biological components for novel purposes (Jacob, 1977). One such manifestation of evolutionary ‘tinkering’ is protein domain shuffling. The concept of the protein domain as a structural unit was first proposed in 1970, on the elucidation of the structure of IgG (Edelman, 1970, Williams and Barclay, 1988). Each variable and constant

homology region within the molecule was shown to contain one intrachain disulphide bond that stabilises the regions with similar, but separate, tertiary structures. These structures are now known as Ig domains. Over time, the term domain has acquired other definition variations such as the nouns ‘fold’, ‘motif’ and ‘signature sequence’ (Doolittle, 1995). Here, I use the term ‘domain’ to mean a discrete, heritable protein sequence motif that forms a conserved tertiary structure; ‘domain architecture’ to mean structures that arise from protein domain combinations; and ‘module’ as a multidomain functional unit (Hartwell et al., 1999).

The protein domain is a basic evolutionary unit from which proteins are built (Vogel et al., 2005). The architecture that arises from multiple domain arrangements is the fundamental order of protein functional complexity and underlies the concept of modular biology (Buljan and Bateman, 2009, Hartwell et al., 1999, Vogel et al., 2005). Protein domains and multidomain modules have been both co-opted throughout evolution for novel purposes, and often retained owing to evolutionary functional relevance (Bashton and Chothia, 2007, Basu et al., 2008, Doolittle, 1995, Ekman et al., 2007, Patthy, 1999, Soding and Lupas, 2003). Thus, protein domain shuffling might drive the evolution of complexity independently of genome expansion and faster than protein reinvention (Hallböök et al., 2006, Vogel and Chothia, 2006, Bjorklund et al., 2005, Bornberg-Bauer et al., 2005, Hartwell et al., 1999, Moore et al., 2008, Soding and Lupas, 2003). For example, rearrangements of modules resulted in the evolution of the multiple protein blood-clotting cascade (Patthy, 1985).

Expansion of distinct protein domain architectures (both permutations and domain combinations) has accelerated in metazoa, particularly in animals (Ekman et al., 2007). These changes in protein domain architecture can occur by several genetic mechanisms: for example, shuffling of single domain-encoding exons by recombination of exon-flanking introns, alternative splicing of multiple domain-encoding exons, and retrotransposition (Moore et al., 2008, Patthy, 1999, Doolittle, 1995). Approximately 5% of protein domains form promiscuous combinations with other domains, and these domains are generally

involved in protein–protein interactions and signalling pathways, suggesting that their promiscuous co-option was a consequence of their usefulness in many biological contexts (Basu et al., 2008, Bjorklund et al., 2005, Marcotte et al., 1999). However, conservation of domain architectures may only be possible with concordant ligand evolution, since novel receptors will be quickly lost without the corresponding pairing of at least one ligand, co-receptor or adaptor protein (Sossin, 2006).

This thesis focuses on receptors with the LIG module and its constituent domains: LRRs and Ig domains. This introduction also considers TyrKs, as LIG modules and TyrKs constitute the Trk neurotrophin receptors. The hypothesis is that the Trk receptor family diversified in the course of evolution, resulting in partial Trk-like proteins in fruit flies that might have conserved binding to neurotrophin family ligands and nervous system functions.

1.2.2 Leucine Rich Repeats

The primary function of LRRs is ligand binding (Kobe and Deisenhofer, 1995, Kobe and Kajava, 2001). LRR proteins can also form dimers, suggesting that alternative modes of binding to LRRs may underlie signalling (Scott et al., 2006). LRR-containing receptor kinases may form dimers with LRR-containing receptor-like proteins that lack an intracellular signalling domain — for example, CLV1–CLV2 heterodimers are suggested to suppress stem cell differentiation in plants, and Sas may interact with the phosphatase Ptp10D in *Drosophila* axon guidance (Torii, 2004, Lee et al., 2013).

Proteins containing extracellular LRRs (eLRRs) are involved in diverse functions, such as cell adhesion and signalling, platelet aggregation, neuronal development, axon guidance and the immune response (Chen et al., 2006, Ko and Kim, 2007, Ma et al., 2006, Nurnberger et al., 2004). For example, the LRR-containing proteins Nogo-66 receptor, Slit, AMIGO, LINGO, netrin G1 ligand (NGL1) and the neuronal LRR (NLRR) family have roles in neurite outgrowth, axon guidance and targeting, and migration (Ko and Kim, 2007).

Mutant alleles of genes encoding proteins with eLRRs result in defects in axon guidance and cell migration (*Slit/Robo*; Long et al. (2004)), myelination (*LINGO1*;Mi et al. (2005), neuronal survival (*Trks* and *Netrin*; Conover and Yancopoulos (1997), Newquist et al. (2013)), plasticity and nerve regeneration (*Nogo*; McGee et al. (2005)), and learning and memory (*NLRR4*; Bando et al. (2005)). Indeed, LRR-containing proteins are defective in many human diseases and disorders, including schizophrenia, hyperthyroidism and the autoimmune condition Graves' disease, and loss of function of *trkA* is a cause of congenital insensitivity to pain (CIPA; de Wit et al. (2011), Matsushima et al. (2005)). Furthermore, upregulation of *trkB* is associated with multiple myeloma, neuroblastoma and lung adenocarcinoma (Gupta et al., 2013).

The LRR family is greatly expanded in mammals, and to a lesser extent flies, compared to the worm (Dolan et al., 2007). In the *Drosophila* proteome, 9 of the 66 eLRR-containing proteins contain at least one additional Ig domain (Dolan et al., 2007). 16 of the 66 *Drosophila* eLRRs share homology with the eLRRs of Toll proteins. Of these 16, 9 contain an intracellular TIR domain (Dolan et al., 2007). It is interesting to note that certain protein families have expanded faster than others in certain species: *Drosophila* has 9 LIGs, whereas humans have 38, and there are 9 *Drosophila*, 13 human and 253 sea urchin Toll-related eLRRs (Buckley and Rast, 2012, Dolan et al., 2007). The functional consequence of such protein family expansions is uncertain. Within the LIGs, many families and architectures are unique to mammals, including the AMIGO family; others have expanded mainly in mammals (flies have one copy of the Lambik LIG protein, whereas mice encode LRIG1, LRIG2 and LRIG3; Nilsson et al. (2001)); and the Kek family has expanded in insects only (Derheimer et al., 2004, Dolan et al., 2007).

1.2.3 Immunoglobulin domains

Ig domains form a structure stabilised by disulphide bonds (Buljan and Bateman, 2009, Edelman, 1970). On the basis of sequence and structural similarities, four sets of Ig domains were identified: Ig-C1 domains are exclusive to vertebrates, whereas Ig-C2 predate the protostome–deuterostome split; and I and V-set Ig domains are the most ancient (Buljan and Bateman, 2009, Williams and Barclay, 1988). Ig domain-containing proteins have been identified in the parazoa, often with kinase domains. Consequently, the ancestral Ig-containing protein is predicted to have had a role in signalling (Gamulin et al., 1994). Like LRRs, Igs can be strung together in tandem repeats (Vogel and Hedgecock (2001)).

Ig domains have adhesion functions at the cell surface, forming heterophilic and homophilic interactions between Ig-containing molecules across opposing membranes that underlie neuronal cell elongation and migration, fasciculation and synapse maintenance (Lin et al., 1994b, Patel et al., 1987, Snow et al., 1988, Rougon and Hobert, 2003, Williams and Barclay, 1988, Zipursky and Grueber, 2013). Trk Ig domains can bind to neurotrophins *in vitro* and *in vivo* (Bothwell, 2006, Holden et al., 1997, Urfer et al., 1995). Furthermore, polysialic acid–NCAM (neuronal cell adhesion molecule; the vertebrate orthologue of *Drosophila* FasII), which is rich in Ig domains, enhances and facilitates BDNF activation of TrkB (Muller et al., 2000).

Drosophila has 142 Ig-containing proteins, of which half belong to families of at least two closely related proteins derived by gene duplication (Vogel, 2003). In some cases, these duplications were followed by the loss or gain of domains. One of the largest of these families is the insect-specific Kek protein family.

1.2.4 Tyrosine Kinases

Protein kinases are crucial biological signalling components, accounting for 1.5–2.5% of eukaryotic genes (Hanks and Hunter, 1995, Manning et al., 2002). The two most common

protein kinases, protein-serine/threonine and TyrKs, constitute 67% and 17%, respectively, of the kinome (Braconi Quintaje and Orchard, 2008).

All major kinase groups and most kinase families, including two-thirds of TyrKs, are shared among metazoa (Manning et al., 2002, Miranda-Saavedra and Barton, 2007). Most TyrK gene duplications occurred rapidly before the radiata–bilateria divergence (Suga et al., 1997). Gene duplications in tetrapods have been slower, indicating that selection pressures on TyrK evolution have varied and may be species-specific. Indeed, unlike Ig and LRR complements, *C. elegans* has twice as many kinases as the fly and there are no fly specific kinase families (Morrison, 2000). Reasons for such accelerated selection in the worm are unknown.

Transmembrane receptor TyrKs (RTKs), which contain an intracellular TyrK, evolved before the divergence of protostomes and deuterostomes, since sponges contain multiple RTKs, including RTKs with extracellular Ig domains (Muller et al., 1999). Whereas RTKs belonging to the PDGFR, FGFR, Ret, ALK and EGFR families are present in both *Drosophila* and humans, no functional Trk-like RTKs have been found in *Drosophila* (Loren et al., 2001, Manning et al., 2002, Schweitzer and Shilo, 1997).

1.3 LIGs in vertebrates

Many metazoan LIG protein families are specific to or enlarged in the mammalian lineage (Dolan et al., 2007). Here, I focus on the vertebrate LIGs that contain only eLRR and Ig domains (Figure 1.3), and do not describe NLRR and PAL proteins, which contain further fibronectin type III (FN3) repeats (Chen et al., 2006).

1.3.1 Trk receptors

The Trk protein family functions as vertebrate neurotrophin receptors (Huang and Reichardt, 2001). In addition to an extracellular LIG module, TrkA, TrkB and TrkC each contain an intracellular TyrK (Figure 1.3). Both the LRR and Ig domains have been shown to be required

Figure 1.3 **Vertebrate LIG proteins**

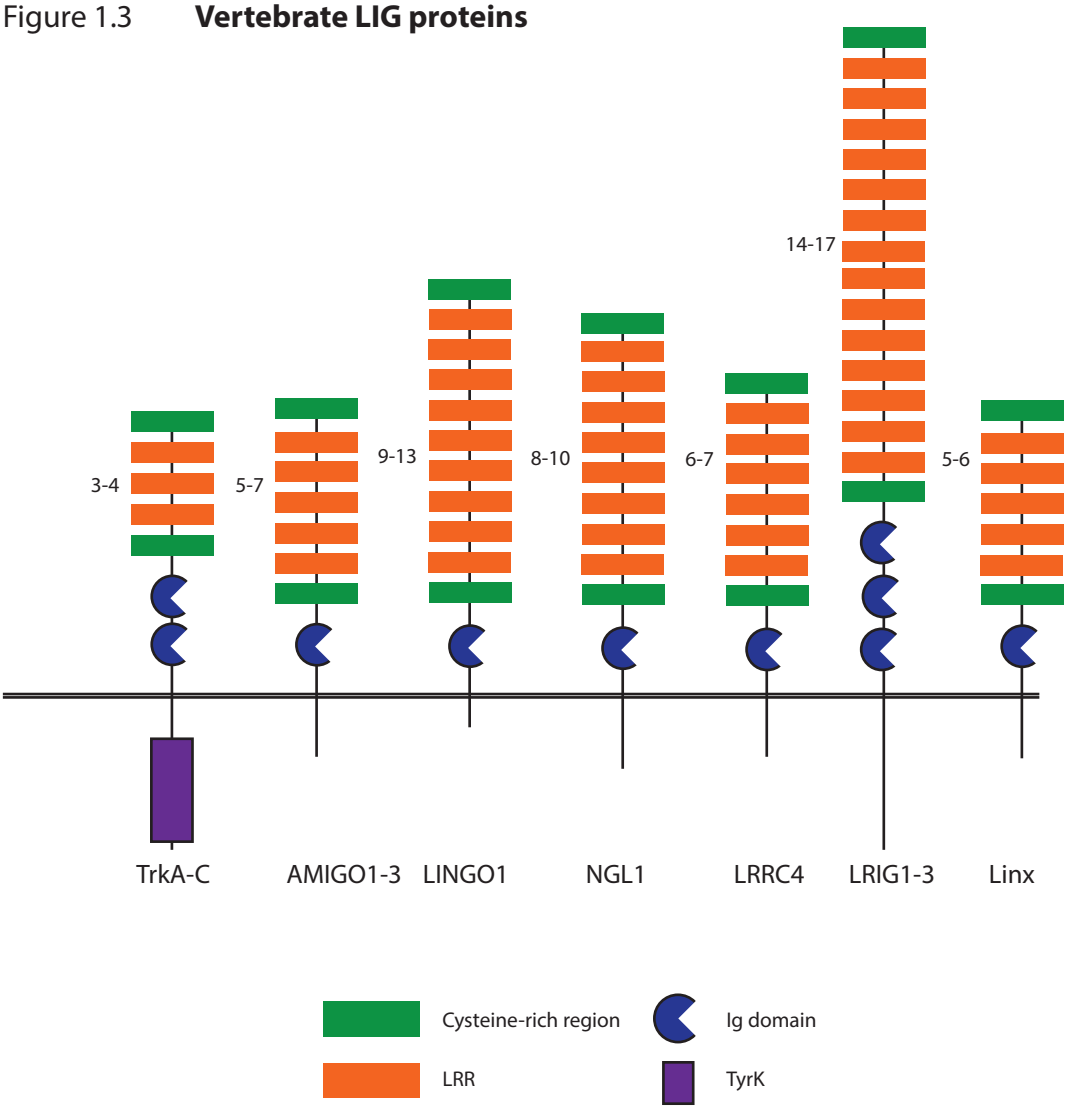

Vertebrate Leucine rich repeat (LRR) and Immunoglobulin (Ig) domain-containing LIG proteins are shown. Extracellular, up. Domain architectures are based on sequences available at UniProt and confirmed using the SMART online tool. Variation in LRR number in the literature is indicated. TyrK, tyrosine kinase. For references, see text.

for neurotrophin binding *in vitro* (Bothwell, 2006, Kobe and Deisenhofer, 1994, Windisch et al., 1995), whereas the Ig domain is sufficient for nerve growth factor (NGF) binding *in vivo* (Bothwell, 2006, Holden et al., 1997, Urfer et al., 1995). Neurotrophin binding to the Trk receptors shows ligand–receptor promiscuity: NGF interacts with TrkA, BDNF and neurotrophin-4/5 (NT-4/5) interact with TrkB, and NT-3 predominantly interacts with TrkC, although it can also bind to both TrkA and TrkB (Huang and Reichardt, 2001). Downstream signalling of the Trk receptors upon ligand binding, and the evolution of the Trk receptors, are discussed below.

1.3.2 Non-Trk vertebrate LIGs

The AMIGO family comprise 5 LRRs and 1 Ig-C2 domain and form homophilic and heterophilic interactions. AMIGO1 is expressed exclusively in the brain, whereas AMIGO2 (also known as Alivin-1) and AMIGO3 are enriched in the brain and in other tissues, such as breast and ovaries (Chen et al., 2006). Ectopic production of substrate-bound AMIGO1 promotes neuron inflammation, whereas elevated levels of soluble AMIGO1 inhibit fasciculation (Chen et al., 2012, Kuja-Panula et al., 2003). Upregulation of both AMIGO1 and AMIGO2 reduces neuronal apoptosis (Ono et al., 2003, Chen et al., 2012). Unlike Trks, AMIGOs have no known intracellular signalling motifs.

LINGO1 is a localized co-receptor of Nogo receptor–$p75^{NTR}$ interactions, which inhibit neuronal regulation and brain injury (Filbin, 2003, Mi et al., 2005). LINGO1 is enriched in the limbic system and neocortex, particularly following BDNF binding (Carim-Todd et al., 2003, Trifunovski et al., 2004).

NGL1 binds the GPI-anchored axon guidance molecule Netrin G1 and is enriched in the cerebral cortex (de Wit et al., 2011). The role of NGL1 is unclear (Chen et al., 2006).

LRRC4 was initially considered to be the vertebrate orthologue of the *Drosophila* protein Kek1. LRRC4 protein is restricted to the adult mammalian brain, with a developmentally

regulated temporal expression profile (Zhang et al., 2005). LRRC4 induces a cell cycle delay, thereby suppressing tumorigenesis.

LRIG proteins contain 14 LRRs and 3 Ig domains, and cluster to the 3p14.3 chromosome, which is often deleted in human cancers (Guo et al., 2004, Hedman et al., 2002). LRIG1 is enriched in the brain in addition to many other tissues, such as skin, kidneys and the stomach, where LRIG2 and LRIG3 are also distributed. LRIGs are present in fish and *Ciona*, and are therefore ancestral to the chordate–urochordate split (Guo et al., 2004). LRIG1 interacts with EGF receptors and thus shares functional similarity with Kek1 (see below; Laederich (2004)). Unlike Kek1, however, LRIG1 upregulation induces EGFR degradation by ubiquitin E3 ligases, and LRIG1 is therefore a negative regulator of TyrK receptor signalling (Gur et al., 2004, Laederich, 2004).

Linx (also known as ISLR2) is localized to sensory and motor neurons and interacts with the Trks and Ret, another RTK (Mandai et al., 2009). *Linx* mutant mice have axonal guidance defects akin to those of NGF- and Trk-null mice. The role of Linx in the specificity of projections and the presence of most vertebrate LIGs in the nervous system highlight the importance of LIGs in nervous system development. Nonetheless, phylogenetic analysis of vertebrate and fruit fly LIGs cluster LRRC4 and the AMIGO, LINGO and LRIG families into the same clade as the *Drosophila* protein Lambik, whereas the *Drosophila* Kek family form a distinct clade with the vertebrate Trks (Mandai et al., 2009). According to this phylogeny, Linx is an outlier of the Trk/Kek clade.

1.4 Evolution of the neurotrophin receptors

1.4.1 Domain shuffling in the Trk superfamily

In addition to the Trk neurotrophin receptors and LIG proteins, the Trk superfamily comprises the Ror, Musk and Ddr families, which are predicted to have evolved from a common ancestral kinase (Figure 1.4; Sossin (2006)).

Figure 1.4 **Trk superfamily evolution by domain shuffling**

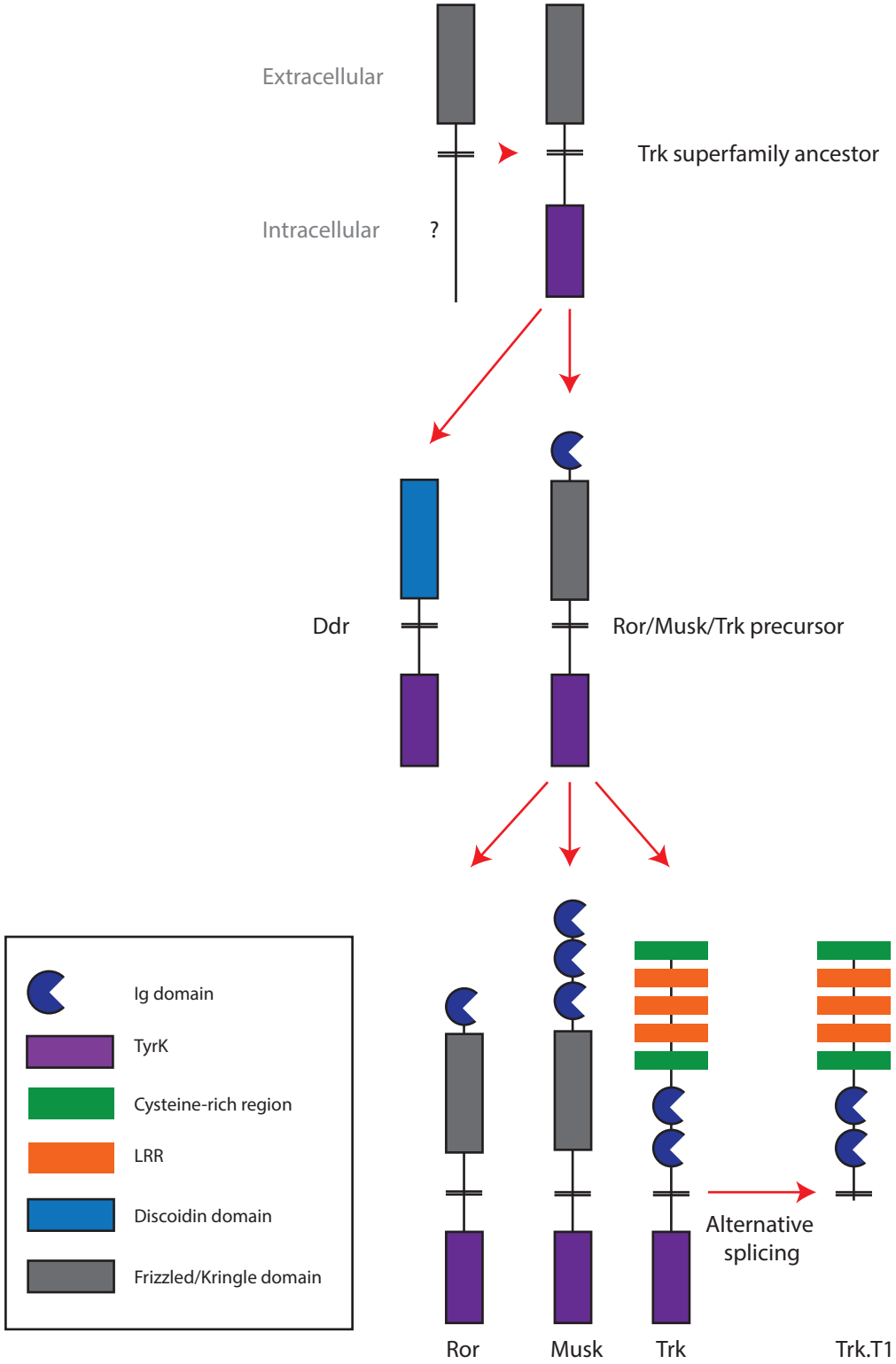

The ancestral Trk protein is predicted to have contained an extracellular Frizzled/Kringle domain and an intracellular tyrosine kinase (TyrK). The ancestral protein subsequently divided into two lineages: Ddr proteins swapped the extracellular Frizzled/Kringle domain for a Discoidin domain, whereas the precursor to the Ror, Musk and Trk families acquired an additional immunoglobulin (Ig) domain. Subsequent domain shuffling of this precursor yielded the three modern protein families. LRR, Leucine rich repeat. Domain shuffling likely occurred by intronic and genomic recombination, alternative splicing. See main text for references.

Ror proteins comprise an extracellular Frizzled/Kringle and Ig domain and an intracellular kinase domain. Fly, rat, mouse and human genomes all encode two Ror proteins, whereas *C. elegans* only encodes one, CAM-1, suggesting that a second Ror was lost in the worm lineage (Forrester, 2002). CAM-1 has roles in neuronal cell migration and is associated with defects in axon outgrowth (Forrester et al., 1999). Vertebrate Rors are also involved in neurite outgrowth, but more generally are involved in cell migration and development, as *mRor2* knockouts have limb, bone and heart defects and die shortly after birth (Takeuchi et al., 2000). The structure of *Drosophila* dRor differs from mammalian Rors in that it lacks an extracellular Ig domain, although this is likely to reflect a recent loss since the Ig domain is present in the bee Ror (Forrester, 2002, Sossin, 2006). dRor may have Trk-like functions in the fly, although the dRor TyrK does not belong to the Trk TyrK family (Jaaro et al., 2001, Manning et al., 2002).

Musk proteins comprise three extracellular Ig domains, a Frizzled/Kringle domain and an intracellular kinase domain (Figure 1.4; Sossin (2006)). Mammalian Musk proteins are expressed in muscles, and cluster neurotransmitter receptors and proteins involved in presynaptic differentiation and synapse formation (Burden et al., 2013, DeChiara et al., 1996). By contrast, zebrafish Musk (also known as Unplugged) induces cellular changes in the extracellular environment around future neuron target locations prior to growth cone arrival (Zhang et al., 2004).

Ddr proteins comprise an extracellular discoidin domain and an intracellular kinase domain (Figure 1.4; Sossin (2006)). Ddrs have crucial roles in cell migration, proliferation and differentiation (Sossin, 2006). *Ddr1* overexpression causes neurite outgrowth reduction in the mouse cerebellum (Bhatt et al., 2000). However, Ddr proteins are more commonly involved in cell–extracellular matrix (ECM) communication, since the ligand of mammalian DDR1 and DDR2 is collagen (Vogel et al., 1997, Vogel, 1999).

Given the presence of a sponge Ddr, *C. elegans* CAM-1 and *Drosophila* dRor, the ancestral protein of the Trk superfamily likely predates both the protostome–deuterostome and parazoa–metazoa evolutionary divides (Sossin, 2006). It is predicted that the vertebrate Trks arose from two separate genome duplications (Hallbook, 1999). TrkA and TrkC arose from the duplication of one ancestral Trk, whereas TrkB and a now-defunct TrkB sister gene arose from a separate duplication from a second ancestral Trk, both occurring between the branch of jawless fish and cartilaginous fish (Hallbook, 1999).

Genealogical analysis can be applied to the wider and older Trk superfamily in combination with the loss and gain of protein domains (Figure 1.4). The ancestral kinase is predicted to have contained an extracellular Frizzled/Kringle domain and a cytoplasmic TyrK domain, since these domains are found in sponge RTKs. The Ddr family first diverged from the ancestor of Rors, Musks and Trks, eventually swapping the Frizzled/Kringle domain for a Discoidin domain (Sossin, 2006). The ancestor of Rors, Musks and Trks subsequently acquired an Ig domain, then simultaneously split into the three separate lineages. Musks acquired further Ig domains, and Trks acquired LRRs. Species-specific domain shuffling further expanded the protein repertoire of the metazoa, for example, in the sea urchin Ror, a further Frizzled/Kringle domain was added; extracellular domains were lost from *Aplysia* Trk-like protein (but not from ApTrk); and sea urchin Trks lack LRRs (see SpBase Annotation SPU_020803; Lapraz et al. (2006)). These domain modifications resulted in the divergence of receptor function (Hu et al., 2004). The acquisition of LRRs and Igs both predate the bilaterian split (Sossin, 2006).

1.4.2 Invertebrate Trks and Trk-like proteins

Trk receptors are present throughout the chordates, in the lamprey and in echinoderms, but are absent from urochordates (Figure 1.5; Hallböök et al. (1998); Lapraz et al. (2006)). *C. elegans* and *Drosophila* lack Trk receptors but Trk-like and full-length Trk receptors have been

Figure 1.5 **Trk proteins in the metazoa**

The Trk and Trk-like isoforms throughout the metazoa are shown above the evolutionary family tree. Structures were determined using the SMART online tool using sequences from Uniprot, except *Hydra* Lemon (Miller and Steele, 2000), ApTrk (Kassabov et al., 2013), LTrk (van Kesteren et al., 1998) and *Daphnia pulex* Trk (Wilson, 2009). *Caenorhabditis elegans* Trk-1 is predicted from the genome, but has not been characterised. Accession IDs: sea urchin SPU_020803; *C. elegans* Trk-1 UPI0000D7DC75/D1073.1A; ApTrkL Q5IJ68_APLCA/Q5IJ68; Sponge RTK Q9Y1Y8_9METZ/QY1Y8.

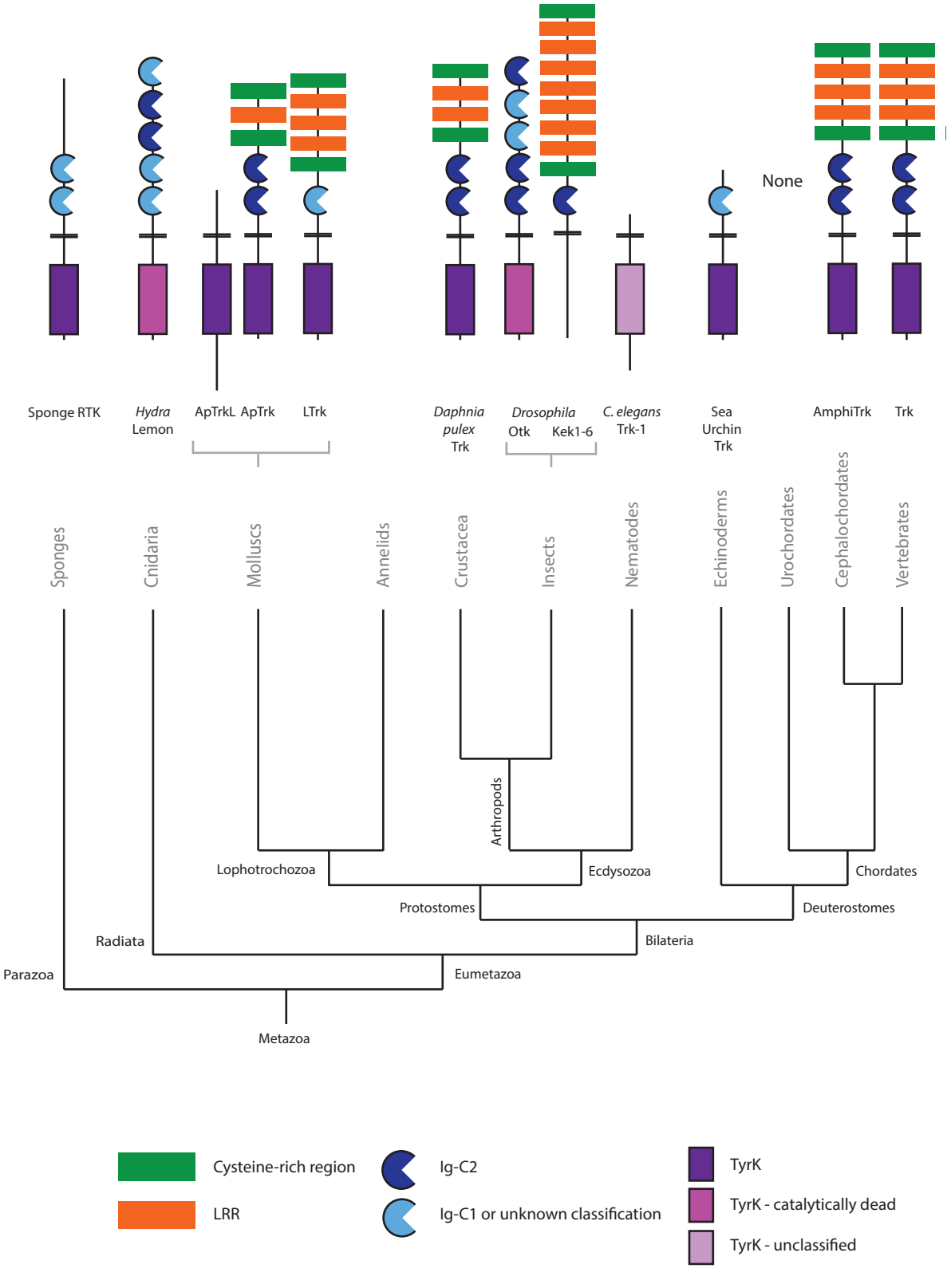
None
Sponge RTK
Hydra
Lemon
ApTrkL
ApTrk
LTrk
Daphnia pulex
Trk
Drosophila
Otk
Kek1-6
C. elegans
Trk-1
Sea Urchin
Trk
AmphiTrk
Trk
Sponges
Cnidaria
Molluscs
Annelids
Crustacea
Insects
Nematodes
Echinoderms
Urochordates
Cephalochordates
Vertebrates
Arthropods
Lophotrochozoa
Ecdysozoa
Chordates
Protostomes
Deuterostomes
Bilateria
Radiata
Eumetazoa
Parazoa
Metazoa
Cysteine-rich region
LRR
Ig-C2
Ig-C1 or unknown classification
TyrK
TyrK - catalytically dead
TyrK - unclassified

isolated from molluscs, and Trk proteins have been identified in the sponges and crustacea (Beck et al., 2004, Benito-Gutiérrez et al., 2006, Bothwell, 2006, Bulloch et al., 2005, Kassabov et al., 2013, Ormond et al., 2004, Suga et al., 2001, van Kesteren et al., 1998, Wilson, 2009). These observations suggest that functional conservation of an ancestral Trk has persisted since the common metazoan ancestor. This is further indicated by the ability of the molluscan *Lymnaea stagnalis* Trk (LTrk; see below) to bind human NT-3 and the ability of the amphioxus AmphiTrk to interact with all vertebrate neurotrophins to induce Akt and extracellular signal-regulated kinase (ERK) signalling (Benito-Gutierrez et al., 2005, van Kesteren et al., 1998).

Nonetheless, structural and functional variation has been introduced over evolutionary time. The LTrk ectodomain comprises 3 LRR motifs but lacks the pair of Ig-C2 domains of vertebrate Trks (van Kesteren et al., 1998). Instead, a putative single Ig-C1, or fragmented single Ig-C2 domain is present, suggesting that Ig domains in LTrk were recently lost. Indeed, LTrk chimaeras with added TrkC Ig-C2 domains can signal via ERK1 and ERK2 in response to NT-3 addition in monkey COS cells (Beck et al., 2004). Furthermore, LTrk may be alternatively spliced with a 100 amino acid N-terminal extension of unknown function (van Kesteren et al., 1998). Endogenous LTrk is located in neurons and dorsal body cells of the CNS in juvenile and adult *Lymnaea* (Bulloch et al., 2005).

The molluscan *Aplysia* Trk-like protein (ApTrkL) is an RTK that lacks extracellular ligand-binding domains (Ormond et al., 2004). ApTrkL is localized to sensory neurons and most likely arose by exon splicing from an ancestral Trk — the TyrK of ApTrkL is most similar to that of the vertebrate Trks, but the ectodomain lacks both LRRs and Ig domains (Ormond et al., 2004). ApTrkL can interact with serotonin in cell culture, but endogenous ligands of ApTrkL are unknown because of the absence of extracellular ligand-binding domains. Recently, a full length Trk was identified in *Aplysia*, formed of two extracellular Ig-C2 domains, a single LRR and an intracellular TyrK (Kassabov et al., 2013). ApTrk is required

for long term facilitation and synaptogenesis, and *ApTrk* mRNA is alternatively spliced to yield different synaptic functions of the ApTrk protein.

The domain architecture of the cephalochordate AmphiTrk resembles that of vertebrate Trks. However, AmphiTrk cannot activate the PLCγ pathway (Benito-Gutierrez et al., 2005, Benito-Gutiérrez et al., 2006). It is likely that this ability has been lost in Amphioxus but was present in the ancestral Trk, since ApTrk has a C terminus SH2 site required for PLCγ signalling (Kassabov et al., 2013).

The lack of *Drosophila* Trks was initially put down to the relative 'simplicity' of flies compared with vertebrates (Jaaro et al., 2001). Furthermore, *Drosophila* neuronal survival could be mediated by alternative mechanisms, such as axon–axon contact and EGF ligand signalling (Benito-Gutiérrez et al., 2006, Hermann et al., 2000, Hidalgo, 2002). However, the genome of the crustacean *Daphnia pulex* encodes a Trk receptor with 2 LRR motifs and 2 Ig domains, thereby resembling vertebrate Trks (Wilson, 2009). This DappuTrk has an intracellular docking site for SHC, which signals through Ras–Raf–ERK and phosphatidylinositol-3-kinase (PI3K)–Akt. The arthropods, to which the crustacea and insects belong, therefore share a Trk-like ancestor, suggesting that *Drosophila* has lost canonical Trk-like protein-encoding genes.

Trk superfamily members were identified in *Drosophila* by homology with the vertebrate TyrK domain or by TyrK-encoding sequence hybridisation screening of cDNA libraries. *Drosophila* Nrk is an atypical Musk orthologue: it is distributed only in neurons (which contrasts with muscle-specific vertebrate Musk signal), and its extracellular domain resembles that of Ror (Oishi et al., 1997). Axonal pathfinding requires Off-track (Otk, previously known as DTrk), which was identified by its Trk-like TyrK domain but which is activated by heterophilic interaction with the semaphorin signalling system (Pulido et al., 1992, Winberg et al., 2001). Otk, its human orthologue CCK4 and the sponge kinase Lemon are distributed

throughout the nervous system, but in each protein the kinase domain is catalytically dead (Kroiher et al., 2001, Miller and Steele, 2000). Nrk, dRor and Otk were identified by research focusing on the Trk TyrK, but no Trk family TyrK is present in flies (Manning et al., 2002).

The protostomes and deuterostomes share a common Trk-like ancestor, but modern full-length Trks are absent from the insects. The above candidate *Drosophila* Trks were detected only from the TyrK domain: phylogenetic analysis comparing mammalian and *Drosophila* protein sequences according to extracellular domains identifies the *Drosophila* Kek family as forming a clade with the Trks (Mandai et al., 2009). The Kek proteins lack an intracellular signalling domain, thus are Trk-like proteins that cannot signal via canonical Trk pathways. The ancestral Trk, therefore, may have contained a TyrK that was subsequently lost in insects, or was a truncated protein that acquired a TyrK domain in other lineages.

1.4.3 Truncated Trks

Naturally occurring truncated forms of TrkB and TrkC that lack an intracellular TyrK are produced by alternative splicing of *TrkB* and *TrkC* (Fenner, 2012). Truncated TrkB.T1 binds BDNF with high affinity, leading to ligand internalization (Fenner, 2012, Renn et al., 2009).

TrkB.T1 was initially thought to function solely as a dominant negative inhibitor of TrkB signalling (Haapasalo et al., 2001). However, TrkB.T1 has a unique expression profile compared to the full length TrkB.TK$^+$. Both TrkB.TK$^+$ and TrkB.T1 are distributed throughout the adult mammalian CNS, but whereas the full length receptor is expressed at birth, TrkB.T1 expression increases postnatally, such that T1–T1 homodimers and T1–TK$^+$ heterodimers are the dominantly expressed forms in the adult brain, with TK$^+$–TK$^+$ homodimers absent (Fenner, 2012, Luberg et al., 2010, Ohira et al., 1999, Ohira and Hayashi, 2009, Sherrard et al., 2009). BDNF is required for adult learning and memory (Bekinschtein et al., 2008); the absence of TK$^+$–TK$^+$ in adults therefore suggests that BDNF may signal via TrkB.T1 during learning.

Despite the absence of a TyrK signalling domain, the short cytoplasmic region of TrkB.T1 is conserved throughout the mammals, indicating that it is important for function (Ohira and Hayashi, 2009). Indeed, overexpression of the truncated TrkB.T1 isoform alters BDNF-triggered calcium release and cell morphology of astrocytes, is required for cochlea development, increases anxiety behaviour in mice, slows the onset of motor neuron degeneration in mouse models, increases muscle contract motility, heightens nociception, decreases apoptosis in the adult cortex, increases neural progenitor proliferation, induces neurite outgrowth and alters dendritic spine density (Carim-Todd et al., 2009, Dorsey et al., 2006, Dorsey et al., 2012, Gestwa et al., 1999, Haapasalo et al., 2001, Michaelsen et al., 2010, Ohira et al., 2007, Renn et al., 2009, Rose et al., 2003, Tervonen et al., 2006, Yanpallewar et al., 2012). A role for TrkB.T1 in synaptic plasticity is implied by its ability to signal via G proteins to PLCγ (Ohira and Hayashi, 2009, Rose et al., 2003). TrkC.T1 misregulation is also implicated in retinal ganglion cell death in glaucoma (Bai et al., 2010).

The mechanism by which truncated Trks signal independently to full length receptors is not fully known. One known interacting partner is Rho GDP dissociation inhibitor 1 (RhoGDI1; Figure 1.6; Ohira et al. (2005)). RhoGDI1 inhibits the activation of RhoA, RhoB, Rac1, Rac2 and Cdc42. These small GTPases are crucial for actin cytoskeleton regulation and mediation of morphological changes throughout neuronal development (Luo, 2000). Unstimulated TrkB.T1 sequesters RhoGDI1, thereby allowing the activation of Rho, leading to actin cytoskeleton rearrangements and glial morphological changes (Figure 1.6a; Ohira et al. (2006), Ohira et al. (2007)). BDNF addition releases RhoGDI1 to inhibit Rho signalling (Figure 1.6b; Ohira et al. (2006), Ohira et al. (2007), Ohira and Hayashi (2009)). By this mechanism it is also suggested that TrkB.T1 can signal via the p21-acivated kinase (PAK), MAPK and PLCγ pathways (Ohira et al., 2006, Ohira et al., 2007, Ohira and Hayashi, 2009). Interestingly, $p75^{NTR}$ can also sequester RhoGDI in vertebrates, a function that is reversed by NGF addition (Yamashita and Tohyama, 2003). It is also suggested that TrkB.T1 interacts

Figure 1.6 **Truncated Trk signalling**

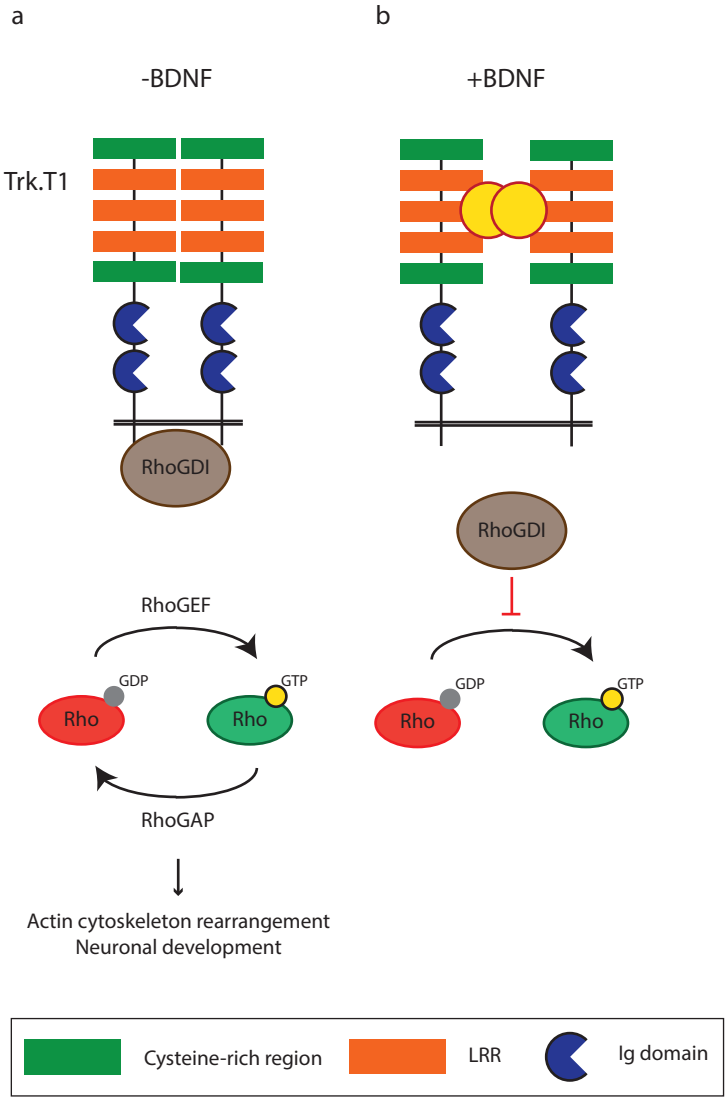

a | The naturally occurring truncated Trk splice isoform TrkB.T1 comprises an extracellular LIG module but lacks an intracellular tyrosine kinase. In the absence of ligand, TrkB.T1 sequesters Rho GDP dissociation inhibitor (RhoGDI). This permits the activation of RhoGTP signalling, and thereby actin cytoskeleton rearrangement and Rac, Rho and Cdc42-dependent neuronal development. **b** | BDNF stimulation releases RhoGDI, thereby inactivating RhoGTP signalling. GAP, GTPase-activating protein; GEF, guanine exchange factor.

with $p75^{NTR}$ to cause unique phenotypes compared with full length TrkB–$p75^{NTR}$ interactions (Hartmann et al., 2004, Michaelsen et al., 2010).

The ability of truncated Trks to signal raises the question: has domain shuffling produced further proteins that lack signalling domains but can function in neurotrophic contexts?

1.4.4 Evolution of the $p75^{NTR}$ superfamily

Neurotrophin signalling modulation and complexity arises from the interaction of $p75^{NTR}$ with the Trks. $p75^{NTR}$ comprises four extracellular TNF receptor (TNFR) domains and an intracellular DEATH domain (see Figure 1.2; Rabizadeh and Bredesen (2003)). The role of $p75^{NTR}$ in neurotrophin signalling is ligand-dependent: pro-neurotrophins promote cell death through Jnk, whereas cleaved neurotrophins promote cell survival through NFκB (Huang and Reichardt, 2001). $p75^{NTR}$ paralogues — NRH1, NRH2, PLAIDD and NRADD — can also modulate Trk signalling (Murray et al., 2004). These proteins are members of the TNFR superfamily (Bothwell, 2006). $p75^{NTR}$ further interacts with Nogo receptor and the LIG protein LINGO1 to mediate axon repellent responses to myelin proteins, as does the TNF receptor protein Troy (Mi et al., 2005). Troy and $p75^{NTR}$ do not share overall sequence similarity, except in their intra-transmembrane domain cysteine residues, but the ligand for the Troy subfamily protein EDAR is the most similar vertebrate protein to *Drosophila* Eiger, the ligand for the only *Drosophila* TNF receptor, Wengen (Igaki et al., 2002, Kanda et al., 2002, Schecterson and Bothwell, 2010). This suggests that a functional interaction between the TNF superfamily and LIG proteins may be conserved between vertebrates and flies.

1.5 LIGs and candidate invertebrate neurotrophin receptors

Has domain shuffling of the ancestral Trk proteins produced novel receptors with roles in the nervous system of *Drosophila*, and that can interact with the DNTs? The primary candidates for such receptors are the LIGs, which contain the extracellular domains required for neurotrophin binding in vertebrates. The 9 dLIGs are Kek1–6, Lambik (Lbk), CG15744 and

CG16974 (Figure 1.7; Dolan et al. (2007)): each are studied here, in addition to three other candidate receptors, to address the above question.

1.5.1 Lambik

Lbk is a transmembrane receptor comprising a large extracellular domain containing 16–17 LRR repeats and 2–3 Ig domains (Figure 1.7; Dolan et al. (2007). The closest vertebrate orthologues of Lbk are the LRIG1–3 family.

The function of Lbk is unknown. The *C. elegans* orthologue SMA-10 is a positive extracellular regulator of bone morphogenetic protein (BMP) receptor signalling, required downstream of the BMP ligand DBL-1 but upstream of the BMP receptor SMA-6 (Gumienny et al., 2010). *Drosophila lbk* cDNA driven by an *SMA-10* promoter rescued the body size defect of *SMA-10* mutants to wild type body size (Gumienny et al., 2010).

1.5.2 CG17839, Rickets and Wengen

Three non-LIG candidates are also studied in this thesis. Rickets (Rk) and the uncharacterised CG17839 are studied owing to their LRR and/or Ig-rich ectodomains, through which they may bind ligands. Rk is a multiple LRR-containing receptor of the CysKnot neuropeptide ligand Bursicon (Dewey et al., 2004, Luo, 2005, Nässel and Winther, 2010). The eLRRs of Rk resemble those of the Trk receptors, although the transmembrane and intracellular domains are G protein linked. The third additional candidate, Wengen (Wgn), is the only *Drosophila* TNFR superfamily member. The Wgn ligand Eiger shares most homology with the vertebrate EDA ligand (see above; Bothwell (2006), Igaki et al. (2002), Kanda et al. (2002), Kauppila et al. (2003)). Wgn interacts with Moesin to control R2–R5 and R8 photoreceptor axon targeting (Ruan et al., 2013).

Figure 1.7 **Candidate neurotrophin receptors in *Drosophila***

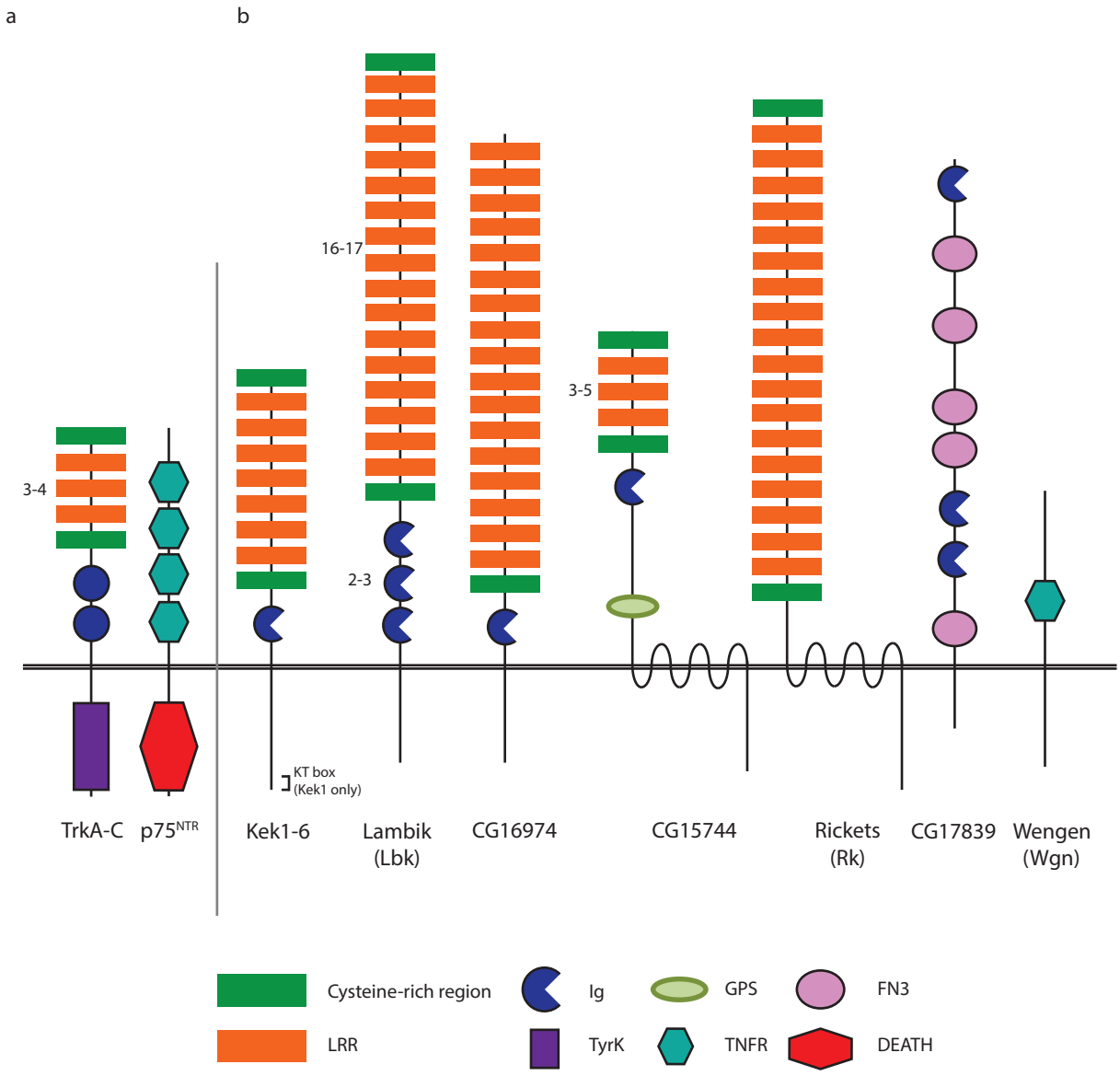

a | The structures of vertebrate Trk and p75^{NTR} receptors are shown. **b** | *Drosophila* LIG and non-LIG candidate receptors. Kek, Lbk, CG16974, CG15744 and Rk domain architectures are based on structures as stated in Dolan et al. (2007). CG17839 and Wgn structures were determined using the SMART online tool (EMBL) using sequences from FlyBase. Domains: FN3, fibronectin 3; GPS, G protein receptor proteolytic site; Ig, immunoglobulin; KT, Kek terminal; LRR, leucine-rich repeat; TNFR, tumour necrosis factor receptor; TyrK, tyrosine kinase.

1.5.3 The Kek protein family

Kek1 and Kek2 were first identified by Musacchio and Perrimon (1996). They comprise 6 eLRR repeats and one extracellular Ig domain, with divergent intracellular domains that lack signalling motifs. Sequence comparison between Kek proteins in other *Drosophila* species reveals that Kek1 has a conserved Kek-specific cytoplasmic 'KT' domain of unknown function (Derheimer et al., 2004). *kek1* is expressed in neurons of the embryonic CNS and PNS (Musacchio and Perrimon, 1996). *kek1* is further expressed in oocyte follicle cells and larval eye and wing discs (Derheimer et al., 2004, Musacchio and Perrimon, 1996, Ghiglione et al., 1999, Ghiglione, 2003). *kek2* is expressed in dorsal cells of the embryonic VNC, in ventral midline cells and ventral muscle groups (Musacchio and Perrimon, 1996). *kek2* is also expressed in neurons of the adult brain and presynaptic punctae at larval NMJs (Guan et al., 2005). *kek5* is expressed in the embryonic CNS, but *kek5*$^{+}$ neuronal cell types have not been determined (Evans et al., 2009). The Kek family are putative cell adhesion proteins as they can form homotypic and heterotypic interactions (MacLaren et al., 2004).

Only the roles of Kek1 and Kek5 are known. Kek1 is an antagonist of EGFR signalling during oogenesis, eye development and the formation of bract cells, which are required for the formation of mechanosensory bristles (Alvarado et al., 2004b, Alvarado et al., 2004a, Derheimer et al., 2004, Ghiglione et al., 1999, Ghiglione, 2003, Layalle et al., 2004, Zartman et al., 2009). By comparison, *kek5* overexpression suppressed ectopic wing vein phenotypes in hypermorphs of the BMP ligand Gbb, whereas phenotypes caused by activated BMP receptors could not be rescued by *kek5* overexpression (Evans et al., 2009). This suggested that Kek5 is an extracellular, rather than intracellular, antagonist of BMP signalling, although whether Kek5 modulates BMP receptors or is a ligand sink was not tested. eLRRs, rather than the Ig domains, are sufficient for Kek1 and Kek5 function (Evans et al., 2009, Alvarado et al., 2004b). Kek6 shares conserved intracellular motifs with Kek5 (MacLaren et al., 2004), and is not involved in EGFR signalling (Alvarado et al., 2004a).

Kek1 is conserved within the *Drosophila* genus and in the mosquito, and orthologues of Kek1, Kek2, Kek5 and Kek6 are also found in the honeybee (Derheimer et al., 2004, MacLaren et al., 2004). Although Kek proteins were initially considered absent outside of the insects, they structurally resemble truncated Trks (Derheimer et al., 2004). Furthermore, phylogenetic analysis places the Kek family together with the Trks (Mandai et al., 2009). This places these two protein families closer together structurally and evolutionarily than the fly and mammalian Tolls (Imler and Zheng, 2004). Thus the Kek family belong to the Trk family, and structurally resemble truncated Trks. This thesis tests this hypothesis by examining the nine dLIGs, including the Trk-like Kek family, plus Rk, Wgn and CG17839. The thesis aimed to investigate the function of the dLIGs in the CNS, where the Trks function in vertebrates. It further aimed to test the ability of the dLIGs to interact with the *Drosophila* neurotrophins (DNTs), given that the ectodomain of dLIGs resembles the neurotrophin binding domain of the Trks.

1.5.4 Potential signalling downstream of Keks or dLIGs

Truncated Trks and $p75^{NTR}$ signal via the RhoGTPases by sequestering RhoGDI (see above). The RhoGTPases regulate the actin cytoskeleton, and thereby underlie axonal growth, axonal targeting and synaptogenesis (Luo, 2000). In neurotrophin signalling, phosphorylated Trk receptors recruit the SOS complex, which can mediate the activation of Rac, in addition to Ras–MEK–ERK signalling (see above). Indeed, NGF treatment can induce axonal branching through Rac1 and actin filament formation (Spillane et al., 2012), and loss of BDNF reduces actin filament formation in adult hippocampal neurons (Rex et al., 2007). Given their similarity to neurotrophin-binding receptors, and truncated Trks, it is possible that the dLIGs, including the Kek proteins, may signal via the RhoGTPases or RasGTPases. Here I briefly review the roles of the RhoGTPases and RasGTPases in axon growth and guidance.

The RhoGTPase family members Rho, Rac and Cdc42 were identified for unique roles in fibroblasts: Rho mediates stress fibre and focal adhesion formation, Rac is required for lamellipodia formation, and Cdc42 mediates filopodia formation (Ridley and Hall, 1992, Ridley et al., 1992, Kozma et al., 1995). Cdc42 activation leads to the sequential activation of Rac, followed by Rho (Nobes and Hall, 1995). Growth cones at the leading edge of advancing neurons are structurally similar to migrating fibroblasts, driven by the assembly and disassembly of actin filaments, crosstalk between the actin cytoskeleton and microtubules, and actin monomer recycling, within filopodia and lamellipodia (Lin et al., 1994a, Lowery and Van Vactor, 2009, Prokop et al., 2013a, Sanchez-Soriano et al., 2009, Sánchez-Soriano et al., 2010). In neuronal development, however, RhoGTPase functions differ depending on cellular context and between axonal growth and targeting.

Axonal growth is defective in both loss and gain of function *Rac* and *Cdc42* mutants (Govek et al., 2005, Hakeda-Suzuki et al., 2002, Luo et al., 1994, Ng et al., 2002). Conversely, dendritic growth is promoted by Cdc42 but not by Rac (Luo et al., 1996). Equivalent phenotypes are also observed in mutants of Rac activating GEFs, such as *Trio* (Bateman et al., 2000). Rac and Cdc42 share a common signalling cascade via PAK; mutants of *Drosophila PAK* display photoreceptor axon mistargeting (Hing et al., 1999, Manser et al., 1994). Rac and Cdc42 also signal via separate cascades — Cdc42 via N-WASP to promote filamentous actin assembly, and Rac via Stathmin to mediate microtubule stabilization (Hall and Lalli, 2010, Luo, 2000). In general, Rac and Cdc42 are required for axonal growth (Albertinazzi et al., 1998, Brown et al., 2000, Kuhn et al., 1998, Luo et al., 1996, Luo et al., 1994); conversely, Rho mediates growth cone collapse via the cytoplasmic kinase Rho-associated protein kinase (ROCK) in response to negative chemotactic cues, such as Sema3A (Gallo, 2006, Kozma et al., 1997, Leeuwen et al., 1997, Yamashita et al., 1999). Indeed, activation of Rho induces growth cone retraction, and lipophosphatidic acid-induced neurite retraction is prevented in a dominant negative Rho genetic background (Jalink et al., 1994). During axon

guidance, loss of Rac causes motor axon guidance defects in the intersegmental nerve branch b (ISNb; Kaufmann et al. (1998); see below). In addition, *Drosophila* mushroom body dendrites overshoot their target in *Rho* loss of function mutants, suggesting that Rho attenuates dendritic growth (Lee et al., 2000). RhoGTPase roles in axon growth and guidance are cell type-specific, as loss or gain of Rac in *Drosophila* sensory neurons arrests axonal growth, whereas dominant negative Rac disrupts axon targeting but not growth in *Drosophila* motor neurons (Kaufmann et al., 1998, Luo et al., 1994). Rac and Cdc42 are also required for acetylcholine receptor clustering at the vertebrate NMJ (Weston et al., 2000).

RasGTPase signalling is required for NGF-mediated axonal initiation, growth and neuronal survival (Hall and Lalli, 2010). Constitutively active R-Ras induces ectopic axonal sprouting in hippocampal neuron cultures, whereas RNAi-mediated knockdown of R-Ras inhibits axon formation (Oinuma et al., 2007). This function of Ras requires PI3K, which in turn promotes Ras upregulation via a positive feedback loop (Schwamborn and Puschel, 2004). PI3K can also signal via mTor to control neuronal polarization (Li et al., 2008). However, Ras signalling can also control neuronal architecture independently of PI3K: in sensory neurons, activated Raf promotes axon growth via ERK, whereas activated PI3K–Akt signalling promotes axon branching (Markus et al., 2002).

1.6 *Drosophila* as a model organism

Drosophila is an ideal genetic model to study neurobiology (Prokop et al., 2013b, Sánchez-Soriano et al., 2007). Furthermore, its nervous system is amenable for experimentation, from histological phenotypes to behaviour (Nichols et al., 2012). *Drosophila* is also a simple model for the study of hormonal regulation, which is manifested by changes in developmental timing (Tennessen and Thummel, 2011b). Given the focus on the nervous system of this work, a behavioural output is essential for putting subcellular and cellular phenotypes into perspective (Guo et al., 2009, Heisenberg, 1997). This section outlines the morphology of the *Drosophila*

CNS and the ring gland as model tissues; and introduces methods for assaying phenotypes in axon guidance and developmental timing.

1.6.1 The *Drosophila* nervous system

The *Drosophila* CNS originates from neural stem cells, called neuroblasts, that are specified in the embryonic ectoderm and invaginate to segregate from the epidermal layer. Neuroblasts originate in several waves during *Drosophila* embryogenesis, starting from stage 9 (Hartenstein, 1993). (See Campos-Ortega and Hartenstein (1985) for embryonic staging.) Neuroblasts divide into a further neuroblast and a ganglion mother cell, which further divides into two neurons or glia (Doe, 1992). Individual neurons and glia begin to differentiate at stage 12. Dorsal closure occurs at stage 15, after which the VNC shortens and thickens up to stage 17 (Figure 1.8a,b).

At stage 12, early neuronal cell bodies (MP1, dMP2, vMP2 and pCC neurons) project pioneer axons that extend along the nerve cord, either side of the midline, to build the longitudinal tracts (Figure 1.8c,d) (Bate and Grunewald, 1981, Hidalgo and Brand, 1997, Lin et al., 1994b, Sánchez-Soriano et al., 2007). MP1 and dMP2 axons extend posteriorly along the nerve cord, whereas the projecting axons of pCC and vMP2 neurons build the longitudinal tracts anteriorly (Hidalgo and Brand, 1997). At stage 13, projecting growth cones within the VNC meet at segmental boundaries, and at stage 14, fascicles separate to form two separate pathways (Hidalgo and Brand, 1997). Subsequent rearrangements result in three longitudinal fascicles by stage 17 (Hidalgo and Brand, 1997). Other axons cross the midline, forming an anterior and posterior commissure per segment (Sánchez-Soriano et al., 2007). Growth cones of the pioneer commissure neurons follow guidance cues released from midline glia and neurons (Hummel et al., 1999). The commissures are subsequently used by midline neurons, such as the neuromodulatory ventral unpaired median (VUM) neurons, to guide axonal

Figure 1.8 **The *Drosophila* nervous system**

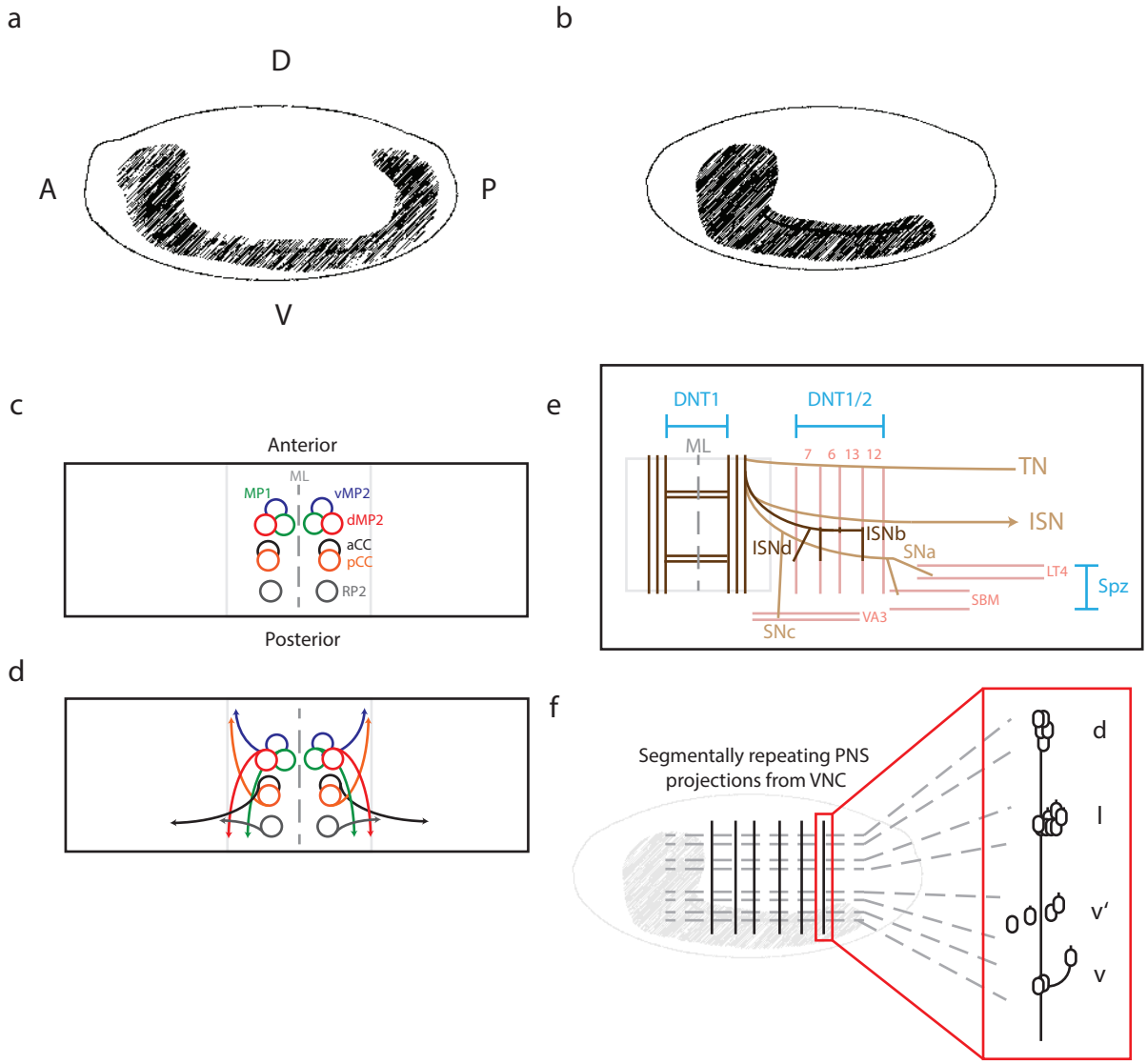

a | Individual neurons and glia begin to differentiate from stage 12 (CNS shaded). **b** | By stage 17, the embryonic ventral nerve cord (VNC) has shortened and thickened and the embryonic brain occupies the anterior of the embryo. **c**,**d** | Segmentally-repeating pioneer neurons project axons towards the anterior (pCC and vMP2) or posterior (dMP2 and MP1) to form the longitudinal tracts, whereas aCC and RP2 pioneer neurons project away from the midline (ML) to form the motor neurons. **e** | Motor axons project from the ladder-shaped neuropil of the VNC to target specific muscles. Intersegmental nerve b (ISNb) motor axons target muscles 6–7, 6–13 and 13–12 to form a characteristic 'E' shape. Not all muscles are shown. Regions of known DNT1, DNT2 and Spz expression are shown in blue (based on Zhu et al. 2008). **f** | ventral (v, v'), lateral (l) and dorsal (d) clusters of the PNS project from the VNC in each segment. LT4, lateral transverse muscle 4; SBM, segment border muscle; SN, segmental nerve; TN, transverse nerve; VA3, ventral acute muscle 3.See main text for references.

projections away from the midline into the longitudinal tracts and/or the muscle (Bossing and Technau, 1994).

In the larva, the CNS comprises the central brain, two optic lobes and the VNC, which in the adult will form the adult central brain, optic lobes and VNC (Hartenstein, 1993). In the embryonic and larval VNC, the central neuropil is enwrapped by interface glia and midline glia, the nerves are enwrapped by peripheral glia, the cortex outside the neuropil comprises the neuronal cell bodies and cortex or cell body glia, and the whole VNC is enveloped by the sub-perineural and perineural glia (Beckervordersandforth et al., 2008).

CNS axons can be labelled with anti-BP102, which labels the entire neuropil, revealing possibly all dendrites or axons along the longitudinal connectives and commissures, or anti-Fasciclin II (ID4), which labels the pioneer neurons, the three main longitudinal connective fascicles and all the motor neurons. Ventral motor neurons can be identified by co-localization with the motor neuron nuclear markers HB9 or Islet, or *lim3Gal4*-driven reporters (axons), and dorsal motor neurons can be identified by co-localization with the motor neuron nuclear marker Eve (Landgraf and Thor, 2006b, Odden et al., 2002). ISNb motor neuron nuclei are $HB9^{+}$, except for the dorsal VUM neuron, which is $Islet^{+}$ (Kim et al., 2009, Landgraf et al., 1997, Landgraf and Thor, 2006b).

Motor neurons terminate at their muscle target, whereupon they form NMJs. The three major ventral motor neuron trunks exiting the embryonic VNC to the muscles are the transverse nerve (TN), ISN and the segmental nerve (SN), which divide into further branches, including the ISNb, ISNd, SNa and SNc branches (Figure 1.8e; Landgraf and Thor (2006b)). The TN marks the border of adjacent body segments, SN motor axons innervate muscular targets in the same segment as their cell body and ISN motor axons innervate muscles in adjacent segments (Landgraf et al., 1997, Landgraf et al., 2003, Landgraf and Thor, 2006a). TN and SN motor neurons innervate transverse external muscles (SNa targets the segment border

muscle (SBM) and lateral transverse (LT) muscles), whereas ISN motor neurons target longitudinal internal muscles (Landgraf et al., 1997, Landgraf et al., 2003).

Pioneer axons of the ISN originate from aCC and RP2 motor neurons in the VNC (Figure 1.8d; Sanchez-Soriano and Prokop (2005)). Follower neurons — including U and VUM motor neurons — project along the pioneer axonal tracts to fasciculate the ISN trunk (Landgraf et al., 1997, Sanchez-Soriano and Prokop, 2005). Conversely, the V and RP1–5 axons fasciculate the SN trunk (Landgraf et al., 1997). By late stage 17, the ISNb motor neuron branch has a characteristic morphology in which three projections target muscles 12–13, 6–13 and 6–7 (Figure 1.8e). Mistargeting of these three ISNb projections can be used as an assay to test the function of genes of interest in target innervation (Bateman et al., 2000, Kaufmann et al., 1998). Here, this paradigm is used to quantify axon misrouting resulting from *kek6* mutations.

DNTs are distributed in the muscle and function as trophic factors in axon targeting (Zhu et al., 2008). In $DNT1^{41}$ and $DNT2^{e03444}/Df(3R)ED6092$ single mutants and $DNT2^{e03444}DNT1^{41}$ double mutants ISNb projection mistargeting increases to 40–50% penetrance, compared to wild type misrouting in ~20% of hemisegments (Zhu et al., 2008). ISNb projection mistargeting is also observed in $toll6^{31}/Df(3L)XG4$ and $toll7^{P8}/Df(2R)BSC22$ single receptor mutants (McIlroy et al., 2013). Therefore, this assay is an ideal context to test the role of *kek6* in DNT signalling.

The PNS is formed of the cell bodies and dendrites of neurons located laterally on the epidermis, and which extend axons towards and into the CNS, and the axons of the motor neurons, which have the cell bodies and dendrites located in the CNS and project their axons to the muscles. This pattern is repeated laterally from the midline in each hemisegment (Figure 1.8f). By stage 17 and from ventral to dorsal, four clusters of cells are present, designated the v, v′, l and d clusters and are detectable with anti-Fusch (22C10) antibodies

(Hidalgo et al., 1995, Ruiz-Gómez and Ghysen, 1990). The ‘l’ cluster comprises the neurons of the chordotonal organ, which are mechanoreceptors. (Field and Matheson, 1998).

1.6.2 The *Drosophila* ring gland and developmental timing

The larval ring gland is one of two body organs required for postembryonic insect development by neuroendocrine signalling (Siegmund and Korge, 2001). It is composed of three endocrine glands: the prothoracic gland (PG), which releases ecdysone; the corpora allata (CA), which releases juvenile hormone (JH) into the haemolymph; and the paired corpora cardiaca (CC), which releases adipokinetic hormone (AKH) with functions comparable to glucagon (Figure 1.9; Edgar (2006)). These glands are stimulated by neuropeptide release from secretory neurons that innervate the CA and PG from the protocerebrum (Nässel and Winther, 2010). The CA and PG have reciprocal roles in developmental timing throughout larval and pupal development (Tennessen and Thummel, 2011a).

With the exception of the CC, the glands of the ring gland are responsible for developmental timing: ecdysone secretion pulses from the PG further larval development, whereas the presence of JH acts as a brake to development, inhibiting ecdysone signalling and preventing pupariation until the larva is large enough to survive metamorphosis (Flatt et al., 2005, King-Jones et al., 2005, Richard et al., 1989).

Distinct stages and checkpoints control larval–pupal development: the *minimum viable weight*, below which the larva will not survive metamorphosis, the *critical weight*, which marks the end of feeding, an *interval to cessation of growth*, and the *onset of larval wandering* (Edgar, 2006). The critical weight is measured by abdominal mecahnoreceptors (Davidowitz et al., 2003, Nijhout, 2003). Prior to this checkpoint, insulin-like signalling drives and regulates growth via PI3K; beyond this checkpoint, starvation or changes in food nutritional quality do not halt metamorphosis (Davidowitz et al., 2003, Mirth and Riddiford,

Figure 1.9 **The *Drosophila* ring gland**

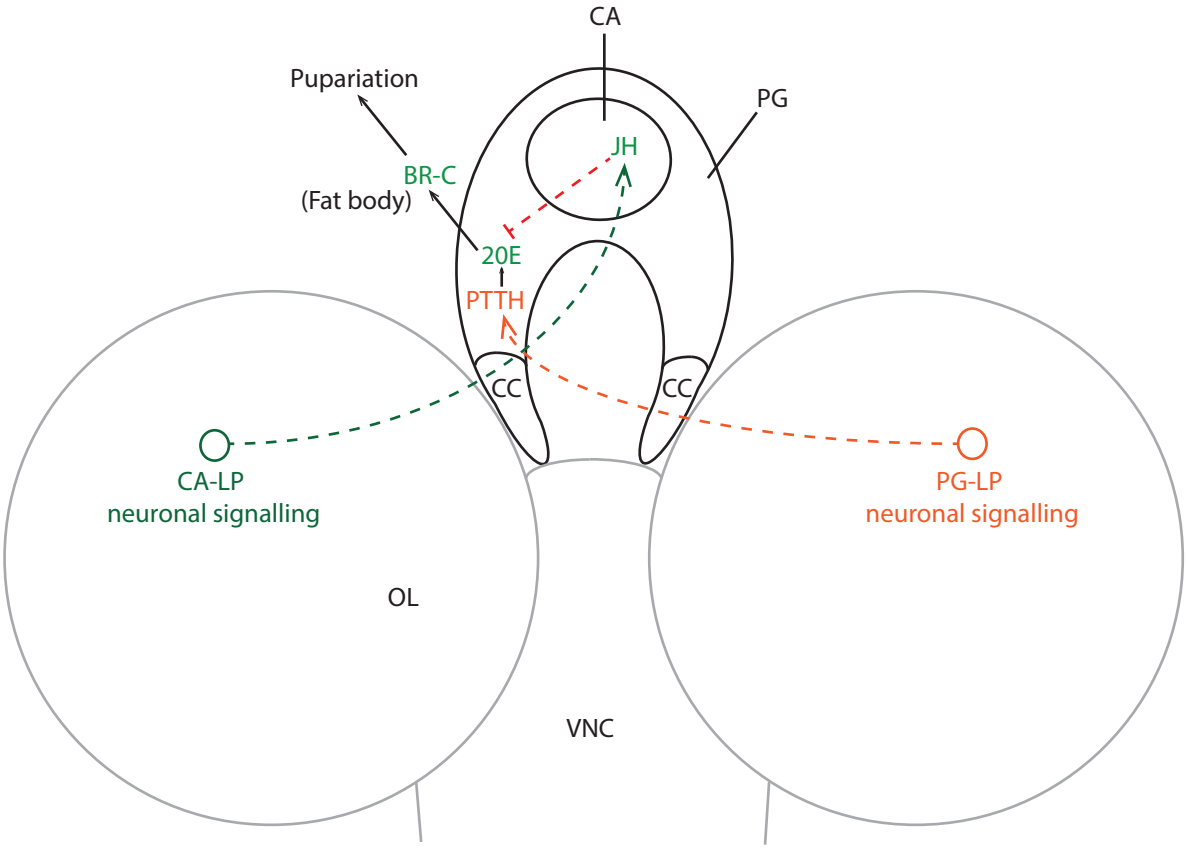

The larval ring gland is positioned anterior to the larval brain and is innervated by neurosecretory neurons from the lateral protocerebrum (LP). The ring gland comprises the corpus allatum (CA), which secretes juvenile hormone (JH); the prothoracic gland (PG); and the pair of corpora cardiaca (CC), which are involved in glucagon-like signalling. Ecdysone released from the PG is converted to 20-hydroxyecdysone (20E) and targets Broad-Core (BR-C), a transcription factor that is upregulated in the fat body to activate signalling required for pupariation and metamorphosis. 20E signalling is triggered by prothoracicotropic hormone (PTTH) release from PG-LP neurons, and is inhibited by the presence of JH. OL, optic lobe; VNC, ventral nerve cord.

2007). In *Drosophila*, the critical weight checkpoint is delayed if food quality is low throughout growth, since proceeding beyond the critical weight checkpoint precociously hinders chances of survival, as the pupa can no longer feed (Beadle, 1938, King-Jones et al., 2005, Tennessen and Thummel, 2011a). During the interval to cessation of growth, larval volume may quadruple (Beadle, 1938, Edgar, 2006). Larval wandering is preceded by an *intermediate surfacing transition (IST)* behaviour, when larvae only temporarily leave their food (Wegman et al., 2010). Full wandering behaviour then follows, whereby larvae permanently leave the food prior to pupariation. Pupariation refers to the pre-pupal transition period during which the white-coloured cuticle of the final larval instar hardens. Within the puparia or prepupa, the epidermis detaches from the cuticle and, after 12 hours, the head everts. Head eversion is the beginning of the pupal state (Chadfield and Sparrow, 1984).

In insects, the CA secretes JH into the haemolymph in response to pro- (allatotropin) and anti- (allatostatin) neuropeptide stimulation. However, in *Drosophila*, no allatotropins have been identified (Nässel and Winther, 2010). JH has a crucial role in maintaining larval growth, as flies with ablated CA pupated prematurely, had gross morphological defects and died before adult eclosion (Riddiford et al., 2010). Prior to the critical weight, JH suppresses ecdysone signalling; after this checkpoint, JH levels drop and the ecdysone signalling cascade begins, resulting in the cessation of feeding and onset of wandering (Dubrovsky et al., 2000, Edgar, 2006, Flatt et al., 2005). The direct downstream targets of JH signalling are unknown, although mutants of the receptor *Met* phenocopy loss of the CA (Riddiford et al., 2010). JH levels rise again after metamorphosis initiation, and are required for the final stages of fat body histolysis (Postlethwait and Jones, 2005).

The ecdysone cascade begins with the release of prothoracicotropic hormone (PTTH) directly into the PG from a pair of neurosecretory neurons that originate in the larval brain (McBrayer et al., 2007, Nässel and Winther, 2010, Siegmund and Korge, 2001). PTTH is a neuropeptide homodimer that forms a CysKnot structure resembling NGF (Nässel and Winther, 2010,

Noguti et al., 1995). PTTH binds the RTK Torso in the PG, and signals via the ERK cascade (Rewitz et al., 2009).

PTTH–Torso signalling leads to the release of ecdysone to peripheral targets, including the fat body, via the haemolymph (Henrich et al., 1987, McBrayer et al., 2007, Pak et al., 1992, Rewitz et al., 2009). Ecdysone is subsequently processed to the active form, 20-hydroxyecdysone (20E; Thummel and Chory (2002)). 20E activates early regulatory transcription factors, including Broad-Core (BR-C); this is repressed by the 20E target receptor DHR4, thereby creating a negative feedback loop (Ou et al., 2011). *DHR4* mutants begin wandering earlier than controls and have smaller adult volumes (King-Jones et al., 2005).

PTTH transcripts are present in the larval brain throughout the L3 instar, oscillating with an 8 hour rhythm (McBrayer et al., 2007). The brain is thus primed for metamorphic changes, subject to the loss of JH upon obtaining the critical weight. Three peaks of 20E release then follow, which correspond to the critical weight checkpoint; the onset of wandering; and the transcription and translation of *sgs3*, which adheres the pupae to solid surfaces for metamorphosis. Each peak activates different early onset genes (Georgel et al., 1991, Karim and Thummel, 1992, Warren et al., 2006).

1.7 Aims

The aim of my thesis was to investigate whether genes encoding non-canonical membrane proteins structurally and phylogenetically related to the Trks may function in fruit flies as receptors for *Drosophila* neurotrophins.

Trk proteins are the receptors of the vertebrate neurotrophins, but are absent from *Drosophila*, despite evidence suggesting that a Trk-like protein was present in the bilaterian ancestor and the presence of Trks in the protostomes (Bothwell, 2006, Jaaro and Fainzilber, 2006, Sossin, 2006). *Drosophila* encodes 9 LIG proteins derived by domain shuffling, of which the Kek

family clusters phylogenetically with the vertebrate Trks (Dolan et al., 2007, Mandai et al., 2009). All 9 dLIGs resemble the extracellular ligand-binding structure of vertebrate Trks.

The specific objectives were:

(1) To characterise the expression patterns of the Trk-like dLIGs, plus *CG17839*, *rk* and *wgn*, and analyse lethality and locomotion phenotypes of available mutant alleles. From this, the most suitable candidates as DNT interacting partners, or neurodevelopment genes, would be selected for further study according to three criteria: neuronal expression, display of nervous system phenotypes and genetic interaction with the DNTs.

(2) To test by expression of Kek≡Toll6 chimaeric receptors in S2 cell culture signalling assays whether any of the Kek proteins could potentially bind DNT1 and DNT2 and trigger a luciferase signalling readout.

(3) To generate tools to enable loss and gain of function analysis of candidate genes for *in vivo* functional genetic analyses. Thus, I generated upstream activation sequence (UAS)-containing overexpression constructs for each of the *kek* genes, and null mutant alleles for *kek3*, *kek4* and *kek6*. With these tools, I tested genetic interactions between the candidate genes and the DNTs to determine whether the receptors were involved in similar signalling pathways and whether their overexpression could rescue *DNT* mutants.

(4) To determine whether the candidate genes had functions in nervous system development, I used the mutants and overexpression constructs I generated to test their functions by analysing and quantifying motor axon targeting defects and locomotion behaviour in larvae in loss of function mutants and upon overexpression of the receptors in neurons.

(5) I serendipitously discovered that *kek4* is expressed in the ring gland, and thus I investigated its function in the temporal control of growth.

CHAPTER 2

METHODS

2.1 Genetics

2.1.1 Genetic protocols

Except where indicated, genetic protocols were carried out at 25^0C in a 12 hour light/dark cycle, and stocks maintained at 18^0C. Flies were reared on cornmeal agar medium. See Table 2.1 for full list of fly stocks in this work, by genotype and by experiment.

Standard fly pushing protocols were used to make chromosome X+II and II+III double mutant stocks, and recombinant alleles on chromosome III (Greenspan (2004); Figures 2.1–2.3). At the F_2 cross of the recombination protocol, deficiencies were used that would be embryonic lethal in progeny heteroallelic with the putative recombined alleles (for example, *Df(3L)ED4342/TM6B* for *Df(3L)ED4342kek6*^{34}*/TM6B* recombinants). Successful recombination of alleles balanced on chromosome III was verified by use of reporter lines for *Gal4* recombinants and/or PCR as applicable. Context-specific Gal4 initiation of transgene expression was used for genetic overexpression (Brand and Perrimon, 1993). Genetic drivers used: *elavGal4* (all neurons), *GMRGal4* (retina), *24BGal4* (muscle) and gene promoter-specific Gal4 lines. Transgenic P element insertions were mapped according to the protocol in Figure 2.4.

2.1.2 Null mutagenesis

Null mutants of *kek3*, *kek4* and *kek6* were generated according to the protocol of Parks et al. (2004) (Figures 2.5–2.7). Genetic work for the generation of the *kek3* deletion was carried out by Alicia Hidalgo. *piggyBac* variants and genomic orientation were selected according to compatibility criteria outlined in Parks et al. (2004). In each case, the start codon of the gene of interest was deleted (Figures 5.1, 5.3, 5.5). Flies containing compatible *piggyBac* elements

Figure 2.1 **Genetic protocol: double mutants, chromosomes II & III**

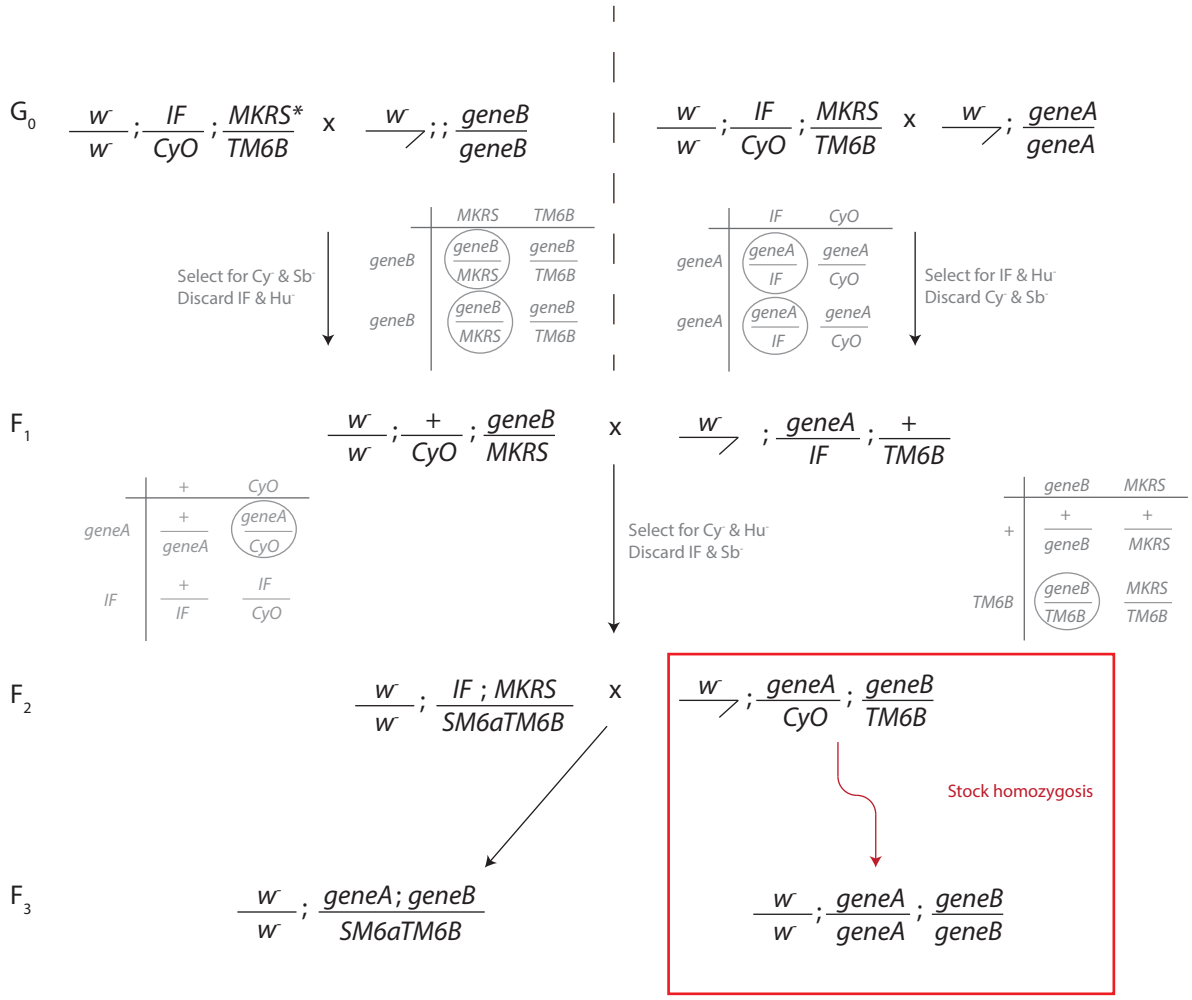

*(or w;IF/CyO lacZ;MKRS/TM6B lacZ)

Genetic protocol for combining alleles on chromosomes II and III. Punnett squares are shown to illustrate balancer selection

Figure 2.2 **Genetic protocol: double mutants, chromosomes X & III**

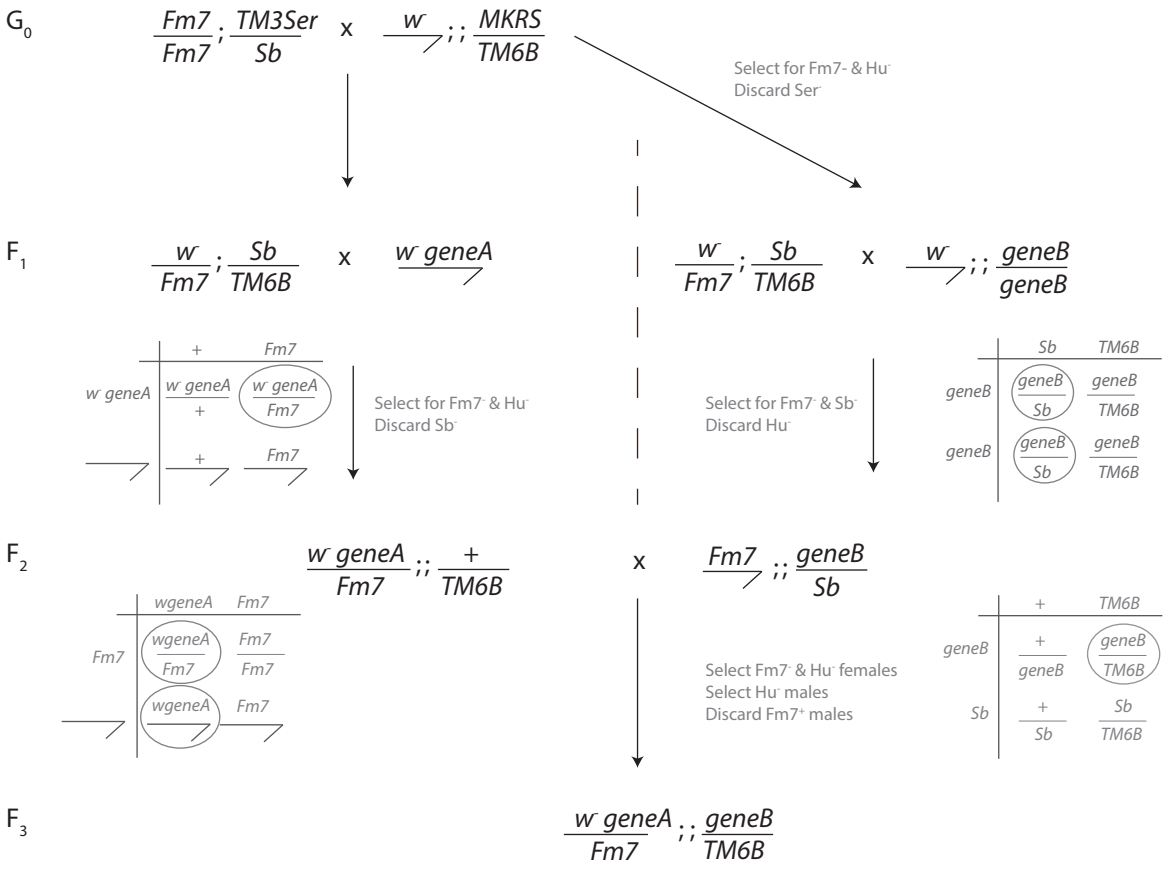

Genetic protocol for combining alleles on chromosomes X and III. Punnett squares are shown to illustrate balancer selection.

Figure 2.3 **Genetic protocol: recombination on chromosome III**

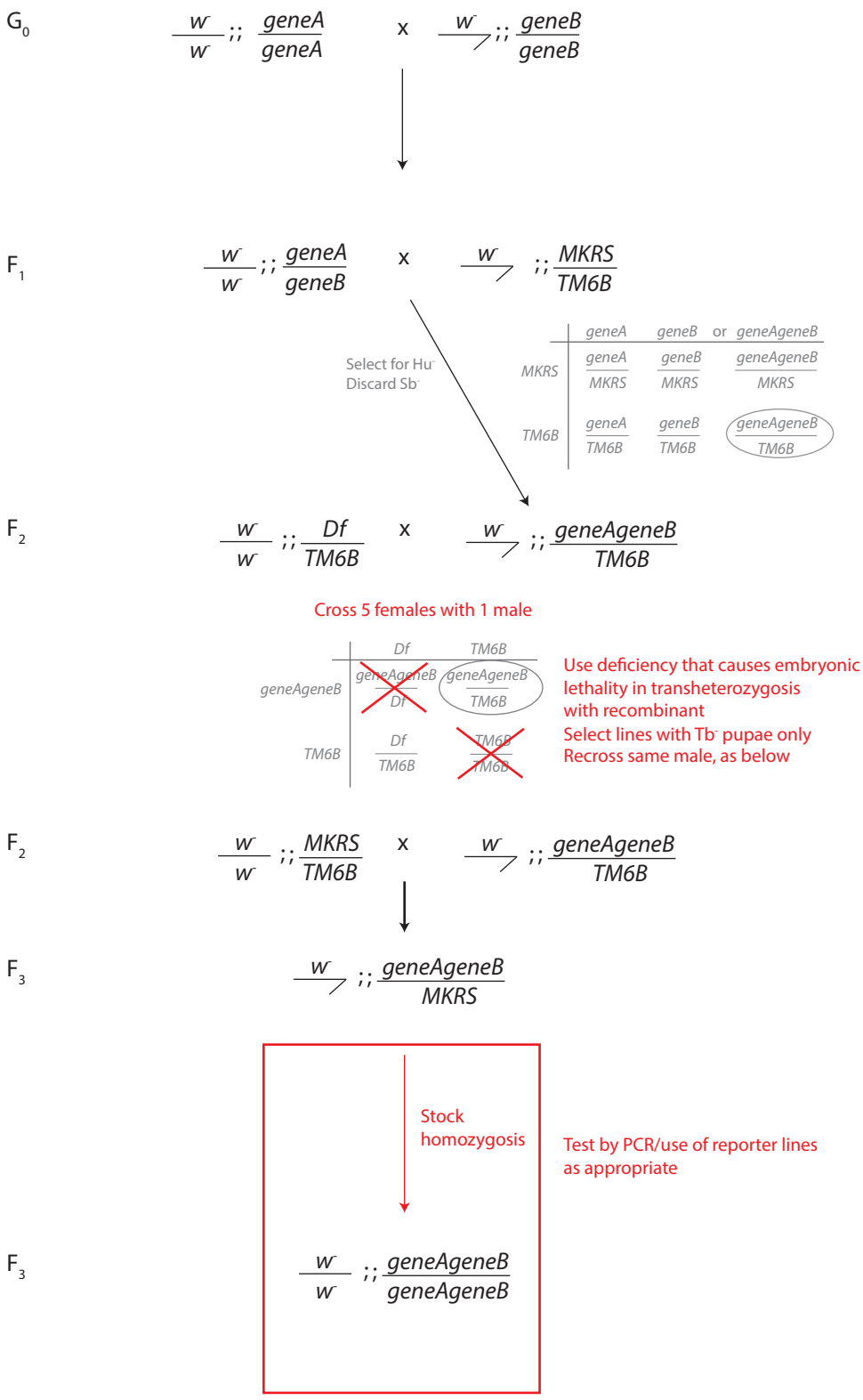

Genetic protocol for combining two alleles by recombination on chromosome III. Punnett squares are shown to illustrate balancer selection. At the F2 cross, multiple unique putative recombinant lines were established by crossing 5 virgin females to 1 male putative recombinant.

Figure 2.4 **Genetic protocol: mapping transgenic constructs**

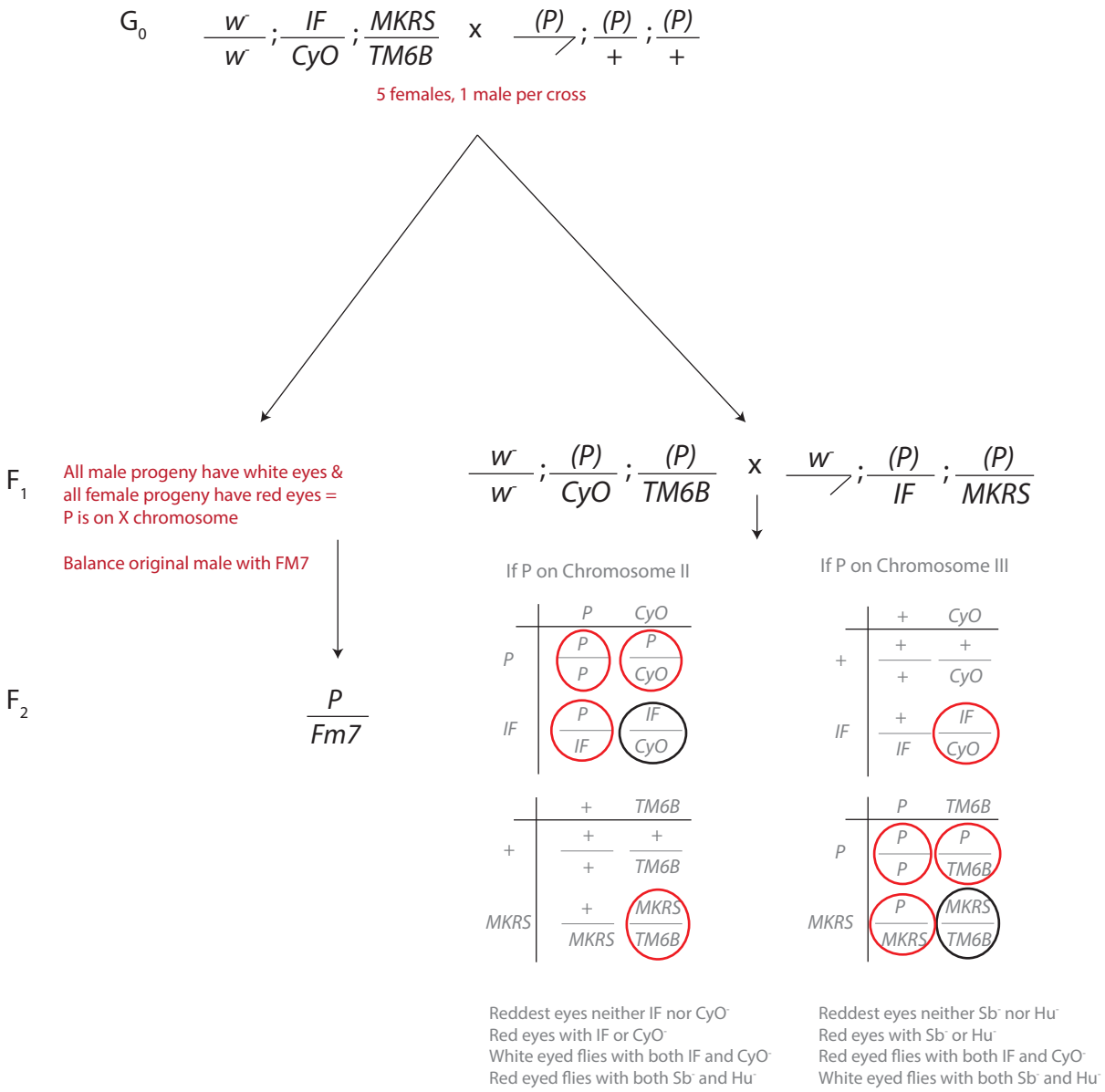

Genetic protocol to map the chromosomal position of transgenic constructs (*kek1-6+pTWR*) received from BestGene. *pTWR* contains a *mini-white* gene that generated red/orange eyes that could be used as a marker for construct mapping.

Figure 2.5 **Genetic Protocol: Heat-shock Flippase-mediated mutagenesis Chromosome II**

piggyBacA and *piggyBacB* denote the FRT-containing transposons that flank the deleted region

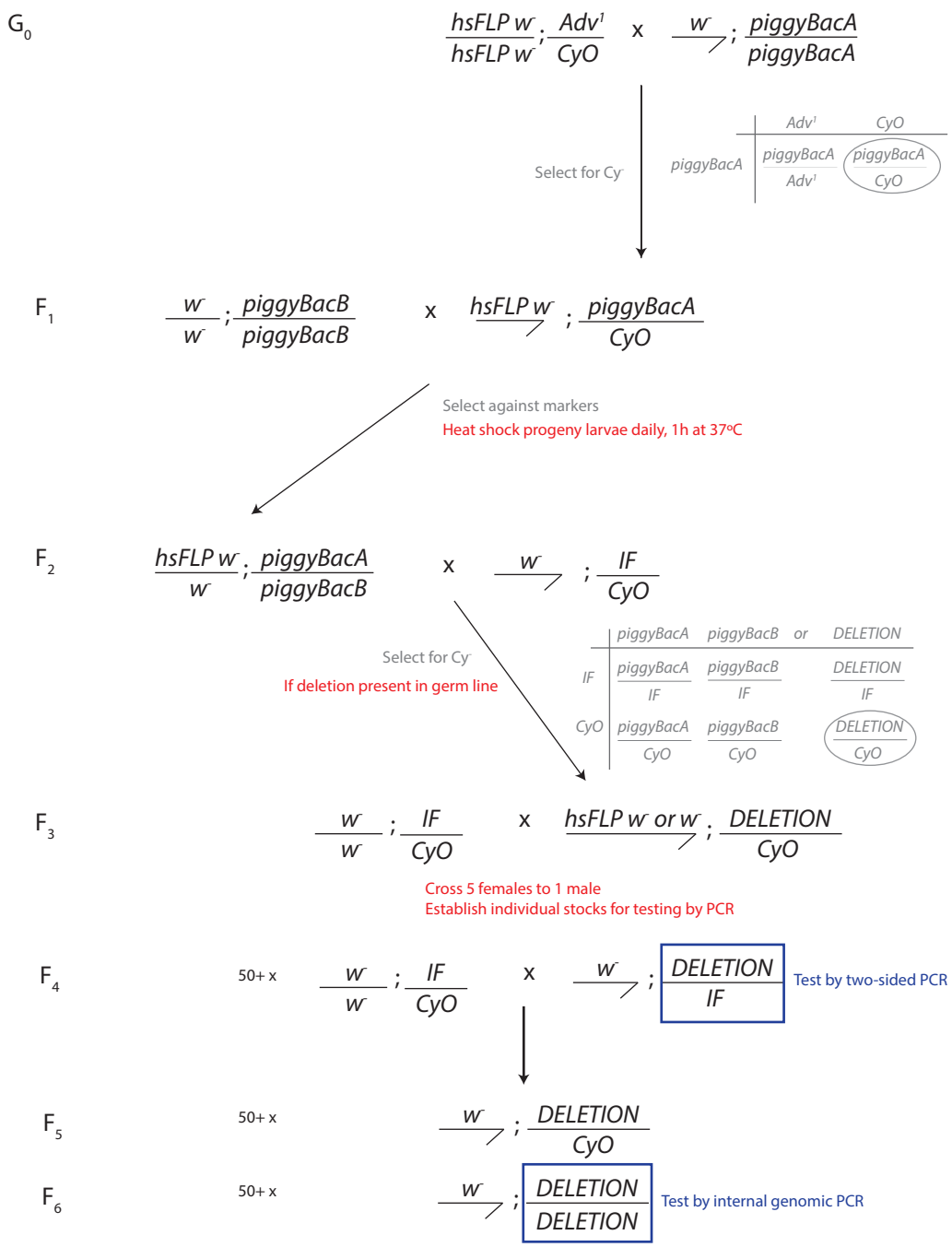

Genetic protocol for null mutagenesis by FRT transposon mutagenesis on chromosome II. F_1 progeny larvae with transheterozygous parental transposons were heat shocked at 37^{0}C for 1 hour daily to induce transposon fusion. If fusion occured in the germ line of these larvae, F_2 progeny carried heritable gene deletions. Multiple putative deletion lines were established at the F_3 cross by crossing 5 virgin isogenic females to 1 mutagenised male. Putative mutants were tested by PCR.

Figure 2.6 **Genetic protocol: Heat-shock Flippase-mediated mutagenesis Chromosome III**

piggyBacA and *piggyBacB* denote the FRT-containing transposons that flank the deleted region

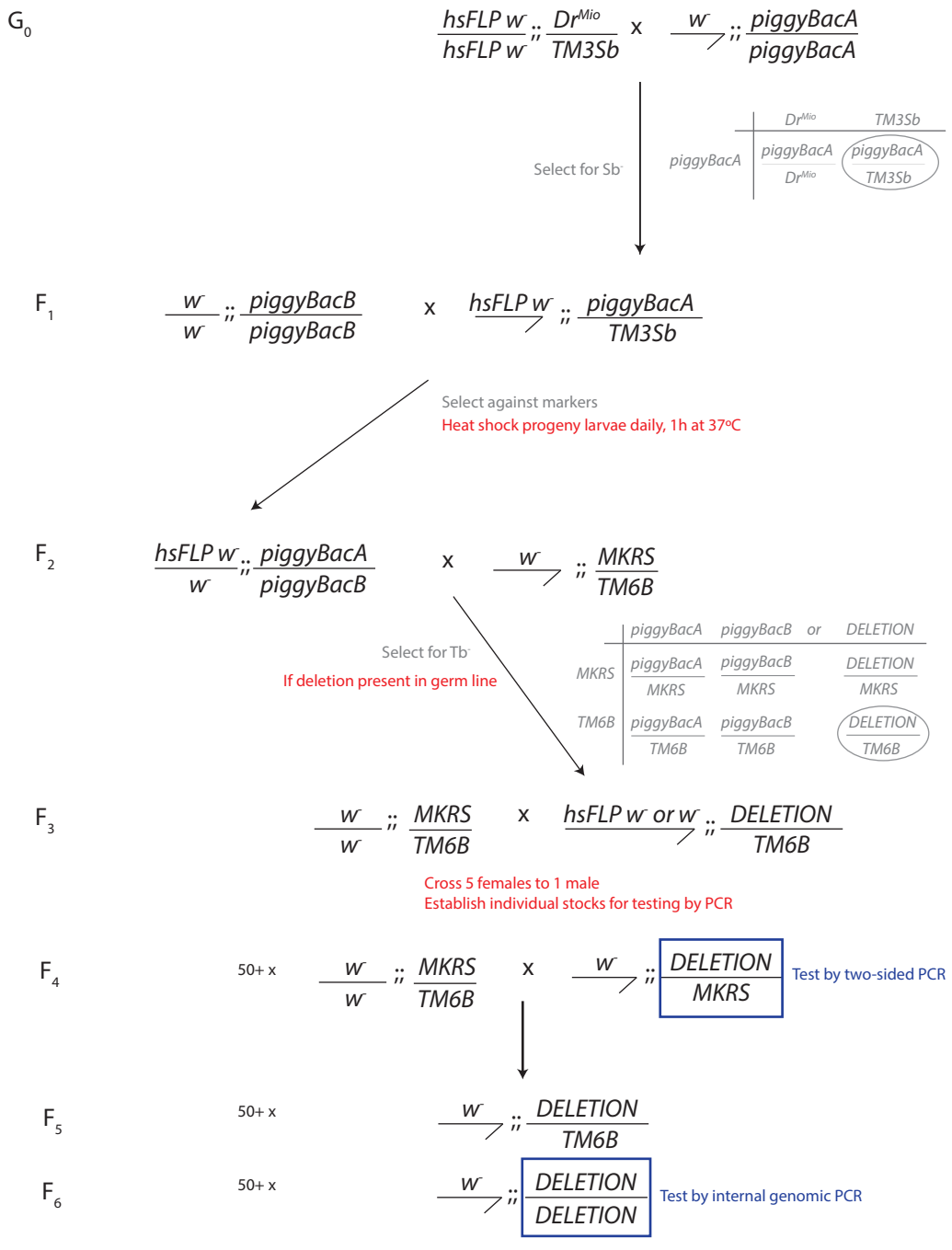

Genetic protocol for null mutagenesis by FRT transposon mutagenesis on chromosome III. Heat shock protocol was followed as per Figure 2.5.

Figure 2.7 **Deletion of *kek3*, *kek4* and *kek6* by FRT transposon mutagenesis**

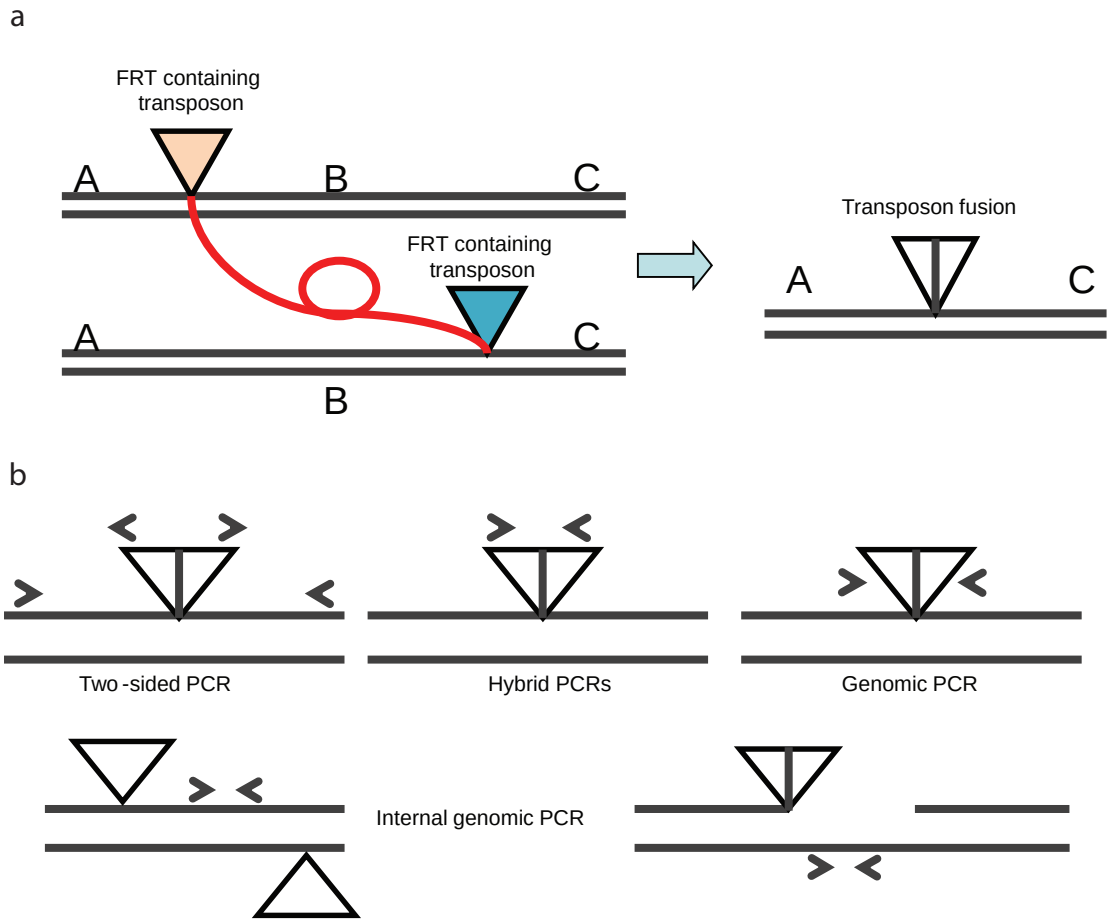

Excision of P elements by genetic and heat-shock activated Flippase-mediated recombination of *piggyBac* transposons to generate *kek3*, *kek4* and *kek6* null mutant alleles.
a | Heat shock activated Flippase induced transposon fusion between two FRT-containing parental transposon lines, deleting the genomic region in between. **b** | Transposon fusions could be tested by PCR. Two sided PCRs amplify from the transposon fusion into the flanking genomic region on both sides of the deletion. Only lines in which both fragments are amplified indicate a successful transposon fusion. Compatible *piggyBac* elements comprise three genetic compositions — WH, RB and XP elements — and either forward or reverse orientation relative to the genome; transposon fusions thus generate distinct sequences that can be amplified by Hybrid PCR. Genomic PCR amplifies the genomic region, including the transposon fusion, either side of the deltion. Internal genomic PCR amplifies a region internal to the putative deletion; bands were absent in homozygous genomic DNA. Here, two-sided and internal genomic PCR were used to verify generated nulls.

Table 2.1 **Fly stocks**

Genotype		Source	Use
Stocks			
yw		Bloomington #6420	
OregonR		Bloomington #5	
w;IF/CyO;MKRS;TM2		Bloomington #3042	
w;IF/CyO;MKRS;TM6B		Bloomington #3703	
w;IF/CyOlacZ;MKRS;TM6BlacZ		Zhu et al. 2008	
w;IF;MKRS/SM6aTM6B		Bloomington #5687, Zhu et al. 2008	
F263 vn^{y3}/TM3lacZ		Hidalgo et al. 2001	
Fm7/Fm7;;TM3Ser/Sb		Bloomington #8599	
P{hsFLP}1, w;Adv^{1}/CyO		Kyoto #105670	FRT mutagenesis
P{hsFLP}1, yw;;Dr^{Mio}/TM3Sb		Kyoto #105671	FRT mutagenesis
w;P{UAS-Cdc42.N17}3	II	Bloomington #6288	*UAS DN Cdc42*
UASMycAFGDP110	III	Bloomington #25918	*UAS DN PI3K*
w;P{UAS-Rac1.L89}6	II	Bloomington #6290	*UAS DN Rac1*
P{UAS-Ras85D.N17}	II	Bloomington #4845	*UAS DN Ras85D*
w;;P{UAS-Rho1.N19}2.1	III	Bloomington #7327	*UAS DN Rho1*
w;P{UAS-Cdc42.V12}2	II	Bloomington #6287	*UAS Act Cdc42*
P{Dp110-CAAX}1, w	X	Bloomington #8294	*UAS Act PI3K*
w;;P{UAS-Rac1.V12}1	III	Bloomington #6291	*UAS Act Rac1*
w;;P{UAS-Ras85D.V12}	III	Bloomington #4847	*UAS Act Ras85D*
w;P{UAS-Rho1.V14.E40L}/CyO	II	Bloomington #7333	*UAS Act Rho1*
Tie^{5}		A. Lowry, Hidalgo laboratory	
Deficiencies			
$15A6^{RA5}$/CyO;ry^{506}/+		Musacchio & Perrimon, 1996	*kek1* deficiency, Axon guidance
Df(2L)$15A6^{RM2}$/CyO		Musacchio & Perrimon, 1996	*kek1* deficiency, Axon guidance
Df(2L)BSC768/SM6a		Bloomington #26865	*kek4* deficiency
Df(2L)ED1050/SM6a		Kyoto #150105	*kek3* deficiency
Df(3R)ED6361/TM6B		Kyoto #150478	*kek6* deficiency, rebalanced
Df(3L)ED4342/TM6BlacZ		Bloomington #8062	*DNT1*/*tie* Deficiency
Df(3L)Exel6101/TM6B		Bloomington #7580	*DNT1* Deficiency
Df(3L)ED6092/TM6B		Bloomington #7571	*DNT2* Deficiency
Driver lines			
24BGal4		Bloomington #1767	Muscle driver
elavGal4		Bloomington #23867	Neurons driver
GMRGal4		M. Freeman	Eye driver
GMRGal4;roTaulacZ		Garrity el al. 1999	Eye driver
spz6Gal4		S. AlAhmed, Hidalgo laboratory	Ring gland driver
Reporters			
UASmCD8GFP		Kyoto #108068	Expression profiles
UASmyrTOMATO		M. Landgraff	Expression profiles
***DNT* alleles**			
$DNT1^{41}$/$DNT1^{41}$		Zhu et al. 2008	Survival index, Axon guidance
$DNT1^{55}$/$DNT1^{55}$		Zhu et al. 2008	Genetics, Survival index

DNT2^{e03444}/DNT2^{e03444}		Zhu et al. 2008	Survival index, Axon guidance
DNT2^{e03444}DNT1^{41}elavGal4/TM6BlacZ		Zhu et al. 2008	Survival index, Axon guidance
w;UASDNT1CK3'+;+/MKRS		Zhu et al. 2008	Axon guidance
DNT2^{37}/TM6B		J Wentzell, Hidalgo laboratory	Genetics
kek1			
15A6(ry^{+});ry^{506}		Musacchio & Perrimon, 1996	
pBac{XP}kek1^{d03841}		Harvard d03841	
		kek1 overexpression	
w;;UASkek1RFP/TM2		Cloning: This work; Transgenesis: BestGene #8547-1-1M	
w;UASkek1RFP/CyO;MKRS/TM6B		Cloning: This work; Transgenesis: BestGene #8547-1-2M	
w;;UASkek1RFP/TM2		Cloning: This work; Transgenesis: BestGene #8547-1-3M	
w;UASkek1RFP/CyO;+/MKRS	*	Cloning: This work; Transgenesis: BestGene #8547-1-4M	Rough eye phenotype, Axon guidance
w;UASkek1RFP/CyO;UASkek1RFP/MKRS		Cloning: This work; Transgenesis: BestGene #8547-1-5M	
w;+/CyO;UASkek1RFP/TM2		Cloning: This work; Transgenesis: BestGene #8547-1-6M	
UASkek1RFP;DNT1^{41}DNT2^{e03444}/SM6aTM6B		This work	DNT rescue, Survival index
kek2			
		kek2 overexpression	
w;UASkek2RFP/CyO;MKRS or TM6B	*	Cloning: This work; Transgenesis: BestGene #9179-1-1M	Rough eye phenotype
w;UASkek2RFP/CyO;MKRS/TM6B		Cloning: This work; Transgenesis: BestGene #9179-1-2F	
w;UASkek2RFP/CyO;UASkek2RFP/MKRS		Cloning: This work; Transgenesis: BestGene #9179-1-3M	
w;UASkek2RFP/CyO		Cloning: This work; Transgenesis: BestGene #9179-1-4M	
w;UASkek2RFP/CyO		Cloning: This work; Transgenesis: BestGene #9179-1-5M	
w;UASkek2RFP/CyO		Cloning: This work; Transgenesis: BestGene #9179-1-7M	
UASkek2RFP;DNT1^{41}DNT2^{e03444}/SM6aTM6B		This work	DNT rescue, Survival index
kek3			
pBac{WH}kek3^{f07027}/CyOlacZ		Harvard f07027	Null mutagenesis
pBac{WH}kek3^{f04709}		Harvard f04709	Null mutagenesis
pBac{WH}kek3^{f07029}		Harvard f07029	Genetics, Null mutagenesis
pBac{WH}kek3^{f07041}		Harvard f07041	Null mutagenesis
w;Mi{ET1}CG15256^{MB09797}		Bloomington #27806	*kek3Gal4*, Expression profiles
		kek3 LOF	
kek3^{f07029};+/SM6aTM6B		This work	Survival index, Locomotion
kek3^{f07029};DNT1^{41}/SM6aTM6B		This work	Kek-DNT interactions, Survival index, Locomotion
kek3^{f07029};DNT2^{e03444}/SM6aTM6B		This work	Kek-DNT interactions, Survival index, Locomotion
kek3^{12}		A Hidalgo/S Bishop, This work	Survival index, Locomotion
kek3^{26}		A Hidalgo/S Bishop, This work	Survival index, Locomotion
kek3^{12};+/SM6aTM6B		This work	Survival index
kek3^{26};+/SM6aTM6B		This work	Survival index
kek3^{12};DNT1^{55}/SM6aTM6B		This work	Kek-DNT interactions, Survival index
kek3^{26};Df(3L)Exel6101/SM6aTM6B		This work	Kek-DNT interactions, Survival index
kek3^{12};DNT2^{37}/SM6aTM6B		This work	Kek-DNT interactions, Survival index
kek3^{12};DNT2^{e0344}/SM6aTM6B		This work	Kek-DNT interactions, Survival index
kek3^{26};Df(3L)6092/SM6aTM6B		This work	Kek-DNT interactions, Survival index

kek3^{12};roTaulacZ		This work	Photoreceptor axon targeting, see Chapter 8
		kek3 overexpression	
w;;UASkek3RFP/TM6B		Cloning: This work; Transgenesis: BestGene #8547-2-1M	
w;UASkek3RFP/CyO		Cloning: This work; Transgenesis: BestGene #8547-2-2M	
w;;UASkek3RFP/MKRS	*	Cloning: This work; Transgenesis: BestGene #8547-2-3M	Locomotion, Rough eye
UASkek3RFP;DNT1^{41}DNT2^{e03444}/SM6aTM6B		This work	DNT rescue, Survival index
kek4			
pBac{WH}kek4^{f05454}		Harvard f05454	Genetics, Null mutagenesis
pBac{RB}kek4^{e04257}		Harvard e04257	Null mutagenesis
w;P{GT1}BG00800		Bloomington #12509	*kek4Gal4*, Expression profiles
		kek4 LOF	
kek4^{f05454};+/SM6aTM6B		This work	Survival index, Locomotion
kek4^{f05454};DNT1^{55}/SM6aTM6B		This work	Kek-DNT interactions, Survival index, Locomotion
kek4^{f05454};DNT2^{e03444}/SM6aTM6B		This work	Kek-DNT interactions, Survival index, Locomotion
kek4^{20}		This work	Survival index, Locomotion, Developmental timing, BR-C staining
kek4^{23}		This work	Survival index, Locomotion, Developmental timing, BR-C staining
kek4^{42}/CyO		This work	
kek4^{20};+/SM6aTM6B		This work	Survival index
kek4^{23};+/SM6aTM6B		This work	Survival index
kek4^{20}/CyO;DNT1^{55}/TM6B		This work	Kek-DNT interactions, Survival index
kek4^{23}/CyO;Df(3L)Exel6101/TM6B		This work	Kek-DNT interactions, Survival index
kek4^{20}/CyO;DNT2^{37}/TM6B		This work	Kek-DNT interactions, Survival index
kek4^{20}/CyOlacZ;DNT2^{e03444}/TM6BlacZ		This work	Kek-DNT interactions, Survival index
kek4^{23}/CyO;Df(3L)6092/TM6B		This work	Kek-DNT interactions, Survival index
		kek4 overexpression	
w;UASkek4RFP/CyO		Cloning: This work; Transgenesis: BestGene #9179-2-1M	
w;(UASkek4RFP)/CyO;(UASkek4RFP)/MKRS		Cloning: This work; Transgenesis: BestGene #9179-2-2M	
w;;UASkek4RFP/MKRS	*	Cloning: This work; Transgenesis: BestGene #9179-2-3M	Developmental timing, Locomotion, BR-C staining, Rough eye
UASkek4RFP;DNT1^{41}DNT2^{e03444}/SM6aTM6B		This work	DNT rescue, Survival index
kek5			
pBac{RB}kek5^{e02482}		Harvard e02482	Genetics
P{GawB}NP5933		Kyoto #105058	*kek5Gal4*, Expression profiles
		kek5 LOF	
kek5^{e02482};;+/TM6B		This work	Survival index, Locomotion
kek5^{e02482};;DNT1^{55}/TM6B		This work	Kek-DNT interactions, Survival index, Locomotion
kek5^{e02482};;DNT2^{e03444}/TM6B		This work	Kek-DNT interactions, Survival index, Locomotion
		kek5 overexpression	
w;IF/CyO;UASkek5RFP/MKRS		Cloning: This work; Transgenesis: BestGene #9179-3-1M	
w;;UASkek5RFP/TM6B		Cloning: This work; Transgenesis: BestGene #9179-3-2M	
w;+/CyO;UASkek5RFP/TM6B		Cloning: This work; Transgenesis: BestGene #9179-3-3M	
w;;UASkek5RFP/MKRS	*	Cloning: This work; Transgenesis: BestGene #9179-3-4M	Rough eye phenotype
w;UASkek5		Cloning: This work; Transgenesis: BestGene #9179-3-8M	
UASkek5RFP;DNT1^{41}DNT2^{e03444}/SM6aTM6B		This work	DNT rescue, Survival index

kek6			
pBac{RB}kek6^{e00907}		Harvard e00907	Null mutagenesis
pBac{RB}kek6^{e05733}		Harvard e05733	Null mutagenesis
		kek6 LOF	
kek6^{34}/TM3lacZ		This work	Axon guidance
kek6^{34}/TM6B		This work	Survival index, Locomotion
kek6^{35}/TM3lacZ		This work	Axon guidance
kek6^{35}/TM6B		This work	Survival index, Locomotion
kek6^{34}Df(3L)ED4342/TM6B		This work	Kek-DNT interactions, Survival index, Locomotion
kek6^{34}Df6092/TM6B		This work	Kek-DNT interactions, Survival index, Locomotion
Df(3R)ED6361DNT1^{55}/TM6B		This work	Kek-DNT interactions, Survival index, Locomotion
Df(3R)ED6361DNT2^{e03444}/TM6B		This work	Kek-DNT interactions, Survival index, Locomotion
Df(3R)ED6361Tie^{5}/TM6B		This work	Kek-DNT interactions, Survival index, Locomotion
kek6^{34}24BGal4/TM6BlacZ		This work	Axon guidance, Survival index
UASDNT1CK3'+;kek6^{35}/TM6BlacZ		This work	Axon guidance, Survival index
UASRho1$^{V14\text{-}E4DL}$;kek6^{35}/TM6B		This work	*kek6-,* Act *Rho*: Survival index
UAScdc42^{V12};kek6^{35}/TM6BlacZ		This work	*kek6-,* Act *cdc42*: Survival index
Toll7^{P8};Df(3R)ED6361/SM6aTM6B		This work	Future use: see Chapter 6 Discussion
		kek6 overexpression	
UASkek6RFP/Fm7		Cloning: This work; Transgenesis: BestGene #8547-3-2F	
w;;UASkek6RFP/TM2		Cloning: This work; Transgenesis: BestGene #8547-3-3M	
w;;UASkek6RFP/TM2	*	Cloning: This work; Transgenesis: BestGene #8547-3-4M	Survival index, Locomotion, Axon guidance, Rough eye
w;UASkek6RFP/CyO	*	Cloning: This work; Transgenesis: BestGene #8547-3-5M	
w;;UASkek6RFP/MKRS		Cloning: This work; Transgenesis: BestGene #8547-3-6M	
w;UASkek6RFP/CyO;UASkek6RFP/MKRS		Cloning: This work; Transgenesis: BestGene #8547-3-7M	
UASkek6RFP/Fm7		Cloning: This work; Transgenesis: BestGene #8547-3-8M	
w;UASkek6RFP/CyO;UASkek6RFP/MKRS		Cloning: This work; Transgenesis: BestGene #8547-3-9M	
w;;UASkek6RFP/MKRS		Cloning: This work; Transgenesis: BestGene #8547-3-10M	
UASkek6RFP;DNT1^{41}DNT2^{e03444}/SM6aTM6B		This work	DNT rescue, Survival index, Axon guidance
UAScdc42$^{N17.3}$;UASkek6RFP		This work	UAS *kek6*, DN cdc42: Axon guidance, locomotion
UASkek6RFP/CyOlacZ;UASMycAFGDP110		This work	UAS *kek6*, DN PI3K: Axon guidance, locomotion
UASRas^{N17};UASkek6RFP		This work	UAS *kek6*, DN Ras: Axon guidance, locomotion
UASdRac$^{L89.6}$;UASkek6RFP		This work	UAS *kek6*, DN Rac: Axon guidance, locomotion
UASkek6RFP;UASRho^{N19}/SM6aTM6B		This work	UAS *kek6*, DN Rho: Axon guidance, locomotion
		kek6 rescue	
kek6^{34}elavGal4/TM6BlacZ		This work	Survival index, Axon guidance, Locomotion
UASkek6RFP;Df(3R)ED6361/SM6aTM6B		This work	Survival index, Axon guidance, Locomotion
UASkek6RFP;kek6^{35}/SM6aTM6B		This work	Survival index
Lambik			
p{GSV2}lbk^{GS50104}/SM1		Kyoto #204812	Genetics
		lbk LOF	
lbk^{GS50104};+/SM6aTM6B		This work	Survival index, Locomotion
lbk^{GS50104};DNT1^{55}/SM6aTM6B		This work	Kek-DNT interactions, Survival index
lbk^{GS50104};DNT2^{e03444}/SM6aTM6B		This work	Kek-DNT interactions, Survival index

Rickets		
rk^{4}	Bloomington #3590	Genetics
	rk LOF	
w;rk^{4}*;+/SM6aTM6B*	This work	Survival index
w;rk^{4}*;DNT1*^{55}*/SM6aTM6B*	This work	Kek-DNT interactions, Survival index
w;rk^{4}*;DNT2*^{e03444}*/SM6aTM6B*	This work	Kek-DNT interactions, Survival index
Wengen		
pBac{RB}wgn^{e00637}	Bloomington #17874	Genetics
	wgn LOF	
pBacwgn^{e00637}*;;+/TM6B*	This work	Survival index, Locomotion
pBacwgn^{e00637}*;;DNT1*^{55}*/TM6B*	This work	Kek-DNT interactions, Survival index
pBacwgn^{e00637}*;;DNT2*^{e03444}*/TM6B*	This work	Kek-DNT interactions, Survival index
CG17839		
pBac{Gal4D,EYFP}CG17839^{PL00504}	Flybase #7366	*CG17839Gal4*, Expression profiles

Transgenic lines used in experiments are indicated with a *.

flanking the genes of interest were crossed such that the parental transposons were held in heterozygosis in combination with heat shock-inducible Flippase recombinase. F_1 parental flies were transferred into duplicate vials 3, 5 and 7 days after crossing; heterozygous larvae in each vial were subjected to 7 daily 2 hour heat shocks at 37^0C in a water bath from 2 days after parental crossing. Adult progeny were balanced using *CyO* (*kek3*, *kek4*) or *TM6B* (*kek6*) balancer chromosomes. At least 50 lines (Appendix III) for each putative deletion were set up at the F_3 cross using 5 pairwise virgin females and 1 putative mutant male. Progeny were screened by polymerase chain reaction (PCR; Figures 5.1–5.5).

Two methods for mutagenesis verification were used (Figure 2.7). Two-sided PCR using genomic DNA from heterozygous putative mutants and parental lines amplified genomic regions flanking the insertion sites either side of the deletion; one primer from each reaction hybridised within the P element insertion. Only lines from which fragments could be amplified on both sides of the putative deletion had undergone a transposon fusion. Internal genomic PCR using genomic DNA from homozygous putative mutants (*kek3*, *kek4*) or heterozygous mutant/deficiency stocks (*kek6*) amplified genomic regions internal to the deletion. Only lines that failed to amplify this fragment, but tested positive for fragments outside of the deleted region, were successful deletions. For primers used and regions of amplification, see Figures 5.1–5.5.

2.1.3 Survival index

Survival index (S.I.) calculations were applied to pupal counts to determine embryonic lethality resulting from mutant alleles. Alleles were balanced over *TM6B* or *SM6aTM6B*, and flies incubated at 18^0C. Pupal progeny of heterozygous flies or crossed heterozygous parents reared in these conditions were scored for Tb^- (*TM6B*) or Tb^+ (homozygotes) markers.

The S.I. of heterozygous flies was calculated as 2 x (number of Tb^+ pupae/number of Tb^- pupae). Heterozygous parents with viable alleles yield an expected Mendelian ratio of 1/3 Tb^+

(*allele*/*allele*):2/3 Tb^{-} (*allele*/*TM6B*) progeny (*TM6B*/*TM6B* is embryonic lethal); thus, viable alleles yield a S.I. of 1. Alleles that impair viability produce more Tb^{-} progeny and thus have survival indices <1.

Transposon-derived alleles for use in initial survival index results (Chapter 3) are summarised in Table 2.2 and Figure 2.8.To determine most suitable candidate genes for further study, *dLIG–Drosophila* neurotrophin (*DNT*) genetic combinations were studied using viable *dLIG* alleles, in which the coding sequence or regulatory regions were disrupted by transposon insertion and/or point mutation. The choice of allele reflected the intention to quickly screen the genes for notable phenotypic differences with DNT combinations: given the lack of knowledge of how these alleles manifest phenotypes, initial survival index results shown in Chapter 3 are not intended for publication.

2.2 Molecular biology

Primers and plasmids used or generated in this work are listed in Tables 2.3 and 2.4, respectively. Origins of *kek* cDNAs for coding sequence amplification are given in Table 2.4.

2.2.1 Genomic DNA isolation

Genomic DNA was isolated from flies for null mutagenesis verification. 15 flies were collected under anaesthetic and chilled in 400µl DNA extraction buffer (0.1M Tris-HCl pH8, 0.05M EDTA pH8, 1% SDS). Flies were homogenised and incubated at 37^{0}C for 15 minutes. Samples were treated with 1µl RNaseA (4mg/ml) for 15 minutes at 37^{0}C and inactivated at 65^{0}C for 15 minutes. Protein was precipitated by mixing 300µl 7.5M ammonium acetate to chilled samples and cooling on ice. Following centrifugation, supernatant was extracted and precipitated in 500µl isopropanol, cooled on ice for 10 minutes and centrifuged at 15,000rpm for 15 minutes. Pelleted DNA was washed in 70% ethanol, dried and dissolved in 60µl TE for 1 hour at 65^{0}C. Samples were cooled prior to use in PCR.

Figure 2.8 **Candidate gene models, P elements and probe hybridisation**

Candidate DNT receptor gene models are shown. Genome locations are indicated above each model, including chromosome. Transposon insertion sites of alleles used in initial genetic studies (Figure 3.11) are indicated (red triangle). The rk^4 point mutation is labelled in red. *In situ* antisense probe hybridisation is labelled in blue. Distances between Gal4 insertions and the start codons of corresponding genes are shown.

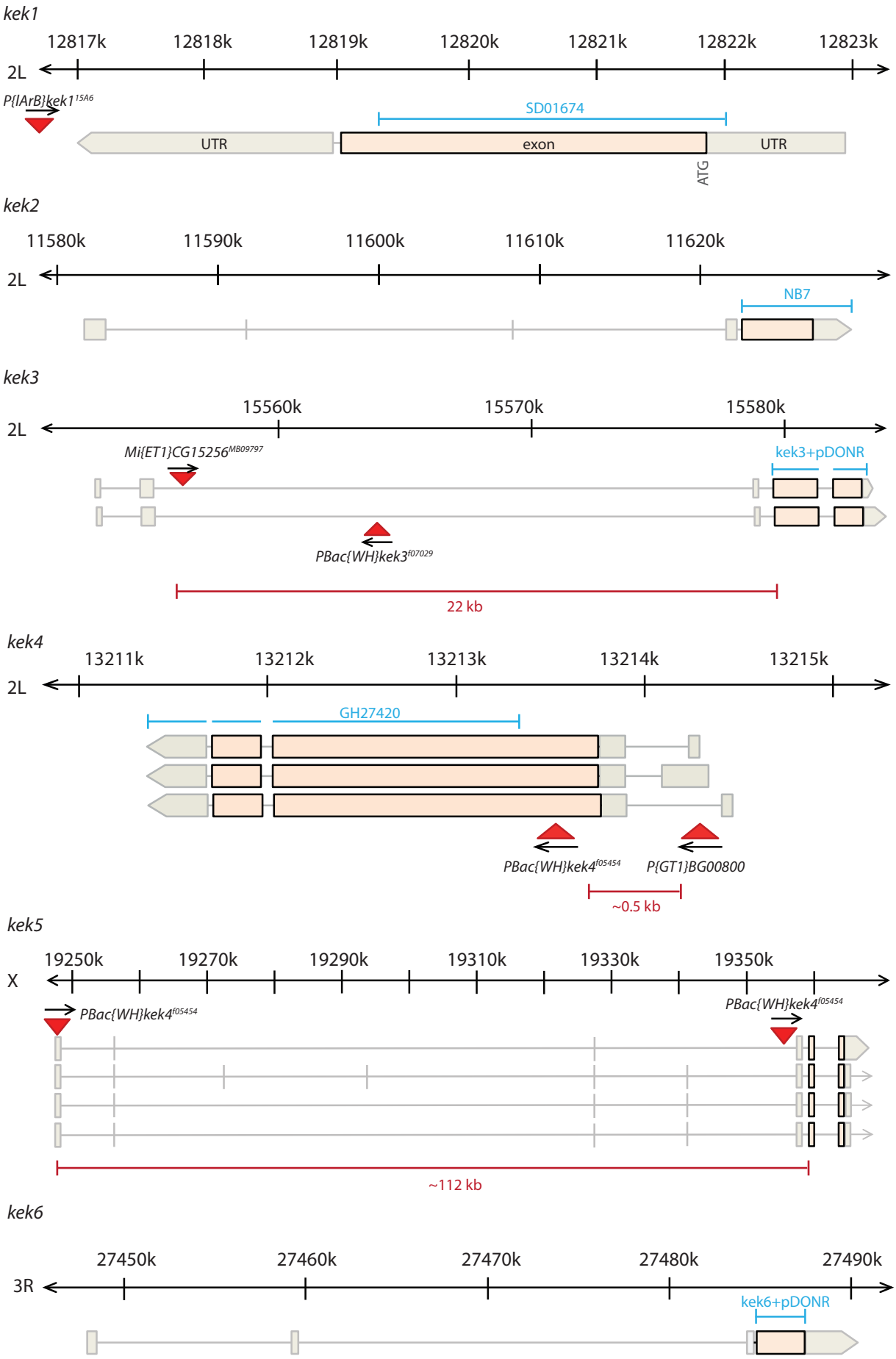
kek1
12817k
12818k
12819k
12820k
12821k
12822k
12823k
2L
P{lArB}kek1^15A6
SD01674
UTR
exon
UTR
ATG
kek2
11580k
11590k
11600k
11610k
11620k
2L
NB7
kek3
15560k
15570k
15580k
2L
Mi{ET1}CG15256^MB09797
kek3+pDONR
PBac{WH}kek3^f07029
22 kb
kek4
13211k
13212k
13213k
13214k
13215k
2L
GH27420
PBac{WH}kek4^f05454
P{GT1}BG00800
~0.5 kb
kek5
19250k
19270k
19290k
19310k
19330k
19350k
X
PBac{WH}kek4^f05454
PBac{WH}kek4^f05454
~112 kb
kek6
27450k
27460k
27470k
27480k
27490k
3R
kek6+pDONR

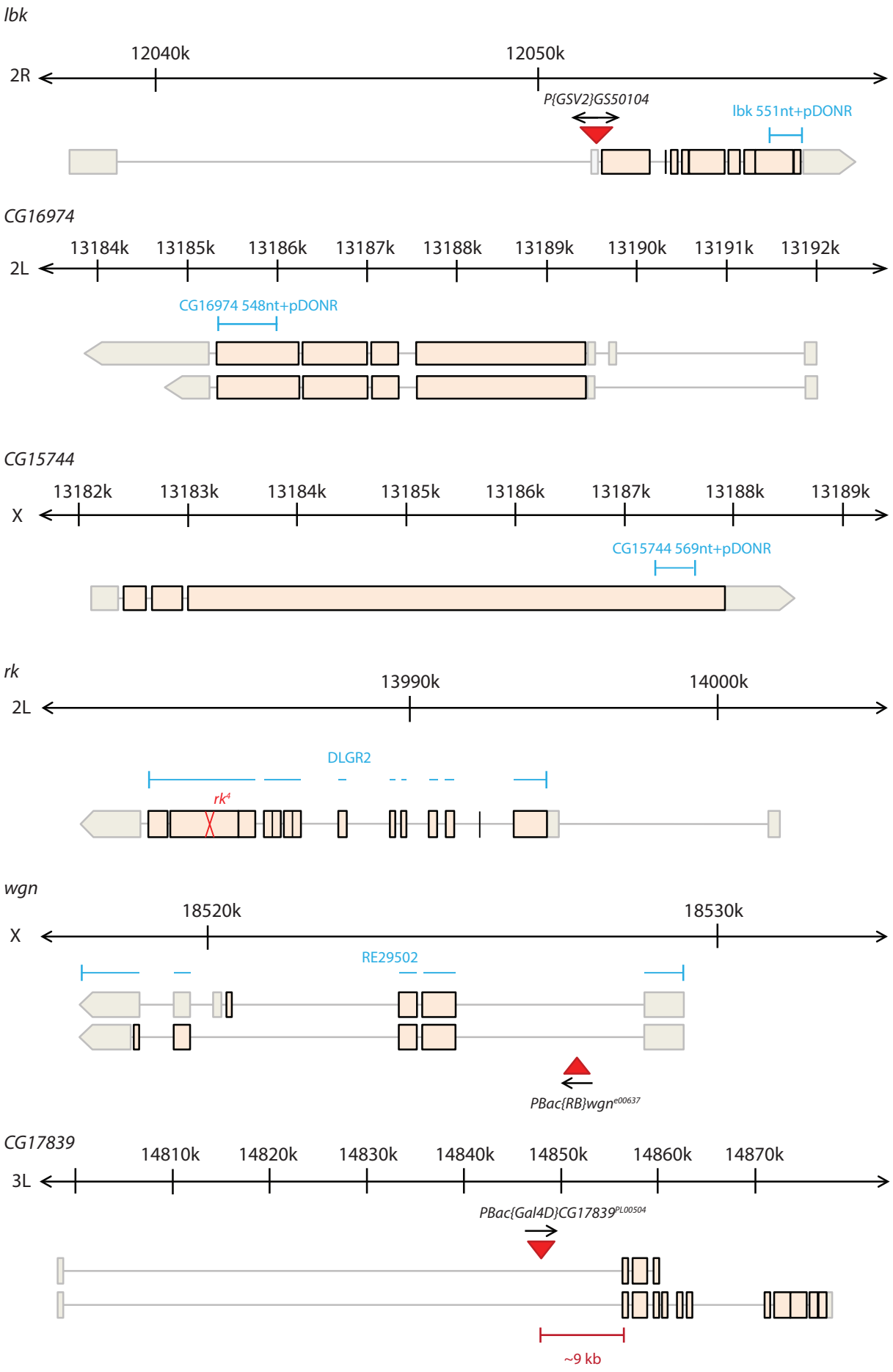
lbk
12040k
12050k
2R
P{GSV2}GS50104
lbk 551nt+pDONR
CG16974
13184k
13185k
13186k
13187k
13188k
13189k
13190k
13191k
13192k
2L
CG16974 548nt+pDONR
CG15744
13182k
13183k
13184k
13185k
13186k
13187k
13188k
13189k
X
CG15744 569nt+pDONR
rk
13990k
14000k
2L
DLGR2
rk4
wgn
18520k
18530k
X
RE29502
PBac{RB}wgne00637
CG17839
14810k
14820k
14830k
14840k
14850k
14860k
14870k
3L
PBac{Gal4D}CG17839PL00504
~9 kb

Table 2.2 **Summary of transposon alleles for survival index**

Allele	Nature of allele	Genomic position	Known phenotypes
kek3^{f07029}	piggyBac transposon insertion, 3′–5′ relative to gene	Intronic; 15kb upstream of ATG	Viable
kek4^{f05454}	piggyBac transposon insertion, 5′–3′ relative to gene	Exonic; 0.5kb downstream of ATG	Viable
kek5^{e02482}	piggyBac transposon insertion, 5′–3′ relative to gene	Intronic; 2kb upstream of ATG	Viable
lbk^{GS50104}	UAS-containing transposon insertion, orientation unknown	UTR; <0.5kb upstream of ATG	Viable
rk^{4}	Missense point mutation	Exonic; <2kb upstream of stop codon	Viable, fertile, behavioural and mating phenotypes, phenotypes in cuticle, leg, neurons and wing
wgn^{e00637}	Transposon insertion, 5′–3′ relative to gene	Intronic; 3kb upstream of ATG	Viable, fertile, neuroanatomy phenotypes

ATG, start codon; UAS, upstream activating sequence; UTR, untranslated region.

Table 2.3 **Primers**

Primer name	Sequence	RE	Amplifies	Use
		kek1		
kek1CDSattB5'Fw	GGGGACAAGTTTGTAC AAA AAA GCA GGC TCA TCC AGG AAA **ATG** CAT ATC A	-	2443nt (9nt+CDS, no STOP)	Gateway cloning, sequencing
kek1CDSattB3'Rv	GGGGACCAC TTT GTA CAA GAA AGC TGG GTA GTC AGT TCT TGG TTT GGT TT	-		
kek1seqFwd1	GCAAGATCGGCGAAATCGAG	-		*kek1* sequencing primer
kek1seqFwd2	GACCGGAGATGTTGCCCATA	-		*kek1* sequencing primer
kek1seqFwd3	TAACAAACAAGACGCAGCCC	-		*kek1* sequencing primer
kek1seqFwd4	GATGACCTCTTCATGAAGCG	-		*kek1* sequencing primer
kek1seqRev1	TCCCACAGACCCGAAGGATA	-		*kek1* sequencing primer
kek1seqRev2	CATGTGATTGGGCGTCTTGC	-		*kek1* sequencing primer
kek1seqRev3	ATCGATAATCCTTTCGGGGC	-		*kek1* sequencing primer
kek1seqRev4	GATTTAGCAGATTCGCACGG	-		*kek1* sequencing primer
		kek2		
kek2CDSattB5'Fw	GGGGACAAGTTTGTAC AAA AAA GCA GGC TCA **ATG** AGT GGT CTG CCA ATC T	-	2682nt (CDS, no STOP)	Gateway cloning, sequencing
kek2CDSattB3'Rv	GGGGACCAC TTT GTA CAA GAA AGC TGG GTA AAT GTC GCT GGT TTC CTG GC	-		
kek2seqFwd1	GGCACTTGTCTTTTCTCACG	-		*kek2* sequencing primer
kek2seqFwd2	CAACGTTGGTGCCGAGGATA	-		*kek2* sequencing primer
kek2seqFwd3	AGCAGCAGCTGCAGCTGAAT	-		*kek2* sequencing primer
kek2seqFwd4	AACAGGTGCAGCCTGCCAAT	-		*kek2* sequencing primer
kek2seqFwd5	CCATTCCGGAGCTGGATGAA	-		*kek2* sequencing primer
kek2seqRev1	GCTGGTACTTCTCGTAGCTC	-		*kek2* sequencing primer
kek2seqRev2	GACACTCTCCGCATCGTTGA	-		*kek2* sequencing primer
kek2seqRev3	AAGATAATGCCGCCTCCGGC	-		*kek2* sequencing primer

kek2seqRev4	CAGCCAGAAGTGGATGTCTA	-		*kek2* sequencing primer
kek2seqRev5	TAAAGTTGAGGACCTGGGTG	-		*kek2* sequencing primer
		kek3		
kek3CDS#2Fwd	GGGGACAAGTTTGTAC AAA AAA GCA GGC TCA TAT GCG **ATG** GCA GCG GGA A	-	3069nt (6nt+CDS, no STOP)	Gateway cloning, sequencing
kek3CDS3'endRev	GGGGACCAC TTT GTA CAA GAA AGC TGG GTA GCT CTT GAA AAT ATC CTG TC	-		
kek3558ntattBFw	GGGGACAAGTTTGTAC AAA AAA GCA GGC TCA AAC TAT TCA AGC ACG GCC	-	558nt (fragment of CDS with Gateway sequences)	*In situ*, cDNA library detection
kek3558ntattBRv	GGGGACCAC TTT GTA CAA GAA AGC TGG GTTAC CAG CAC TTC CAT CAC CA	-		
kek3upCDS-5'Fwd	CAGCCACATCAACATTGGCA	-	3281nt (145nt + CDS + 50nt downstream)	Gateway cloning
kek3dwnCDS-3'Rev	TTGGCGGACCAAAGTCTATC	-		
kek3seqFwd1	AGTGGAACTGGATCTAAGCC	-		*kek3* sequencing primer
kek3seqFwd2	GAGTGGAGGGCAGGAACATA	-		*kek3* sequencing primer
kek3seqFwd3	ATCGAGATGACGGCCAGAAC	-		*kek3* sequencing primer
kek3seqFwd4	GAAGACCACACCCATTGCCA	-		*kek3* sequencing primer
kek3seqFwd5	CAGCGGGCCAATAGTTTCCT	-		*kek3* sequencing primer
kek3seqFwd6	CGCCATGTTGAAGCGGTTAA	-		*kek3* sequencing primer
kek3seqRev1	AGATGACTCGGCAGCAGTTT	-		*kek3* sequencing primer
kek3seqRev2	CGAGGTCACTGGTTTGCTGT	-		*kek3* sequencing primer
kek3seqRev3	AACTAGCCCCTCCTCCCAGA	-		*kek3* sequencing primer
kek3seqRev4	TTGGGGTACTCCTTCCACGT	-		*kek3* sequencing primer
kek3seqRev5	GTAGAGCGCCAATGAGGGTA	-		*kek3* sequencing primer
kek3seqRev6	CTTTTCGACGCACCTTCGTC	-		*kek3* sequencing primer
kek3FRT1.5kbupLI	CAGGACGCGAATGTTGTCCT	-	1.5kb with WH-WH- 2sid LI R	Null verification,~1.5kb upstream of *pBac[WH]kek3[f04709]*
kek3FRT2.5kbdnRI	TTGGATTGAGGAGAAGCCTC	-	2.7kb with WH-WH- 2sid RI F	Null verification, ~2.5kb downstream of *pBac[WH]kek3[f07027]*
kek3f07041Rev	AGTACCCTAACCAATGCTC	-	~250nt with WH-WH- 2sid LI R	Null verification, ~250nt downstream of *pBac[WH]f07041*
kek3FRT GP Fwd	CGAAGAGAATTCAAGACGGG	-	7.4kb genomic region including P element fusion, ~200nt using WH-WH-2sid LI R and RI F two-sided PCR primers	Null verification, ~100nt upstream of *pBac[WH]kek3[f04709]*
kek3FRT GP Rev	GTGTGAAGAAGTTCATCCCC	-		Null verification, ~100nt downstream of *pBac[WH]kek3[f07027]*

kek3intgenF	GGACAGGGGCATGTGTATAT	-	543 nt	In *kek3* intron, for verifying homozygous *kek3* nulls
kek3intgenR	ATTCCGGGAAGGTTGAAAGC	-		In *kek3* intron, for verifying homozygous *kek3* nulls
kek3-EC-TM-RI	CGAT-GAATTC-AGGTACAGAGTTCCAGAGAC	EcoRI	Kek3 juxtamembrane domain towards N terminus	Chimaera cloning
		kek4		
kek4CDSattB5'Fw	GGGGACAAGTTTGTAC AAA AAA GCA GGC TCA CTA GAC CTT CCG TTC CTT A (ga aaa atc tca **atg**)	-	1977nt (30nt+CDS, no STOP)	Gateway cloning, sequencing
kek4CDSattB3'Rv	GGGGACCAC TTT GTA CAA GAA AGC TGG GTA TAT TGA GAT ATC AAC ACC AG	-		
Kek4 1.6kb in Fwd	TAGTTTGCCCGTTCAGTCAC	-	514nt	cDNA library detection
Kek4 2kbin Rev	GGTATTGTACTTGCTTCGGG	-		
kek4seqFwd1	CTGTTGCAAGCACTTCGCCA	-		*kek4* sequencing primer
kek4seqFwd2	GCTCCAAGCCGGTGAAAAGT	-		*kek4* sequencing primer
kek4seqFwd3	CATCCAATTCGAATGGCAGC	-		*kek4* sequencing primer
kek4seqRev1	ACTCCAGAACTTAGGGCGCT	-		*kek4* sequencing primer
kek4seqRev2	TATTGGGAGATCCGTGGACG	-		*kek4* sequencing primer
kek4seqRev3	ACACATTGGGTAGCAGGTCG	-		*kek4* sequencing primer
kek4FRT GP Fwd	CTTGCCAGAGTTCCATTTGC	-	100nt with WH-WH- 2sid LI F	Null verification, ~100nt upstream of *pBac[WH]kek4[f05454]*
kek4FRT GP Rev	CAGTAGCTGTCTATAAGTTAATG	-	100nt with WH-WH- 2sid RI F	Null verification, ~100nt downstream of *pBac[RB]kek4[e04257]*
kek4intgenF	GGAACGGAAGGTCTAGCACA	-	561nt	In *kek4* transcribed region, for verifying homozygous *kek4* nulls
kek4intgenR	AATCTACTTGACATGCGCCG	-		Within *kek4* gene span, for verifying homozygous *kek4* nulls
k4-EC-TM-EcoRI	CGCG-GAATTC-TTGCAAATAAGTGTGCTGGC	EcoRI	Kek4 juxtamembrane domain towards N terminus	Chimaera cloning
		kek5		
kek5CDSattB5'Fw	GGGGACAAGTTTGTAC AAA AAA GCA GGC T AG CTA GAC GCA GAC TTA GAG (cca cag cca gcg **atg**)	-	2825nt (35nt+CDS, no STOP)	Gateway cloning, sequencing
kek5CDSattB3'Rv	GGGGACCAC TTT GTA CAA GAA AGC TGG GTA GAC CTC GGT GCC ATC CTC GC	-		
kek5seqFwd1	GCGCAACGTGATCATCAACA	-		*kek5* sequencing primer
kek5seqFwd2	AAGCGGCCATTGCAGCAGTA	-		*kek5* sequencing primer
kek5seqFwd3	GGTCAATCCAGTCGAGAAGC	-		*kek5* sequencing primer

kek5seqFwd4	ACCACCACCAGCAGCAACAA	-		*kek5* sequencing primer
kek5seqFwd5	GCAACAGCAGTTGCAACAAC	-		*kek5* sequencing primer
kek5seqRev1	GTGGTTCGCAATCCCAAGTT	-		*kek5* sequencing primer
kek5seqRev2	TTGGTGCCGTAGATGCCGTG	-		*kek5* sequencing primer
kek5seqRev3	GGTGGTGTCCTTTTGATAGG	-		*kek5* sequencing primer
kek5seqRev4	GAAGTTCTCCGATGGCACCT	-		*kek5* sequencing primer
kek5seqRev5	TGGATGGTGCAGTTGCGCAA	-		*kek5* sequencing primer
K5-EC-TM-BamHI	CTAT-GGATCC-GCTCATCATGGTGGTGTCCT	BamHI	Kek5 juxtamembrane domain towards N terminus	Chimaera cloning
		kek6		
kek6 5'end Fwd	GGGGACAAGTTTGTAC AAA AAA GCA GGC TCA **ATG** CAT CGC AGC ATG GAT C	-	2508nt (CDS, no STOP)	Gateway cloning, sequencing
kek6 3'end Rev	GGGGACCAC TTT GTA CAA GAA AGC TGG GTA GAG CGA CAC GAA CTC GCC AG	-		
kek6seqFwd1	GTTTCCTATTCTGCCCCATC	-		*kek6* sequencing primer
kek6seqFwd2	CATCGCCTCGGATAAGCTGT	-		*kek6* sequencing primer
kek6seqFwd3	GAAGCATGTTGGTGCAGCAG	-		*kek6* sequencing primer
kek6seqFwd4	ATACAGCAGCAGCAGCACCA	-		*kek6* sequencing primer
kek6seqRev1	TTGCTGTTGCAGCTGCTGGT	-		*kek6* sequencing primer
kek6seqRev2	TGCAACCTGTTGCTGTTGCG	-		*kek6* sequencing primer
kek6seqRev3	TACTCCACAGCTTATCCGAG	-		*kek6* sequencing primer
kek6seqRev4	CTAGGCGCTTGAGGGGATTT	-		*kek6* sequencing primer
kek6FRT GP Fwd	GCAGCATATGCTCCAAGCTG	-	100nt with WH-WH- 2sid LI F	Null verification, ~100nt upstream of *pBac[RB]kek6[e00907]*
kek6FRT GP Rev	CACAGTGACAGAATCCAAAC	-	100nt with WH-WH- 2sid RI F	Null verification, ~100nt downstream of *pBac[WH]kek6[f05733]*
kek6intgenF	GCCTGGACTGTTGCAGATGA	-	513nt	In *kek6* CDS, for verifying homozygous *kek6* nulls
kek6intgenR	GTTGAGGAACTCCAGCAGAT	-		In *kek6* CDS, for verifying homozygous *kek6* nulls
k6-EC-TM-BamHI	GTAT-GAATTC-ACGCCGGCCTTGTTGGCATG	BamHI	Kek6 juxtamembrane domain towards N terminus	Chimaera cloning
		lbk		
LbkCDS5'endFwd	GGGGACAAGTTTGTAC AAA AAA GCA GGC TCA **ATG** CAC GTT TCA GCC ATA A	-	3756nt (CDS, no STOP)	Gateway cloning

LbkCDS3'endRev	GGGGACCAC TTT GTA CAA GAA AGC TGG GTA AAT GTC CAC TGT TGT GCA CT	-		
lbk551ntattBFwd	GGGGACAAGTTTGTAC AAA AAA GCA GGC T AG AAA CTA CGC ATG AGC CTG	-	551nt (fragment of CDS with Gateway sequences)	*In situ*
lbk551ntattBRev	GGGGACCAC TTT GTA CAA GAA AGC TGG GT A CCG CTC AAA TGT CCA CTG T	-		
		CG15744		
CG15744 5kbinFwd	GGGGACAAGTTTGTAC AAA AAA GCA GGC T GG ATT GGA TAG CCT TGG TGA	-	569nt (fragment of CDS)	*In situ*
CG15744 5kbinRev	GGGGACCAC TTT GTA CAA GAA AGC TGG GT T TCG CTT CCA TCT CCA TCT C	-		
		CG16974		
16974Fwd548nt	GGGGACAAGTTTGTAC AAA AAA GCA GGC T TA TAT GAA TCC CGA AGG CGC	-	548nt (fragment of CDS with Gateway sequences)	*In situ*
16974Rev548nt	GGGGACCAC TTT GTA CAA GAA AGC TGG GT T TGG GGG GAG TAG ATG GTA A	-		
		FRT mutagenesis		
WH-WH- 2sid LI R	TCCAAGCGGCGACTGAGATG	-		Null verification, 2-sided primers (Parks et al. 2004)
WH-WH- 2sid RI F	CCTCGATATACAGACCGATAAAAC	-		Null verification, 2-sided primers (Parks et al. 2004)
WH-RB+ hyb	TGCATTTGCCTTTCGCCTTAT	-		Null verification, hybrid primers (Parks et al. 2004)
RB+WH- hyb	GACGCATGATTATCTTTTACGTGAC	-		Null verification, hybrid primers (Parks et al. 2004)
		Toll6		
Tl6-EcoRI-IC	CATG-GAATTC-AACTTCTGCTACAAGTCACC	EcoRI	Toll6 juxtamembrane domain towards C terminus	Chimaera cloning
Tl6-BamHI-IC	CATG-GGATCC-AACTTCTGCTACAAGTCACC	BamHI	Toll6 juxtamembrane domain towards C terminus	Chimaera cloning
Toll6attB2RevTag	GGGGACCAC TTT GTA CAA GAA AGC TGG GT C CGC CCA CAG GTT CTT CTG CT			Chimaera cloning
		Other primers		
UASSeqFor	AAAGTAACCAGCAACCAAGT		Upstream of MCS in UAS element	Colony PCR, Gateway cloning
pAct5.1B4MCSFwd	TTCCGGATTATTCATACCGTC		Upstream of MCS in actin promoter	Colony PCR, Gateway cloning

Sequences internal to gene coding sequences are underlined; start codons are in bold. Reading frames are denoted by spaced codons (lower case letters in parentheses are used to show sequences downstream of primers up to the start codon where appropriate). Gateway sequences are marked in orange, restriction enzyme sites are marked in blue. CDS, coding sequence; MCS, multiple cloning site; UAS, upstream activating sequence.

Table 2.4 **Cloning constructs**

Construct	Abbreviated name	Antibiotic	Inserts	mRNA/Insert size	Source	Comments
		Kek1		**3595**		
pOT2-SD01674		Chloramphenicol	*kek1* cDNA SD01674 into *pOT2*	3618	BDGP	For *in situ*
pDONR-kek1	*pDONR+kek1*	Kanamycin	Full length *kek1* CDS from clone SD01674. No stop codon. In frame with Gateway sequences for subsequent cloning	2443	This work	Entry clone
pAct5C-kek1-mCFP	*pAWC+kek1*	Ampicillin	Full length *kek1* CDS, N-terminal Actin promoter, C-terminal mCFP; attB sites		This work	For cell culture
pAct5C-kek1-FLAG	*pAWF+kek1*	Ampicillin	Full length *kek1*, N-terminal Actin promoter, C-terminal FLAG; attB sites	(*kek1* + attB = 2480)	This work	For cell culture
pUAS-kek1-mRFP	*pTWR+kek1*	Ampicillin	Full length *kek1*, N-terminal UAS promoter, C-terminal mRFP; attB sites		This work	For fly transgenesis
		Kek2		**4318**		
pNB40-NB7		Ampicillin	*kek2* cDNA NB7 into *pNB40*	~4200	Musacchio & Perrimon, 1996	For *in situ*
pDONR-kek2	*pDONR+kek2*	Kanamycin	Full length *kek2* CDS from clone NB7. No stop codon. In frame with Gateway sequences for subsequent cloning	2682	This work	Entry clone
pAct5C-kek2-mCFP	*pAWC+kek2*	Ampicillin	Full length *kek2* CDS, N-terminal Actin promoter, C-terminal mCFP; attB sites		This work	For cell culture
pAct5C-kek2-FLAG	*pAWF+kek2*	Ampicillin	Full length *kek2* CDS, N-terminal Actin promoter, C-terminal FLAG; attB sites	(*kek2* + attB = 2719)	This work	For cell culture
pUAS-kek2-mRFP	*pTWR+kek2*	Ampicillin	Full length *kek2* CDS, N-terminal UAS promoter, C-terminal mRFP; attB sites		This work	For fly transgenesis
		Kek3		**4361**		
pDONR-kek3	*pDONR+kek3*	Kanamycin	Full length *kek3* CDS from GH cDNA library. No stop codon. In frame with Gateway sequences for subsequent cloning	3069	This work	Entry clone For *in situ*
pAct5C-kek3-mCFP	*pAWC+kek3*	Ampicillin	Full length *kek3* CDS, N-terminal Actin promoter, C-terminal mCFP; attB sites		This work	For cell culture
pAct5C-kek3-FLAG	*pAWF+kek3*	Ampicillin	Full length *kek3* CDS, N-terminal Actin promoter, C-terminal FLAG; attB sites	(*kek3* + attB = 3106)	This work	For cell culture
pUAS-kek3-mRFP	*pTWR+kek3*	Ampicillin	Full length *kek3* CDS, N-terminal UAS promoter, C-terminal mRFP; attB sites		This work	For fly transgenesis

pDONR-kek3ECD+TM≡ Toll6ICD	*pDONR+kek3≡ Toll6*	Kanamycin	Kek3 ICD + TM domain fused to Toll6 ICD. In frame with Gateway sequences		This work	Entry clone, EcoRI link between *kek* and *toll6*
pAct5c-kek3ECD+TM≡ Toll6ICD-3HA	*pAWH+kek3≡Toll6*	Ampicillin	Kek3 ICD + TM domain fused to Toll6 ICD, N-terminal Actin promoter, C-terminal 3xHA tag; attB sites	(*kek3* EC: 1392) (*toll6* IC: 1260)	This work	For cell culture, luciferase assay
		Kek4		**2497**		
pOT2-GH27420		Chloramphenicol	*kek4* cDNA GH27420 into *pOT2*	1737	BDGP	For *in situ*
pDONR-kek4	*pDONR+kek4*	Kanamycin	Full length *kek4* CDS from larvae/pupae RT-PCR. No stop codon. In frame with Gateway sequences for subsequent cloning	1977	This work	Entry clone
pAct5C-kek4-mCFP	*pAWC+kek4*	Ampicillin	Full length *kek4* CDS, N-terminal Actin promoter, C-terminal mCFP; attB sites		This work	For cell culture
pAct5C-kek4-FLAG	*pAWF+kek4*	Ampicillin	Full length *kek4* CDS, N-terminal Actin promoter, C-terminal FLAG; attB sites	(*kek4* + attB = 2014)	This work	For cell culture
pUAS-kek4-mRFP	*pTWR+kek4*	Ampicillin	Full length *kek4* CDS, N-terminal UAS promoter, C-terminal mRFP; attB sites		This work	For fly transgenesis
pDONR-kek4ECD+TM≡ Toll6ICD	*pDONR+kek4≡ Toll6*	Kanamycin	Kek4 ICD + TM domain fused to Toll6 ICD. In frame with Gateway sequences		This work	Entry clone, EcoRI link between *kek* and *toll6*
pAct5c-kek4ECD+TM≡ Toll6ICD-3HA	*pAWH+kek4≡Toll6*	Ampicillin	Kek4 ICD + TM domain fused to Toll6 ICD, N-terminal Actin promoter, C-terminal 3xHA tag; attB sites	(*kek4* EC: 1290) (*toll6* IC: 1260)	This work	For cell culture, luciferase assay
		Kek5		**4357**		
pDONR-kek5	*pDONR+kek5*	Kanamycin	Full length *kek5* CDS from LD cDNA library. No stop codon. In frame with Gateway sequences for subsequent cloning	2825	This work	Entry clone
pAct5C-kek5-mCFP	*pAWC+kek5*	Ampicillin	Full length *kek5* CDS, N-terminal Actin promoter, C-terminal mCFP; attB sites	(*kek5* + attB = 2860)	This work	For cell culture
pAct5C-kek5-FLAG	*pAWF+kek5*	Ampicillin	Full length *kek5* CDS, N-terminal Actin promoter, C-terminal FLAG; attB sites		This work	For cell culture
pUAS-kek5-mRFP	*pTWR+kek5*	Ampicillin	Full length *kek5* CDS, N-terminal UAS promoter, C-terminal mRFP; attB sites		This work	For fly transgenesis
pDONR-kek5ECD+TM≡Toll6ICD	*pDONR+kek5≡ Toll6*	Kanamycin	Kek5 ICD + TM domain fused to Toll6 ICD. In frame with Gateway sequences	(*kek5* EC: 1302) (*toll6* IC: 1260)	This work	Entry clone, BamHI link between *kek* and *toll6*
pAct5c-kek5ECD+TM≡ Toll6ICD-3HA	*pAWH+kek5≡Toll6*	Ampicillin	Kek5 ICD + TM domain fused to Toll6 ICD, N-terminal Actin promoter, C-terminal 3xHA tag; attB sites		This work	For cell culture, luciferase assay

		Kek6		**2511**		
pDONR-kek6	*pDONR+kek6*	Kanamycin	Full length *kek6* CDS from GH cDNA library. No stop codon. In frame with Gateway sequences for subsequent cloning	2508	This work	Entry clone For *in situ*
pAct5C-kek6-mCFP	*pAWC+kek6*	Ampicillin	Full length *kek6* CDS, N-terminal Actin promoter, C-terminal mCFP; attB sites	(*kek6* + attB = 2545)	This work	For cell culture
pAct5C-kek6-FLAG	*pAWF+kek6*	Ampicillin	Full length *kek6* CDS, N-terminal Actin promoter, C-terminal FLAG; attB sites		This work	For cell culture
pUAS-kek6-mRFP	*pTWR+kek6*	Ampicillin	Full length *kek6* CDS, N-terminal UAS promoter, C-terminal mRFP; attB sites		This work	For fly transgenesis
pDONR-kek6ECD+TM≡Toll6ICD	*pDONR+kek6≡ Toll6*	Kanamycin	Kek6 ICD + TM domain fused to Toll6 ICD. In frame with Gateway sequences	(*kek6* EC: 1284) (*toll6* IC: 1260)	This work	Entry clone, BamHI link between *kek* and *toll6*
pAct5c-kek6ECD+TM≡ Toll6ICD-3HA	*pAWH+kek6≡Toll6*	Ampicillin	Kek6 ICD + TM domain fused to Toll6 ICD, N-terminal Actin promoter, C-terminal 3xHA tag; attB sites		This work	For cell culture, luciferase assay
		Wengen		**2403**		
pFLC-I-RE29502		Ampicillin	*Wg* cDNA RE29502 into *pFLC-I*	2425	BDGP	Already in the lab
		Lambik		**4423**		
pDONR-lbk 551nt		Kanamycin	551nt *lbk* fragment from library into *pDONR* by Gateway cloning	551	This work	For *in situ*
		Rickets		**5407**		
pCR2.1-TOPO-DLGR2		Ampicillin, Kanamycin	*Rk* cDNA into pCR2.1-TOPO	5399	Eriksen *et al.*, 2000	For *in situ*
		CG15744		**5952**		
pDONR-CG15744 569nt		Kanamycin	569bp fragment of *CG15744* from cDNA library into *pDONR* by Gateway cloning	569	This work	For *in situ*
		CG16974		**4340**		
pDONR-CG16974 548nt		Kanamycin	548nt fragment of *CG16974* from cDNA library into *pDONR* by Gateway cloning	548	This work	For *in situ*
		DNTs				
pAct5c-DNT1 (Pro-TEV-6H-V5-CK+CTD)		Ampicillin	DNT1 CysKnot, Prodomain and 3′ tail, V5 and 6xHis tags, N terminal Actin promoter		G. McIlroy	For cell culture
pAct5c-DNT2 (Pro-TEV-6H-V5-CK)		Ampicillin	DNT2 CysKnot and Prodomain, V5 and 6xHis tags, N terminal Actin promoter		G. McIlroy	For cell culture
pAct-renilla luciferase			Renilla luciferase, N terminal Actin promoter		S. Brogna	For cell culture

2.2.2 Cloning summary

kek1–6 coding sequences were amplified from cDNA clones (*kek1*, *SD01674*; *kek2*, *NB7*), LD cDNA library (*kek5*), GH cDNA library (*kek3*; *kek6*) or reverse transcription PCR (*kek4*). These sources were used so that the amplified fragments were uninterrupted *kek* exons only. Primers used incorporated flanking *attB* sites for use in Gateway cloning. *kek* CDS-containing entry clones were further recombined into one of three destination clones: *pAct5c-attR-mCFP* (*pAWC*), *pAct5c-attR-FLAG* (*pAWF*) or *pUASt-attR-mRFP* (*pTWR*). Details of each procedure in the cloning process are given below. Details of primers used and restriction digest verification of *kek* CDS cloning are given in Chapter 4.

Protein domains of Kek3–6 and Toll6 were predicted using ProSite (ExPASy), PFAM, SMART, TMHMM (http://www.cbs.dtu.dk/services/TMHMM/) and TMPred (ExPASy) algorithms and PubMed data (Table 2.5; Figure 2.9); longest possible predicted peptide regions were assumed. Primers were designed to amplify the sequences that encode the extracellular and transmembrane domains of Kek3–6 and the intracellular domain of Toll6. A unique enzyme site (BamHI or EcoRI) was introduced 3′ to the *kek* sequence and 5′ to the *toll6* sequence during PCR. Purified fragments were digested at these unique sites and ligated. In addition, attB sites were introduced during PCR to the 5′ and 3′ ends of ligated fragments for Gateway cloning into *pDONR*^{221} and the actin promoter-driven construct *pAct5c-attR-3xHA* (*pAWH*; see cloning strategy, Appendix II). Encoded chimaeric proteins were designed to fuse 15 amino acids C-terminal to the Kek transmembrane region, halfway between the Toll6 transmembrane region and the Toll/Interleukin-1 receptor (TIR) domain. Full details of primers used and restriction digest verification of *kek≡toll6* chimaeras are given in Chapter 4.

2.2.3 PCR

DNA was amplified from genomic DNA, cDNA clones or cDNA libraries (see above) by PCR. Diagnostic PCRs used Taq DNA polymerase (Invitrogen); 50µl master mixes (5µl 10X

Figure 2.9 **Protein sequences of Kek3, Kek4, Kek5, Kek6 and Toll6**

Protein domains were estimated using prediction algorithms (see Table 2.5). Cysteine-rich regions are marked in green; LRRs in yellow; Ig domains in blue; transmembrane domains in red and the Toll6 TIR domain in grey. The position of chimaera fusion between Kek extracellular and transmembrane domains and the Toll6 intracellular domain is noted by [xxxx]. Peptides used for the generation of custom antibodies to Kek3, Kek4 and Kek6 are indicated.

Kek3

Anti-Kek3 peptide

MAAGRAAATLEAPGPPSGQDIASDNSAQRRTLATKVRRKGPRPQRRLHPPLRPRLPLHLHLLLWLLCCCSQLGQL
RAECPAVCECKWKSGKESVLCLNANLTHIPQPLDAGTQLLDLSGNEIQLIPDDSFATAQLLNLQKVYLARCHLRL
IERHAFRKLINLVELDLSQNLLSAIPSLALYHVSELRELRLSGNPILRVPDDAFGHVPQLVKLELSDCRLSHIAV
RAFAGLESSLEWLKLDGNRLSEVRSGTITSLASLHGLELARNTWNCSCSLRPLRAWMLQQNIPSGIPPTCESPPR
LSGRAWDKLDVDDFACVPQIVATDTTAHGVEGRNITMSCYVEGVPQPAVKWLLKNRLIANLSAGGDGDSDSEPRT
AAATQGRKTYVVNMLRNASNLTILTADMQDAGIYTCAAENKAGKVEASVTLAVSRRPPEAPWGVRIILLGAVAAL
LLVGGSSFAAICLCSLQRRRKLRLWNSVP[xxxx]PVRRSESYEKIEMTARTRPDLGGGASCGGGSATGAGLFHD
AEEQGYLRAAHTPLNDNDAGQAAAIVNPSAGSAQRRNGDYLHVSTHCDDEEEDQQLHHHPQQQPASQHHPHPNQQ
QHQQRKGSQGHVVSASGANNSAPLEETDLHIPRLIDIGGTDSASSSISSQVDAAARLAGYAGHTWKTTPIATTKI
NSPHSKPVTSAAPSSLNTQATPYAHYGNHPADEMATSVFCSEGQESDLFDSNYPDLLDIAKYAVAQAQQEGRGQG
YAQATTTPNGGLCTLPRKLKTSGKYFRNSSDSQSPLLADNSSKYGSSTLGDGSFLNEAMGLGRRYSAESSYANYS
STATYTGGGQRANSFLNLVQSGAHQGKLLPSHLGQKPSLPSSPVQHQRSLSSAATPLLDFSALASRAAGAANTSV
AAYDYHAAQLERFLEEYRNLQDQLCKMKETCDTIRKKETPLRVAIGQSAAQLADPVMYSAASHSPKPPATSNLKT
KTLLPGQPPDPPPYWLHRNAMLKRLNGDGSAGTNGSGGSPASPQPRQDIFKS

Kek4

Anti-Kek4 peptide

MAIKLSFDPCSISLKHLSLFLFKIYCLALIFRSASADWLLDCGNCHCKWNSGKKTADCRNLSLSGVPEYLSPEVQ
VLDLSHNHIFYLEENAFLTTHLQNLQKLLIRNGTLKYLNQRSFTQLQILIELDLSNNLLVDLLPNVFDCLSKVRA
IFLNGNLLQALRHGVFRNLKYLHKIELKRNRLVSIDAKAFVGVPLLSQIYLDNNELTKLRVESFQDLTKLTALSL
VENPWNCTCDLQMFRDFVIGMNLYTPPTSCHYPLQLRGRLWIEDQPEAFACKPKIVYPTLSTSINTSKENVTLIC
RVHGSPNTVIAWDYTNQVYESRSKPVKSLQKQRIYIELLREDESKIRKFGHDVFVSRLTIVNARKSDEGVYTCLA
ENPGGKDSVHISVVVQKDMERISLIDSNFFAIVCLIAMGFLSMSILFSLVTCLIFKRFKQFHPGQHTYLQ[xxxx
]PTSLPVQSPGSEEATAISALSSGVIRESKIVLDPLSAINEPSNKNYTLFKTSNSNGSEYMHTRNYKDVRLNSNT
YTENLDNQAESISSRNRELYSNIAGDREKEELKQKDELDKDSRQSSLQSTGCSRKKGQIDELQPDLLPSTQPTAL
KNINETFGPSAKKAEVNPRSKYNTNVQKYLKEKYGSVRIKNISTKEPITGVDISI

Kek5

MMGNRTERSGRRLGMILLLLGVLVVLMALPPPTAGTTDWMQSCGTCHCQWNSGKKSADCKNKALTKIPQDMSNEM
QVLDFAHNQIPELRREEFLLAGLPNVHKIFLRNCTIQEVHREAFKGLHILIELDLSGNRIRELHPGTFAGLEKLR
NVIINNNEIEVLPNHLFVNLSFLSRIEFRNNRLRQVQLHVFAGTMALSAISLEQNRLSHLHKETFKDLQKLMHLS
LQGNAWNCSCELQDFRDFAISKRLYTPPTDCQEPPQLRGKLWSEVPSENFACRPRILGSVRSFIEANHDNISLPC
RIVGSPRPNVTWVYNKRPLQQYDPRVRVLTSVEQMPEQPSQVLTSELRIVGVRASDKGAYTCVADNRGGRAEAEF
QLLVSGDYAGAVSASDGMGMGAIGAPTIDPQTNMFLIICLIITTLLLLLLVAVLTLFWYCRRIKTYQKDTTMMS[
xxxx]GDGLISSKMDKTHNGSMLEGSVIMEMQKSLLNEVNPVEKPPRRTDIESVDGGDDVLEIKKTLLDDTVYVA
NHSRDEEAVSVAMSDTTTTPRSRHTYVDDAYANSLPPDLLAFPARVPPTSPSMQSSQSNIPDQVIYGIRSPPSLT
SPVYTHMTPHGIYGTKTMTAPHNGFMTLQHPKSRNLALIATTNSSRQHQHHHQLQQQQQHHHHHQQQQQQQQQQQ
HPLATTSPFLPAPVVYSPATGVVMKQGYMTIPRKPRAPSWAPSTSGAAGHGSIQLSEFQSPTSPNPSETGTATTA
ELQAEPVYDNLGLRTTAGGNSTLNLTKIAGSQGGAGQQYSMRDRPLPATPSLTSVSSATNASKIYEPIHELIQQQ
QQLQQQQQQQQQQRLGSMDTEPLYGVRQQGITILPGSSISGAGLGHAAYLSPGSGAAVSPSHASSSGDSPKAAKIP
PRPPPKPKKKMSVTTTRSGQGSTSQLFDDEGEDGTEV

Kek6

Anti-Kek6 peptide

MHRSMDRRRSRTPRTLPVCWILLCLVAWTVADDWSLSCASNCTCKWTNGKKSAICSSLQLTTIPNTLSTELQVLV
LNDNHIPYLNREEFSTLGLLNLQRIYLKKSEVQYIHKESFRNLKILVEIDLSDNKLEMLDKDTFMGNDRLRILYL
NGNPLKRLAAYQFPILPHLRTLDMHDCLISYIDPMSLANLNLLEFLNLKNNLLESLSEYVFQHMANLKTLSLEEN
PWQCNCKLRKFRGWYVNSRLSSVSLVCKGPPAQKDRTWDSVDDELFGCPPRVEIFNNEEVQNIDIGSNTTFSCLV
YGDPLPEVAWELNGKILDNDNVLFESESIASDKLWSNLTVFNVTSLDAGTYACTGSNSIGSMTQNISIYLSEIVQ
HVLEKTPETFWYFGLIMGIFGTVFLLISISFVVCLCKRTTRQHRHANKAGV[xxxx]SSVSFNDQEKKLLDSSVT
TTTNDRGDSYGIDNQPTSIGMNKGDSAGMGFNQIEIHAVESHRHGSMLVQQQPQQQQVAGGGGMRQQLMQVKDST
CGMMSVPTSMAGHAHSHPAQISEEFPLNVGVFPPPPEFCSNIVPNPAFGGNIFIRVSVTQDMLDGADLNMYPDLL
NIPKRMQDVQESGAGAVAVPEGQFATLPRHTARRGILKKDTSLQQQQQQHQQQHQHQQQQQQQQIQQQQHQQLQQ
QHQPSGLYTHDEIVTYNLEASGYDPHQSGYHSNAMELPPPPPPPAVTAVVQCHHPSPNNCASCINNAPPPPSACQ
SPPVEVTPMRPLDSSAYPKYDNMGRRITASGGLGGSNLSLHDEERYENETLFGQAESQTKGMPEQSQDLHQPQEV
TQGQDKGGGPGEFVSL

Toll6

MIYYMLLILPVVLAQDQQHTTESLSTKHHQQQQLSHSNAIMGEAGVSNSQLMQPSTPARTLRPLTAGAGGDPSLY
DAPDDCHFMPAAGLDQPEIALTCNLRTVNSEFDTTNFSVIPAEHTIALHILCNDEIMAKSRLEAQSFAHLVRLQQ
LSIQYCKLGRLGRQVLDGLEQLRNLTLRTHNILWPALNFEIEADAFSVTRRLERLDLSSNNIWSLPDNIFCTLSE
LSALNMSENRLQDVNELGFRDRSKEPTNGSTESTSTTESAKKSSSSSTSCSLDLEYLDVSHNDFVVLPANGFGTL
RRLRVLSVNNNGISMIADKALSGLKNLQILNLSSNKIVALPTELFAEQAKIIQEVYLQNNSISVLNPQLFSNLDQ
LQALDLSMNQITSTWIDKNTFVGLIRLVLLNLSHNKLTKLEPEIFSDLYTLQILNLRHNQLENIAADTFAPMNNL
HTLLLSHNKLKYLDAYALNGLYVLSLLSLDNNALIGVHPDAFRNCSALQDLNLNGNQLKTVPLALRNMRHLRTVD
LGENMITVMEDSAFKGLGNLYGLRLIGNYLENITMHTFRDLPNLQILNLARNRIAVVEPGAFEMTSSIQAVRLDG
NELNDINGLFSNMPSLLWLNISDNRLESFDYGHVPSTLQWLDLHKNRLSSLSNRFGLDSELKLQTLDVSFNQLQR
IGPSSIPNSIELLFLNDNLITTVDPDTFMHKTNLTRVDLYANQITTLDIKSLRILPVWEHRALPEFYIGGNPFTC
DCNIDWLQKINHITSRQYPRIMDLETIYCKLLNNRERAYIPLIEAEPKHFLCTYKTHCFAVCHCCEFDACDCEMT
CPTNCTCFHDQTWSTNIVECSGAAYSEMPRRVPMDTSELYIDGNNFVELAGHSFLGRKNLAVLYANNSNVAHIYN
TTFSGLKRLLILHLEDNHIISLEGNEFHNLENLRELYLQSNKIASIANGSFQMLRKLEVLRLDGNRLMHFEVWQL
SANPYLVEISLADNQWSCECGYLARFRNYLGQSSEKIIDASRVSCIYNNATSVLREKNGTKCTLRDGVAHYMHTN
EIEGLLPLLLVATCAFVAFFGLIFGLFCYRHELKIWAHSTNCLM[xxxx]NFCYKSPRFVDQLDKERPNDAYFAY
SLQDEHFVNQILAQTLENDIGYRLCLHYRDVNINAYITDALIEAAESAKQFVLVLSKNFLYNEWSRFEYKSALHE
LVKRRKRVVFILYGDLPQRDIDMDMRHYLRTSTCIEWDDKKFWQKLRLALPLPNGRGNNNKRVVSGCLSGRTPSV
NMYATSHEYQAGNGGVIPPPSARYADCGSNNYATINECAAAGGGRGYKPIPTSASAAAAACKFNTMNQLSKKQQR
DLSVAGMAKTLEHQHHHNHQANRRSQHEYAVPSYLPSAAPAYDSVDYAKQQIRNNANCECVNLGTAKRAAGKNPA
SGLPSSFSSNFVPPGGASYNCKKSCSCIGDDELLCSCGGGGGIGVNLLESGTQSSVTMSSSSNNSRQPELTHYES
NLSLNDDEDEDHDQQKNLWA

Table 2.5 **Estimated protein domain spans for chimaera cloning**

Tool Used	LRR span	Ig span	Transmembrane span
Kek3			
Prosite	111-132 209-230 161-182 234-255 185-206	318-427	
PFAM	136-180 184-232	318-428	
SMART	78-114 183-206 113-132 207-230 135-158 233-255 159-182 267-317	330-418	
PubMed	267-316	319-428	
TMHMM			No region with probability of 1; two possible peaks ~450-480 and ~500-520
TMPred			441-466
Kek4			
Prosite	73-94 171-192 123-145 195-216	278-387	
PFAM	194-232	279-390	
SMART	72-94 169-192 121-144 193-216 145-168 228-277	291-380	404-426
PubMed	228-277	296-387	
TMHMM			404-426
TMPred			404-430
Kek5			
Prosite		279-380	
PFAM	74-121 125-175 254-278	279-379	
SMART	98-121 170-193 122-145 196-217 146-169 229-278	291-369	13-35 411-433
PubMed	64-229? 229-277	296-376	
TMHMM			411-433
TMPred			410-434
Kek6			
Prosite	70-91 168-189 120-141 192-213 144-165 216-237	275-367	
PFAM	116-165 167-210	277-370	
SMART	37-73 166-189 69-91 190-213 94-117 225-274 118–141	289-360	385-407

PubMed	225-274	295-367	
TMHMM			385-407
TMPred			390-411 388-411
SignalP			388-411
Toll6			
Prosite	201-222 544-565 225-246 568-589 278-299 592-613 302-323 615-635 326-347 637-658 351-372 662-683 375-396 684-705 401-422 708-728 425-446 860-881 449-470 908-929 497-519 932-953 520-541 956-977	1111-1247	
PFAM	200-243? 496-542? 278-300 544-586? 302-345? 591-632? 352-396? 636-683? 401-423 683-728? 424-470 931-980?	1115-1243	
SMART	145-168 495-517 199-222 518-541 223-246 542-565 279-299 566-589 300-323 613-633 324-347 638-657 353-372 662-683 373-398 684-705 399-422 825-863 423-446 906-929 447-470 930-953 471-494 954-977	1112-1247	1055-1077
PubMed	278-465 401-649 862-990?	1114-1247	
TMHMM			1055-1077
TMPred			1058-1079 1443-1469

Amino acid positions of LRRs, Ig and transmembrane domains are shown

PCR buffer (200mM Tris-HCl pH8.4, 500mM KCl; Invitrogen), 1.5µl 50mM MgCl (Invitrogen), 0.5µl Taq DNA polymerase) were divided into 5x10µl reaction volumes. For *kek* CDS and *kek≡toll6* chimaera cloning, Phusion High-Fidelity DNA polymerase (NEB) was used; 50µl reaction volumes (10µl 5X HF buffer (NEB), 0.5µl Phusion polymerase). For all PCR reaction mixtures, 1µl 10mM dNTP mix (Roche), 4pmol forward and reverse primers, 1µl DNA template were used. A PTC-200 thermal cycler (MJ Research) or myCycler thermal cycler (BioRad) were used to run the following PCR cycle for null mutagenesis verification:

95^0C 1'30	(x1 cycle)
95^0C 45" → 55^0C 30" → 72^0C 1'30	(x35 cycles)
72^0C 10'	(x1 cycle)
4^0C ∞	

Primers used for null verification are listed in Figures 5.2 and 5.4.

Phusion polymerase PCR program:

98^0C 2'	(x1 cycle)
98^0C 30" → T_m-3^0C 30" → 72^0C 30"/kb	(x35 cycles)
72^0C 15'	(x1 cycle)
4^0C ∞	

where T_m is the melting temperature of the primers

Primers used for *kek* CDS amplification are marked in cloning maps, Appendix II. Primers for *kek≡toll6* chimaera amplification are listed in chimaera cloning strategy, Appendix II.

2.2.4 Reverse Transcription-PCR

kek4 CDS was amplified from larval and pupal RNA by RT-PCR. 10 *yw* larvae and 10 *yw* pupae were frozen in liquid nitrogen and homogenized. RNA was extracted using the RNeasy Mini Kit (Qiagen) as per kit instructions. Genomic DNA was removed using TurboDNase

(Ambion) as per kit instructions. *kek4* cDNA was synthesized from purified ssRNA using Superscript II reverse transcriptase (Invitrogen) and primer *kek4CDSattB3'Rv*. *kek4* CDS was amplified from cDNA by Phusion PCR using primers *kek4CDSattB5'Fw* and *kek4CDSattB3'Rv* as per section 2.2.3.

2.2.5 Gel electrophoresis and DNA purification

DNA fragments and Phusion DNA polymerase products were run at 60V on 0.8% agarose (Bioline) gels in 1X TAE buffer with ethidium bromide (Sigma) for DNA detection. DNA was labelled using DNA loading buffer and compared with 5ng/µl 1kb DNA ladder (NEB) run in outside lanes. Gels were photographed under UV light using a G:BOX Chemi gel dock (Syngene). *kek* CDS and *toll6* DNA fragments were excised from gels under UV and purified using the QIAquick Gel Extraction kit (Qiagen) as per kit instructions for 'gel extraction'.

2.2.6 DNA ligation

Purified *kek3–6* and *toll6* DNA fragments were digested using EcoRI (*kek3*, *kek4*, *kek6* and *toll6*) or BamHI (*kek5* and *toll6*). Digested fragments were purified using the QIAquick Gel Extraction kit (Qiagen) as per instructions for 'PCR clean up'. Digested fragments were ligated at 18^0C using 1µl T4 DNA ligase (NEB), 2µl 10X T4 DNA Ligase Buffer (NEB) and ddH_2O up to 20µl. Ligated fragments were subsequently cloned into *pDONR*^{221} by Gateway cloning.

2.2.7 Gateway cloning

kek overexpression and *kek≡toll6* constructs were generated by Gateway (Invitrogen) cloning. Gateway cloning involves the enzyme-mediated recombination of gene-flanking *attB* sites with entry clone attP sites. The kanamycin-resistant *pDONR*^{221} entry vector contains *attP* sites that flank a chloramphenicol resistance gene and the lethal DNA gyrase gene *ccdB*. Successful Gateway cloning using BP clonase II (Invitrogen) exchanges the

chloramphenicol–ccdB cassette for the gene of interest; thus, only successful clones will grow on kanamycin-containing media following bacterial transformation. Fusion of *attB* and *attP* sites forms a *pDONR*^{221} construct containing the gene of interest, flanked by *attL* sites. Entry clones can subsequently by recombined into destination vectors that contain a range of promoters and encode terminal tags. Recombination of *attL* sites with *attR* sites in ampicillin-resistant destination vectors by LR clonase II (Invitrogen) exchanges a second lethal cassette for the gene of interest; thus, only successful clones will grow on ampicillin-containing media following bacterial transformation. BP and LR reactions were done following Invitrogen instructions. C terminal tag vectors were selected to minimise disruption to gene function by tag insertion into the intracellular Kek domain, which has no known functional domains.

For use in cell culture, *kek* overexpression constructs were cloned from entry vectors into *pAWC*, which contained an N-terminal actin promoter and encoded C-terminal monomeric CFP tag, and *pAWF*, which encoded an N-terminal FLAG tag. *kek≡toll6* chimaeras were cloned from entry vectors into *pAWH*, which encoded an N-terminal HA tag in each reading frame. For transgenesis, *kek* overexpression constructs were cloned from entry vectors into *pTWR*, which contained a *UAS* promoter and encoded a C-terminal monomeric RFP tag. At each stage, cloning was verified by restriction digests (see Chapter 4). Successfully cloned *kek1–6+pTWR* constructs were sent to BestGene, Inc. for transgenesis.

2.2.8 Transformation of *E. coli* and DNA amplification

All cloning constructs and template clones used for RNA probe synthesis were transformed into chemically competent DH5α or DH10β (small constructs; Invitrogen) or One Shot OmniMAX (large constructs; Invitrogen) *E. coli* cells prior to amplification. 1µl plasmid DNA was added to 25µl cells on ice for 30 minutes (for cDNA clones received from the DGRC, 25µl cells were added to pre-hydrated Whatman FTA clone discs). Cells were heat shocked at 42^{0}C for 30 seconds in a water bath, cooled and grown for at least 1 hour at 37^{0}C

with shaking (225rpm) in SOC media. Transformed media was spread on to LB agar plates with antibiotic and grown overnight at 37^0C.

Individual *E. coli* colonies were picked from plates and grown overnight in 2ml of LB media with antibiotic. DNA was harvested by miniprep boiling protocol: 1.5ml overnight media was pelleted at 13k rpm for <1 minute and supernatant discarded. Resuspended pellets were boiled at 100^0C for 1 minute in 350µl pH8 STET buffer and 30µl 5mg/ml lysozyme solution (Sigma), cooled and centrifuged for 20 minutes. Pellets contained *E. coli* cell debris and were removed using a sterile pipette tip. DNA in the supernatant was precipitated with 5M ammonium acetate and 2 volumes isopropanol, frozen for ≥30 minutes, and pelleted by 15 minute centrifugation. Washed DNA pellets were resuspended in TE. Miniprep DNA was tested by restriction digests. Colonies containing a successful clone were amplified by inoculating 100ml fresh LB+antibiotic media with 100µl of the corresponding single colony overnight miniprep culture, and growing overnight at 37^0C with shaking (225rpm). DNA was harvested from large scale cultures using a PureLink HiPure Plasmid Filter Maxiprep Kit (Invitrogen) as per kit instructions.

2.2.9 DNA sequencing

kek1–6+pAWC and *kek3–6≡toll6* constructs were sequenced. In each case, if the destination construct sequence was correct, the entry clone from which other constructs were generated was therefore assumed to be correct also. For each reaction, ≥500ng clone DNA was mixed with 3pmol primer and ddH_2O and sequenced by the Genomics Facility, School of Biosciences, University of Birmingham. Full inserts (*kek* CDS or *kek≡toll6* chimaera CDS) were sequenced. Sequencing primers were spaced 500nt apart and each nucleotide was verified by 2–3 overlapping sequences. Sequencing reaction data were aligned using the Kalign tool (European Bioinformatics Institute) against predicted sequence data obtained from FlyBase. No mutations were detected in *kek* CDS or *kek≡toll6* inserts.

2.3 Cell culture

2.3.1 S2 cell culture

S2 cells (gift from Saverio Brogna, University of Birmingham) were maintained at 27^0C in Insect-Xpress medium (Lonza)+penicillin/streptomycin/L-glutamine mix (Lonza) and 10% foetal bovine serum (Lonza). S2 cells stably transfected with *drosomycin-luciferase* (gift of Lynne Prince; Weber et al. (2003)) were grown in identical conditions, with media further supplemented with 1µg/ml puromycin (Invitrogen). 1ml suspended cells were passaged every two days into 4ml fresh medium. 6-well plate experiments required $3x10^6$ cells seeded per 2ml media, 24 hours prior to transfection. Per well of experiment, 250µl serum-free media, 3µl TransIT-2020 (Mirus), and 2µg DNA (*kek1–6+pAWC*) or 2µg (*kek3–6≡toll6+pAWH*) plus 1µg (*pAct-renilla-luciferase*) were incubated at room temperature for 30 minutes, supplemented with 350µl serum-free media and added to aspirated cells. After 4 hours, transfection mixture was removed and 2ml supplemented medium added. All experiments were conducted 48 hours after transfection; imaging of Kek or Kek≡Toll6 distribution required 6h serum starvation prior to antibody labelling.

2.3.2 Luciferase reporter assay

S2 cells stably transfected with *drosomycin-luciferas*e and transiently transfected with chimaeric constructs and *pAct-renilla-luciferase* were stimulated with DNT protein and Dif signalling quantified by luminescence. *pAct-renilla* was a gift from Saverio Brogna, University of Birmingham, and used as an internal control for transfection efficiency. DNT ligand (6 wells of S2 cell culture-produced DNT1/2 per 6-well plate experiment; 50nM Baculovirus DNT2 per well) was added 48 hours after transfection and luminescence quantified 24 hours after DNT stimulation. Transfected and stimulated cells were pelleted from single wells, resuspended in 400µl media and separated into three 50µl aliquots in an opaque 96-well plate. 40µl of Firefly Luciferase Substrate (Dual-Glo Luciferase Assay

System; Promega) was added per 50µl aliquot. Luminescence was measured after 10 minutes of incubation at room temperature using a Mithras LB 940 Multimode Microplate Reader (Berthold). 40µl Stop & Glo substrate (Dual-Glo Luciferase Assay System; Promega) was added to halt Dif signalling and to activate Renilla Luciferase. Renilla luminescence data was used to normalize Firefly Luciferase data.

2.4 Protein expression and purification

DNT1 and DNT2 were expressed in S2 cells transfected with V5-tagged *pAct5c-DNT1/DNT2* constructs generated by Graham McIlroy (University of Birmingham; see constructs in Table 2.4), and purified from conditioned medium according to Arnot et al. (2010) (see below). Baculovirus DNT2 was produced by Graham McIlroy and Jukka Aurikko (University of Cambridge).

2.4.1 DNT purification

S2 cell-produced His-tagged DNT was generated in 6 well plates and purified 48 hours after transfection. 12ml supernatant was harvested by centrifugation and filtered through a 0.2µm Acrodisc (Pall) filter. Two rounds of centrifugation at 4^0C and 5,000g were required to buffer exchange filtered supernatant to chilled PBS+20mM imidazole using a Vivaspin6 500MWCO Concentrator (Sartorius). Supernatant was concentrated to 400µl. Concentrated supernatant was purified using NiNTA spin columns (Qiagen) according to kit protocol. Purified protein in 500mM imidazole was subsequently further buffer exchanged to PBS without imidazole by further concentration at 5,000g. V5-tagged DNT1 and DNT2 were detected by dot blot: 10µl of each protein were blotted on to nitrocellulose membrane, blocked in 5% milk powder in TBS+0.05% Tween20 (Sigma), labelled using anti-V5 and peroxidase-labelled anti-mouse, and developed using SuperSignal West Pico Chemiluminescent Substrate (Thermo; Table 2.6). Dot blots were photographed using a G:BOX Chemi dock (Syngene; Figure 4.4).

Table 2.6 **Antibodies**

Antibody	Dilution	Donor	Source		Use
Primary antibodies					
Anti-GFP	1:1000	Rabbit	Molecular probes	A11122	Embryonic expression profiles, S2 cell protein distribution
Anti-βgal	1:5000	Rabbit	Cappel		Embryonic expression profiles, Axon guidance
Anti-dsRed	1:100	Rabbit	Clonteck	632496	Embryonic/larval expression profiles
Anti-HA	1:200	Mouse	Roche	11583816001	S2 cell protein distribution
Anti-V5	1:5000	Mouse	Invitrogen	46-0705	Dot blot, Western
Anti-Broad	1:100	Mouse	Dshb	25E9.D7	Ecdysone signalling
Anti-FasII ID4	1:5	Mouse	Hybridoma Bank	ID4	Axon guidance
Anti-Kek3 ASDN	1:100	Guinea Pig	Davids Biotechnologie		Kek3 protein distribution
Anti-Kek4 DCG	1:50	Guinea Pig	Davids Biotechnologie		Kek4 protein distribution
Anti-Kek6 HRS	1:1	Guinea Pig	Davids Biotechnologie		Kek6 protein distribution
Anti-HB9	1:1000	Rabbit	Gift of H T Broihier		Motor neuron marker
Anti-DIG-AP	1:1000	Sheep	Boehringer Mannheim		In situ hybridisation
Anti-DIG-POD	1:500	Sheep	Roche	11207733910	In situ hybridisation
Secondary antibodies					
Biotinylated anti-guinea pig	1:300	Donkey	Jackson	706-066-148	Immunohistochemistry
Biotinylated anti-rabbit	1:300	Goat	Vector	BA-1000	Embryonic expression profiles, Axon guidance
Biotinylated anti-mouse	1:300	Horse	Vector	BA-2000	Axon guidance
Peroxidase-labelled anti-mouse	1:1000	Horse	Vector	PI-2000	Dot blot, Western
Alexa488 anti-rabbit	1:250	Goat	Molecular Probes	A11034	Immunohistochemistry, Immunocytochemistry
Alexa647 anti-rabbit	1:250	Goat	Molecular Probes	A21245	Immunohistochemistry
Alexa488 anti-mouse	1:250	Mouse	Molecular Probes	A11029	Immunohistochemistry, Immunocytochemistry
Alexa647 anti-mouse	1:250	Donkey	Molecular Probes	A31571	Immunohistochemistry
Streptavidin488	1:250		Molecular Probes	S11223	Immunohistochemistry

2.4.2 SDS-PAGE and Western blot

Purified protein was boiled for 5 minutes in 4% SDS loading buffer (Maniatis et al., 1982), chilling on ice, then centrifuged for 3 minutes. Samples were run through a 5% stacking gel (5% acrylamide (Fisher), 0.1% ammonium persulfate (National Diagnostics), 0.1% TEMED (Sigma), 125 mM Tris pH6.8, 0.1% SDS) and a 12% resolving gel (12% acrylamide, 0.1% ammonium persulfate, 0.04% TEMED, 375mM Tris pH8.8, 0.1% SDS) at 100V for ~90 minutes in a mini-PROTEAN 3 system (BioRad). Molecular weights were determined using the Prestained Protein Marker, Broad Range (NEB).

Proteins were transferred to a nitrocellulose membrane at 30V, 4°C for 1 hour using an Xcell SureLock Mini-Cell at 30V for 1 hour. blocked for 1 hour in 5% non-fat milk powder in 0.05% PBTween and incubated in primary antibody overnight at 4°C. Membranes were washed in in PBTween, incubated in secondary antibody in blocking solution for 2 hours at room temperature, then washed again. Luminescence was detected by a G:BOX Chemi (Syngene) and Genesnap software after incubation with SuperSignal West Pico (Thermo) kit, as per kit instructions.

2.5 Immunochemistry

2.5.1 Fixation

S2 cells used to detect Kek distribution were transfected on sterile coverslips; 48 hours post-transfection, medium was aspirated and coverslips were removed to separate small Petri dishes. Coverslips were washed with PBS+0.1% Tween20 and fixed for 15 minutes with 4% formaldehyde in a humid chamber. Fixed cells were washed and blocked in 4% BSA (Sigma) prior to immunolabelling.

Embryos were collected overnight (17 hours, 25^0C) on grape juice agar plates. Collected embryos were dechorionated in 1:5 bleach solution and washed carefully prior to fixation. For

antibody labelling, dechorionated embryos were immediately added to a pre-mixed solution of 300µl 37% formaldehyde, 2700µl PBS, 3ml heptane, and fixed for 20 minutes at room temperature with rolling. For *in situ* hybridisation, dechorionated embryos were immediately added to a pre-mixed solution of 3ml 4% paraformaldehyde, 3ml heptane, and fixed for 20 minutes at room temperature with rolling. Embryos were washed in methanol, and excess vitelline membrane removed by vortexing.

L3 instar larvae were collected and stored in PBS on ice. Larval brains were dissected in PBS and fixed immediately in 4% formaldehyde in PEM during a 20 minute dissection window. Formaldehyde was then refreshed and samples fixed for a further 50 minutes, with rolling. Larval brains were washed in PBS with 0.3% Triton-X-100 and blocked in 10% normal goat serum (Vector labs) for 1 hour prior to storage or immunolabelling.

2.5.2 Immunolabelling

Antibodies used in this work are summarised in Table 2.6. Custom antibodies were raised against Kek3, Kek4 and Kek6 peptides. Unique peptide sequences from each protein were chosen in the N-terminal region to avoid labelling of repetitive, common domain sequences. Peptide selection was validated and approved, and antibodies purified from guinea pig polyclonal serum, by Davids Biotechnologie (Germany). Peptides chosen were: ASDNSAQRRTLATKVRRK (Kek3), DCGNCHCKWNSGKKTADC (Kek4) and HRSMDRRRSRTPRTLPVC (Kek6). These peptide sequences are highlighted in Figure 2.9 (black brackets). Anti-Kek6 antibodies were validated by comparing immunolabelling in *yw* and $kek6^{34}/Df(kek6)$ mutants (see Chapter 6).

Antibody labelling was detected by HRP or fluorescence. Blocked S2 cells were washed with PBS+0.1% Tween20 and 60µl primary antibody was added per coverslip; coverslips were incubated overnight in a humid chamber, at 4^0C with rocking. Coverslips were washed with PBS+0.1% Tween20 in 6 well plates and further stained with fluorescent secondary

antibodies, in a humid chamber, for 2 hours at room temperature in the dark. Washed coverslips were inverted and mounted on microscope slides using Vectashield with DAPI (Vector Labs).

Fixed embryos were incubated overnight in primary antibody dilution, at 4^0C with rocking. Stained embryos were washed for 1 hour in PBS+0.1% Triton-X-100. The correct secondary antibody dilution was added and embryos incubated for 2 hours at room temperature with rocking (in darkness for fluorescent secondary antibodies). Embryos were washed for a further 1 hour in PBS+0.1% Triton-X-100. Samples for fluorescence microscopy were mounted in Vectashield mounting medium (Vector Labs). Larval stains were conducted as per embryo stains but with PBS+0.3% Triton-X-100.

For antibody labelling detection by HRP, secondary antibody-labelled embryos were incubated at room temperature, 30 minutes, in 0.5% Vectastain ABC reagent solution (Vector Labs) in PBS+0.1% Triton-X-100. ABC reagent was removed and embryos washed for 1 hour. Embryos were aspirated in a clean 24-well plate and 300µl 0.7mg/ml SIGMAFAST 3,3′-diaminobenzidine (DAB) solution (Sigma) in PBS+0.1% Triton-X-100 was added. Labelling patterns were detected with 3% final concentration H_2O_2 solution (Sigma). Reactions were stopped with ≥1 hour washing in PBS+0.1% Triton-X-100 and embryos mounted in 70% glycerol. For double immunolabelling, the procedure was repeated and separate labels detected separately, with black HRP staining generated by addition of 5µl 8% $NiCl_2$ (Sigma) during H_2O_2 development.

2.5.3 Antisense RNA probe transcription

Antisense RNA probes were transcribed from linearised constructs as follows: *kek1* (*SD01674+pOT2* cDNA clone; linearised with EcoRI, transcribed with SP6 RNA polymerase); *kek2* (*NB7+pNB40*; HindIII; T7 RNA polymerase); *kek3* (*kek3* 558nt+*pDONR*^{221}; HpaI; T7); *kek4* (*GH27420+pOT2*; EcoRI; SP6); *kek6* (*kek6+pDONR*^{221};

HpaI; T7); *CG15744* (*CG15744* 569nt+*pDONR*^{221}; HpaI; T7); *CG16974* (*CG16974* 548nt+*pDONR*^{221}; HpaI; T7); *lambik* (*lbk* 551nt+*pDONR*^{221}; HpaI; T7); rickets (*DLGR2+pCR2.1-TOPO*; HindIII; T7); *wengen* (*RE29502+pFLC-I*; SacI; T3 RNA polymerase). Restriction enzymes linearised 10µg of construct 5′ relative to the cDNA. All digests at 37^{0}C. Linearised DNA was verified by agarose gel electrophoresis compared to uncut plasmid. To purify linearised DNA, 50µl phenol (Sigma), 49µl chloroform (Fisher) and 1µl isoamyl alcohol (Fisher) were added to 50µl linearised DNA, samples centrifuged for 5 minutes and the aqueous layer precipitated in 5µl 3M sodium acetate and 3 volumes ethanol. Samples were stored at -80^{0}C for ≥30 minutes, DNA pelleted at 13k rpm for 10 minutes, washed in 70% ethanol and stored at -20^{0}C in 20µl ddH_2O+DEPC. Transcription reactions were conducted as follows: 1µg linearised template DNA, 2µl DIG RNA labelling mix (Roche), 2µl suitable RNA polymerase (see above), 2µl 20X transcription buffer (specific to polymerase); 1µl Recombinant RNasin Ribonuclease Inhibitor (Promega) in ddH_2O+DEPC up to 20µl total volume; 2 hour incubation time at 37^{0}C. Transcription reactions were stopped with 1µl DNase (RNase-free; NEB), incubated for 15 minutes 37^{0}C and all enzymatic activity terminated by heat shock at 65^{0}C for 15 minutes. Probes were precipitated in 2.5µl 4M LiCl (Fisher) plus 75µl ethanol and stored at -80^{0}C for ≥30 minutes. Probes were pelleted by 15 minutes centrifugation, washed with 70% ethanol in ddH_2O+DEPC, dried and stored at -20^{0}C in 50µl ddH_2O+DEPC with 1µl Recombinant RNasin Ribonuclease Inhibitor.

2.5.4 *In situ* hybridisation

In situ hybridisation of antisense RNA probes was used in embryos to determine mRNA expression patterns of putative receptor genes.

Day one of *in situ* hybridisation protocol: Fixed embryos were warmed slowly to room temperature and rehydrated by washing in 50% methanol:50% PBS+0.1% Tween20 for 15 minutes, then for 15 minutes in PBS+0.1% Tween20. Washed samples were fixed again in

4% paraformaldehyde for 20 minutes with rolling and washed again in PBS+0.1% Tween20. Embryos were digested for 90 seconds in 125ng/ml RNase-free Proteinase K (Sigma) in PBS+0.1% Tween20. Digestion was halted by washing twice with 0.2% glycine (Fisher) in PBS+0.1% Tween20 and twice with PBS+0.1% Tween20. Samples were fixed for a third time in 4% paraformaldehyde for 30 minutes and washed for 30 minutes in PBS+0.1% Tween20. Hybridisation buffer was prepared by mixing 5ml formamide (MP Biomedicals), 2.5ml 20X SSC, 100µl 10% Tween20 in PBS, 10µl heparin (50mg/ml stock; Sigma) and 2.3ml ddH_2O+DEPC and stored in a water bath at 55^0C. Fixed and washed samples were gently warmed to 55^0C by washing in 50% PBS+0.1% Tween20:50% hybridisation buffer for 10 minutes at room temperature and 10 minutes at 55^0C in the water bath. 100µl salmon testes ssDNA (10mg/ml stock; Sigma) was denatured for 10 minutes at 95^0C, cooled on ice+methanol and added to the hybridisation buffer at 55^0C (Complete hybridisation buffer). Warmed embryos were incubated in complete hybridisation buffer for 3 hours at 55^0C. Antisense DIG-labelled RNA probe was denatured at 95^0C for 10 minutes, cooled on ice+methanol for 10 minutes and added to samples at 1:20, 1:40 and 1:100 titrations in complete hybridisation buffer. Hybridisation mixtures were left overnight at 55^0C.

Day two of *in situ* hybridisation protocol: A 1:1000 dilution of alkaline-phosphatase (AP)-conjugated anti-DIG in PBS+0.1% Tween20 was pre-absorbed with paraformaldehyde-fixed embryos for ≥1 hour at room temperature on a windmill mixer. Meanwhile, at 55^0C, embryos were washed for 20 minutes in complete hybridisation buffer, 20 minutes in 50% PBS+0.1% Tween20:50% complete hybridisation buffer, and 5 x 20 minutes in PBS+0.1% Tween20. After the final wash, embryos were slowly cooled to room temperature. Washed embryos were incubated with rocking for 1 hour at room temperature in 1:100 pre-absorbed AP-conjugated anti-DIG. Incubated samples were washed with PBS+0.1% Tween20 for 1 hour 20 minutes and 3 x 5 minutes in staining solution (250µl 4M NaCl, 500µl 1M MgCl2, 1ml 1M Tris-HCl pH9.5 and 100µl 10% Tween20 in PBS, made up to 10 ml total volume with

ddH_2O+DEPC). Samples were developed in the dark in a 24-well plate in 500µl volume of staining solution supplemented with 2.25µl NBT (100mg/ml) and 1.75µl BCIP (50mg/ml). Development was halted by washing with PBS+0.1% Tween20 and samples stored in 70% glycerol at 4^0C prior to mounting.

2.5.5 Fluorescent *in situ* hybridisation

Fluorescent *in situ* hybridisation was used to detect *kek6* mRNA localization in the embryo. The protocol is adapted from that of A. Bustos (Benjamin Altenhein laboratory, Johannes Gutenberg University, Mainz, Germany, personal communication).

Day one: Fixed embryos were warmed slowly to room temperature and rehydrated by washing in 50% methanol:50% PBS+0.1% Triton-X-100 for 15 minutes, then 3 x 10 minutes in PBS+0.1% Triton-X-100 at room temperature. Embryos were next incubated at room temperature for 10 minutes in 50% PBS+0.1% Triton-X-100:50% hybridisation solution (5ml formamide, 2.5ml 20X SSC+DEPC, 2.5ml H_2O+DEPC, 50µl Tween20) and 10 minutes in hybridisation solution. 100µl salmon testes ssDNA (10mg/ml stock; Sigma) was denatured for 10 minutes at 95^0C, cooled on ice+methanol and added to the hybridisation solution (complete hybridisation solution) at 55^0C in a water bath. Embryos were incubated in complete hybridisation solution at 55^0C for 3 hours. Antisense DIG-labelled RNA probe was denatured at 95^0C for 10 minutes, cooled on ice+methanol for 10 minutes and added to samples at 1:20, 1:40 and 1:100 titrations in complete hybridisation solution. Hybridisation mixtures were left overnight at 55^0C.

Day two: Samples were washed in complete hybridisation solution for 30 minutes at 65^0C, 30 minutes in 50% complete hybridisation solution:50% PBS+0.1% Triton-X-100 at 65^0C and 4 x 20 minutes in PBS+0.1% Triton-X-100 at 65^0C. After the final wash, embryos were cooled slowly to room temperature. Embryos were blocked for 30 minutes in TNB buffer (0.1M Tris-HCl pH 7.5, 0.15M NaCl, 0.5% blocking reagent (TSA Fluorescein System; Perkin Elmer)).

Blocked embryos were incubated overnight at 4^0C with rocking in 1:500 POD-conjugated anti-DIG (Roche) in TNB buffer.

Day three: Samples were washed with PBS+0.1% Triton-X-100 for 1 hour and for 10 minutes with TNT buffer (0.1M Tris-HCl pH7.5, 0.15M NaCl, 0.05% Tween20). Tyramide Fluorescein (TSA Fluorescein System; Perkin Elmer) was pre-mixed 1:50 in amplification diluent and added to embryos (100µl per sample). Embryos were incubated for 10 minutes in the dark and amplification terminated by washing with TNT buffer.

2.6 Microscopy

Whole mount and dissected HRP-stained embryos (Gal4-driven expression patterns, anti-Kek6 labelling, ISNb axon guidance), adult wings, fluorescent anti-Broad stained fat bodies and anti-Kek4 stained ring glands were viewed using an Axioplan 2 (Zeiss) light microscope at 20x, 40x (differential interference contrast (DIC), oil) and/or 63x (DIC, oil) magnification using Nomarski optics. Images were captured using a JVC 3CCD camera and Image Grabber software (Neotech) or AxioCam HRc (Zeiss) camera and Zen2012 (Zeiss) software.

Fluorescent images of S2 cells (63x oil), anti-Kek4 stained larval ring glands (40x oil) and putative *kek3Gal4>UASmyrTOMATO* larval brains (20x oil) stained fluorescently with anti-dsRed were captured using a Leica SP2 AOBS inverted laser scanning confocal microscope. Fluorescent images of anti-Kek6-stained embryos (40x oil) were captured using a Leica SP2 upright laser scanning confocal microscope. Both microscopes are maintained by the Birmingham Advanced Light Microscope Facility (BALM, University of Birmingham). Images were captured at 200Hz, 1024x1024 pixel resolution and averaging of 3 slices. All images were processed in ImageJ (NIH), Photoshop (Adobe) and compiled using Illustrator (Adobe).

2.7 Phenotypic analysis

2.7.1 Axon guidance

Anti-FasII and HRP-stained late stage 17 embryos were filleted and imaged by light microscopy. Embryos with genotypes containing the *lacZ*-expressing enhancer trap *15A6* were further stained using anti-βgal and NiCl to separate homozygous and heterozygous progeny. Abdominal segments A1–A5 were scored on both sides of the embryo for ISNb motor nerve terminal misrouting, loss and fan phenotypes at muscles 6, 7, 12 and 13.

2.7.2 Locomotion

Locomotion phenotypes were detected according to protocols outlined in McIlroy et al. (2013) and Sutcliffe (2010). Larvae and adults were incubated at 25^0C in a 12 hour light/dark cycle (8am–8pm) and filmed between 10am and 12pm. Larvae were filmed crawling across a humid agar plate, and adult flies were filmed walking around the rim of a 46mm diameter Petri dish, using a Moticam 2000 camera (Motic) and Motic Images Plus 2.0 ML software. Dishes were placed on a LP812 light box (Jessops) to backlight the experimental setup. For larval recordings, the camera was clamped above the setup such that the dish perimeter was just outside the field of view; for adult recordings, the camera was positioned 95mm above the dish. Adult flies were anaesthetised and wings clipped using micro scissors; 1 hour of recovery time was permitted prior to filming. Videos were decompressed using VirtualDub software (www.virtualdub.org), and stacks of the first 400 continuous greyscale frames were compiled in ImageJ. Stacks were processed with the FlyTracker ImageJ plugin (Manuel Forero, Hidalgo laboratory; McIlroy et al. (2013)) to give trajectories and quantified speed, distance, resting and wobbling.

2.7.3 Developmental timing

To determine phenotypes in developmental timing caused by ring gland gene mutations, cages of *yw*, *kek4*^{20} x *kek4*^{23} and *spz6Gal4* x *UASkek4RFP* adults were incubated at 25^{0}C with a 12 hour light/dark cycle in cages closed with a grape juice agar plate. Grape juice plates were replaced at 9am, 10am and 2pm daily to stage embryo collections. Plates removed at 9am and 10am were discarded, whereas plates removed at 2pm were incubated overnight. After 24 hours incubation (12.30pm), 50 L1 larvae of each genotype were transferred to vials containing blue food. Food was prepared by pre-mixing 10ml Formula 4-24 Instant Medium, Blue (Carolina), 0.1g dried yeast and 20ml H_2O. Excess water was removed and food left to set at room temperature prior to larvae addition. Vials were incubated at 25^{0}C in an empty pipette tip box filled with 2cm water to create a humid microenvironment. At 4 hour intervals throughout the day, the number of L1/L2 instar larvae, wandering L3 instar (blue gut), wandering L3 instar (white gut), white puparia, brown pupae, black pupae and eclosed adults were scored until all flies were eclosed. Adult flies were removed upon eclosion to avoid miscounting a second generation of progeny. At each time point, cumulative percentage of larvae having passed an individual moult or developmental stage were calculated by deducting the percentage of larvae observed at all preceding stages from 100% (for example, if 80% of larvae are still at L1/L2 instar stage, and 10% are observed to be wandering L3 larvae with blue guts, only 10% will have reached at least the white gut wandering L3 stage).

2.7.4 Body growth assays

Wandering L3 larvae, brown pupae and eclosed adults of *yw*, *kek4*^{20} x *kek4*^{23} and *spz6Gal4* x *UASkek4RFP* crosses were collected and adhered to glass slides. All three genotypes were assembled on each slide. Slides were illuminated using a LP812 light box and photographed using a Moticam 2000 (Motic) camera or Pentax K-30 camera clamped above the slide. Body

lengths were measured using the ImageJ line tool, and body sizes measured using the ImageJ ROI manager tool.

Adult wings were cut from flies using microscissors and mounted in glycerol on glass slides. Wing hairs were photographed using an AxioCam HRc (Zeiss) camera and Zen2012 (Zeiss) software at 20x magnification with the anterior crossvein aligned vertically on the left of the image (see (Gidaszewski et al., 2009) as a guide to wing morphology). Wing hair number was scored manually in a 700x450 pixel region of interest between longitudinal veins L3 and L4 where the left side of the ROI connects the two veins. Each wing was counted three times and hair cell counts from the third count were used to maximise scoring proficiency.

2.8 Statistical analysis

Data was input to Excel (Microsoft) and analysed in SPSS Statistics 21 (IBM) and GraphPad Prism 6. Categorical data were tested using χ^2, and χ^2 with a Bonferroni correction for multiple comparisons. Distribution of continuous data with natural distribution was determined by kurtosis, skewness and Levene's Test for Homogeneity of Variance. Data were considered not normally distributed if absolute kurtosis and skewness values for each genotype were greater than 1.96 x standard error of kurtosis/skewness. Variance of the populations of different samples were considered unequal if Levene's test for homogeneity of variance gave a P value of <0.05. Means of parametric data were compared by One-Way ANOVA, unless data failed distribution or variance tests, in which case data were tested by Welch ANOVA. Multiple post hoc comparisons were compared using a Dunnett test (to compare all samples to a control), a Games-Howell test (to compare all samples to a control when a Welch ANOVA is required) or Student's t-test with Bonferroni correction (comparisons between samples). Non-parametric data were analysed using a Kruskal-Wallis test around the median and multiple comparisons were made using a post-hoc Dunn test. In all results, * indicates $P<0.05$, ** indicates $P<0.01$ and *** indicates $P<0.005$.

CHAPTER 3

CHARACTERISATION OF THE *DROSOPHILA* LIGs

3.1 INTRODUCTION

In this chapter, I investigated whether any of the nine *Drosophila* LIG proteins, as well as the non-LIGs *CG17839*, *rk* and *wgn*, could function as *Drosophila* neurotrophin (DNT) receptors according to three criteria.

First, candidate genes were screened for neuronal central nervous system (CNS) gene expression. *kek1*, *kek2* and *kek5* are expressed in the embryonic CNS (Evans et al., 2009, Musacchio and Perrimon, 1996). Furthermore, Kek2 protein has been detected at the larval neuromuscular junction (NMJ; Guan et al. (2005)). To determine the embryonic expression patterns of each candidate gene, I followed three strategies: (1) RNA probes that hybridise to the mRNA of the genes of interest were transcribed for *in situ* hybridisation; (2) for *kek3*, *kek5* and *CG17839*, Gal4 insertion lines were available. These were crossed to a *UASmyrTOMATO* (red fluorescent protein) reporter, and expression was visualized in fixed embryos by immunolabelling. (3) To detect protein distribution, custom antibodies were generated to immunolabel unique peptide sequences of Kek3, Kek4 (Chapter 7) and Kek6 (Chapter 6).

Second, candidate receptors were screened for genetic interaction with ligand mutants using the survival index (S.I.; see below)..

Third, interactions between the dLIGs and the DNTs were determined using adult locomotion as a behavioural readout. Behavioural output is essential for putting subcellular and cellular phenotypes into perspective: “Nothing in neurobiology makes sense except in the light of behaviour” (Guo et al., 2009, Heisenberg, 1997). Using locomotion, the aim was to select the receptor candidates with suggested DNT interactions and/or suggested behavioural roles.

The aim of the chapter was to select the most suitable receptor candidates in the context of DNT signalling and nervous system development for further study.

3.2 RESULTS

3.2.1 Candidate receptor expression profiles

The DNTs are expressed in the CNS and muscular targets (Sutcliffe et al., 2013, Zhu et al., 2008). Therefore, a putative receptor for the DNTs is anticipated to be expressed in cell types that could interact with the ligand expressing cells and thus receive the ligand. This could include cells that express both the ligands and the receptors.

3.2.1.1 dLIG expression profiles

Expression profiles of candidate genes were determined by *in situ* hybridisation using antisense RNA probes. Hybridisation region of probes is shown in Figure 2.8. The primary aim of profiling was to identify genes clearly expressed in the CNS, for further analysis. Consequently, sense probes were not used to validate expression profiles.

In situ hybridisation (Figure 3.1a) revealed that *CG15744* may have early embryonic stage signal in the CNS (Figure 3.1b). By stage 16, signal was also observed in the gut (Figure 3.1c). By stage 17, signal and background noise were difficult to distinguish (Figure 3.1d). Viewed ventrally, stage 14 embryos did reveal *CG15744* signal in the ventral nerve cord (VNC; Figure 3.1e). Signal was detected in midline cells in stage 13 embryos (Figure 3.1f, arrowhead). From stage 15, *CG15744* signal was detected throughout the VNC in the intra-longitudinal axonal tract space (Figure 3.1g–h). Pairs of *CG15744*$^{+}$ cells were observed adjacent to the midline in stage 16 embryos (Fig 3.1g, arrowheads). Stage 17 embryos expressed *CG15744* in many neurons ventral to the neuropil (Figure 3.1h, left image). In addition, no signal was detected in longitudinal or midline glia in filleted stage 17 embryos (Figure 3.1h, white neuropil). Cell types could not be verified throughout.

Figure 3.1 ***CG15744* is expressed in the CNS**

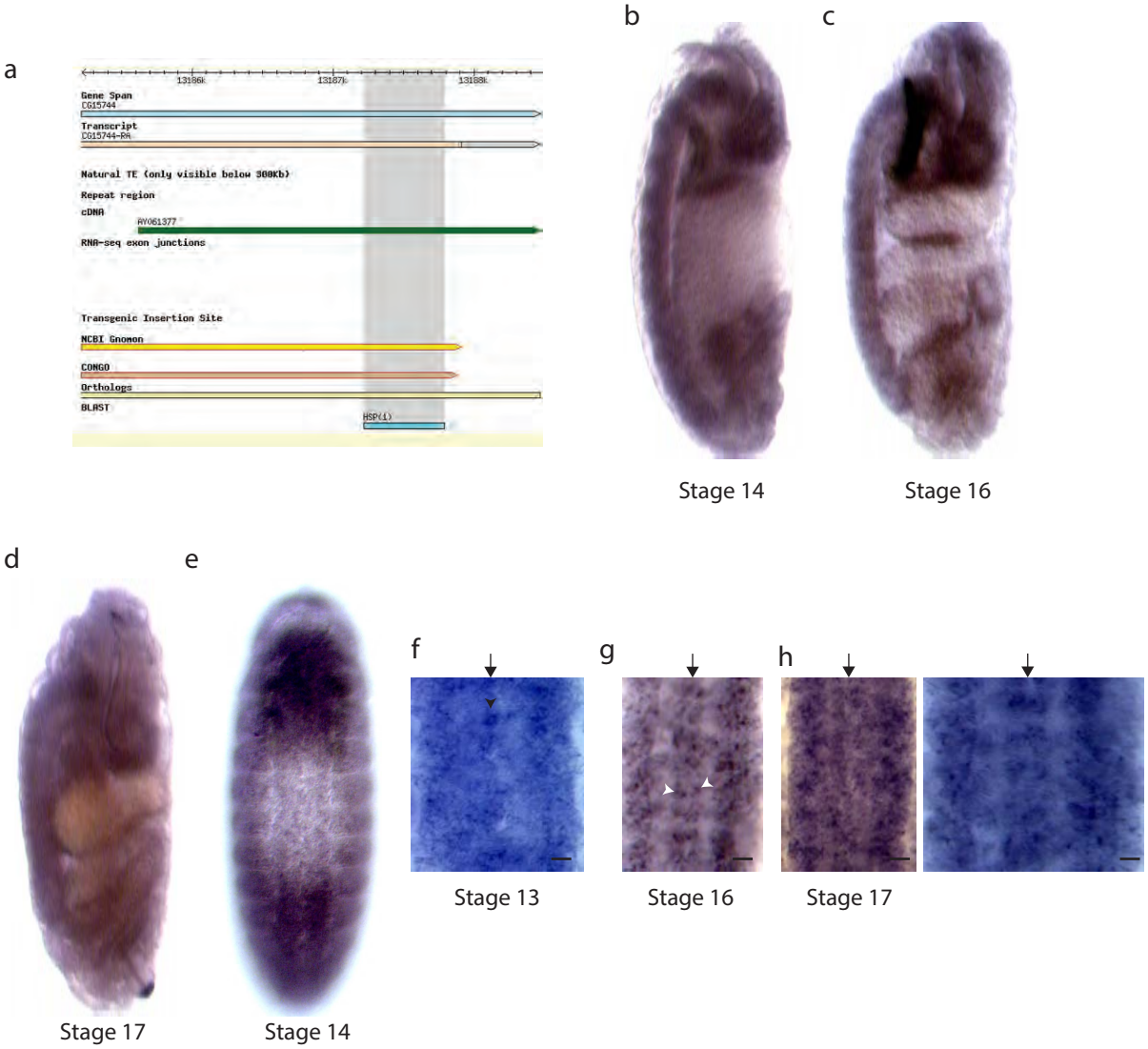

a | BLAST search of the sequence of an antisense *CG15744* RNA probe uncovers the exonic coding sequence of *CG15744*. **b-e** | Hybridisation of *CG15744* mRNA in the CNS od whole mount embryos. **f-h** | Dissected embryos reveal VNC signal including midline cells (black arrowhead) and cells immediately adjacent to the midline (white arrowhead). The embryonic midline is labelled with a black arrow. Scale bar, 10µm.

By contrast, *CG16974* and *lambik* formed an outlier group with markedly different expression profiles to the other dLIGs (Figures 3.2–3.3). *CG16974* signal was absent from the VNC throughout development (Figure 3.2b–d). Instead, *CG16974* was detected from stage 14 in the periphery of the embryo in cell clusters. These may represent the peripheral nervous system (PNS) or muscle (Figure 3.2e–h). *CG16974*$^{+}$ cell number in the periphery increased with development. Dissected embryos revealed *CG16974* is expressed in stripes at the intersegmental boundaries of stage 13 embryos (Figure 3.2i, arrowheads). These resembled the expression pattern of the border cell transcription factor *stripe* at muscle attachment sites, which is required for muscle development (Frommer et al., 1996). Lateral cell clusters that resemble central PNS clusters were *CG16974*$^{+}$ in stage 15 embryos (Figure 3.2j). Last, ventral muscle groups or muscle attachment sites adjacent to the VNC in stage 17 embryos were *CG16974*$^{+}$ (Figure 3.2k).

Lambik, similarly, was absent from the CNS in embryos, as determined by *in situ* hybridisation (Figure 3.3b–e). Instead, *lambik* transcript was enriched in the epidermis (Figure 3.3f–h). *Lambik* was first detected in the periphery by stage 13 (Figure 3.3f). In stage 14 embryos, *lambik* transcript formed two stripes of single cells or cell clusters along the length of the body (Figure 3.3g, boxed). These may be myoblast muscle precursors (Rau et al., 2001). *lambik*$^{+}$ cell number in the lateral flank of the embryo increased up to stage 17 (Figure 3.3h).

3.2.1.2 The *kek* genes are expressed in the CNS

Embryos of the lacZ-containing *P[1ArB]* transposon insertion line *15A6* (located at *33F1–2* on the second chromosome, adjacent to the *kek1* gene at *34A1*; Musacchio and Perrimon (1996)) were stained with anti-βgal and detected using HRP (Figure 3.4). In stage 12 embryos, *kek1* transcript was localised in discrete cells along the VNC (Figure 3.4a). By stage 16, strong expression was observed in the VNC and central brain (Figure 3.4b). In stage 17

Figure 3.2 ***CG16974* is expressed in the PNS**

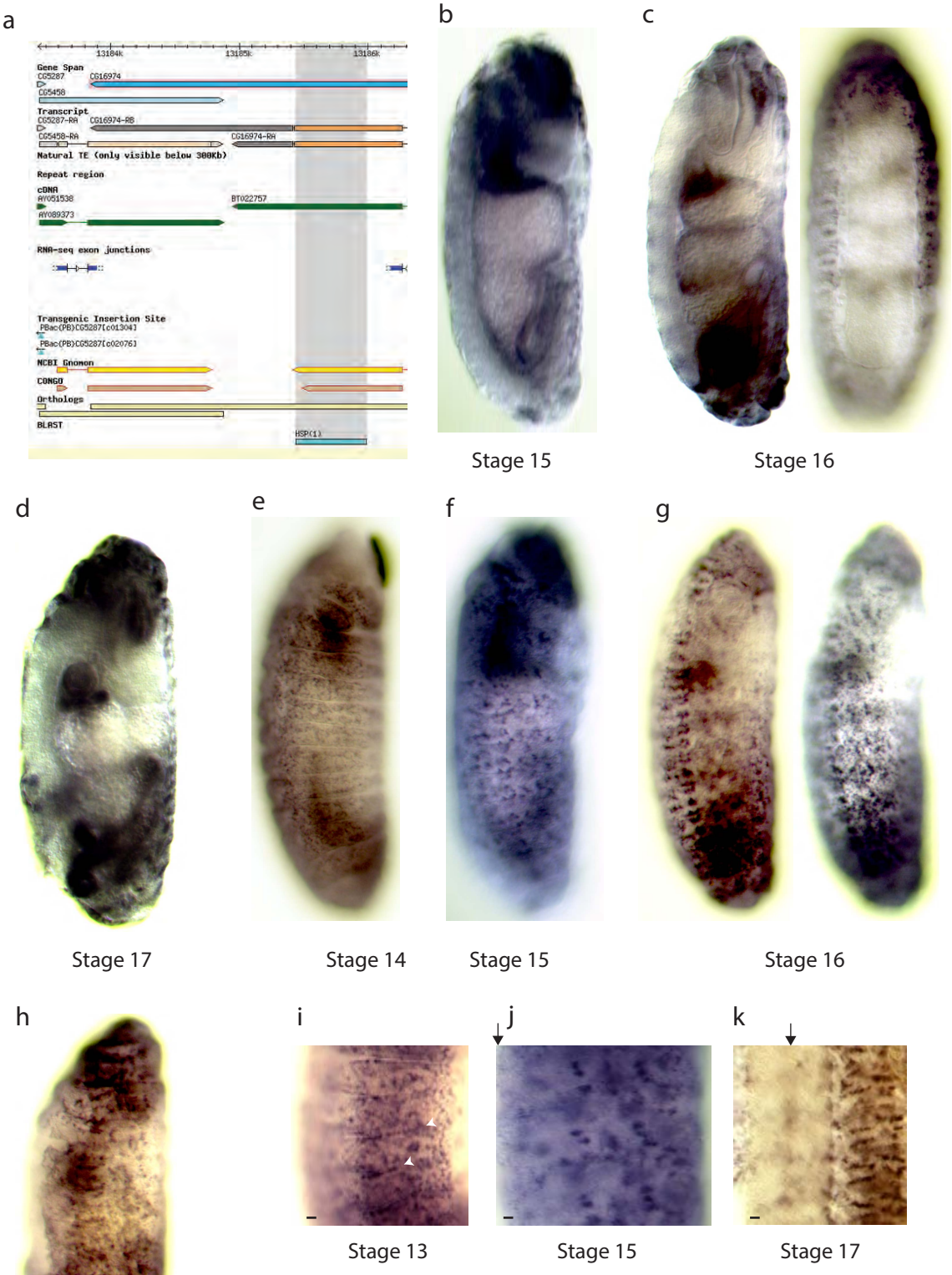

a | BLAST search of the antisense *CG16974* RNA probe sequence uncovers exonic coding sequence of the *CG16974* gene. **b-d** | *In situ* hybridisation reveals that *CG16974* transcript is not present in the embryonic CNS. **e-h** | *CG16974* mRNA is enriched in the epidermis in the periphery of the embryo. **i-k** | *CG16974* transcript was detected in stripes at the intersegmental boundaries of stage 13 embryos (**i**), lateral cell clusters of stage 15 embryos (**j**) and ventral muscle attachment sites (**k**). The embryonic midline is labelled with a black arrow. Scale bar, 10µm.

Figure 3.3 ***lambik* is expressed in the PNS**

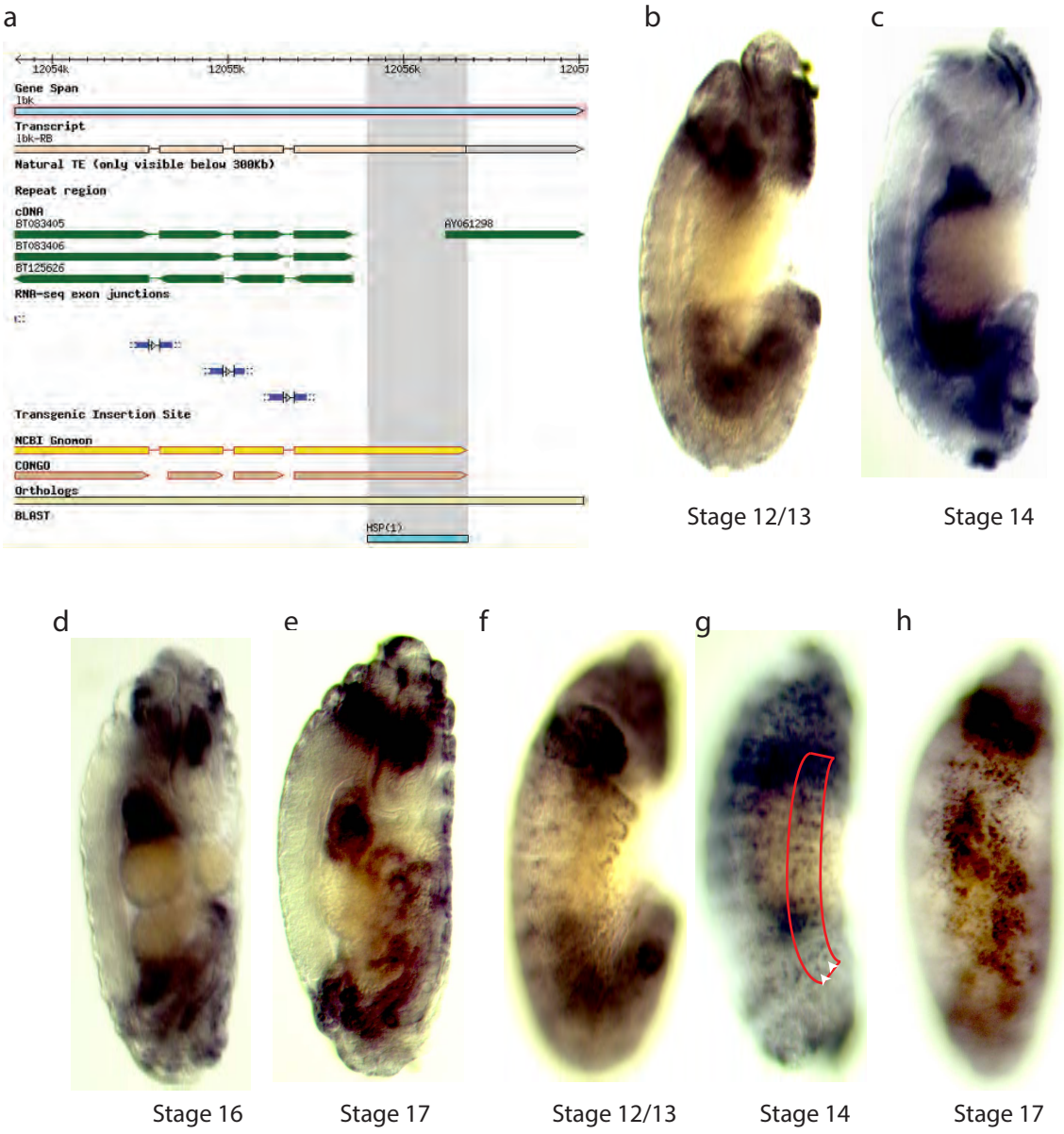

a | BLAST search of the antisense *lbk* RNA probe sequence uncovers exonic coding sequence of the *lbk* gene. **a-e** | *lbk* mRNA could not be detected in the CNS by *in situ* hybridisation. **f-h** | *lbk* mRNA was detected in the periphery, in epidermis, muscle or the PNS.

Figure 3.4 ***kek1* is expressed in the CNS**

15A6 lacZ transposon insertion line, stained with anti-βgal

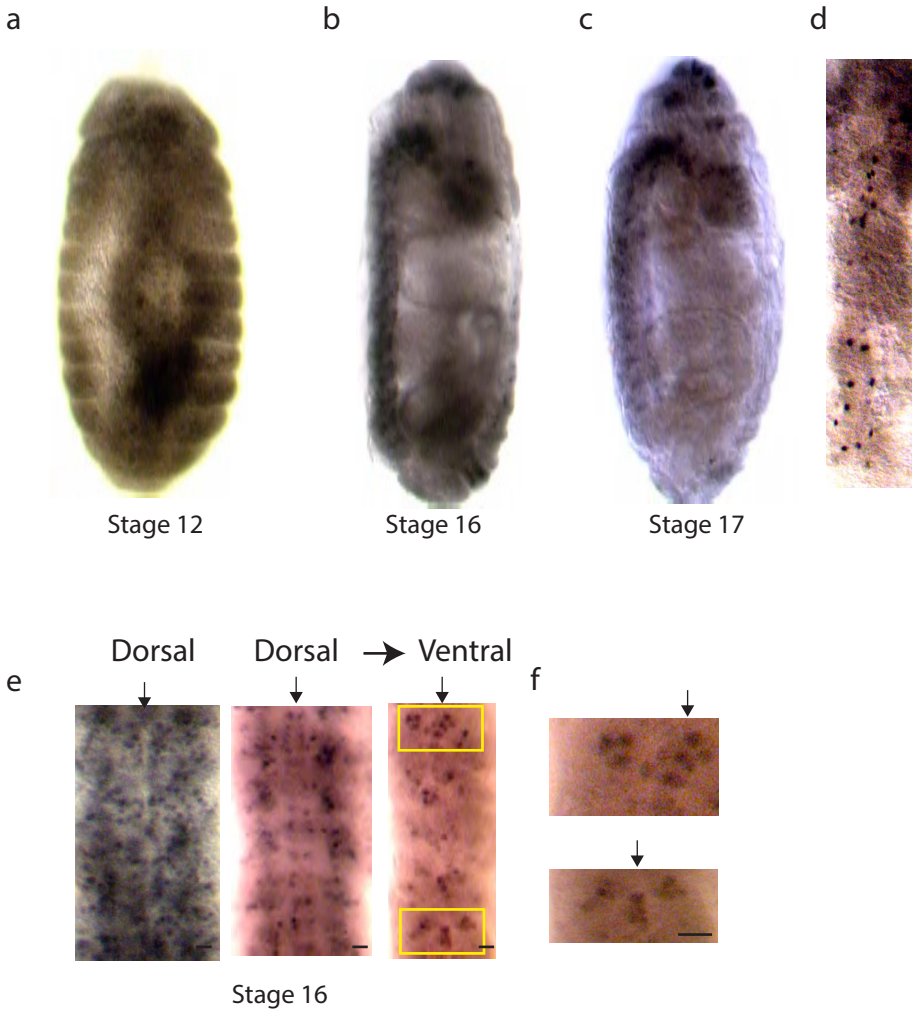

Embryos containing the lacZ reporter enhancer trap *15A6* (Musacchio and Perrimon, 1996) were labelled with anti-βgal and detected using HRP. **a-c** | *kek1* expression was detected within the ventral nerve cord from stage 12 to stage 17. **d** | Anti-βgal labels *kek1*$^{+}$ cells at the dorsal midline. **e-f** | Dorsal–ventral arranged whole mount VNC images and magnifications. The embryonic midline is labelled with a black arrow. Scale bar, 10μm.

embryos, signal remained exclusive to the CNS (Figure 3.4c), except for select cells along the dorsal midline (Figure 3.4d). These cells formed an elongated loop shape in the middle of the embryo, and may be cardioblasts or pericardial cells of the early *Drosophila* heart (Tao and Schulz, 2007). The VNC of whole mount embryos revealed *kek1*$^{+}$ cells either side of the neuropil and the midline (Figure 3.4e). In the dorsal VNC, signal was detected in a repeating four cell pattern either side of the midline (Figure 3.4e, middle). Ventral to this, signal was detected in cell clusters that overlay the midline and longitudinal tracts (Figure 3.4f, magnified view 3.4g).

In situ hybridisation using a full-length *kek1* antisense probe (Figure 3.5a) revealed signal in putative cardioblasts along the epidermal leading edge, on the dorsal flank of the germ band (Figure 3.5b). In the CNS, *kek1* transcript was strongly localized to the VNC by stage 14 (Figure 3.5c). Additional lateral signal was detected at stage 14 in the epidermis. From stage 15, *kek1* signal was strongly detected in the VNC and brain (Figure 3.5d–f). In stage 16 embryos, signal was further detected in discrete PNS clusters (Figure 3.5e,f). *kek1* transcript may also have been present in the Bolwig's organ, which is a cluster of photoreceptors (Figure 3.5e, arrowhead; Friedrich (2008)). In early embryos and eggs, *kek1* transcript was localized in dorsal stripes (Figure 3.5g).

kek1 signal was detected in the CNS from stage 12, in large cell bodies (Figure 3.5i). *kek1*$^{+}$ cell number increased by stage 13 (Figure 3.5k). By stage 14, VNC signal remained strongest in cells ventral to the longitudinal axon tracts (Figure 3.5k). By stage 15, *kek1*$^{+}$ signal ventral to the neuropil formed a distinct 'V' shape that resembles *HB9*$^{+}$ motor neuron staining (Figure 3.5l). Paired cells adjacent to the midline, one pair per hemisegment, also revealed *kek1* transcript signal (Figure 3.5l, arrowheads). By stage 16, *kek1* was detected in touching paired cell bodies immediately adjacent to the midline (Figure 3.5m, boxed). Signal was further detected in paired nuclei either side of the midline in stage 17 embryos (Figure 3.5n).

Figure 3.5 ***kek1* is expressed in the CNS and PNS**

a | Probe hybridisation confirmed by BLAST. **b–g** | *kek1* mRNA was detected in the embryonic CNS. Cardioblast signal was detected at stage 12. VNC expression was detected from stage 14. *kek1* mRNA was detected in the epidermis from stage 14, and the PNS from stage 16 (Bolwig's organ, arrowhead). **h** | *kek1* transcript is enriched in the dorsal pole of the early embryo. **i-n** | Dissected embryos reveal *kek1* trancript in the VNC (arrowheads, cells flanking the midline; box, paired cells adjacent to the midline). The embryonic midline is labelled with a black arrow. Scale bar, 10µm.

a

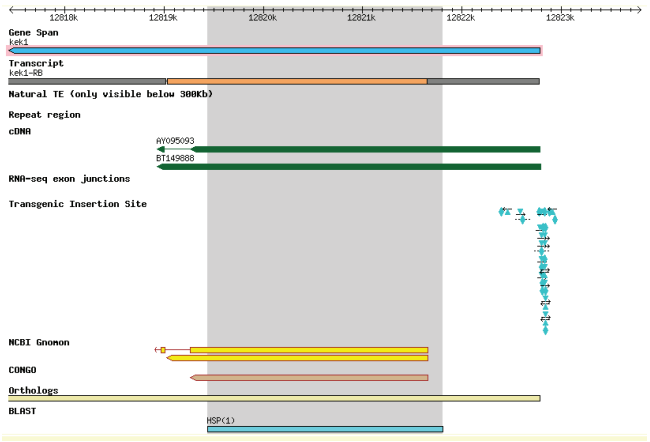

b c d e

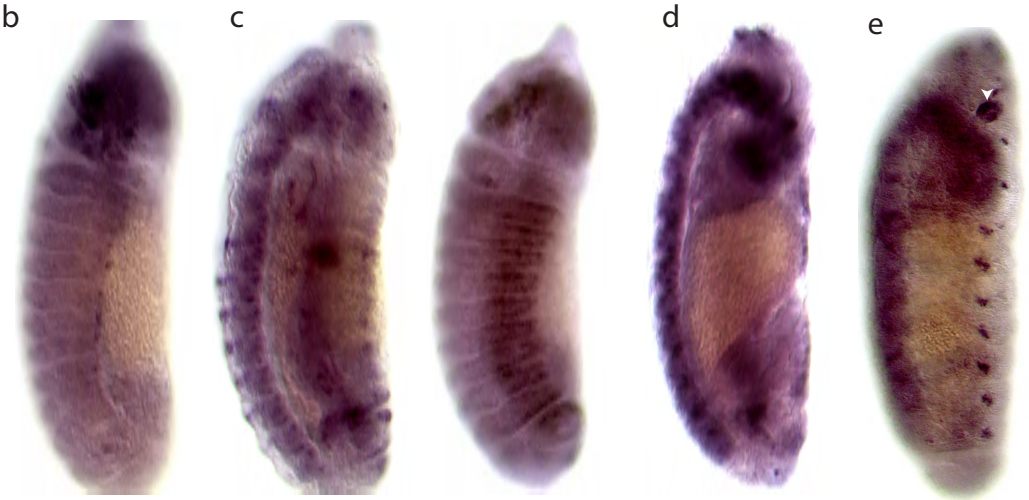

Stage 12 Stage 14 Stage 15 Stage 16

f g h

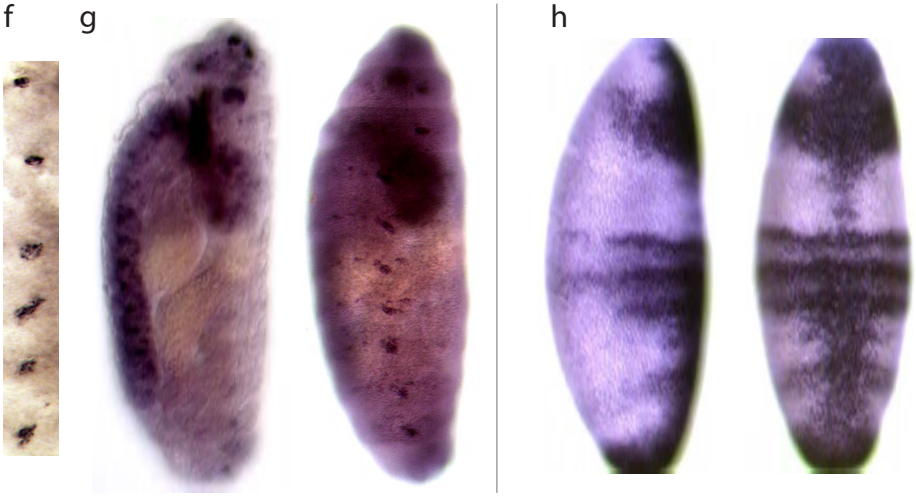

Stage 17 lateral dorsal

i j k l m n

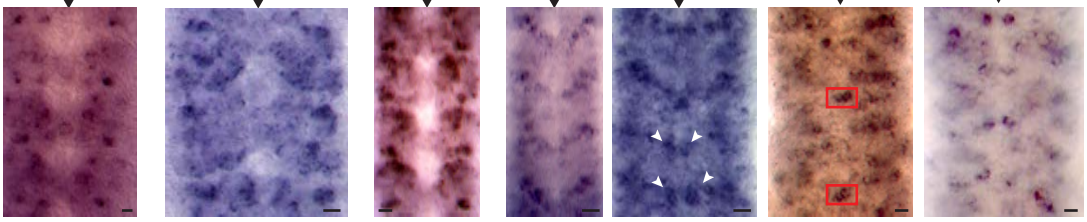

Stage 12 Stage 13 Stage 14 Stage 15 Stage 16 Stage 17

15A6 embryos stained with anti-βgal and *in situ* hybridisation using a *kek1* antisense RNA probe both reveal *kek1* signal in the embryonic VNC and central brain (Figure 3.4c, 3.5e), and signal in 2 paired cells either side of the midline (Figure 3.4e, 3.5o). Nonetheless, differences were observed: anti-βgal revealed 4 *kek1*$^{+}$ paired cells per segment and ventral cell clusters overlaying the midline, whereas *in situ* hybridisation revealed putative *kek1*$^{+}$ MP1 cells, V-shaped *kek1* signal suggestive of HB9^{+} cells, in addition to putative Bolwig's organ signal (Figure 3.4e,f, 3.5a,d,j,l). Since the *kek1* probe used hybridises to the *kek1* mRNA (Figure 3.5a), this signal can be attributed to *kek1* gene activation and thus the cell-specific expression revealed by in situ hybridisation is more reliable than that of *15A6* embryos. Nonetheless, expression profile overlap across the CNS between both detection methods confirms the expression of *kek1* in the CNS.

kek2 transcript was enriched in the VNC and brain (Figure 3.6a–d). From stage 15, signal was detected in stripes along the flank of the embryo (Figure 3.6e–g). These stripes comprised the clusters of the PNS. By Stage 17, PNS signal was restricted to discrete clusters per hemisegment, ventral to the chordotonal organs (Figure 3.6g). *kek2* signal was detected in the VNC from stage 13 in the intra-axonal tract region (Figure 3.6h,i), and later in the lower lateral muscle precursors or exit glia flanking the VNC (Figure 3.6h–j arrowheads).

kek2 signal in the VNC was enriched in four cells per segment, akin to the aCC or pCC and RP2 pattern (Figures 1.8, 3.6j–n). Cells ventral to the neuropil also became *kek2*$^{+}$ as the embryo developed (Figure 3.6l,n). In Stage 16 and 17 embryos, signal was absent from longitudinal and midline glia (Figure 3.6m,n). Ventral midline cell bodies were detected to be *kek2*$^{+}$ in stage 17 embryos (Figure 3.6n).

PCR amplification of ~500nt fragments (primers *kek3558ntattBFw* & *kek3558ntattBRv* and *kek41.6kbinFwd* & *kek42kbinRev*; see Table 2.3) was attempted from LD embryo cDNA

Figure 3.6 ***kek2* is expressed in the CNS**

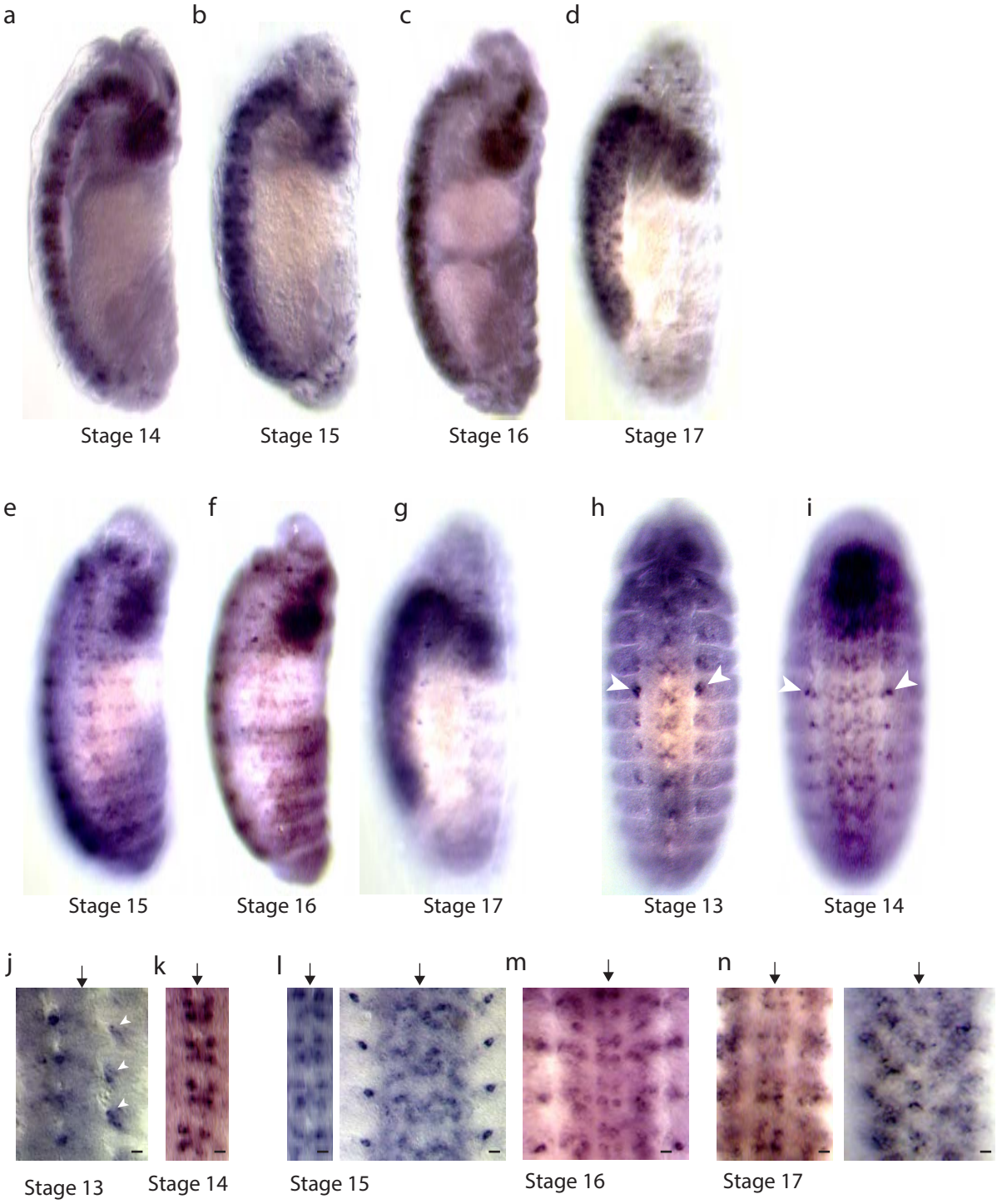

a-g | *In situ* hybridisation reveals *kek2* mRNA is enriched in the embryonic CNS. **h,i** | *kek2* mRNA was detected in lower lateral muscle precursors or exit glia (arrowheads). **j-n** | Dissected embryos reveal *kek2* transcript in increasing numbers of neurons from stage 13. Signal was also detected in lower lateral muscle precursors or exit glia (arrowheads). The embryonic midline is labelled with a black arrow. Scale bar, 10µm.

libraries. *kek3* and *kek4* cDNA could not be detected in this library, suggesting that these genes are not expressed in embryos, or mRNA levels are extremely low.

In situ hybridisation using a *kek3* antisense probe (Figure 3.7a) revealed weak signal in the VNC of stage 17 embryos, evident in only isolated cells in each segment (Figure 3.7b,c). By comparison, *kek3* was enriched in the larval brain, as detected by putative *kek3Gal4*-driven reporters (Figure 3.7d–f). However, it must be noted that this Gal4 insertion (*Mi[ET1]CG15256*^{MB09797}) is 22kb upstream of the first exon (Figure 2.8), thus expression detected may be unrelated to normal expression. Viewed along the frontal plane (a cross section of the brain), membrane-tethered signal was observed throughout the nerve cord in discrete cell bodies and connections, and around the outside of the central brain (Figure 3.7d, left image). Viewed along the horizontal plane (ventral–dorsal), putative *kek3Gal4* signal reached up to the boundary between the central brain and the optic lobe (Figure 3.7d, right image). Putative *kek3Gal4* signal was absent from the majority of the optic lobe, apart from a single axon and cluster of cell bodies in the centre of the optic lobe (Figure 3.7d,e). Putative *kek3Gal4* signal in the nerve cord was confined to repeating stripes of cell bodies detected dorsal to the neuropil, but only in the periphery of the nerve cord more ventrally, leaving the neuropil unstained (Figure 3.7f). Thus, this distant Gal4 insertion suggests that cell bodies of cortex or peripheral glia may be *kek3*$^{+}$. Last, we raised custom antibodies against a non-leucine rich repeat, non-immunoglobulin, unique extracellular Kek3 peptide sequence (see Chapter 2.5.2). Nerve cords labelled with Anti-Kek3 revealed Kek3 signal in the upper layer of the neuropil (Figure 3.7g).

Putative *kek5Gal4* (*P[GawB]NP5933*) was crossed to *UASmCD8GFP* (Figure 3.8a–f) or *UASmyrTOMATO* (Figure 3.8g–k) and stained with fluorescent secondary antibodies. As with *kek3*, it should be noted that the *kek5Gal4* insertion is very far upstream (112kb) of the first *kek5* exon (Figure 2.8), thus expression detected may be unrelated to normal *kek5* expression. Putative *kek5Gal4*-driven GFP signal was detected in stage 10 embryos in isolated medial

Figure 3.7 ***kek3* is expressed in the larval CNS**

In situ hybridisation

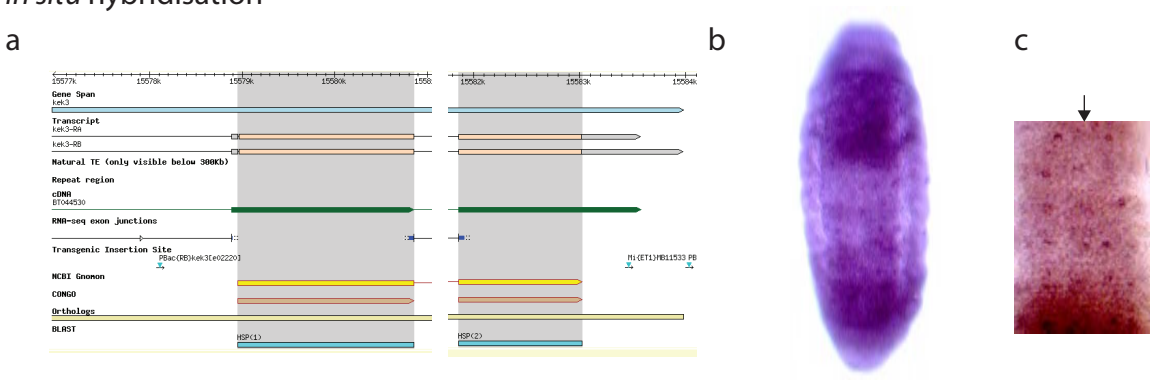

Putative *kek3Gal4>UASmyrTomato*

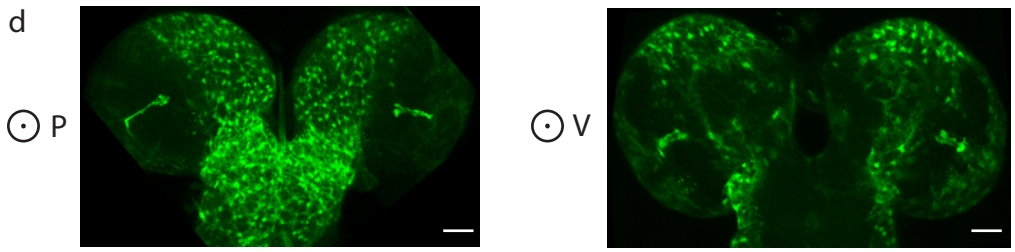

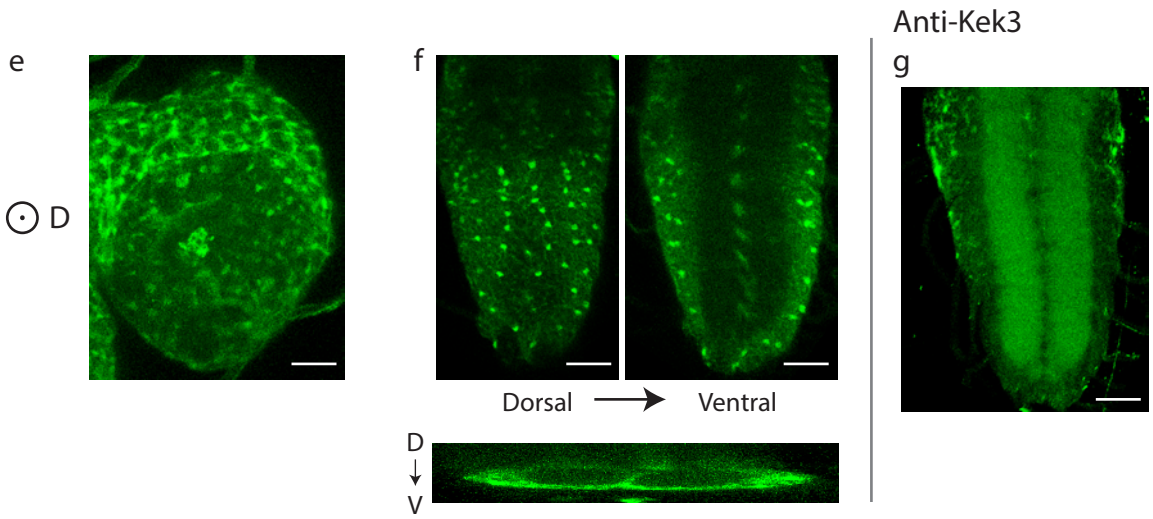

a | Verification of probe hybridisation by BLAST. **b,c** | *In situ* hybridisation revealed only weak detection of *kek3* mRNA in the embryonic CNS. **d-f** | Putative *kek3Gal4*-driven *UASmyrTOMATO* was detected in the larval ventral nerve cord, central brain, and a cell cluster and axon in the medial optic lobe. **f** | Putative *kek3Gal4* signal surrounds the neuropil. **g** | anti-Kek3 reveals Kek3 protein in the upper layer of the neuropil. Target symbols indicate plane of view closest to the viewer, e.g. posterior (P) closest along posterior-anterior axis. Scale bar, 50µm.

Figure 3.8 ***kek5* is expressed in the embryonic and larval CNS**

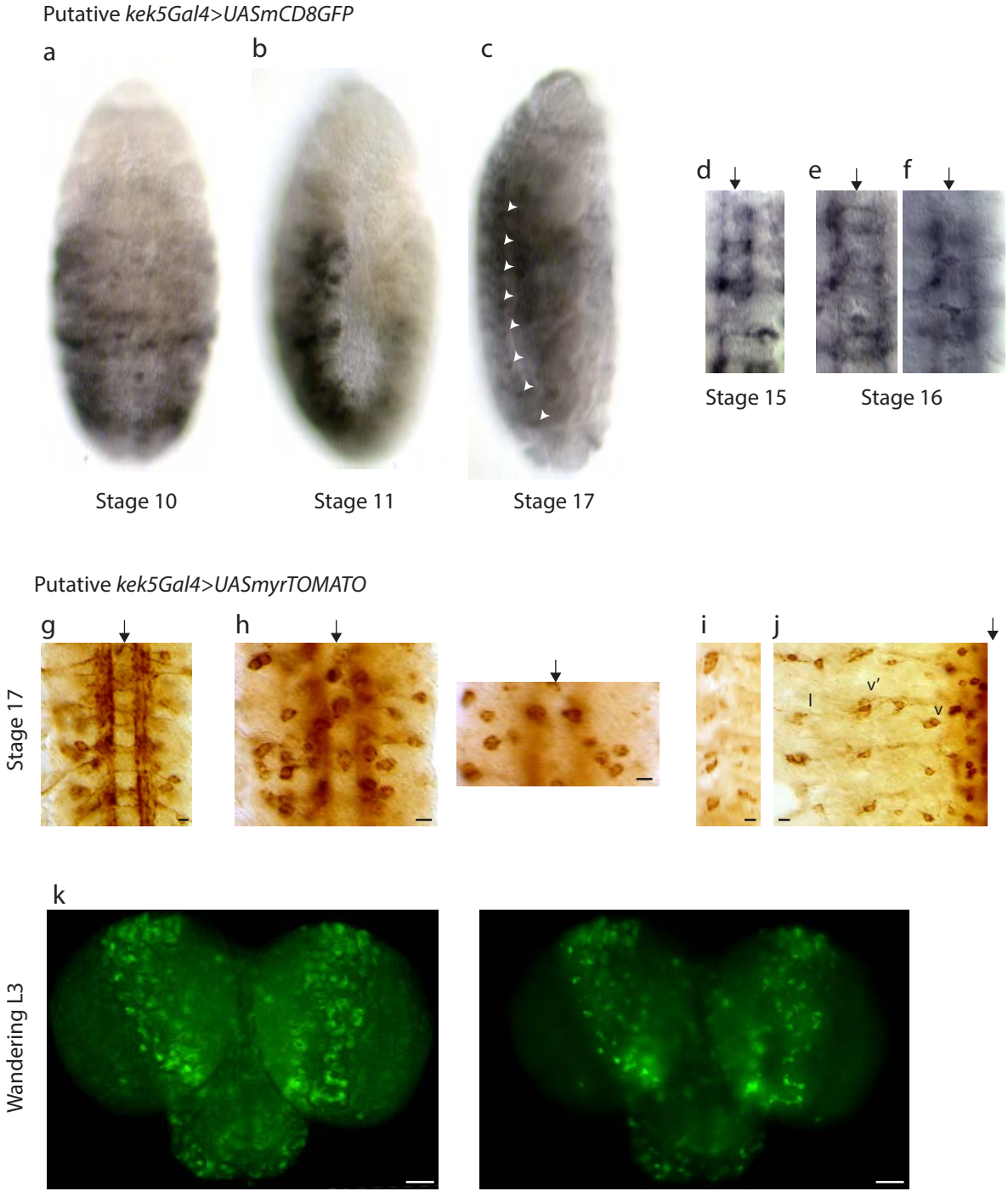

a-c | Membrane-tethered GFP reporter was detected in the VNC in dorsal clusters (arrowheads). **d-f** | Membrane-tethered GFP was detected in midline crossing contralateral neurons and neuronal cell bodies on the midline. **g-j** | myrTomato reporter indicates expression of *kek5* in stage 17 embryos in longitudinal axons, commissures, ventral cell bodies and ventral (v) and lateral (l) PNS clusters. The embryonic midline is labelled with a black arrow. **k** | myrTomato reporter is detected in the larval ventral nerve cord and central brain. Scale bars: 10µm (embryos), 50µm (larvae).

cells parallel to the midline (Figure 3.8a). By stage 11, putative *kek5Gal4*-driven GFP was detected along the germ band in large cell clusters (Figure 3.8b). By stage 17, expression was restricted to the VNC, in localised dorsal clusters in each segment (Figure 3.8c, arrowheads). Dissected embryos revealed *kek5Gal4*-driven GFP expression in stage 15 and 16 midline-crossing contralateral neurons (Figure 3.8d,e). *kek5* GFP was also detected in neuronal cell bodies and axons ventral to and overlying the midline (Figure 3.8f).

The membrane-tethered marker *UASmyrTOMATO* revealed very clear *kek5*$^{+}$ CNS axonal signal in the stage 17 embryo (Figure 3.8g). Neuronal cell bodies lateral to the VNC projected *kek5*$^{+}$ axons into the commissures and motor neurons that exit the VNC Putative *kek5Gal4*-driven myrTomato was also present in neuronal cell bodies ventral to the neuropil, including cell bodies directly ventral to the longitudinal axon tracts and to the midline (Figure 3.8h). Stage 17 PNS cell bodies were also shown to be *kek5*$^{+}$ (Figure 3.8i). *kek5*$^{+}$ neurons were observed in the ventral (v and v′) and lateral (l) PNS neuronal clusters (Figure 3.8j). *kek5*-driven myrTomato expression was also observed in the larval brain. Signal was enriched in the central brain and VNC (Figure 3.8k).

The expression patterns of *kek6* and *kek4* are shown in Chapters 6 and Chapter 7, respectively.

3.2.1.3 Expression profiles of non-LIG candidates

Rickets could not be detected consistently in the embryonic nervous system (Figure 3.9a–c). Non-specific signal was observed adjacent to the midline in stage 12 embryos (Figure 3.9a). However, no VNC signal was detected in stage 16 embryos (Figure 3.9b) apart from a few, isolated ventral midline cells (Figure 3.9c, amplified in 3.9d). *rk*$^{+}$ signal was detected in the brain and hindgut of stage 16 embryos (Figure 3.9b).

CG17839-driven GFP was not detected in the stage 12 embryos (Figure 3.9e). Expression was observed in the VNC from stage 14, at the most ventral and most dorsal planes only (Figure

Figure 3.9 ***rickets* and *CG17839* expression profiles**

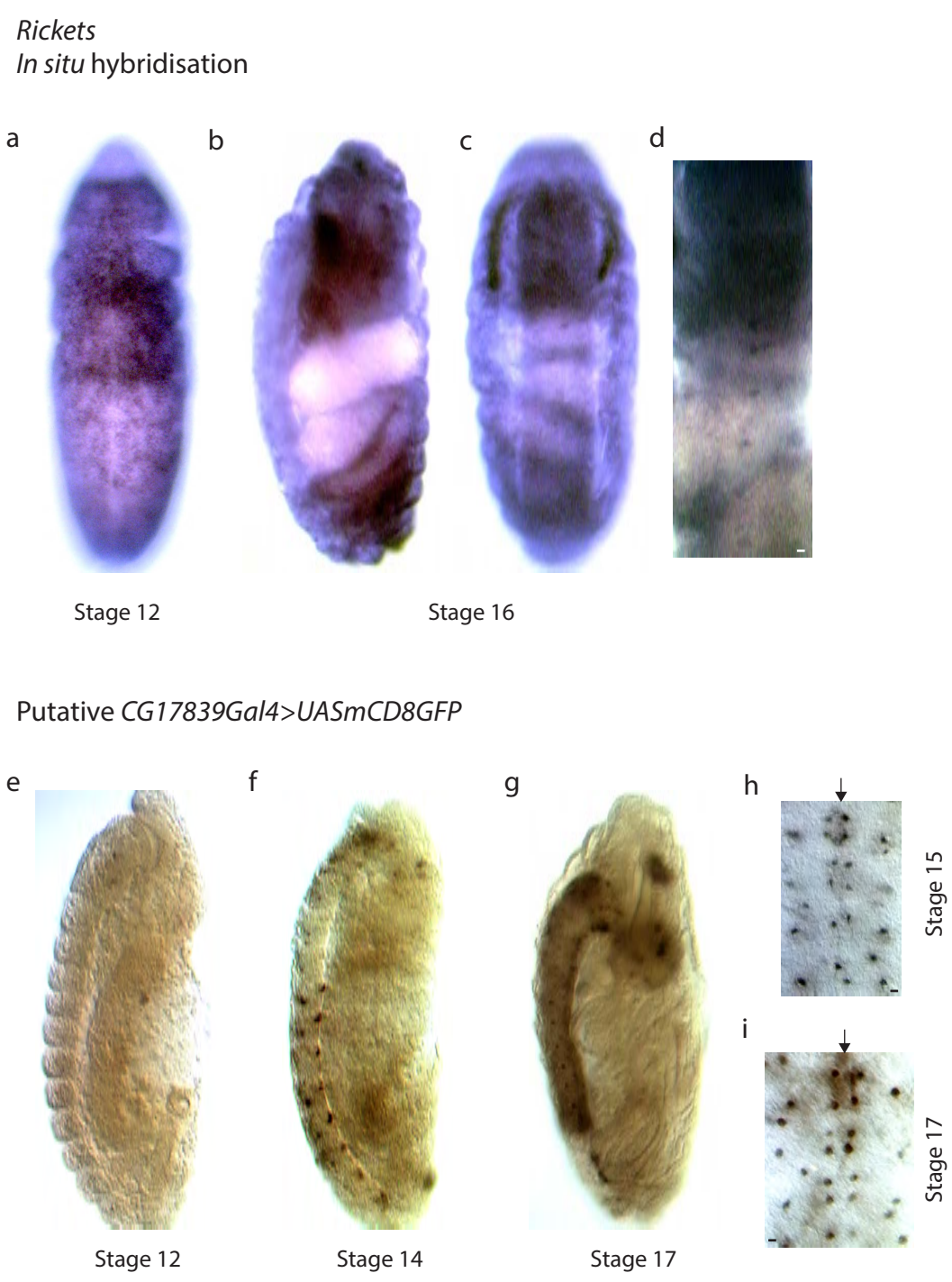

a-d | *In situ* hybridisation reveals only weak rickets signal in the CNS. **d** | Magnified view of VNC in image **c** reveals individual *rickets*$^{+}$ cells along the midline. **e-i** | Putative *CG17839Gal4*-driven mCD8GFP reveals *CG17839*$^{+}$ cells in the ventral and dorsal VNC from stage 14. CG17839 is enriched in the CNS by stage 17. **h-i** | Dissected embryos reveal four *CG17839*$^{+}$ cells per segment. The embryonic midline is labelled with a black arrow. Scale bar, 10µm.

3.9f). *CG17839*>GFP was enriched in the stage 17 VNC (Figure 3.9g). Dissected stage 15 and 17 embryos revealed four *CG17839*$^{+}$ cells per segment (Figure 3.9h,i).

The expression profile of *wengen* was markedly different. *In situ* hybridisation using an antisense RNA probe revealed clusters of *wengen* transcript throughout the germ band of stage 11 embryos (Figure 3.10a–c). These clusters resemble oenocytes and tracheal precursors (Ebner et al., 2002, Sotillos et al., 2010). By stage 15, two bands of signal could be detected — one in the lateral musculature precursors or epidermis (Figure 3.10d, left image), and one in the tracheal system (Figure 3.10d, right image). By stage 16, signal was detected in segmental boundaries (Figure 3.10e, arrowheads). Dorsal and ventral views of whole mount stage 11 embryos revealed *wengen* transcript in large single cells along the germ band, medial to the midline (Figure 3.10f–h). *Wengen* transcript was also present in repeating U-shaped clusters throughout the germ band. These resemble the expression of *tinman*, which is required for the positioning of the *Drosophila* heart (Lockwood and Bodmer, 2002).

Wengen^{+} cells in the VNC of stage 11 and stage 12 embryos divided to produce repeating pairs of cells over the longitudinal axonal tracts (Figure 3.10i). *Wengen* signal was also seen on the midline, suggesting that the role of *wengen* is glial (Figure 3.10j, arrowheads). In later stage embryos, *wengen*$^{+}$ cells extended projections away from (arrowhead) and towards (white arrow) the midline (Figure 3.10k,l). These may be exit glia. *Wengen* transcript was enriched in the ventral lateral muscles or muscle attachment sites of stage 15 embryos (Figure 3.10m).

3.2.2 The dLIGs interact with the DNTs

To determine whether the dLIGs interact with the DNTs, two assays were performed on *dLIG–DNT* combinations: a lethality assay, and a locomotion assay to determine behavioural phenotypes.

Figure 3.10 ***wengen* is expressed in trachea, the heart and glia**

a | Probe hybridisation confirmed by BLAST. **b,c** | *In situ* hybridisation reveals *wgn* mRNA is localized to tracheal and oeonocyte precursors in the early embryo. **d,e** | *wgn* mRNA is enriched in the trachea by stage 15 and segmental boundaries by stage 16 (arrowheads). **f-h** | *wgn* mRNA was detected in single cells along the future nerve cord in stage 11 embryos. Lateral *wgn* mRNA signal resembles the U-shaped expression pattern of the heart positioning gene, *tinman*. **i-m** | Dissected embryos reveal *wgn* mRNA on the midline, between the longitudinal tracts and in putative exit glia. Scale bar, 10μm.

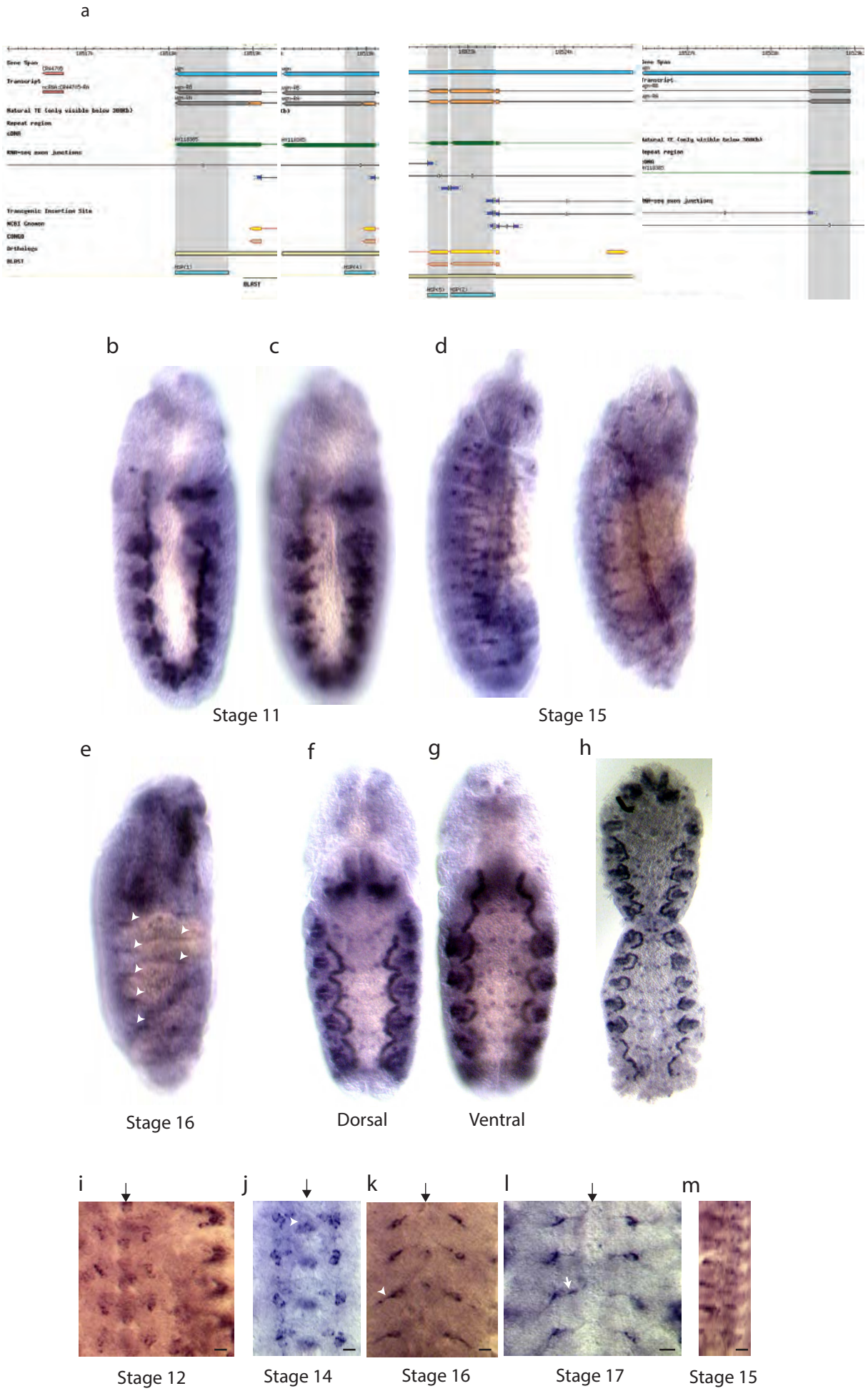
a
b
c
d
Stage 11
Stage 15
e
f
g
h
Stage 16
Dorsal
Ventral
i
j
k
l
m
Stage 12
Stage 14
Stage 16
Stage 17
Stage 15

3.2.2.1 Genetic interactions of the dLIGs

At 18^0C, $DNT1^{41}$ and $DNT2^{e03444}$ single mutant alleles are viable (McIlroy et al., 2013): when crossed, $DNT1^{41}/TM6B$ or $DNT2^{e03444}/TM6B$ parental lines yield homozygous $DNT1^{41}/DNT1^{41}$ (hereafter $DNT1^{-/-}$) or $DNT2^{e03444}/DNT2^{e03444}$ (hereafter $DNT2^{-/-}$) progeny, in addition to allele/balancer progeny. This can be quantified by scoring pupal phenotypes, since homozygous pupae are Tb^+, whereas *TM6B*-balanced pupae are Tb^- (tubby). Using the survival index (S.I.), a wild type S.I. of 1 equates to an expected Mendelian Tb^+:Tb^- progeny ratio of 1:2 (see Methods for further details). Under these conditions, $DNT2^{e03444}DNT1^{41}$ double mutants are homozygous lethal (hereafter $DNT2^{-/-}DNT1^{-/-}$), as there are no Tb^+ progeny pupae from a cross of $DNT2^{e03444}DNT1^{41}/TM6B$ parents (Figure 3.11a). This suggests that DNT1 and DNT2 are functionally redundant (Zhu et al., 2008). If mutants for the 12 candidate genes in this study interact with *DNT* mutants, *dLIG–DNT* double combinations may deviate the S.I. away from a S.I. of 1. Thus, dLIG–DNT combinations were balanced over *TM6B* and bred at 18^0C, and pupal phenotypes were scored. Full genotypes and survival indices are shown in Table 3.1.

Transposon-derived alleles used are summarised in Table 2.2 and Figure 2.8, and described in Chapter 2.1.3. In each protocol, isogenic balancer stocks were used at the G_0 cross, and F_2 progeny double mutants were self-crossed en masse (10♀:8♂) to form stable stocks but not isogenized by 1:1 matings. Given the isogenic background, this was deemed unnecessary since phenotypes would derive only from the introduced alleles. How these alleles manifest phenotypes, and whether 1:1 stock matings would affect results, was unknown: this experiment was intended to diagnose notable phenotypic differences between different *dLIG–DNT* genetic combinations only. *kek1*, *kek2* and *kek6* genetic interactions could not be assayed owing to a lack of available viable alleles.

Figure 3.11 ***dLIGs* interact genetically with the *DNTs***

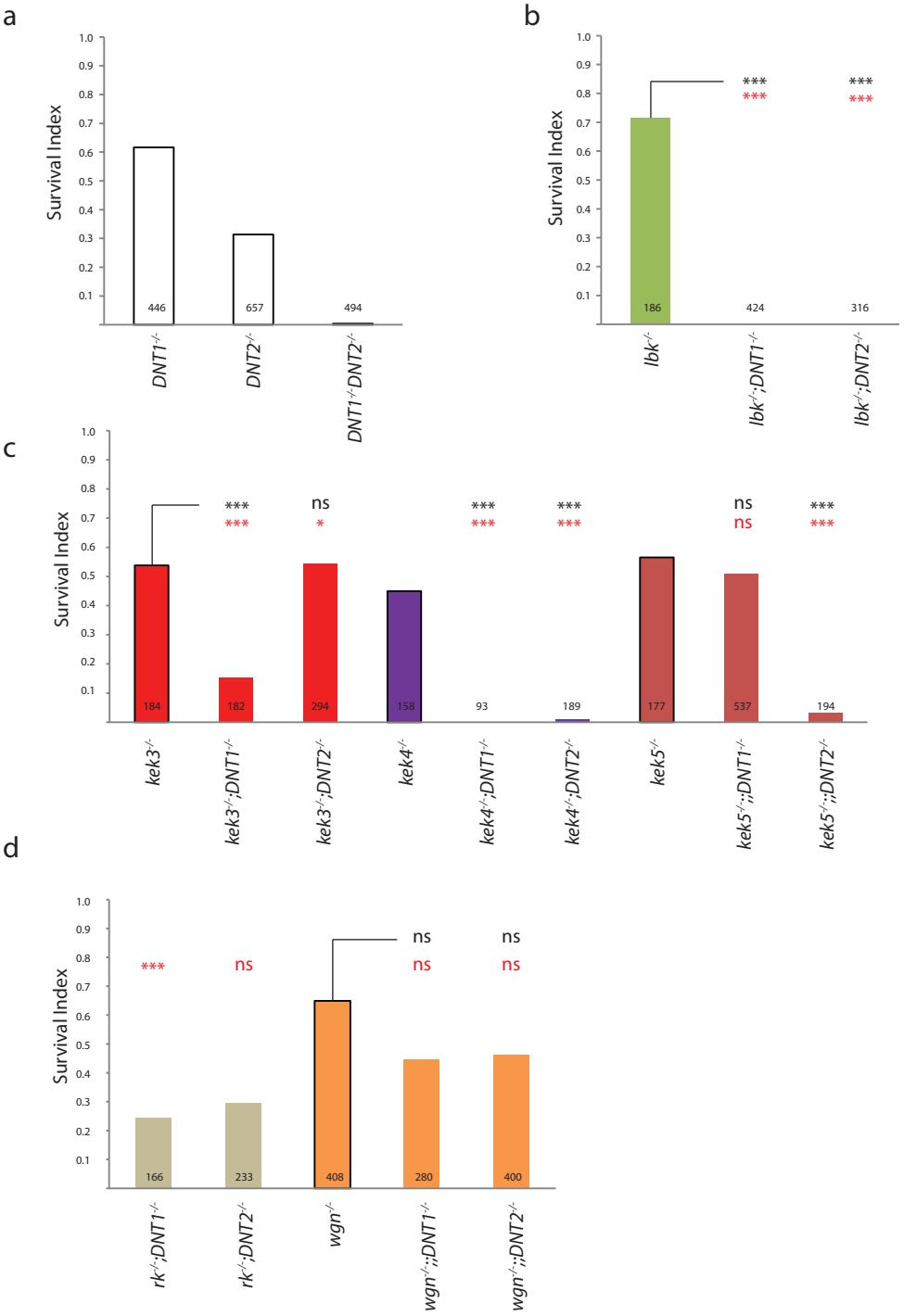

a | The survival index of single *DNT1*, *DNT2* and double *DNT2DNT1* mutants is shown. At 18°C, *DNT2DNT1/TM6B* mutants are embryonic lethal in homozygosis (no $DNT2^{-/-}DNT1^{-/-}$ pupae detected, survival index=0), whereas single *DNT1/TM6B* or *DNT2/TM6B* mutants are not. Expected Mendelian segregation of viable alleles give a survival index value of 1. Double mutants combining *DNT1* or *DNT2* mutations with *lbk* (**b**), *kek3*, *kek4* and *kek5* (**c**) or *rk* and *wgn* mutations (**d**) are shown. Survival indices of double mutants are compared to single receptor mutants (black stars; χ2 with Bonferroni correction) and single *DNT* mutations (red stars; χ2 with Bonferroni correction). See Table 3.1 for full genotypes and raw data, and Appendix I for statistical values.

Table 3.1 ***DNT–dLIG* survival assays, Raw data, 18^{0}C experiments**

Abbreviation	Progeny of	n	Tb$^-$	Tb$^+$	Survival index
DNT1$^{-/-}$	*DNT1^{41}/TM6B*	446	341	105	0.616
DNT2$^{-/-}$	*DNT2^{e03444}/TM6B*	657	568	89	0.313
DNT1$^{-/-}$DNT2$^{-/-}$	*DNT1^{41}DNT2^{e03444}/TM6B*	494	493	1	0.004
lbk$^{-/-}$	*lbk^{GS50104};+/SM6aTM6B*	186	137	49	0.715
lbk$^{-/-}$;DNT1$^{-/-}$	*lbk^{GS50104};DNT1^{55}/SM6aTM6B*	424	424	0	0.000
lbk$^{-/-}$;DNT2$^{-/-}$	*lbk^{GS50104};DNT2^{e03444}/SM6aTM6B*	316	316	0	0.000
kek3$^{-/-}$	*kek3^{f07029};+/SM6aTM6B*	184	145	39	0.538
kek3$^{-/-}$;DNT1$^{-/-}$	*kek3^{f07029};DNT1^{55}/SM6aTM6B*	182	169	13	0.154
kek3$^{-/-}$;DNT2$^{-/-}$	*kek3^{f07029};DNT2^{e03444}/SM6aTM6B*	294	231	63	0.545
kek4$^{-/-}$	*kek4^{f05454};+/SM6aTM6B*	158	129	29	0.450
kek4$^{-/-}$;DNT1$^{-/-}$	*kek4^{f05454};DNT1^{55}/SM6aTM6B*	93	93	0	0.000
kek4$^{-/-}$;DNT2$^{-/-}$	*kek4^{f05454};DNT2^{e03444}/SM6aTM6B*	189	188	1	0.011
kek5$^{-/-}$	*kek5^{e02482};;+/TM6B*	177	138	39	0.565
kek5$^{-/-}$;;DNT1$^{-/-}$	*kek5^{e02482};;DNT1^{55}/TM6B*	537	428	109	0.509
kek5$^{-/-}$;;DNT2$^{-/-}$	*kek5^{e02482};;DNT2^{e03444}/TM6B*	194	191	3	0.031
rk$^{-/-}$;DNT1$^{-/-}$	*w;rk^{4};DNT1^{55}/SM6aTM6B*	166	148	18	0.243
rk$^{-/-}$;DNT2$^{-/-}$	*w;rk^{4};DNT2^{e03444}/SM6aTM6B*	233	203	30	0.296
wgn$^{-/-}$	*pBacwgn^{e00637};;+/TM6B*	408	308	100	0.649
wgn$^{-/-}$;;DNT1$^{-/-}$	*pBacwgn^{e00637};;DNT1^{55}/TM6B*	280	229	51	0.445
wgn$^{-/-}$;;DNT2$^{-/-}$	*pBacwgn^{e00637};;DNT2^{e03444}/TM6B*	400	325	75	0.462

The *lambik* allele *P[GSV2]GS50104* (hereafter lbk^{-}) caused partially reduced embryonic viability. *lbk* mutants were homozygous lethal in combination with mutations of either *DNT1* or *DNT2* (Figure 3.11b). Both combinations were statistically significant compared to $lbk^{-/-}$ (black stars; χ^2 with Bonferroni correction applied in all S.I. cases) and to the respective single *DNT* mutation (red stars).

Single $kek3^{f07029}$, $kek4^{f05454}$ or $kek5^{e02482}$ mutations (hereafter $kek3^{-}$, $kek4^{-}$, $kek5^{-}$) partially impaired viability (Figure 3.11c). Compared to $kek3^{-/-}$ single mutations, *kek3DNT1* double mutants resulted in viability being further reduced. Furthermore, compared to single $DNT1^{-/-}$ mutants, *kek3DNT1* double mutants had reduced viability. *kek4DNT1* and *kek4DNT2* double mutants were homozygous lethal and significantly different compared to single receptor and single *DNT* mutations. *kek5DNT2* double mutants were semi-lethal and significantly different from $kek5^{-/-}$ and $DNT2^{-/-}$ single mutants. This suggested specific interactions between kek3–5 and the DNTs, discussed below.

Combinations of the rickets allele rk^{4} (hereafter rk^{-}) with *DNT* alleles also reduced viability. However, there was no difference between the two combinations (Figure 3.11d). Similarly, although combinations of $wengen^{e00637}$ (hereafter wgn^{-}) and the *DNTs* partially reduced viability compared with single receptor mutants, no difference was observed between the combinations. Survival indices of *wgnDNT* combinations were not significantly different from either $wgn^{-/-}$ mutants alone or the single *DNT* mutation.

3.2.2.2 *kek3* and *kek4* interact with *DNTs* to effect locomotion phenotypes

Mutant alleles of *toll6* and *toll7* cause motor axon and locomotion phenotypes (McIlroy et al., 2013). Additional putative receptors could have related or reciprocal phenotypes, depending on their ligand and whether they have functions in activating, inhibiting or modulating signalling.

In *Drosophila*, involuntary locomotion behaviour is controlled by rhythmic firing within the motor circuit, which can persist in an uncoordinated fashion in the absence of sensory input (Brown, 1911, Wilson, 1961, Glanzman, 2010, Suster and Bate, 2002). Locomotion can be measured by a number of assays. Climbing assays, as well as horizontal phototaxis, smell or taste chemotaxis assays require minimal setup, but results vary significantly between trials and measure only voluntary behaviour, thus requiring central processing of stimuli — indeed, these assays are used to assess neurodegeneration in fly disease models (Barone and Bohmann, 2013, Feany and Bender, 2000, Nichols et al., 2012, Vang et al., 2012). Data of involuntary locomotion and movement in response to stimuli can be obtained en masse using systems that record adult movement as it interrupts an infrared beam (Chiu et al., 2010, Dimitrijevic et al., 2004, Parr et al., 2001), but data output is binary.

Tracking software can determine single fly location or track multiple flies simultaneously to yield custom parameter data (Branson et al., 2009, Diaper et al., 2013, Donelson et al., 2012, Humphrey et al., 2012, Kabra et al., 2012, Simon and Dickinson, 2010). Here, an inexpensive setup was used to record single receptor or receptor–DNT double mutant adults walking around a Petri dish. Flies were tracked and trajectories quantified using the FlyTracker ImageJ plugin (McIlroy et al., 2013), a modification of the MTrack2 ImageJ plugin (Hand et al., 2009) that tracks migrating cells. FlyTracker provided distance, moving speed, resting and wobbling data from individual films of flies (McIlroy et al., 2013, Sutcliffe, 2010). The method was used to identify dLIG–DNT interactions, rather than mechanisms of receptor function.

All single DNT and receptor mutations caused a decrease in total distance and speed travelled. *DNT2*$^{-/-}$ mutants had a more pronounced locomotion phenotype than *DNT1*$^{-/-}$ (Figure 3.12).

With regards to moving speed, *kek3*$^{-/-}$*DNT1*$^{-/-}$ and *kek3*$^{-/-}$*DNT2*$^{-/-}$ double mutants travelled faster than *kek3*$^{-/-}$ single mutants (Figure 3.12b). Furthermore, the moving speed variation

Figure 3.12 ***dLIGs* interact with *DNTs* to induce locomotion phenotypes**

Adult single and double mutant flies were filmed walking around a Petri dish and their trajectory parameters quantified. **a** | Example trajectories of control (*yw*) and mutant genotypes. **b** | Speed histograms of double receptor-ligand mutants compared with single receptor mutants. Statistics shown compare double mutants. Frame numbers, full genotypes and statistical values are shown in Appendix I. **c-e** | *DNT1* and *DNT2* mutations interact differently with *kek3* and *kek4* mutations in the context of total distance travelled (**c**), time spent resting (**d**) and wobbling (**e**). Total film numbers are shown for each genotype in **c**; frame numbers for wobbling and resting calculations are shown in Appendix I. Statistics compare double mutants against single mutants (black stars) and double mutants against single *DNT* mutations (red stars).

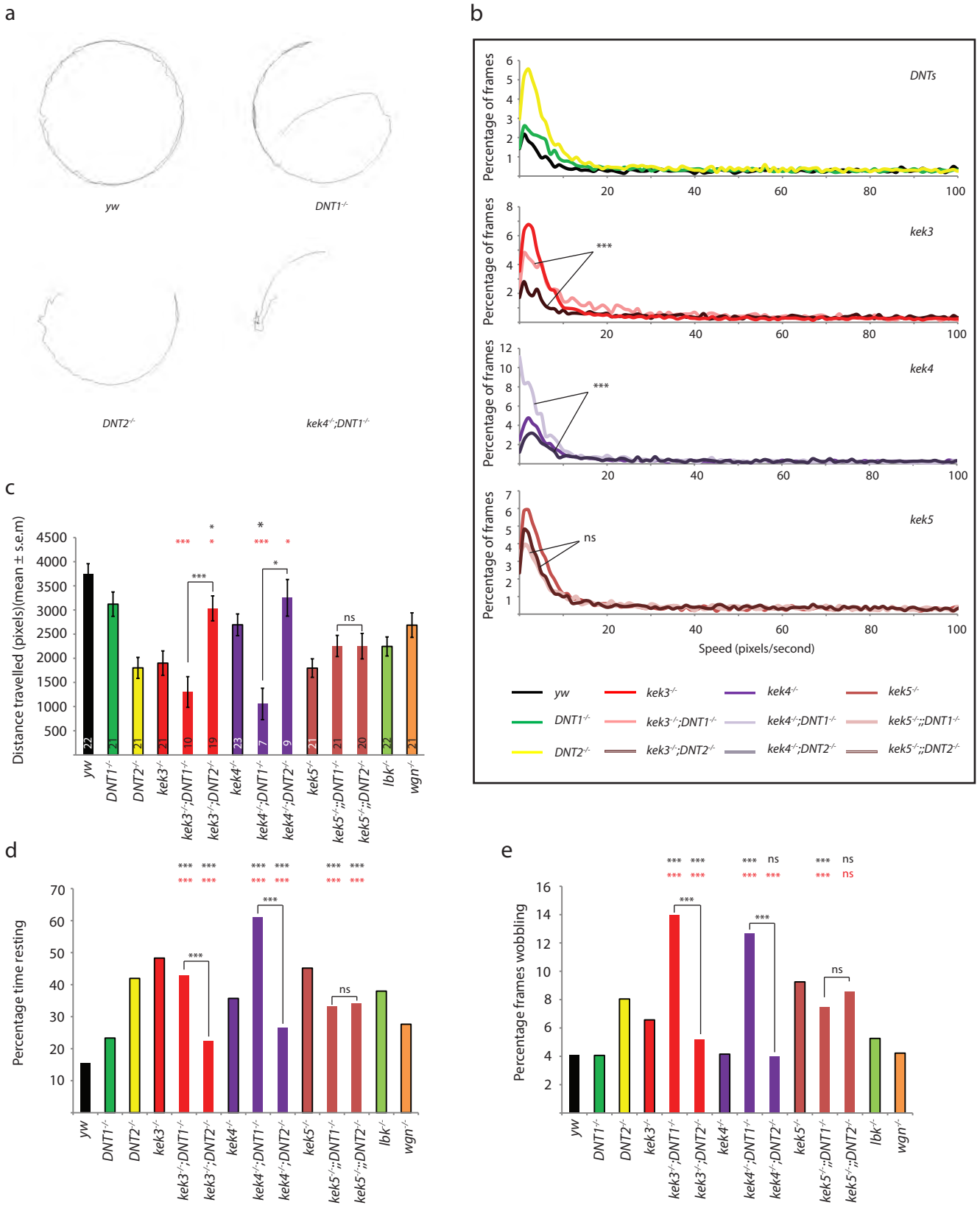
a
yw
DNT1-/-
DNT2-/-
kek4-/-;DNT1-/-
b
DNTs
kek3
kek4
kek5
Percentage of frames
Speed (pixels/second)
yw
DNT1-/-
DNT2-/-
kek3-/-
kek3-/-;DNT1-/-
kek3-/-;DNT2-/-
kek4-/-
kek4-/-;DNT1-/-
kek4-/-;DNT2-/-
kek5-/-
kek5-/-;;DNT1-/-
kek5-/-;;DNT2-/-
c
Distance travelled (pixels)(mean ± s.e.m)
d
Percentage time resting
e
Percentage frames wobbling

between these two double mutants was significant, indicating specificity in ligand–receptor interactions (Kruskal-Wallis with Dunn's post hoc; see Appendix I for statistical values). Similarly, *kek4*$^{-/-}$*DNT1*$^{-/-}$ and *kek4*$^{-/-}$*DNT2*$^{-/-}$ double mutants displayed significantly different speed behaviours from each other. *kek4*$^{-/-}$*DNT1*$^{-/-}$ double mutants walked slower, and *kek4*$^{-/-}$ *DNT2*$^{-/-}$ double mutants travelled faster, than *kek4*$^{-/-}$ single mutants. Differences in moving speed variation were not observed between *kek5*$^{-/-}$*DNT1*$^{-/-}$ and *kek5*$^{-/-}$*DNT2*$^{-/-}$ double mutants.

In accordance with speed results, *kek3*$^{-/-}$*DNT2*$^{-/-}$ double mutants travelled further than *kek3*$^{-/-}$ single mutants (Figure 3.12c; Student's t-test with Bonferroni correction applied in all cases). Furthermore, *kek3*$^{-/-}$*DNT1*$^{-/-}$ and *kek3*$^{-/-}$*DNT2*$^{-/-}$ travelled significantly different distances compared to one another, indicating ligand specificity. *kek4*$^{-/-}$*DNT1*$^{-}$ and *kek4*$^{-/-}$*DNT2*$^{-/-}$ displayed opposite distance phenotypes. *kek4*$^{-/-}$*DNT1*$^{-/-}$ double mutants travelled less far than *kek4*$^{-/-}$ single mutants. Conversely, *kek5*$^{-/-}$*DNT1*$^{-/-}$ and *kek5*$^{-/-}$*DNT2*$^{-/-}$ double mutants did not display different distance phenotypes compared to one another or to *kek5*$^{-/-}$ single mutants.

kek4$^{-/-}$*DNT1*$^{-/-}$ double mutants had the strongest phenotype of all genotypes tested (Figure 3.12a). The interaction of *kek4*$^{-/-}$ and *DNT1*$^{-/-}$ produced flies that rested much more than single receptor mutants (Figure 3.12d; χ^2 with Bonferroni correction in all cases).When moving, *kek4*$^{-/-}$*DNT1*$^{-/-}$ double mutants wobbled extensively (Figure 3.12e; χ^2 with Bonferroni correction in all cases). *kek3*$^{-/-}$*DNT1*$^{-/-}$ adults also wobbled more than *kek3*$^{-/-}$ *DNT2*$^{-/-}$ double mutants and *kek3*$^{-/-}$ single mutants. It is possible that wobbling data may have skewed speed data, which could account for the conflicting conclusions that *kek3*$^{-/-}$*DNT1*$^{-/-}$ double mutants travelled faster, but less far, than *kek3*$^{-/-}$ single mutants. Indeed, time spent resting by *kek3*$^{-/-}$*DNT1*$^{-/-}$ adults was comparable to *kek3*$^{-/-}$. Conversely, *kek3*$^{-/-}$*DNT2*$^{-/-}$ double mutants rested significantly less than single receptor mutants (Figure 3.12c).

For all four locomotion variables, *kek3*$^{-/-}$*DNT1*$^{-/-}$ double mutants behaved differently to *kek3*$^{-/-}$*DNT2*$^{-/-}$, and *kek4*$^{-/-}$*DNT1*$^{-/-}$ double mutants behaved differently to *kek4*$^{-/-}$*DNT2*$^{-/-}$ double mutants. Results suggested an interaction between *kek3*$^{-}$ or *kek4*$^{-}$ with *DNT1* alleles in the control of locomotor behaviour.

3.3 DISCUSSION

In this chapter, experiments showed that the *kek* family and *CG15744* are expressed in the CNS; whereas *lambik* and *CG16974* are absent from the CNS but present in the PNS. Of the other genes tested, *rickets* was detected weakly in the VNC and more strongly in the brain, *CG17839* was localized to a low number of specific CNS cells, and *wengen* was expressed in glia of early embryos, the trachea and a low number of VNC cells.

My data concur with the published expression patterns of *kek1* localization (Derheimer et al., 2004, Ghiglione, 2003, Ghiglione et al., 1999, Musacchio and Perrimon, 1996). Further *kek1* signal in midline cells was detected in some samples (Figure 3.5m). Loss of *kek1* leads to dorsalized egg shells (Zartman et al., 2009). Furthermore, Kek1 upregulation antagonizes EGFR signalling to induce ventralized embryos (Ghiglione et al., 1999); in this respect, the role of Kek1 resembles Spz–Toll signalling, as gain of function *spz* and *toll* alleles also produce ventralized embryos (Anderson et al., 1985, Morisato and Anderson, 1994). The dorsal localization of *kek1* in early embryos observed here confirms that *kek1* has a role in the establishment of polarity (Figure 3.5g), and the presence of *kek1* mRNA in the dorsal embryo warrants further investigation. Last, the possible detection of *kek1* in cardioblasts suggests a further function of the gene outside of the nervous system.

kek2 mRNA localization concurred with published expression data. Furthermore, *kek2* expression was detected in a segmentally repeating 4 cell pattern along the VNC. This pattern resembles aCC/RP2 or pCC/RP2 pioneer motor neuron pairings (Hidalgo and Brand, 1997,

Sanchez-Soriano and Prokop, 2005). Therefore, the role of *kek2* in motor neuron development could be investigated.

There are restrictions to interpretation inherent in the use of the Gal4/UAS system. First, the further away from the start codon a Gal4 element is inserted, the lower the likelihood it is positioned in the promoter of the gene of interest. At 22kb upstream of the *kek3* coding sequence and 112kb upstream of *kek5*, the expression profiles driven by *Mi[ET1]CG15256*^{MB09797} and *P[GawB]NP5933* should be interpreted as not fully representative of *kek3* or *kek5* localization (Figure 2.8). The expression profile of *kek3* had not previously been reported, and cell-specific expression of *kek5* in the CNS was unknown. Putative *kek3Gal4*-driven reporter was detected in the optic lobe and in glia that surround the neuropil and central brain. Given the detection of putative *kek3Gal4* in the optic lobe, larval photoreceptor axon guidance would be the ideal place to start in the analysis of *kek3* function. Genetic stocks combining *kek3* null mutants and *roTaulacZ* have been generated for this purpose. Putative *kek5Gal4* data suggest that *kek5* is present in axons of the longitudinal axon tract, commissures, motor neurons and the PNS. Furthermore, *kek5* may be expressed in large cell clusters throughout the larval central brain.

Both putative *kek3* and *kek5* expression were determined here using the same reporter line, and similarities in larval VNC and optic lobe signal were detected between the two genes. To exclude signal noise caused by the reporter, expression results should be separately verified by antibody labelling and/or *in situ* hybridisation. Nonetheless, the putative *kek3* and *kek5* Gal4 results using the *UASmyrTOMATO* reporter did show gene-specific expression — *kek3* in the centre of the larval optic lobe, and *kek5* in the embryonic VNC and PNS clusters.

The remaining candidate genes had interesting expression profiles, between them displaying expression in the PNS and glia. However, the abundant expression of the *kek* genes

throughout the CNS made them the more important candidates for further study, subject to interaction with the DNTs.

The S.I. assay indicates that DNT1 and DNT2 may be redundant (Figure 3.11a; Zhu et al. (2008)). The difference in the effect of *DNT* mutant allele combinations with *kek3*$^{-}$, *kek4*$^{-}$ and *kek5*$^{-}$ highlighted potential specificities of receptor–ligand interactions. If the assumption is made that Kek receptors interact with specific DNT ligands, the redundancy of DNT1 and DNT2 suggests that the loss of DNT1 and its Kek receptor should be viable, because neurotrophin signalling can still occur via DNT2 and a different Kek. Conversely, the loss of DNT1 and the Kek that might bind DNT2 will increase lethality in the S.I. assay because both pathways have been interrupted. By this model, data here suggest that Kek3 protein may bind DNT2, Kek5 protein may bind DNT1, and Kek4 protein bind either DNT1 or DNT2. Of note also is the Lambik protein, which may bind DNT1 or DNT2.

The phenotypic effect of these genetic combinations was determined by locomotion assay. Again, *kek3*$^{-/-}$*DNT1*$^{-/-}$ and *kek4*$^{-/-}$*DNT1*$^{-/-}$ double mutants displayed enhanced phenotypes compared to single mutations, further suggesting that the Kek3 and Kek4 proteins may interact with DNT2.

Two points should be considered regarding the locomotion data. First, the n numbers of *kek3*$^{-/-}$*DNT1*$^{-/-}$ and *kek4*$^{-/-}$*DNT1*$^{-/-}$, which exhibit prominent phenotypes, are low. This resulted from the strong homozygous lethality of these genotypes (Figure 3.11). *kek3*$^{-/-}$*DNT1*$^{-/-}$ and *kek4*$^{-/-}$*DNT1*$^{-/-}$ were viable at 25^{0}C, but lethality remained high and flies were difficult to breed. By contrast, *lbk*$^{-/-}$*DNT1*$^{-/-}$ and *lbk*$^{-/-}$*DNT2*$^{-/-}$ homozygous flies were lethal at 25^{0}C, and could not be tested by the locomotion assay. It is possible that higher n numbers would dilute these results, although traces do suggest a behavioural phenotype was induced.

Second, adult flies may not have been the most suitable developmental stage to study locomotion. Adult gene expression was not studied, so it is not possible to compare *kek*$^{+}$

embryonic and adult cell types, nor whether embryonic expression is maintained through to adulthood. The larval nervous system is extensively remodelled during metamorphosis; thus, the effect on the adult locomotor circuit of a mutation in a gene required in the embryo is undefined and not possible to deduce (Tissot M and RF, 2000, Truman, 1990). The effect of genetic interactions on locomotion behaviour is more reliably translated to embryonic expression when studied in larvae, a method adopted in later chapters. However, the purpose of the locomotion assay in this chapter was not to link embryonic expression to adult function but to test whether the *kek* genes interact with the *DNTs*. To this end, Kek3 and Kek4 interactions with DNT2 were suggested.

The positions of the P element transposon insertion lines are shown in Figure 2.8. It is unclear how significant the genetic interactions observed were, since the phenotypic effect of the mutations was unknown. Nonetheless, distinct interactions were observed with the DNTs, indicating indirect or direct receptor–ligand specificity. Such interactions need to be confirmed using null mutants and overexpression constructs in which the nature of the alleles is known. The purpose of this chapter was to identify candidate genes for further study; in Chapters 4 and 5 the generation of overexpression constructs and null mutants is discussed.

Based on initial criteria, the Kek family were selected for further study: they were expressed in the CNS; *kek3*$^{-}$, *kek4*$^{-}$ and *kek5*$^{-}$ interacted genetically with specific DNTs; and *kek3*$^{-}$ and *kek4*$^{-}$ interacted with *DNT1*$^{-}$ to manifest behavioural phenotypes. The remaining candidates, although interesting, were excluded. The most promising remaining candidate for further study was *lbk*, which interacted genetically with both DNTs. Lbk function is not considered further in this thesis, but should be investigated further in future work in the context of PNS functions of the DNTs.

CHAPTER 4

GAIN OF FUNCTION ANALYSIS REVEALS KEK INTERACTIONS WITH THE DNTS

4.1 INTRODUCTION

To study the function of the *kek* genes, overexpression and loss of function tools needed to be built. This chapter focuses on the generation of overexpression tools for *kek1–6* for use in cell culture and *in vivo*, and to assay putative *Drosophila* neurotrophin (DNT)–Kek interactions.

There are a number of methods to create overexpression constructs for activated receptors. One option is to mutagenize key amino acids required for ligand-specific activation. In the case of the $Toll^{10b}$ allele, for example, a Cys–Tyr substitution in the juxtamembrane cysteine-rich region releases receptor autoinhibition, a function that is usually ligand-dependent (Schneider et al., 1991, Hu, 2004). Another option is to delete the entire ligand-binding region to release the requirement of ligand for activation, as is the case for $Toll^{\Delta LRR}$ (Winans and Hashimoto, 1995). However, because the Kek proteins lack intracellular signalling domains, the mechanism of signalling, the key intracellular residues for signalling, and whether the proteins dimerize or interact with a co-receptor, are all unknown. As such, the region of the protein to target by point mutation or peptide deletion was unknown. Instead, wild type, full length forms were cloned.

The resulting overexpression constructs may not induce activity alone except by membrane saturation and ectopic dimerization. However, TrkA can exist as an inactive, preformed dimer in cell culture (Shen and Maruyama, 2011); thus ectopic Kek6 dimerization might still require ligand or point mutation to signal. Nevertheless, others have used overexpression of wild type

forms, e.g. of the Tolls, resulting in gain of function phenotypes (for example, Yagi et al. (2010)).

Putative receptor–ligand interactions can be tested biochemically, as in the case of Toll7 and Toll6 with DNT1 and DNT2 (McIlroy et al., 2013), or functionally, as in the case of Jellybelly (Jeb) and ALK (Englund et al., 2003). Mutation of a receptor may phenocopy loss of the ligand (for example, mesodermal disorganization in *jeb* and *ALK* mutants (Englund et al., 2003) or developmental delays induced by prothoracicotropic hormone (*PTTH*) and *torso* mutants in the PG (Rewitz et al., 2009)). Alternatively, receptor and ligand mutations may have reciprocal phenotypes owing to the release of an endogenous inhibitory function (for example, BDNF)-mediated inhibition of RhoGTPase signalling via release of RhoGDI sequestration by TrkB.T1 (Ohira et al., 2005)). A simple readout of functional interactions can be determined in cell culture by quantifying signalling of expressed receptors in response to ligand stimulation. To this end, here, Kek≡Toll6 chimaeras were generated for use in cell culture. Chimaeric proteins have been used previously to determine interactions or signalling ability of transmembrane receptors lacking signalling domains (Alvarado et al., 2004a, Ormond et al., 2004). In this chapter, the intracellular domain of Toll6 was chosen because it signals via NFκB.

4.2 RESULTS

4.2.1 Molecular cloning of *kek* genes into *pAct5c* and *UAS* vectors

The coding sequences of *kek1–6* were amplified by PCR from cDNA libraries, genomic clones or RT-PCR from larval and pupal tissue (see Appendix II for maps and supporting data). Amplified coding sequences were recombined into *pDONR*^{221} and verified using restriction digests. *pDONR+kek1–6* entry clones were further recombined with *pAct5c-attR-mCFP* (*pAWC*) and verified by restriction digests and sequencing (Appendix II; 5′ and 3′ fragment ends are shown; no mutations or nucleotide omissions were detected throughout the

fragments). Since the destination insert sequence was correct, the *pDONR*^{221} insert sequence was also correct and therefore *pDONR+kek1–6* could be used for further cloning. *actin* promoter-driven expression of *kek* genes in S2 cells revealed outer membrane-localised expression of Kek2–6, indicating that the constructs were correctly processed (Figure 4.1). Sites of receptor enrichment at sites of cell–cell contact were detected for Kek2, Kek3 and Kek6 (arrows).

pDONR+kek1–6 entry clones were used to further recombine the *kek* genes into *pAct–attR–FLAG* (*pAWF*) for use in cell culture (Appendix II, verified by restriction digests), and *pUASt–attR–mRFP* (*pTWR*) for fly transgenesis (Appendix II, verified by restriction digests and PCR).

4.2.2 Phenotypic analysis of *kek* overexpression mutants

Overexpression of the EGFR antagonist *kek1* in the eye, using the *GMRGal4* driver, induces a rough eye phenotype (Alvarado et al., 2004b). The mode of function of other *kek* genes is unknown. To ascertain whether other *kek* genes might share the same signalling properties as *kek1*s, and whether to investigate *kek2-6* signalling via EGFR,*UASkek1RFP–UASkek6RFP* (*kek1–6+pTWR*; hereafter *UASkek1–UASkek6*) were overexpressed in the eye and flies were inspected for rough eye phenotypes. *GMRGal4*-driven expression of *UASkek1* resulted in a rough eye phenotype (Figure 4.2). *GMRGal4>UASkek2–6*, conversely, did not induce eye phenotypes. This suggested that the different *kek* genes activate different signalling pathways or bind specific co-receptors. This agrees with Alvarado et al. (2004a), which finds that Kek1 is the only family member involved in EGFR signalling.

The double mutant *DNT2*^{e03444}*DNT1*^{41} is semi-lethal at 18^{0}C when balanced over *TM6B* (no *DNT2*$^{-/-}$*DNT1*$^{-/-}$ progeny survive to pupation; see Chapter 3.2.2.1). At 25^{0}C, *DNT2*$^{-/-}$*DNT1*$^{-/-}$ homozygotes have a S.I. of 0.02 (Table 4.1). Neuronal expression of *UASkek2*, *UASkek3* and *UASkek6* in a double *DNT* mutant background rescued this lethality (Figure 4.3; χ^2 analysis

Figure 4.1 **Overexpression constructs target the cell membrane in S2 cells**

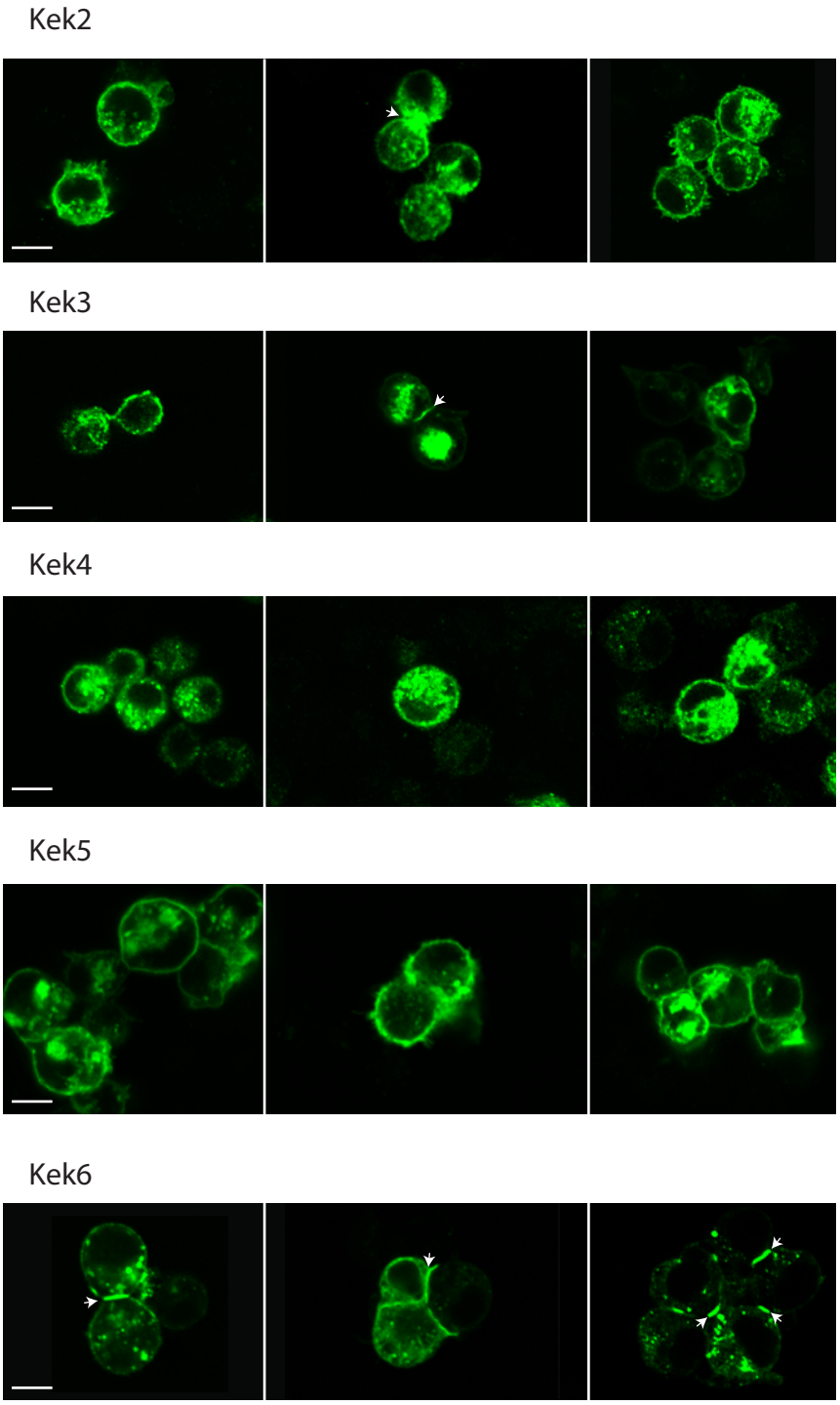

kek2-6+pAWC constructs were expressed in S2 cells and fluorescently stained with anti-GFP. mCFP would be detected at the cell membrane for each construct, suggesting that constructs had been correctly processed. Enrichment of protein at sites of intercellular contact is highlighted with an arrow. Scale bar, 10µm.

Figure 4.2 ***kek1* overexpression induces a rough eye phenotype**

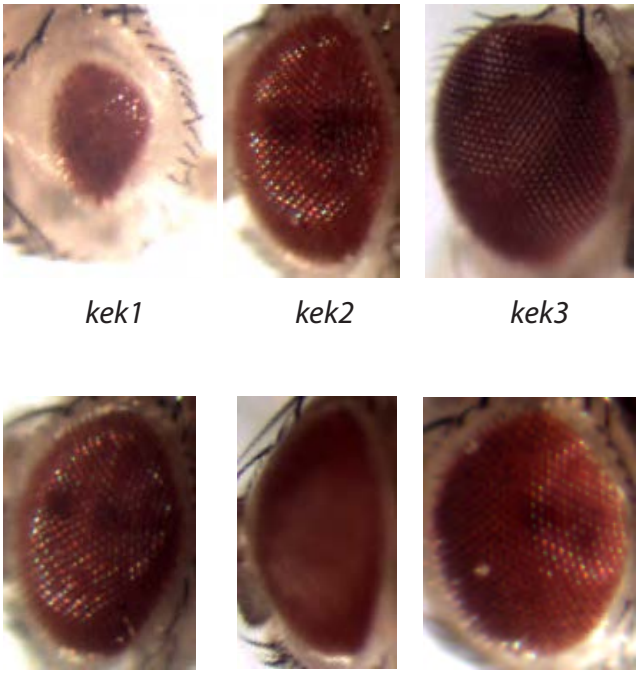

Transgenic *UASkek1-6* constructs were overexpressed in the eye using *GMRGal4*. Of these, *GMRGal4>UASkek1RFP* induced a rough eye phenotype, whereas the other transgenic kek constructs displayed no abnormal eye phenotype.

Figure 4.3 **_kek_ gene overexpression rescues lethality in _DNT_ mutants**

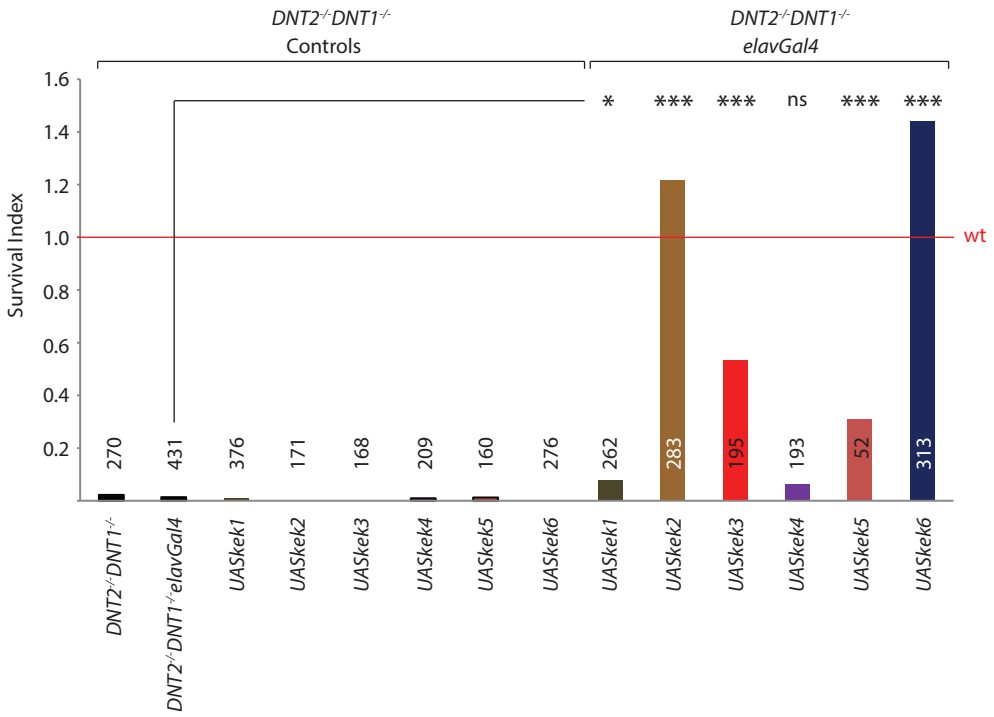

Survival index of *UASkek1-6* constructs alone and driven by *elavGal4* in a *DNT2*^{e03444}*DNT1*^{41}*/TM6B* background at 25ºC was calculated. Neuronal overexpression of *kek2*, *kek3*, *kek5* and *kek6* rescued the lethality of homozygous *DNT* double mutations. Wild type viability is indicated by the red line. Statistics compare genetic rescues with *DNT2*$^{-/-}$*DNT1*$^{-/-}$*elavGal4* (black stars). See Table 4.1 for full genotypes and raw data, and Appendix I for statistical values.

Table 4.1 ***kek* overexpression rescues *DNT2*$^{-/-}$*DNT1*$^{-/-}$ lethality, Raw data, 25^{0}C experiments**

Abbreviation	Progeny of	n	Tb^{-}	Tb^{+}	Survival index
DNT2$^{-/-}$*DNT1*$^{-/-}$	*DNT2*^{e03444}*DNT1*^{41}/*TM6B*	270	267	3	0.02247191
DNT2$^{-/-}$*DNT1*$^{-/-}$*elavGal4*	*DNT2*^{e03444}*DNT1*^{41}*elavGal4/TM6B*	431	428	3	0.014018692
DNT2$^{-/-}$ *DNT1*$^{-/-}$					
UASkek1	*UASkek1RFP; DNT2*^{e03444}*DNT1*^{41}*/SM6aTM6B*	376	374	2	0.010695187
UASkek2	*UASkek2RFP; DNT2*^{e03444}*DNT1*^{41}*/SM6aTM6B*	171	171	0	0
UASkek3	*UASkek3RFP; DNT2*^{e03444}*DNT1*^{41}*/SM6aTM6B*	168	168	0	0
UASkek4	*UASkek4RFP; DNT2*^{e03444}*DNT1*^{41}*/SM6aTM6B*	209	208	1	0.009615385
UASkek5	*UASkek5RFP; DNT2*^{e03444}*DNT1*^{41}*/SM6aTM6B*	160	159	1	0.012578616
UASkek6	*UASkek6RFP; DNT2*^{e03444}*DNT1*^{41}*/SM6aTM6B*	276	276	0	0
DNT2$^{-/-}$*DNT1*$^{-/-}$ *elavGal4>*					
UASkek1	*DNT2*^{e03444}*DNT1*^{41}*elavGal4/TM6B x UASkek1RFP; DNT2*^{e03444}*DNT1*^{41}*/SM6aTM6B*	262	252	10	0.079365079
UASkek2	*DNT2*^{e03444}*DNT1*^{41}*elavGal4/TM6B x UASkek2RFP; DNT2*^{e03444}*DNT1*^{41}*/SM6aTM6B*	283	176	107	1.215909091
UASkek3	*DNT2*^{e03444}*DNT1*^{41}*elavGal4/TM6B x UASkek3RFP; DNT2*^{e03444}*DNT1*^{41}*/SM6aTM6B*	195	154	41	0.532467532
UASkek4	*DNT2*^{e03444}*DNT1*^{41}*elavGal4/TM6B x UASkek4RFP; DNT2*^{e03444}*DNT1*^{41}*/SM6aTM6B*	193	187	6	0.064171123
UASkek5	*DNT2*^{e03444}*DNT1*^{41}*elavGal4/TM6B x UASkek5RFP; DNT2*^{e03444}*DNT1*^{41}*/SM6aTM6B*	52	45	7	0.311111111
UASkek6	*DNT2*^{e03444}*DNT1*^{41}*elavGal4/TM6B x UASkek6RFP; DNT2*^{e03444}*DNT1*^{41}*/SM6aTM6B*	313	182	131	1.43956044

with Bonferroni correction in all cases; see Appendix I for statistical values). Conversely, neuronal expression of *UASkek1* and *UASkek4* did not rescue this lethality. The S.I. of *DNT2*$^{-/-}$*DNT1*$^{-/-}$*neurons>UASkek5* flies was increased compared to *DNT1*$^{-/-}$*DNT2*$^{-/-}$ double mutants, but the observed n number was low; it is thus likely that with a larger sample size, viability would be more apparent. The ability of *kek3* overexpression to rescue *DNT2*$^{-/-}$*DNT1*$^{-/-}$ lethality matches its genetic interaction with *DNT2* shown in Chapter 3.

4.2.3 DNT2 can interact with Kek≡Toll6 chimaera receptors to induce NFκB signalling

DNT1 and DNT2 binding to full length Toll6 induces nuclear localization of the NFκB homologue Dif (McIlroy et al., 2013). In the innate immune response to fungal infection, Spz binding to Toll stimulates translation of the peptide Drosomycin via Dif nuclear localization (Manfruelli et al., 1999, Meng et al., 1999, Hu, 2004, Zhang and Zhu, 2009). S2 cells stably transfected with a *drosomycin* promoter–*luciferase* coding sequence fusion construct provide a means to quantify stimulation of *drosomycin* expression, and thereby upstream Spz–Toll and DNT–Toll6 receptor activation, by measuring luminescence (Tauszig et al., 2000, McIlroy et al., 2013, Weber et al., 2003). Potential DNT–Kek interactions were tested by measuring luminescence of *drosomycin-luciferase* S2 cells expressing Kek≡Toll6 chimaeras and stimulated by DNT1 and DNT2 (purified according to Arnot et al. (2010)) or DNT2 produced using the Baculovirus system (McIlroy et al., 2013).

First, Kek≡Toll6 chimaeras were cloned for use in cell culture. Kek3, Kek4, Kek5 and Kek6 ectodomains and Toll6 intracellular regions were amplified by PCR (see Appendix II). *kek1* and *kek2* mutants are embryonic lethal (Musacchio and Perrimon, 1996), and thus no data could be obtained to indicate putative *kek1*/*2–DNT* interactions in Chapter 3. It was decided to focus on *kek3–kek6*, for which a complete data set could be obtained, and for which few data have been published. Kek3, Kek4, Kek5, Kek6 and Toll6 fragments were ligated, recombined into *pDONR*^{221} and confirmed by restriction digests (see Appendix II for maps and supporting

data). Entry clones were subsequently recombined into the destination vector *pAct5c-attR-3xHA* (*pAWH*) and confirmed by restriction digests and sequencing. No mutations or nucleotide omissions were detected in the chimaera sequences.

48 hours post-transfection, Kek3≡Toll6, Kek4≡Toll6, Kek5≡Toll6 and Kek6≡Toll6 chimaeras were detected at the cell membrane of S2 cells, thus indicating that the proteins were processed normally (Figure 4.4a). V5-tagged constructs used to synthesize full length DNT1 pro-domain, CysKnot and C-terminal domain, and DNT2 pro-domain (subsequently cleaved in cell culture) and CysKnot, from 6-well plates of seeded S2 cells, were a gift from Graham McIlroy (Hidalgo laboratory; Figure 4.4b): pro-domains of both proteins were cleaved in cell culture, as verified by Western blot (Figure 4.4c). Stimulation of chimaera-expressing cells with DNT1 and DNT2 produced and purified from S2 cell culture induced an increase in luciferase activity in positive controls — S2 cells transfected with *pAct-Toll6* (full length Toll6) — compared to cells transfected with a blank *pDONR*^{221} plasmid (Figure 4.5a,b, all results were normalized against *pActin-renilla* luciferase luminescence). For all statistical values, see Appendix I.

Although stimulation with DNT1 in PBS induced a significant increase in luciferase activity in S2 cells transfected with Kek3≡Toll6, Kek4≡Toll6 and Kek6≡Toll6 chimaeras compared to the blank plasmid control (Figure 4.5a, black labels; Student's t-test with Bonferroni correction applied in all cases; see Appendix I for statistical values), this increase was not significant compared to the chimaeras with PBS alone (red labels). Similarly, addition of DNT2 in PBS induced a significant increase in luciferase activity in S2 cells transfected with Kek3≡Toll6, Kek4≡Toll6 and Kek6≡Toll6 chimaeras only when compared to the blank plasmid control (Figure 4.5b; black stars), not when compared to chimaeras overexpression alone (red labels). This indicated that chimaera overexpression was sufficient to increase endogenous NFκB signalling, perhaps by ectopic dimerization of Toll6 Toll/Interleukin-1 receptor (TIR) domains.

Figure 4.4 **KekΞToll6 chimaeras localize to the cell membrane**

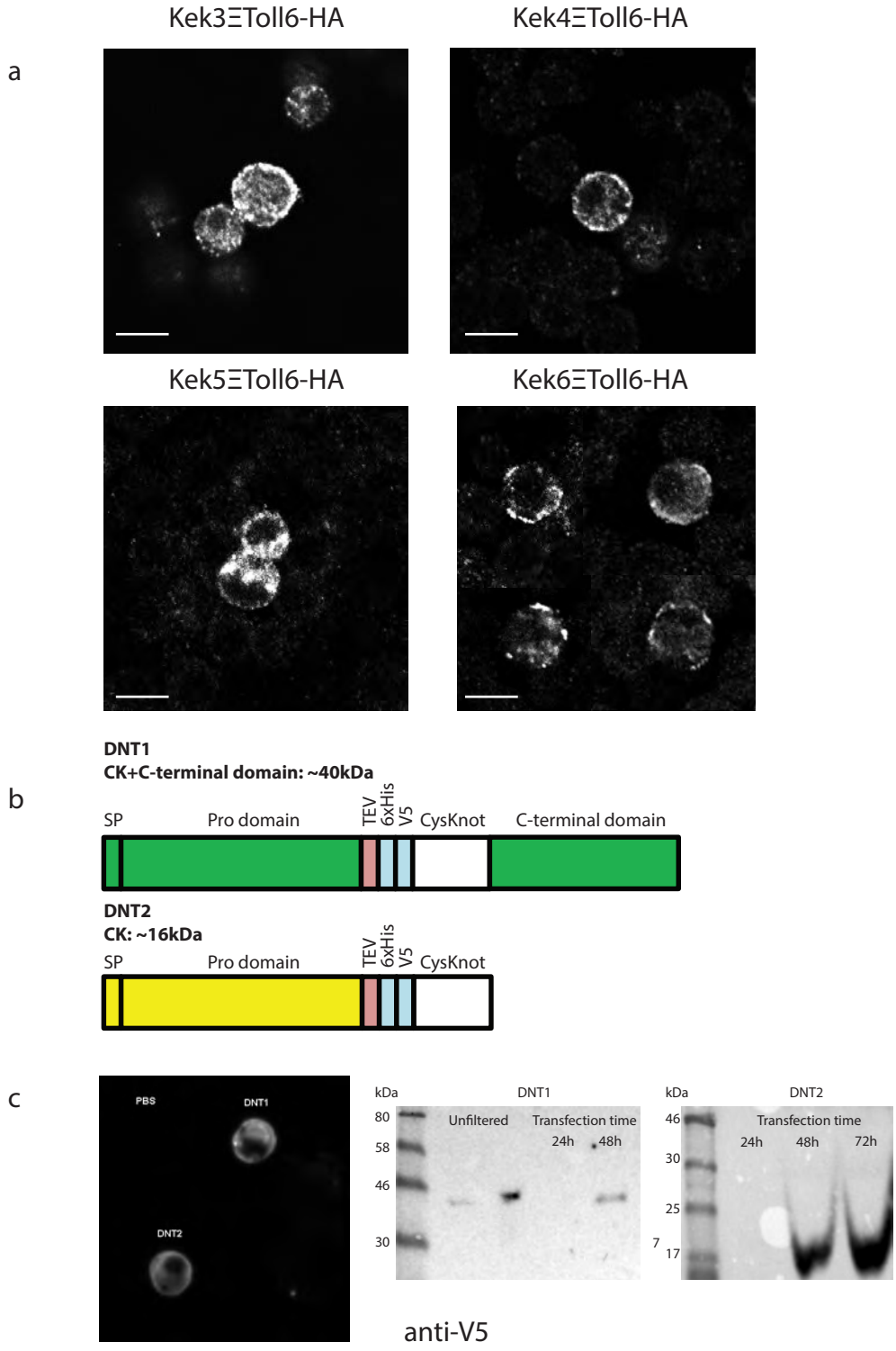

a | HA-tagged *kek3-6Ξtoll6* chimaeras were transfected into S2 cells and fluorescently labelled with anti-HA. Translated chimaeras were distributed at the cell membrane 48 hours after transfection. Kek6 images are a composite of 4 different cells. Scale bar, 10µm. **b** | *pAct5c-DNT1/2* construct models, showing the proteins produced by translation, including protein sizes, His/V5 tags and TEV site for artificial pro-domain cleavage. Both DNT1 and DNT2 spontaneously cleaved in S2 cells and TEV cleavage was unnecessary. Constructs were driven by an *actin* promoter. **c** | Protein purified according to the method in Chapter 2.4.1 was verified by dot blot analysis and Western blot using anti-V5. SP, signal peptide.

Figure 4.5 **DNT2 can interact with KekΞToll6 chimaeras to induce NFκB signalling**

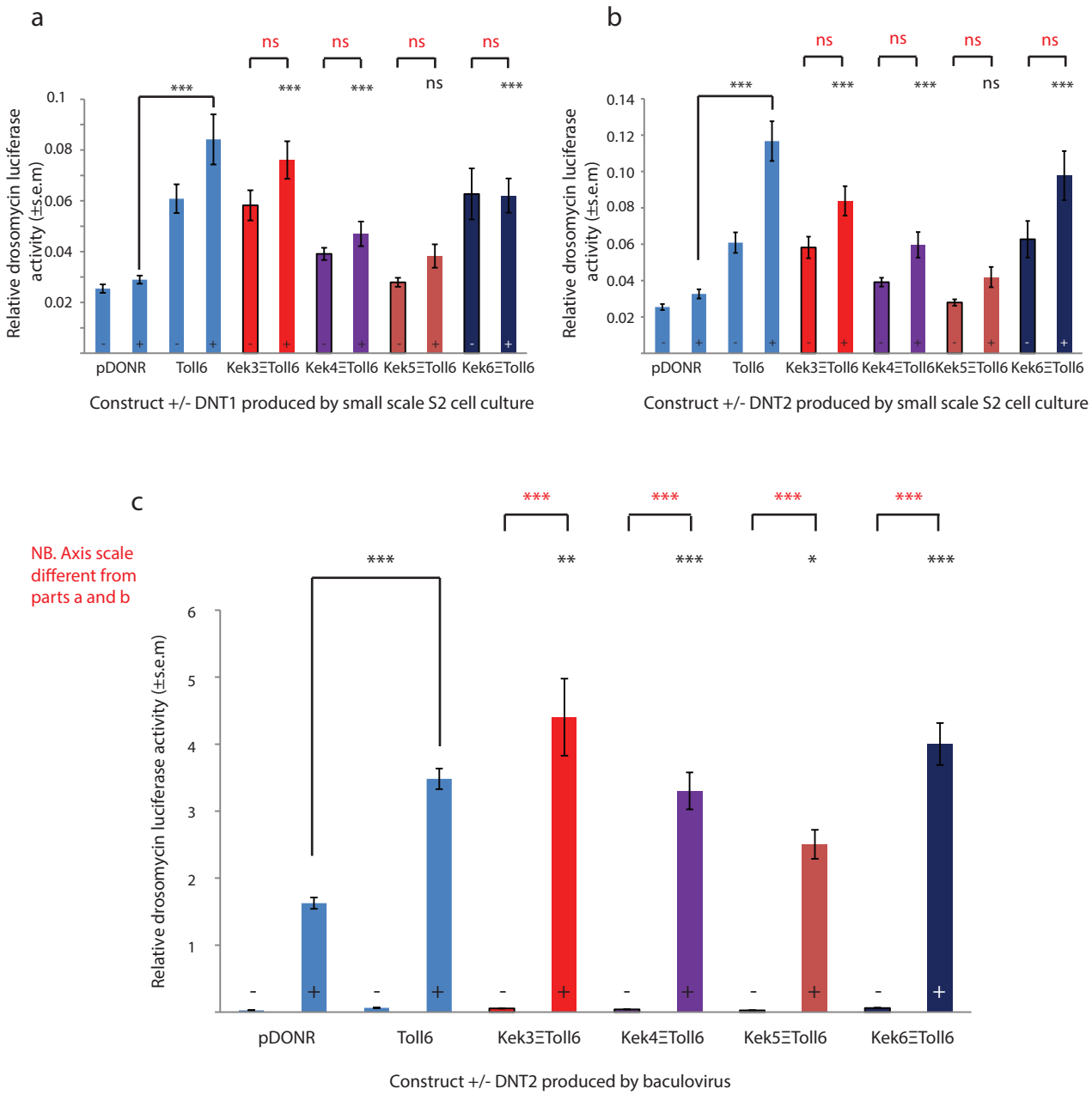

S2 cells stably transfected with *drosomycin-luciferase* and transiently transfected with *kekΞtoll6* chimaera constructs were stimulated (+) by DNT1 or DNT2 produced by small scale DNT culture from S2 cells (**a,b**) or Baculovirus (**c**). Unstimulated controls were treated with PBS (-). Luciferase activity was measured by luminescence upon addition of DualGlo substrate. **a,b** | S2 cell-produced DNT1 and DNT2 stimulation induced an increase in signalling by Kek3, Kek4 and Kek6 chimaeras compared with untranfected controls (black stars) but not with unstimulated transfected controls (red stars). **c** | Baculovirus DNT2 stimulation induced a notable increase in signalling by all chimaeras compared with untranfected controls and with unstimulated transfected controls. Kek3ΞToll6 and Kek6ΞToll6 chimaera signalling exceeded that of full length Toll6.

Baculovirus-derived DNT2, by contrast, induced a marked increase in NFκB luciferase activity (Figure 4.5c, note the increased order of magnitude compared with Figure 4.5a,b). DNT2 stimulation induced a two–three-fold increase in luciferase activity in all chimaeras compared to the blank plasmid control (black stars). DNT2 stimulation also triggered a significant increase in signalling in all chimaeras compared to chimaera upregulation alone (red stars). The greatest increase in activity was shown by Kek3≡Toll6, which had a 78-fold increase in luciferase activity. Furthermore, both Kek3≡Toll6 and Kek6≡Toll6 had increased activity compared to Toll6 upregulation alone. This suggested that Kek3 and Kek6 can signal upon binding DNT2.

The different responses to the two sources of DNT may reflect differences in ligand folding or sensitivity caused by their methods of production. The pro-domain was cleaved from both proteins in S2 cell culture, a step that is required for signalling (DeLotto and DeLotto, 1998, McIlroy, 2011). However it is unknown whether S2 cell produced DNTs are correctly folded (Arnot et al., 2010). The Baculovirus system, by comparison, uses insect cells to generate and fold proteins prior to secretion.

4.3 DISCUSSION

In this chapter, I cloned the coding sequence of the six Kek family members into Gateway entry vectors, and subsequently into *pAct5c-attR-FLAG* (*pAWF*), *pAct5c-attR-mCFP* (*pAWC*) and *pUASt-attR-mRFP* (*pTWR*) for use in cell culture and for transgenesis.

Next, I cloned Kek≡Toll6 chimaeras comprising the extracellular (ligand-binding), transmembrane and juxtamembrane regions of Kek3–6. Differences in luminescence in cells expressing these constructs reflected differences in Dif signalling by the chimaeras in response to DNT stimulation. Although the endogenous signalling role of Kek proteins remains unknown, these data indicate that DNT2–Kek interactions can induce signalling.

S2 cells express Toll family members, but lack many surface proteins present in neurons *in vivo* (Brillet et al., 2010, Tauszig et al., 2000). It was therefore important to compare signalling results with *pDONR*^{221}-transfected cells exposed to DNT stimulation to account for endogenous Toll6 signalling. Such signalling could be induced by ligand binding, or ectopic dimerization caused by Toll6 ICD overexpression.

A negative control comprising a blank or absent ectodomain with the Toll6 TIR domain was not used. The purpose of the experiment was to determine whether DNT addition could induce an increase in signalling by Kek chimaeras. Therefore, of interest was whether a difference in signalling could be induced by ligand addition, indicative of a ligand–receptor interaction, regardless of whether a basal level of NFκB signalling was induced by negative control. Without a ligand-binding site, signalling via a blank negative control would not be induced by ligand addition but by Toll6 ICD overexpression, which may result in release of signalling autoinhibition via homotypic dimerization or heterotypic dimerization with endogenous S2 cell-expressed Toll6. This basal level of signalling was therefore represented in the experimental setup by the PBS-induced chimaeras, e.g. in the chimaera+PBS to chimaera+DNT comparisons. The effect of DNT addition on endogenous Toll6 signalling was accounted for by the *pDONR*+DNT control. Nonetheless, of note were DNT2 stimulated Kek3≡Toll6 and Kek6≡Toll6, which had increased luciferase activity compared to Toll6+DNT2, thus greater than the combination of activity induced by endogenous Toll6 and by upregulation of the Toll6 TIR domain.

These results agreed with indications from Chapter 3 that the Kek proteins have roles related to the DNTs, and can bind them to induce signalling. In the next Chapter, loss of function tools were engineered for further study of this family.

CHAPTER 5

LOSS OF FUNCTION ANALYSIS REVEALS KEK INTERACTIONS WITH THE DNTS

5.1 INTRODUCTION

In Chapter 3, *kek3* and *kek4* were identified as potential *Drosophila* neurotrophin (DNT) interacting partners. In Chapter 4, a potential interaction between *kek6* and *DNT2* was also identified. However, the functions of *kek6* could not be analysed further, as alleles were unavailable. Furthermore, *kek3* and *kek4* mutants used in Chapter 3 were transposon insertions, rather than gene deletions. In this chapter, loss of function mutants for *kek3*, *kek4* and *kek6* were generated by Flippase recognition target (FRT)-mediated null mutagenesis according to the protocol in Parks et al. (2004). I determined *DNT–kek* genetic interactions using these alleles and survival assays. Furthermore, behavioural phenotypes of *kek3* and *kek4* were quantified. The mutants are then studied in further detail in Chapters 6 and 7.

Drosophila is ideally suited to genetic manipulation. Deletions can be generated by imprecise excision of P elements or chemical mutagenesis (Hummel and Klambt, 2007, Bökel, 2007). Excision of transposons by FRT-mediated null mutagenesis requires two FRT-containing *piggyBac* transposons that flank the region of interest, and that are in the correct orientation relative to the genome and to each other (Parks et al., 2004). An advantage of this method is that it creates a mutation of predictable size in the region of interest. The transposons are genetically combined with heat-shock Flippase, and crossed to one another. Heterozygous progeny bearing both transposons are subjected to heat shocks to induce recombination between the FRT elements, resulting in the break and elimination of the intervening sequences and creating a deletion (Figure 2.7). Putative mutants are then balanced to generate a stable stock. Recombination success is determined by at least two methods of PCR verification: internal genomic PCRs amplify a region internal to the deletion that should be

absent in successful recombinants, and two-sided PCR, which amplifies DNA fragments from the transposon to the flanking genomic region for each parental transposon (see Methods). This protocol is dependent on the availability of suitable transposons: *kek3*, *kek4* and *kek6*-flanking transposon lines were available, whereas suitable *kek5* transposons could not be obtained for the generation of a *kek5* null mutant by this method. Results in previous chapters identified *kek5* as a putative DNT-interacting partner; a *kek5* null, $kek5^{fe148}$, is published, but could not be obtained (Evans et al., 2009). Consequently, the role of *kek5* was not studied further.

kek3, *kek4* and *kek6* null mutants were here used to identify and verify *DNT–kek* genetic interactions, as per Chapter 3. This chapter further aimed to identify potential downstream components of Kek signalling by means of genetic rescue. Last, null mutants were used to determine adult locomotion phenotypes corresponding to total loss of function of *kek3* and *kek4*.

5.2 RESULTS

5.2.1 Generation of *kek3, kek4* and *kek6* null mutants by FRT mediated mutagenesis

I first tried to generate *kek3* null mutants using the 5′–3′ parental insertion lines $PBac[WH]CG15256^{f04709}$ (left isolate) and $PBac[WH]kek3^{f07027}$ (right isolate), which would have resulted in a 21 kb deletion (Figure 5.1a). 50 lines were generated using these parental transposons and tested by internal genomic PCR and two-sided PCR (Figure 5.2, see Appendix III for all lines tested). 42 lines produced an internal *kek3* 500nt fragment and were discarded. 2 lines did not yield an internal *kek3* fragment using internal genomic primers. (To confirm that the absence of a band was not the result of a poor DNA preparation, the 2 lines were tested by internal genomic PCR to the unaffected *kek6* CDS. For both lines a 500nt *kek6* fragment was obtained) Two-sided PCR using these lines did not yield expected 200nt bands. Thus, the lines were disregarded. The parental line $kek3^{f04709}$ did not yield an expected 200nt

Figure 5.1 ***kek3* mutagenesis**

a

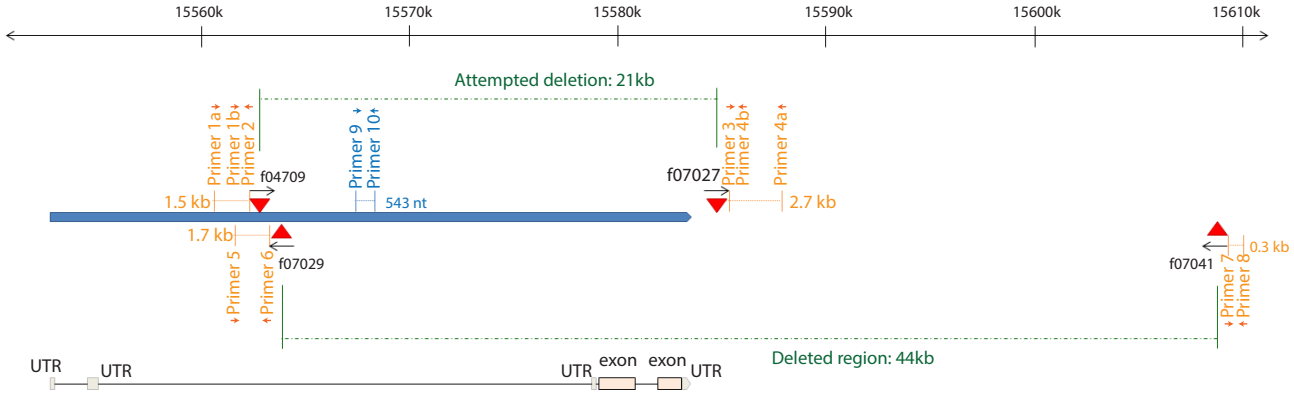

b Two-sided PCR

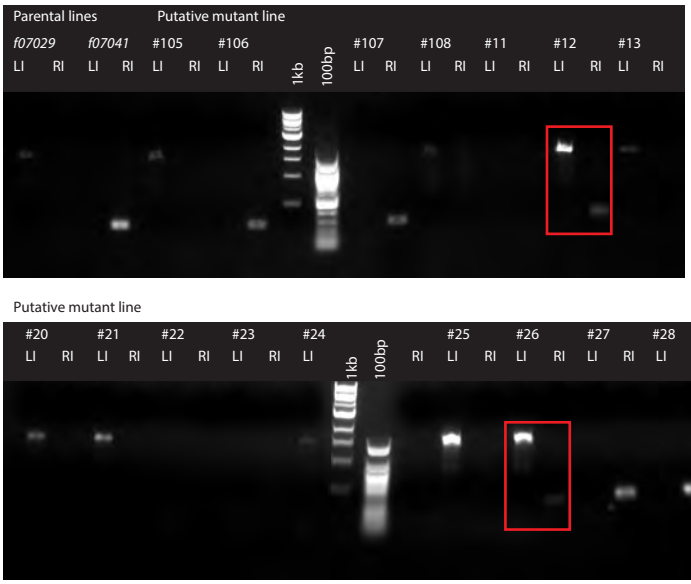

LI/RI = Two-sided PCR for 5′ (left)/3′ (right) transposon

c Internal genomic PCR

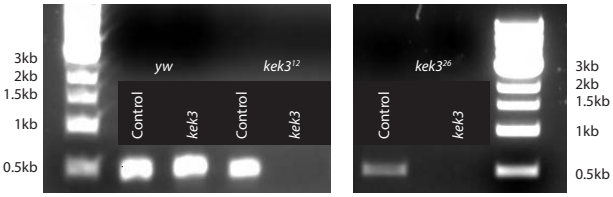

Control fragment: *kek6* internal genomic PCR

a | *piggyBac* transposon lines *kek3*^{f07029} and *kek3*^{f07041} were used to generate a 44kb deletion encompassing the entire coding sequence of *kek3*. **b** | Two mutant alleles, *kek3*^{12} and *kek3*^{26} were identified by two-sided PCR. Both lines tested positive for both left and right isolate parental transposon elements. **c** | *kek3* deletion was verified in both lines by internal genomic PCR. Homozygous *kek3*^{12} and *kek3*^{26} flies lacked an internal *kek3* fragment.

Figure 5.2 ***kek3* null verification primers**

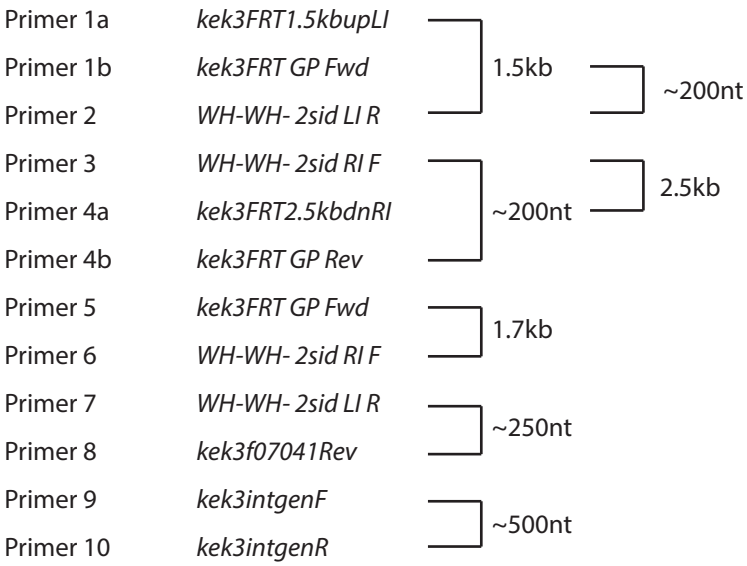

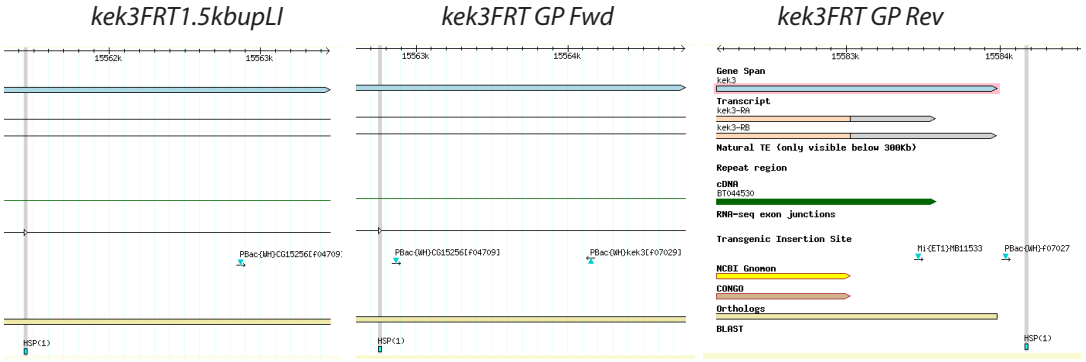

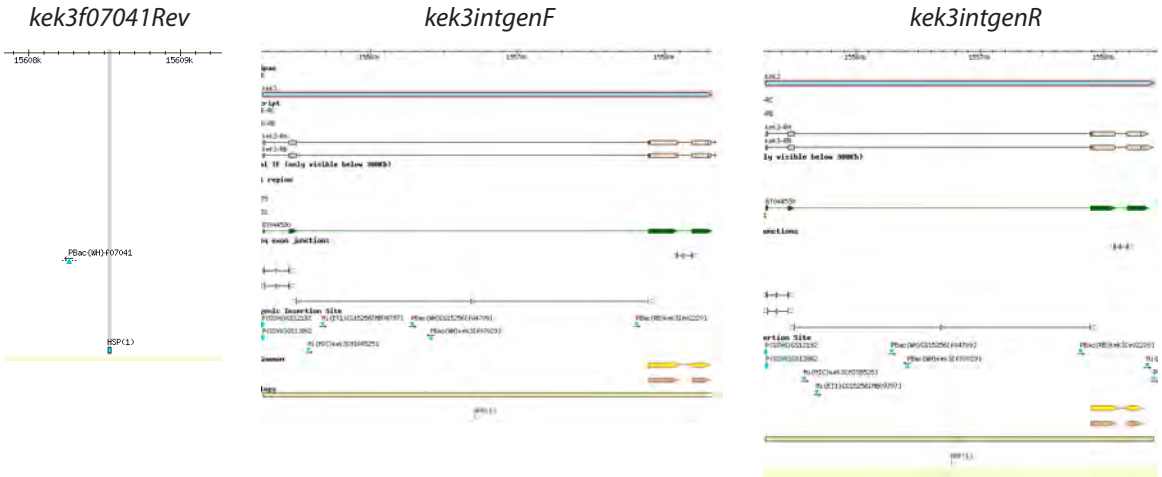

Primer details for Figure 5.1a. Primer hybridisation to regions identified in Figure 5.1 is highlighted by BLAST searches of the *Drosophila* genome.

fragment from left isolate two-sided PCR primers, and was therefore deemed to be the cause of the unsuccessful mutagenesis. Thus, this method was unsuccessful.

The generation of an alternative 44 kb deletion between the 3′–5′ parental insertion lines *PBac[WH]kek3*^{f07029} (left isolate) and *pBac[WH]f07041* (right isolate) was attempted (Figure 5.1a). Parental lines tested positive for two-sided PCR fragments (Appendix III). 108 lines were generated by Alicia Hidalgo, of which 54 were tested by myself by two-sided and internal genomic PCRs (Figure 5.2). 13 lines tested positive for the left isolate two-sided PCR fragment (Figure 5.1b). Of these, 2 lines, *kek3*^{12} and *kek3*^{26}, further tested positive for the right isolate two-sided PCR fragment (Figure 5.1b). *kek3*^{12} and *kek3*^{26} were verified as nulls by internal genomic PCR using homozygous flies (Figure 5.1c).

The generation of a 0.9 kb *kek4* deletion between the 3′–5′ parental insertion line *pBac[WH]kek4*^{f05454} (left isolate) and the 5′–3′ parental line *pBac[RB]e04257* (right isolate) was attempted (Figure 5.3a). I generated 50 lines using these parental transposons and tested by PCR (Appendix III, Figure 5.4). No nulls were generated, but parental lines tested positive using respective two-sided PCR primersThe protocol was repeated and a further 63 lines were generated and tested. 35 lines tested positive for the left isolate two-sided PCR fragment (Figure 5.3b). Four of these lines — *kek4*^{20}, *kek4*^{23}, *kek4*^{42}, *kek4*^{50} — also tested positive for the right isolate two-sided PCR fragment (Figure 5.3b). *kek4*^{20} and *kek4*^{23} were confirmed as successful mutants by internal genomic PCR (Figure 5.3c).

The generation of a 41.9 kb *kek6* deletion between the 5′–3′ parental insertion line *pBac[RB]e00907* (left isolate) and the 3′–5′ parental line *pBac[WH]f05733* (right isolate) were attempted (Figure 5.5a). Parental lines tested positive for respective two-sided PCR fragments. I generated 50 lines using these parental transposons and tested by PCR (Appendix III, Figure 5.4). Two lines —*kek6*^{34} and *kek6*^{35} — tested positive for the left isolate two-sided PCR fragment (Figure 5.5b). Both of these lines also tested positive for the right isolate two-

Figure 5.3 ***kek4* mutagenesis**

a

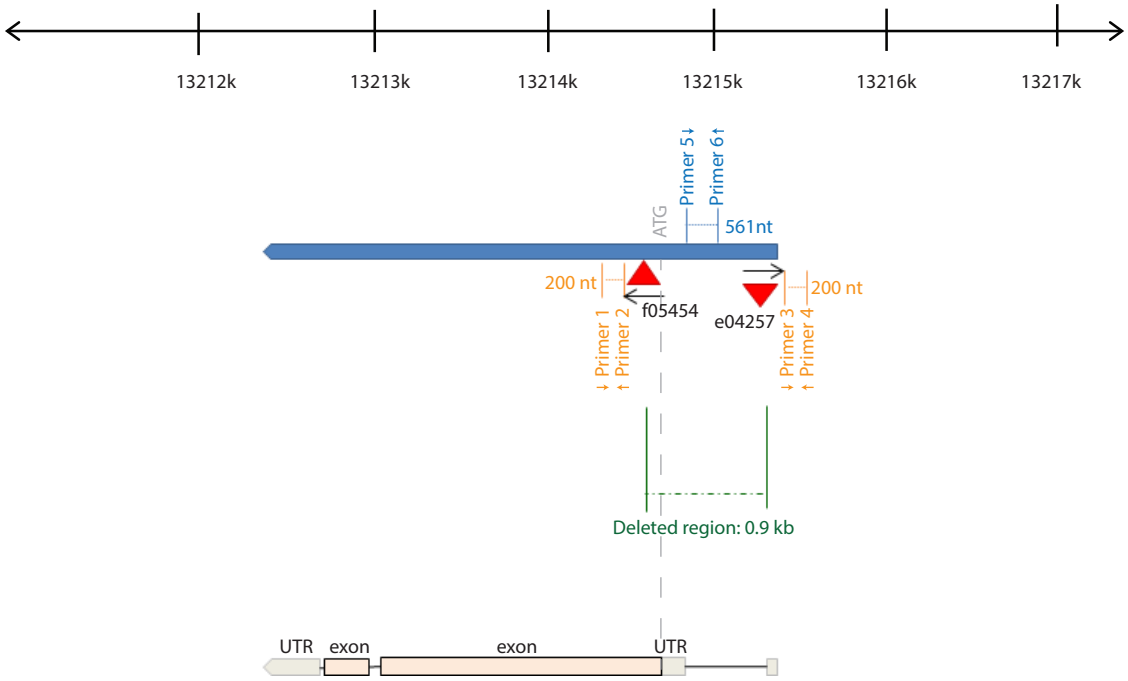

b Two-sided PCR

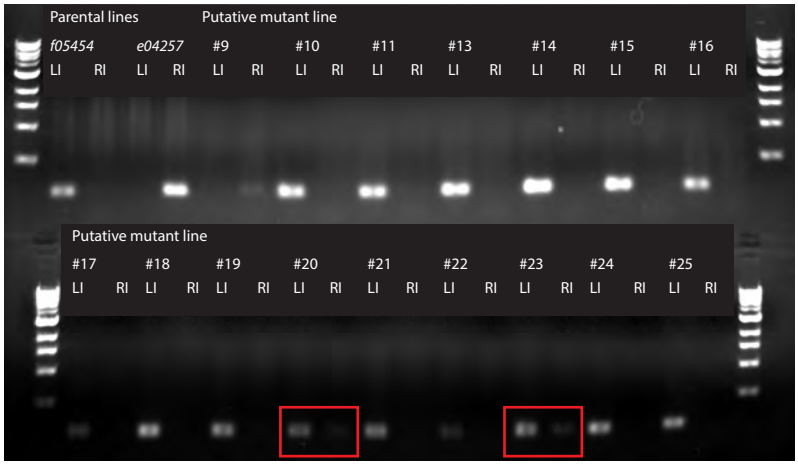

LI/RI = Two-sided PCR for 5′ (left)/3′ (right) transposon

c Internal genomic PCR

Control fragment: *kek6* internal genomic PCR

a | *piggyBac* transposon lines *kek4*^{f05454} and *kek4*^{e04257} were used to generate a 0.9kb deletion encompassing the start codon of *kek4*. **b** | Four mutant alleles, including *kek4*^{20} and *kek4*^{23} were identified by two-sided PCR. Both lines tested positive for both left and right isolate parental transposon elements. **c** | *kek4* deletion was verified in both lines by internal genomic PCR. Homozygous *kek4*^{20} and *kek4*^{23} flies lacked an internal *kek4* fragment.

Figure 5.4 ***kek4* and *kek6* null verification primers**

kek4

Primer 1	*kek4FRT GP Fwd*	~200nt
Primer 2	*WH-WH- 2sid RI F*	
Primer 3	*WH-WH- 2sid RI F*	~200nt
Primer 4	*kek4FRT GP Rev*	
Primer 5	*kek4intgenF*	~500nt
Primer 6	*kek4intgenR*	

kek4intgenF

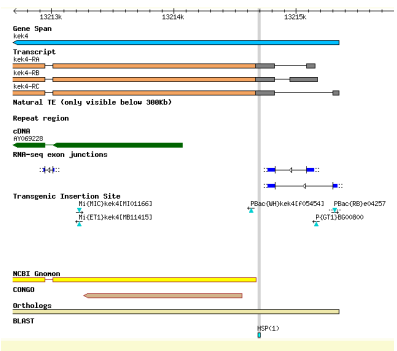

kekFRT GP Fwd

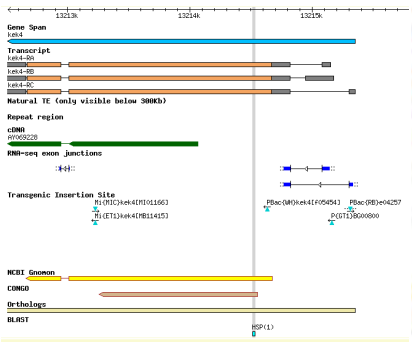

kek4FRT GP Rev

kek4intgenR

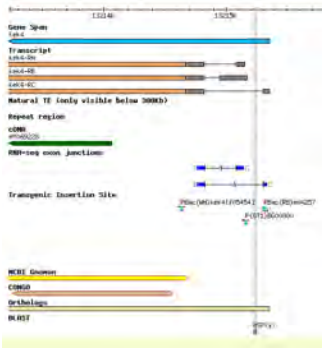

kek6

Primer 1	*kek6FRT GP Fwd*	~200nt
Primer 2	*WH-WH- 2sid LI R*	
Primer 3	*WH-WH- 2sid LI R*	~200nt
Primer 4	*kek6FRT GP Rev*	
Primer 5	*kek6intgenF*	~500nt
Primer 6	*kek6intgenR*	

kek6intgenF

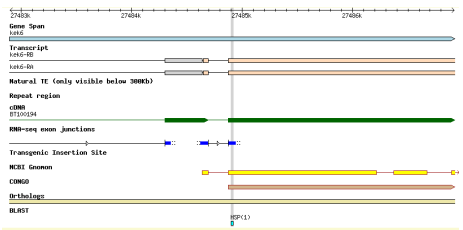

kek6FRT GP Fwd

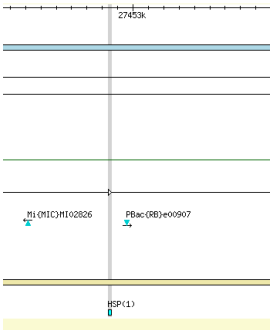

kek6FRT GP Rev

kek6intgenR

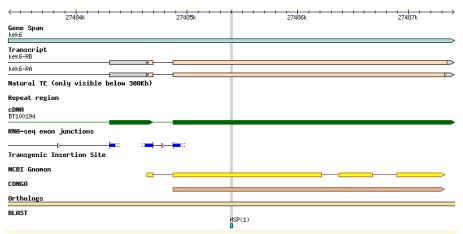

Primer details for Figure 5.3a and 5.5a. Primer hybridisation to regions identified in each figure is highlighted by BLAST searches of the *Drosophila* genome.

Figure 5.5 ***kek6* mutagenesis**

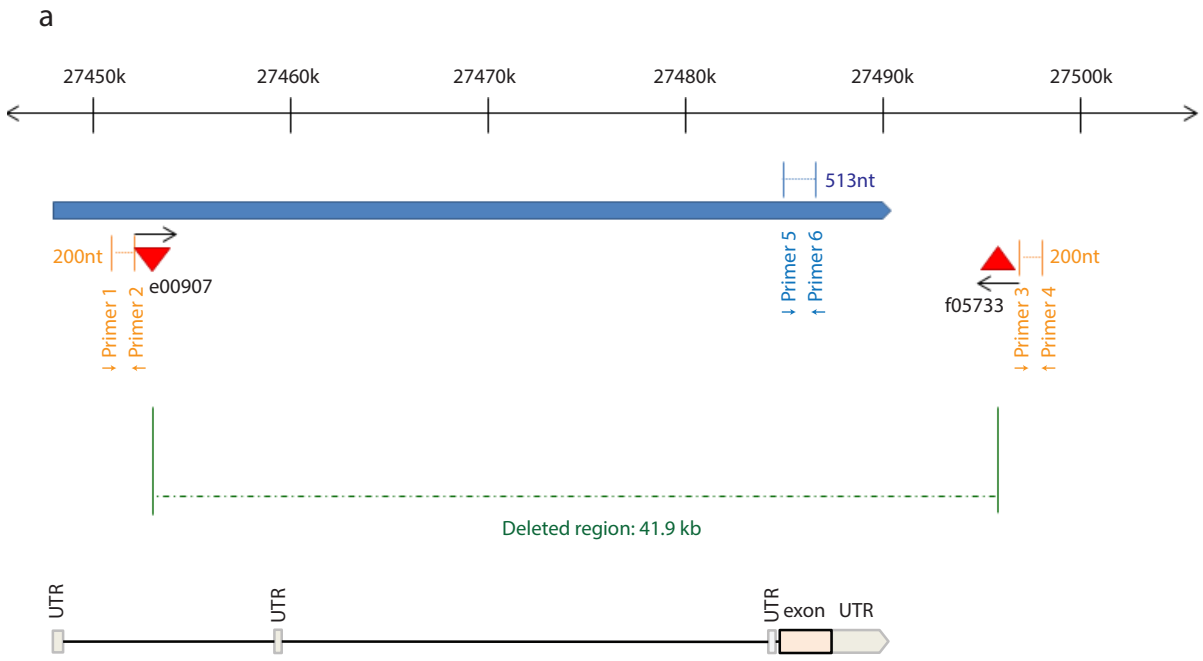

b Two-sided PCR

LI/RI = Two-sided PCR for 5′ (left)/3′ (right) transposon

c Internal genomic PCR

Control fragment: *kek3* internal genomic PCR

a | *piggyBac* transposon lines *kek6*^{e00907} and *kek6*^{f05733} were used to generate a 41.9kb deletion encompassing the entire coding sequence of *kek6*. **b** | Two mutant alleles, *kek6*^{34} and *kek6*^{35} were identified by two-sided PCR. Both lines tested positive for both left and right isolate parental transposon elements. **c** | *kek6* deletion was verified in both lines by internal genomic PCR. Heterozygous *kek6*^{34}*/Df(3R)ED6361* and *kek6*^{35}*/Df(3R)ED6361* flies lacked an internal *kek6* fragment.

sided PCR fragment (Figure 5.5b). *kek6*^{34} and *kek6*^{35} were crossed *in trans* with *Df(3R)ED6361* (hereafter *Df(kek6)*) to test by internal genomic PCR. No internal band could be amplified, thereby confirming the lines as mutants (Figure 5.5c). DNA preparation validity was confirmed by internal genomic PCR to the unaffected *kek3* locus.

Parental transposon lines chosen for *kek3* and *kek6* mutagenesis flanked the entire translated region of the genes, whereas parental transposon lines for the *kek4* deletion exposed some of the *kek4* coding sequence but deleted the start codon (Figures 5.1, 5.3, 5.5).

5.2.2 *DNT–kek* genetic interactions

When balanced over *TM6B* and kept at 18^{0}C, the viability of single *DNT* mutant alleles is impaired relative to an expected Mendelian S.I. of 1 (Figure 3.11a, Figure 5.6). Under these same conditions, the double mutant *DNT2*^{e03444}*DNT1*^{41} is homozygous lethal (*DNT2*$^{-/-}$*DNT1*$^{-/-}$; see Chapter 3.2.2.1). In Chapter 3, I recreated these conditions and tested the survival of single and double mutants of the candidate receptors, using transposon insertion alleles. Here, I test the viability of FRT mutagenesis-derived *kek3*, *kek4* and *kek6* null mutants. I calculated the S.I. for *kek3*^{12}, *kek3*^{26}, *kek4*^{20}, *kek4*^{23}, *kek6*^{34} and *kek6*^{35} alleles. Furthermore, I tested the viability of *DNT–kek* double mutants to determine ligand–receptor genetic interactions. Raw data and full genotypes are shown in Tables 5.1 and 5.2, statistical values are shown in Appendix I.

At 18°C, parental *kek3*^{12}*/TM6B* flies were crossed and pupal phenotypes of progeny were scored. If *kek3*^{12} were lethal, only heterozygous, *Tb*$^{-}$ pupae would be observed, whereas a viable allele would yield *Tb*$^{+}$ (*kek3*$^{12/12}$) progeny. Using this experimental setup, the single alleles *kek3*^{12}, *kek3*^{26}, *kek4*^{20}, *kek4*^{23} were viable (Figure 5.6a, Table 5.1). In addition, the heteroallelic mutants *kek3*$^{12/26}$ and *kek4*$^{20/23}$ were viable, as determined by crossing *kek3*^{12}*/TM6B* with *kek3*^{26}*/TM6B* and *kek4*^{20}*/TM6B* with *kek4*^{23}*/TM6B*, and scoring pupal phenotypes. Under these same experimental conditions, *kek3*$^{12/12}$;*DNT1*$^{-/-}$ and

Figure 5.6 ***kek3* and *kek4* interact genetically with the *DNTs***

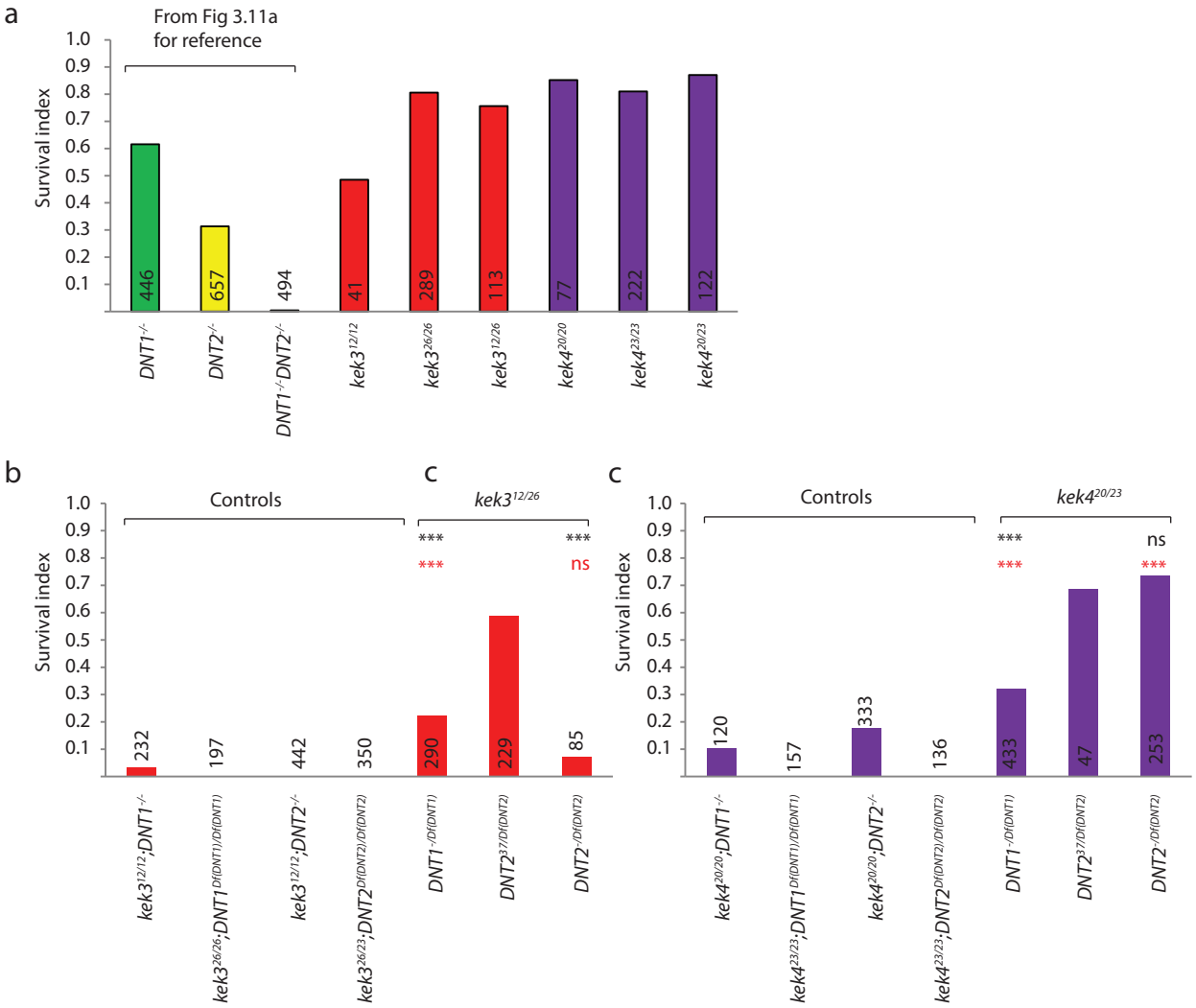

Interactions between *kek3* and *kek4* alleles and *DNT* alleles were determined using the survival index. **a** | Single receptor mutants are not lethal. **b,c** | Survival indices of *kek3DNT* and *kek4DNT* double mutants in homozygosis and heteroallelic combinations are compared. *kek3* mutants genetically interact with both *DNT1* and *DNT2*, whereas in heteroallelic genotypes, *kek4* mutants interact genetically with *DNT1* alleles only. All parental lines balanced over *TM6B* and reared at 18ºC. Statistics compare double mutants with single receptor mutants (black stars) or with single *DNT* mutants (red stars). See Table 5.1 for full genotypes and raw data, and Appendix I for statistical vaues. *Df(DNT1)* = *Df(3L)Exel6101*, *Df(DNT2)* = *Df(3L)ED6092*.

Table 5.1 ***kek* null allele survival assays, Raw data, 18^{0}C experiments**

Abbreviation	Progeny of	n	Tb$^-$	Tb$^+$	Survival index
DNT1$^{-/-}$	*DNT1*^{41}/*TM6B*	446	341	105	0.616
DNT2$^{-/-}$	*DNT2*^{e03444}/*TM6B*	657	568	89	0.313
DNT1$^{-/-}$*DNT2*$^{-/-}$	*DNT1*^{41} *DNT2*^{e03444}/*TM6B*	494	493	1	0.004
kek3$^{12/12}$	*kek3*^{12};+/*SM6aTM6B*	41	33	8	0.485
kek3$^{26/26}$	*kek3*^{26};+/*SM6aTM6B*	289	206	83	0.806
kek3$^{12/26}$	*kek3*^{12};+/*SM6aTM6B* x *kek3*^{26};+/*SM6aTM6B*	113	82	31	0.756
kek4$^{20/20}$	*kek4*^{20};+/*SM6aTM6B*	77	54	23	0.852
kek4$^{23/23}$	*kek4*^{23};+/*SM6aTM6B*	222	158	64	0.810
kek4$^{20/23}$	*kek4*^{20};+/*SM6aTM6B* x *kek4*^{23};+/*SM6aTM6B*	122	85	37	0.871
kek3$^{12/12}$*DNT1*$^{-/-}$	*kek3*^{12};*DNT1*^{55}/*SM6aTM6B*	232	228	4	0.035
kek3$^{26/26}$*DNT1*$^{Df(DNT1)/Df(DNT1)}$	*kek3*^{26};*Df(3L)Exel6101/SM6aTM6B*	197	197	0	0
kek3$^{12/12}$*DNT2*$^{-/-}$	*kek3*^{12};*DNT2*^{e03444}/*SM6aTM6B*	442	442	0	0
kek3$^{26/26}$*DNT2*$^{Df(DNT2)/Df(DNT2)}$	*kek3*^{26};*Df(3L)ED6092/SM6aTM6B*	350	350	0	0
kek3$^{12/26}$ *DNT1*$^{-/Df(DNT1)}$	*kek3*^{26};*Df(3L)Exel6101/SM6aTM6B* x *kek3*^{12};*DNT1*^{55}/*SM6aTM6B*	290	261	29	0.222
DNT2$^{37/Df(DNT2)}$	*kek3*^{12};*DNT2*^{37}/*SM6aTM6B* x *kek3*^{26};*Df(3L)ED6092/SM6aTM6B*	229	177	52	0.588
DNT2$^{-/Df(DNT2)}$	*kek3*^{12};*DNT2*^{e03444}/*SM6aTM6B* x *kek3*^{26};*Df(3L)ED6092/SM6aTM6B*	85	82	3	0.073
kek4$^{20/20}$*DNT1*$^{-/-}$	*kek4*^{20};*DNT1*^{55}/*SM6aTM6B*	120	114	6	0.105
kek4$^{23/23}$*DNT1*$^{Df(DNT1)/Df(DNT1)}$	*kek4*^{23};*Df(3L)Exel6101/SM6aTM6B*	157	157	0	0
kek4$^{20/20}$*DNT2*$^{-/-}$	*kek4*^{20};*DNT2*^{e03444}/*SM6aTM6B*	333	306	27	0.176
kek4$^{23/23}$*DNT2*$^{Df(DNT2)/Df(DNT2)}$	*kek4*^{23};*Df(3L)ED6092/SM6aTM6B*	136	136	0	0
kek4$^{20/23}$ *DNT1*$^{-/Df(DNT1)}$	*kek4*^{20};*DNT1*^{55}/*SM6aTM6B* x *kek4*^{23};*Df(3L)Exel6101/SM6aTM6B*	433	373	60	0.322
DNT2$^{37/Df(DNT2)}$	*kek4*^{23};*Df(3L)ED6092/SM6aTM6B* x *kek4*^{20};*DNT2*^{37}/*SM6aTM6B*	47	35	12	0.686
DNT2$^{-/Df(DNT2)}$	*kek4*^{20};*DNT2*^{e03444}/*SM6aTM6B* x *kek4*^{23};*Df(3L)ED6092/SM6aTM6B*	253	185	68	0.735
kek6^{34}	*kek6*^{34}/*TM6B*	482	482	0	0
kek6$^{34/Df(kek6)}$	*kek6*^{34}/*TM6B* x *Df(3R)ED6361/TM6BlacZ*	479	263	216	1.643
kek6^{35}	*kek6*^{35}/*TM6B*	190	187	3	0.032
kek6$^{35/Df(kek6)}$	*kek6*^{35}/*TM6B* x *Df(3R)ED6361/TM6BlacZ*	87	64	23	0.719
kek6$^{34/35}$	*kek6*^{34}/*TM6B* x *kek6*^{35}/*TM6B*	392	379	13	0.069
kek6$^{34/35}$ *DNT1*$^{-/Df(DNT1)}$	*kek6*^{34}*Df(3L)ED4342/TM6B* x *DNT1*^{41}*Df(3R)ED6361/TM6B*	169	102	67	1.314
DNT2$^{-/Df(DNT2)}$	*Df(3R)ED6361DNT2*^{e03444}/*TM6B* x *kek6*^{34}*Df(3L)6092/TM6B*	78	61	17	0.557
Tie$^{5/Df(Tie)}$	*kek6*^{34}*Df(3L)ED4342/TM6B* x *Tie*^{5}*Df(Q3R)ED6361/TM6B*	236	168	68	0.810

Table 5.2 ***kek* null allele survival assays, Raw data, 25^{0}C experiments**

Abbreviation	Progeny of	n	Tb^-	Tb^+	Survival index
kek6$^{34/35}$	*kek6^{34}/TM6B* x *kek6^{35}/TM6B*	435	400	35	0.175
kek6$^{34/34}$elavGal4	*kek6^{34}elavGal4/TM6BlacZ*	148	147	1	0.014
kek6$^{34/342}$4BGal4	*kek6^{34}24BGal4*	401	401	0	0
UASDNT1CK3'+;kek6$^{35/35}$	*UASDNT1CK3'+;kek6^{35}/TM6BlacZ*	208	207	1	0.010
UASkek6;kek6$^{35/35}$	*UASkek6RFP;kek6^{35}/SM6aTM6B*	110	110	0	0
kek6$^{34/35}$					
elavGal4>UASDNT1CK3'+	*kek6^{34}elavGal4/TM6BlacZ* x *UASDNT1CK3'+;kek6^{35}/TM6BlacZ*	251	178	73	0.820
24BGal4>UASDNT1CK3'+	*kek6^{34}24BGal4/TM6BlacZ* x *UASDNT1CK3'+;kek6^{35}/TM6BlacZ*	97	90	7	0.156
kek6$^{34/35}$, elavGal4					
UASactRho	*kek6^{34}elavGal4/TM6B* x *UASRho1$^{V14-E40L}$;kek6^{35}/TM6B*	188	158	30	0.380
UASactCdc42	*kek6^{34}elavGal4/TM6B* x *UAScdc42^{V12};kek6^{35}/TM6B*	162	130	32	0.492
UASkek6	*kek6^{34}elavGal4/TM6B* x *UASkek6RFP;kek6^{35}/SM6aTM6B*	245	211	34	0.323

kek3$^{12/12}$;*DNT2*$^{-/-}$ double mutants were lethal (Figure 5.6b). Comparing heteroallelic double mutants, viability was reduced in *kek3*$^{12/26}$;*DNT1*$^{-/Df(DNT1)}$ and *kek3*$^{12/26}$;*DNT2*$^{-/Df(DNT2)}$ double mutants compared to *kek3*$^{12/26}$ (Figure 5.6b, black stars; χ^2 with Bonferroni correction in all cases — *Df(DNT1)* is *Df(3L)Exel6101*, and *Df(DNT2)* is *Df(3L)ED6092*). Viability was also reduced in *kek3*$^{12/26}$;*DNT1*$^{-/Df(DNT1)}$ double mutants compared to *DNT1*$^{-/-}$ (red stars).This suggested a genetic interaction between *kek3* and *DNT1* alleles.

Homozygous *kek4*$^{20/20}$;*DNT1*$^{-/-}$ and *kek4*$^{20/20}$;*DNT2*$^{-/-}$ double mutants had reduced viability compared to single receptor mutants (Figure 5.6c). Viability of heteroallelic *kek4*$^{20/23}$;*DNT1*$^{-/Df(DNT1)}$ double mutants was reduced compared to *kek4*$^{20/23}$ (Figure 5.6c; black stars), and compared to *DNT1*$^{-/-}$ (red stars). Conversely, *kek4*$^{20/23}$;*DNT2*$^{-/Df(DNT2)}$ and *kek4*$^{20/23}$;*DNT2*$^{37/Df(DNT2)}$ double mutants were viable (Figure 5.6c). This suggested a genetic interaction between *kek4* and *DNT1* alleles.

The two *kek6* null alleles *kek6*^{34} and *kek6*^{35} caused embryonic lethality in homozygosis but were viable over *Df(kek6)* (Figure 5.7a; see Appendix I for full genotypes and statistics). Heteroallelic *kek6*$^{34/35}$ single mutants were also lethal.

The heteroallelic *DNT1*$^{-/Df(DNT1)}$*kek6*$^{34/Df(kek6)}$ double mutant was viable (Figure 5.7b). Conversely, viability was reduced in *DNT2*$^{-/Df(DNT2)}$*kek6*$^{34/Df(kek6)}$ and Tie$^{5/Df(Tie)}$*kek6*$^{34/Df(kek6)}$ double mutants compared with *kek6*$^{34/Df(kek6)}$ (Figure 5.7b; black stars — *Df(Tie)* is *Df(3L)ED4342*). The *tie*^{5} mutant allele was generated by Alice Lowry, in our laboratory, by FRT-mediated mutagenesis. This result suggested a genetic interaction between *kek6* and *DNT2*, and *kek6* and *tie*.

At 25^{0}C, *kek6*$^{34/35}$ single mutants were partially viable (Figure 5.7c, Table 5.2). This was rescued by neuronal expression of *UASDNT1CK3′*+, which encodes the DNT1 CysKnot and a 3′ tail. By contrast, overexpression of *UASDNT1CK3′*+ at the muscle did not rescue *kek6*$^{34/35}$ lethality. Furthermore, *kek6*$^{34/35}$ lethality was rescued by neuronal expression of activated *Rho*

Figure 5.7 ***kek6* genetically interacts with *DNT2***

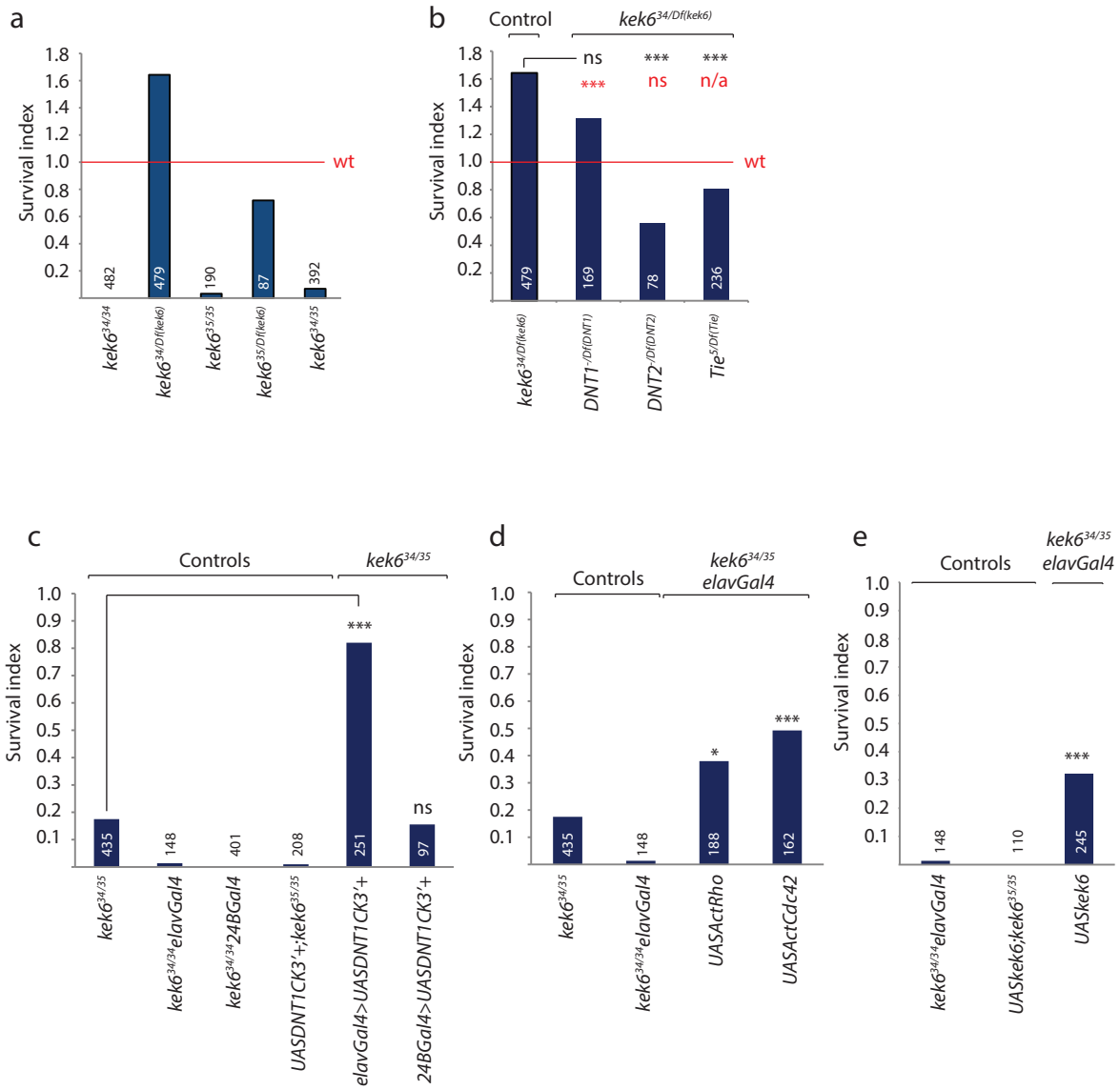

Interactions between *kek6* null alleles and DNT alleles were determined using the survival index. **a** | Single receptor mutants were lethal in homozygosis and in heteroallelic combinations, but were viable over the deficiency *Df(kek6)*. **b** | *kek6* mutants interacted genetically with *DNT2* and *Tie* to reduce viability. *kek6DNT1* double mutants were viable. Statistics compare double mutants with single receptor mutants (black stars) or with single *DNT* mutants (red stars). **c** | The lethality of heteroallelic *kek6* loss of function alleles could be rescued by neuronal, but not muscular, upregulation of the DNT1 CysKnot and 3' tail. **d,e** | The lethality of heteroallelic *kek6* loss of function alleles could be partially rescued by neuronal upregulation of activated Rho and Cdc42 (**d**), and by neuronal overexpression of *kek6* (**e**). See Tables 5.1-5.2 for full genotypes and raw data, and Appendix I for statistical values. *Df(kek6)* = *Df(3R)ED6361*, *Df(Tie)* and *Df(DNT1)* = *Df(3L)ED4342*. *Df(DNT2)* = *Df(3L)ED6092*.

and activated *Cdc42* alleles (Figure 5.7d). *kek6*$^{34/35}$ lethality was partially rescued by neuronal expression of *UASkek6* (Figure 5.7e).

5.2.3 *kek3* and *kek4* nulls affect locomotion

To test the function of *kek3* and *kek4*, homozygous *kek3*$^{12/12}$ and *kek4*$^{20/20}$ adults were filmed as per the locomotion assay used in Chapter 3. *kek3*^{12} and *kek4*^{20} alleles were generated in a w^- background. Both *kek3*$^{12/12}$ and *kek4*$^{20/20}$ travelled significantly less far than *yw* (Figure 5.8a; One-Way ANOVA with Dunnett's post hoc, see Appendix I for statistical values). *kek3* and *kek4* nulls rested significantly more often than *yw* (Figure 5.8b; χ^2 with Bonferroni correction in both cases). When moving, both null alleles wobbled more than *yw* controls, the phenotype strongest in *kek4*$^{20/20}$ adults (Figure 5.8c; χ^2 with Bonferroni correction in both cases). The stronger phenotype of *kek4*$^{20/20}$ adults was reflected by short locomotion traces (Figure 5.8d). Both null allele traces revealed that movement of *kek3* and *kek4* mutant adult flies was dramatically reduced compared to *yw* controls, which walked around the perimeter of the Petri dish. Travelling speed histograms reveal that both *kek3*$^{12/12}$ and *kek4*$^{20/20}$ flies moved at slower speeds far more frequently than *yw* (Figure 5.8e; Kruskal-Wallis with Dunn's post hoc).

5.3 DISCUSSION

In this chapter, I generated null mutant alleles of *kek3*, *kek4* and *kek6*, with the help of A. Hidalgo, by a genetic method that recombines FRT-containing transposons, deleting the genomic region in between. Using these mutants, I determined interactions between these genes and the *DNTs*. Potential components in the *kek6* signalling pathway were also identified using genetics. Last, *kek3* and *kek4* null adults had locomotion phenotypes.

Of the Kek family, transposon lines were only available to carry out the genomic deletion of *kek3, kek4* and *kek6* by the Parks et al. (2004) method. Along with the *kek1*^{RM2} and *kek1*^{RA5} (Musacchio and Perrimon, 1996), and *kek5*^{fe148} alleles (Evans et al., 2009), these new alleles

Figure 5.8 ***kek3* and *kek4* are required for adult locomotion**

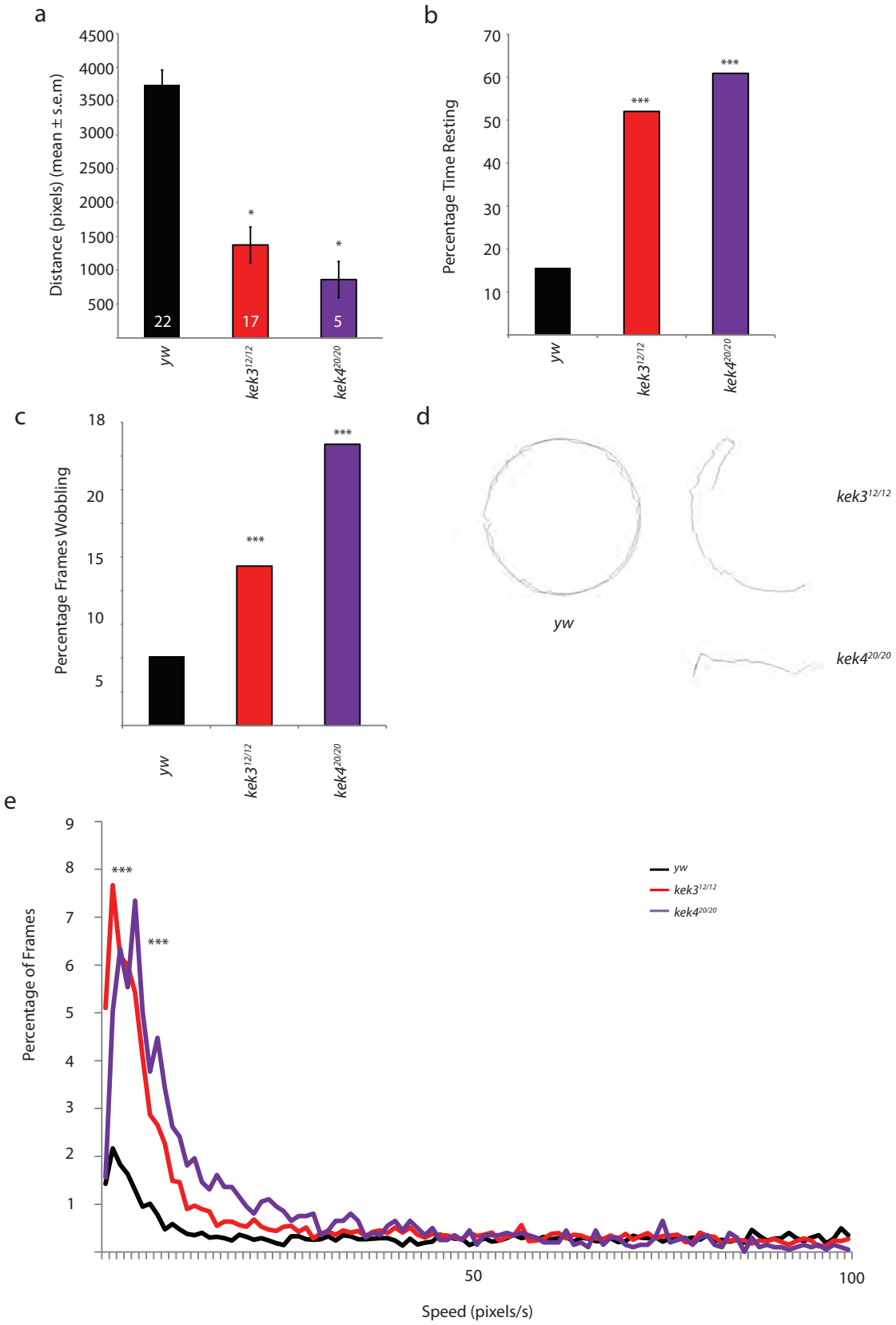

Adult single and double mutant flies were filmed walking around a Petri dish and their trajectory parameters quantified. **a-c** | *kek3*$^{12/12}$ and *kek4*$^{20/20}$ mutant flies travel shorter distances (**a**), rest more frequently (**b**) and wobble more (**c**) compared with *yw* controls. Total film numbers are shown for each genotype in **a**. **d** | Example trajectories of control (*yw*) and mutant genotypes. **e** | Speed histograms of mutant flies compared with *yw*. *kek3* and *kek4* alleles significantly reduce adult walking speed. Frame numbers, full genotypes and statistical values are shown in Appendix I.

create a set of null mutants for all *kek* genes, except *kek2*. *kek2* knockdown could be studied using available RNAi lines in future studies (Guan et al., 2005).

kek3^{12}, *kek3*^{26}, *kek4*^{20} and *kek4*^{23} alleles were viable in homozygosis. Furthermore, each line had a comparable effect on lethality. The lower S.I. of *kek3*$^{12;+}$*/SM6aTM6B* may be attributed to a low sample size.

It is unclear which S.I. results to focus on among the *DNT–kek* combinations. In Chapter 3, viability was assessed in homozygous single and double mutant progeny — for example, *kek4*$^{f05454/f05454}$ (*kek4*$^{-/-}$) — by crossing parents with the allele balanced over *TM6B*. In this chapter, heterozygous single and double mutant progeny were scored as well as homozygous progeny — for example, *kek4*$^{20/23}$ as well as *kek4*$^{20/20}$. These revealed that *kek3*$^{12/12}$;*DNT1*$^{-/-}$ and *kek3*$^{12/12}$*;DNT2*$^{-/-}$ double mutants were homozygous lethal. *kek4*$^{20/20}$*;DNT1*$^{-/-}$ and *kek4*$^{20/20}$*;DNT2*$^{-/-}$ double mutants were partially viable in homozygosis. These results confirm the findings of Chapter 3, from which Kek3 and Kek4 were thought to bind DNT2. The results in this chapter also suggest that Kek3 could interact with DNT1.

However, conclusions differ when comparing heteroallelic single and double mutants (Figure 5.6b,c). In these cases, *kek3*$^{12/26}$*;DNT1*$^{-/Df(DNT1)}$ and *kek3*$^{12/26}$*;DNT2*$^{-/Df(DNT2)}$ double mutants had reduced viability. However, *kek4*$^{20/23}$*;DNT2*$^{-}$*/*$^{Df(DNT2)}$ double mutants were viable. Nonetheless, interactions between *kek3* and both *DNTs*, and *kek4* and *DNT1*, agreed with the same interactions implied from genetic and locomotion data in Chapter 3.

Although *kek3* and *kek4* null alleles were viable in homozygosis, *kek6*^{34} and *kek6*^{35} were not. However, these lines were viable when crossed with *Df(kek6)*. This suggested that there was something in the genetic background of the *kek6* parental transposon lines, as opposed to the deletion itself, that caused lethality in homozygosis and had been retained throughout the mutagenesis protocol. A second possibility is that the genetic discrepancy arose from the third chromosome of the parental heat-shock Flippase line used at the G_0 generation for *kek6*

mutagenesis. Alternatively, the heat shock-activated Flippase method may have deleted additional genomic regions in these lines.

The viability of *kek6*^{34} and *kek6*^{35} over the *Df(kek6)* deficiency shows that loss of *kek6* function does not affect viability. Therefore, the rescue of *kek6*$^{34/35}$ by neuronal upregulation of Kek6, DNT1 CysKnot, activated Rho and activated Cdc42 could simply result from consequences of genetic debris within these lines. It was interesting, nonetheless, that neuronal, but not muscular, overexpression of *UASDNT1CK3'*+ could rescue this phenotype.

The reduction in viability in *DNT2*$^{-/Df(DNT2)}$*kek6*$^{34/Df(kek6)}$ mutants was suggestive of weak interactions between Kek6 and DNT1. This will need to be studied by further phenotypic analysis and biochemical means. Interactions between Kek6 and Tie, as a co-receptor, were not implied, since *Tie*$^{5/Df(Tie)}$*kek6*$^{34/Df(kek6)}$ had a nearly wild type S.I.

Locomotion analyses were not conducted with *DNT–kek* double mutants. Nonetheless, it was interesting to see what phenotypes these mutations alone could cause. Loss of *kek3* and *kek4* mutants travelled significantly shorter distances than *yw* control flies. Consequently, these mutants moved slower than controls. Furthermore, *kek3* and *kek4* mutants rested and wobbled more than *yw*. These results concurred with the phenotypes of transposon lines used in Chapter 3. The phenotypes of *kek4*$^{20/20}$ were more pronounced than those of *kek4*$^{-/-}$ (*kek4*^{f05454}), although the sample size was small. Because of the problems associated with studying adult locomotion behaviour discussed in Chapter 3, locomotion phenotypes in *kek3* and *kek4* mutant larvae were studied in Chapter 7.

kek3, *kek4* and *kek6* are the least studied Kek family members. Thus, for the rest of this thesis I made use of loss and overexpression tools. Experiments focused primarily on *kek4* and *kek6*. With these tools it was possible to study the roles of the genes alone, regardless of any context with the DNTs, as well as their roles in combination with the DNTs.

CHAPTER 6

KEK6 FUNCTION IN THE CENTRAL NERVOUS SYSTEM

6.1 INTRODUCTION

In Chapter 3, *kek1*, *kek2* and *kek5* were detected in the embryonic central nervous system (CNS). This chapter aimed to: (1) investigate the function of Kek6 in the CNS; (2) test functional interactions between Kek6 and the *Drosophila* neurotrophins (DNTs), (3) and investigate potential downstream pathways. To do this, the expression pattern of *kek6* was analysed by *in situ* hybridisation and antibody staining. The developmental expression of *kek6* was profiled in the embryonic CNS, in order to test if it could correspond functionally with the localisation of DNTs, and motor neurons. modENCODE and FlyAtlas data reveal that *kek6* is expressed strongly in the larval CNS and adult brain, in addition to the gut, adult heart and adult female gonads (Celniker et al., 2009, Chintapalli et al., 2007). However, detailed embryonic expression patterns have not been published, and the function of Kek6 is unknown for any tissue.

I next tested whether interfering with *kek6* function either in loss of function mutants, or upon *kek6* overexpression, resulted in axon guidance phenotypes in the intersegmental nerve b (ISNb) motor neuron projections. I used antibodies to FasII to label all motor neurons (FasII; Lin et al. (1994b)).

Finally, using the same loss and gain of function alleles, I tested whether *kek6* is necessary for normal locomotion behaviour. In Chapters 3 and 5, adult locomotion was used as an assay for behaviour, although embryonic expression profiles were detailed. However, the embryonic CNS and peripheral nervous system (PNS) are remodelled throughout metamorphosis (Tissot and Stocker, 2000, Truman, 1990). Furthermore, the central pattern generator underlying larval locomotion behaviour includes the segmental nerve (SN) and ISN nerves (Fox et al.,

2006). Thus, it was more appropriate to compare *kek6* embryonic expression patterns and misrouting in ISNb motor axons with larval locomotion, prior to metamorphic rewiring. I tested whether *kek6* loss and gain of function have locomotion phenotypes.

Using the same phenotypic assays, I also tested interactions between Kek6 and the DNTs, and whether interfering with downstream signalling components could rescue *kek6* overexpression phenotypes. Growth cone extension is controlled by rearrangements of microtubules and the actin cytoskeleton (Dent and Gertler, 2003). Growth cone movement requires the growth and retraction of filopodia and lamellipodia, which are supported by actin microfilaments and microtubules. Actin rearrangements are also required for the formation of synapses (Dillon and Goda, 2005). In neurons, actin rearrangements are controlled by the Rho GTPase superfamily, including Rho, Rac and Cdc42, which are activated and deactivated by Guanine exchange factor (GEF; including ephexin1) and GTPase-activating protein (GAP) proteins, respectively (Dent and Gertler, 2003, Dillon and Goda, 2005, Huang and Reichardt, 2001, Shi et al., 2010). RhoGTPase signalling is downstream of Ras–phosphatidylinositol 3-kinase (PI3K) signalling, and Ras can further promote axon growth via extracellular signal-regulated kinase (ERK; Markus et al. (2002).

6.2 RESULTS

6.2.1 *kek6* is expressed in the embryonic nervous system

The distribution of *kek6* transcripts was analysed by *in situ* hybridisation (Figure 6.1). *kek6* mRNA was present from stage 13 along the length of the ventral nerve cord (VNC), with signal detected in each segment. By stage 15, *kek6* mRNA expression was enriched along the VNC in a distinct segmented pattern on either side of the midline (Figure 6.1b). Four stripes of transcript were observed in the VNC (arrowheads). By stage 16, mRNA signal was seen throughout the VNC in two distinct stripes parallel but lateral to the midline (Figure 6.1c). By stage 17, transcript signal was uniform throughout the CNS, and therefore indicated a likely

Figure 6.1 ***kek6* is expressed in the CNS**
In situ hybridisation

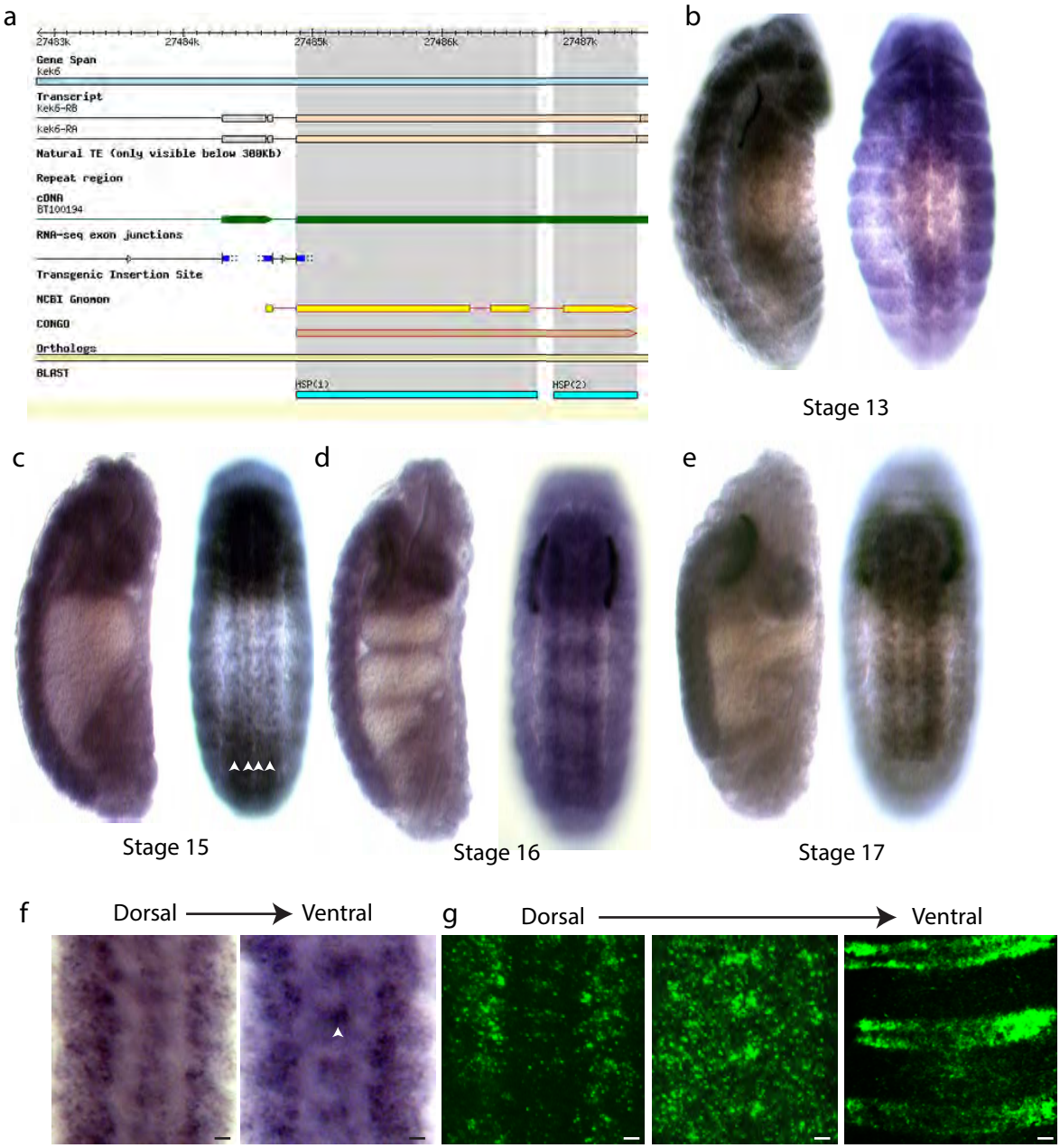

a | Probe hybridisation confirmed by BLAST. **b-e** | *In situ* hybridisation of antisense *kek6* RNA probe reveals hybridisation with *kek6* mRNA in the VNC and embryonic brain from stage 13. Transcript was detected in stripes along the VNC (arrowheads). **f** | Dissected embryos reveal *kek6* mRNA is enriched in the VNC surrounding the neuropil and on the midline (arrowhead). **g** | Slices of the VNC fluorescently labelled using an antisense *kek6* RNA probe reveals kek6 mRNA flanking the neuropil in the dorsal VNC, pairs of *kek6*$^{+}$ neuronal cell bodies ventral to the neuropil, and epidermal stripes. Scale bar, 10µm.

neuronal role for *kek6* (Figure 6.1d). Filleted stage 16 and 17 embryos showed *kek6* expression surrounding the axons of the longitudinal tracts (Figure 6.1e,f). Kek6 transcript was also detected in the cortex, ventral to the neuropil (Figure 6.1f, arrowhead).

Fluorescent *in situ* hybridisation revealed *kek6* transcript throughout the VNC in stage 17 embryos (Figure 6.1g). *kek6* mRNA was detected in soma lateral to the neuropil in the dorsal VNC, and pairs of *kek6*$^{+}$ nuclei were detected ventral to the neuropil, either side of the midline. On the epidermis, *kek6* signal was detected in stripes. This was not detected by alkaline phosphatase (non-fluorescent) *in situ* hybridisation, and may reflect background sticking of the RNA probe to the embryo.

Kek6 protein was detected in the longitudinal axons of the VNC with anti-Kek6 (Figure 6.2a): antibodies were designed by selecting a unique peptide sequence from Kek6 in the N-terminal region to avoid labelling of repetitive, common domain sequences (see Chapter 2.5.2). Anti-Kek6 did not stain neurons in *kek6*$^{34/Df(kek6)}$ null mutant embryos at any developmental stage (Figure 6.2d; *Df(kek6)* is *Df(3R)ED6361*). HRP developed embryos revealed Kek6 distribution along the neuropil (Figure 6.2a, left image). Kek6^{+} signal was detected both in longitudinal connectives and along commissures crossing the midline (Figure 6.2a, right image). Fluorescent anti-Kek6 stains further revealed the presence of Kek6 in pioneer neurons in stage 12 embryos (Figure 6.2b). The arc away from the midline and the proximity of the start of these axons suggested an MP1 or ventral unpaired median (VUM; arrowhead) neuron-like origin, although cell bodies could not be discerned. In stage 16 and 17 embryos, Kek6 was present in many CNS axons. Kek6^{+} axons extended along the length of the VNC and crossed the midline. By stage 17, signal was detected in axons leaving the VNC perpendicular to the midline (Figure 6.2b, right image; Figure 6.2c, arrowheads). These projections are likely to be motor neurons.

Figure 6.2 **Kek6 is distributed in motor neurons**

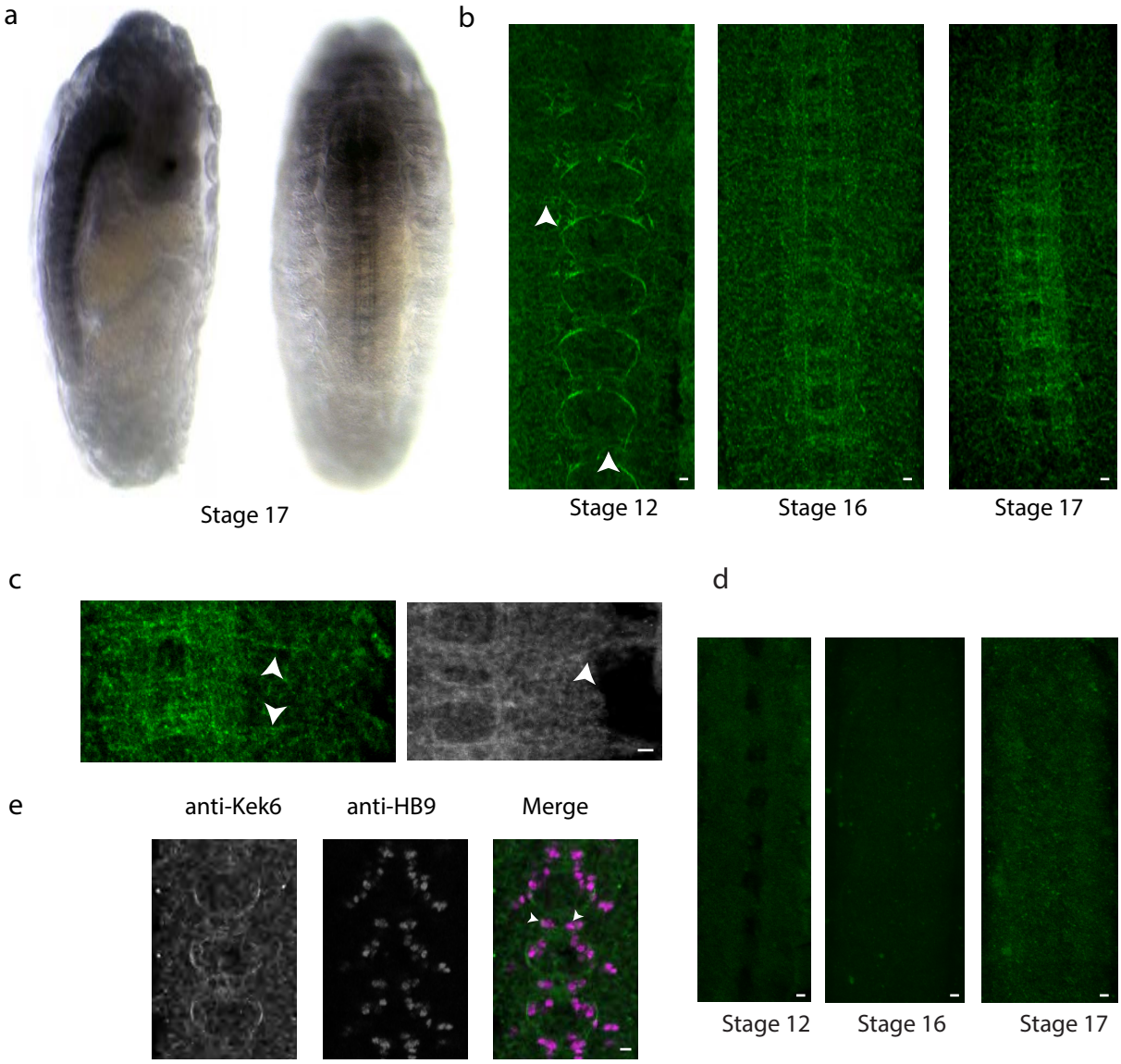

a | HRP-detected anti-Kek6 labels axons in the embryonic longitudinal tracts and the commissures in stage 17 embryos. **b** | Fluorescent anti-Kek6 labelling reveals Kek6 is distributed in pioneer interneurons and putative motor neurons (arrowheads) in stage 12 embryos, throughout the VNC, and in motor neurons in stage 17 embryos. **c** | Magnified view of Kek6^{+} motor neurons in stage 17 embryos (arrowheads). **d** | Anti-Kek6 does not label *kek6^{34}/Df(3R)ED6361* embryos. **e** | Stage 12 embryos co-labelled with anti-Kek6 (green) and anti-HB9 (magenta). Scale bars, 10μm.

To determine whether the neuronal signal observed from *kek6 in situ* hybridisations is present in motor neurons, *yw* embryos were double stained with anti-Kek6 and anti-HB9. $HB9^+$ is a nuclear marker. I detected $HB9^+$ signal in the nuclei of cells that were surrounded by $Kek6^+$ cell membrane signal: given their location relative to the pioneer axon projections, these cells may correspond to the MP2 (arrowhead) pioneer neurons, and the RP motor neurons, which are posterior to the aCC and the Us (Figure 1.8; Figure 6.2e).

In situ hybridisation and anti-Kek6 staining both confirm that kek6 is required in the CNS, in the embryonic brain and VNC. *In situ* stains reveal *kek6* mRNA expression in nuclei throughout the VNC, suggestive of a neuronal localization: anti-Kek6 staining localizes to axons along the VNC, and motor neurons that exit perpendicular to the VNC. The *in situ* and antibody expression profiles therefore overlap.

6.2.2 *kek6* is required for axon targeting

To test if *kek6* is involved in axon targeting, I studied the effect of *kek6* loss and gain of function on ISNb motor neuron projection targeting to the boundaries of muscles 12–13, 6–13 and 6–7. Late stage 17 embryos were stained with the motor axon marker anti-FasII and ISNb projections in abdominal hemisegments A1–A5 (10 hemisegments per embryo) were scored for misrouting phenotypes. Phenotypes were scored for each projection in each hemisegment, then grouped into the categories ‘fan’, ‘loss of 1 projection’ and ‘misrouting and 2 or more projections affected’ (Zhu et al., 2008). A fan phenotype was defined as multiple, misdirected thin projections originating from the location of an absent ‘b’ projection. Loss of 1 projection and fan phenotypes occur at a combined basal rate of around 12–15% of hemisegments. This did not vary between genotypes. Misrouting refers to aberrant projections to another muscle or axon, an unusual route taken by the axon or lack of final targeting.

All lines tested had a w^- genetic background, and transgenes bore the w^+ minigene. In *yw* controls, 20% of hemisegments exhibited a misrouting phenotype. Neuronal overexpression

of *kek6* resulted in an increase in misrouting (Figure 6.3a; χ^2 with Bonferroni correction applied in all cases, see Appendix I for statistical values). *kek6* overexpression using the *elavGal4* neuronal driver introduced novel misrouting phenotypes, including bifurcation and overgrowth of projection 'b', and looping and overshooting of projection 'a' (Figure 6.3b, red arrowheads). Misrouting also increased in *kek6* loss of function mutants. Typically, $kek6^{34/Df(kek6)}$ embryos had similar misrouting phenotypes to *yw*, although anterior targeting of projection 'b', projection sprouting at muscle boundary 6–13, and lack of projection 'a' targeting was observed (Figure 6.3b, blue arrowheads). Finally, *elavGal4*-driven *kek6* overexpression rescued projection misrouting caused by $kek6^{34/Df(kek6)}$ loss of function (Figure 6.3a). Motor axon misrouting caused by *kek6* loss of function and overexpression contrasted with the lack of an overall effect induced by *kek1* loss and overexpression (Figure 6.3c,d), despite *kek1* being similarly expressed in the embryonic CNS. Nonetheless, unique misrouting phenotypes, including ectopic projection sprouting, were observed for both *kek1* genotypes, suggesting that a statistical difference might be observed with a larger sample size (Figure 6.3d, arrowheads).

Phenotypes associated with loss of *kek6* function correlate with loss of DNT1, but not DNT2 (Zhu et al., 2008). Loss of DNT1 induced misrouting of projection a and projection b towards adjacent segments, and bifurcation of projection b (Zhu et al., 2008), as observed in the images shown in Figure 6.3b. The correlation of phenotypes, however, does not imply that Kek6 and the DNTs are in the same functional pathway, simply that Kek6 has a role in motor axon targeting.

To test the function of *kek6* in relation to DNT signalling, I quantified motor axon mistargeting in two genetic contexts: (1) to test whether *kek6* null embryos could rescue the sprouting induced by overexpression of *UASDNT1CK3'*+ in the muscle (with *24BGAL4*); (2) and to test whether neuronal overexpression of *kek6* could rescue the phenotype of $DNT2^{e03444}DNT1^{41}$ double mutant embryos. Muscle-driven expression of the DNT1 CysKnot-

Figure 6.3 ***kek6* is required for motor axon targeting**

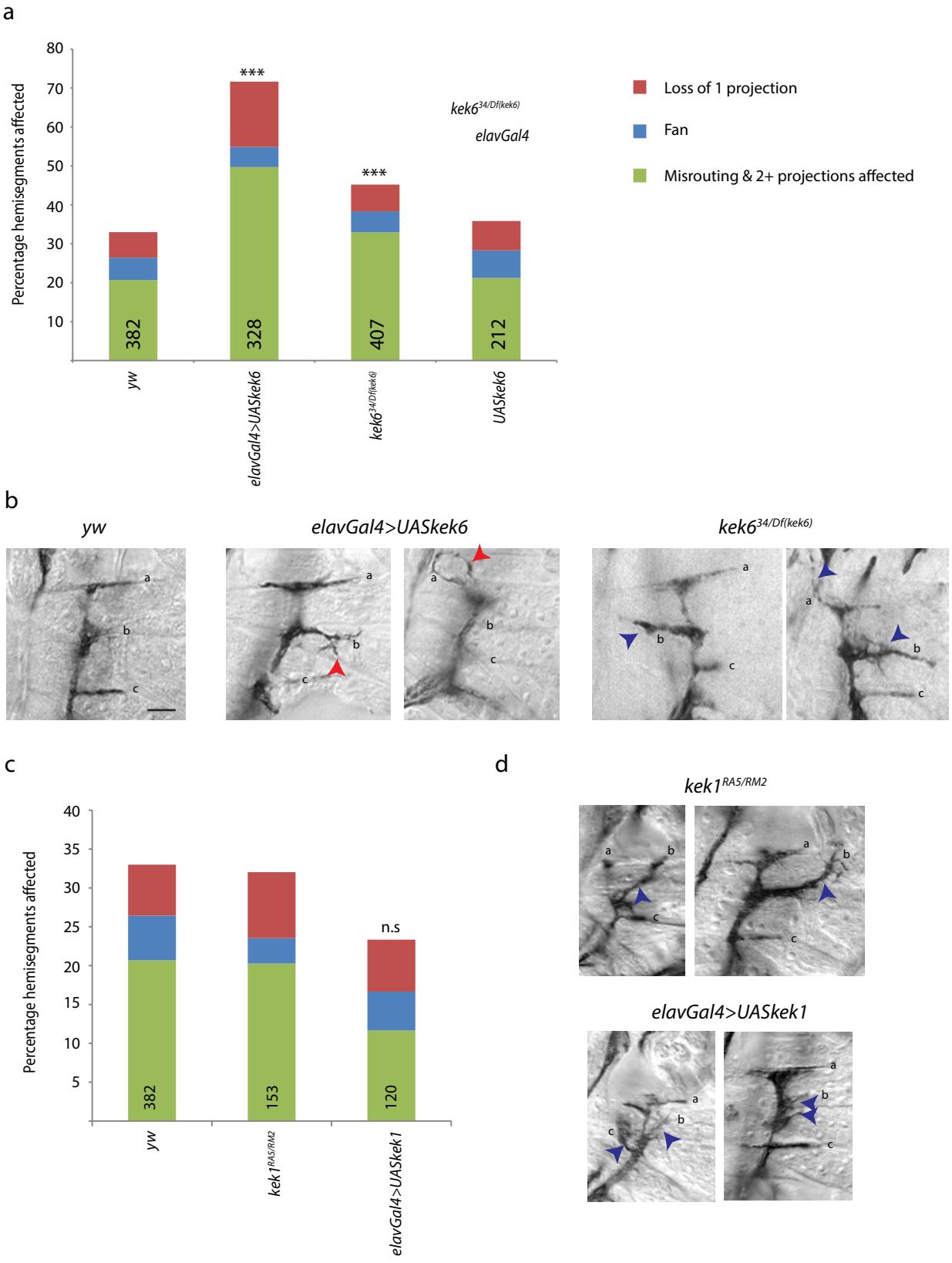

ISNb motor neurons were labelled with anti-FasII and projections to muscles 6–7, 6–13 and 12–13 were scored for misrouting or loss phenotypes. **a** | Neuronal overexpression and *kek6* loss of function mutations induced an increase in axon misrouting compared to *yw*. Misrouting phenotypes were rescued by *kek6* overexpression in a *kek6* mutant background. **b** | ISNb misrouting phenotypes in *yw* and *kek6* mutants. **c,d** | Loss or gain of function of *kek1* had no overall effect on motor axon targeting compared to *yw*. See Appendix I for statistical values. Arrowheads label misrouting phenotypes referenced in main text. Scale bar, 15µm. *Df(kek6) = Df(3R)ED6361*

3'+ induced motor axon projection misrouting and ectopic sprouting (Figure 6.4a,b, red arrowheads). These phenotypes were rescued when DNT1 was overexpressed in a *kek6* null genetic background (Figure 6.4a; χ^2 with Bonferroni correction applied in all cases, see Appendix I for statistical values). This suggests that Kek6 functions downstream of DNT1. By contrast, neuronal overexpression of *kek6* in a $DNT2^{e03444}DNT1^{41}$ genetic background did not rescue the sprouting (red arrowheads) and misrouting (blue arrowheads) phenotypes of the double *DNT* mutant (Figure 6.4a,b). This suggests that Kek6 is not sufficient for signalling downstream of the DNTs.

I next asked what downstream signalling pathway may function downstream of *kek6*. For this, I tested whether mutations in downstream signalling components might suppress or enhance the *kek6* loss of function or overexpression phenotypes. For example, to test if *kek6* might activate Ras, I asked whether a dominant negative form of Ras might rescue the *kek6* overexpression misrouting phenotype. Since Kek6 lacks a tyrosine kinase (TyrK) domain, I did not explore whether it can directly influence cell survival or cell proliferation. Instead, I focused on signalling components known to influence the actin cytoskeleton directly, or those known to influence cell migration and cell shape. Kek6 could influence these events by directly recruiting such components without the need of a catalytic motif. Thus, I tested dominant negative forms of Cdc42, PI3K, Rac, Ras and Rho.

Of these, dominant negative Ras and PI3K rescued motor axon misrouting induced by neuronal overexpression of *kek6* (Figure 6.5a,b; χ^2 with Bonferroni correction applied in all cases, see Appendix I for statistical values). This suggests that Kek6 may signal via Ras and PI3K pathways. Conversely, dominant negative Rac, Rho and Cdc42 did not rescue axon misrouting caused by *kek6* gain of function (Figure 6.5a,b). This suggests that Kek6 does not function via activation of RhoGTPase signalling. In the *kek6* overexpression background, dominant negative Cdc42 embryos had ectopic projections (Figure 6.5b, red arrowheads); dominant negative Rac induced some super-sprouting (blue arrowhead); and dominant

Figure 6.4 **_kek6_ interacts with DNTs in motor axon targeting**

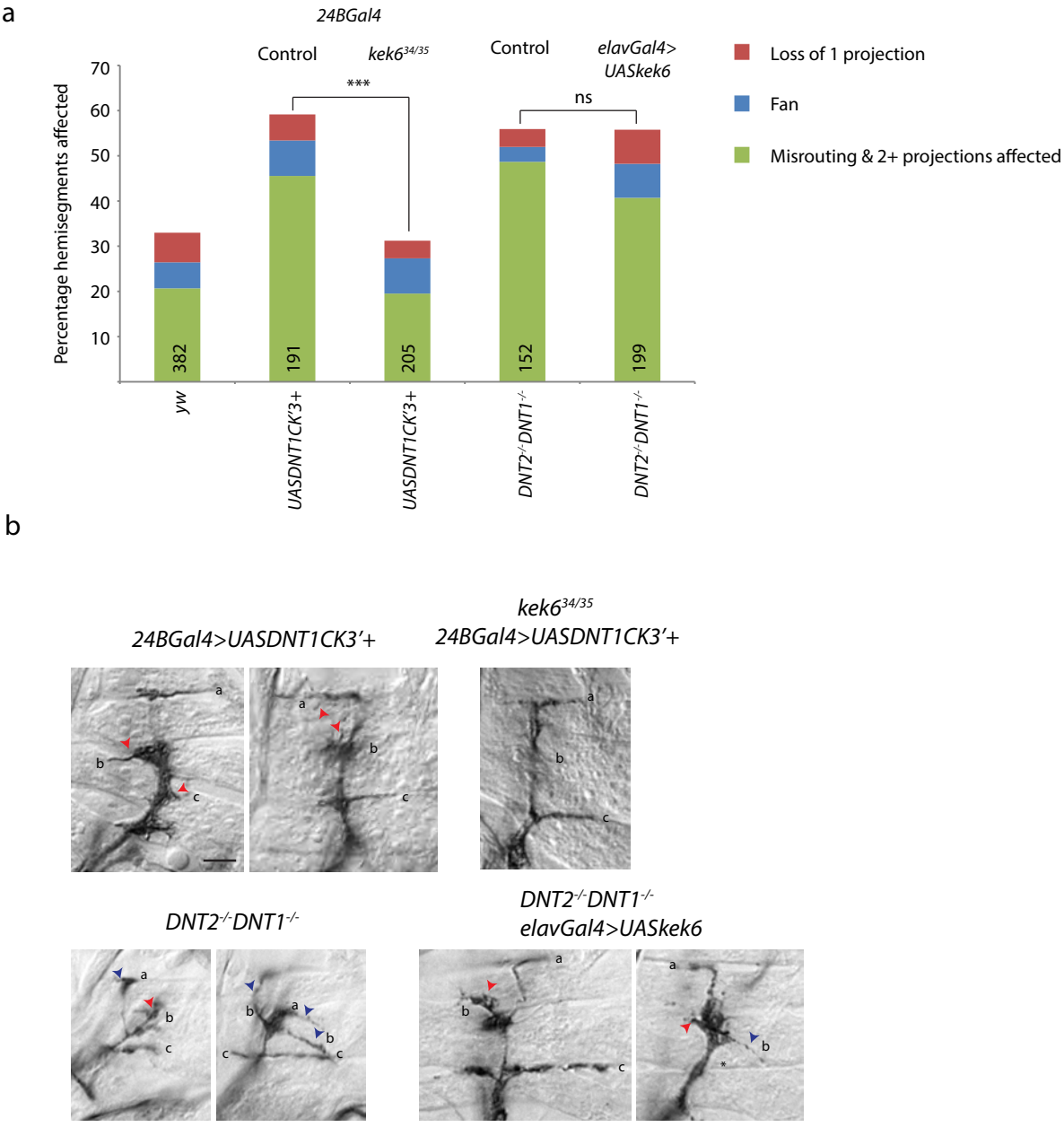

a | ISNb motor axons labelled with anti-FasII reveal that axon misrouting induced by muscle-driven overexpression of DNT1 did not occur in a *kek6* null genetic background. Conversely, misrouting phenotypes induced by homozygous *DNT2*^{e03444}*DNT1*^{41} (*DNT2*$^{-/-}$*DNT1*$^{-/-}$) double mutations could not be rescued by neuronal *kek6* overexpression. **b** | ISNb misrouting phenotypes exhibited by genotypes in part **a**. Arrowheads label misrouting phenotypes referenced in main text. See Appendix I for statistical values. Scale bar, 15µm.

Figure 6.5 ***kek6* is upstream of Ras and PI3K in motor axon targeting**

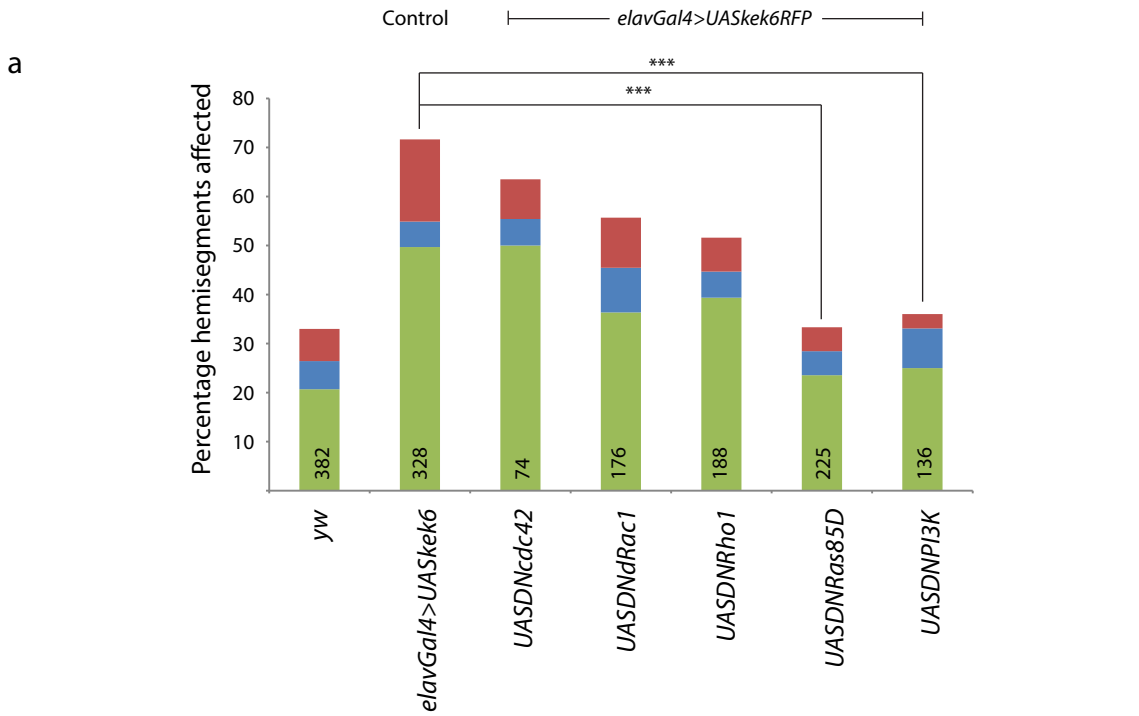

a | ISNb motor axons labelled with anti-FasII reveal that axon misrouting induced by neuronal overexpression of *kek6* can be rescued by simultaneous expression of dominant-negative Ras and PI3K, but not dominant-negative Cdc42, Rac or Rho. **b** | ISNb misrouting phenotypes exhibited by genotypes in part **a**. Arrowheads indicate phenotypes referenced in main text. See Appendix I for statistical values. Scale bar, 15µm.

negative Rho induced predominantly misrouting phenotypes, including a looped projection 'b' (green arrowhead). In a *kek6* gain of function background, dominant negative Ras and PI3K resulted in motor axons that looked predominantly wild type. Any misrouting phenotypes observed in these genotypes were shared with *kek6* overexpression mutants. This suggests that Kek6 is upstream of Ras-activated PI3K signalling.

6.2.3 *kek6* is required for normal larval locomotion behaviour

To investigate whether loss or gain of *kek6* function affected locomotion, I filmed mutant larvae crawling on agar plates for 1 minute, using the ImageJ plugin FlyTracker, modified by Manuel Forero in our lab from an existing plug-in, to quantify speed and to plot larval movement (McIlroy et al., 2013). Three separate controls were tested — *yw*, *yw/OregonR* and *elavGal4* — to account for the potential impact of the *white* gene on locomotor behaviour, given its role in serotonin and dopamine uptake (Borycz et al., 2008, McIlroy et al., 2013). Thus, the three controls were w^{-}, w^{+}/w^{-} and homozygous *mini-white*, respectively. All transgenic and mutant lines had w^{-} backgrounds, but insertions and Flippase recognition target (FRT)-mediated null alleles bore *mini-white* constructs (one per null, Gal4 or UAS allele).

Larva movement traces suggested that all three controls travelled similar distances. Furthermore, all three controls had comparable speed profiles, although *yw/OregonR* heterozygotes travelled at slower speeds slightly less frequently (Figure 6.6a,b). Homozygous *elavGal4* was used as the control for future analysis because it contains 2 *miniwhite* constructs, as do most mutant genotypes tested. *kek6* loss of function resulted in an increase in crawling speed (Figure 6.6b; Kruskal-Wallis with Dunn's post hoc, see Appendix I for statistical values). Neuronal overexpression of *kek6* also increased crawling speed.

Although not obvious from trajectories, neuronal overexpression of *kek6* partially rescued the speed phenotype of *kek6* loss of function (Figure 6.7a,b; Dunn's post hoc).

Figure 6.6 ***kek6* is required for larval locomotion behaviour**

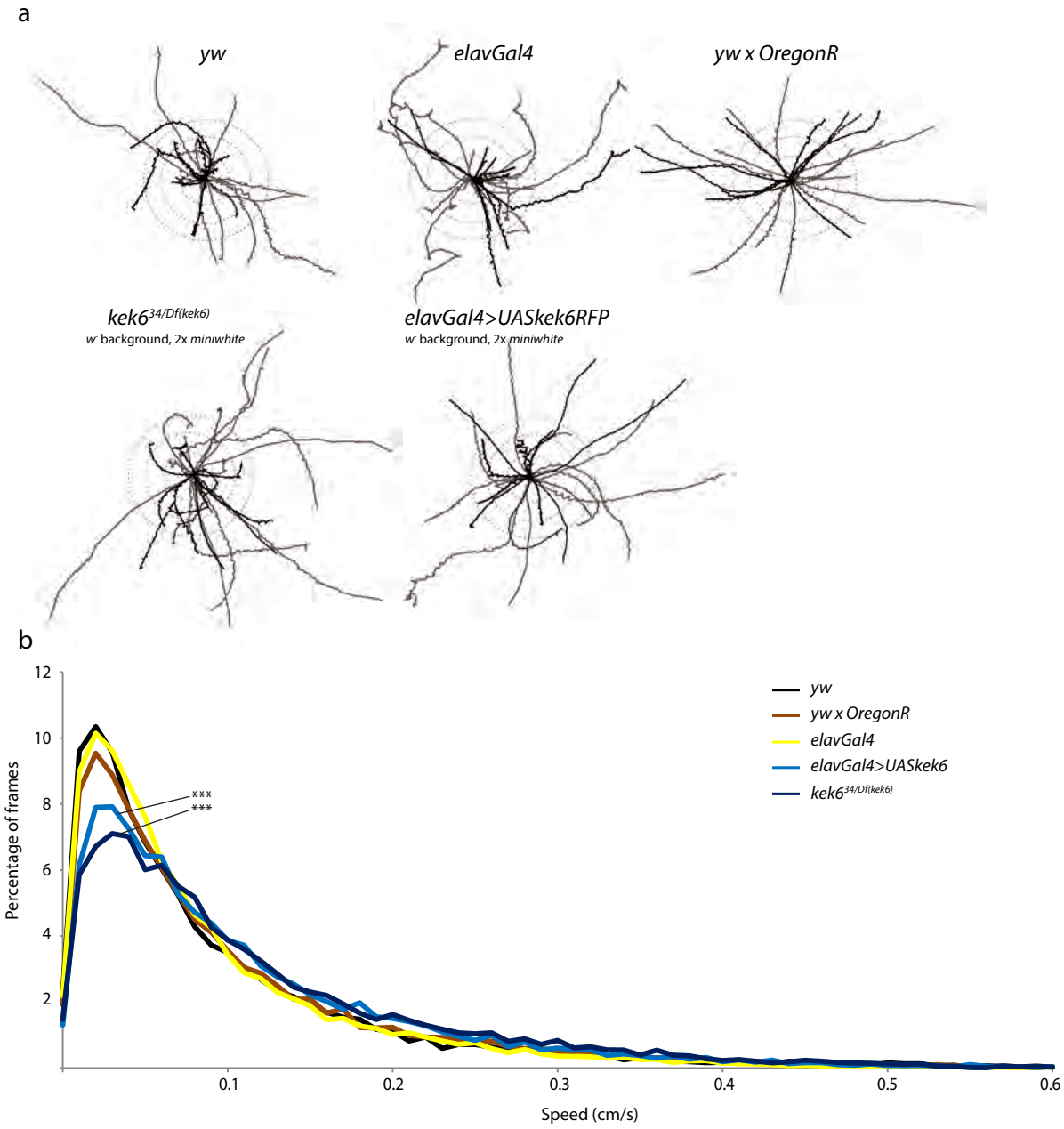

a | Trajectories of control and *kek6* mutant larvae reveal different larval activity.
b | Speed histogram of larval movement per video frame reveals *kek6* loss and gain of function mutations increase larval speed. See Appendix I for statistical values and frame numbers. *Df(kek6)* = *Df(3R)ED6361*

Figure 6.7 **Neuronal overexpression of *kek6* partially rescues *kek6* loss of function locomotion phenotypes**

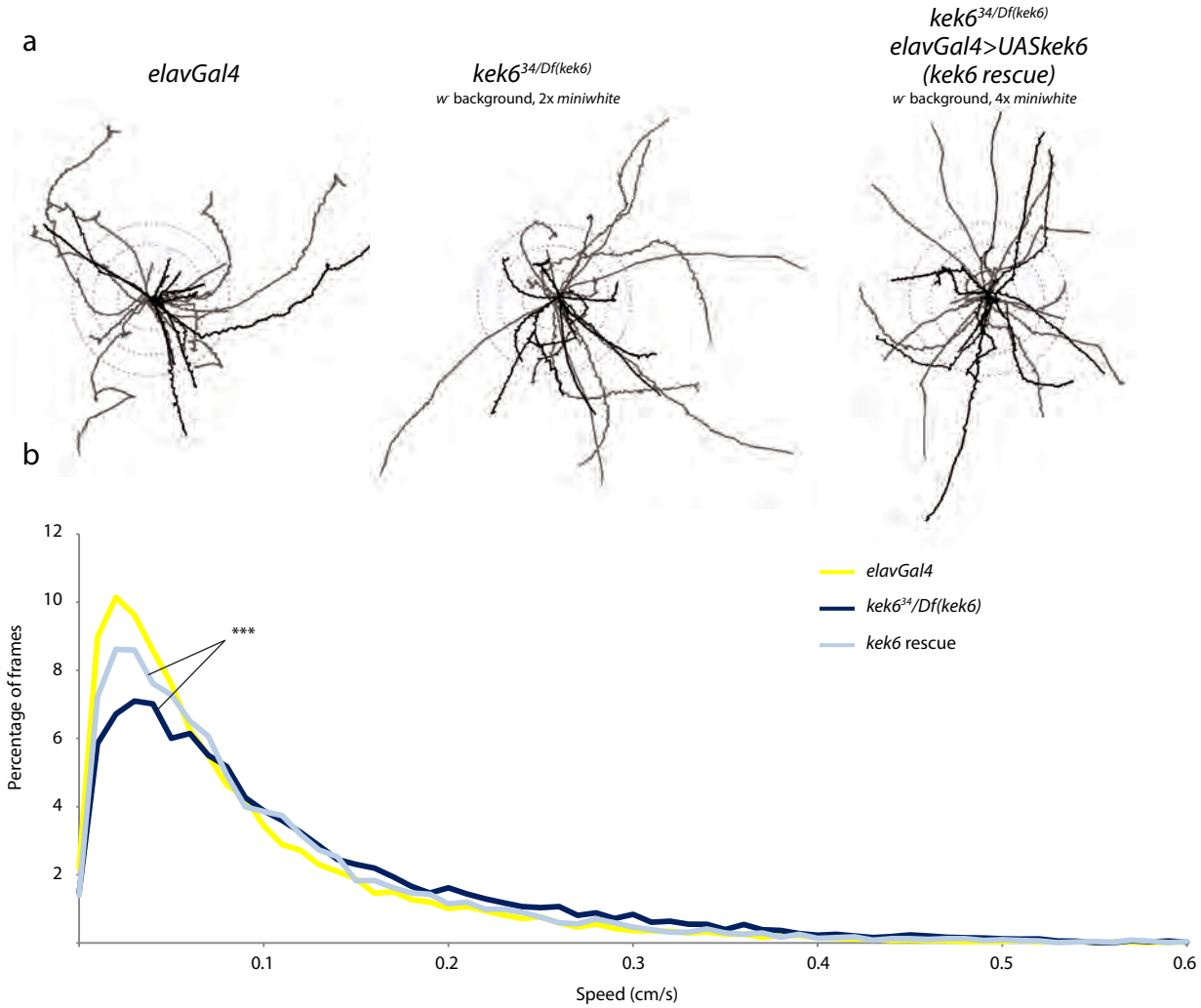

a | Trajectories of control, *kek6* mutant and *kek6* rescue larvae. **b** | Neuronal overexpression of *kek6* in *kek6* null mutant larvae partially rescues movement speed. Comparison of speeds between loss of *kek6* and *kek6* rescue is significant. See Appendix I for statistical values and frame numbers. *Df(kek6) = Df(3R)ED6361*

To examine interactions between Kek6 and the DNTs, *kek6–DNT* double mutants were tested for locomotion phenotypes. In addition, the *tie*^{5} mutant allele (generated by Alice Lowry, Hidalgo laboratory) was combined with *kek6*^{34} to test Tie as a potential downstream partner of the receptor. Trajectories revealed that *DNT1*$^{-/Df(DNT1)}$*kek6*^{34}*/Df(kek6)* and Tie$^{5/Df(Tie)}$*kek6*$^{34/Df(kek6)}$ double mutants had similar locomotion behaviours to *kek6*$^{34/Df(kek6)}$ single mutants (Figure 6.8a — *Df(Tie)* and *Df(DNT1)* are *Df(3L)ED4342*). However, *DNT2*$^{-/Df(DNT2)}$*kek6*$^{34/Df(kek6)}$ double mutant larvae crawled more slowly, as their trajectories were considerably shorter (*Df(DNT2)* is *Df(3L)ED6092*). Contrary to the increased distance observed in *kek6* mutants, the distance travelled by *DNT2*$^{-/Df(DNT2)}$*kek6*$^{34/Df(kek6)}$ double mutants was comparable to that by *elavGal4* control larvae (Figure 6.8b). However, the decrease in travelling distance of *DNT2*$^{-/Df(DNT2)}$*kek6*$^{34/Df(kek6)}$ double mutants was not statistically significant when compared with single *kek6*$^{34/Df(kek6)}$ heteroalleles (Student's t-test with Bonferroni correction, see Appendix I for statistical values). It is likely that this would be significant with a sample size n>25. By contrast, when analysing speed, *DNT2*$^{-/Df(DNT2)}$*kek6*$^{34/Df(kek6)}$ double mutants crawled significantly slower than *kek6*$^{34/Df(kek6)}$ single mutants (Figure 6.8c; Dunn's post hoc). Together, these data suggest that there is a functional relationship between Kek6 and the DNTs.

To test whether the loss of signalling components downstream of Kek6 could rescue behavioural phenotypes as well as motor axon guidance phenotypes, I filmed larvae co-expressing *kek6* and dominant negative *Ras*, *PI3K* or *Rho* alleles under the control of the *elavGAL4* neuronal promoter. Trajectories revealed that dominant negative PI3K and Rho were unable to rescue the locomotion phenotype of larvae overexpressing *kek6* (Figure 6.9a). By comparison, co-expression of dominant negative *Ras* and *kek6* by *elavGal4* decreased distance travelled compared with *kek6* overexpression alone (Figures 6.9a,b; Student's t-test with Bonferroni correction, see Appendix I for statistical values). Larvae with neuronal co-expression of *kek6* and dominant negative *Ras* also travelled significantly slower than *kek6*

Figure 6.8 ***kek6* interacts with *DNTs* in locomotion behaviour**

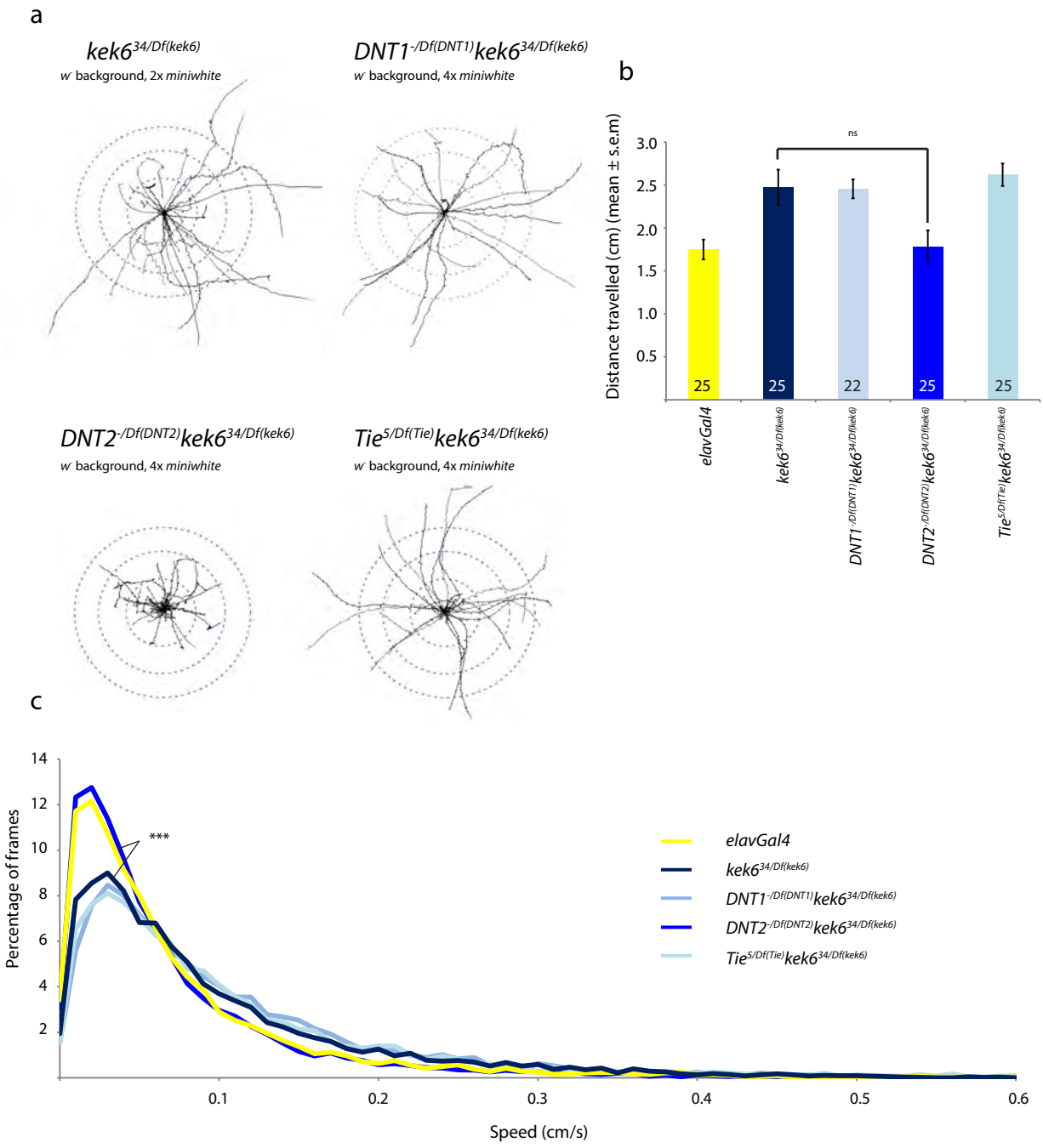

a | Trajectories of *kek6* single and double mutants reveal a genetic interaction between *kek6* and *DNT2* in locomotion behaviour. **b** | *kek6DNT2* larvae travel shorter distances than $kek6^{34/Df(kek6)}$ single mutants. **c** | *kek6DNT2* larvae move significantly slower than $kek6^{34/Df(kek6)}$ single mutants and at speeds comparable to controls. See Appendix I for statistical values and frame numbers. *Df(kek6)* = *Df(3R)ED6361*, *Df(Tie)* and *Df(DNT1)* = *Df(3L)ED4342*, *Df(DNT2)* = *Df(3L)ED6092*.

Figure 6.9 **_kek6_ is upstream of Ras in locomotion behaviour**

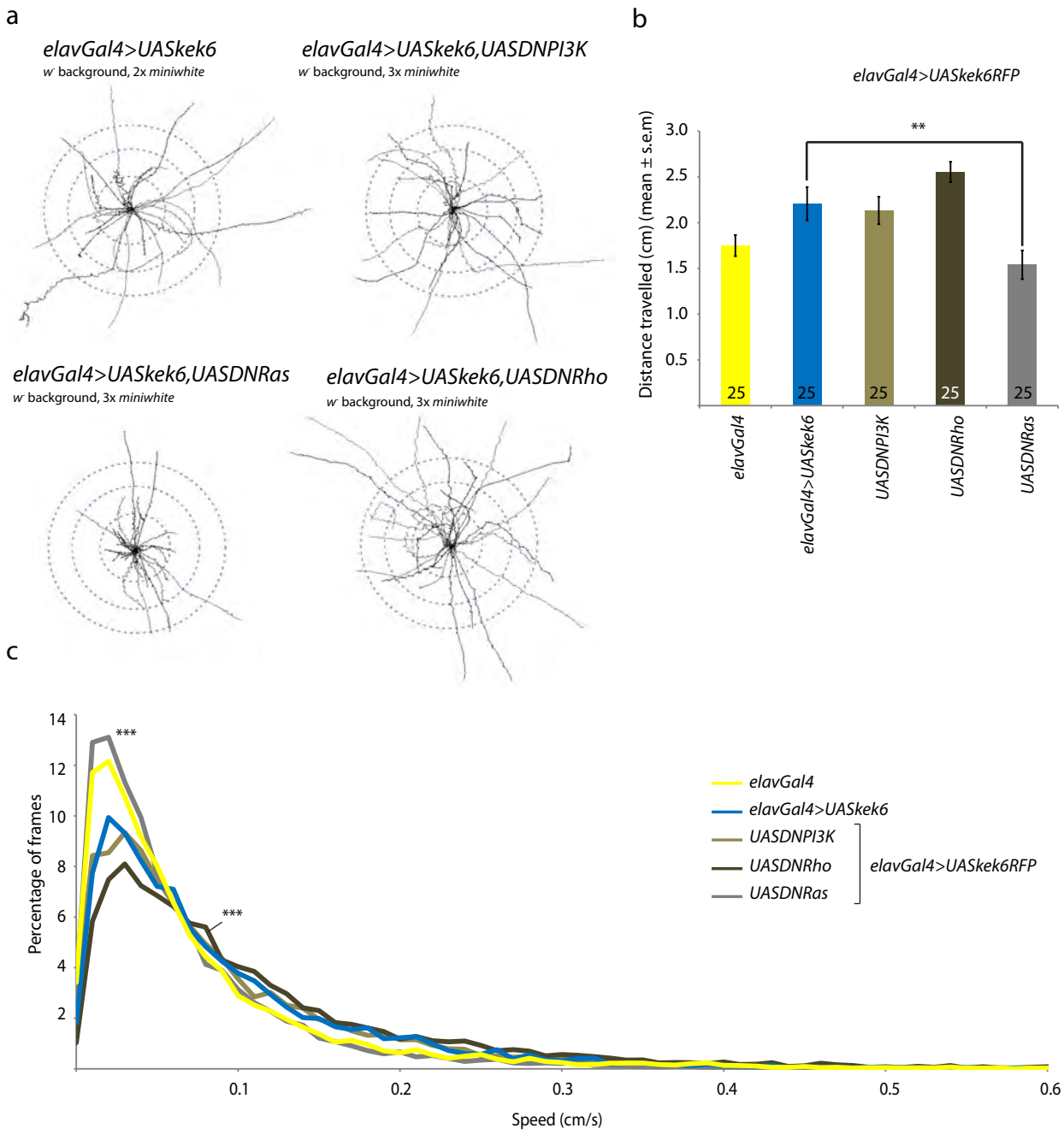

a | Trajectories of *kek6* overexpression mutants reveal simultaneous neuronal overexpression of dominant negative Ras reduces locomotion activity in larvae. **b** | *elavGal4>UASkek6,UASDNRas* larvae travel shorter distances than *elavGal4>UASkek6* mutants. **c** | Neuronal overexpression of dominant negative PI3K or Rho do not affect locomotion behaviour in an *elavGal4>UASkek6* background. By contrast, co-expression of dominant negative Ras and *UASkek6* results in larvae that crawl as slowly as wild type larvae. See Appendix I for statistical values and frame numbers.

overexpression alone (Figure 6.9c). Furthermore, larvae in which dominant negative *Rho* was co-expressed with *kek6* travelled significantly faster than *elavGal4>UASkek6* (Dunn's post hoc). Altogether, these data suggest that Ras and Rho function downstream of Kek6, possibly in an antagonistic manner.

6.3 DISCUSSION

In this chapter, *kek6* mRNA expression and protein distribution were visualised by *in situ* hybridisation and antibody labelling, respectively. *kek6* mRNA was enriched in the embryonic CNS, in the VNC and brain from stage 13 to stage 17. Kek6 protein was localized to pioneer neurons of the VNC in stage 12 embryos, and longitudinal tract fascicles in stage 16 and stage 17 embryos. Kek6 protein was also detected in motor axons.

The role of *kek6* in nervous system development was tested by quantifying misrouting of ISNb motor axons. Loss and gain of function of *kek6* caused an increase in projection misrouting compared to *yw* controls. Neuronal expression of *kek6* in *kek6* null embryos was sufficient to rescue misrouting phenotypes. Misrouting of projections associated with muscle-driven expression of the *UASDNT1CK3'*+ did not occur in a *kek6* null genetic background; by contrast, the misrouting phenotypes of $DNT1^{-/-}DNT2^{-/-}$ double mutants could not be rescued by *kek6* overexpression. Last, simultaneous neuronal overexpression of *kek6* and dominant negative alleles of *Rho*, *Rac* and *Cdc42* did not rescue projection misrouting induced by *kek6* overexpression, whereas overexpression of dominant negative *Ras* and *PI3K* did.

The function of *kek6* in behaviour was tested by recording larval locomotion. Loss and gain of function *kek6* mutants moved faster than controls. This phenotype was partially rescued by the overexpression of *kek6* in a *kek6* null background. *kek6DNT* interactions revealed locomotion phenotypes for $DNT2^{-/Df(DNT2)}kek6^{34/Df(kek6)}$ double mutants, but not $DNT1^{-/Df(DNT1)}kek6^{34/Df(kek6)}$ or $Tie^{5/Df(Tie)}kek6^{34/Df(kek6)}$. Last, overexpression of dominant negative Ras rescued the locomotion phenotype induced by *kek6* overexpression in neurons, whereas

dominant negative *Rho* or *PI3K* could not. Thus, *kek6* is neuronal, and *kek6* mutants have neuronal phenotypes in axon guidance and locomotion.

Although I have not been able to identify the specific motor neurons expressing *kek6*, there is abundant evidence that motor neurons express *kek6*. First, FISH labelling of *kek6* mRNA revealed ventral cells. Second, Kek6 antibodies revealed signal in axons extending anteriorly from the midline; this could correspond to the VUMs, which project anteriorly then away from the midline (Landgraf et al., 2003). Finally, anti-Kek6 antibodies reveal signal along the motor axons exiting the CNS.

Consistently with its neuronal expression, misrouting and locomotion data revealed that *kek6* has roles in neuronal development. Furthermore, neuronal expression of *kek6* in a *kek6* null background was sufficient to rescue ISNb projection misrouting in embryos, and partially rescued locomotion phenotypes in larvae. The partial rescue of the *kek6* null larval locomotion phenotype suggests that further roles of Kek6 may exist in other tissues, such as muscle; that overexpression did not restore endogenous protein levels; or that the construct is not functional (for example, the RFP tag may interfere with function). Nonetheless, both loss and gain of function of *kek6* resulted in phenotypes, suggesting that Kek6 levels are important for normal function. This confirms that the phenotypes I reported for the mutants were indeed caused by the specific loss of *kek6*.

Since it was not known how Kek6 signals, there was uncertainty as to whether *kek6* overexpression would have any effect *in vivo*. In survival assays (Chapter 5), overexpression of *kek6* only partially rescued the lethality of $kek6^{34/35}$ heteroallelic flies. However, each of these alleles over the deficiency for the locus was fully viable, implying that the lethality of single homozygous mutants for each of the $kek6^{34}$ and $kek6^{35}$ alleles is unrelated to the loss of *kek6*. Hence, the partial rescue of overexpressing *kek6* in a $kek6^{34/Df(kek6)}$ heteroallelic background indicates that the *kek6* transgene is functional.

There is further evidence that the *kek6* transgene used for overexpression is functional: (1) the fact that *kek6* overexpression rescues the loss of function mutant *kek6* phenotype in axon guidance and (2) larval locomotion, and (3) the rescue of $DNT2^{-/-}DNT1^{-/-}$ lethality by neuronal expression of *kek6* in the survival assay (see Chapter 5). Furthermore, motor axon misrouting caused by *kek6* overexpression was reproducible. How *kek6* overexpression phenotypes were manifested is an unsolved question, although a role in cell adhesion cannot be discounted, given that Kek6 was detected at cell–cell boundaries in Figure 4.1.

I have provided multiple evidence that Kek6 interacts with the DNTs: (1) In motor axon targeting, overexpression of *kek6* could not induce signalling in the absence of DNTs. (2) In motor axon targeting, loss of *kek6* rescued the phenotype caused by ectopic DNT1. (3) NFκB signalling was induced in response to DNT2 stimulation in S2 cells transfected with Kek6≡Toll6 chimaeric constructs (Figure 4.5); (4) genetic interaction data in survival assays (Figure 5.7), and (5) the synergistic locomotion phenotype of $DNT2^{-/Df(DNT2)}kek6^{34/Df(kek6)}$ double mutants.

My data suggest that Kek6 signals via Ras and PI3K. Dominant negative Ras and PI3K rescued the misrouting of ISNb projections caused by *kek6* overexpression. In addition, dominant negative Ras could rescue the locomotion phenotype of larvae overexpressing *kek6*. Ras is a signalling hub protein upstream of ERK, CREB, Rho, Akt and BAD signalling (Figure 1.2). The role of PI3K in axon guidance, but not locomotion, indicates that Kek6 may function via specific signalling pathways depending on functional context.

In this chapter I showed that *kek6* is neuronal and has important roles in CNS development. Vertebrate neurotrophins also have roles in immunity and the systemic control of growth. In the next chapter, I tested the expression pattern and function of *kek4* in hormonal regulation and whole organism development.

CHAPTER 7

KEK4 FUNCTION IN THE RING GLAND

7.1 INTRODUCTION

This chapter aimed to investigate the functions of Kek4 in the systemic control of growth. In previous chapters I showed that *kek4* can interact with both *Drosophila* neurotrophin 1 (*DNT1*) and *DNT2* genetically. Furthermore, in adults, $kek4^{-/-}DNT1^{-/-}$ double mutants, using $kek4^{f05454}$, had locomotion phenotypes. FlyAtlas data reports *kek4* to be abundantly expressed in the larva (Chintapalli et al., 2007), and preliminary analysis of the *kek4* expression pattern here detected Kek4 in the ring gland rather than the central nervous system (CNS). Mammalian neurotrophins have functions involved in the systemic, hormonal control of growth (Levi-Montalcini et al., 1990). Since the *kek* genes interact with the *DNTs*, it is conceivable that members of the *kek* family might also have non-neuronal functions. Thus, in this chapter I investigated the functions of *kek4* in the ring gland.

7.2 RESULTS

7.2.1 *kek4* is expressed in the ring gland

The expression profile of *kek4* was analysed by *in situ* hybridisation to *kek4* mRNA transcripts, and antibody stains using anti-Kek4 (Figures 7.1,7.2). *kek4* mRNA was not detected in the embryonic ventral nerve cord (VNC) in stages 15, 16 or 17 (Figure 7.1a,b). Instead, *kek4* transcript was detected in the mid- and hindgut, and in structures anterior to the developing central brain. These structures may include the ring gland and/or stomatogastric nervous system.

To analyse Kek4 distribution in the larval brain, the putative *kek4Gal4* line *P[GT1]BG00800* was crossed with *UASmyrTOMATO* and larval brains were fluorescently stained with anti-dsRed (Figure 7.1c). *kek4Gal4*-driven myrTomato was detected in a single axonal stripe along

Figure 7.1 ***kek4* is expressed in the ring gland**

a

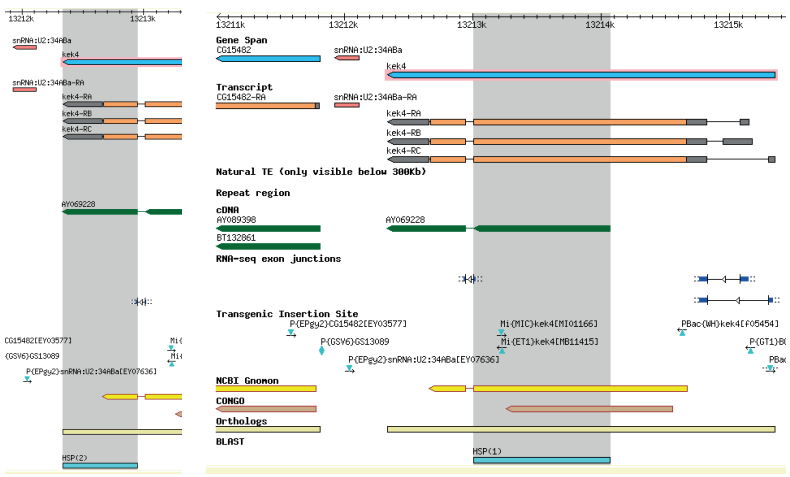

b

In situ hybridisation

Stage 15 Stage 16 Stage 17

c

kek4Gal4>UASmyrTOMATO

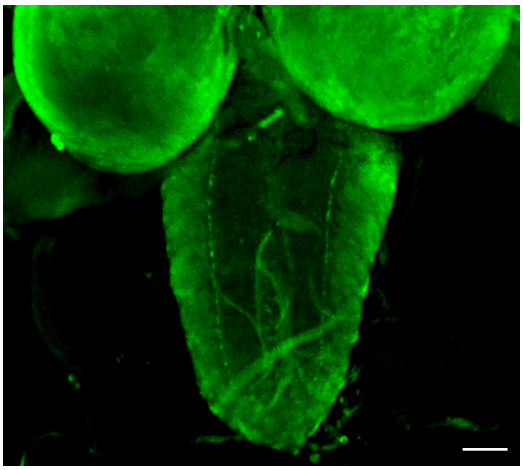

d

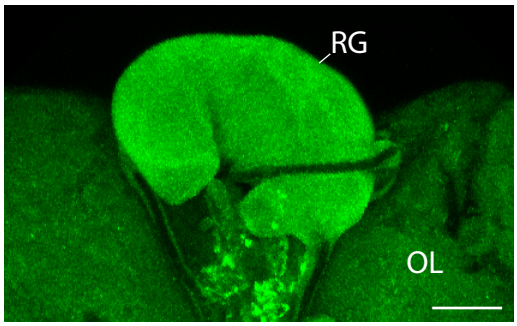

a | Hybridisation of RNA probe, transcribed from DGRC clone, confirmed by BLAST (probe spans exon). **b** | *In situ* hybridisation reveals *kek4* mRNA is absent from the embryonic CNS. **c,d** | Putative *kek4Gal4* (*P[GT1]BG00800*)-driven UASmyrTOMATO was detected in axons of the larval VNC and enriched in the ring gland (RG). OL, optic lobe. Scale bar, 50µm.

Figure 7.2 ***kek4* is expressed in the corpus allatum and corpora cardiaca**

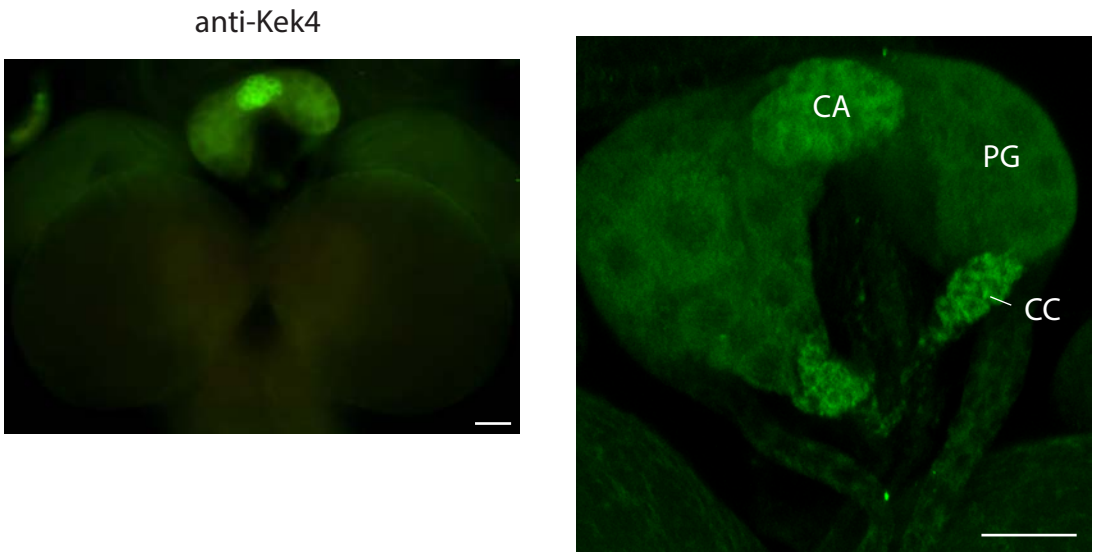

Anti-Kek4 reveals Kek4 protein in the ring gland. Kek4 is enriched in the corpus allatum (CA) and corpora cardiaca (CC), but is absent from the prothoracic gland (PG). Scale bar, 50µm.

the length of the nerve cord, either side of the neuropil (Figure 7.1c). Putative *kek4Gal4*-driven reporter was also detected in the ring gland (Figure 7.1d).

To further determine Kek4 distribution, custom anti-Kek4 antibodies were raised from peptides. Unique peptide sequences from Kek4 were chosen in the N-terminal region to avoid labelling of repetitive, common domain sequences (see Chapter 2.5.2). Strikingly, anti-Kek4 labelled specific glands of the ring gland, and did not label the CNS (Figure 7.2). The ring gland is composed of three endocrine glands (Figure 1.9) (Edgar, 2006, Richard et al., 1989, Siegmund and Korge, 2001). The prothoracic gland (PG) releases ecdysone, which is processed to an active form, 20E, and furthers larval development (Riddiford, 1993). The corpus allatum (CA) releases juvenile hormone (JH), which prohibits 20E signalling and maintains the larval state (Richard et al., 1989, Flatt et al., 2005). The paired corpora cardiaca (CC) release the lipid and sugar mobilising adipokinetic hormone (AKH) (Nässel and Winther, 2010). Kek4 was detected specifically in the CA and the CC, but absent from the PG (Figure 1.9; Figure 7.2).

7.2.2 *kek4* controls larval developmental timing

The period between the final larval moult (L3) and pupariation is defined by distinct stages and checkpoints (Edgar, 2006): the *minimum viable weight,* below which the larva will not survive metamorphosis (Edgar, 2006); the *critical weight*, which marks the end of feeding; and the onset of larval wandering. Wandering larvae permanently leave the food prior to pupariation and can no longer feed. To determine variation in checkpoint timing in mutants, larval instars can be temporally staged and moults can be timed by onset of morphological changes in mouth hooks or behavioural traits such as wandering (King-Jones et al., 2005, Mirth et al., 2005, Ou et al., 2011, Rewitz et al., 2009). Furthermore, the timing of the critical weight can be determined using larvae reared on food supplemented with blue colouring, which is cleared from the gut once feeding has ended (King-Jones et al., 2005, Ou et al.,

2011). To determine whether Kek4 has a role in the timing of larval development, pupariation and pupation, controls, *kek4*$^{20/23}$ heteroallelic mutants and larvae overexpressing *kek4* in the whole ring gland (*spz6Gal4>UASkek4*) were staged at the L1 larval instar and timed as they progressed through L3 wandering instar, white pupa (puparia or prepupa), brown pupa, black pupa and eclosed adult stages (Figure 7.3). *spz6Gal4* was used as a ring gland-specific driver, as it drives expression in CA, PG and CC cells (S. AlAhmed, Hidalgo laboratory, personal communication). 'Wandering L3, clear gut' was also recorded as a developmental marker, corresponding to the wandering L3 larvae that have digested all food consumed during the terminal growth period.

Both *yw* and *spz6Gal4* larvae had very similar developmental profiles at 25^{0}C (Figure 7.3a,b). L3 larvae began to wander out of their food from 76 hours after L1 staging (T_{50}=86 hours, where T_{50} corresponds to the time at which half of recorded larvae have passed the development stage). Subsequent stages up to forming brown pupae followed in quick succession. Full pupation of all larvae was reached at ~104 hours post-L1 staging. Adult eclosion followed approximately 4.5 days later (T_{50}= ~218 hours). Compared to controls, *spz6Gal4>UASkek4* L3 larvae moulted early (Figure 7.3c). By contrast, the *kek4*$^{20/23}$ L3 larvae moult was delayed (Figure 7.3d). Timing between moults, post-wandering L3 instar, was similar for all genotypes.

Phenotypic effects were also compared by stage (Figure 7.4). Compared to controls, *spz6Gal4>UASkek4* L3 larvae wandering was premature (Figure 7.4a; χ^2 with Bonferroni correction in all cases, see Appendix I for statistical values). *kek4*$^{20/23}$ single mutants, conversely, displayed delayed onset of wandering. Thus, *spz6Gal4>UASkek4* accelerated larval wandering, whereas *kek4* mutation significantly delayed development. Subsequent development through pupariation and pupation was concordantly brought forward or delayed (Figure 7.4b,c).

Figure 7.3 ***kek4* controls developmental timing, by genotype**

Developmental profiles of *yw* (**a**), *spz6Gal4* (**b**), *spz6Gal4>UASkek4* (**c**) and *kek4*$^{20/23}$ (***d***) larvae were recorded. *kek4* overexpression accelerated larval developmental stages, but caused 40% pupal lethality: *kek4* loss of function delayed larval development.

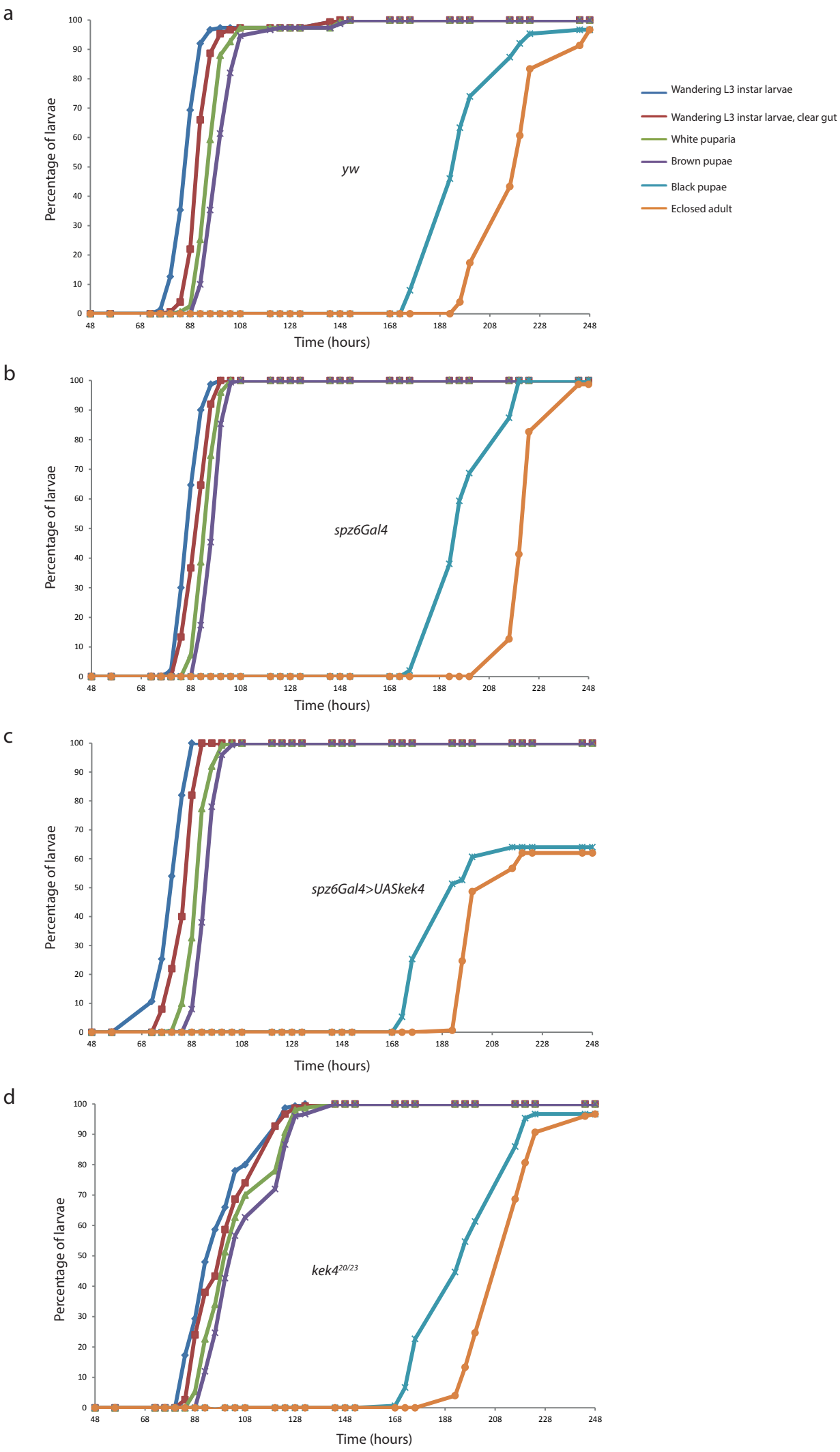
a
b
c
d
Percentage of larvae
Time (hours)
yw
spz6Gal4
spz6Gal4>UASkek4
kek4^20/23
Wandering L3 instar larvae
Wandering L3 instar larvae, clear gut
White puparia
Brown pupae
Black pupae
Eclosed adult

Figure 7.4 ***kek4* controls developmental timing, by stage**

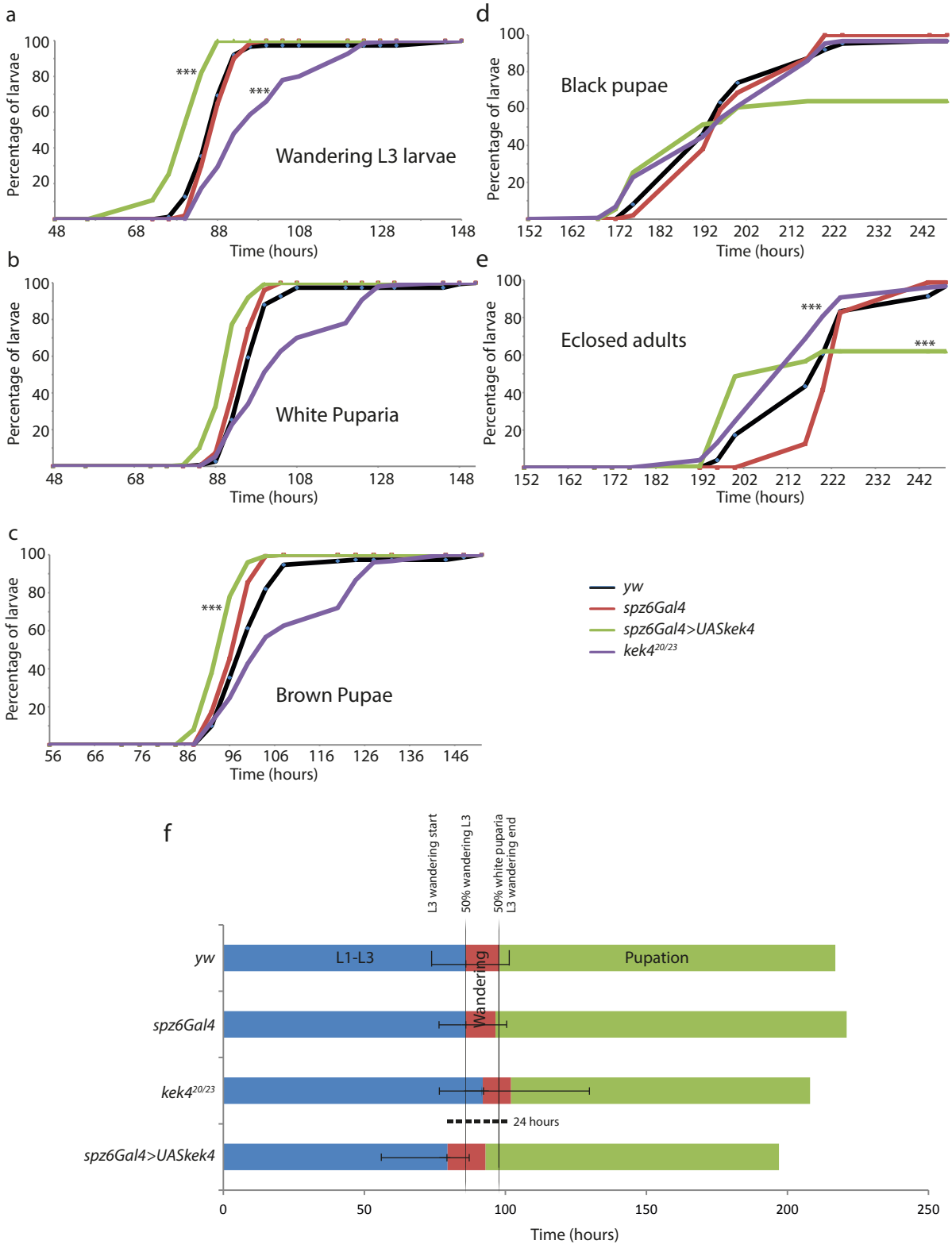

a-e | *kek4* gain of function accelerates larval development. Comparison by developmental stage reveals timing differences originate pre-L3 larval moult, as delays are consistent for later stages. **f** | Development time courses highlight shifts in developmental timing. *kek4*$^{20/23}$ wandering onset occurs over an extended period compared with controls and *spz6Gal4>UASkek4*. n=150 for each genotype. See Appendix I for statistical values.

Control genotypes and *kek4*$^{20/23}$ mutants reached T_{50} black pupae at the same time (~190–194 hours; Figure 7.4d). Not all *Spz6Gal4>UASkek4* pupae, by comparison, reached this stage. When recalculated to consider only those pupae that reached eclosion, *spz6Gal4>UASkek4* T_{50}=~178 hours, nearly one day earlier than controls. Accordingly, *spz6Gal4>UASkek4* adult eclosion was premature compared with controls (Figure 7.4e). Nearly half of *spz6Gal4>UASkek4* larvae died during metamorphosis and did not eclose (Figure 7.4e). Developmental time courses confirmed that *kek4*$^{20/23}$ mutants had delayed development, whereas *kek4* overexpression accelerated development (Figure 7.4f).

7.2.3 *kek4* inhibits juvenile hormone signalling

JH has a crucial role in maintaining larval growth, since loss of JH-secreting cells in the CA accelerates pupation (Riddiford et al., 2010). The direct downstream targets of JH signalling are not known (Riddiford et al., 2010). Therefore, an alternative is to test for ecdysone target activation, which coincides with termination of JH signalling at the critical weight checkpoint.

20E activates early regulatory transcription factors, including Broad-Core (BR-C). JH and 20E signalling were tested by labelling BR-C in the fat body. *BR-C* is an early 20E-regulated gene required for successful metamorphosis (Guay and Guild, 1991, Kiss et al., 1988). *BR-C* is directly stimulated by 20E, but this is inhibited by JH (Huang et al., 2011a, Konopova and Jindra, 2008). Therefore, BR-C should only be detected during the larval–pupal transition. However, *BR-C* transcript is present in the early L3 instar, and thus aberrant JH signalling can result in early *BR-C* upregulation (Galcerán et al., 1990, Huang et al., 2011a).

BR-C was absent from the fat body of *yw* larvae (Figure 7.5). Fat body BR-C was also absent in *kek4*$^{20/23}$ mutants. However, BR-C was upregulated in the fat body cells of *spz6Gal4>UASkek4* larvae. This suggested that ectopic *kek4* signalling inhibits JH signalling or activates ecdysone, permitting BR-C upregulation. Given that *kek4* is not expressed in the

Figure 7.5 ***kek4* inhibits juvenile hormone signalling**

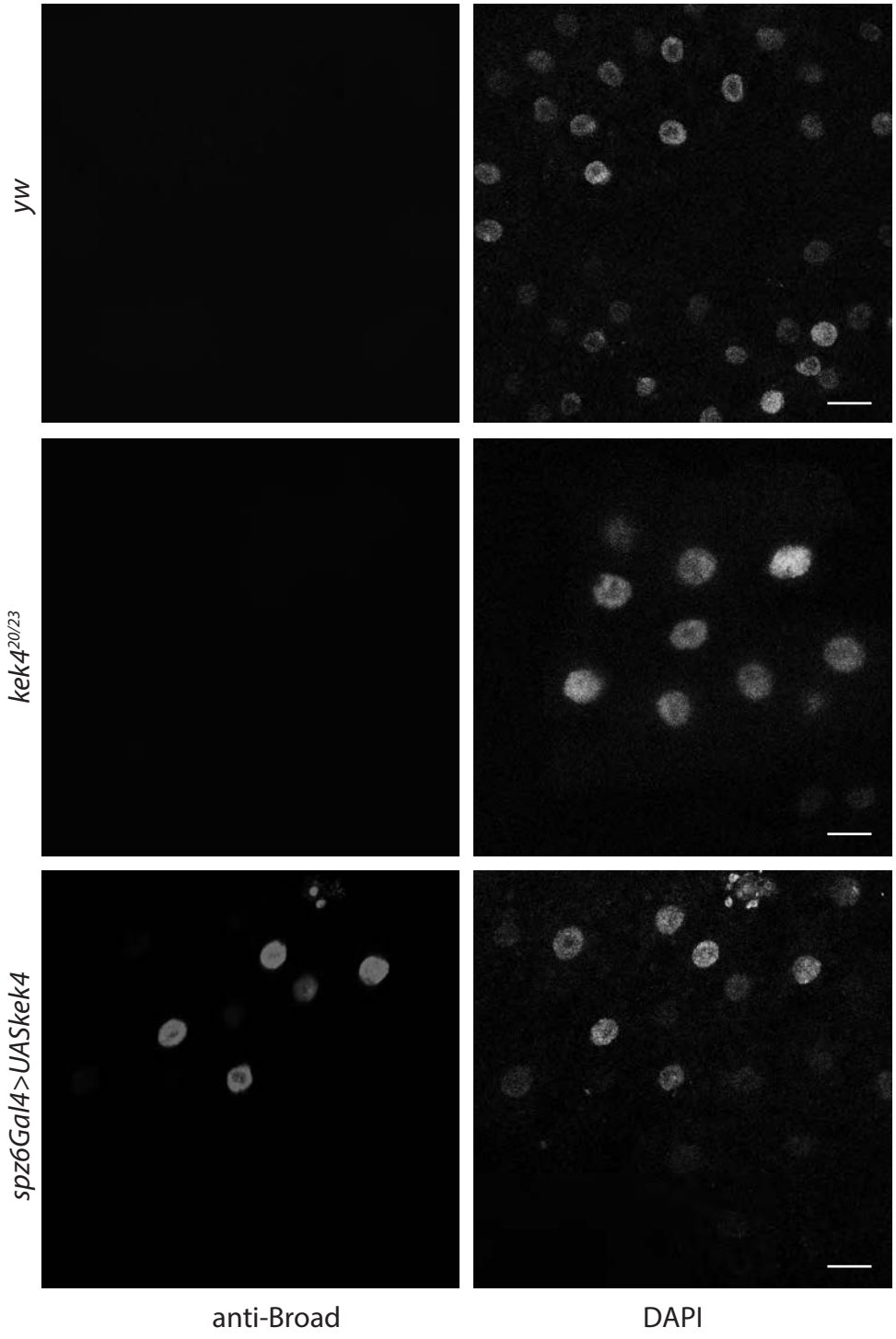

Fat bodies of early L3 larvae were fluorescently labelled with anti-Broad, which labels the pro-metamorphosis early transcription factor Broad-Core (BR-C). BR-C is activated by ecdysone signalling only in the absence of juvenile hormone. *yw* and *kek4*$^{20/23}$ mutant larval fat bodies displayed no BR-C upregulation, whereas *spz6Gal4>UASkek4* mutants did. Thus, *kek4* overexpression in the ring gland may reduce juvenile hormone signalling and permit BR-C upregulation. Scale bar, 10µm.

PG, and JH signalling must be terminated prior to BR-C upregulation, this implied that *kek4* most likely inhibits JH.

7.2.4 *kek4* does not influence larval or pupal body size

Altered timing of wandering onset would affect total feeding time and thereby nutritional uptake (Wegman et al., 2010). Therefore, I next asked whether the delayed or accelerated developmental phenotypes of *kek4* mutants affected body size. 20E-dependent developmental progression forms a negative feedback loop with insulin-like growth (Colombani et al., 2005). Induced overexpression of phosphatidylinositol 3-kinase (PI3K) in the CA and PG increases ring gland growth, but decreases larval and adult body sizes through premature 20E activation (Caldwell et al., 2005, Colombani et al., 2005, Mirth et al., 2005). The same phenotypes are induced by activation of Ras and Raf, and 20E food supplements (Caldwell et al., 2005). Conversely, loss of insulin signalling, 20E or PTTH in the ring gland, and ecdysone receptors in the fat body, delay wandering, and produce smaller ring glands and larger adults (Colombani et al., 2005, McBrayer et al., 2007). Therefore, the PG and CA regulate incoming signals from stretch receptors, insulin, 20E and the fat body to define the critical weight checkpoint and body size. Body size can be measured by organism volume, according to Colombani et al. (2005).

Larval, pupal and adult body sizes and lengths were measured using the ImageJ ROI manager (Figure 7.6a). Body size was measured as the area within the maximum circumference of the body stage, as photographed from above. Larval body size did not significantly vary between *yw*, *kek4*$^{20/23}$ and *spz6Gal4>UASkek4* genotypes (Figure 7.6b). Furthermore, pupal length did not vary between genotypes (Figure 7.6c). By comparison, *spz6Gal4>UASkek4* pupal body size was slightly increased compared with *yw* (Figure 7.6d; Welch ANOVA with Games-Howell post hoc, see Appendix I for statistical values). No difference was observed in adult body size between genotypes (Figure 7.6e).

Figure 7.6 ***kek4* does not control body size**

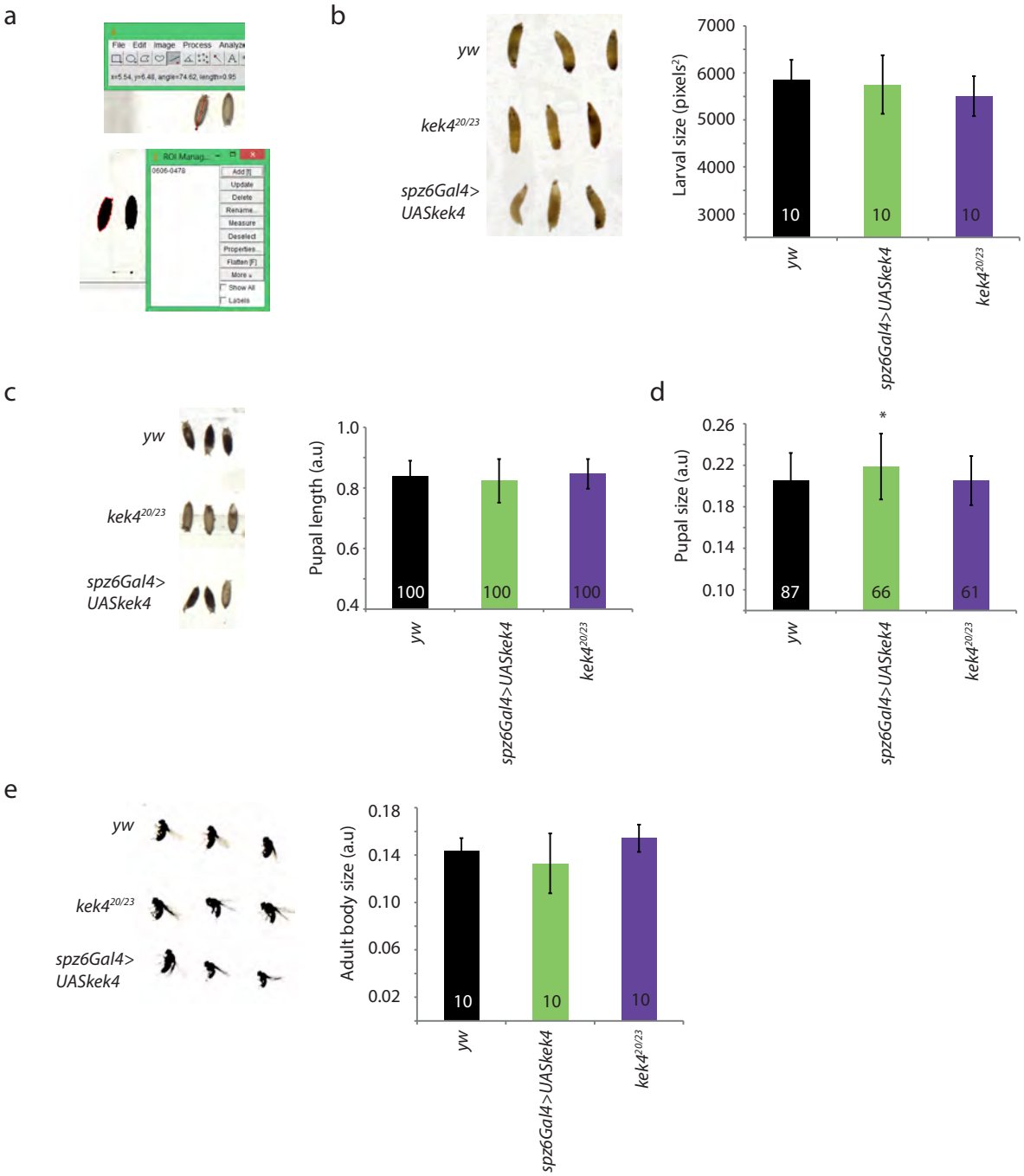

a | *yw*, *kek4*$^{20/23}$ and *spz6Gal4>UASkek4* body sizes were measured using the ImageJ ROI manager tool. **b** | No effect was observed in larval sizes by genotype. **c** | No change in body length could be observed between genotypes. **d** | *spz6Gal4>UASkek4* pupae were slightly bigger than *yw* and *kek4* loss of function mutants. **e** | No effect on adult body size was observed between genotypes. See Appendix I for statistical values and larval/pupal/adult numbers.

An alternative method to assay body growth is to count wing hairs in a defined area of the wing (McBrayer et al., 2007). Each hair correlates with one cell. Since body size did not change in *kek4* mutants, a change in wing cell density might indicate changes in wing cell division or wing cell size. I counted the hairs in a region of interest of female wings for each genotype (Figure 7.7a). Compared to *yw*, *kek4* loss of function significantly increased hair, and therefore cell, density (Figure 7.7b; Welch ANOVA with Games-Howell post hoc, see Appendix I for statistical values). This implied that cell size must be smaller in *kek4* mutants.

7.2.5 *kek4* is required for normal locomotion behaviour

The CC is not involved in developmental timing. Instead it releases AKH to metabolise stored sugars and lipids in the fat body (Kim and Rulifson, 2004, Nässel and Winther, 2010). AKH controls heartbeat, life span, starvation response and locomotion. For example, starvation results in hyperactivity in *Drosophila* adults as the animal searches for food; this response was lost when AKH neurons were ablated (Lee and Park, 2004). Furthermore, AKH can directly stimulate motor neurons in other insects, and AKH loss leads to docile *Drosophila* adults (Isabel et al., 2005, Milde et al., 1995, Nässel and Winther, 2010). Here, I tested the role of Kek4 in locomotion behaviour.

To do this, I analysed the locomotion behaviour of *elavGal4>kek4* and $kek4^{20/23}$ larvae (Figure 7.8). Trajectories of larval movement revealed that loss of *kek4* function resulted in increased locomotion of larvae, whereas gain of *kek4* function resulted in reduced locomotion (Fig.7.8a). $kek4^{20/23}$ larvae also travelled significantly further than *elavGal4* controls, as defined by the sum of distances moved by larvae between each video frame (Figure 7.8b; Welch ANOVA with Games-Howell post hoc, see Appendix I for statistical values), whereas *kek4* overexpression produced larvae that travelled significantly less far. Furthermore, *kek4* mutants travelled significantly faster than controls (Figure 7.8c; Kruskal-Wallis with Dunn's post hoc), whereas the opposite phenotype was observed with *elavGal4>UASkek4* larvae.

Figure 7.7 ***kek4* controls cell number in the wing**

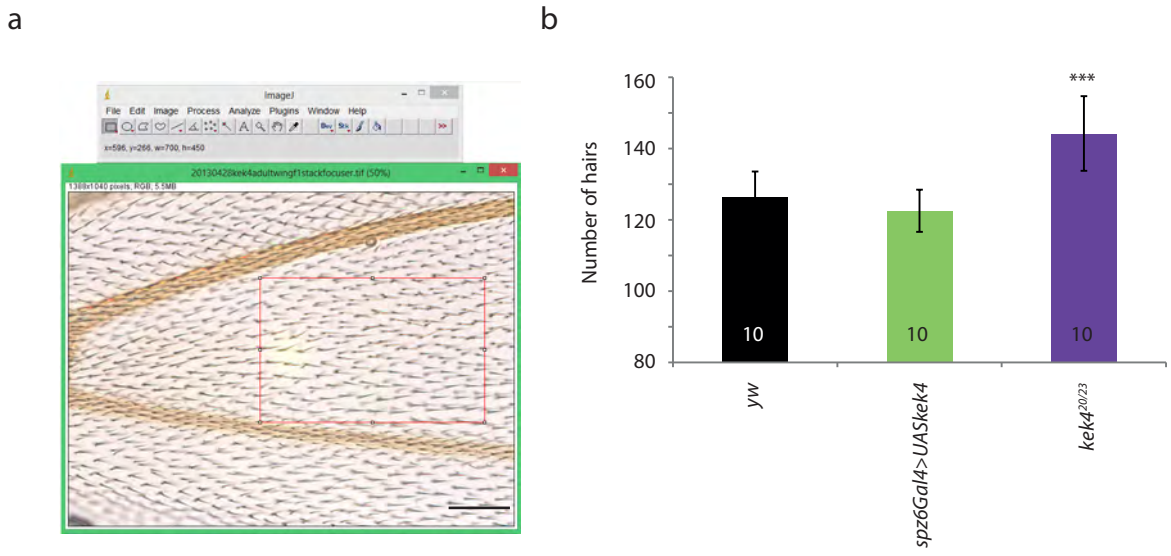

a | Hairs were scored in a defined ROI in the adult wing (see Methods). **b** | *kek4* loss of function mutants displayed increased cell number in the adult wing. See Appendix I for statistical values. Scale bar, 50µm.

Figure 7.8 ***kek4* is required for larval locomotion**

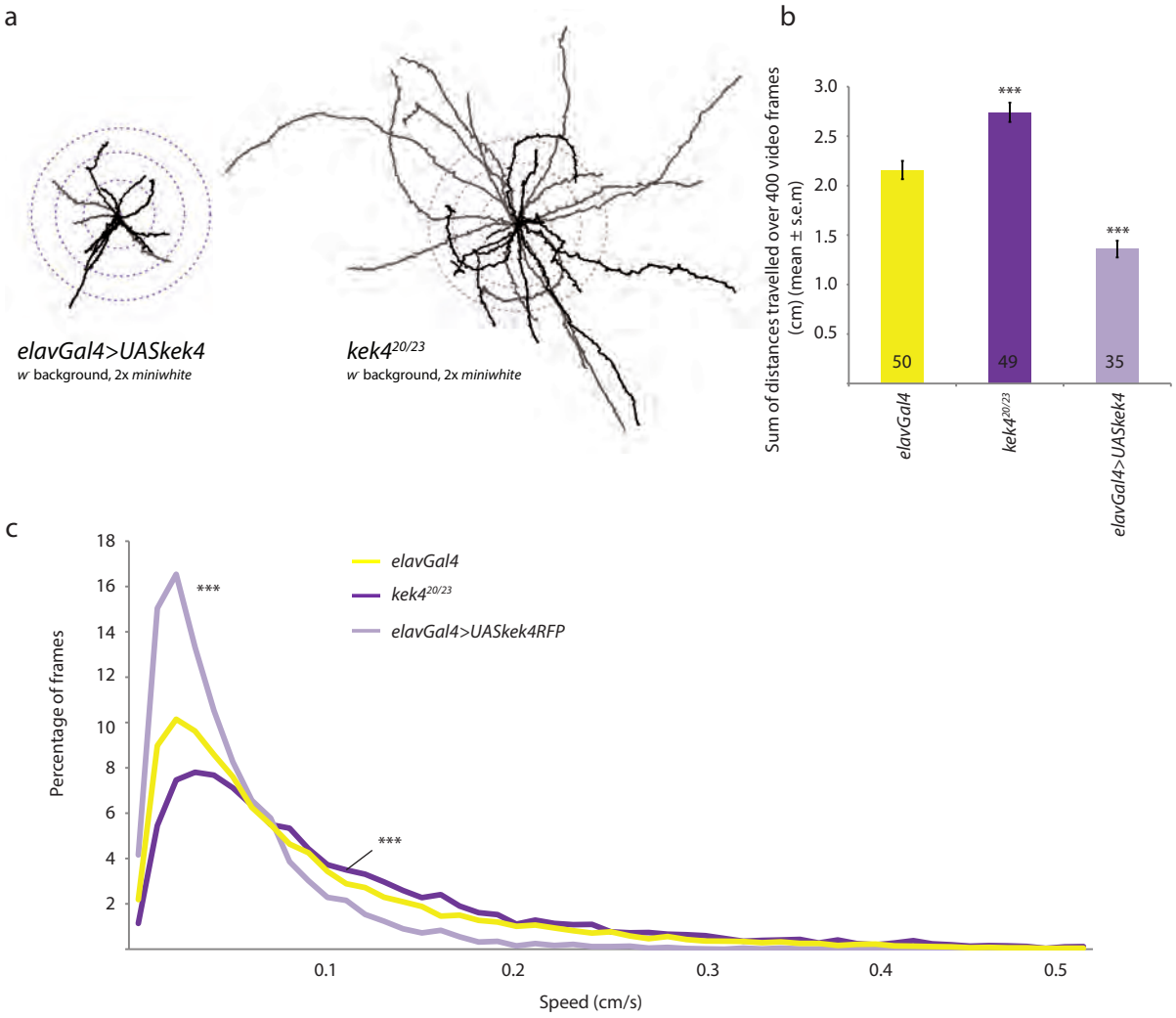

a | Trajectories of *kek4* overexpression and loss of function mutants reveal dramatic differences in locomotion behaviour. **b** | *kek4*$^{20/23}$ mutant larvae travel longer distances than controls, whereas *elavGal4>UASkek4* move less far. **c** | Neuronal overexpression of *kek4* significantly slowed larval movement compared with control larvae. Reciprocally, *kek4* loss accelerated larval movement behaviour. See Appendix I for statistical values and frame numbers.

To control for phenotypes caused by unwanted genetic changes introduced during tool generation, the locomotion assay was repeated using *kek3* mutants, also generated in Chapters 4 and 5. Neither loss nor gain of Kek3 protein resulted in locomotion speed phenotypes compared with *elavGal4* (Figure 7.9a,b). These results indicate that *kek4* loss and gain of function had reciprocal phenotypic effects in these experiments.

7.3 DISCUSSION

In this chapter, *kek4* expression patterns were detected by *in situ* hybridisation and antibody labelling of both a *kek4Gal4* insertion reporter and of endogenous Kek4 protein. Notably, anti-Kek4 showed striking specificity to the CA and CC of the ring gland, but not the PG.

Development of *kek4* loss of function mutants was delayed up to pupariation compared to controls; conversely, larvae in which *kek4* was overexpressed by *spz6Gal4* displayed accelerated pupariation and pupation. Furthermore, nearly half of the *spz6Gal4>UASkek4* mutants tested died prior to adult eclosion. BR-C was upregulated in *spz6Gal4>UASkek4* mutants. Together, these data suggested that Kek4 inhibits JH, thereby promoting 20E signalling through BR-C.

The role of Kek4 in systemic control of growth was tested by measuring body sizes and counting wing hair cell number. No difference in larval area, pupal length or adult area could be detected between *yw* controls, $kek4^{20/23}$ or *spz6Gal4>UASkek4* mutants. By contrast, *spz6Gal4>UASkek4* pupae were mildly larger than controls. Cell number increased in *kek4* loss of function mutants, suggesting that cells are smaller in these mutants. One method to verify this might be clonal analysis, whereby the growth of an individual cell (wing, or elsewhere) and its daughter cells could be labelled and directly compared between genotypes (Petit et al., 2005).

The absence of Kek4 from the larval brain, particularly the neurosecretory neuron clusters that innervate the CA, suggests that Kek4 is a receptor of secreted or paracrine ligands that

Figure 7.9 ***kek3* is not required for larval locomotion**

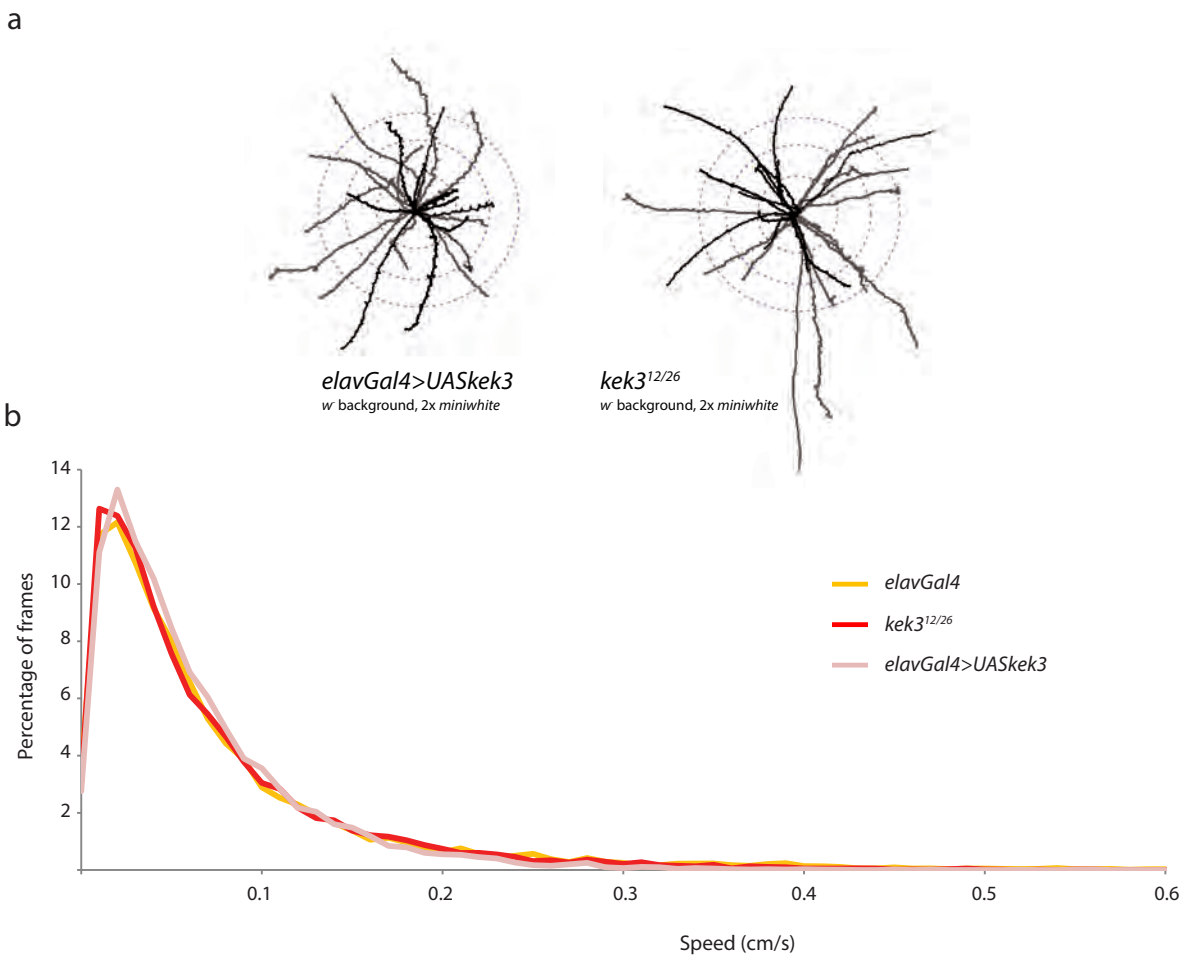

a | Trajectories of *kek3* overexpression and loss of function mutants reveal no noticeable differences in locomotion behaviour. **b** | Speed histogram revealing *kek3*$^{12/26}$ and *elavGal4>UASkek3* mutants do not behave differently to controls. See Appendix I for statistical values and frame numbers.

target the CA. In moths, the pro-JH neuropeptide allatotropin is detected in the CC; signalling is then relayed to the CA by the inhibition of short neuropeptide F (sNPF), which targets the CA and inhibits JH production (Yamanaka et al., 2008). In *Drosophila*, no allatotropins or true allatostatins have been identified (Yoon and Stay, 1995). However, the *Drosophila* CC does express sNPF (Nassel et al., 2008). It would be interesting to test whether Kek4 can interact with CC-derived sNPF. Alternatively, Kek4 may interact with neuropeptides released from neurosecretory cells that directly innervate the CA, such as ion transport peptide (ITP; Dircksen et al. (2008)).

Loss of *kek4* delayed the onset of wandering in L3 larvae, whereas *kek4* overexpression accelerated development. This is consistent with the finding that *kek4* functions upstream of and antagonizes JH function. The accelerated development of *spz6Gal4>UASkek4* larvae resulted in ~40% pupal lethality. Thus, *kek4* overexpression alone can initiate metamorphosis before the critical weight checkpoint has been passed. Ectopic PI3K signalling in the ring gland can also initiate precocious metamorphosis, regardless of larval size (Colombani et al., 2005). Thus, Kek4 may signal via PI3K. To investigate this, the phenotypes of *kek4* loss and gain of function mutations combined with dominant negative and activated forms of PI3K should be tested: *kek4* loss of function should delay accelerated development caused by ring gland upregulation of PI3K signalling. Observed delays could not be attributed to specific larval stages, which each undergo distinct morphological and signalling changes. To delineate the contribution of each larval instar to observed delays, the experiment should be repeated with larvae separately staged at L1, L2 and L3 instars.

Ectopic Kek4 signalling induced BR-C activity in the fat body. This agreed with the hypothesis that Kek4 inhibits JH signalling, since endogenous *BR-C* transcript cannot be translated in the presence of JH (Huang et al., 2011a). This result does not preclude the possibility that Kek4 signalling simultaneously promotes the 20E cascade, rather than simply

permitting it, although secondary messengers that link these processes and their distinct tissue localizations are unclear.

Given that development was slowed in *kek4* mutants, it was a surprise that this was not reflected in the body size of larvae, pupae or adults. It would be expected that longer developmental times would increase body size. This would probably be remedied with larger sample sizes, particularly in adult body sizes (n=10, P=0.116). Nevertheless, the increased wing hair number in *kek4* mutants suggested that body cell density was increased by the delay in development.

kek4 loss and gain of function mutants had reciprocal locomotion phenotypes. It is likely that these phenotypes are the result of Kek4 function in AKH signalling within the CC: AKH promotes activity via motor neurons (Isabel et al., 2005, Milde et al., 1995, Nässel and Winther, 2010). These results suggest that Kek4 antagonises or inhibits AKH signalling.

CC cells secrete sNPF, which must be downregulated to permit JH release from the CA (see above). However, sNPF downregulation also corresponds with the onset of wandering (Wu et al., 2003). Furthermore, sNPF also promotes feeding behaviours and enhances activity during starvation (Lee et al., 2004). In this respect it has similar roles to AKH; thus sNPF–Kek4 interactions could be tested in the context of locomotion, as well as JH signalling.

In conclusion, Kek4 has a role in the systemic control of timing. Next, studies could attempt to decipher the downstream signalling response to Kek4 activation, to determine how Kek4 activation inhibits JH signalling and thereby permits the PTTH–20E cascade. Furthermore, the Kek4 ligand should be searched for: it would be interesting to repeat the above experiments incorporating *DNT* mutants, since putative interactions were suggested in Chapters 3–5. This would provide another example of non-CNS functions of the neurotrophin family, along with the endocrine and immune system roles outlined in Chapter 1.1.4.

CHAPTER 8

DISCUSSION AND CONCLUSIONS

8.1 Main outcomes

This thesis provides evidence of genetic and functional interactions — *in vivo* and in cell culture — between the *Drosophila* neurotrophins (DNTs) and the Kek family, as DNT receptors, in the central nervous system (CNS). Specifically, it provides functional evidence of neurotrophic roles of Kek6 in axon guidance and behaviour, and of a role for Kek4 in developmental timing. Individual findings by gene are summarised in Table 8.1.

These findings are important because *Drosophila* was long presumed to lack neurotrophin-binding Trk receptors. Initially, *Drosophila melanogaster* was considered too simplistic to require and use neurotrophism (Jaaro et al., 2001). Furthermore, analysis of the *Drosophila* kinome showed a complete absence of proteins containing a Trk family TyrK (Manning et al., 2002). Nonetheless, evidence emerged of neurotrophism in insects, and the *Drosophila* neurotrophins DNT1 and DNT2 were recently discovered (Hidalgo, 2002, Zhu et al., 2008). DNT1 and DNT2 can bind and signal via Toll receptors (McIlroy et al., 2013), but reasons to search for Trk proteins in *Drosophila* remained: *vertebrate* neurotrophic ligand–receptor interactions are promiscuous (Huang and Reichardt, 2001), suggesting that *Drosophila* neurotrophin interactions might also require other receptors ; Trk proteins were found in non-insect invertebrates (for example, (Kassabov et al., 2013)), and thus Trks are evolutionarily ancient ; and domain shuffling from ancestral Trk superfamily proteins yielded *Drosophila* leucine rich repeat (LRR) and immunoglobulin (Ig)-containing (LIG) proteins (Dolan et al., 2007), of which the Kek family cluster phylogenetically with the vertebrate Trks, despite lacking intracellular TyrK domains (Mandai et al., 2009). Evidence provided here suggests that the Kek proteins are insect Trks.

Table 8.1 **Summary of thesis, by gene**

Gene	Expression	Figure	Functional analysis	Figure	Genetic analysis	Figure
kek1	Embryo: CNS: VNC and brain; neuronal nuclei PNS: chordotonal organs Heart precursors	3.4,3.5	Axon guidance assay: LOF/GOF mutants exhibit ISNb phenotypes *GMRGal4* assay: *UASkek1* induces a rough eye phenotype	 6.4 4.32	SurvivaI Index assay: Neuronal overexpression of *kek1*: no effect	 4.33
kek2	Embryo: CNS: VNC and brain; neuronal nuclei PNS: ventral clusters Muscle precursors	3.6	*GMRGal4* assay: No phenotype	 4.32	SurvivaI Index assay: Neuronal overexpression of *kek2* rescues $DNT2^{-/-}DNT1^{-/-}$ lethality	 4.33
kek3	Embryo: weak/absent expression Larva: CNS: Central brain and glia surrounding VNC; central optic lobe axon	3.7	Locomotion assay: $kek3^{f07029}$ interacts with *DNTs* *kek3* nulls exhibit adult, but not larval, phenotypes Luciferase assay: DNT2 induces Kek3≡Toll6 signalling in culture *GMRGal4* assay: No phenotype	 3.12 5.8,7.8 4.47 4.32	SurvivaI Index assay: $kek3^{f07029}$ interacts with *DNTs* $kek3^{12}$ and $kek3^{26}$ interact with DNTs Neuronal overexpression of *kek3* rescues $DNT2^{-/-}DNT1^{-/-}$ lethality	 3.11 5.6 4.33
kek4	Embryo: mid/hindgut, ring gland precursors Larva: CA and CC of ring gland	7.1	Locomotion assay: $kek4^{f05454}$interacts with *DNTs* *kek4* nulls exhibit adult and larval locomotion phenotypes Luciferase assay: DNT2 induces Kek4≡Toll6 signalling in culture Ring gland assays: Kek4 delays developmental timing Kek4 inhibits juvenile hormone signalling Kek4 controls cell number, but not body size *GMRGal4* assay: No phenotype	 3.12 5.8,7.7 4.47 7.2,7.3 7.4 7.5,7.6 4.32	SurvivaI Index assay: $kek4^{f05454}$ interacts with *DNTs* $kek4^{20}$ and $kek4^{23}$ interact with *DNT1* Neuronal overexpression of *kek4*: no effect	 3.11 5.6 4.33
kek5	Embryo: CNS: contralateral neurons and longitudinal fascicles of VNC PNS: chordotonal organs and ventral/lateral neuron clusters Larva: VNC and central brain	3.8	Locomotion assay: $kek5^{e02482}$ does not interact with *DNTs* Luciferase assay: DNT2 induces Kek5≡Toll6 signalling in culture *GMRGal4* assay: No phenotype	 3.12 4.47 4.32	SurvivaI Index assay: $kek5^{e02482}$ interacts with *DNTs* Neuronal overexpression of *kek5* may rescue $DNT2^{-/-}DNT1^{-/-}$ lethality	 3.11 4.33
kek6	Embryo: CNS: brain and VNC: longitudinal axons, pioneer neurons and motorneurons	6.1,6.2	Axon guidance assay: LOF/GOF mutants exhibit ISNb phenotypes LOF rescues DNT1 overexpression ISNb phenotypes Kek6 is upstream of Ras and PI3K	 6.4 6.5 6.6	SurvivaI Index assay: $kek6^{34}$ interacts with *DNT2* and *tie* *DNT1* GOF rescues *kek6* null lethality Rho and Cdc42 rescue *kek6* lethality	 5.7 5.7 5.7

			Locomotion assay:		*kek6* is neuronal	5.7
			LOF/GOF mutants exhibit locomotion phenotypes	6.7	Neuronal overexpression of *kek6* rescues $DNT2^{-/-}DNT1^{-/-}$ lethality	4.33
			Kek6 function is neuronal	6.8		
			kek6 interacts with *DNT2*	6.9		
			Kek6 is upstream of Ras	6.10		
			Luciferase assay:			
			DNT2 induces Kek6≡Toll6 signalling in culture	4.47		
			GMRGal4 assay:			
			No phenotype	4.32		
lbk	Embryo: CNS: absent Epidermis and/or muscle precursors or PNS neuronal clusters	3.3			SurvivaI Index assay: $lbk^{PGS50104}$ interacts with *DNTs*	3.11
CG15744	Embryo: CNS: VNC and brain; undefined signal Hindgut	3.1				
CG16974	Embryo: CNS: absent Epidermis and/or PNS neuronal clusters Muscle precursors and/or muscle attachment sites	3.2				
rk	Embryo: CNS: weak signal in early embryo VNC Brain and hindgut signal by stage 16	3.9			SurvivaI Index assay: rk^{4} does not interact with *DNTs*	3.11
wgn	Embryo: CNS: select nuclei in VNC, exit glia Oenocytes and tracheal precursors Heart precursors Lateral muscles/attachment sites	3.10			SurvivaI Index assay: wgn^{e00637} does not interact with *DNTs*	3.11
CG17839	Embryo: CNS: VNC and brain	3.9				

That a TyrK-lacking protein could be considered a Trk might be controversial. However, these results are important because they provide an invertebrate example of a functional role for truncated Trks, naturally expressed TyrK-less Trk isoforms found in vertebrates (Ohira and Hayashi, 2009). Truncated Trks were originally assumed to be dominant negative Trk receptors that function as ligand sinks. This work indicates that, in the absence of full length Trks, invertebrate truncated Trks can function as neurotrophin receptors.

In the absence of full length Trks in insects, *Drosophila* neurotrophin signalling therefore occurs via NGF CysKnot-containing ligands and LIG-containing truncated Trks — the Keks — in addition to Tolls. This work is the first to support this neurotrophic model in *Drosophila*, supports the recognition of neurotrophism outside of the vertebrates, and indicates the importance of evolutionary conservation of protein modules in neurotrophism throughout the metazoa.

8.2 The LIGs function in the *Drosophila* nervous system

Data in this thesis reveal that the dLIGs have distinct roles in the *Drosophila* nervous system. Each gene had a distinct expression profile; only *kek1* overexpression in the eye induced a rough eye phenotype; *kek4* mutants affected JH signalling and developmental timing in larvae; *kek6* mutants displayed motor axon misrouting phenotypes, whereas *kek1* mutants did not; and both *kek4* and *kek6* mutant larvae had locomotion phenotypes, whereas *kek3* mutant larvae did not. Thus, diversification of Kek functions in the nervous system paralleled their duplication. It was not determined whether *kek1–3*, *kek5* and *kek6* have larval brain expression or whether the Kek family are involved in adult brain function. It would therefore be a natural extension of the project to determine the roles of these genes in such contexts. For Kek6, the first step would be to determine synaptogenesis phenotypes in the larval neuromuscular junction (NMJ), a common paradigm for testing the roles of genes in synaptic plasticity. Furthermore, the function of Kek3 in the adult should be tested: *kek3* loss of

function had no effect on larval locomotion, but Kek3 was required for normal adult behaviour. It is possible, therefore, that the temporal expression of *kek3* function is delayed compared to the other Kek protein family members and that *kek3* is required in the adult. Indeed, FlyAtlas and modENCODE data suggest that *kek3* is weakly expressed in the larval brain and abundantly expressed in the adult brain (Celniker et al., 2009, Chintapalli et al., 2007).

The specificity of *lambik* and *CG16974* expression in the peripheral nervous system (PNS) warrants further attention. In particular, localized expression to the chordotonal organs suggests that these proteins are required for behavioural responses. Chordotonal organs are internal mechanoreceptors, including stretch receptors, and provide sensory feedback to the locomotor central pattern generator circuit (Field and Matheson, 1998, Caldwell et al., 2003). Thus, *lambik* and *CG16974* may also exhibit locomotion phenotypes or, via their stretch receptor role, be required at the critical weight checkpoint. The roles of *lambik* and *CG16974* in sensory perception would be interesting to pursue further. The genetic interactions suggested by $lbk^{-}DNT1^{-}$ and $lbk^{-}DNT2^{-}$ double mutants suggests an interplay between the PNS and the neurotrophins, thereby linking the roles of the DNTs in the CNS with systemic growth and behaviour. In vertebrates, peripheral nerves are enriched in truncated Trks, and NGF supports the growth of PNS neurons throughout development and into adulthood (Raivich and Kreutzberg, 1993, Valenzuela et al., 1993).

8.3 dLIGs and the DNTs

The 12 candidate receptor genes were initially characterised with a view to selecting candidates for further study. The candidates were chosen according to the following criteria:

1. *dLIG expression enriched in the neurons of the CNS. DNTs* are expressed in neuronal targets and have trophic effects on innervating neurons, including motor neurons, and interneurons within the ventral nerve cord (VNC; Zhu et al. (2008). Neurotrophin–

receptor signalling can also be autocrine, or create coincident positive feedback loops; for example, during exercise and learning, synaptic BDNF upregulates transcription of *TrkB* and *BDNF* itself (Vaynman et al., 2003). Receptors with complementary or coincident expression profiles to the *DNTs* would therefore be strong candidates to function as DNT receptors. By this criterion, *lbk*, *CG16974*, *rk*, *CG17839* and *wgn* were eliminated as candidates because they were detected primarily in the PNS, glia or were absent from the VNC. This does not preclude a role for these genes in the nervous system, but allowed the project to focus on a subset of candidates.

2. *dLIGs with a role in CNS development and function.* The DNTs maintain neuronal survival and targeting (Zhu et al., 2008). Putative receptors, therefore, are likely to share similar or related phenotypes in CNS development, although ligand and receptor promiscuity, antagonistic functions of ligands and domineering non-autonomous phenotypes caused by receptor mutations must be considered. Roles for the dLIGs in the CNS were initially selected using adult locomotion as a phenotype. These data highlighted the Kek protein family as the most suitable receptor candidates. Subsequently, *kek6* was shown to be required for motor axon targeting and correct locomotion behaviour in larvae.

3. *dLIGs that interact with the DNTs in vivo and/or in cell culture.* This was assessed by genetic interactions and using lethality as a phenotype. Survival assays revealed transposon-derived alleles of *kek3*, *kek4*, *kek5* and *lambik* genetically interacted with specific *DNT* alleles. Subsequent genetic analysis with Flippase recognition target (FRT)-derived null alleles confirmed the importance of *kek3* and *kek4* genetic interactions with the DNTs. Furthermore, survival indices of *kek6–DNT* double mutants revealed a potential interaction between Kek6 and DNT1.
   dLIG–DNT interactions were next tested in cell culture, by expressing Kek≡Toll6 chimaeras, stimulating with DNT protein, and measuring activation of NFkB

signalling as readout. NFkB has a role in synaptic plasticity and is conserved throughout the bilateria (for example, NFkB is involved in the induction of long term memory in crabs (Freudenthal and Romano, 2000)). In flies, NFkB signalling is triggered in response to DNT binding to Toll6 and Toll7 (McIlroy et al., 2013). It is not known whether endogenous Kek proteins can signal via NFkB, although this is unlikely due to the absence of appropriate intracellular domains in full length Keks. Nonetheless, the ability of Kek≡Toll6 chimaeras to signal through NFkB indicated an ability of the extracellular domain of Kek proteins, Kek3 and Kek6, in particular, to functionally interact with the DNTs.

According to these criteria, the Kek protein family were selected for further study.

Putative DNT–Kek interactions do not preclude the possibility of alternative Kek ligands. Vertebrate neurotrophins have a conserved six cysteine CysKnot homodimer structure, defined by the first defined neurotrophin, NGF (Sun, 1995). Active DNT1, DNT2 and Spz form CysKnot dimers, and the tertiary structure of Spz overlaps closely with NGF (Arnot et al., 2010, Zhu et al., 2008). The Kek protein family may interact with other CysKnot dimers. Alternatively, EGF- or Dpp-like TGFβ ligands may signal through the Kek family. Kek1 interacts with EGFR, whereas Kek5 extracellular LRRs bind and sequester bone morphogenetic protein (BMP) (Derheimer et al., 2004, Evans et al., 2009, Ghiglione et al., 1999, Ghiglione, 2003). The possibility of Kek ligand promiscuity warrants further investigation.

8.4. Downstream signalling of Kek6

Ras and phosphatidylinositol 3-kinase (PI3K) belong to many essential pathways, including the actin cytoskeleton-regulating pathways. It was therefore unsurprising that dominant negative forms of these hub proteins disrupted phenotypes caused by *kek6* overexpression in

neurons. More surprising was the absence of an effect caused by dominant negative Cdc42, Rac or Rho, which should suppress ectopic cytoskeletal rearrangements during growth cone targeting in a *kek6* neuronal overexpression background.

In canonical Trk signalling, ligand-induced receptor activation leads to Ras, PI3K and phospholipase Cγ (PLCγ; signalling (Figure 1.2). Furthermore, the recruitment of the SHC–SOS complex to phosphorylated tyrosine residues on the intracellular TyrK domain facilitates the activation of Rac and subsequent Rho-mediated cytoskeletal rearrangements. Rac GEF activity of SOS is further enhanced by Ras signalling through PI3K (Nimnual et al., 1998). Thus, phenotypes caused by excessive signalling could be rescued by expression of dominant negative Rho, Rac or Cdc42 alleles. However, dominant negative Rho, Rac or Cdc42 did not rescue axon misrouting phenotypes induced by neuronal overexpression of *kek6*. By contrast, binding of BDNF to truncated TrkB.T1 provokes its dissociation from RhoGDI1, an inhibitor of Rho, thus permitting Rho inactivation (Figure 1.6; Ohira et al. (2006)). If the mechanism of Kek6 signalling resembles that of truncated Trks, activated Kek6 signalling might also result in the inhibition of Rho. This might explain why dominant negative Rho did not rescue *kek6* overexpression phenotypes in these assays. To test this hypothesis, simultaneous *elavGal4*-driven *kek6* and constitutively-activated *rho* should be compared for axon guidance defects and locomotion phenotypes; *kek6* overexpression-mediated RhoGTPase inhibition could be rescued by expression of activated *rho*. Since Rac and Cdc42 are required for axon growth, it is possible that dominant negative isoforms in these assays generated axon misrouting phenotypes independently of aberrant Kek6 levels.

The ability of Kek6 to signal via CREB was not considered and would be a logical extension of the work. CREB proteins are associated with memory formation, a role that is conserved from mammals to *Lymnaea*, and neurogenesis (Dworkin and Mantamadiotis, 2010, Kandel,

2012, Merz et al., 2011). *CREB* transcription increases in response to BDNF signalling through TrkB (Vaynman et al., 2003), linking the CREB pathway to the neurotrophins. CREB signalling can be activated by phosphorylated ERK, CREB-1 is phosphorylated by protein kinase A and the memory suppressor protein CREB-2 is downregulated by MAPK signalling (Kandel, 2012, Xing et al., 1998). The role of Kek signalling in the CREB pathway via Ras therefore warrants investigation.

As previously discussed, Kek6 may signal to the actin cytoskeleton directly via a RhoGDI-type mechanism. Alternatively, since LRR and Ig domains are associated with protein–protein interactions, and the extracellular domain of Kek1 can bind EGFR, Kek6 may function via a co-receptor (de Wit et al., 2011, Ghiglione, 2003, Kobe and Kajava, 2001, Vaughn and Bjorkman, 1996, Williams and Barclay, 1988). The protein–protein interaction prediction database STRING (Search Tool for the Retrieval of Interacting Genes) is unable to identify interacting partners with Kek6 (Szklarczyk et al. (2011); http://string-db.org/).

The effect on protein function of combining protein domains with distinct roles is synergistic (Bashton and Chothia, 2007). As such, single domain proteins from the same protein family have a 67% chance of having similar functions, whereas two multidomain proteins with one domain in common have similar functions only 35% of the time (Hegyi and Gerstein, 2001). For example, ‘paired receptors’, which have similar extracellular domains but have different cytoplasmic domains, often have opposing functions as activators and inhibitors (Akkaya and Barclay, 2013). These opposing functions arise because of pathogen-driven evolutionary pressures, and are implemented through protein–protein communication via their extracellular Ig domains or specific amino acids in their transmembrane domains (Akkaya and Barclay, 2013, Nakayama et al., 2007). These receptors may hint at potential Kek6-interacting partners.

‘Activating paired receptors’ with one or more Ig domains contain a characteristic positively charged arginine, lysine or histidine in their transmembrane domain (Takai, 2005). These residues interact with the ITAM (immunoreceptor tyrosine-based activation motif) domains of adaptor proteins and co-receptors. ‘Inhibitory paired receptors’, by comparison, contain cytoplasmic ITIM domains, which recruit phosphatases upon ligand binding. An example of an inhibitory paired receptor is PIR-B, which interacts with Toll-like receptor 2 (TLR-2) in response to *Staphylococcus aureus* infection to modulate cytokine release (Nakayama et al., 2007).

ITAM domains are characterised by the consensus motif YxxI/Lx(6–12)YxxI/L, and ITIM domains by S/I/V/LxYxxI/V/L (Takai, 2005). The Kek proteins lack ITAM and ITIM sequences. However, the transmembrane domains of the Kek proteins are rich in positively-charged lysine residues (Figure 2.9), and thus may interact with ITAM domain-containing adaptors or co-receptors, in the manner of activating paired receptors. An example of receptor–ITAM domain binding in *Drosophila* involves Draper, which recognises and promotes the engulfment of axonal debris and dying neuronal cells (Logan et al., 2012). The intracellular ITAM domain of Draper forms a complex with the cytosolic TyrKs Src42A and Shark (Ziegenfuss et al., 2008). Src42A is predicted to interact with Ras85D (Therrien et al. (2000); and Shark has a role upstream of the JNK pathway during dorsal closure (Fernandez et al., 2000).

An alternative co-receptor is Tie. Tie was discovered by homology to the TyrK of PDGFR, and is characterised by an intracellular TyrK, a transmembrane domain, and no recognisable extracellular domains (Mitsuhiro et al., 1994). It therefore resembles the intracellular portion of Trks, although predicted phosphorylation sites differ between the TyrK domains of Tie and human TrkB (NetPhos2.0; Blom et al. (1999)). Known roles of Tie include border cell migration in egg chambers, and it is involved in JAK/STAT and Hedgehog signalling (Wang et al., 2006, Nybakken et al., 2005). In this thesis, Tie was briefly studied in combination with

kek6 alleles. *kek6* viability was slightly reduced in *kek6Tie* double mutants, but this combination had no discernible locomotion phenotype compared with $kek6^{34/Df(kek6)}$ alone.

In Chapter 5, $DNT2^{-/Df(DNT2)}kek6^{34/Df(kek6)}$ double mutants had impaired viability compared with *kek6* loss alone (Figure 5.7). These data might suggest that Kek6 is a receptor for DNT1: if DNT2 simply bound Kek6, then the phenotype of loss of DNT2 should be equivalent to that of *kek6* mutants, and of the double mutants. If Kek6 binds DNT1, then losing both DNT2 and Kek6 in the double mutants is equivalent to losing two ligand-receptor pathways rather than one. However, this conclusion is difficult to draw in the light of axon misrouting data presented in Chapter 6, and is further complicated by the fact that DNTs bind Toll6 and Toll7 receptors (McIlroy et al., 2013). Overexpression of *DNT1* in muscles resulted in intersegmental nerve b (ISNb) projection misrouting, which was rescued in a *kek6* null genetic background. This is consistent with the fact that the loss of a receptor should abrogate the effect of exogenous ligand. However, $kek6^{34}$*24BGal4* x *UASDNT1CK3'+*;$kek6^{35}$ rescued misrouting to the level of the *yw* control, rather than to the level of *kek6* loss of function alone (Figure 6.4). DNT1 binds the Toll7 receptor, also in the context of motor axon targeting (McIlroy et al., 2013). One possible interpretation for these data is that Kek6 may interact with Toll7, modulating its function. On the other hand, luciferase assay data revealed that Kek6 can bind DNT2 (Figure 4.5). If Kek6 binds DNT2, $DNT2^{-/Df(DNT2)}kek6^{34/Df(kek6)}$ double mutants should not have different phenotypes to *kek6* or *DNT2* single mutants. However, in the locomotion assay, $DNT2^{-/Df(DNT2)}kek6^{34/Df(kek6)}$ larvae crawled significantly slower than $kek6^{34/Df(kek6)}$ single mutants. These conflicting data suggest that Kek6 ligand binding is promiscuous, that other receptors are required for Kek6 function and/or Kek6 is a co-receptor that modulates other receptors, perhaps Toll6 and Toll7.

One possibility to test whether Kek6 may modulate Toll6 or Toll7 function is to manipulate Toll6 or Toll7 and Kek6 simultaneously. If Kek6 modulates Toll6 or Toll7, this could result in synergistic activation or in repression, in two possible scenarios: (1) If Kek6 represses

Toll6 function: the rescue of axon targeting in *kek6*^{34}*24BGal4* x *UASDNT1CK3'+;kek6*^{35} may result from the enhancement of the DNT2–Toll6 pathway in the absence of Kek6, plus the combined activation of the Toll7 pathway when *DNT1* is overexpressed (McIlroy et al., 2013, Zhu et al., 2008). (2) If Kek6 activates Toll7 function: the loss of *kek6* may impair the function of Toll7 if DNT1 is in limiting levels, and this is overcome by the overexpression of *DNT1*, which activates Toll7.

To test the hypothesis that Kek6 modulates Toll6 or Toll7, *kek6* and *toll6* or *toll7* could be simultaneously overexpressed in neurons (e.g. *elavGal4>UASkek6RFP;UASToll6*). If Kek6 negatively modulates Toll6, then *kek6* overexpression should partially rescue any phenotype caused by the overexpression of *toll6* (for example, upregulation of Toll6 downstream signalling, as measured by immunolabelling and detection by Western blot). If Kek6 were to promote Toll7 signalling, then overexpression of both *toll7* and *kek6* could result in a stronger phenotype than overexpressing either *kek6* or *toll7* alone. For instance, overexpression of one dose of either *toll6* or *toll7* in neurons (with *elavGAL4*) is not sufficient to cause misrouting phenotypes in axon guidance (McIlroy et al., 2013). To affect axon guidance, either two copies of *UASToll6* or two copies of GAL4 (*Toll7GAL4;elavGAL4*) had to be employed (McIlroy et al., 2013). If Kek6 enhances the functions of Toll6 or Toll7, expressing both *kek6* and *toll6* or *toll7* may induce a stronger axon guidance phenotype than expressing either of them alone.

8.5 Evolution of domain shuffling

Exon shuffling by intronic recombination, gene rearrangements and intronic mutations expands proteomes. Organism complexity correspondingly increases. But complexity alone is not an advantageous trait without a selective pressure that necessitated expanded domain architecture repertoires: thus, what is the evolutionary driving force behind domain shuffling?

Domain shuffling allows for rapid novelty in protein evolution, which is required for the myriad self–non-self and antigen recognition combinations for which the immune system is responsible (Soding and Lupas, 2003). This same process drives the evolution of pathogen surface proteins seeking to evade immune capture. Alternative splicing of Ig domain proteins is essential in *Drosophila* innate immunity, and the adaptive immune system of jawless vertebrates relies on the recombination of a large cluster of diverse LRR sequences (Hirano et al., 2011, Kurata, 2010). Indeed, since LRRs and Igs are involved in protein–protein interactions, they are frequently involved in the innate immune system (Nurnberger et al., 2004). Pattern recognition receptors (PRRs), such as Tolls and TLRs, which recognise microbial-associated molecular patterns, are typically rich in LRRs (Dishaw et al., 2012, Tauszig et al., 2000). Furthermore, the innate immune system of *Amphioxus* has an extensively expanded repertoire of intracellular PRRs compared with sea urchin, of which LIG proteins are one of the most expanded families (Dishaw et al., 2012, Huang et al., 2008, Huang et al., 2011b).

On a molecular level, the immune and nervous systems have many common links. Many gene and protein families have roles in both immunity and the nervous system. For example, in *C. elegans*, innate immunity and pathogen avoidance is regulated by NPR-1^{+} neurons (Aballay, 2009, Styer et al., 2008). Some mammalian *TLRs*, which are involved in the innate immune system, are expressed and function in neurons (Ma et al., 2006); and *Drosophila* Toll6 and Toll7 can interact with the DNTs in the CNS (McIlroy et al., 2013). p75^{NTR} belongs to the tumour necrosis factor (TNF) receptor superfamily, members of which are primarily involved in the innate/adaptive immune system, making the role of p75^{NTR} in nervous system development ‘atypical’ (Bothwell, 2006). It is uncertain whether TNF receptor superfamily roles in immunity or the nervous system are the ancestral function.

The CNS is immunologically active: the blood–brain barrier, which is rich in LRR and Ig domain-rich cell–cell adhesion molecules, is the first line of defence against brain infections

and CNS injuries (Lampron et al., 2013, Schulze and Firth, 1993). Microglia, astrocytes, oligodendrocytes, endothelial cells and neurons also express functional PRRs (Hanamsagar et al., 2012). When the pro-inflammatory cytokine IL-1β is activated in response to TLR activation, subsequent signalling enhances the production of insulin-like growth factor-1 and NGF (Mason et al., 2001, Spranger et al., 1990).

The characteristics that make tandem, shuffled domains suitable for innate and adaptive immunity also support nervous system functions. For example, alternative splicing can create functionally distinct cell adhesion molecules, such as FasII, in neurons (Walsh and Doherty, 1997). Alternative splicing of Ig and LRR domains also underlie neurite self-avoidance during neurodevelopment (Zipursky and Grueber, 2013). DSCAM, which is an Ig domain-rich transmembrane protein required for neuronal connectivity, has >38,000 splice isoforms (Wojtowicz et al., 2004), permitting complexity of neuron to neuron contacts. Indeed, the mechanism of alternative splicing balances the mathematical conundrum posed within the nervous system: the human brain, for example, comprises 10^{12} neurons with at least 1,000 more connections, but axonal and synaptic development rely on a limited repertoire of signalling factors (Loya et al., 2010). Such components are enriched in Ig and/or LRR domains, for example, NCAM, Semaphorins, Robo and Slit (Tessier-Lavigne and Goodman, 1996). Alternative splicing amplifies this repertoire, often from single loci, to thousands of components required throughout the development of connectivity. In vertebrates, for example, alternative splicing of neurexins and neuroligins mediates synapse differentiation. In *Drosophila*, alternative splicing of Robo3 generates proteins with reciprocal functions, as Robo3.1 promotes midline crossing of axons, whereas Robo3.2 repels contralateral commissural neuron growth cones once they have crossed the midline (Chen et al., 2008).

Thus, the mechanisms that underlie the diversity of protein domains in the immune system overlap with the nervous system. A system that creates cell–cell signalling complexity to evade infection produced domains and modules that could be co-opted by domain shuffling

into proteins with roles in the nervous system, and/or vice versa. It is unclear which arose first, although it is interesting that the ability to signal via action potentials, and thus a defining characteristic of the nervous system, is conserved throughout the eukaryotes (including in plants; Volkov et al. (2013)). Here, I showed that a protein family unique to the insects that features commonly shuffled domains is required for nervous system development.

8.6 Implications: Evolution of receptors in the nervous system by domain shuffling

Above I considered the Keks as co-receptors or novel modulators of DNT receptor signalling, focusing on models of Kek6–Toll6/7 interactions. Alternatively, Keks may function as ligand sinks and dominant negative inhibitors of DNT signalling, as was the presumed role of truncated Trks on their discovery; this would tally with the known antagonistic roles of Kek1 and Kek5. Because they are unique to the insects, the Keks may be evolutionary artefacts that arose by retrotransposition of truncated Trk-like proteins and that were subsequently retained in the insect lineage. Below, I consider the evolution of the Trk family, and of Keks as Trk-like proteins,

The TyrK of Trks, which has traditionally been used as the defining feature from which to identify Trk orthologues, is one of three domains that are essential for its functions. The remaining domains, Igs and LRRs, in combination, are essential for ligand identification and binding to Trks. Thus, the contention that there are no Trks in *Drosophila* is not very helpful. Whilst there may not be full length canonical Trks, by comparing full length protein sequences that include LIG modules, the Kek protein sequences cluster phylogenetically with the vertebrate Trks (Mandai et al., 2009), implying that, regarding the extracellular domain, the Keks are possibly orthologues of TrkB.T1.

Domain shuffling throughout evolution has created separate protein families with distinct roles and highlights modular conservation between species. On a smaller scale, domain splicing and recombination mediate receptor specificity to neurotrophins (Clary and

Reichardt, 1994). For example, TrkA has an alternative splice form containing an additional 18bp exon that translates to the extracellular domain. This mediates the specificity of TrkA ligand binding: NT-3 binding requires the translation of the exon, whereas NGF does not (Clary and Reichardt, 1994). TrkB splice variants also have different affinities for BDNF (Strohmaier et al., 1996). TrkB.T1, TrkB.T2 and TrkC.T1 are functional isoforms with roles distinct from full length Trks (Ohira and Hayashi, 2009). In addition, cell type-specific binding of co-receptors such as Linx mediate neurotrophic signalling in vertebrates (Mandai et al., 2009). Thus, the context-specific use of protein domains and peptides complements the promiscuity of neurotrophin ligand–receptor interactions that underlie neuronal network complexity. In *Drosophila*, LIG proteins may have arisen from a common metazoan ancestor, and the generation of lineage-specific proteins by domain shuffling permitted the co-option of the LIG module for novel functions.

This domain shuffling yielded Kek6, which can interact with the DNTs *in vivo* and is required for motor axon targeting and locomotion; Kek4, which is required in the ring gland for temporal regulation of development; and Lbk and CG16974 in the PNS. I have also shown that Kek3 and Kek4 can functionally interact with the DNTs in cell culture and *in vivo*. Despite the lack of an intracellular TyrK, therefore, the Kek protein family appear to be functional truncated Trk-like proteins. The LIG module is thus a crucial component of the nervous system throughout metazoan proteomes.

It is unclear whether the ancestral protein from which the Trk and Kek families arose contained an intracellular kinase. On the one hand, the conservation of the TyrK in Trk and Trk-like proteins in other invertebrates suggests that an ancestral kinase was lost in the insect lineage (Figure 8.1) (Kassabov et al., 2013, van Kesteren et al., 1998, Wilson, 2009). The loss of the TyrK would have impacted the signalling ability of these proteins and necessitated signalling diversity by means of, for example, gene duplication, co-receptor binding or ligand promiscuity. On the other hand, truncated Trks are naturally occurring isoforms in vertebrates

Figure 8.1 **Evolution of the Trk family**

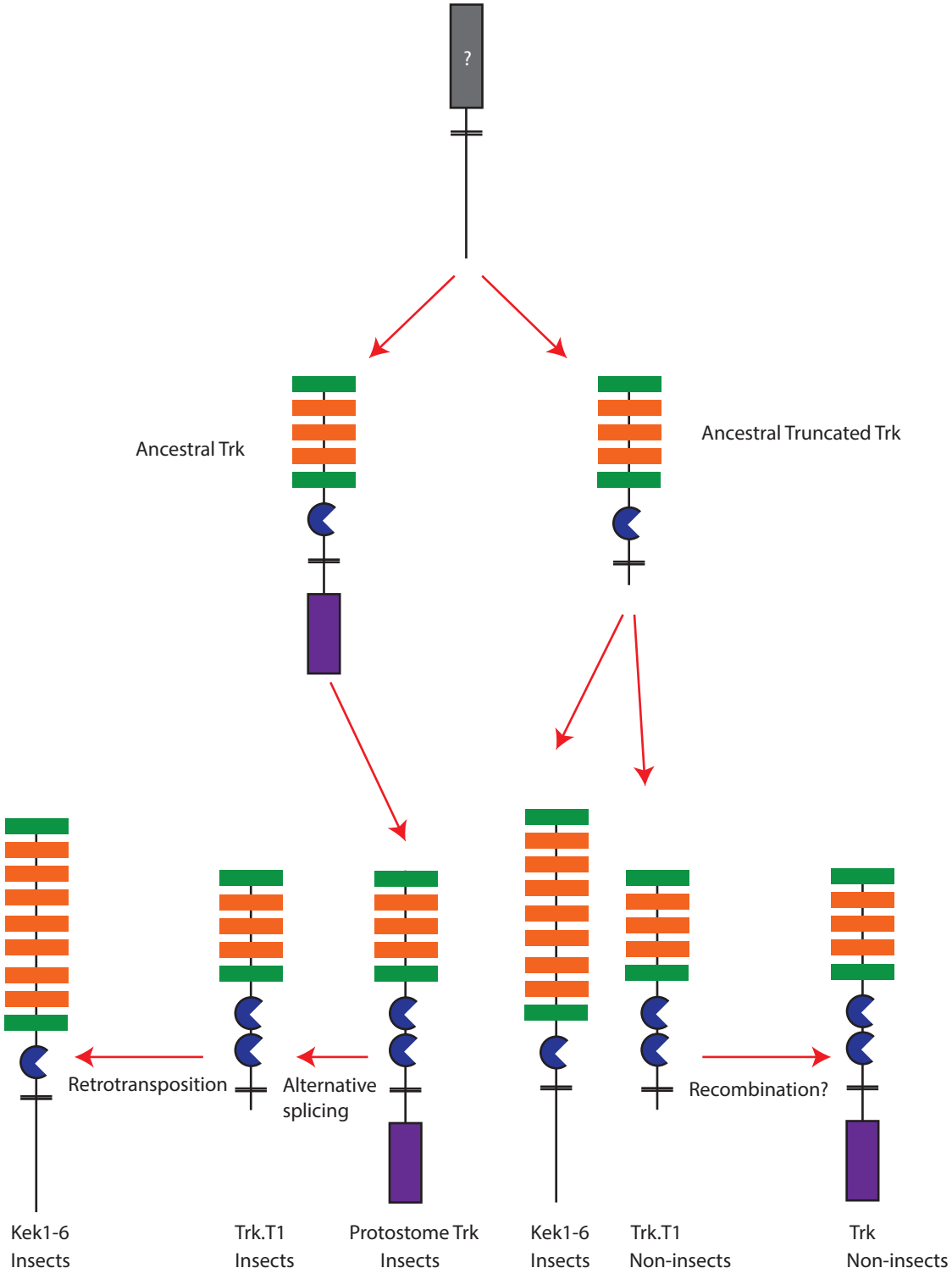

Potential evolutionary expansion of the Trk and Trk-like families in the metazoa. Kek proteins are Trk-like proteins that lack an intracellular tyrosine kinase (TyrK) domain. Potential mechanisms of TyrK acquisition or loss from an ancestral Trk or truncated Trk are shown.

with distinct roles. Such roles could be an ancestral function that was subsequently supplemented by the addition of a kinase, except in the insects (Figure 8.1). If the former is true, *Drosophila* may encode further receptors that are distinct from the Trk family TyrK domain-containing receptor TyrKs (RTKs) but fulfil the role of the Trk TyrK, and may function as co-receptors to the Kek proteins; in the latter scenario, other protostomes may encode functional truncated Trk-like proteins comprising extracellular LIG motifs but lack an intracellular kinase. Given the presence of an LIG module-lacking Trk-like transmembrane TyrK protein in *Aplysia*, it would be interesting to explore metazoan proteomes further for conservation of truncated proteins. Kek downstream signalling must next be investigated, to determine whether the mechanism of truncated Trk signalling has been conserved in *Drosophila*: if so, there is a possibility that this is an ancestral role or that the Keks arose from truncated Trk retrotransposition. If Kek proteins signal differently to truncated Trks, this would suggest that the TyrK-lacking domain of Kek proteins is a recent loss from a metazoan TyrK-containing Trk precursor and that the truncated Kek protein has been co-opted for another role. Last, the importance of the LIGs in modulating vertebrate neurotrophic signalling strongly suggests that the dLIGs modulate Toll6 and Toll7; this should be explored further.

REFERENCES

ABALLAY, A. 2009. Neural regulation of immunity: role of NPR-1 in pathogen avoidance and regulation of innate immunity. *Cell Cycle,* 8**,** 966-9.

AKKAYA, M. & BARCLAY, A. N. 2013. How do pathogens drive the evolution of paired receptors? *European Journal of Immunology,* 43**,** 303-313.

ALBERTINAZZI, C., GILARDELLI, D., PARIS, S., LONGHI, R. & DE CURTIS, I. 1998. Overexpression of a neural-specific rho family GTPase, cRac1B, selectively induces enhanced neuritogenesis and neurite branching in primary neurons. *J Cell Biol,* 142**,** 815-25.

ALOE, L. & LEVI-MONTALCINI, R. 1977. Mast cells increase in tissues of neonatal rats injected with the nerve growth factor. *Brain Res,* 133**,** 358-66.

ALOE, L., PROBERT, L., KOLLIAS, G., BRACCI-LAUDIERO, L., SPILLANTINI, M. G. & LEVI-MONTALCINI, R. 1993. The synovium of transgenic arthritic mice expressing human tumor necrosis factor contains a high level of nerve growth factor. *Growth Factors,* 9**,** 149-155.

ALOE, L., SKAPER, S. D., LEON, A. & LEVI-MONTALCINI, R. 1994. Nerve growth factor and autoimmune diseases. *Autoimmunity,* 19**,** 141-150.

ALOE, L., TUVERI, M. A., CARCASSI, U. & LEVI-MONTALCINI, R. 1992. Nerve growth factor in the synovial fluid of patients with chronic arthritis. *Arthritis Rheum.,* 35**,** 351-355.

ALOYZ, R. S., BAMJI, S. X., POZNIAK, C. D., TOMA, J. G., ATWAL, J., KAPLAN, D. R. & MILLER, F. D. 1998. p53 is essential for developmental neuron death as regulated by the TrkA and p75 neurotrophin receptors. *J Cell Biol,* 143**,** 1691-703.

ALVARADO, D., RICE, A. H. & DUFFY, J. B. 2004a. Bipartite Inhibition of *Drosophila* Epidermal Growth Factor Receptor by the Extracellular and Transmembrane Domains of Kekkon1. *Genetics,* 167**,** 187-202.

ALVARADO, D., RICE, A. H. & DUFFY, J. B. 2004b. Knockouts of Kekkon1 Define Sequence Elements Essential for *Drosophila* Epidermal Growth Factor Receptor Inhibition. *Genetics,* 166**,** 201-211.

ANDERSON, K. V., JURGENS, G. & NUSSLEIN-VOLHARD, C. 1985. Establishment of dorsal-ventral polarity in the Drosophila embryo: genetic studies on the role of the Toll gene product. *Cell,* 42**,** 779-89.

ANGELETTI, R. H. & BRADSHAW, R. A. 1971. Nerve Growth Factor from Mouse Submaxillary Gland: Amino Acid Sequence. *Proceedings of the National Academy of Sciences,* 68**,** 2417-2420.

ARNOT, C. J., GAY, N. J. & GANGLOFF, M. 2010. Molecular Mechanism That Induces Activation of Spatzle, the Ligand for the Drosophila Toll Receptor. *Journal of Biological Chemistry,* 285**,** 19502-19509.

AYYAR, S., PISTILLO, D., CALLEJA, M., BROOKFIELD, A., GITTINS, K., GOLDSTONE, C. & SIMPSON, P. 2007. NF-kB/Rel-Mediated Regulation of the Neural Fate in Drosophila. *PLoS One,* 2**,** e1178.

BAI, Y., SHI, Z., ZHUO, Y., LIU, J., MALAKHOV, A., KO, E., BURGESS, K., SCHAEFER, H., ESTEBAN, P. F., TESSAROLLO, L. & SARAGOVI, H. U. 2010. In Glaucoma the Upregulated Truncated TrkC.T1 Receptor Isoform in Glia Causes Increased TNF- Production, Leading to Retinal Ganglion Cell Death. *Investigative Ophthalmology & Visual Science,* 51**,** 6639-6651.

BANDO, T., SEKINE, K., KOBAYASHI, S., WATABE, A. M., RUMP, A., TANAKA, M., SUDA, Y., KATO, S., MORIKAWA, Y., MANABE, T. & MIYAJIMA, A. 2005. Neuronal leucine-rich repeat protein 4 functions in hippocampus-dependent long-lasting memory. *Mol Cell Biol,* 25**,** 4166-75.

BARONE, M. C. & BOHMANN, D. 2013. Assessing neurodegenerative phenotypes in Drosophila dopaminergic neurons by climbing assays and whole brain immunostaining. *J Vis Exp***,** e50339.
BASHTON, M. & CHOTHIA, C. 2007. The Generation of New Protein Functions by the Combination of Domains. *Structure,* 15**,** 85-99.
BASU, M. K., CARMEL, L., ROGOZIN, I. B. & KOONIN, E. V. 2008. Evolution of protein domain promiscuity in eukaryotes. *Genome Res,* 18**,** 449-61.
BATE, C. M. & GRUNEWALD, E. B. 1981. Embryogenesis of an insect nervous system II: A second class of neuron precursor cells and the origin of the intersegmental connectives. *Journal of Embryology and Experimental Morphology,* 61**,** 317-330.
BATEMAN, J., SHU, H. & VAN VACTOR, D. 2000. The Guanine Nucleotide Exchange Factor Trio Mediates Axonal Development in the Drosophila Embryo. *Neuron,* 26**,** 93-106.
BEADLE, G. W. T., EDWARD L CLANCY, C W 1938. FOOD LEVEL IN RELATION TO RATE OF DEVELOPMENT AND EYE PIGMENTATION IN DROSOPHILA MELANOGASTER. *Biol Bull,* 75.
BECK, G. & FAINZILBER, M. 2002. Genetic Models Meet Trophic Mechanisms: EGF Family Members Are Gliatrophins in Drosophila. *Neuron,* 33**,** 673-675.
BECK, G., MUNNO, D. W., LEVY, Z., DISSEL, H. M., VAN-MINNEN, J., SYED, N. I. & FAINZILBER, M. 2004. Neurotrophic activities of trk receptors conserved over 600 million years of evolution. *Journal of Neurobiology,* 60**,** 12-20.
BECKERVORDERSANDFORTH, R. M., RICKERT, C., ALTENHEIN, B. & TECHNAU, G. M. 2008. Subtypes of glial cells in the Drosophila embryonic ventral nerve cord as related to lineage and gene expression. *Mechanisms of Development,* 125**,** 542-557.
BEKINSCHTEIN, P., CAMMAROTA, M., KATCHE, C., SLIPCZUK, L., ROSSATO, J. I., GOLDIN, A., IZQUIERDO, I. & MEDINA, J. H. 2008. BDNF is essential to promote persistence of long-term memory storage. *Proceedings of the National Academy of Sciences,* 105**,** 2711-2716.
BENITO-GUTIÉRREZ, È., GARCIA-FERNÀNDEZ, J. & COMELLA, J. X. 2006. Origin and evolution of the Trk family of neurotrophic receptors. *Molecular and Cellular Neuroscience,* 31**,** 179-192.
BENITO-GUTIERREZ, E., NAKE, C., LLOVERA, M., COMELLA, J. X. & GARCIA-FERNANDEZ, J. 2005. The single AmphiTrk receptor highlights increased complexity of neurotrophin signalling in vertebrates and suggests an early role in developing sensory neuroepidermal cells. *Development,* 132**,** 2191-202.
BERAMENDI, A., PERON, S., MEGIGHIAN, A., REGGIANI, C. & CANTERA, R. 2005. The inhibitorκB-ortholog Cactus is necessary for normal neuromuscular function in Drosophila melanogaster. *Neuroscience,* 134**,** 397-406.
BERGMANN, A., TUGENTMAN, M., SHILO, B.-Z. & STELLER, H. 2002. Regulation of Cell Number by MAPK-Dependent Control of Apoptosis: A Mechanism for Trophic Survival Signaling. *Developmental Cell,* 2**,** 159-170.
BERKEMEIER, L. R., WINSLOW, J. W., KAPLAN, D. R., NIKOLICS, K., GOEDDEL, D. V. & ROSENTHAL, A. 1991. Neurotrophin-5: a novel neurotrophic factor that activates trk and trkB. *Neuron,* 7**,** 857-66.
BHATT, R. S., TOMODA, T., FANG, Y. & HATTEN, M. E. 2000. Discoidin domain receptor 1 functions in axon extension of cerebellar granule neurons. *Genes & Development,* 14**,** 2216-2228.
BILLEN, L. P., KOKOSKI, C. L., LOVELL, J. F., LEBER, B. & ANDREWS, D. W. 2008. Bcl-XL inhibits membrane permeabilization by competing with Bax. *PLoS Biol,* 6**,** e147.
BJORKLUND, A. K., EKMAN, D., LIGHT, S., FREY-SKOTT, J. & ELOFSSON, A. 2005. Domain rearrangements in protein evolution. *J Mol Biol,* 353**,** 911-23.

BLOM, N., GAMMELTOFT, S. & BRUNAK, S. 1999. Sequence and structure-based prediction of eukaryotic protein phosphorylation sites. *J Mol Biol,* 294**,** 1351-62.
BÖKEL, C. 2007. EMS Screens: From Mutagenesis to Screening and Mapping. *In:* DAHMANN, C. (ed.) *Drosophila : Methods and Protocols.* Humana Press.
BORNBERG-BAUER, E., BEAUSSART, F., KUMMERFELD, S. K., TEICHMANN, S. A. & WEINER, J., 3RD 2005. The evolution of domain arrangements in proteins and interaction networks. *Cell Mol Life Sci,* 62**,** 435-45.
BORYCZ, J., BORYCZ, J. A., KUBÓW, A., LLOYD, V. & MEINERTZHAGEN, I. A. 2008. Drosophila ABC transporter mutants white, brown and scarlet have altered contents and distribution of biogenic amines in the brain. *Journal of Experimental Biology,* 211**,** 3454-3466.
BOSSING, T. & TECHNAU, G. M. 1994. The fate of the CNS midline progenitors in Drosophila as revealed by a new method for single cell labelling. *Development,* 120**,** 1895-906.
BOTHWELL, M. 2006. Evolution of the Neurotrophin Signaling System in Invertebrates. *Brain, Behaviour and Evolution,* 68**,** 124-132.
BRACCI-LAUDIERO, L., ALOE, L., LEVI-MONTALCINI, R., GALEAZZI, M., SCHILTER, D., SCULLY, J. L. & OTTEN, U. 1993. Increased levels of NGF in sera of systemic lupus erythematosus patients. *Neuroreport,* 4**,** 565-565.
BRACONI QUINTAJE, S. & ORCHARD, S. 2008. The annotation of both human and mouse kinomes in UniProtKB/Swiss-Prot: one small step in manual annotation, one giant leap for full comprehension of genomes. *Mol Cell Proteomics,* 7**,** 1409-19.
BRADSHAW, R. A., BLUNDELL, T. L., LAPATTO, R., MCDONALD, N. Q. & MURRAY-RUST, J. 1993. Nerve growth factor revisited. *Trends in Biochemical Sciences,* 18**,** 48-52.
BRAND, A. H. & PERRIMON, N. 1993. Targeted gene expression as a means of altering cell fates and generating dominant phenotypes. *Development,* 118**,** 401-415.
BRANSON, K., ROBIE, A. A., BENDER, J., PERONA, P. & DICKINSON, M. H. 2009. High-throughput ethomics in large groups of Drosophila. *Nat Meth,* 6**,** 451-457.
BRILLET, K., PEREIRA, C. A. & WAGNER, R. 2010. Expression of Membrane Proteins in Drosophila Melanogaster S2 Cells: Production and Analysis of a EGFP-Fused G Protein-Coupled Receptor as a Model. 601**,** 119-133.
BROWN, M. D., CORNEJO, B. J., KUHN, T. B. & BAMBURG, J. R. 2000. Cdc42 stimulates neurite outgrowth and formation of growth cone filopodia and lamellipodia. *J Neurobiol,* 43**,** 352-64.
BROWN, T. G. 1911. The Intrinsic Factors in the Act of Progression in the Mammal. *Proceedings of the Royal Society of London. Series B, Containing Papers of a Biological Character,* 84**,** 308-319.
BUCKLEY, K. M. & RAST, J. P. 2012. Dynamic evolution of toll-like receptor multigene families in echinoderms. *Frontiers in Immunology,* 3.
BULJAN, M. & BATEMAN, A. 2009. The evolution of protein domain families. *Biochem Soc Trans,* 37**,** 751-5.
BULLOCH, A. G. M., DIEP, C. Q., LOGAN, C. C., BULLOCH, E. S., ROBBINS, S. M., HISLOP, J. & SOSSIN, W. S. 2005. Ltrk is differentially expressed in developing and adult neurons of the Lymnaea central nervous system. *The Journal of Comparative Neurology,* 487**,** 240-254.
BURDEN, S. J., YUMOTO, N. & ZHANG, W. 2013. The Role of MuSK in Synapse Formation and Neuromuscular Disease. *Cold Spring Harbor Perspectives in Biology,* 5.
CALDWELL, J. C., MILLER, M. M., WING, S., SOLL, D. R. & EBERL, D. F. 2003. Dynamic analysis of larval locomotion in Drosophila chordotonal organ mutants. *Proc Natl Acad Sci U S A,* 100**,** 16053-8.

CALDWELL, P. E., WALKIEWICZ, M. & STERN, M. 2005. Ras activity in the Drosophila prothoracic gland regulates body size and developmental rate via ecdysone release. *Curr Biol,* 15**,** 1785-95.
CALZA, A., FERNANDEZ, M., GIULIANI, A., PIRONDI, S., D'INTINO, G. & GIARDINO, L. 2003. NERVE GROWTH FACTOR IN THE CENTRAL NERVOUS SYSTEM: MORE THAN NEURONAL SURVIVAL. *Archives Italiennes de Biologie,* 141**,** 93-102.
CAMPOS-ORTEGA, J. A. & HARTENSTEIN, V. 1985. *The embryonic development of Drosophila melanogaster,* Berlin, Springer-Verlag.
CANTERA, R., ROOS, E. & ENGSTROM, Y. 1999. Dif and Cactus Are Colocalized in the Larval Nervous System of Drosophila melanogaster. *J. Neurobiol.,* 38**,** 16-26.
CARIM-TODD, L., BATH, K. G., FULGENZI, G., YANPALLEWAR, S., JING, D., BARRICK, C. A., BECKER, J., BUCKLEY, H., DORSEY, S. G., LEE, F. S. & TESSAROLLO, L. 2009. Endogenous Truncated TrkB.T1 Receptor Regulates Neuronal Complexity and TrkB Kinase Receptor Function In Vivo. *Journal of Neuroscience,* 29**,** 678-685.
CARIM-TODD, L., ESCARCELLER, M., ESTIVILL, X. & SUMOY, L. 2003. LRRN6A/LERN1 (leucine-rich repeat neuronal protein 1), a novel gene with enriched expression in limbic system and neocortex. *Eur J Neurosci,* 18**,** 3167-82.
CELNIKER, S. E., DILLON, L. A., GERSTEIN, M. B., GUNSALUS, K. C., HENIKOFF, S., KARPEN, G. H., KELLIS, M., LAI, E. C., LIEB, J. D., MACALPINE, D. M., MICKLEM, G., PIANO, F., SNYDER, M., STEIN, L., WHITE, K. P. & WATERSTON, R. H. 2009. Unlocking the secrets of the genome. *Nature,* 459**,** 927-30.
CHADFIELD, C. G. & SPARROW, J. C. 1984. Pupation in drosophila melanogaster and the effect of the Lethalcryptocephal mutation. *Developmental Genetics,* 5**,** 103-114.
CHAO, M. V. 2003. Neurotrophins and their receptors: a convergence point for many signalling pathways. *Nat Rev Neurosci,* 4**,** 299-309.
CHAO, M. V., RAJAGOPAL, R. & LEE, F. S. 2006. Neurotrophin signalling in health and disease. *Clin Sci (Lond),* 110**,** 167-73.
CHEN, Y., AULIA, S., LI, L. & TANG, B. L. 2006. AMIGO and friends: An emerging family of brain-enriched, neuronal growth modulating, type I transmembrane proteins with leucine-rich repeats (LRR) and cell adhesion molecule motifs. *Brain Research Reviews,* 51**,** 265-274.
CHEN, Y., HOR, H. H. & TANG, B. L. 2012. AMIGO is expressed in multiple brain cell types and may regulate dendritic growth and neuronal survival. *Journal of Cellular Physiology,* 227**,** 2217-2229.
CHEN, Z., GORE, B. B., LONG, H., MA, L. & TESSIER-LAVIGNE, M. 2008. Alternative splicing of the Robo3 axon guidance receptor governs the midline switch from attraction to repulsion. *Neuron,* 58**,** 325-32.
CHINTAPALLI, V. R., WANG, J. & DOW, J. A. T. 2007. Using FlyAtlas to identify better Drosophila melanogaster models of human disease. *Nat Genet,* 39**,** 715-720.
CHIU, J. C., LOW, K. H., PIKE, D. H., YILDIRIM, E. & EDERY, I. 2010. Assaying locomotor activity to study circadian rhythms and sleep parameters in Drosophila. *J Vis Exp*.
CLARY, D. O. & REICHARDT, L. F. 1994. An alternatively spliced form of the nerve growth factor receptor TrkA confers an enhanced response to neurotrophin 3. *Proc Natl Acad Sci U S A,* 91**,** 11133-7.
COLOMBANI, J., BIANCHINI, L., LAYALLE, S., PONDEVILLE, E., DAUPHIN-VILLEMANT, C., ANTONIEWSKI, C., CARRÉ, C., NOSELLI, S. & LÉOPOLD, P. 2005. Antagonistic Actions of Ecdysone and Insulins Determine Final Size in Drosophila. *Science,* 310**,** 667-670.

CONOVER, J. C. & YANCOPOULOS, G. D. 1997. Neurotrophin regulation of the developing nervous system: analyses of knockout mice. *Rev Neurosci,* 8**,** 13-27.
CORBIT, K. C., FOSTER, D. A. & ROSNER, M. R. 1999. Protein Kinase Cδ Mediates Neurogenic but Not Mitogenic Activation of Mitogen-Activated Protein Kinase in Neuronal Cells. *Molecular and Cellular Biology,* 19**,** 4209-4218.
DAOPIN, S., PIEZ, K. A., OGAWA, Y. & DAVIES, D. R. 1992. Crystal structure of transforming growth factor-beta 2: an unusual fold for the superfamily. *Science,* 257**,** 369-73.
DATTA, S. R., DUDEK, H., TAO, X., MASTERS, S., FU, H., GOTOH, Y. & GREENBERG, M. E. 1997. Akt phosphorylation of BAD couples survival signals to the cell-intrinsic death machinery. *Cell,* 91**,** 231-41.
DAVIDOWITZ, G., D'AMICO, L. J. & NIJHOUT, H. F. 2003. Critical weight in the development of insect body size. *Evol Dev,* 5**,** 188-97.
DE WIT, J., HONG, W., LUO, L. & GHOSH, A. 2011. Role of leucine-rich repeat proteins in the development and function of neural circuits. *Annu Rev Cell Dev Biol,* 27**,** 697-729.
DECHIARA, T. M., BOWEN, D. C., VALENZUELA, D. M., SIMMONS, M. V., POUEYMIROU, W. T., THOMAS, S., KINETZ, E., COMPTON, D. L., ROJAS, E., PARK, J. S., SMITH, C., DISTEFANO, P. S., GLASS, D. J., BURDEN, S. J. & YANCOPOULOS, G. D. 1996. The Receptor Tyrosine Kinase MuSK Is Required for Neuromuscular Junction Formation In Vivo. *Cell,* 85**,** 501-512.
DELOTTO, Y. & DELOTTO, R. 1998. Proteolytic processing of the Drosophila Spatzle protein by Easter generates a dimeric NGF-like molecule with ventralising activity. *Mechanisms of Development,* 72**,** 141-148.
DENT, E. W. & GERTLER, F. B. 2003. Cytoskeletal Dynamics and Transport in Growth Cone Motility and Axon Guidance. *Neuron,* 40**,** 209-227.
DERHEIMER, F. A., MACLAREN, C. M., WEASNER, B. P., ALVARADO, D. & DUFFY, J. B. 2004. Conservation of an Inhibitor of the Epidermal Growth Factor Receptor, Kekkon1, in Dipterans. *Genetics,* 166**,** 213-224.
DEWEY, E. M., MCNABB, S. L., EWER, J., KUO, G. R., TAKANISHI, C. L., TRUMAN, J. W. & HONEGGER, H.-W. 2004. Identification of the Gene Encoding Bursicon, an Insect Neuropeptide Responsible for Cuticle Sclerotization and Wing Spreading. *Current Biology,* 14**,** 1208-1213.
DIAPER, D. C., ADACHI, Y., SUTCLIFFE, B., HUMPHREY, D. M., ELLIOTT, C. J., STEPTO, A., LUDLOW, Z. N., VANDEN BROECK, L., CALLAERTS, P., DERMAUT, B., AL-CHALABI, A., SHAW, C. E., ROBINSON, I. M. & HIRTH, F. 2013. Loss and gain of Drosophila TDP-43 impair synaptic efficacy and motor control leading to age-related neurodegeneration by loss-of-function phenotypes. *Hum Mol Genet,* 22**,** 1539-57.
DIERING, G. H., NUMATA, Y., FAN, S., CHURCH, J. & NUMATA, M. 2013. Endosomal Acidification by Na,+/H+ Exchanger NHE5 Regulates TrkA Cell-Surface Targeting and NGF-Induced PI3K Signaling. *Mol Biol Cell*.
DILLON, C. & GODA, Y. 2005. The actin cytoskeleton: integrating form and function at the synapse. *Annu Rev Neurosci,* 28**,** 25-55.
DIMITRIJEVIC, N., DZITOYEVA, S. & MANEV, H. 2004. An automated assay of the behavioral effects of cocaine injections in adult Drosophila. *J Neurosci Methods,* 137**,** 181-4.
DIRCKSEN, H., TESFAI, L. K., ALBUS, C. & NASSEL, D. R. 2008. Ion transport peptide splice forms in central and peripheral neurons throughout postembryogenesis of Drosophila melanogaster. *J Comp Neurol,* 509**,** 23-41.
DISHAW, L. J., HAIRE, R. N. & LITMAN, G. W. 2012. The amphioxus genome provides unique insight into the evolution of immunity. *Briefings in Functional Genomics,* 11**,** 167-176.

DOE, C. Q. 1992. Molecular markers for identified neuroblasts and ganglion mother cells in the Drosophila central nervous system. *Development,* 116**,** 855-863.
DOLAN, J., WALSHE, K., ALSBURY, S., HOKAMP, K., O'KEEFFE, S., OKAFUJI, T., MILLER, S. F. C., TEAR, G. & MITCHELL, K. J. 2007. The extracellular Leucine-Rich Repeat superfamily; a comparative survey and analysis of evolutionary relationships and expression patterns. *BMC Genomics,* 8**,** 320.
DONELSON, N., KIM, E. Z., SLAWSON, J. B., VECSEY, C. G., HUBER, R. & GRIFFITH, L. C. 2012. High-Resolution Positional Tracking for Long-Term Analysis of <italic>Drosophila</italic> Sleep and Locomotion Using the "Tracker" Program. *PLoS ONE,* 7**,** e37250.
DOOLITTLE, R. F. 1995. The multiplicity of domains in proteins. *Annu Rev Biochem,* 64**,** 287-314.
DORSEY, S. G., LOVERING, R. M., RENN, C. L., LEITCH, C. C., LIU, X., TALLON, L. J., SADZEWICZ, L. D., PRATAP, A., OTT, S., SENGAMALAY, N., JONES, K. M., BARRICK, C., FULGENZI, G., BECKER, J., VOELKER, K., TALMADGE, R., HARVEY, B. K., WYATT, R. M., VERNON-PITTS, E., ZHANG, C., SHOKAT, K., FRASER-LIGGETT, C., BALICE-GORDON, R. J., TESSAROLLO, L. & WARD, C. W. 2012. Genetic deletion of trkB.T1 increases neuromuscular function. *Am J Physiol Cell Physiol,* 302**,** C141-53.
DORSEY, S. G., RENN, C. L., CARIM-TODD, L., BARRICK, C. A., BAMBRICK, L., KRUEGER, B. K., WARD, C. W. & TESSAROLLO, L. 2006. In vivo restoration of physiological levels of truncated TrkB.T1 receptor rescues neuronal cell death in a trisomic mouse model. *Neuron,* 51**,** 21-8.
DUBROVSKY, E. B., DUBROVSKAYA, V. A., BILDERBACK, A. L. & BERGER, E. M. 2000. The Isolation of Two Juvenile Hormone-Inducible Genes in Drosophila melanogaster. *Developmental Biology,* 224**,** 486-495.
DWORKIN, S. & MANTAMADIOTIS, T. 2010. Targeting CREB signalling in neurogenesis. *Expert Opin Ther Targets,* 14**,** 869-79.
EBNER, A., FABRICE, N. K., RIBEIRO, C., PETITE, V., NUSSBAUMER, U. & AFFOLTER, M. 2002. Tracheal development in Drosophila melanogaster as a model system for studying the development of a branched organ. *Gene,* 287**,** 55-66.
EDELMAN, G. M. 1970. Covalent structure of a human γG-immunoglobulin. XI. Functional implications. *Biochemistry,* 9**,** 3197-3205.
EDGAR, B. A. 2006. How flies get their size: genetics meets physiology. *Nat Rev Genet,* 7**,** 907-16.
EKMAN, D., BJORKLUND, A. K. & ELOFSSON, A. 2007. Quantification of the elevated rate of domain rearrangements in metazoa. *J Mol Biol,* 372**,** 1337-48.
ENGLUND, C., LOREN, C. E., GRABBE, C., VARSHNEY, G. K., DELEUIL, F., HALLBERG, B. & PALMER, R. H. 2003. Jeb signals through the Alk receptor tyrosine kinase to drive visceral muscle fusion. *Nature,* 425**,** 512-6.
ERNST, A. F., GALLO, G., LETOURNEAU, P. C. & MCLOON, S. C. 2000. Stabilization of growing retinal axons by the combined signaling of nitric oxide and brain-derived neurotrophic factor. *J Neurosci,* 20**,** 1458-69.
EVANS, T. A., HARIDAS, H. & DUFFY, J. B. 2009. Kekkon5 is an extracellular regulator of BMP signaling. *Developmental Biology,* 326**,** 36-46.
FAINZILBER, M., SMIT, A. B., SYED, N. I., WILDERING, W. C., HERMANN, VAN DER SCHORS, R. C., JIMENEZ, C., LI, K. W., VAN MINNEN, J., BULLOCH, A. G., IBANEZ, C. F. & GERAERTS, W. P. 1996. CRNF, a molluscan neurotrophic factor that interacts with the p75 neurotrophin receptor. *Science,* 274**,** 1540-3.
FEANY, M. B. & BENDER, W. W. 2000. A Drosophila model of Parkinson's disease. *Nature,* 404**,** 394-8.

FENNER, B. M. 2012. Truncated TrkB: beyond a dominant negative receptor. *Cytokine Growth Factor Rev,* 23**,** 15-24.
FERNANDEZ, R., TAKAHASHI, F., LIU, Z., STEWARD, R., STEIN, D. & STANLEY, E. R. 2000. The Drosophila shark tyrosine kinase is required for embryonic dorsal closure. *Genes & Development,* 14**,** 604-614.
FIELD, L. H. & MATHESON, T. 1998. Chordotonal organs of insects. *Advances in Insect Physiology,* 27**,** 1-228.
FILBIN, M. T. 2003. Myelin-associated inhibitors of axonal regeneration in the adult mammalian CNS. *Nat Rev Neurosci,* 4**,** 703-13.
FLATT, T., TU, M. P. & TATAR, M. 2005. Hormonal pleiotropy and the juvenile hormone regulation of Drosophila development and life history. *Bioessays,* 27**,** 999-1010.
FORRESTER, W. C. 2002. The Ror receptor tyrosine kinase family. *Cell Mol Life Sci,* 59**,** 83-96.
FORRESTER, W. C., DELL, M., PERENS, E. & GARRIGA, G. 1999. A C. elegans Ror receptor tyrosine kinase regulates cell motility and asymmetric cell division. *Nature,* 400**,** 881-5.
FOX, L. E., SOLL, D. R. & WU, C. F. 2006. Coordination and modulation of locomotion pattern generators in Drosophila larvae: effects of altered biogenic amine levels by the tyramine beta hydroxlyase mutation. *J Neurosci,* 26**,** 1486-98.
FREUDENTHAL, R. & ROMANO, A. 2000. Participation of Rel/NF-kappaB transcription factors in long-term memory in the crab Chasmagnathus. *Brain Res,* 855**,** 274-81.
FRIEDRICH, M. 2008. Opsins and cell fate in the Drosophila Bolwig organ: tricky lessons in homology inference. *BioEssays,* 30**,** 980-993.
FROMMER, G., VORBRUGGEN, G., PASCA, G., JAECKLE, H. & VOLK, T. 1996. Epidermal egr-like zinc finger protein of Drosophila participates in myotube guidance. *The EMBO Journal,* 15**,** 1642-1649.
GALCERÁN, J., LLANOS, J., SAMPEDRO, J., PONGS, O. & IZQUIERDO, M. 1990. Transcription at the ecdysone-inducible locus 2B5 in Drosophila. *Nucleic Acids Research,* 18**,** 539-545.
GALLO, G. 2006. RhoA-kinase coordinates F-actin organization and myosin II activity during semaphorin-3A-induced axon retraction. *J Cell Sci,* 119**,** 3413-23.
GAMULIN, V., RINKEVICH, B., SCHACKE, H., KRUSE, M., MULLER, I. M. & MULLER, W. E. 1994. Cell adhesion receptors and nuclear receptors are highly conserved from the lowest metazoa (marine sponges) to vertebrates. *Biol Chem Hoppe Seyler,* 375**,** 583-8.
GEORGEL, P., RAMAIN, P., GIANGRANDE, A., DRETZEN, G., RICHARDS, G. & BELLARD, M. 1991. Sgs-3 chromatin structure and trans-activators: developmental and ecdysone induction of a glue enhancer-binding factor, GEBF-I, in Drosophila larvae. *Molecular and Cellular Biology,* 11**,** 523-532.
GESTWA, G., WIECHERS, B., ZIMMERMANN, U., PRAETORIUS, M., ROHBOCK, K., KOPSCHALL, I., ZENNER, H. P. & KNIPPER, M. 1999. Differential expression of trkB.T1 and trkB.T2, truncated trkC, and p75(NGFR) in the cochlea prior to hearing function. *J Comp Neurol,* 414**,** 33-49.
GHIGLIONE, C. 2003. Mechanism of inhibition of the Drosophila and mammalian EGF receptors by the transmembrane protein Kekkon 1. *Development,* 130**,** 4483-4493.
GHIGLIONE, C., CARRAWAY, K. L., AMUNDADOTTIR, L. T., BOSWELL, R. E., PERRIMON, N. & DUFFY, J. B. 1999. The Transmembrane Molecule Kekkon 1 Acts in a Feedback Loop to Negatively Regulate the Activity of the *Drosophila* EGF Receptor during Oogenesis. *Cell,* 96**,** 847-856.
GIDASZEWSKI, N., BAYLAC, M. & KLINGENBERG, C. 2009. Evolution of sexual dimorphism of wing shape in the Drosophila melanogaster subgroup. *BMC Evolutionary Biology,* 9**,** 110.

GLANZMAN, D. L. 2010. Ion pumps get more glamorous. *Nat Neurosci,* 13**,** 4-5.
GÖTZ, R., RAULF, F. & SCHARTL, M. 1992. Brain-Derived Neurotrophic Factor Is More Highly Conserved in Structure and Function than Nerve Growth Factor During Vertebrate Evolution. *Journal of Neurochemistry,* 59**,** 432-442.
GOVEK, E. E., NEWEY, S. E. & VAN AELST, L. 2005. The role of the Rho GTPases in neuronal development. *Genes Dev,* 19**,** 1-49.
GREENSPAN, R. J. 2004. *Fly Pushing: The Theory and Practice of Drosophila Genetics*, Cold Spring Harbor Laboratory Press.
GUAN, Z., SARASWATI, S., ADOLFSEN, B. & LITTLETON, J. T. 2005. Genome-Wide Transcriptional Changes Associated with Enhanced Activity in the Drosophila Nervous System. *Neuron,* 48**,** 91-107.
GUAY, P. S. & GUILD, G. M. 1991. The ecdysone-induced puffing cascade in Drosophila salivary glands: a Broad-Complex early gene regulates intermolt and late gene transcription. *Genetics,* 129**,** 169-75.
GUMIENNY, T. L., MACNEIL, L., ZIMMERMAN, C. M., WANG, H., CHIN, L., WRANA, J. L. & PADGETT, R. W. 2010. Caenorhabditis elegans SMA-10/LRIG is a conserved transmembrane protein that enhances bone morphogenetic protein signaling. *PLoS Genet,* 6**,** e1000963.
GUO, A., ZHANG, K., PENG, Y. & XI, W. 2009. Heisenberg's roadmap guides our journey to the small cognitive world of Drosophila. *J Neurogenet,* 23**,** 100-3.
GUO, D., HOLMLUND, C., HENRIKSSON, R. & HEDMAN, H. 2004. The LRIG gene family has three vertebrate paralogs widely expressed in human and mouse tissues and a homolog in Ascidiacea. *Genomics,* 84**,** 157-165.
GUPTA, V. K., YOU, Y., GUPTA, V. B., KLISTORNER, A. & GRAHAM, S. L. 2013. TrkB Receptor Signalling: Implications in Neurodegenerative, Psychiatric and Proliferative Disorders. *Int J Mol Sci,* 14**,** 10122-42.
GUR, G., RUBIN, C., KATZ, M., AMIT, I., CITRI, A., NILSSON, J., AMARIGLIO, N., ROGER, HENRIKSSON & RECHAVI, G. 2004. LRIG1 restricts growth factor signaling by enhancing receptor ubiquitylation and degradation. *EMBO Journal,* 23**,** 3270-3281.
HAAPASALO, A., KOPONEN, E., HOPPE, E., WONG, G. & CASTREN, E. 2001. Truncated trkB.T1 is dominant negative inhibitor of trkB.TK+-mediated cell survival. *Biochem Biophys Res Commun,* 280**,** 1352-8.
HAKEDA-SUZUKI, S., NG, J., TZU, J., DIETZL, G., SUN, Y., HARMS, M., NARDINE, T., LUO, L. & DICKSON, B. J. 2002. Rac function and regulation during Drosophila development. *Nature,* 416**,** 438-42.
HALL, A. & LALLI, G. 2010. Rho and Ras GTPases in axon growth, guidance, and branching. *Cold Spring Harb Perspect Biol,* 2**,** a001818.
HALLBOOK, F. 1999. Evolution of the vertebrate neurotrophin and Trk receptor gene families. *Curr Opin Neurobiol,* 9**,** 616-21.
HALLBOOK, F., IBANEZ, C. F. & PERSSON, H. 1991. Evolutionary studies of the nerve growth factor family reveal a novel member abundantly expressed in Xenopus ovary. *Neuron,* 6**,** 845-58.
HALLBÖÖK, F., LUNDIN, L.-G. & KULLANDER, K. 1998. Lampetra fluviatilis Neurotrophin Homolog, Descendant of a Neurotrophin Ancestor, Discloses the Early Molecular Evolution of Neurotrophins in the Vertebrate Subphylum. *The Journal of Neuroscience,* 18**,** 8700-8711.
HALLBÖÖK, F., WILSON, K., THORNDYKE, M. & OLINSKI, R. P. 2006. Formation and Evolution of the Chordate Neurotrophin and Trk Receptor Genes. *Brain, Behavior and Evolution,* 68**,** 133-144.
HANAMSAGAR, R., HANKE, M. L. & KIELIAN, T. 2012. Toll-like receptor (TLR) and inflammasome actions in the central nervous system. *Trends Immunol,* 33**,** 333-42.

HAND, A. J., SUN, T., BARBER, D. C., HOSE, D. R. & MACNEIL, S. 2009. Automated tracking of migrating cells in phase-contrast video microscopy sequences using image registration. *Journal of Microscopy,* 234**,** 62-79.

HANKS, S. K. & HUNTER, T. 1995. Protein kinases 6. The eukaryotic protein kinase superfamily: kinase (catalytic) domain structure and classification. *FASEB J,* 9**,** 576-96.

HARTENSTEIN, V. 1993. *Atlas of Drosophila Development*, Cold Spring Harbor Laboratory Press.

HARTMANN, M., BRIGADSKI, T., ERDMANN, K. S., HOLTMANN, B., SENDTNER, M., NARZ, F. & LESSMANN, V. 2004. Truncated TrkB receptor-induced outgrowth of dendritic filopodia involves the p75 neurotrophin receptor. *J Cell Sci,* 117**,** 5803-14.

HARTWELL, L. H., HOPFIELD, J. J., LEIBLER, S. & MURRAY, A. W. 1999. From molecular to modular cell biology. *Nature,* 402**,** C47-52.

HEDMAN, H., NILSSON, J., GUO, D. & HENRIKSSON, R. 2002. Is LRIG1 a tumour suppressor gene at chromosome 3p14.3? *Acta Oncol,* 41**,** 352-354.

HEGYI, H. & GERSTEIN, M. 2001. Annotation transfer for genomics: measuring functional divergence in multi-domain proteins. *Genome Res,* 11**,** 1632-40.

HEISENBERG, M. 1997. Genetic approach to neuroethology. *BioEssays,* 19**,** 1065-1073.

HENRICH, V. C., PAK, M. D. & GILBERT, L. I. 1987. Neural factors that stimulate ecdysteroid synthesis by the larval ring gland of *Drosophila melanogaster*. *Journal of Comparative Physiology B,* 157**,** 543-549.

HERMANN, P. M., VAN KESTEREN, R. E., WILDERING, W. C., PAINTER, S. D., RENO, J. M., SMITH, J. S., KUMAR, S. B., GERAERTS, W. P., ERICSSON, L. H., SMIT, A. B., BULLOCH, A. G. & NAGLE, G. T. 2000. Neurotrophic actions of a novel molluscan epidermal growth factor. *J Neurosci,* 20**,** 6355-64.

HIDALGO, A. 2002. Interactive nervous system development: control of cell survival in Drosophila. *Trends in Neuroscience,* 25**,** 365-370.

HIDALGO, A. & BRAND, A. H. 1997. Targeted neuronal ablation: the role of pioneer neurons in guidance and fasciculation in the CNS of Drosophila. *Development,* 124**,** 3253-3262.

HIDALGO, A., KINRADE, E. F. V. & GEORGIOU, M. 2001. The Drosophila Neuregulin Vein Maintains Glial Survival during Axon Guidance in the CNS. *Developmental Cell,* 1**,** 679-690.

HIDALGO, A., URBAN, J. & BRAND, A. H. 1995. Targeted ablation of glia disrupts axon tract formation in the Drosophila CNS. *Development,* 121**,** 3703-12.

HING, H., XIAO, J., HARDEN, N., LIM, L. & ZIPURSKY, S. L. 1999. Pak Functions Downstream of Dock to Regulate Photoreceptor Axon Guidance in Drosophila. *Cell,* 97**,** 853-863.

HIRAMOTO, M., HIROMI, Y., GINIGER, E. & HOTTA, Y. 2000. The Drosophila Netrin receptor Frazzled guides axons by controlling Netrin distribution. *Nature,* 406**,** 886-9.

HIRANO, M., DAS, S., GUO, P. & COOPER, M. D. 2011. Chapter 4 - The Evolution of Adaptive Immunity in Vertebrates. *In:* FREDERICK, W. A. (ed.) *Advances in Immunology.* Academic Press.

HOLDEN, P. H., ASOPA, V., ROBERTSON, A. G. S., CLARKE, A. R., TYLER, S., BENNETT, G. S., BRAIN, S. D., WILCOCK, G. K., ALLEN, S. J., SMITH, S. K. F. & DAWBARN, D. 1997. Immunoglobulin-like domains define the nerve growth factor binding site of the TrkA receptor. *Nature Biotechnology,* 15**,** 668-672.

HU, J. Y., GLICKMAN, L., WU, F. & SCHACHER, S. 2004. Serotonin regulates the secretion and autocrine action of a neuropeptide to activate MAPK required for long-term facilitation in Aplysia. *Neuron,* 43**,** 373-85.

HU, X. 2004. Multimerization and interaction of Toll and Spatzle in Drosophila. *Proceedings of the National Academy of Sciences,* 101**,** 9369-9374.

HUANG, E. J. & REICHARDT, L. F. 2001. Neurotrophins: roles in neuronal development and function. *Annu Rev Neurosci,* 24**,** 677-736.
HUANG, J., TIAN, L., PENG, C., ABDOU, M., WEN, D., WANG, Y., LI, S. & WANG, J. 2011a. DPP-mediated TGF signaling regulates juvenile hormone biosynthesis by activating the expression of juvenile hormone acid methyltransferase. *Development,* 138**,** 2283-2291.
HUANG, S., WANG, X., YAN, Q., GUO, L., YUAN, S., HUANG, G., HUANG, H., LI, J., DONG, M., CHEN, S. & XU, A. 2011b. The Evolution and Regulation of the Mucosal Immune Complexity in the Basal Chordate Amphioxus. *The Journal of Immunology,* 186**,** 2042-2055.
HUANG, S., YUAN, S., GUO, L., YU, Y., LI, J., WU, T., LIU, T., YANG, M., WU, K., LIU, H., GE, J., YU, Y., HUANG, H., DONG, M., YU, C., CHEN, S. & XU, A. 2008. Genomic analysis of the immune gene repertoire of amphioxus reveals extraordinary innate complexity and diversity. *Genome Research,* 18**,** 1112-1126.
HUMMEL, T. & KLAMBT, C. 2007. P-Element Mutagenesis. *In:* DAHMANN, C. (ed.) *Drosophila: Methods and Protocols.* Humana Press.
HUMMEL, T., SCHIMMELPFENG, K. & KLAMBT, C. 1999. Commissure formation in the embryonic CNS of Drosophila. *Development,* 126**,** 771-9.
HUMPHREY, D. M., PARSONS, R. B., LUDLOW, Z. N., RIEMENSPERGER, T., ESPOSITO, G., VERSTREKEN, P., JACOBS, H. T., BIRMAN, S. & HIRTH, F. 2012. Alternative oxidase rescues mitochondria-mediated dopaminergic cell loss in Drosophila. *Human Molecular Genetics,* 21**,** 2698-2712.
IGAKI, T., KANDA, H., YAMAMOTO-GOTO, Y., KANUKA, H., KURANAGA, E., AIGAKI, T. & MIURA, M. 2002. Eiger, a TNF superfamily ligand that triggers the *Drosophila* JNK pathway. *EMBO Journal,* 21**,** 3009-3018.
IMLER, J. L. & ZHENG, L. 2004. Biology of Toll receptors: lessons from insects and mammals. *J Leukoc Biol,* 75**,** 18-26.
INAMORI, K., ARIKI, S. & KAWABATA, S. 2004. A Toll-like receptor in horseshoe crabs. *Immunol Rev,* 198**,** 106-15.
ISABEL, G., MARTIN, J. R., CHIDAMI, S., VEENSTRA, J. A. & ROSAY, P. 2005. AKH-producing neuroendocrine cell ablation decreases trehalose and induces behavioral changes in Drosophila. *Am J Physiol Regul Integr Comp Physiol,* 288**,** R531-8.
JAARO, H., BECK, G., CONTICELLO, S. G. & FAINZILBER, M. 2001. Evolving better brains:a need for neurotrophins? *Trends in Neuroscience,* 24**,** 79-85.
JAARO, H. & FAINZILBER, M. 2006. Building Complex Brains – Missing Pieces in an Evolutionary Puzzle. *Brain, Behavior and Evolution,* 68**,** 191-195.
JACOB, F. 1977. Evolution and tinkering. *Science,* 196**,** 1161-1166.
JALINK, K., VAN CORVEN, E. J., HENGEVELD, T., MORII, N., NARUMIYA, S. & MOOLENAAR, W. H. 1994. Inhibition of lysophosphatidate- and thrombin-induced neurite retraction and neuronal cell rounding by ADP ribosylation of the small GTP-binding protein Rho. *J Cell Biol,* 126**,** 801-10.
JOHNSON, C., CHUN-JEN LIN, C. & STERN, M. 2012. Ras-dependent and Ras-independent effects of PI3K in Drosophila motor neurons. *Genes Brain Behav,* 11**,** 848-58.
JONES, K. R. & REICHARDT, L. F. 1990. Molecular cloning of a human gene that is a member of the nerve growth factor family. *Proc Natl Acad Sci U S A,* 87**,** 8060-4.
KABRA, M., ROBIE, A. A., RIVERA-ALBA, M., BRANSON, S. & BRANSON, K. 2012. JAABA: interactive machine learning for automatic annotation of animal behavior. *Nature Methods,* 10**,** 64-67.
KANCZKOWSKI, W., ZIEGLER, C. G., ZACHAROWSKI, K. & BORNSTEIN, S. R. 2008. Toll-like receptors in endocrine disease and diabetes. *Neuroimmunomodulation,* 15**,** 54-60.

KANDA, H., IGAKI, T., KANUKA, H., YAGI, T. & MIURA, M. 2002. Wengen, a Member of the Drosophila Tumor Necrosis Factor Receptor Superfamily, Is Required for Eiger Signaling. *Journal of Biological Chemistry,* 277**,** 28372-28375.

KANDEL, E. R. 2012. The molecular biology of memory: cAMP, PKA, CRE, CREB-1, CREB-2, and CPEB. *Mol Brain,* 5**,** 14.

KAPLAN, D. R. & MILLER, F. D. 2000. Neurotrophin signal transduction in the nervous system. *Curr Opin Neurobiol,* 10**,** 381-91.

KARIM, F. D. & THUMMEL, C. S. 1992. Temporal coordination of regulatory gene expression by the steroid hormone ecdysone. *EMBO J,* 11**,** 4083-4093.

KASSABOV, STEFAN R., CHOI, Y.-B., KARL, KEVIN A., VISHWASRAO, HARSHAD D., BAILEY, CRAIG H. & KANDEL, ERIC R. 2013. A Single Aplysia Neurotrophin Mediates Synaptic Facilitation via Differentially Processed Isoforms. *Cell Reports,* 3**,** 1213-1227.

KAUFMANN, N., WILLS, Z. P. & VAN VACTOR, D. 1998. Drosophila Rac1 controls motor axon guidance. *Development,* 125**,** 453-61.

KAUPPILA, S., MAATY, W. S. A., CHEN, P., TOMAR, R. S., EBY, M. T., CHAPO, J., CHEW, S., RATHORE, N., ZACHARIAH, S., SINHA, S. K., ABRAMS, J. M. & CHAUDHARY, P. M. 2003. Eiger and its receptor, Wengen, comprise a TNF-like system in Drosophila. *Oncogene,* 22**,** 4860-4867.

KIM, M. D., WEN, Y. & JAN, Y.-N. 2009. Patterning and organization of motor neuron dendrites in the Drosophila larva. *Developmental Biology,* 336**,** 213-221.

KIM, S. K. & RULIFSON, E. J. 2004. Conserved mechanisms of glucose sensing and regulation by Drosophila corpora cardiaca cells. *Nature,* 431**,** 316-20.

KING-JONES, K., CHARLES, J.-P., LAM, G. & THUMMEL, C. S. 2005. The Ecdysone-Induced DHR4 Orphan Nuclear Receptor Coordinates Growth and Maturation in Drosophila. *Cell,* 121**,** 773-784.

KISS, I., BEATON, A. H., TARDIFF, J., FRISTROM, D. & FRISTROM, J. W. 1988. Interactions and developmental effects of mutations in the Broad-Complex of Drosophila melanogaster. *Genetics,* 118**,** 247-59.

KO, J. & KIM, E. 2007. Leucine-rich repeat proteins of synapses. *J Neurosci Res,* 85**,** 2824-32.

KOBE, B. & DEISENHOFER, J. 1994. The leucine-rich repeat: a versatile binding motif. *Trends in Biochemical Sciences,* 19**,** 415-421.

KOBE, B. & DEISENHOFER, J. 1995. A Structural Basis of the Interactions Between Leucine-Rich Repeats and Protein Ligands. *Nature,* 374**,** 183-186.

KOBE, B. & KAJAVA, A. V. 2001. The leucine-rich repeat as a protein recognition motif. *Curr Opin Struct Biol,* 11**,** 725-32.

KONOPOVA, B. & JINDRA, M. 2008. Broad-Complex acts downstream of Met in juvenile hormone signaling to coordinate primitive holometabolan metamorphosis. *Development,* 135**,** 559-568.

KOZMA, R., AHMED, S., BEST, A. & LIM, L. 1995. The Ras-related protein Cdc42Hs and bradykinin promote formation of peripheral actin microspikes and filopodia in Swiss 3T3 fibroblasts. *Molecular and Cellular Biology,* 15**,** 1942-52.

KOZMA, R., SARNER, S., AHMED, S. & LIM, L. 1997. Rho family GTPases and neuronal growth cone remodelling: relationship between increased complexity induced by Cdc42Hs, Rac1, and acetylcholine and collapse induced by RhoA and lysophosphatidic acid. *Mol Cell Biol,* 17**,** 1201-11.

KROIHER, M., MILLER, M. A. & STEELE, R. E. 2001. Deceiving appearances: signaling by "dead" and "fractured" receptor protein-tyrosine kinases. *Bioessays,* 23**,** 69-76.

KUHN, T. B., BROWN, M. D. & BAMBURG, J. R. 1998. Rac1-dependent actin filament organization in growth cones is necessary for beta1-integrin-mediated advance but not for growth on poly-D-lysine. *J Neurobiol,* 37**,** 524-40.

KUJA-PANULA, J., KIILTOMÄKI, M., YAMASHIRO, T., ROUHIAINEN, A. & RAUVALA, H. 2003. AMIGO, a transmembrane protein implicated in axon tract development, defines a novel protein family with leucine-rich repeats. *Journal of Cell Biology,* 160**,** 963-974.

KUMAR, S. & HEDGES, S. B. 1998. A molecular timescale for vertebrate evolution. *Nature,* 392**,** 917-20.

KURATA, S. 2010. Fly immunity: recognition of pathogens and induction of immune responses. *Adv Exp Med Biol,* 708**,** 205-17.

KUWANA, T., MACKEY, M. R., PERKINS, G., ELLISMAN, M. H., LATTERICH, M., SCHNEITER, R., GREEN, D. R. & NEWMEYER, D. D. 2002. Bid, Bax, and lipids cooperate to form supramolecular openings in the outer mitochondrial membrane. *Cell,* 111**,** 331-42.

LAEDERICH, M. B. 2004. The Leucine-rich Repeat Protein LRIG1 Is a Negative Regulator of ErbB Family Receptor Tyrosine Kinases. *Journal of Biological Chemistry,* 279**,** 47050-47056.

LAMPRON, A., ELALI, A. & RIVEST, S. 2013. Innate Immunity in the CNS: Redefining the Relationship between the CNS and Its Environment. *Neuron,* 78**,** 214-232.

LANDGRAF, M., BOSSING, T., TECHNAU, G. M. & BATE, M. 1997. The Origin, Location, and Projections of the Embryonic Abdominal Motorneurons of Drosophila. *Journal of Neuroscience,* 17**,** 9642-9655.

LANDGRAF, M., JEFFREY, V., FUJIOKA, M., JAYNES, J. B. & BATE, M. 2003. Embryonic Origins of a Motor System: Motor Dendrites Form a Myotopic Map in Drosophila. *PLoS Biology,* 1**,** 221-230.

LANDGRAF, M. & THOR, S. 2006a. Development and structure of motoneurons. *Int Rev Neurobiol,* 75**,** 33-53.

LANDGRAF, M. & THOR, S. 2006b. Development of Drosophila motoneurons: specification and morphology. *Semin Cell Dev Biol,* 17**,** 3-11.

LAPRAZ, F., RÖTTINGER, E., DUBOC, V., RANGE, R., DULOQUIN, L., WALTON, K., WU, S.-Y., BRADHAM, C., LOZA, M. A., HIBINO, T., WILSON, K., POUSTKA, A., MCCLAY, D., ANGERER, L., GACHE, C. & LEPAGE, T. 2006. RTK and TGF-β signaling pathways genes in the sea urchin genome. *Developmental Biology,* 300**,** 132-152.

LAUDIERO, L. B., ALOE, L., LEVI-MONTALCINI, R., BUTTINELLI, C., SCHILTER, D., GILLESSEN, S. & OTTEN, U. 1992. Multiple sclerosis patients express increased levels of nerve growth factor in cerebrospinal fluid. *Neuroscience Letters,* 147**,** 9-12.

LAYALLE, S., RAGONE, G., GIANGRANDE, A., GHYSEN, A. & DAMBLY-CHAUDIERE, C. 2004. Control of bract formation inDrosophila: poxn, kek1, and the EGF-R pathway. *genesis,* 39**,** 246-255.

LEE, G. & PARK, J. H. 2004. Hemolymph Sugar Homeostasis and Starvation-Induced Hyperactivity Affected by Genetic Manipulations of the Adipokinetic Hormone-Encoding Gene in Drosophila melanogaster. *Genetics,* 167**,** 311-323.

LEE, H.-K., CORDING, A., VIELMETTER, J. & ZINN, K. 2013. Interactions between a Receptor Tyrosine Phosphatase and a Cell Surface Ligand Regulate Axon Guidance and Glial-Neuronal Communication. *Neuron,* 78**,** 813-826.

LEE, K. S., YOU, K. H., CHOO, J. K., HAN, Y. M. & YU, K. 2004. Drosophila short neuropeptide F regulates food intake and body size. *J Biol Chem,* 279**,** 50781-9.

LEE, T., WINTER, C., MARTICKE, S. S., LEE, A. & LUO, L. 2000. Essential Roles of Drosophila RhoA in the Regulation of Neuroblast Proliferation and Dendritic but Not Axonal Morphogenesis. *Neuron,* 25**,** 307-316.

LEEUWEN, F. N., KAIN, H. E., KAMMEN, R. A., MICHIELS, F., KRANENBURG, O. W. & COLLARD, J. G. 1997. The guanine nucleotide exchange factor Tiam1 affects

neuronal morphology; opposing roles for the small GTPases Rac and Rho. *J Cell Biol,* 139**,** 797-807.
LEVI-MONTALCINI, R. 1976. Nerve-growth factor in familial dysautonomia. *New England Journal of Medicine,* 295**,** 671-673.
LEVI-MONTALCINI, R. 1987. The nerve growth factor: thirty-five years later. *EMBO J,* 6**,** 1145-1154.
LEVI-MONTALCINI, R., ALOE, L. & ALLEVO, E. 1990. A Role for Nerve Growth Factor in Nervous, Endocrine and Immune Systems. *Progress in Neuroendocrinimmunology,* 3**,** 1-10.
LEVI-MONTALCINI, R. & HAMBURGER, V. 1951. Selective growth stimulating effects of mouse sarcoma on the sensory and sympathetic nervous system of the chick embryo. *Journal of Experimental Zoology,* 116**,** 321-361.
LI, Y. H., WERNER, H. & PUSCHEL, A. W. 2008. Rheb and mTOR regulate neuronal polarity through Rap1B. *J Biol Chem,* 283**,** 33784-92.
LIN, C.-H., THOMPSON, C. A. & FORSCHER, P. 1994a. Cytoskeletal reorganization underlying growth cone motility. *Current Opinion in Neurobiology,* 4**,** 640-647.
LIN, D. M., FETTER, R. D., KOPCZYNSKI, C., GRENNINGLOH, G. & GOODMAN, C. S. 1994b. Genetic analysis of Fasciclin II in drosophila: Defasciculation, refasciculation, and altered fasciculation. *Neuron,* 13**,** 1055-1069.
LOCKWOOD, W. K. & BODMER, R. 2002. The patterns of wingless, decapentaplegic, and tinman position the Drosophila heart. *Mechanisms of Development,* 114**,** 13-26.
LOGAN, M. A., HACKETT, R., DOHERTY, J., SHEEHAN, A., SPEESE, S. D. & FREEMAN, M. R. 2012. Negative regulation of glial engulfment activity by Draper terminates glial responses to axon injury. *Nat Neurosci,* 15**,** 722-30.
LONG, H., SABATIER, C., MA, L., PLUMP, A., YUAN, W., ORNITZ, D. M., TAMADA, A., MURAKAMI, F., GOODMAN, C. S. & TESSIER-LAVIGNE, M. 2004. Conserved roles for Slit and Robo proteins in midline commissural axon guidance. *Neuron,* 42**,** 213-23.
LOREN, C. E., SCULLY, A., GRABBE, C., EDEEN, P. T., THOMAS, J., MCKEOWN, M., HUNTER, T. & PALMER, R. H. 2001. Identification and characterization of DAlk: a novel Drosophila melanogaster RTK which drives ERK activation in vivo. *Genes Cells,* 6**,** 531-44.
LOWERY, L. A. & VAN VACTOR, D. 2009. The trip of the tip: understanding the growth cone machinery. *Nat Rev Mol Cell Biol,* 10**,** 332-43.
LOYA, C. M., VAN VACTOR, D. & FULGA, T. A. 2010. Understanding neuronal connectivity through the post-transcriptional toolkit. *Genes & Development,* 24**,** 625-635.
LU, B., PANG, P. T. & WOO, N. H. 2005. The yin and yang of neurotrophin action. *Nat Rev Neurosci,* 6**,** 603-14.
LUBERG, K., WONG, J., WEICKERT, C. S. & TIMMUSK, T. 2010. Human TrkB gene: novel alternative transcripts, protein isoforms and expression pattern in the prefrontal cerebral cortex during postnatal development. *Journal of Neurochemistry,* 113**,** 952-964.
LUO, C. W. 2005. Bursicon, the insect cuticle-hardening hormone, is a heterodimeric cystine knot protein that activates G protein-coupled receptor LGR2. *Proceedings of the National Academy of Sciences,* 102**,** 2820-2825.
LUO, L. 2000. Rho GTPases in neuronal morphogenesis. *Nat Rev Neurosci,* 1**,** 173-80.
LUO, L., HENSCH, T. K., ACKERMAN, L., BARBEL, S., JAN, L. Y. & JAN, Y. N. 1996. Differential effects of the Rac GTPase on Purkinje cell axons and dendritic trunks and spines. *Nature,* 379**,** 837-40.

LUO, L., LIAO, Y. J., JAN, L. Y. & JAN, Y. N. 1994. Distinct morphogenetic functions of similar small GTPases: Drosophila Drac1 is involved in axonal outgrowth and myoblast fusion. *Genes Dev,* 8**,** 1787-802.

MA, Y., LI, J., CHIU, I., WANG, Y., SLOANE, J. A., LÜ, J., KOSARAS, B., SIDMAN, R. L., VOLPE, J. J. & VARTANIAN, T. 2006. Toll-like receptor 8 functions as a negative regulator of neurite outgrowth and inducer of neuronal apoptosis. *The Journal of Cell Biology,* 175**,** 209-215.

MACLAREN, C. M., EVANS, T. A., ALVARADO, D. & DUFFY, J. B. 2004. Comparative analysis of the Kekkon molecules, related members of the LIG superfamily. *Development Genes and Evolution,* 214.

MAGGIRWAR, S. B., SARMIERE, P. D., DEWHURST, S. & FREEMAN, R. S. 1998. Nerve growth factor-dependent activation of NF-kappaB contributes to survival of sympathetic neurons. *J Neurosci,* 18**,** 10356-65.

MANDAI, K., GUO, T., ST. HILLAIRE, C., MEABON, J. S., KANNING, K. C., BOTHWELL, M. & GINTY, D. D. 2009. LIG Family Receptor Tyrosine Kinase-Associated Proteins Modulate Growth Factor Signals during Neural Development. *Neuron,* 63**,** 614-627.

MANFRUELLI, P., REICHHART, J.-M., STEWARD, R., HOFFMANN, J. A. & LEMAITRE, B. 1999. A mosaic analysis in fat body cells of the control of antimicrobial peptide genes by the Rel proteins Dorsal and DIF. *EMBO Journal,* 18**,** 3380-3391.

MANIATIS, T., FRITSCH, E. F. & SAMBROOK, J. 1982. *Molecular cloning: a laboratory manual*, Cold Spring Harbor Laboratory, New York.

MANNING, G., PLOWMAN, G. D., HUNTER, T. & SUDARSANAM, S. 2002. Evolution of protein kinase signaling from yeast to man. *Trends in Biochemical Sciences,* 27**,** 514-520.

MANSER, E., LEUNG, T., SALIHUDDIN, H., ZHAO, Z. S. & LIM, L. 1994. A brain serine/threonine protein kinase activated by Cdc42 and Rac1. *Nature,* 367**,** 40-6.

MARCOTTE, E. M., PELLEGRINI, M., NG, H.-L., RICE, D. W., YEATES, T. O. & EISENBERG, D. 1999. Detecting Protein Function and Protein-Protein Interactions from Genome Sequences. *Science,* 285**,** 751-753.

MARKUS, A., ZHONG, J. & SNIDER, W. D. 2002. Raf and akt mediate distinct aspects of sensory axon growth. *Neuron,* 35**,** 65-76.

MASON, J. L., SUZUKI, K., CHAPLIN, D. D. & MATSUSHIMA, G. K. 2001. Interleukin-1β Promotes Repair of the CNS. *The Journal of Neuroscience,* 21**,** 7046-7052.

MATSUSHIMA, N., TACHI, N., KUROKI, Y., ENKHBAYAR, P., OSAKI, M., KAMIYA, M. & KRETSINGER, R. H. 2005. Structural analysis of leucine-rich-repeat variants in proteins associated with human diseases. *Cellular and Molecular Life Sciences,* 62**,** 2771-2791.

MCBRAYER, Z., ONO, H., SHIMELL, M., PARVY, J.-P., BECKSTEAD, R. B., WARREN, J. T., THUMMEL, C. S., DAUPHIN-VILLEMANT, C., GILBERT, L. I. & O'CONNOR, M. B. 2007. Prothoracicotropic Hormone Regulates Developmental Timing and Body Size in Drosophila. *Developmental Cell,* 13**,** 857-871.

MCGEE, A. W., YANG, Y., FISCHER, Q. S., DAW, N. W. & STRITTMATTER, S. M. 2005. Experience-driven plasticity of visual cortex limited by myelin and Nogo receptor. *Science,* 309**,** 2222-6.

MCILROY, G. 2011. *Toll-7 and Toll-6: Central Nervous System Functions as Drosophila Neurotrophin Receptors.* Doctor of Philosophy, University of Birmingham.

MCILROY, G., FOLDI, I., AURIKKO, J., WENTZELL, J. S., LIM, M. A., FENTON, J. C., GAY, N. J. & HIDALGO, A. 2013. Toll-6 and Toll-7 function as neurotrophin receptors in the Drosophila melanogaster CNS. *Nat Neurosci,* advance online publication.

MELLOR, H. & PARKER, P. J. 1998. The extended protein kinase C superfamily. *Biochem J,* 332 (Pt 2)**,** 281-92.
MENG, X., KHANUJA, B. S. & IP, Y. T. 1999. Toll receptor-mediated Drosophila immune response requires Dif, an NF- κ B factor. *Genes & Development,* 13**,** 792-797.
MERZ, K., HEROLD, S. & LIE, D. C. 2011. CREB in adult neurogenesis--master and partner in the development of adult-born neurons? *Eur J Neurosci,* 33**,** 1078-86.
MI, S., MILLER, R. H., LEE, X., SCOTT, M. L., SHULAG-MORSKAYA, S., SHAO, Z., CHANG, J., THILL, G., LEVESQUE, M., ZHANG, M., HESSION, C., SAH, D., TRAPP, B., HE, Z., JUNG, V., MCCOY, J. M. & PEPINSKY, R. B. 2005. LINGO-1 negatively regulates myelination by oligodendrocytes. *Nat Neurosci,* 8**,** 745-51.
MICHAELSEN, K., ZAGREBELSKY, M., BERNDT-HUCH, J., POLACK, M., BUSCHLER, A., SENDTNER, M. & KORTE, M. 2010. Neurotrophin receptors TrkB.T1 and p75NTR cooperate in modulating both functional and structural plasticity in mature hippocampal neurons. *European Journal of Neuroscience,* 32**,** 1854-1865.
MILDE, J. J., ZIEGLER, R. & WALLSTEIN, M. 1995. Adipokinetic hormone stimulates neurones in the insect central nervous system. *Journal of Experimental Biology,* 198**,** 1307-11.
MILLER, M. A. & STEELE, R. E. 2000. Lemon encodes an unusual receptor protein-tyrosine kinase expressed during gametogenesis in Hydra. *Dev Biol,* 224**,** 286-98.
MINDORFF, E. N., O'KEEFE, D. D., LABBE, A., YANG, J. P., OU, Y., YOSHIKAWA, S. & VAN MEYEL, D. J. 2007. A Gain-of-Function Screen for Genes That Influence Axon Guidance Identifies the NF- B Protein Dorsal and Reveals a Requirement for the Kinase Pelle in Drosophila Photoreceptor Axon Targeting. *Genetics,* 176**,** 2247-2263.
MIRANDA-SAAVEDRA, D. & BARTON, G. J. 2007. Classification and functional annotation of eukaryotic protein kinases. *Proteins: Structure, Function, and Bioinformatics,* 68**,** 893-914.
MIRTH, C., TRUMAN, J. W. & RIDDIFORD, L. M. 2005. The role of the prothoracic gland in determining critical weight for metamorphosis in Drosophila melanogaster. *Curr Biol,* 15**,** 1796-807.
MIRTH, C. K. & RIDDIFORD, L. M. 2007. Size assessment and growth control: how adult size is determined in insects. *BioEssays,* 29**,** 344-355.
MITCHELL, K. J., DOYLE, J. L., SERAFINI, T., KENNEDY, T. E., TESSIER-LAVIGNE, M., GOODMAN, C. S. & DICKSON, B. J. 1996. Genetic analysis of Netrin genes in Drosophila: Netrins guide CNS commissural axons and peripheral motor axons. *Neuron,* 17**,** 203-15.
MITSUHIRO, I., TOSHIMITSU, M., TAIZO, T. & KAZUO, C. 1994. Alternative splicing generates two distinct transcripts for the Drosophila melanogaster fibroblast growth factor receptor homolog. *Gene,* 139**,** 215-218.
MIYASHITA, T. & REED, J. C. 1995. Tumor suppressor p53 is a direct transcriptional activator of the human bax gene. *Cell,* 80**,** 293-9.
MIZUGUCHI, K., PARKER, J. S., BLUNDELL, T. L. & GAY, N. J. 1998. Getting knotted: a model for the structure and activation of Spätzle. *Trends in Biochemical Sciences,* 23**,** 239-242.
MOORE, A. D., BJÖRKLUND, Å. K., EKMAN, D., BORNBERG-BAUER, E. & ELOFSSON, A. 2008. Arrangements in the modular evolution of proteins. *Trends in Biochemical Sciences,* 33**,** 444-451.
MORISATO, D. & ANDERSON, K. V. 1994. The spatzle gene encodes a component of the extracellular signaling pathway establishing the dorsal-ventral pattern of the Drosophila embryo. *Cell,* 76**,** 677-88.
MORRISON, D. K., MURAKAMI, M.S., CLEGHON, V. 2000. Protein Kinases and Phosphatases in the Drosophila Genome. *Journal of Cell Biology,* 150**,** F57-F62.

MULLER, D., DJEBBARA-HANNAS, Z., JOURDAIN, P., VUTSKITS, L., DURBEC, P., ROUGON, G. & KISS, J. Z. 2000. Brain-derived neurotrophic factor restores long-term potentiation in polysialic acid-neural cell adhesion molecule-deficient hippocampus. *Proceedings of the National Academy of Sciences,* 97**,** 4315-4320.

MULLER, W. E., SKOROKHOD, A. & MULLER, I. M. 1999. Receptor tyrosine kinase, an autapomorphic character of metazoa: identification in marine sponges. *Acta Biol Hung,* 50**,** 395-411.

MURRAY, S. S., PEREZ, P., LEE, R., HEMPSTEAD, B. L. & CHAO, M. V. 2004. A novel p75 neurotrophin receptor-related protein, NRH2, regulates nerve growth factor binding to the TrkA receptor. *J Neurosci,* 24**,** 2742-9.

MUSACCHIO, M. & PERRIMON, N. 1996. The Drosophila kekkon Genes: Novel Members of both the Leucine-Rich Repeat and Immunoglobulin Superfamilies Expressed in the CNS. *Developmental Biology,* 178**,** 63-76.

NAKAYAMA, M., UNDERHILL, D. M., PETERSEN, T. W., LI, B., KITAMURA, T., TAKAI, T. & ADEREM, A. 2007. Paired Ig-Like Receptors Bind to Bacteria and Shape TLR-Mediated Cytokine Production. *The Journal of Immunology,* 178**,** 4250-4259.

NASSEL, D. R., ENELL, L. E., SANTOS, J. G., WEGENER, C. & JOHARD, H. A. 2008. A large population of diverse neurons in the Drosophila central nervous system expresses short neuropeptide F, suggesting multiple distributed peptide functions. *BMC Neurosci,* 9**,** 90.

NÄSSEL, D. R. & WINTHER, Å. M. E. 2010. Drosophila neuropeptides in regulation of physiology and behavior. *Progress in Neurobiology,* 92**,** 42-104.

NEWQUIST, G., DRENNAN, J. M., LAMANUZZI, M., WALKER, K., CLEMENS, J. C. & KIDD, T. 2013. Blocking apoptotic signaling rescues axon guidance in Netrin mutants. *Cell Rep,* 3**,** 595-606.

NG, J., NARDINE, T., HARMS, M., TZU, J., GOLDSTEIN, A., SUN, Y., DIETZL, G., DICKSON, B. J. & LUO, L. 2002. Rac GTPases control axon growth, guidance and branching. *Nature,* 416**,** 442-7.

NICHOLS, C. D., BECNEL, J. & PANDEY, U. B. 2012. Methods to assay Drosophila behavior. *J Vis Exp*.

NIJHOUT, H. F. 2003. The control of body size in insects. *Dev Biol,* 261**,** 1-9.

NILSSON, J., VALLBO, C., GUO, D., GOLOVLEVA, I., HALLBERG, B., HENRIKSSON, R. & HEDMAN, H. 2001. Cloning, characterization, and expression of human LIG1. *Biochem Biophys Res Commun,* 284**,** 1155-61.

NIMNUAL, A. S., YATSULA, B. A. & BAR-SAGI, D. 1998. Coupling of Ras and Rac guanosine triphosphatases through the Ras exchanger Sos. *Science,* 279**,** 560-3.

NOBES, C. D. & HALL, A. 1995. Rho, Rac, and Cdc42 GTPases regulate the assembly of multimolecular focal complexes associated with actin stress fibers, lamellipodia, and filopodia. *Cell,* 81**,** 53-62.

NOGUTI, T., ADACHI-YAMADA, T., KATAGIRI, T., KAWAKAMI, A., IWAMI, M., ISHIBASHI, J., KATAOKA, H., SUZUKI, A., GŌ, M. & ISHIZAKI, H. 1995. Insect prothoracicotropic hormone: a new member of the vertebrate growth factor superfamily. *FEBS Letters,* 376**,** 251-256.

NURNBERGER, T., BRUNNER, F., KEMMERLING, B. & PIATER, L. 2004. Innate immunity in plants and animals: striking similarities and obvious differences. *Immunol Rev,* 198**,** 249-66.

NYBAKKEN, K., VOKES, S. A., LIN, T. Y., MCMAHON, A. P. & PERRIMON, N. 2005. A genome-wide RNA interference screen in Drosophila melanogaster cells for new components of the Hh signaling pathway. *Nature Genetics,* 37**,** 1323-1332.

ODDEN, J. P., HOLBROOK, S. & DOE, C. Q. 2002. Drosophila HB9 Is Expressed in a Subset of Motoneurons and Interneurons, Where It Regulates Gene Expression and Axon Pathfinding. *The Journal of Neuroscience,* 22**,** 9143-9149.

OEFNER, C., D'ARCY, A., WINKLER, F. K., EGGIMANN, B. & HOSANG, M. 1992. Crystal structure of human platelet-derived growth factor BB. *EMBO J,* 11**,** 3921-6.

OHIRA, K., FUNATSU, N., HOMMA, K. J., SAHARA, Y., HAYASHI, M., KANEKO, T. & NAKAMURA, S. 2007. Truncated TrkB-T1 regulates the morphology of neocortical layer I astrocytes in adult rat brain slices. *Eur J Neurosci,* 25**,** 406-16.

OHIRA, K. & HAYASHI, M. 2009. A New Aspect of the TrkB Signaling Pathway in Neural Plasticity. *Current Neuropharmacology,* 7**,** 276-285.

OHIRA, K., HOMMA, K. J., HIRAI, H., NAKAMURA, S. & HAYASHI, M. 2006. TrkB-T1 regulates the RhoA signaling and actin cytoskeleton in glioma cells. *Biochem Biophys Res Commun,* 342**,** 867-74.

OHIRA, K., KUMANOGOH, H., SAHARA, Y., HOMMA, K. J., HIRAI, H., NAKAMURA, S. & HAYASHI, M. 2005. A Truncated Tropo-Myosine-Related Kinase B Receptor, T1, Regulates Glial Cell Morphology via Rho GDP Dissociation Inhibitor 1. *The Journal of Neuroscience,* 25**,** 1343-1353.

OHIRA, K., SHIMIZU, K. & HAYASHI, M. 1999. Change of expression of full-length and truncated TrkBs in the developing monkey central nervous system. *Brain Res Dev Brain Res,* 112**,** 21-9.

OINUMA, I., KATOH, H. & NEGISHI, M. 2007. R-Ras controls axon specification upstream of glycogen synthase kinase-3beta through integrin-linked kinase. *J Biol Chem,* 282**,** 303-18.

OISHI, I., SUGIYAMA, S., LIU, Z. J., YAMAMURA, H., NISHIDA, Y. & MINAMI, Y. 1997. A novel Drosophila receptor tyrosine kinase expressed specifically in the nervous system. Unique structural features and implication in developmental signaling. *J Biol Chem,* 272**,** 11916-23.

OLTVAI, Z. N., MILLIMAN, C. L. & KORSMEYER, S. J. 1993. Bcl-2 heterodimerizes in vivo with a conserved homolog, Bax, that accelerates programmed cell death. *Cell,* 74**,** 609-19.

ONO, T., SEKINO-SUZUKI, N., KIKKAWA, Y., YONEKAWA, H. & KAWASHIMA, S. 2003. Alivin 1, a novel neuronal activity-dependent gene, inhibits apoptosis and promotes survival of cerebellar granule neurons. *J Neurosci,* 23**,** 5887-96.

ORMOND, J., HISLOP, J., ZHAO, Y., WEBB, N., VAILLAINCOURT, F., DYER, J. R., FERRARO, G., BARKER, P., MARTIN, K. C. & SOSSIN, W. S. 2004. ApTrkl, a Trk-like Receptor, Mediates Serotonin- Dependent ERK Activation and Long-Term Facilitation in Aplysia Sensory Neurons. *Neuron,* 44**,** 715-728.

OU, Q., MAGICO, A. & KING-JONES, K. 2011. Nuclear Receptor DHR4 Controls the Timing of Steroid Hormone Pulses During <italic>Drosophila</italic> Development. *PLoS Biol,* 9**,** e1001160.

PAK, J. W., CHUNG, K. W., LEE, C. C., KIM, K., NAMKOONG, Y. & KOOLMAN, J. 1992. Evidence for multiple forms of the prothoracicotropic hormone in Drosophila melanogaster and indication of a new function. *Journal of Insect Physiology,* 38**,** 167-176.

PALGI, M., LINDSTROM, R., PERANEN, J., PIEPPONEN, T. P., SAARMA, M. & HEINO, T. I. 2009. Evidence that DmMANF is an invertebrate neurotrophic factor supporting dopaminergic neurons. *Proceedings of the National Academy of Sciences,* 106**,** 2429-2434.

PANG, P. T., TENG, H. K., ZAITSEV, E., WOO, N. T., SAKATA, K., ZHEN, S., TENG, K. K., YUNG, W. H., HEMPSTEAD, B. L. & LU, B. 2004. Cleavage of proBDNF by tPA/plasmin is essential for long-term hippocampal plasticity. *Science,* 306**,** 487-91.

PARKER, J. S., MIZUGUCHI, K. & GAY, N. J. 2001. A family of proteins related to Spätzle, the toll receptor ligand, are encoded in the Drosophila genome. *Proteins: Structure, Function, and Bioinformatics,* 45**,** 71-80.

PARKS, A. L., COOK, K. R., BELVIN, M., DOMPE, N. A., FAWCETT, R., HUPPERT, K., TAN, L. R., WINTER, C. G., BOGART, K. P., DEAL, J. E., DEAL-HERR, M. E., GRANT, D., MARCINKO, M., MIYAZAKI, W. Y., ROBERTSON, S., SHAW, K. J., TABIOS, M., VYSOTSKAIA, V., ZHAO, L., ANDRADE, R. S., EDGAR, K. A., HOWIE, E., KILLPACK, K., MILASH, B., NORTON, A., THAO, D., WHITTAKER, K., WINNER, M. A., FRIEDMAN, L., MARGOLIS, J., SINGER, M. A., KOPCZYNSKI, C., CURTIS, D., KAUFMAN, T. C., PLOWMAN, G. D., DUYK, G. & FRANCIS-LANG, H. L. 2004. Systematic generation of high-resolution deletion coverage of the Drosophila melanogaster genome. *Nature Genetics,* 36**,** 288-292.

PARR, J., LARGE, A., WANG, X., FOWLER, S. C., RATZLAFF, K. L. & RUDEN, D. M. 2001. The inebri-actometer: a device for measuring the locomotor activity of Drosophila exposed to ethanol vapor. *J Neurosci Methods,* 107**,** 93-9.

PATEL, N. H., SNOW, P. M. & GOODMAN, C. S. 1987. Characterization and cloning of fasciclin III: a glycoprotein expressed on a subset of neurons and axon pathways in Drosophila. *Cell,* 48**,** 975-88.

PATTHY, L. 1985. Evolution of the proteases of blood coagulation and fibrinolysis by assembly from modules. *Cell,* 41**,** 657-663.

PATTHY, L. 1999. Genome evolution and the evolution of exon-shuffling — a review. *Gene,* 238**,** 103-114.

PETIT, A. C., LEGUE, E. & NICOLAS, J. F. 2005. Methods in clonal analysis and applications. *Reprod Nutr Dev,* 45**,** 321-39.

POSTLETHWAIT, J. H. & JONES, G. J. 2005. Endocrine control of larval fat body histolysis in normal and mutant Drosophila melanogaster. *Journal of Experimental Zoology,* 203**,** 207-214.

PROKOP, A., BEAVEN, R., QU, Y. & SANCHEZ-SORIANO, N. 2013a. Using fly genetics to dissect the cytoskeletal machinery of neurons during axonal growth and maintenance. *J Cell Sci,* 126**,** 2331-41.

PROKOP, A., BEAVEN, R., QU, Y. & SÁNCHEZ-SORIANO, N. 2013b. Using fly genetics to dissect the cytoskeletal machinery of neurons during axonal growth and maintenance. *Journal of Cell Science,* 126**,** 2331-2341.

PULIDO, D., CAMPUZANO, S., KODA, T., MODOLELL, J. & BARBACID, M. 1992. Dtrk, a Drosophila gene related to the trk family of neurotrophin receptors, encodes a novel class of neural cell adhesion molecule. *EMBO J,* 11**,** 391-404.

RABIZADEH, S. & BREDESEN, D. E. 2003. Ten years on: mediation of cell death by the common neurotrophin receptor p75NTR. *Cytokine & Growth Factor Reviews,* 14**,** 225-239.

RAIVICH, G. & KREUTZBERG, G. W. 1993. Nerve growth factor and regeneration of peripheral nervous system. *Clin Neurol Neurosurg,* 95 Suppl**,** S84-8.

RAU, A., BUTTGEREIT, D., HOLZ, A., FETTER, R., DOBERSTEIN, S. K., PAULULAT, A., STAUDT, N., SKEATH, J., MICHELSON, A. M. & RENKAWITZ-POHL, R. 2001. rolling pebbles (rols) is required in Drosophila muscle precursors for recruitment of myoblasts for fusion. *Development,* 128**,** 5061-5073.

RENN, C. L., LEITCH, C. C. & DORSEY, S. G. 2009. In vivo evidence that truncated trkB.T1 participates in nociception. *Mol Pain,* 5**,** 61.

REWITZ, K. F., YAMANAKA, N., GILBERT, L. I. & O'CONNOR, M. B. 2009. The Insect Neuropeptide PTTH Activates Receptor Tyrosine Kinase Torso to Initiate Metamorphosis. *Science,* 326**,** 1403-1405.

REX, C. S., LIN, C. Y., KRAMAR, E. A., CHEN, L. Y., GALL, C. M. & LYNCH, G. 2007. Brain-derived neurotrophic factor promotes long-term potentiation-related cytoskeletal changes in adult hippocampus. *J Neurosci,* 27**,** 3017-29.

RICHARD, D. S., APPLEBAUM, S. B., SLITER, T. J., BAKER, F. C., SCHOOLEYO, D. A., REUTER, C. C., HENRICH, V. C. & GILBER, L. 1989. Juvenile hormone bisepoxide biosynthesis in vitro by the ring gland of Drosophila melanogaster: A putative juvenile hormone in the higher Diptera. *Proceedings of the National Academy of Sciences,* 86**,** 1421-1425.

RIDDIFORD, L. M. 1993. Hormone receptors and the regulation of insect metamorphosis. *Receptor,* 3**,** 203-9.

RIDDIFORD, L. M., TRUMAN, J. W., MIRTH, C. K. & SHEN, Y. C. 2010. A role for juvenile hormone in the prepupal development of Drosophila melanogaster. *Development,* 137**,** 1117-26.

RIDLEY, A. J. & HALL, A. 1992. The small GTP-binding protein rho regulates the assembly of focal adhesions and actin stress fibers in response to growth factors. *Cell,* 70**,** 389-99.

RIDLEY, A. J., PATERSON, H. F., JOHNSTON, C. L., DIEKMANN, D. & HALL, A. 1992. The small GTP-binding protein rac regulates growth factor-induced membrane ruffling. *Cell,* 70**,** 401-10.

ROSE, C. R., BLUM, R., PICHLER, B., LEPIER, A., KAFITZ, K. W. & KONNERTH, A. 2003. Truncated TrkB-T1 mediates neurotrophin-evoked calcium signalling in glia cells. *Nature,* 426**,** 74-8.

ROSENFELD, R. D., ZENI, L., HANIU, M., TALVENHEIMO, J., RADKA, S. F., BENNETT, L., MILLER, J. A. & WELCHER, A. A. 1995. Purification and identification of brain-derived neurotrophic factor from human serum. *Protein Expr Purif,* 6**,** 465-71.

ROUGON, G. & HOBERT, O. 2003. New insights into the diversity and function of neuronal immunoglobulin superfamily molecules. *Annu Rev Neurosci,* 26**,** 207-38.

RUAN, W., UNSAIN, N., DESBARATS, J., FON, E. A. & BARKER, P. A. 2013. Wengen, the Sole Tumour Necrosis Factor Receptor in <italic>Drosophila</italic>, Collaborates with Moesin to Control Photoreceptor Axon Targeting during Development. *PLoS ONE,* 8**,** e60091.

RUIZ-GÓMEZ, M. & GHYSEN, A. 1990. Development of the Peripheral Nervous System in Drosophila. *In:* RAYMOND, P., EASTER, S., JR. & INNOCENTI, G. (eds.) *Systems Approaches to Developmental Neurobiology.* Springer US.

SÁNCHEZ-SORIANO, N., GONÇALVES-PIMENTEL, C., BEAVEN, R., HAESSLER, U., OFNER-ZIEGENFUSS, L., BALLESTREM, C. & PROKOP, A. 2010. Drosophila growth cones: A genetically tractable platform for the analysis of axonal growth dynamics. *Developmental Neurobiology,* 70**,** 58-71.

SANCHEZ-SORIANO, N. & PROKOP, A. 2005. The influence of pioneer neurons on a growing motor nerve in Drosophila requires the neural cell adhesion molecule homolog FasciclinII. *J Neurosci,* 25**,** 78-87.

SÁNCHEZ-SORIANO, N., TEAR, G., WHITINGTON, P. & PROKOP, A. 2007. Drosophila as a genetic and cellular model for studies on axonal growth. *Neural Development,* 2**,** 9.

SANCHEZ-SORIANO, N., TRAVIS, M., DAJAS-BAILADOR, F., GONÇALVES-PIMENTEL, C., WHITMARSH, A. J. & PROKOP, A. 2009. Mouse ACF7 and Drosophila Short stop modulate filopodia formation and microtubule organisation during neuronal growth. *Journal of Cell Science,* 122**,** 2534-2542.

SCHECTERSON, L. C. & BOTHWELL, M. 2010. Neurotrophin receptors: Old friends with new partners. *Developmental Neurobiology,* 70**,** 332-338.

SCHECTERSON, L. C., HUDSON, M. P., KO, M., PHILIPPIDOU, P., AKMENTIN, W., WILEY, J., ROSENBLUM, E., CHAO, M. V., HALEGOUA, S. & BOTHWELL, M. 2010. Trk activation in the secretory pathway promotes Golgi fragmentation. *Molecular and Cellular Neuroscience,* 43**,** 403-413.

SCHNEIDER, D. S., HUDSON, K. L., LIN, T. Y. & ANDERSON, K. V. 1991. Dominant and recessive mutations define functional domains of Toll, a transmembrane protein required for dorsal-ventral polarity in the Drosophila embryo. *Genes & Development,* 5**,** 797-807.

SCHULZE, C. & FIRTH, J. A. 1993. Immunohistochemical localization of adherens junction components in blood-brain barrier microvessels of the rat. *J Cell Sci,* 104 (Pt 3)**,** 773-82.

SCHWAMBORN, J. C. & PUSCHEL, A. W. 2004. The sequential activity of the GTPases Rap1B and Cdc42 determines neuronal polarity. *Nat Neurosci,* 7**,** 923-9.

SCHWEITZER, R. & SHILO, B. Z. 1997. A thousand and one roles for the Drosophila EGF receptor. *Trends Genet,* 13**,** 191-6.

SCOTT, P. G., DODD, C. M., BERGMANN, E. M., SHEEHAN, J. K. & BISHOP, P. N. 2006. Crystal structure of the biglycan dimer and evidence that dimerization is essential for folding and stability of class I small leucine-rich repeat proteoglycans. *J Biol Chem,* 281**,** 13324-32.

SEIDAH, N. G., BENJANNET, S., PAREEK, S., CHRETIEN, M. & MURPHY, R. A. 1996. Cellular processing of the neurotrophin precursors of NT3 and BDNF by the mammalian proprotein convertases. *FEBS Lett,* 379**,** 247-50.

SHAMAS-DIN, A., KALE, J., LEBER, B. & ANDREWS, D. W. 2013. Mechanisms of Action of Bcl-2 Family Proteins. *Cold Spring Harbor Perspectives in Biology,* 5.

SHEN, J. & MARUYAMA, I. N. 2011. Nerve growth factor receptor TrkA exists as a preformed, yet inactive, dimer in living cells. *FEBS Lett,* 585**,** 295-9.

SHERRARD, R. M., DIXON, K. J., BAKOUCHE, J., RODGER, J., LEMAIGRE-DUBREUIL, Y. & MARIANI, J. 2009. Differential expression of TrkB isoforms switches climbing fiber-Purkinje cell synaptogenesis to selective synapse elimination. *Developmental Neurobiology,* 69**,** 647-662.

SHI, L., FU, A. K. & IP, N. Y. 2010. Multiple roles of the Rho GEF ephexin1 in synapse remodeling. *Commun Integr Biol,* 3**,** 622-4.

SIEGMUND, T. & KORGE, G. 2001. Innervation of the Ring Gland of Drosophila melanogaster. *Journal of Comparative Neurology,* 431**,** 481-491.

SIGGERS, D. C., ROGERS, J. G., BOYER, S. H., MARGOLET, L., DORKIN, H., BANERJEE, S. P. & SHOOTER, E. M. 1976. Increased Nerve-Growth-Factor β-Chain Cross-Reacting Material in Familial Dysautonomia. *New England Journal of Medicine,* 295**,** 629-634.

SIMON, J. C. & DICKINSON, M. H. 2010. A New Chamber for Studying the Behavior of <italic>Drosophila</italic>. *PLoS ONE,* 5**,** e8793.

SKELDAL, S., SYKES, A. M., GLERUP, S., MATUSICA, D., PALSTRA, N., AUTIO, H., BOSKOVIC, Z., MADSEN, P., CASTREN, E., NYKJAER, A. & COULSON, E. J. 2012. Mapping of the interaction site between sortilin and the p75 neurotrophin receptor reveals a regulatory role for the sortilin intracellular domain in p75 neurotrophin receptor shedding and apoptosis. *J Biol Chem,* 287**,** 43798-809.

SKRZYPIEC, A. E., W. BUCZKO & PAWLAK, R. 2008. TISSUE PLASMINOGEN ACTIVATOR IN THE AMYGDALA: ANEW ROLE FOR AN OLD PROTEASE. *J Physiol Pharmacol,* 59**,** 135-146.

SMEYNE, R. J., KLEIN, R., SCHNAPP, A., LONG, L. K., BRYANT, S., LEWIN, A., LIRA, S. A. & BARBACID, M. 1994. Severe sensory and sympathetic neuropathies in mice carrying a disrupted Trk/NGF receptor gene. *Nature,* 368**,** 246-9.

SNOW, P. M., ZINN, K., HARRELSON, A. L., MCALLISTER, L., SCHILLING, J., BASTIANI, M. J., MAKK, G. & GOODMAN, C. S. 1988. Characterization and cloning of fasciclin I and fasciclin II glycoproteins in the grasshopper. *Proc Natl Acad Sci U S A,* 85**,** 5291-5.

SODING, J. & LUPAS, A. N. 2003. More than the sum of their parts: on the evolution of proteins from peptides. *Bioessays,* 25**,** 837-46.

SOSSIN, W. S. 2006. Tracing the Evolution and Function of the Trk Superfamily of Receptor Tyrosine Kinases. *Brain, Behavior and Evolution,* 68**,** 145-156.

SOTILLOS, S., ESPINOSA-VAZQUEZ, J. M., FOGLIA, F., HU, N. & HOMBRIA, J. C. 2010. An efficient approach to isolate STAT regulated enhancers uncovers STAT92E fundamental role in Drosophila tracheal development. *Dev Biol,* 340**,** 571-82.

SPILLANE, M., KETSCHEK, A., DONNELLY, C. J., PACHECO, A., TWISS, J. L. & GALLO, G. 2012. Nerve growth factor-induced formation of axonal filopodia and collateral branches involves the intra-axonal synthesis of regulators of the actin-nucleating Arp2/3 complex. *J Neurosci,* 32**,** 17671-89.

SPRANGER, M., LINDHOLM, D., BANDTLOW, C., HEUMANN, R., GNAHN, H., NAHER-NOE, M. & THOENEN, H. 1990. Regulation of Nerve Growth Factor (NGF) Synthesis in the Rat Central Nervous System: Comparison between the Effects of Interleukin-1 and Various Growth Factors in Astrocyte Cultures and in vivo. *Eur J Neurosci,* 2**,** 69-76.

STROHMAIER, C., CARTER, B. D., URFER, R., BARDE, Y. A. & DECHANT, G. 1996. A splice variant of the neurotrophin receptor trkB with increased specificity for brain-derived neurotrophic factor. *EMBO J,* 15**,** 3332-7.

STYER, K. L., SINGH, V., MACOSKO, E., STEELE, S. E., BARGMANN, C. I. & ABALLAY, A. 2008. Innate immunity in Caenorhabditis elegans is regulated by neurons expressing NPR-1/GPCR. *Science,* 322**,** 460-4.

SUGA, H., KATOH, K. & MIYATA, T. 2001. Sponge homologs of vertebrate protein tyrosine kinases and frequent domain shufflings in the early evolution of animals before the parazoan-eumetazoan split. *Gene,* 280**,** 195-201.

SUGA, H., KUMA, K.-I., IWABE, N., NIKOH, N., ONO, K., KOYANAGI, M., HOSHIYAMA, D. & MIYATA, T. 1997. Intermittent divergence of the protein tyrosine kinase family during animal evolution. *FEBS Letters,* 412**,** 540-546.

SUN, P. D. 1995. The Cystine-Knot Growth-Factor Superfamily. *Annu. Rev. Biophys. Biomol. Struct.,* 24**,** 269-291.

SUSTER, M. L. & BATE, M. 2002. Embryonic assembly of a central pattern generator without sensory input. *Nature,* 416**,** 174-8.

SUTCLIFFE, B. 2010. *Functional analysis of Drosophila neurotrophins: from neuronal survival to behaviour. University of Birmingham.* PhD, University of Birmingham.

SUTCLIFFE, B., ZHU, B., FORERO, M. G., ROBINSON, I. M. & HIDALGO, A. 2013. Neuron-type specific functions of DNT1, DNT2 and Spz at the *Drosophila* neuromuscular junction. *PLoS One,* In press.

SZKLARCZYK, D., FRANCESCHINI, A., KUHN, M., SIMONOVIC, M., ROTH, A., MINGUEZ, P., DOERKS, T., STARK, M., MULLER, J., BORK, P., JENSEN, L. J. & VON MERING, C. 2011. The STRING database in 2011: functional interaction networks of proteins, globally integrated and scored. *Nucleic Acids Res,* 39**,** D561-8.

TAKAI, T. 2005. A Novel Recognition System for MHC Class I Molecules Constituted by PIR. *Advances in Immunology,* 88**,** 161-192.

TAKEUCHI, S., TAKEDA, K., OISHI, I., NOMI, M., IKEYA, M., ITOH, K., TAMURA, S., UEDA, T., HATTA, T., OTANI, H., TERASHIMA, T., TAKADA, S., YAMAMURA, H., AKIRA, S. & MINAMI, Y. 2000. Mouse Ror2 receptor tyrosine kinase is required for the heart development and limb formation. *Genes Cells,* 5**,** 71-8.

TAO, Y. & SCHULZ, R. A. 2007. Heart development in *Drosophila*. *Seminars in Cell & Developmental Biology,* 18**,** 3-15.
TAUSZIG, S., JOUANGUY, E., HOFFMANN, J. A. & IMLER, J. L. 2000. Toll-related receptors and the control of antimicrobial peptide expression in *Drosophila*. *Proceedings of the National Academy of Sciences,* 97**,** 10520-10525.
TENNESSEN, J. M. & THUMMEL, C. S. 2011a. Coordinating growth and maturation - insights from Drosophila. *Curr Biol,* 21**,** R750-7.
TENNESSEN, JASON M. & THUMMEL, CARL S. 2011b. Coordinating Growth and Maturation — Insights from Drosophila. *Current Biology,* 21**,** R750-R757.
TERVONEN, T. A., AJAMIAN, F., DE WIT, J., VERHAAGEN, J., CASTREN, E. & CASTREN, M. 2006. Overexpression of a truncated TrkB isoform increases the proliferation of neural progenitors. *Eur J Neurosci,* 24**,** 1277-85.
TESSIER-LAVIGNE, M. & GOODMAN, C. S. 1996. The Molecular Biology of Axon Guidance. *Science,* 274**,** 1123-1133.
THERRIEN, M., MORRISON, D. K., WONG, A. M. & RUBIN, G. M. 2000. A genetic screen for modifiers of a kinase suppressor of Ras-dependent rough eye phenotype in Drosophila. *Genetics,* 156**,** 1231-42.
THOMSON, T. M., RETTIG, W. J., CHESA, P. G., GREEN, S. H., MENA, A. C. & OLD, L. J. 1988. Expression of human nerve growth factor receptor on cells derived from all three germ layers. *Exp Cell Res,* 174**,** 533-9.
THUMMEL, C. S. & CHORY, J. 2002. Steroid signaling in plants and insects—common themes, different pathways. *Genes & Development,* 16**,** 3113-3129.
TISSOT M & RF, S. 2000. Metamorphosis in drosophila and other insects: the fate of neurons throughout the stages. *Prog Neurobiol,* 62**,** 89-111.
TISSOT, M. & STOCKER, R. F. 2000. Metamorphosis in Drosophila and other insects: the fate of neurons throughout the stages. *Progress in Neurobiology,* 62**,** 89-111.
TOMETTEN, M., BLOIS, S. & ARCK, P. C. 2005. Nerve growth factor in reproductive biology: link between the immune, endocrine and nervous system? *Chem Immunol Allergy,* 89**,** 135-48.
TORII, K. U. 2004. Leucine-Rich Repeat Receptor Kinases in Plants: Structure, Function, and Signal Transduction Pathways. *International Review of Cytology.* Academic Press.
TRIACA, V. & TIRASSA, P. 2003. Circulating NGF antibody alters the distribution of NG2 and CD56 positive cells in the brain of an animal model of inflammatory disorder. *Archives Italiennes de Biologie,* 141**,** 127-139.
TRIFUNOVSKI, A., JOSEPHSON, A., RINGMAN, A., BRENE, S., SPENGER, C. & OLSON, L. 2004. Neuronal activity-induced regulation of Lingo-1. *Neuroreport,* 15**,** 2397-400.
TRUMAN, J. W. 1990. Metamorphosis of the central nervous system of Drosophila. *Journal of Neurobiology,* 21**,** 1072-1084.
URFER, R., TSOULFAS, P., O'CONNELL, L., L.SHELTON, D., F.PARADA, L. & G.PRESTA, L. 1995. An immunoglobulin-like domain determines the specificity of neurotrophin receptors. *EMBO J,* 14**,** 2795-2805.
VALENZUELA, D. M., MAISONPIERRE, P. C., GLASS, D. J., ROJAS, E., NUNEZ, L., KONG, Y., GIES, D. R., STITT, T. N., IP, N. Y. & YANCOPOULOS, G. D. 1993. Alternative forms of rat TrkC with different functional capabilities. *Neuron,* 10**,** 963-74.
VAN KESTEREN, R. E., FAINZILBER, M., HAUSER, G., VAN MINNEN, J., VREUGDENHIL, E., SMIT, A. B., IBANEZ, C. F., GERAERTS, W. P. M. & BULLOCH, A. G. M. 1998. Early evolutionary origin of the neurotrophin receptor family. *EMBO Journal,* 17**,** 2534-2542.

VANG, L. L., MEDVEDEV, A. V. & ADLER, J. 2012. Simple Ways to Measure Behavioral Responses of *Drosophila* to Stimuli and Use of These Methods to Characterize a Novel Mutant. *PLoS ONE,* 7**,** e37495.
VAUGHN, D. E. & BJORKMAN, P. J. 1996. The (Greek) key to structures of neural adhesion molecules. *Neuron,* 16**,** 261-73.
VAYNMAN, S., YING, Z. & GOMEZ-PINILLA, F. 2003. Interplay between brain-derived neurotrophic factor and signal transduction modulators in the regulation of the effects of exercise on synaptic-plasticity. *Neuroscience,* 122**,** 647-657.
VETTER, M. L., MARTIN-ZANCA, D., PARADA, L. F., BISHOP, J. M. & KAPLAN, D. R. 1991. Nerve growth factor rapidly stimulates tyrosine phosphorylation of phospholipase C-gamma 1 by a kinase activity associated with the product of the trk protooncogene. *Proc Natl Acad Sci U S A,* 88**,** 5650-4.
VILAR, M., CHARALAMPOPOULOS, I., KENCHAPPA, R. S., SIMI, A., KARACA, E., REVERSI, A., CHOI, S., BOTHWELL, M., MINGARRO, I., FRIEDMAN, W. J., SCHIAVO, G., BASTIAENS, P. I. H., VERVEER, P. J., CARTER, B. D. & IBÁÑEZ, C. F. 2009. Activation of the p75 Neurotrophin Receptor through Conformational Rearrangement of Disulphide-Linked Receptor Dimers. *Neuron,* 62**,** 72-83.
VOGEL, B. E. & HEDGECOCK, E. M. 2001. Hemicentin, a conserved extracellular member of the immunoglobulin superfamily, organizes epithelial and other cell attachments into oriented line-shaped junctions. *Development,* 128**,** 883-94.
VOGEL, C. 2003. The immunoglobulin superfamily in Drosophila melanogaster and Caenorhabditis elegans and the evolution of complexity. *Development,* 130**,** 6317-6328.
VOGEL, C. & CHOTHIA, C. 2006. Protein Family Expansions and Biological Complexity. *PLoS Comput Biol,* 2**,** e48.
VOGEL, C., TEICHMANN, S. A. & PEREIRA-LEAL, J. 2005. The relationship between domain duplication and recombination. *J Mol Biol,* 346**,** 355-65.
VOGEL, W. 1999. Discoidin domain receptors: structural relations and functional implications. *FASEB J,* 13 Suppl**,** S77-82.
VOGEL, W., GISH, G. D., ALVES, F. & PAWSON, T. 1997. The Discoidin Domain Receptor Tyrosine Kinases Are Activated by Collagen. *Molecular Cell,* 1**,** 13-23.
VOLKOV, A. G., VILFRANC, C. L., MURPHY, V. A., MITCHELL, C. M., VOLKOVA, M. I., O'NEAL, L. & MARKIN, V. S. 2013. Electrotonic and action potentials in the Venus flytrap. *Journal of Plant Physiology,* 170**,** 838-846.
WALSH, F. S. & DOHERTY, P. 1997. Neural cell adhesion molecules of the immunoglobulin superfamily: role in axon growth and guidance. *Annu Rev Cell Dev Biol,* 13**,** 425-56.
WANG, X., BO, J., BRIDGES, T., DUGAN, K. D., PAN, T.-C., CHODOSH, L. A. & MONTELL, D. J. 2006. Analysis of Cell Migration Using Whole-Genome Expression Profiling of Migratory Cells in the Drosophila Ovary. *Developmental Cell,* 10**,** 483-495.
WARREN, J. T., YERUSHALMI, Y., SHIMELL, M. J., O'CONNOR, M. B., RESTIFO, L. L. & GILBERT, L. I. 2006. Discrete pulses of molting hormone, 20-hydroxyecdysone, during late larval development of Drosophila melanogaster: correlations with changes in gene activity. *Dev Dyn,* 235**,** 315-26.
WEBER, A. N. R., TAUSZIG-DELAMASURE, S., HOFFMANN, J. A., LELIÈVRE, E., GASCAN, H., RAY, K. P., MORSE, M. A., IMLER, J. L. & GAY, N. J. 2003. Binding of the Drosophila cytokine Spätzle to Toll is direct and establishes signaling. *Nature Immunology,* 4**,** 794-800.

WEGMAN, L. J., AINSLEY, J. A. & JOHNSON, W. A. 2010. Developmental timing of a sensory-mediated larval surfacing behavior correlates with cessation of feeding and determination of final adult size. *Developmental Biology,* 345**,** 170-179.
WEHRMAN, T., HE, X., RAAB, B., DUKIPATTI, A., BLAU, H. & GARCIA, K. C. 2007. Structural and Mechanistic Insights into Nerve Growth Factor Interactions with the TrkA and p75 Receptors. *Neuron,* 53**,** 25-38.
WEI, M. C., ZONG, W. X., CHENG, E. H., LINDSTEN, T., PANOUTSAKOPOULOU, V., ROSS, A. J., ROTH, K. A., MACGREGOR, G. R., THOMPSON, C. B. & KORSMEYER, S. J. 2001. Proapoptotic BAX and BAK: a requisite gateway to mitochondrial dysfunction and death. *Science,* 292**,** 727-30.
WESTON, C., YEE, B., HOD, E. & PRIVES, J. 2000. Agrin-induced acetylcholine receptor clustering is mediated by the small guanosine triphosphatases Rac and Cdc42. *J Cell Biol,* 150**,** 205-12.
WILLIAMS, A. F. & BARCLAY, A. N. 1988. The immunoglobulin superfamily--domains for cell surface recognition. *Annu Rev Immunol,* 6**,** 381-405.
WILSON, D. M. 1961. The Central Nervous Control of Flight in a Locust. *Journal of Experimental Biology,* 38**,** 471-490.
WILSON, K. H. S. 2009. The genome sequence of the protostome Daphnia pulex encodes respective orthologues of a neurotrophin, a Trk and a p75NTR: Evolution of neurotrophin signaling components and related proteins in the bilateria. *BMC Evolutionary Biology,* 9**,** 243.
WINANS, K. A. & HASHIMOTO, C. 1995. Ventralization of the Drosophila embryo by deletion of extracellular leucine-rich repeats in the Toll protein. *Mol Biol Cell,* 6**,** 587-96.
WINBERG, M. L., TAMAGNONE, L., BAI, J., COMOGLIO, P. M., MONTELL, D. & GOODMAN, C. S. 2001. The transmembrane protein Off-track associates with Plexins and functions downstream of Semaphorin signaling during axon guidance. *Neuron,* 32**,** 53-62.
WINDISCH, J. M., AUER, B., MARKSTEINER, R., LANG, M. E. & SCHNEIDER, R. 1995. Specific neurotrophin binding to leucine-rich motif peptides of TrkA and TrkB. *FEBS Letters,* 374**,** 125-129.
WOJTOWICZ, W. M., FLANAGAN, J. J., MILLARD, S. S., ZIPURSKY, S. L. & CLEMENS, J. C. 2004. Alternative splicing of Drosophila Dscam generates axon guidance receptors that exhibit isoform-specific homophilic binding. *Cell,* 118**,** 619-33.
WU, Q., WEN, T., LEE, G., PARK, J. H., CAI, H. N. & SHEN, P. 2003. Developmental control of foraging and social behavior by the Drosophila neuropeptide Y-like system. *Neuron,* 39**,** 147-61.
XING, J., KORNHAUSER, J. M., XIA, Z., THIELE, E. A. & GREENBERG, M. E. 1998. Nerve growth factor activates extracellular signal-regulated kinase and p38 mitogen-activated protein kinase pathways to stimulate CREB serine 133 phosphorylation. *Mol Cell Biol,* 18**,** 1946-55.
YAGI, Y., NISHIDA, Y. & IP, Y. T. 2010. Functional analysis of Toll-related genes in Drosophila. *Development, Growth & Differentiation,* 52**,** 771-783.
YAMANAKA, N., YAMAMOTO, S., ŽITŇAN, D., WATANABE, K., KAWADA, T., SATAKE, H., KANEKO, Y., HIRUMA, K., TANAKA, Y., SHINODA, T. & KATAOKA, H. 2008. Neuropeptide Receptor Transcriptome Reveals Unidentified Neuroendocrine Pathways. *PLoS ONE,* 3**,** e3048.
YAMASHITA, T. & TOHYAMA, M. 2003. The p75 receptor acts as a displacement factor that releases Rho from Rho-GDI. *Nat Neurosci,* 6**,** 461-7.
YAMASHITA, T., TUCKER, K. L. & BARDE, Y. A. 1999. Neurotrophin binding to the p75 receptor modulates Rho activity and axonal outgrowth. *Neuron,* 24**,** 585-93.

YANPALLEWAR, S. U., BARRICK, C. A., BUCKLEY, H., BECKER, J. & TESSAROLLO, L. 2012. Deletion of the BDNF truncated receptor TrkB.T1 delays disease onset in a mouse model of amyotrophic lateral sclerosis. *PLoS One,* 7**,** e39946.

YOON, J. G. & STAY, B. 1995. Immunocytochemical localization of Diploptera punctata allatostatin-like peptide in Drosophila melanogaster. *J Comp Neurol,* 363**,** 475-88.

ZAPATA, J. M., MATSUZAWA, S., GODZIK, A., LEO, E., WASSERMAN, S. A. & REED, J. C. 2000. The Drosophila tumor necrosis factor receptor-associated factor-1 (DTRAF1) interacts with Pelle and regulates NFkappaB activity. *J Biol Chem,* 275**,** 12102-7.

ZARTMAN, J. J., KANODIA, J. S., CHEUNG, L. S. & SHVARTSMAN, S. Y. 2009. Feedback control of the EGFR signaling gradient: superposition of domain-splitting events in Drosophila oogenesis. *Development,* 136**,** 2903-2911.

ZHANG, J., LEFEBVRE, J. L., ZHAO, S. & GRANATO, M. 2004. Zebrafish unplugged reveals a role for muscle-specific kinase homologs in axonal pathway choice. *Nat Neurosci,* 7**,** 1303-9.

ZHANG, Q., WANG, J., FAN, S., WANG, L., CAO, L., TANG, K., PENG, C., LI, Z., LI, W., GAN, K., LIU, Z., LI, X., SHEN, S. & LI, G. 2005. Expression and functional characterization of LRRC4, a novel brain-specific member of the LRR superfamily. *FEBS Letters,* 579**,** 3674-3682.

ZHANG, Z. T. & ZHU, S. Y. 2009. Drosomycin, an essential component of antifungal defence in Drosophila. *Insect Molecular Biology,* 18**,** 549-556.

ZHU, B., PENNACK, J. A., MCQUILTON, P., FORERO, M. G., MIZUGUCHI, K., SUTCLIFFE, B., GU, C.-J., FENTON, J. C. & HIDALGO, A. 2008. Drosophila Neurotrophins Reveal a Common Mechanism for Nervous System Formation. *PLoS Biology,* 6**,** e284.

ZIEGENFUSS, J. S., BISWAS, R., AVERY, M. A., HONG, K., SHEEHAN, A. E., YEUNG, Y. G., STANLEY, E. R. & FREEMAN, M. R. 2008. Draper-dependent glial phagocytic activity is mediated by Src and Syk family kinase signalling. *Nature,* 453**,** 935-9.

ZIPURSKY, L. S. & GRUEBER, W. B. 2013. The molecular basis of self-avoidance. *Annu Rev Neurosci,* 36**,** 547-68.

APPENDIX I

STATISTICAL DATA, ALL CHAPTERS

Statistical tests, Chapter 3

GENOTYPE	n	COMPARISON	NORMALITY	H.OF VAR.	DESCRIPTIVE STATISTICS	DF & TEST VALUE	P	MULTIPLE COMPARISONS & CORRECTIONS	
Survival index									
Genotype	**Pupae**		**N/A**	**N/A**	**categorical data**	χ^2	**P**	χ^2	**Bonf.x22**
DNT1[55]/TM6B	446	All together				X=444.984 d.f.=19	**<0.001**		
DNT2[e03444]/TM6B	657								
DNT2[e03444]DNT1[41]/TM6B	494								
w;lbk[PGSV250104];+/SM6aTM6B	186								
w;lbk[PGSV250104];DNT1[55]/ SM6aTM6B	424	*w;lbk[PGSV250104];+/SM6aTM6B* vs *w;lbk[PGSV250104];DNT1[55]/SM6aTM6B*				X=121.455 d.f.=1		<0.001	<0.001
w;lbk[PGSV250104];DNT2[e03444]/ SM6aTM6B	316	*w;lbk[PGSV250104];+/SM6aTM6B* vs *w;lbk[PGSV250104];DNT2[e03444]/SM6aTM6B*				X=92.252 d.f.=1		<0.001	<0.001
		DNT1[55]/TM6B vs *w;lbk[PGSV250104];DNT1[55]/SM6aTM6B*				X=113.521 d.f.=1		<0.001	<0.001
		DNT2[e03444]/TM6B vs *w;lbk[PGSV250104];DNT2[e03444]/SM6aTM6B*				X=47.116 d.f.=1		<0.001	<0.001
w;kek3[f07029];+/SM6aTM6B	184								
w;kek3[f07029];DNT1[55]/ SM6aTM6B	182	*w;kek3[f07029];+/SM6aTM6B* vs *w;kek3[f07029];DNT1[55]/SM6aTM6B*				X=14.824 d.f.=1		<0.001	<0.001
w;kek3[f07029];DNT2[e03444]/ SM6aTM6B	294	*w;kek3[f07029];+/SM6aTM6B* vs *w;kek3[f07029];DNT2[e03444]/SM6aTM6B*				X=0.004 d.f.=1		0.952	20.944
		DNT1[55]/TM6B vs *w;kek3[f07029];DNT1[55]/SM6aTM6B*				X=22.782 d.f.=1		<0.001	<0.001
		DNT2[e03444]/TM6B vs *w;kek3[f07029];DNT2[e03444]/SM6aTM6B*				X=9.397 d.f.=1		0.002	0.044
w;kek4[f05454];+/SM6aTM6B	158								
w;kek4[f05454];DNT1[55]/ SM6aTM6B	93	*w;kek4[f05454];+/SM6aTM6B* vs *w;kek4[f05454];DNT1[55]/SM6aTM6B*				X=19.299 d.f.=1		<0.001	<0.001
w;kek4[f05454];DNT2[e03444]/ SM6aTM6B	189	*w;kek4[f05454];+/SM6aTM6B v w;kek4[f05454];DNT2[e03444]/SM6aTM6B*				X=34.621 d.f.=1		<0.001	<0.001
		DNT1[55]/TM6B vs *w;kek4[f05454];DNT1[55]/SM6aTM6B*				X=27.192 d.f.=1		<0.001	<0.001
		DNT2[e03444]/TM6B vs *w;kek4[f05454];DNT2[e03444]/SM6aTM6B*				X=26.162 d.f.=1		<0.001	<0.001
kek5[e02482];;+/TM6B	177								
kek5[e02482];;DNT1[55]/TM6B	537	*kek5[e02482];;+/TM6B* vs *kek5[e02482];;DNT1[55]/TM6B*				X=0.244 d.f.=1		0.621	13.662
kek5[e02482];;DNT2[e03444]/TM6B	194	*kek5[e02482];;+/TM6B* vs *kek5[e02482];;DNT2[e03444]/TM6B*				X=38.697 d.f.=1		<0.001	<0.001
		DNT1[55]/TM6B vs *kek5[e02482];;DNT1[55]/TM6B*				X=1.506 d.f.=1		0.22	4.84
		DNT2[e03444]/TM6B vs *kek5[e02482];;DNT2[e03444]/TM6B*				X=22.368 d.f.=1		<0.001	<0.001
w;rk[4];DNT1[55]/SM6aTM6B	166	*DNT1[55]/TM6B* vs *w;rk[4];DNT1[55]/SM6aTM6B*				X=12.149 d.f.=1		<0.001	<0.001
w;rk[4];DNT2[e03444]/SM6aTM6B	233	*DNT2[e03444]/TM6B* vs *w;rk[4];DNT2[e03444]/SM6aTM6B*				X=0.067 d.f.=1		0.796	17.512
pBac{RB}wgn[e00637];;+/TM6B	408								

pBac{RB}wgn[e00637];; DNT1[55]/TM6B	280	*pBac{RB}wgn[e00637];;+/TM6B* vs *pBac{RB}wgn[e00637];;DNT1[55]/TM6B*					X=3.842 d.f.=1		0.05	1.1
pBac{RB}wgn[e00637];; DNT2[e03444]/TM6B	400	*pBac{RB}wgn[e00637];;+/TM6B* vs *pBac{RB}wgn[e00637];;DNT2[e03444]/TM6B*					X=3.949 d.f.=1		0.047	1.034
		DNT1[55]/TM6B vs *pBac{RB}wgn[e00637];;DNT1[55]/TM6B*					X=2.895 d.f.=1		0.089	1.958
		DNT2[e03444]/TM6B vs *pBac{RB}wgn[e00637];;DNT2[e03444]/TM6B*					X=5.136 d.f.=1		0.023	0.506

Adult locomotion: Distance

Genotype	Flies		Kurt.	Skew.	Levene's	Mean±s.e.m.	One-Way ANOVA	P	t-test	Bonf.x15
yw	22	All together	-0.112	-0.672	**P=0.792**	3742.13±217.09	F=7.829 d.f.1=13 d.f.2=244	**<0.001**		
DNT1[55]	21		-0.485	0.158		3120.85±252.50				
DNT2[e03444]	21		1.538	0.845		1801.27±217.06				
kek3[f07029]	21		-0.999	0.504		1900.56±252.22				
kek3[f07029]DNT1[55]	10	*kek3[f07029]DNT1[55]* vs *DNT1[55]*	0.871	1.026	0.433	1301.09±317.70	d.f.=29 t=4.259		<0.001	<0.001
		kek3[f07029]DNT1[55] vs *kek3[f07029]*			0.357		d.f.=29 t=1.404		0.171	2.565
kek3[f07029]DNT2[e03444]	19	*kek3[f07029]DNT2[e03444]* vs *DNT2[e03444]*	0.085	-0.455	0.525	3034.00±257.96	d.f.=38 t=-3.679		0.001	0.015
		kek3[f07029]DNT2[e03444] vs *kek3[f07029]*			0.543		d.f.=38 t=-3.137		0.003	0.045
		kek3[f07029]DNT1[55] vs *kek3[f07029]DNT2[e03444]*			0.751		d.f.=27 t=-4.084		<0.001	<0.001
kek4[f05454]	23		-1.187	-0.114		2693.19±224.63				
kek4[f05454]DNT1[55]	7	*kek4[f05454]DNT1[55]* vs *DNT1[55]*	-1.02	0.508	0.318	1054.64±325.21	d.f.=26 t=4.320		<0.001	<0.001
		kek4[f05454]DNT1[55] vs *kek4[f05454]*			0.364		d.f.=28 t=3.669		0.001	0.015
kek4[f05454]DNT2[e03444]	9	*kek4[f05454]DNT2[e03444]* vs *DNT2[e03444]*	-0.894	-0.26	0.564	3252.23±379.80	d.f.=28 t=-3.508		0.002	0.03
		kek4[f05454]DNT2[e03444] vs *kek4[f05454]*			0.872		d.f.=30 t=-1.299		0.204	3.06
		kek4[f05454]DNT1[55] vs *kek4[f05454]DNT2[e03444]*			0.565		d.f.=14 t=-4.237		0.001	0.015
kek5[e02482]	21		-0.496	-0.039		1796.60±191.78				
kek5[e02482]DNT1[55]	21	*kek5[e02482]DNT1[55]* vs *DNT1[55]*	-0.665	-0.262	0.387	2255.64±219.18	d.f.=40 t=2.588		0.013	0.195
		kek5[e02482]DNT1[55] vs *kek5[e02482]*			0.493		d.f.=40 t=-1.576		0.123	1.845
kek5[e02482]DNT2[e03444]	20	*kek5[e02482]DNT2[e03444]* vs *DNT2[e03444]*	-1.162	-0.015	0.166	2251.05±263.63	d.f.=39 t=-1.323		0.194	2.91
		kek5[e02482]DNT2[e03444] vs *kek5[e02482]*			0.077		d.f.=39 t=-1.404		0.168	2.52
		kek5[e02482]DNT1[55] vs *kek5[e02482]DNT2[e03444]*			0.283		d.f.=39 t=0.013		0.989	14.835
lbk[GSV2]50104	22		-0.226	0.12		2245.38±197.63				
wgn[e00637]	21		-0.954	-0.243		2686.04±253.78				

Adult locomotion: Moving speed

Genotype	Frames		distribution not normal	Histogram	Kruskal-Wallis	P	Dunn post-hoc	
yw	8230	All together			d.f.=13, Kruskal-Wallis:6883.510	**<0.001**		
DNT1[55]	7356							
DNT2[e03444]	8179							
kek3[f07029]	8703							
kek3[f07029]DNT1[55]	3612	*kek3[f07029]DNT1[55]* vs *DNT1[55]*			Dunn's: 18919		<0.001	
		kek3[f07029]DNT1[55] vs *kek3[f07029]*			Dunn's: 2620		<0.001	
kek3[f07029]DNT2[e03444]	7149	*kek3[f07029]DNT2[e03444]* vs *DNT2[e03444]*			Dunn's: -12710		<0.001	
		kek3[f07029]DNT2[e03444] vs *kek3[f07029*			Dunn's: -14741		<0.001	
		kek3[f07029]DNT1[55] vs *kek3[f07029]DNT2[e03444]*			Dunn's: -17360		<0.001	
kek4[f05454]	8552							
kek4[f05454]DNT1[55]	2614	*kek4[f05454]DNT1[55]* vs *DNT1[55]*			Dunn's: 28081		<0.001	
		kek4[f05454]DNT1[55] vs *kek4[f05454]*			Dunn's: 21403		<0.001	
kek4[f05454]DNT2[e03444]	3435	*kek4[f05454]DNT2[e03444]* vs *DNT2[e03444]*			Dunn's: -13351		<0.001	
		kek4[f05454]DNT2[e03444] vs *kek4[f05454]*			Dunn's: -5760		<0.001	
		kek4[f05454]DNT1[55] vs *kek4[f05454]DNT2[e03444]*			Dunn's: -27163		<0.001	
kek5[e02482]	8217							
kek5[e02482]DNT1[55]	7927	*kek5[e02482]DNT1[55]* vs *DNT1[55]*			Dunn's: 8704		<0.001	
		kek5[e02482]DNT1[55] vs *kek5[e02482]*			Dunn's: -6639		<0.001	
kek5[e02482]DNT2[e03444]	7953	*kek5[e02482]DNT2[e03444]* vs *DNT2[e03444]*			Dunn's: -4716		<0.001	
		kek5[e02482]DNT2[e03444] vs *kek5[e02482]*			Dunn's: -5791		<0.001	
		kek5[e02482]DNT1[55] vs *kek5[e02482]DNT2[e03444]*			Dunn's: 848.3		n.s	
lbk[GSV2]50104	8453							
wgn[e00637]	7919							

Adult locomotion: Percentage time resting

Genotype	Frames		N/A	N/A	Categorical data	χ^2	P	χ^2	Bonf.x15
yw	8272	All together				X=4805.067 d.f.=13	**<0.001**		
DNT1[55]	7801								
DNT2[e03444]	8230								
kek3[f07029]	8338								
kek3[f07029]DNT1[55]	3850	*kek3[f07029]DNT1[55]* vs *DNT1[55]*				X=472.569 d.f.=1		<0.001	<0.001
		kek3[f07029]DNT1[55] vs *kek3[f07029]*				X=31.023 d.f.=1		<0.001	<0.001
kek3[f07029]DNT2[e03444]	7199	*kek3[f07029]DNT2[e03444]* vs *DNT2[e03444]*				X=656.453 d.f.=1		<0.001	<0.001

		kek3[f07029]DNT2[e03444] vs *kek3[f07029*			X=1108.452 d.f.=1		<0.001	<0.001
		kek3[f07029]DNT1[55] vs *kek3[f07029]DNT2[e03444]*			X=498.399 d.f.=1		<0.001	<0.001
kek4[f05454]	8594							
kek4[f05454]DNT1[55]	2628	*kek4[f05454]DNT1[55]* vs *DNT1[55]*			X=1278.864 d.f.=1		<0.001	<0.001
		kek4[f05454]DNT1[55] vs *kek4[f05454]*			X=482.147 d.f.=1		<0.001	<0.001
kek4[f05454]DNT2[e03444]	3466	*kek4[f05454]DNT2[e03444]* vs *DNT2[e03444]*			X=250.345 d.f.=1		<0.001	<0.001
		kek4[f05454]DNT2[e03444] vs *kek4[f05454]*			X=118.828 d.f.=1		<0.001	<0.001
		kek4[f05454]DNT1[55] vs *kek4[f05454]DNT2[e03444]*			X=742.956 d.f.=1		<0.001	<0.001
kek5[e02482]	8249							
kek5[e02482]DNT1[55]	8113	*kek5[e02482]DNT1[55]* vs *DNT1[55]*			X=191.478 d.f.=1		<0.001	<0.001
		kek5[e02482]DNT1[55] vs *kek5[e02482]*			X=245.564 d.f.=1		<0.001	<0.001
kek5[e02482]DNT2[e03444]	7976	*kek5[e02482]DNT2[e03444]* vs *DNT2[e03444]*			X=102.872 d.f.=1		<0.001	<0.001
		kek5[e02482]DNT2[e03444] vs *kek5[e02482]*			X=202.668 d.f.=1		<0.001	<0.001
		kek5[e02482]DNT1[55] vs *kek5[e02482]DNT2[e03444]*			X=1.878 d.f.=1		0.171	2.565
lbk[GSV2]50104	8343							
wgn[e00637]	7973							

Adult locomotion: percentage wobbling

Genotype	Flies	N/A	N/A	Categorical data	χ^2	P	χ^2	Bonf.x15
yw	8272	All together			X=1083.745 d.f.=13	**<0.001**		
DNT1[55]	7801							
DNT2[e03444]	8230							
kek3[f07029]	8338							
kek3[f07029]DNT1[55]	3850	*kek3[f07029]DNT1[55]* vs *DNT1[55]*			X=372.333 d.f.=1		<0.001	<0.001
		kek3[f07029]DNT1[55] vs *kek3[f07029]*			X=177.782 d.f.=1		<0.001	<0.001
kek3[f07029]DNT2[e03444]	7199	*kek3[f07029]DNT2[e03444]* vs *DNT2[e03444]*			X=50.277 d.f.=1		<0.001	<0.001
		kek3[f07029]DNT2[e03444] vs *kek3[f07029*			X=13.406 d.f. =1		<0.001	<0.001
		kek3[f07029]DNT1[55] vs *kek3[f07029]DNT2[e03444]*			X=256.351 d.f.=1		<0.001	<0.001
kek4[f05454]	8594							
kek4[f05454]DNT1[55]	2628	*kek4[f05454]DNT1[55]* vs *DNT1[55]*			X=249.218 d.f.=1		<0.001	<0.001
		kek4[f05454]DNT1[55] vs *kek4[f05454]*			X=233.242 d.f.=1		<0.001	<0.001
kek4[f05454]DNT2[e03444]	3466	*kek4[f05454]DNT2[e03444]* vs *DNT2[e03444]*			X=64.133 d.f.=1		<0.001	<0.001
		kek4[f05454]DNT2[e03444] vs *kek4[f05454]*			X=0.862 d.f.=1		0.353	5.295
		kek4[f05454]DNT1[55] vs *kek4[f05454]DNT2[e03444]*			X=159.625 d.f.=1		<0.001	<0.001
kek5[e02482]	8249							
kek5[e02482]DNT1[55]	8113	*kek5[e02482]DNT1[55]* vs *DNT1[55]*			X=84.965 d.f.=1		<0.001	<0.001

		kek5[e02482]DNT1[55] vs *kek5[e02482]*	X=16.661 d.f.=1	<0.001	<0.001
kek5[e02482]DNT2[e03444]	7976	*kek5[e02482]DNT2[e03444]* vs *DNT2[e03444]*	X=1.369 d.f.=1	0.242	3.63
		kek5[e02482]DNT2[e03444] vs *kek5[e02482]*	X=2.442 d.f.=1	0.118	1.77
		kek5[e02482]DNT1[55] vs *kek5[e02482]DNT2[e03444]*	X=6.234 d.f.=1	0.013	0.195
lbk[GSV2]50104	8343				
wgn[e00637]	7973				

Statistical tests, Chapter 4

GENOTYPE	n	COMPARISON	NORMALITY	H. OF VAR.	DESCRIPTIVE STATISTICS	DF & TEST VALUE	P	MULTIPLE COMPARISONS & CORRECTIONS	
Survival index									
Genotype	**Pupae**		**N/A**	**N/A**	**categorical data**	χ^2		χ^2	**Bonf.x6**
DNT2[e03444]DNT1[41]/TM6B	270	All together				X=908.085 d.f.=13	**<0.001**		
DNT2[e03444]DNT1[41]elavGal4/TM6B	431								
UASkek1RFP;DNT2[e03444] DNT1[41]/TM6B	376								
UASkek2RFP;DNT2[e03444] DNT1[41]/TM6B	171								
UASkek3RFP;DNT2[e03444] DNT1[41]/TM6B	168								
UASkek4RFP;DNT2[e03444] DNT1[41]/TM6B	209								
UASkek5RFP;DNT2[e03444] DNT1[41]/TM6B	160								
UASkek6RFP;DNT2[e03444] DNT1[41]/TM6B	276								
DNT[e03444]DNT1[41]elavGal4/TM6B x UASkek1RFP;DNT2[e03444] DNT1[41]/SM6aTM6B	262	*DNT[e03444]DNT1[41]elavGal4/TM6B x UASkek1RFP;DNT2[e03444]DNT1[41]/SM6aTM6B vs DNT2[e03444]DNT1[41]elavGal4/TM6B*				X=8.621 d.f.=1		0.003	0.018
DNT[e03444]DNT1[41]elavGal4/TM6B x UASkek2RFP;DNT2[e03444] DNT1[41]/SM6aTM6B	283	*DNT[e03444]DNT1[41]elavGal4/TM6B x UASkek2RFP;DNT2[e03444]DNT1[41]/SM6aTM6B vs DNT2[e03444]DNT1[41]elavGal4/TM6B*				X=180.546 d.f.=1		<0.001	<0.001
DNT[e03444]DNT1[41]elavGal4/TM6B x UASkek3RFP;DNT2[e03444] DNT1[41]/SM6aTM6B	195	*DNT[e03444]DNT1[41]elavGal4/TM6B x UASkek3RFP;DNT2[e03444]DNT1[41]/SM6aTM6B vs DNT2[e03444]DNT1[41]elavGal4/TM6B*				X=84.912 d.f.=1		<0.001	<0.001
DNT[e03444]DNT1[41]elavGal4/TM6B x UASkek4RFP;DNT2[e03444] DNT1[41]/SM6aTM6B	193	*DNT[e03444]DNT1[41]elavGal4/TM6B x UASkek4RFP;DNT2[e03444]DNT1[41]/SM6aTM6B vs DNT2[e03444]DNT1[41]elavGal4/TM6B*				X=5.459 d.f.=1		0.019	0.114
DNT[e03444]DNT1[41]elavGal4/TM6B x UASkek5RFP;DNT2[e03444] DNT1[41]/SM6aTM6B	52	*DNT[e03444]DNT1[41]elavGal4/TM6B x UASkek5RFP;DNT2[e03444]DNT1[41]/SM6aTM6B vs DNT2[e03444]DNT1[41]elavGal4/TM6B*				X=37.294 d.f.=1		<0.001	<0.001
DNT[e03444]DNT1[41]elavGal4/TM6B x UASkek6RFP;DNT2[e03444] DNT1[41]/SM6aTM6B	313	*DNT[e03444]DNT1[41]elavGal4/TM6B x UASkek6RFP;DNT2[e03444]DNT1[41]/SM6aTM6B vs DNT2[e03444]DNT1[41]elavGal4/TM6B*				X=207.992 d.f.=1		<0.001	<0.001

Drosomycin-luciferase: Dif reporter DNT1CK stimulation, small scale DNT production

Genotype	Repeats	N/A	Levene's	Mean±s.e.m.	Welch ANOVA		t-test	Bonf.x9
pDONR	15 (5x in triplicate)	All together	**0**	0.254±0.002	F=14.912 d.f.1=11 d.f.2=39.663	**<0.001**		
pDONR+DNT1CK	15 (5x in triplicate)			0.290±0.002				
Toll6	9 (3x in triplicate)			0.061±0.006				
Toll6+DNT1CK	9 (3x in triplicate)	pDONR+DNT1CK vs Toll6+DNT1CK	**0**	0.084±0.010	d.f.=25 t=-7.651		<0.001	<0.001
kek3≡Toll6 chimaera	9 (3x in triplicate)			0.058±0.006				
kek3≡Toll6 chimaera+DNT1CK	9 (3x in triplicate)	pDONR+DNT1CK vs kek3≡Toll6 chimaera+DNT1CK	**0**	0.076±0.007	d.f.=25 t=-8.374		<0.001	<0.001
		kek3≡Toll6 chimaera vs kek3≡Toll6 chimaera+DNT1CK	**0.366**		d.f.=16 t=-1.883		0.078	0.702
kek4≡Toll6 chimaera	9 (3x in triplicate)			0.039±0.002				
kek4≡Toll6 chimaera+DNT1CK	9 (3x in triplicate)	pDONR+DNT1CK vs kek4≡Toll6 chimaera+DNT1CK	**0.006**	0.047±0.005	d.f.=25 t=-4.398		<0.001	<0.001
		kek4≡Toll6 chimaera vs kek3≡Toll6 chimaera+DNT1CK	**0.042**		d.f.=16 t=-1.453		0.165	1.485
kek5≡Toll6 chimaera	9 (3x in triplicate)			0.028±0.002				
kek5≡Toll6 chimaera+DNT1CK	9 (3x in triplicate)	pDONR+DNT1CK vs kek5≡Toll6 chimaera+DNT1CK	**0.002**	0.038±0.005	d.f.=25 t=-2.358		0.026	0.234
		kek5≡Toll6 chimaera vs kek3≡Toll6 chimaera+DNT1CK	**0.002**		d.f.=16 t=-2.100		0.052	0.468
kek6≡Toll6 chimaera	9 (3x in triplicate)			0.063±0.010				
kek6≡Toll6 chimaera+DNT1CK	9 (3x in triplicate)	pDONR+DNT1CK vs kek6≡Toll6 chimaera+DNT1CK	**0**	0.062±0.007	d.f.=25 t=-6.325		<0.001	<0.001
		kek6≡Toll6 chimaera vs kek3≡Toll6 chimaera+DNT1CK	**0.463**		d.f.=16 t=0.053		0.959	8.631

Drosomycin-luciferase: Dif reporter DNT2CK stimulation, small scale DNT production

Genotype	Repeats	N/A	Levene's	Mean±s.e.m.	Welch ANOVA		t-test	Bonf.x9
pDONR	15 (5x in triplicate)	All together	0	0.025±0.002	F=20.429 d.f.1=11 d.f.2=39.850	**<0.001**		
pDONR+DNT2CK	15 (5x in triplicate)			0.033±0.003				
Toll6	9 (3x in triplicate)			0.061±0.006				
Toll6+DNT2CK	9 (3x in triplicate)	pDONR+DNT2CK vs Toll6+DNT2CK	0.001	0.117±0.011	d.f.=25 t=-10.005		<0.001	<0.001
kek3≡Toll6 chimaera	9 (3x in triplicate)			0.058±0.006				
kek3≡Toll6 chimaera+DNT2CK	9 (3x in triplicate)	pDONR+DNT2CK vs kek3≡Toll6 chimaera+DNT2CK	0.001	0.084±0.008	d.f.=25 t=-7.642		<0.001	<0.001
		kek3≡Toll6 chimaera vs kek3≡Toll6 chimaera+DNT2CK	0.2		d.f.=16 t=-2.546		0.022	0.198
kek4≡Toll6 chimaera	9 (3x in triplicate)			0.039±0.002				
kek4≡Toll6 chimaera+DNT2CK	9 (3x in triplicate)	pDONR+DNT2CK vs kek4≡Toll6 chimaera+DNT2CK	0.006	0.060±0.007	d.f.=25 t=-4.442		<0.001	<0.001
		kek4≡Toll6 chimaera vs kek3≡Toll6 chimaera+DNT2CK	0.003		d.f.=16 t=-2.763		0.014	0.126

kek5≡Toll6 chimaera	9 (3x in triplicate)			0.028±0.002				
kek5≡Toll6 chimaera+DNT2CK	9 (3x in triplicate)	pDONR+DNT2CK vs kek5≡Toll6 chimaera+DNT2CK	0.118	0.042±0.006	d.f.=25 t=-1.741		0.094	0.47
		kek5≡Toll6 chimaera vs kek3≡Toll6 chimaera+DNT2CK	0.012		d.f.=16 t=-2.381		0.03	0.27
kek6≡Toll6 chimaera	9 (3x in triplicate)			0.063±0.010				
kek6≡Toll6 chimaera+DNT2CK	9 (3x in triplicate)	pDONR+DNT2CK vs kek6≡Toll6 chimaera+DNT2CK	0.004	0.100±0.014	d.f.=25 t=-6.481		<0.001	<0.001
		kek6≡Toll6 chimaera vs kek3≡Toll6 chimaera+DNT2CK	0.548		d.f.=16 t=-2.078		0.054	0.486

Drosomycin-luciferase: Dif reporter DNT2CK stimulation, Baculovirus

Genotype	Repeats	N/A	Levene's	Mean±s.e.m.	Welch ANOVA		t-test	Bonf.x9
pDONR	9 (3x in triplicate)	All together	0	0.0277±0.001	F=66.12 d.f.1=11 d.f.2=37.190	**<0.001**		
pDONR+DNT2CK	9 (3x in triplicate)			1.6265±0.085				
Toll6	9 (3x in triplicate)			0.0640±0.003				
Toll6+DNT2CK	9 (3x in triplicate)	pDONR+DNT2CK vs Toll6+DNT2CK	0.112	3.4821±0.154	d.f.=16 t=-10.582		<0.001	<0.001
kek3≡Toll6 chimaera	9 (3x in triplicate)			0.0568±0.003				
kek3≡Toll6 chimaera+DNT2CK	9 (3x in triplicate)	pDONR+DNT2CK vs kek3≡Toll6 chimaera+DNT2CK	0	4.4033±0.575	d.f.=16 t=-4.778		0.001	0.009
		kek3≡Toll6 chimaera vs kek3≡Toll6 chimaera+DNT2CK	0		d.f.=16 t=-7.560		<0.001	<0.001
kek4≡Toll6 chimaera	9 (3x in triplicate)			0.0420±0.002				
kek4≡Toll6 chimaera+DNT2CK	9 (3x in triplicate)	pDONR+DNT2CK vs kek4≡Toll6 chimaera+DNT2CK	0.024	3.3021±0.276	d.f.=16 t=-5.798		<0.001	<0.001
		kek4≡Toll6 chimaera vs kek4≡Toll6 chimaera+DNT2CK	0.001		d.f.=16 t=-11.779		<0.001	<0.001
kek5≡Toll6 chimaera	9 (3x in triplicate)			0.0265±0.001				
kek5≡Toll6 chimaera+DNT2CK	9 (3x in triplicate)	pDONR+DNT2CK vs kek5≡Toll6 chimaera+DNT2CK	0.003	2.5050±0.217	d.f.=16 t=-3.773		0.003	0.027
		kek5≡Toll6 chimaera vs kek5≡Toll6 chimaera+DNT2CK	0		d.f.=16 t=-11.429		<0.001	<0.001
kek6≡Toll6 chimaera	9 (3x in triplicate)			0.0622±0.004				
kek6≡Toll6 chimaera+DNT2CK	9 (3x in triplicate)	pDONR+DNT2CK vs kek6≡Toll6 chimaera+DNT2CK	0.011	4.0023±0.314	d.f.=16 t=-7.303		<0.001	<0.001
		kek6≡Toll6 chimaera vs kek6≡Toll6 chimaera+DNT2CK	0.001		d.f.=16 t=-12.543		<0.001	<0.001

Statistical tests, Chapter 5

GENOTYPE	n	COMPARISON	NORMALITY	H. OF VAR.	DESCRIPTIVE STATISTICS	DF & TEST VALUE	P	MULTIPLE COMPARISONS & CORRECTIONS	
			Survival index						
Genotype	**Pupae**		**N/A**	**N/A**	**categorical data**	χ^2	**P**	χ^2	**Bonf.x21**
DNT1[41]/TM6B	446	All together				X=711.616 d.f.=18	**<0.001**		
DNT2[e03444]/TM6B	657								
DNT2[e03444]DNT1[41]/TM6B	494								
kek3[12];+/SM6aTM6B	41								
kek3[12];+/SM6aTM6B x kek3[26];+/SM6aTM6B	113								
kek3[12];DNT1[55]/TM6B	232	*kek3[12];DNT1[55]/TM6B* vs *kek3[12];+/SM6aTM6B*				X=26.234 d.f.=1		<0.001	<0.001
		kek3[12];DNT1[55]/TM6B vs *DNT1[41]/TM6B*				X=53.847 d.f.=1		<0.001	<0.001
kek3[26];Df(3L)Exel6101/TM6B x kek3[12];DNT1[55]/TM6B	290	*kek3[26];Df(3L)Exel6101/TM6B x kek3[12];DNT1[55]/TM6B* vs *kek3[12];+/SM6aTM6B x kek3[26];+/SM6aTM6B*				X=19.503 d.f.=1		<0.001	<0.001
		kek3[26];Df(3L)Exel6101/TM6B x kek3[12];DNT1[55]/TM6B vs *DNT1[41]/TM6B*				X=21.643 d.f.=1		<0.001	<0.001
kek3[12];DNT2[e03444]/TM6B	442	*kek3[12];DNT2[e03444]/TM6B* vs *kek3[12];+/SM6aTM6B*				X=87.696 d.f.=1		<0.001	<0.001
		kek3[12];DNT2[e03444]/TM6B vs *DNT2[e03444]/TM6B*				X=65.151 d.f.=1		<0.001	<0.001
kek3[12];DNT2[e03444]/TM6B x kek3[26];Df(3L)6092/TM6B	85	*kek3[12];DNT2[e03444]/TM6B x kek3[26];Df(3L)6092/TM6B* vs *kek3[12];+/SM6aTM6B x kek3[26];+/SM6aTM6B*				X=19.489 d.f.=1		<0.001	<0.001
		kek3[12];DNT2[e03444]/TM6B x kek3[26];Df(3L)6092/TM6B vs *DNT2[e03444]/TM6B*				X=6.953 d.f.=1		0.008	0.168
kek4[20];+/SM6aTM6B	77								
kek4[20];+/SM6aTM6B x kek4[23];+/SM6aTM6B	122								
kek4[20];DNT1[55]/TM6B	120	*kek4[20];DNT1[55]/TM6B* vs *kek4[20];+/SM6aTM6B*				X=23.109 d.f.=1		<0.001	<0.001
		kek4[20];DNT1[55]/TM6B vs *DNT1[41]/TM6B*				X=20.622 d.f.=1		<0.001	<0.001
kek4[20];DNT1[55]/TM6B x kek4[23];Df(3L)Exel6101/TM6B	433	*kek4[20];DNT1[55]/TM6B x kek4[23];Df(3L)Exel6101/TM6B* vs *kek4[20];+/SM6aTM6B x kek4[23];+/SM6aTM6B*				X=17.904 d.f.=1		<0.001	<0.001
		kek4[20];DNT1[55]/TM6B x kek4[23];Df(3L)Exel6101/TM6B vs *DNT1[41]/TM6B*				X=13.518 d.f.=1		<0.001	<0.001

kek4[20];DNT2[e03444]/TM6B	333	*kek4[20];DNT2[e03444]/TM6B* vs *kek4[20];+/SM6aTM6B*	X=27.660 d.f.=1	<0.001	<0.001
		kek4[20];DNT2[e03444]/TM6B vs *DNT2[e03444]/TM6B*	X=6.318 d.f.=1	0.012	0.252
kek4[20];DNT2[e03444]/TM6B x kek4[23];Df(3L)6092/TM6B	253	*kek4[20];DNT2[e03444]/TM6B x kek4[23];Df(3L)6092/TM6B* vs *kek4[20];+/SM6aTM6B x kek4[23];+/SM6aTM6B*	X=0.486 d.f.=1	0.486	10.206
		kek4[20];DNT2[e03444]/TM6B x kek4[23];Df(3L)6092/TM6B vs *DNT2[e03444]/TM6B*	X=22.738 d.f.=1	<0.001	<0.001
kek6[34]/TM6B x Df(3R)ED6361/TM6BlacZ	479				
kek6[34]Df(3L)ED4342/TM6B x DNT1[41]Df(3R)ED6361/TM6B	169	*kek6[34]Df(3L)ED4342/TM6B x DNT1[41]Df(3R)ED6361/TM6B* vs *kek6[34]/TM6B x Df(3R)ED6361/TM6BlacZ*	X=1.508 d.f.=1	0.219	
		kek6[34]Df(3L)ED4342/TM6B x DNT1[41]Df(3R)ED6361/TM6B vs *DNT1[41]/TM6B*	X=15.774 d.f.=1	<0.001	<0.001
Df(3R)ED6361DNT2[e03444]/TM6B x kek6[34]Df(3L)6092/TM6B	78	*Df(3R)ED6361DNT2[e03444]/TM6B x kek6[34]Df(3L)6092/TM6B* vs *kek6[34]/TM6B x Df(3R)ED6361/TM6BlacZ*	X=14.964 d.f.=1	<0.001	<0.001
		Df(3R)ED6361DNT2[e03444]/TM6B x kek6[34]Df(3L)6092/TM6B vs *DNT2[e03444]/TM6B*	X= 3.844 d.f.=1	0.05	1.05
kek6[34]Df(3L)ED4342/TM6B x Tie[5]Df(3R)ED6361/TM6B	236	*kek6[34]Df(3L)ED4342/TM6B x Tie[5]Df(3R)ED6361/TM6B* vs *kek6[34]/TM6B x Df(3R)ED6361/TM6BlacZ*	X=17.502 d.f.=1	<0.001	<0.001

Survival index

Genotype	Pupae	N/A	N/A	categorical data	χ^2	P	χ^2	Bonf.x4
kek6[34]/TM6B x kek6[35]/TM6B	*435*	All together			X=218.327 d.f.=7	**<0.001**		
kek6[34]elavGal4/TM6BlacZ	*148*							
kek6[34]24BGal4	*401*							
UASDNT1CK3'+;kek6[35]/TM6BlacZ	208							
kek6[34]elavGal4/TM6BlacZ x UASDNT1CK3'+;kek6[35]/TM6BlacZ	251	*kek6[34]elavGal4/TM6BlacZ x UASDNT1CK3'+;kek6[35]/TM6BlacZ* vs *kek6[34]/TM6B x kek6[35]/TM6B*			X=53.105 d.f.=1		<0.001	<0.001
kek6[34]24BGal4/TM6BlacZ x UASDNT1CK3'+;kek6[35]/TM6BlacZ	97	*kek6[34]24BGal4/TM6BlacZ x UASDNT1CK3'+;kek6[35]/TM6BlacZ* vs *kek6[34]/TM6B x kek6[35]/TM6B*			X=0.075 d.f.=1		0.784	3.136
kek6[34]elavGal4/TM6B x UASActRho;kek6[35]/TM6B	188	*kek6[34]elavGal4/TM6BlacZ x UASActRho;kek6[35]/TM6BlacZ* vs *kek6[34]/TM6B x kek6[35]/TM6B*			X=8.792 d.f.=1		0.003	0.012

kek6[34]elavGal4/TM6B x UASActcdc42;kek6[35]/TM6B	162	*kek6[34]elavGal4/TM6BlacZ x UASActCdc42;kek6[35]/TM6BlacZ* vs *kek6[34]/TM6B x kek6[35]/TM6B*						X=16.238 d.f.=1		<0.001	<0.001

Survival index

Genotype	Pupae		N/A		N/A	categorical data		χ^2	P	χ^2	
kek6[34]elavGal4/TM6BlacZ	148	All together						X=35.368 d.f.=2	**<0.001**		
UASkek6RFP;kek6[35]/SM6aTM6B	110										
kek6[34]elavGal4/TM6B x UASkek6RFP;kek6[35]/SM6aTM6B	245	*kek6[34]elavGal4/TM6BlacZ* vs *kek6[34]elavGal4/TM6B x UASkek6RFP;kek6[35]/SM6aTM6B*						X=19.822 d.f.=1		<0.001	

Adult locomotion: speed

Genotype	Frames		Distribution not normal		N/A	Histogram	Kruskal-Wallis		Dunn	
yw	8230	All together					d.f.=2, Kruskal-Wallis:3859.663	**<0.001**		
kek3[12]	6587	*yw* vs *kek3[12]*					Dunn's: 4472		<0.001	
kek4[20]	1988	*yw* vs *kek4[20]*					Dunn's: 5162		<0.001	

Adult locomotion: Distance

Genotype	Flies		Kurt.	Skew.	Levene's	Mean±s.e.m.	One-Way ANOVA		Dunnett	
yw	22	All together	-0.112	-0.672	**0.369**	3742.13±217.1	F=33.549 d.f.1=2 d.f.2=41	**<0.001**		
kek3[12]	17	*yw* vs *kek3[12]*	-0.133	0.858	0.747	1374.32±263.5	Mean difference: 2367.81		Sig to 0.05 level	
kek4[20]	5	*yw* vs *kek4[20]*	0.025	1.023	0.21	862.53±267.6	Mean difference: 2879.60		Sig to 0.05 level	

Adult locomotion: Resting

Genotype	Frames		N/A	N/A	Categorical data	χ^2		χ^2	Bonf.x2
yw	8272	All together				X=2786.335 d.f.=2	**<0.001**		
kek3[12]	6615	*yw* vs *kek3[12]*				X=2245.728 d.f.=1		<0.001	<0.001
kek4[20]	1994	*yw* vs *kek4[20]*				X=1783.997 d.f.=1		<0.001	<0.001

Adult locomotion: wobbling

Genotype	Frames		N/A	N/A	Categorical data	χ^2		χ^2	Bonf.x2
yw	8272	All together				X=407.725 d.f.=2	**<0.001**		
kek3[12]	6615	*yw* vs *kek3[12]*				X=174.537 d.f.=1		<0.001	<0.001
kek4[20]	1994	*yw* vs *kek4[20]*				X=417.102 d.f.=1		<0.001	<0.001

Statistical tests, Chapter 6

GENOTYPE	n	COMPARISON	NORMALITY	H. OF VAR.	DESCRIPTIVE STATISTICS	DF & TEST VALUE	P	MULTIPLE COMPARISONS & CORRECTION	
Axon guidance									
Genotype	**HS**		**N/A**	**N/A**	**Categorical data**	χ^2		χ^2	**Bonf.x10**
yw	382	All together				X=158.843 d.f.=12	**<0.001**		
elavGal4>UASkek6RFP	328	*yw x elavGal4>UASkek6RFP*				X=66.125 d.f.=1		<0.001	<0.001
kek6[34]/Df(3R)ED6361	407	*yw x kek6[34]/Df(3R)ED6361*				X=14.987 d.f.=1		<0.001	<0.001
kek6[34/Df(3R)ED6361] elavGal4>UASkek6RFP	212	*yw x kek6[34/Df(3R)ED6361]elavGal4>UASkek6RFP*				X=0.025 d.f.=1		0.875	8.75
24BGal4>UASDNT1CK3'+	191								
kek6[34/35]24BGal4>UASDNT1CK3'+	205	*24BGal4>UASDNT1CK3'+* vs *kek6[34/35]24BGal4>UASDNT1CK3'+*				X=30.770 d.f.=1		<0.001	<0.001
DNT2[e03444]DNT1[41]	152								
DNT2[e03444]DNT1[41] elavGal4>UASkek6RFP	199	*DNT2[e03444]DNT1[41]* vs *DNT2[e03444]DNT1[41]elavGal4>UASkek6RFP*				X=2.226 d.f.=1		0.136	1.36
elavGal4>UASDNRas;UASkek6RFP	225	*elavGal4>UASkek6RFP* vs *elavGal4>UASDNRas;UASkek6RFP*				X=38.308 d.f.=1		<0.001	<0.001
elavGal4>UASDNdRac;UASkek6RFP	176	*elavGal4>UASkek6RFP* vs *elavGal4>UASDNdRac;UASkek6RFP*				X=8.224 d.f.=1		0.004	0.1408
elavGal4>UASkek6RFP; UASMycAFGDP110	136	*elavGal4>UASkek6RFP* vs *elavGal4>UASkek6RFP;UASMycAFGDP110*				X=23.998 d.f.=1		<0.001	<0.001
elavGal4>UAScdc42[N17]; UASkek6RFP	74	*elavGal4>UASkek6RFP* vs *elavGal4>UAScdc42[N17];UASkek6RFP*				X=0.002 d.f.=1		0.962	9.62
elavGal4>UASkek6RFP;UASDNRho	188	*elavGal4>UASkek6RFP* vs *elavGal4>UASkek6RFP;UASDNRho*				X=5.138 d.f.=1		0.023	0.23
Axon guidance									
Genotype	**HS**		**N/A**	**N/A**	**Categorical data**	χ^2		χ^2	**Bonf.x2**
yw	382					X=5.064 d.f.=1	**0.079**		
RA5/RM2	153	*yw* vs *RA5/RM2*				X=0.012 d.f.=1		0.914	1.828
elavGal4>UASkek1RFP	120	*yw* vs *elavGal4>UASkek1RFP*				X=4.916 d.f.=1		0.027	0.054
Larval locomotion: speed									
Genotype	**Frames**		**Distribution not normal**		**Histogram**	**Kruskal-Wallis**		**Dunn**	
yw	19837	All together				d.f.=5, Kruskal-Wallis:1414.429	**<0.001**		
yw/OregonR	19497								
elavGal4	19950								

kek6[34]/Df(3R)ED6361	19562	*elavGal4* vs *kek6[34]/Df(3R)ED6361*		Dunn's: -9244	<0.001
elavGal4>UASkek6RFP	19687	*elavGal4* vs *elavGal4>UASkek6RFP*		Dunn's: -7215	<0.001
kek6[34]elavGal4>UASkek6RFP Df(3R)ED6361	9491	*elavGal4* vs *kek6[34]elavGal4>UASkek6RFP Df(3R)ED6361*		Dunn's: -4046	<0.001
		kek6[34]/Df(3R)ED6361 vs *kek6[34]elavGal4>UASkek6RFP Df(3R)ED6361*		Dunn's: 5199	<0.001

Larval locomotion: Speed

Genotype	Frames	Distribution not normal	Histogram	Kruskal-Wallis	P	Dunn
elavGal4	9975	All together		d.f.=8, Kruskal-Wallis:3090.657	**<0.001**	
kek6[34]/Df(3R)ED6361	9826					
kek6[34]DfED4342 /Df(3R)ED6361DNT1[55]	8743	*elavGal4* vs *kek6[34]DfED4342/Df(3R)ED6361DNT1[55]*		Dunn's: -10037		<0.001
kek6[34]Df6092/ Df(3R)ED6361DNT2[e03444]	9975	*elavGal4* vs *kek6[34]Df6092/Df(3R)ED6361DNT2[e03444]*		Dunn's: 1038		<0.05
kek6[34]DfED4342 /Df(3R)ED6361Tie[5]	9928	*elavGal4* vs *kek6[34]DfED4342/Df(3R)ED6361Tie[5]*		Dunn's: -9898		<0.001
		kek6[34]/Df(3R)ED6361 vs *kek6[34]DfED4342/Df(3R)ED6361DNT1[55]*		Dunn's: -2742		<0.001
		kek6[34]/Df(3R)ED6361 vs *kek6[34]Df6092/Df(3R)ED6361DNT2[e03444]*		Dunn's: 8332		<0.001
		kek6[34]/Df(3R)ED6361 vs *kek6[34]DfED4342/Df(3R)ED6361Tie[5]*		Dunn's: -2604		<0.001
elavGal4>UASkek6RFP	9917					
elavGal4>UASkek6RFP; UASMycAFGDP110	9975	*elavGal4* vs *elavGal4>UASkek6RFP;UASMycAFGDP110*		Dunn's: -5673		<0.001
elavGal4>UASDNRas;UASkek6RFP	9880	*elavGal4* vs *elavGal4>UASDNRas;UASkek6RFP*		Dunn's: 2148		<0.001
elavGal4>UASkek6RFP UASDNRho	9902	*elavGal4* vs *elavGal4>UASkek6RFP;UASDNRho*		Dunn's: -10998		<0.001
		elavGal4>UASkek6RFP vs *elavGal4>UASkek6RFP;UASMycAFGDP110*		Dunn's: 389.5		ns
		elavGal4>UASkek6RFP vs *elavGal4>UASDNRas;UASkek6RFP*		Dunn's: 8210		<0.001
		elavGal4>UASkek6RFP vs *elavGal4>UASkek6RFP;UASDNRho*		Dunn's: -4936		<0.001

Larval locomotion: Distance

Genotype	Larvae		Kurt.	Skew.	Levene's	Mean±s.e.m.	Welch ANOVA		t-test	Bonf.x3
elavGal4	25	All together	0.009	0.783	0	1.75±0.12	F=7.054 d.f.1=8 d.f.2=88.542	**<0.001**		
kek6[34]/Df(3R)ED6361	25		-1.525	0.367		2.47±0.21				
kek6[34]DfED4342 /Df(3R)ED6361DNT1[55]	22	*kek6[34]/Df(3R)ED6361* vs *kek6[34]DfED4342/Df(3R)ED6361DNT1[55]*	-0.608	0.218		2.45±0.11	d.f.=45 t=0.078		0.938	2.814
kek6[34]Df6092 /Df(3R)ED6361DNT2[e03444]	25	*kek6[34]/Df(3R)ED6361* vs *kek6[34]Df6092/Df(3R)ED6361DNT2[e03444]*	0.64	1.152		1.78±0.19	d.f.=48 t=2.471		0.017	0.051

kek6[34]DfED4342 /Df(3R)ED6361Tie[5]	25	*kek6[34]/Df(3R)ED6361* vs *kek6[34]DfED4342/Df(3R)ED6361Tie[5]*	-0.547	0.133	2.61±0.13	d.f.=48 t=-0.597	0.553	1.659
elavGal4>UASkek6RFP	25		1.083	0.879	2.21±0.18			
elavGal4>UASkek6RFP; UASMycAFGDP110	25	*elavGal4>UASkek6RFP* vs *elavGal4>UASkek6RFP;UASMycAFGDP110*	0.166	0.187	2.13±0.15	d.f.=48 t=0.309	0.309	0.927
elavGal4>UASDNRas;UASkek6RFP	25	*elavGal4>UASkek6RFP* vs *elavGal4>UASDNRas;UASkek6RFP*	-1.118	-0.031	2.55±0.16	d.f.=48 t=3.129	0.003	0.009
elavGal4>UASkek6RFP UASDNRho	25	*elavGal4>UASkek6RFP* vs *elavGal4>UASkek6RFP UASDNRho*	-0.205	0.737	1.54±0.11	d.f.=48 t=-1.445	0.155	0.465

Statistical tests, Chapter 7

GENOTYPE OR EXPERIMENT	n	COMPARISON	NORMALITY	H. OF VAR.	DESCRIPTIVE STATISTICS	DF & TEST VALUE	P	MULTIPLE COMPARISONS & CORRECTION	
Larval developmental timing – Onset of wandering L3									
Genotype		**Larvae**	**N/A**	**N/A**	**Categorical data**	**χ^2**		**χ^2**	**Bonf.x2**
yw	150	All together				X=317.733 d.f.=81	**<0.001**		
spz6Gal4	150								
spz6Gal4>UASkek4	150	*spz6Gal4 vs spz6Gal4>UASkek4*				X=109.561 d.f=27		<0.001	<0.001
kek4[20/23]	150	*spz6Gal4 vs kek4[20/23]*				X=44.127 d.f.=25		0.01	0.02
Larval developmental timing – Brown pupae									
Genotype		**Larvae**	**N/A**	**N/A**	**Categorical data**	**χ^2**		**χ^2**	**Bonf.x2**
yw	150	All together				X=296.644 d.f.=69	**<0.001**		
spz6Gal4	150								
spz6Gal4>UASkek4	150	*spz6Gal4 vs spz6Gal4>UASkek4*				X=90.701 d.f=23		<0.001	<0.001
kek4[20/23]	150	*spz6Gal4 vs kek4[20/23]*				X=36.551 d.f.=22		0.026	0.052
Larval developmental timing – Eclosed adults									
Genotype		**Larvae**	**N/A**	**N/A**	**Categorical data**	**χ^2**		**χ^2**	**Bonf.x2**
yw	150	All together				X=162.005 d.f.=21	**<0.001**		
spz6Gal4	150								
spz6Gal4>UASkek4	150	*spz6Gal4 vs spz6Gal4>UASkek4*				X=124.648 d.f=7		<0.001	<0.001
kek4[20/23]	150	*spz6Gal4 vs kek4[20/23]*				X=71.438 d.f.=7		<0.001	<0.001
Larval volume									
Genotype		**Larvae**	**Kurt.**	**Skew.**	**Levene's**	**Mean±SD**	**Welch ANOVA**		
yw	10	All together	0.267	-0.887	0.312	5851±428	F=1.252 d.f.1=2 d.f.2=17.588	**0.224**	
spz6Gal4>UASkek4	10		-0.987	0.084		5752±624			
kek4[20/23]	10		-1.81	0.075		5506±424			
Pupal volume									
Genotype		**Pupae**	**Kurt.**	**Skew.**	**Levene's**	**Mean±SD**	**Welch ANOVA**		**Games-Howell**
yw	87	All together	0.032	-0.001	0.02	0.205±0.027	F=5.465 d.f.1=2 d.f.2=133.092	**0.012**	

spz6Gal4>UASkek4	66	*yw vs spz6Gal4>UASkek4*	-0.617	0.206		0.219±0.032	d.f.=151 t=-2.852	0.017
kek4[20/23]	61	*yw vs kek4[20/23]*	-0.17	-0.261		0.205±0.024	d.f.=146 t=0	1

Pupal length

Genotype	Pupae		Kurt.	Skew.	Levene's	Mean±SD	Welch ANOVA		Games-Howell
yw	100	All together	1.127	-0.6	0	0.84±0.05	F=4.161 d.f.1=2 d.f.2=193.592	**0.033**	
spz6Gal4>UASkek4	100	*yw vs spz6Gal4>UASkek4*	-0.1	-0.528		0.82±0.07	d.f.=198 t=1.868		0.151
kek4[20/23]	100	*yw vs kek4[20/23]*	-0.154	-0.029		0.85±0.05	d.f.=198 t=-0.941		0.615

Adult body size

Genotype	Adults		Kurt.	Skew.	Levene's	Mean±SD	Welch ANOVA		Games-Howell
yw	10	All together	-0.713	0.527	P=0.008	0.144±0.01	F=3.821 d.f.1=2 d.f.2=16.795	**0.044**	
spz6Gal4>UASkek4	10	*yw vs spz6Gal4>UASkek4*	-0.631	-0.477		0.133±0.025	d.f.=18 t=1.247		0.45
kek4[20/23]	10	*yw vs kek4[20/23]*	1.726	1.377		0.154±0.012	d.f.=18 t=-2.113		0.116

Wing hair count

Genotype	Adults		Kurt.	Skew.	Levene's	Mean±SD	Welch ANOVA		Games-Howell
yw	10	All together	-0.087	-0.806	P=0.517	126.3±7.2	F=18.702 d.f.1=2 d.f.2=15.882	**<0.001**	
spz6Gal4>UASkek4	10	*yw vs spz6Gal4>UASkek4*	-1.021	-0.573		122.6±5.9	d.f.=17 t=1.225		0.448
kek4[20/23]	10	*yw vs kek4[20/23]*	2.522	-1.65		144.2±10.5	d.f.=17 t=-4.381		0.002

Larval locomotion - speed

Genotype	Frames		Distribution not normal	Histogram	Kruskal-Wallis		Dunn
elavGal4	19950	All together			d.f.=2, Kruskal-Wallis:3459.228	**<0.001**	
kek4[20/23]	19746	*elavGal4 vs kek4[20/23]*			Dunn's: -3424		<0.001
elavGal4>UASkek4RFP	13463	*elavGal4 vs elavGal4>UASkek4*			Dunn's: 6475		<0.001

Larval locomotion - distance

Genotype	Frames		Kurt.	Skew.	Levene's	Mean±s.e.m.	Welch ANOVA		Games-Howell
elavGal4	25	All together	-0.834	-0.013	0.183	2.16±0.09	F=49.329 d.f.1=2 d.f.2=86.267	**<0.001**	
kek4[20/23]	24	*elavGal4 vs kek4[20/23]*	-0.395	-0.145		2.74±0.10	d.f.=47 t=-4.506		<0.001
elavGal4>UASkek4RFP	15	*elavGal4 vs elavGal4>UASkek4*	-0.048	0.784		1.36±0.08	d.f.=38 t=3.183		<0.001

APPENDIX II

CLONING MAPS, SUPPORTING GELS AND SEQUENCING DATA

Cloning of *kek1-kek6* into *pDONR*^{221}

For each construct: **a** | Plasmid maps of cloned constructs. Enzyme sites for restriction digest verification and primer sites for initial sequence amplification are shown. **b** | Amplified PCR fragment. Primers and source DNA are also shown. **c** | Restriction digest verification of cloned plasmids.

Cloning of *kek1-6* into *pAct-attR-mCFP (pAWC), pAct-attR-FLAG (pAWF), pUASt-attR-mRFP (pTWR)*

pDONR+kek1-6 entry clones were recombined into *pAct-attR-FLAG* destination vector by Gateway cloning. For each construct: **a** | Plasmid map of cloned construct. Enzyme sites for restriction digest verification are shown. **b** | Cloned constructs were verified by restriction digest of maxiprep DNA/*pAWC+kek1* only: cloned constructs were initially detected by PCR of transformed colonies - cloning was tested by amplification of the *kek1* CDS into the actin promoter region. **c** | Cloning was verified by PCR amplification of the gene CDS into the UAS element (*pTWR* constructs only).

Cloning of *kek1* into *pDONR*^{221}

a

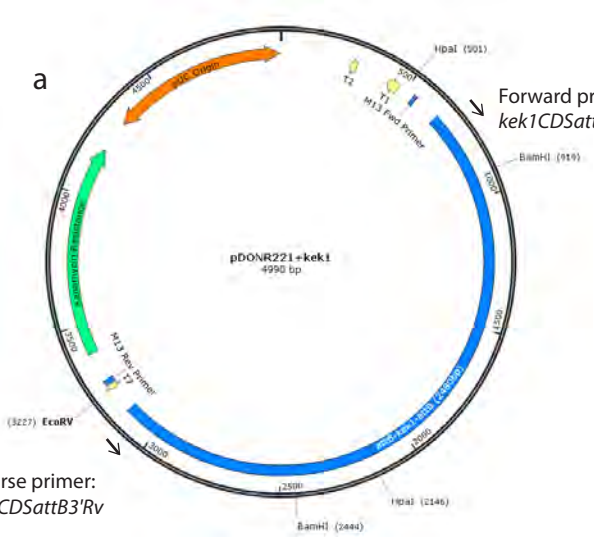

Forward primer:
kek1CDSattB5'Fw

Reverse primer:
kek1CDSattB3'Rv

b

kek1 CDS PCR

SD01674 clone

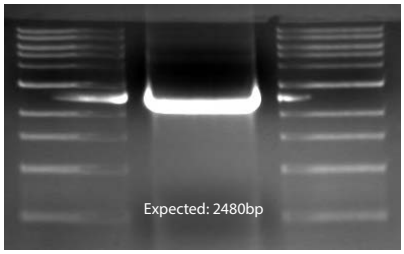

c

pDONR+kek1 Maxiprep digests

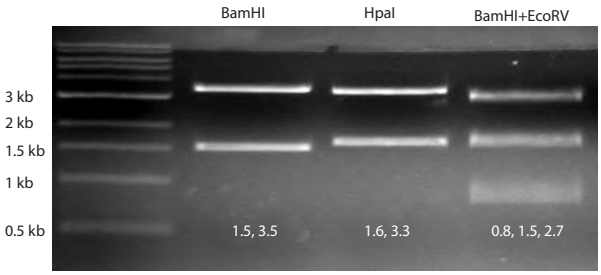

Cloning of *kek2* into *pDONR*^{221}

a

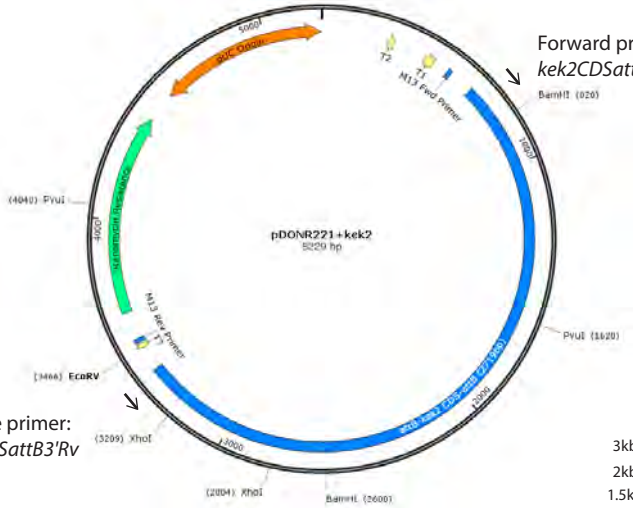

Forward primer:
kek2CDSattB5'Fw

Reverse primer:
kek2CDSattB3'Rv

b

kek2 CDS PCR

NB7 cDNA

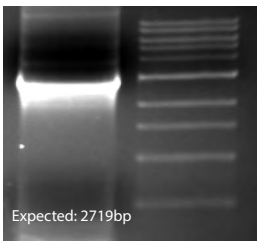

c

pDONR+kek2 Maxiprep digests

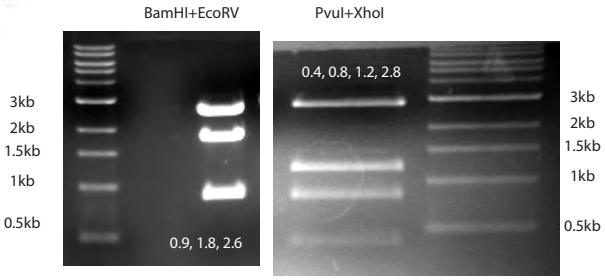

Cloning of *kek3* into *pDONR*^{221}

a

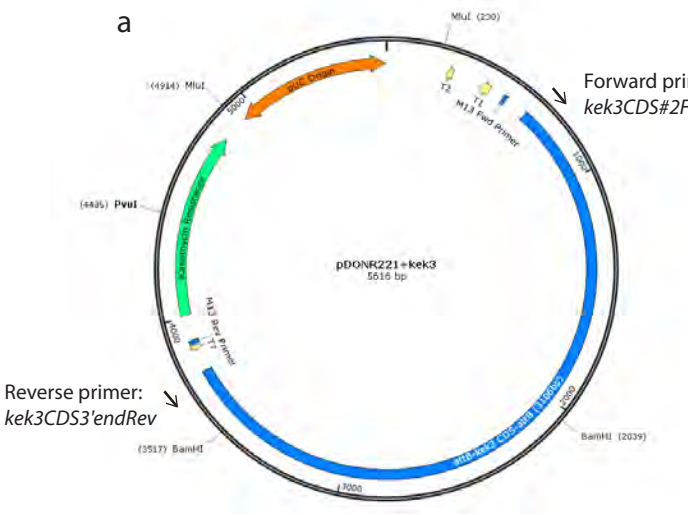

Forward primer:
kek3CDS#2Fwd

Reverse primer:
kek3CDS3'endRev

b

kek3 CDS PCR
GH cDNA library

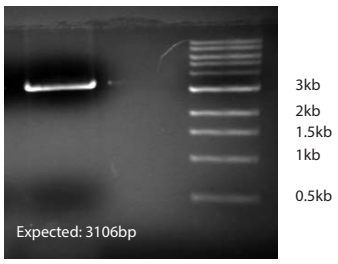

c

pDONR+kek3 Maxiprep digests

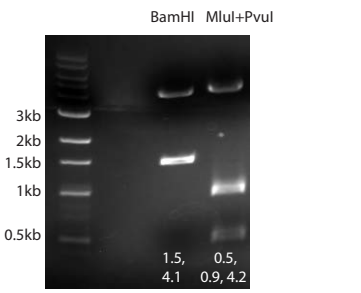

Cloning of *kek4* into *pDONR*^{221}

a

b

kek4 CDS PCR
RT-PCR from larvae/pupae

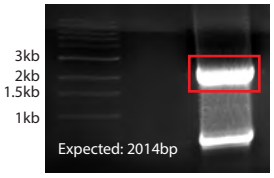

c

pDONR+kek4 Maxiprep digests

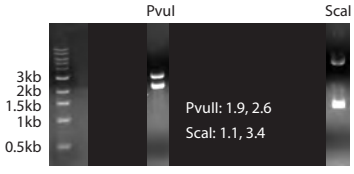

Cloning of *kek5* into *pDONR*^{221}

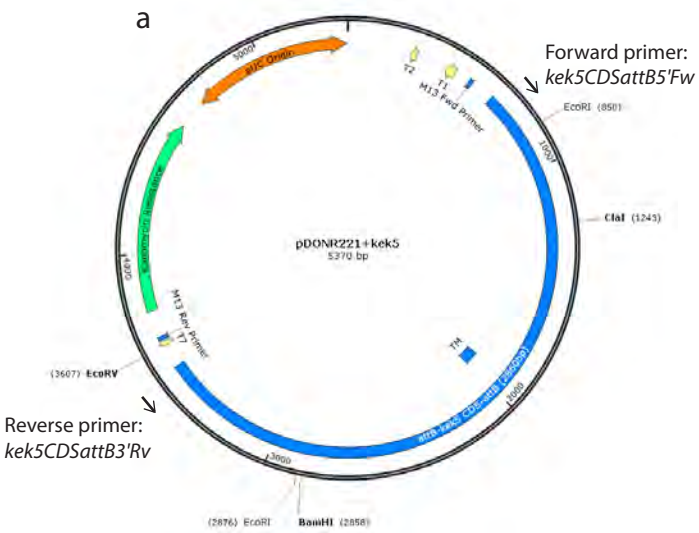

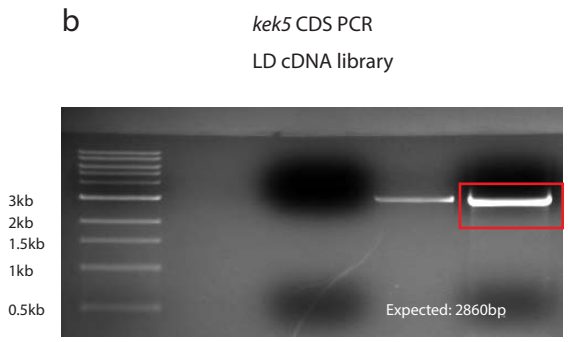

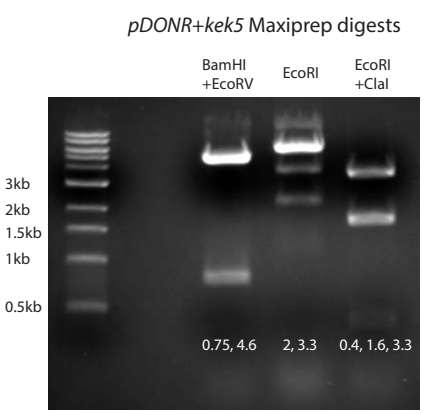

Cloning of *kek6* into *pDONR*^{221}

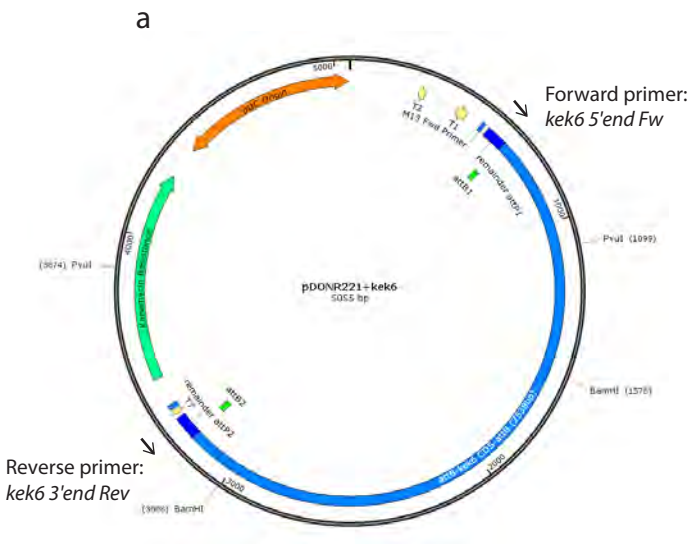

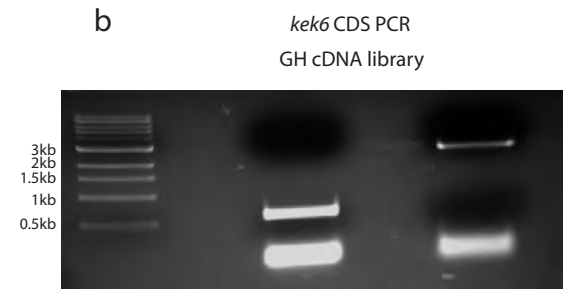

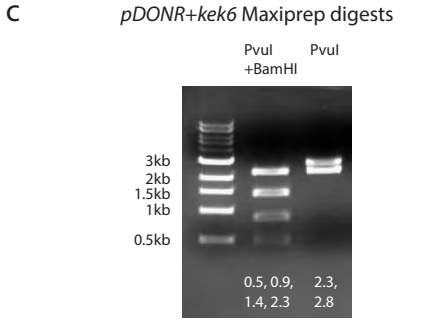

Cloning of *kek1* into *pAct-attR-mCFP*

a

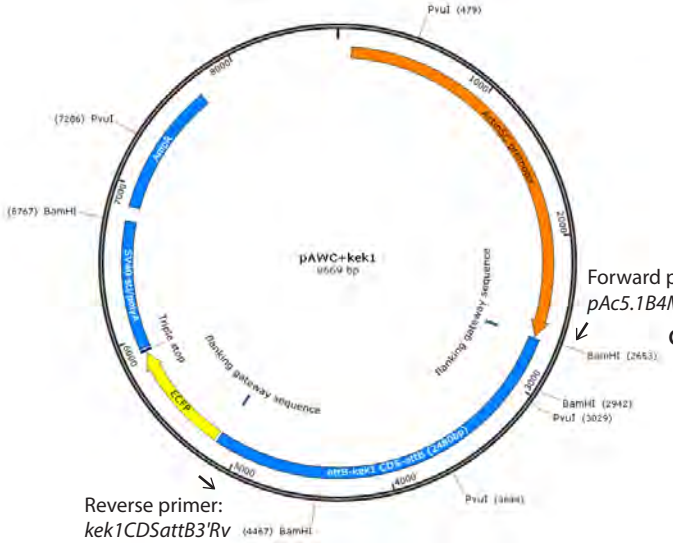

b *pAWC+kek1* colony PCR

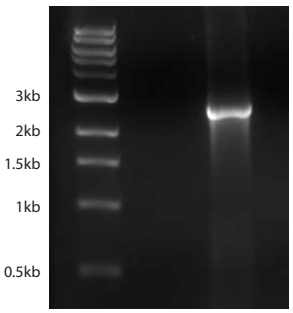

Expected: 2574nt

c *pAWC+kek1* Maxiprep digests

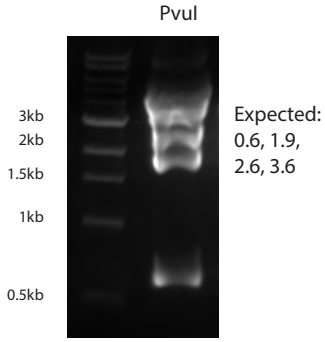

Cloning of *kek2* into *pAct-attR-mCFP*

a

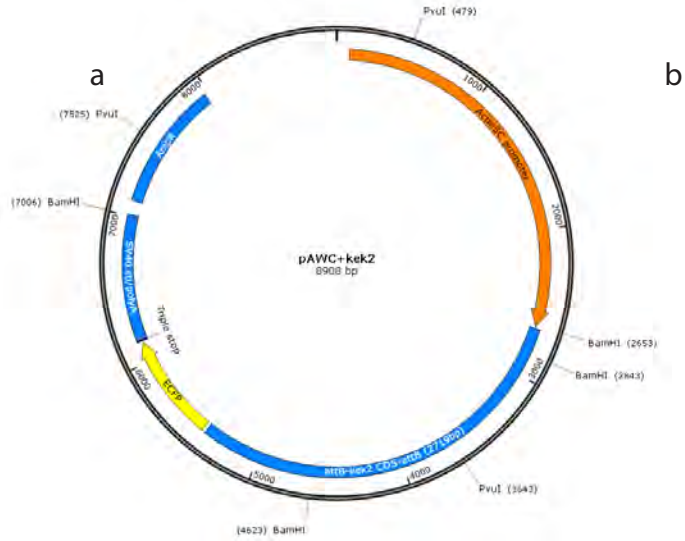

b *pAWC+kek2* Maxiprep digests

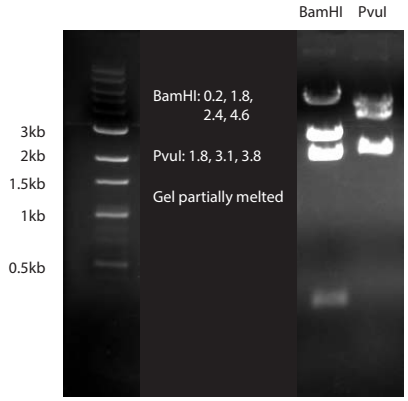

Cloning of *kek3* into *pAct-attR-mCFP*

a

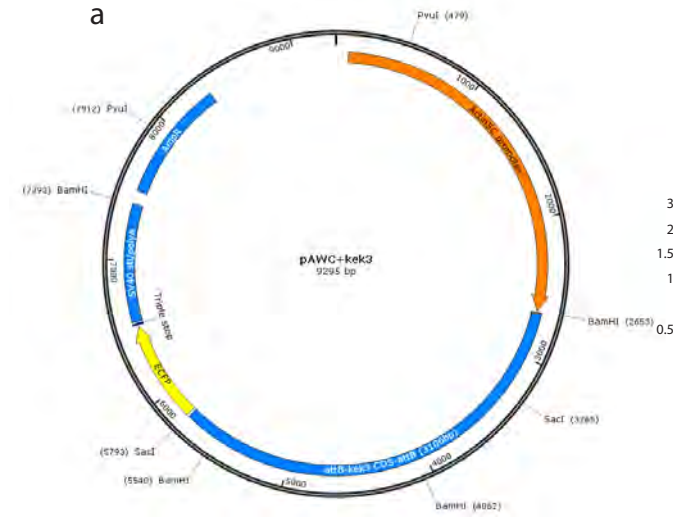

b *pAWC+kek3* Maxiprep digests

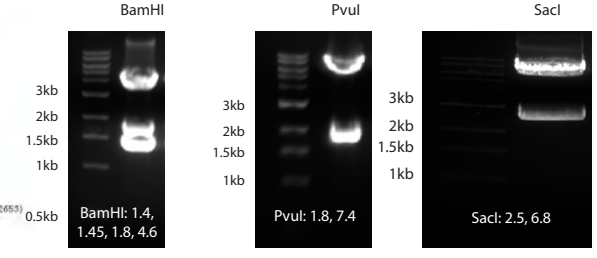

Cloning of *kek4* into *pAct-attR-mCFP*

a

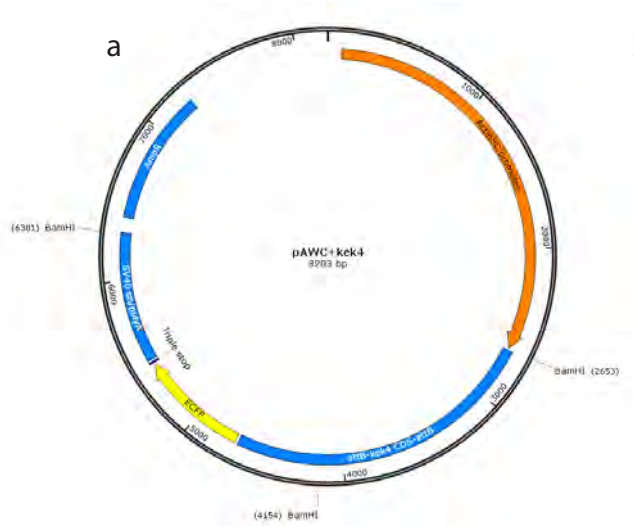

b *pAWC+kek4* Maxiprep digest

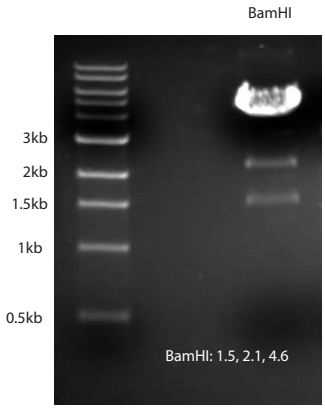

Cloning of *kek5* into *pAct-attR-mCFP*

a

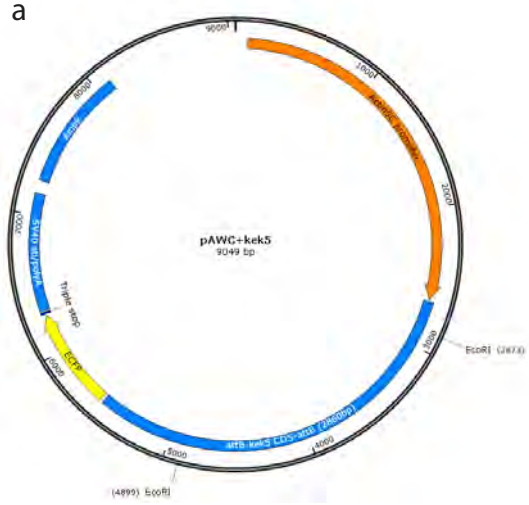

b *pAWC+kek5* Maxiprep digests

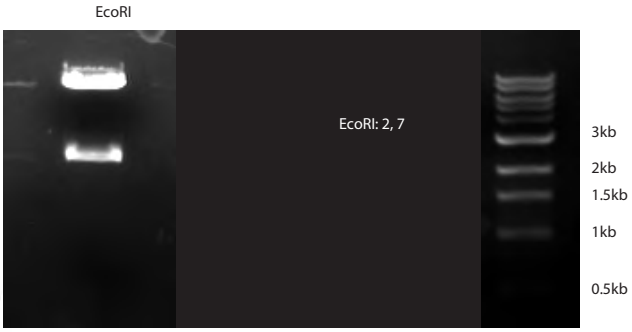

Cloning of *kek6* into *pAct-attR-mCFP*

a

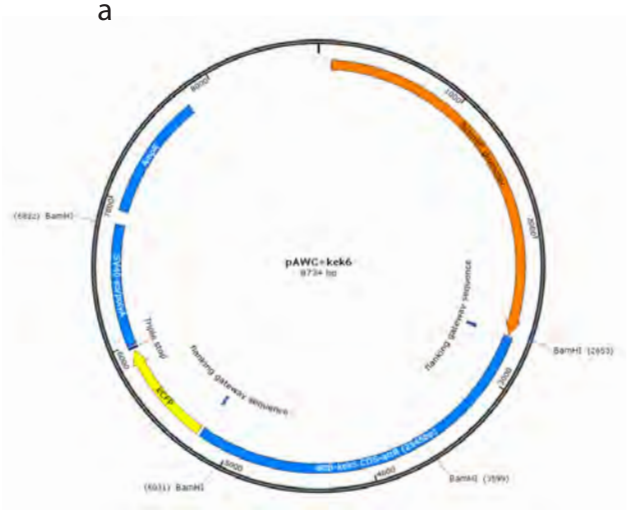

b *pAWC+kek6* Maxiprep digests

Sequencing of *kek1+pAWC*

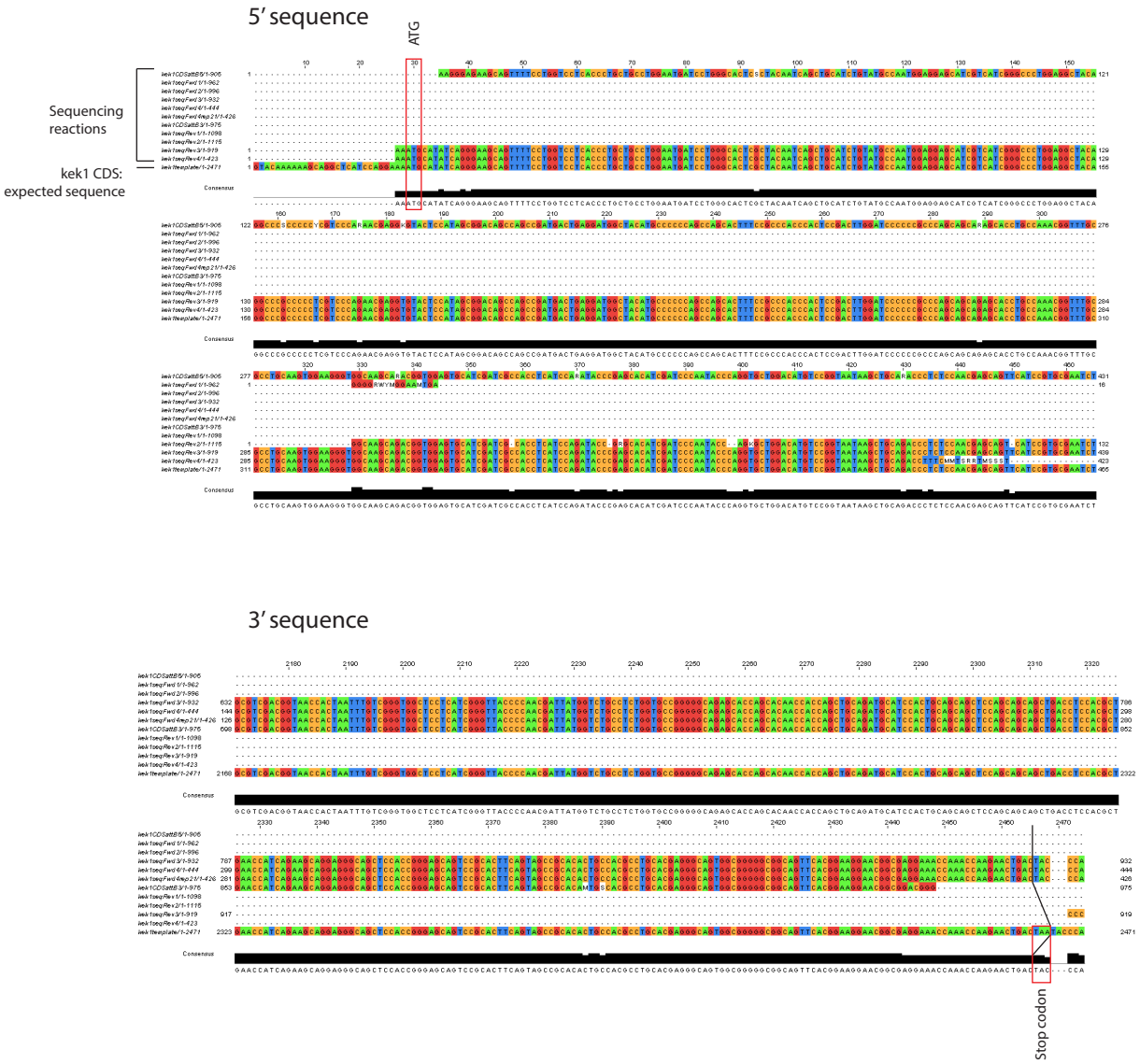

Maxiprepped *pAct-kek1-mCFP* (*kek1+pAWC*) DNA was verified by sequencing. 5′ and 3′ fragment ends are shown only. No point mutations or substitutions were detected in the entire *kek1* CDS. The STOP codon was successfully removed to allow the use of C-terminal Gateway tags.

Sequencing of *kek2+pAWC*

5′ sequence

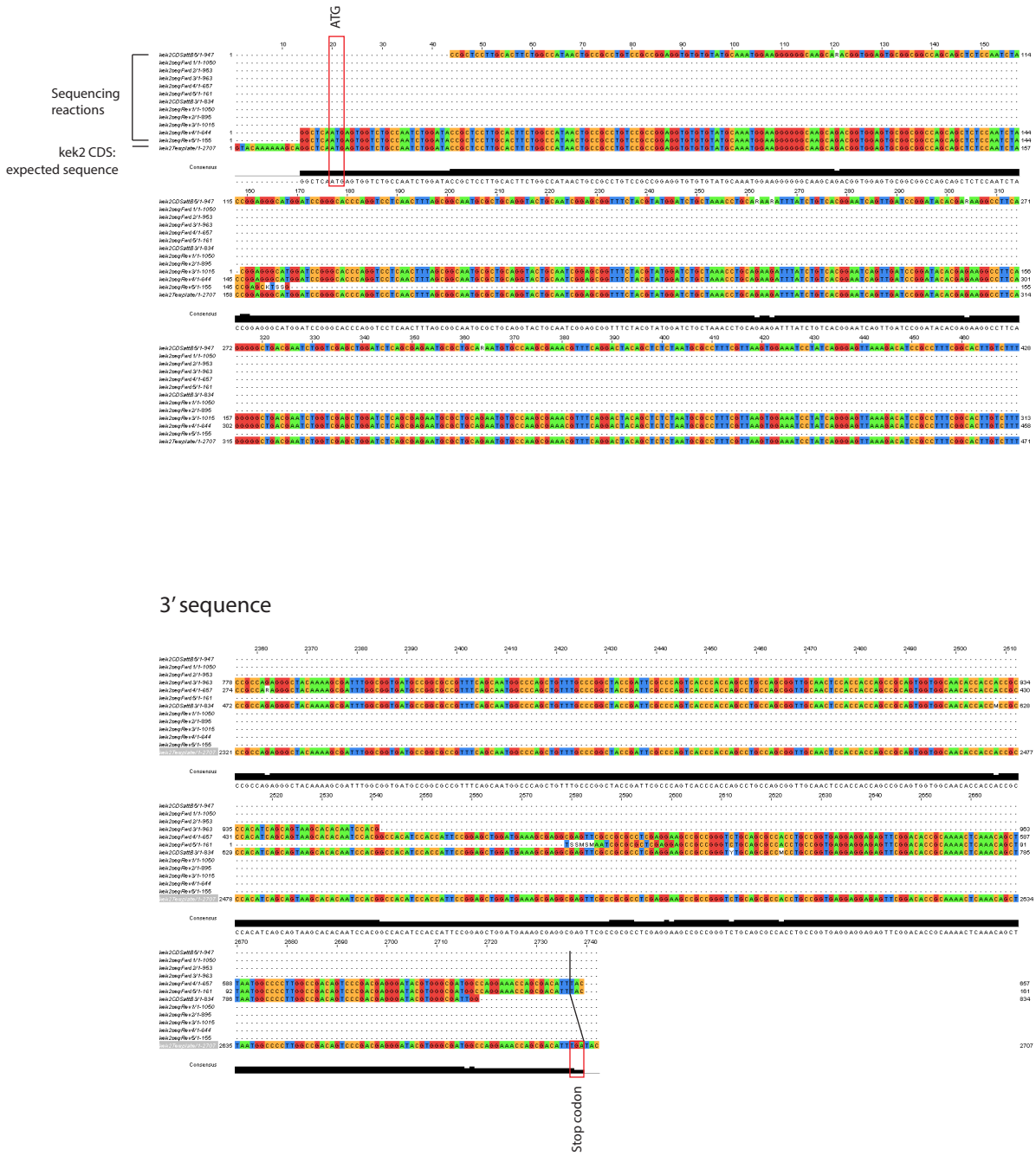

3′ sequence

Maxiprepped *pAct-kek2-mCFP* (*kek2+pAWC*) DNA was verified by sequencing. 5′ and 3′ fragment ends are shown only. No point mutations or substitutions were detected in the entire *kek2* CDS. The STOP codon was successfully removed to allow the use of C-terminal Gateway tags.

Sequencing of *kek3+pAWC*

5′ sequence

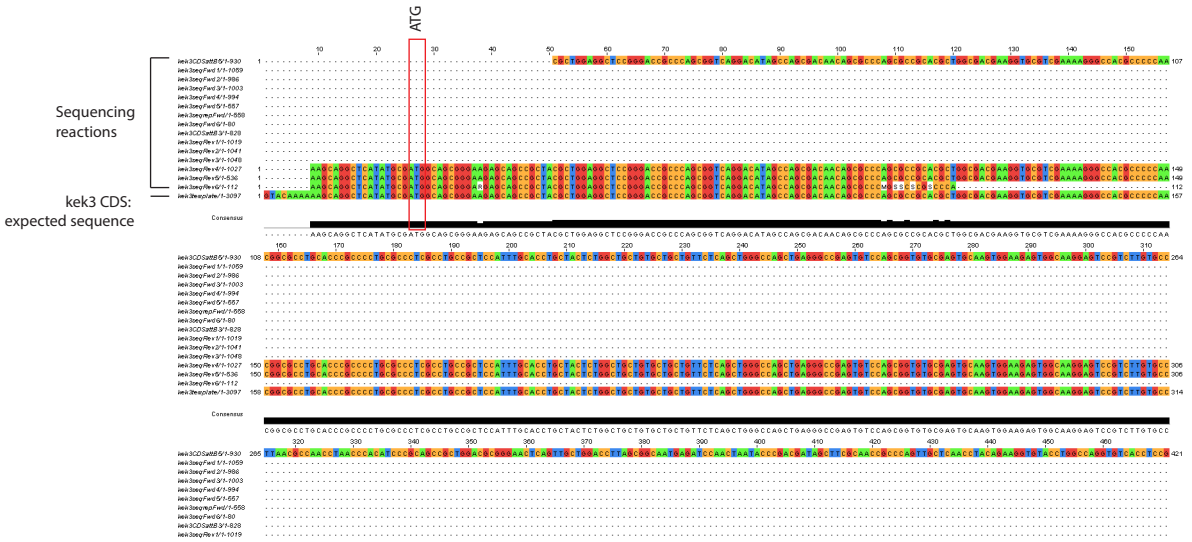

3′ sequence

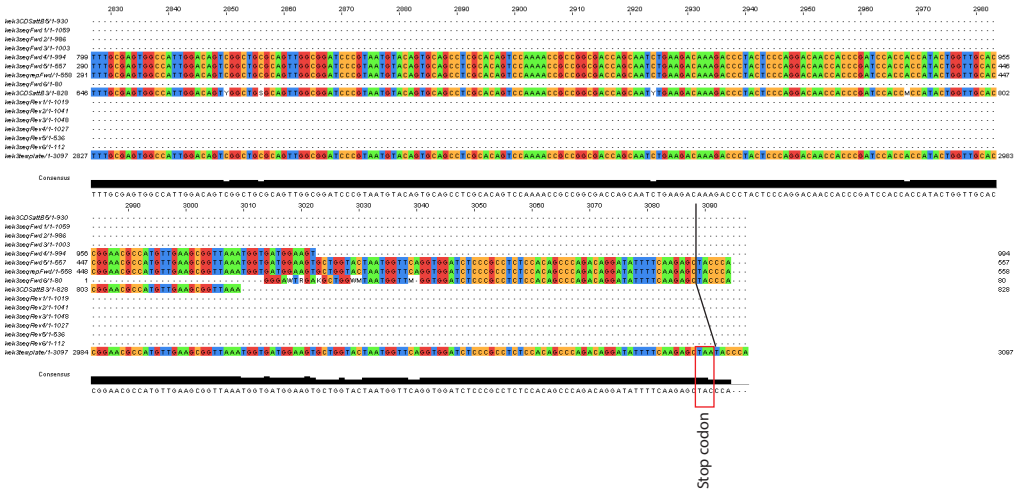

Maxiprepped *pAct-kek3-mCFP* (*kek3+pAWC*) DNA was verified by sequencing. 5′ and 3′ fragment ends are shown only. No point mutations or substitutions were detected in the entire *kek3* CDS. The STOP codon was successfully removed to allow the use of C-terminal Gateway tags.

Sequencing of kek4+pAWC

5′ sequence

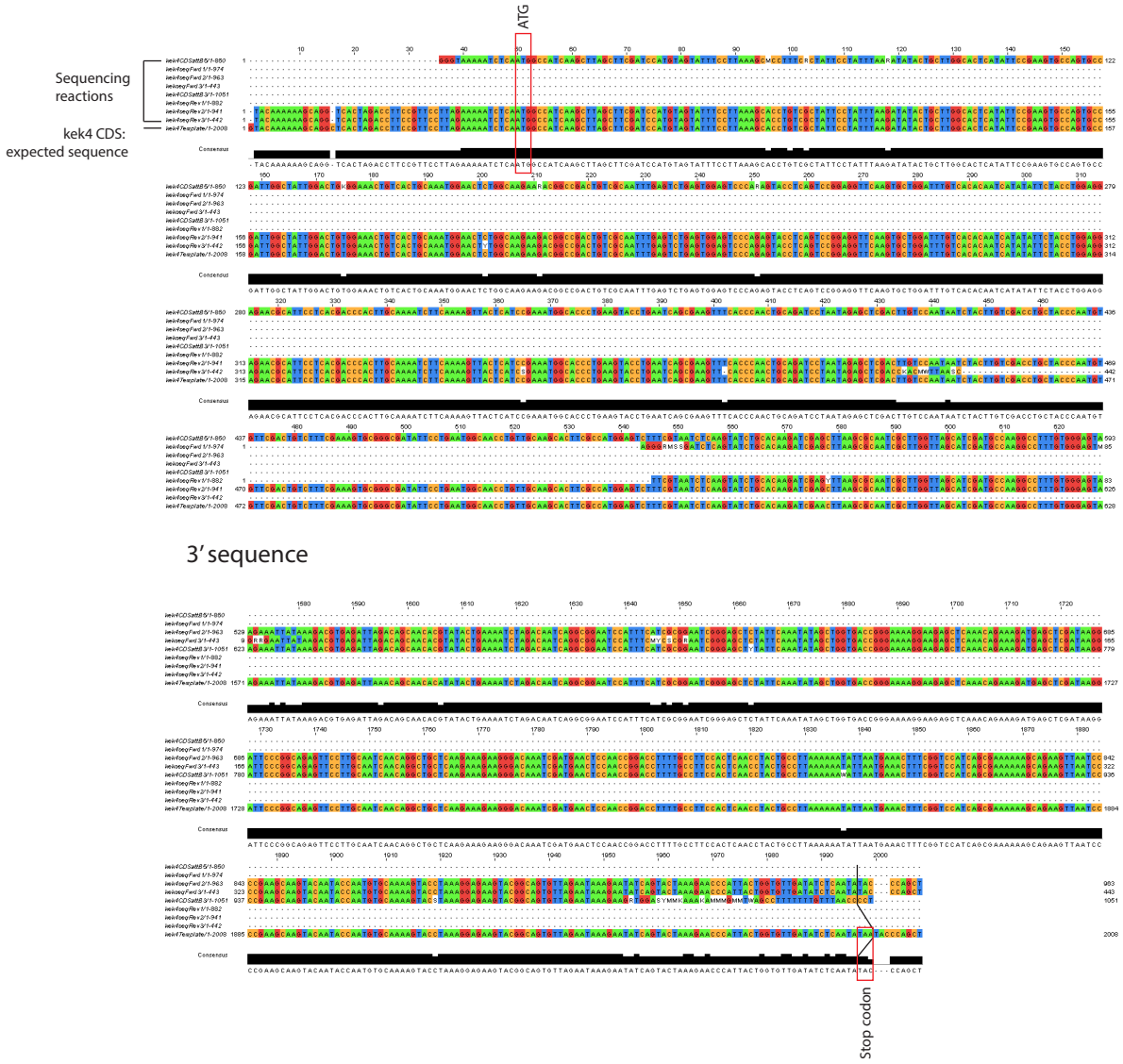

3′ sequence

Maxiprepped *pAct-kek4-mCFP* (*kek4+pAWC*) DNA was verified by sequencing. 5′ and 3′ fragment ends are shown only. No point mutations or substitutions were detected in the entire *kek4* CDS. The STOP codon was successfully removed to allow the use of C-terminal Gateway tags.

Sequencing of *kek5+pAWC*

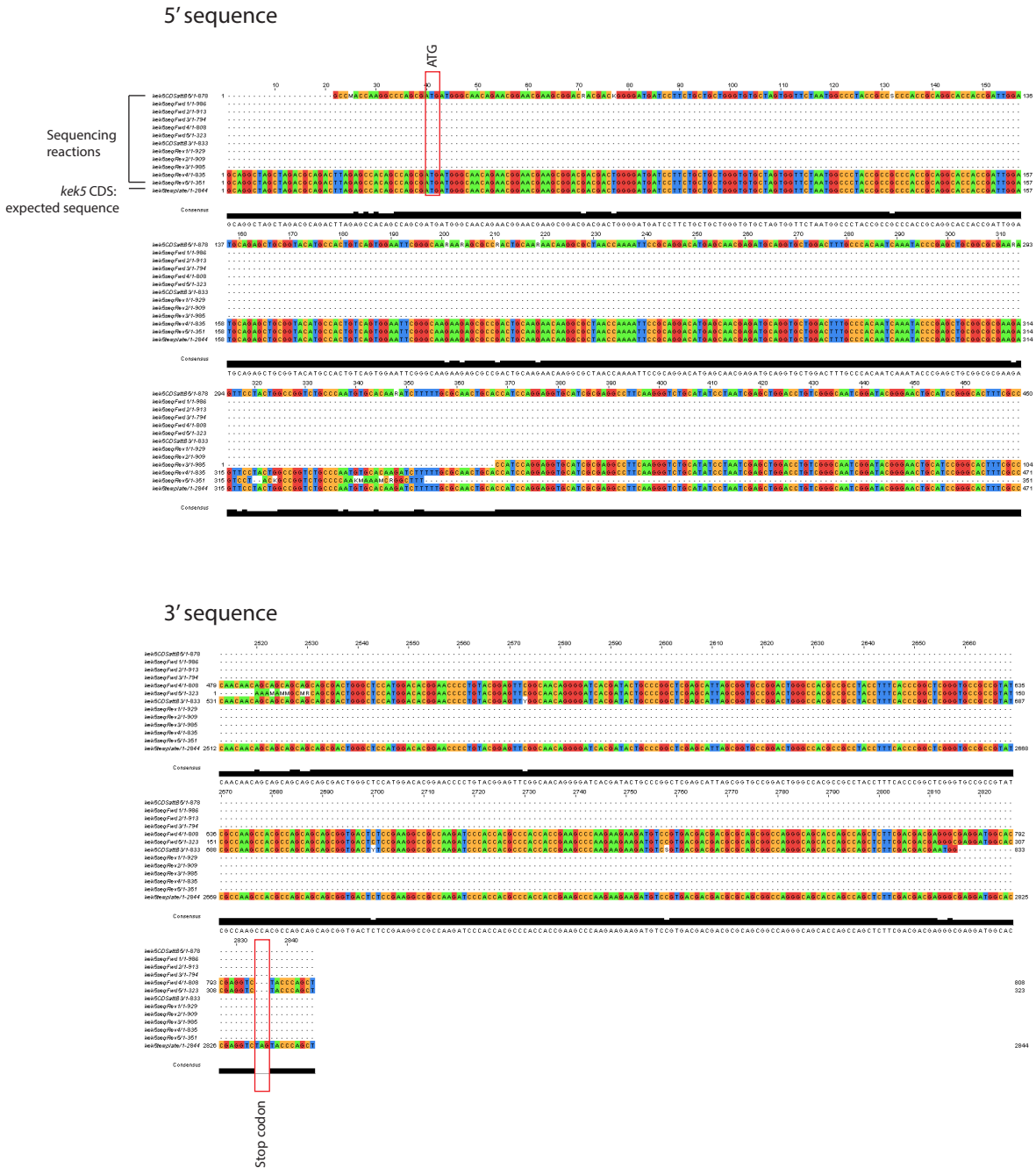

Maxiprepped *pAct-kek5-mCFP* (*kek5+pAWC*) DNA was verified by sequencing. 5′ and 3′ fragment ends are shown only. No point mutations or substitutions were detected in the entire *kek5* CDS. The STOP codon was successfully removed to allow the use of C-terminal Gateway tags.

Sequencing of *kek6+pAWC*

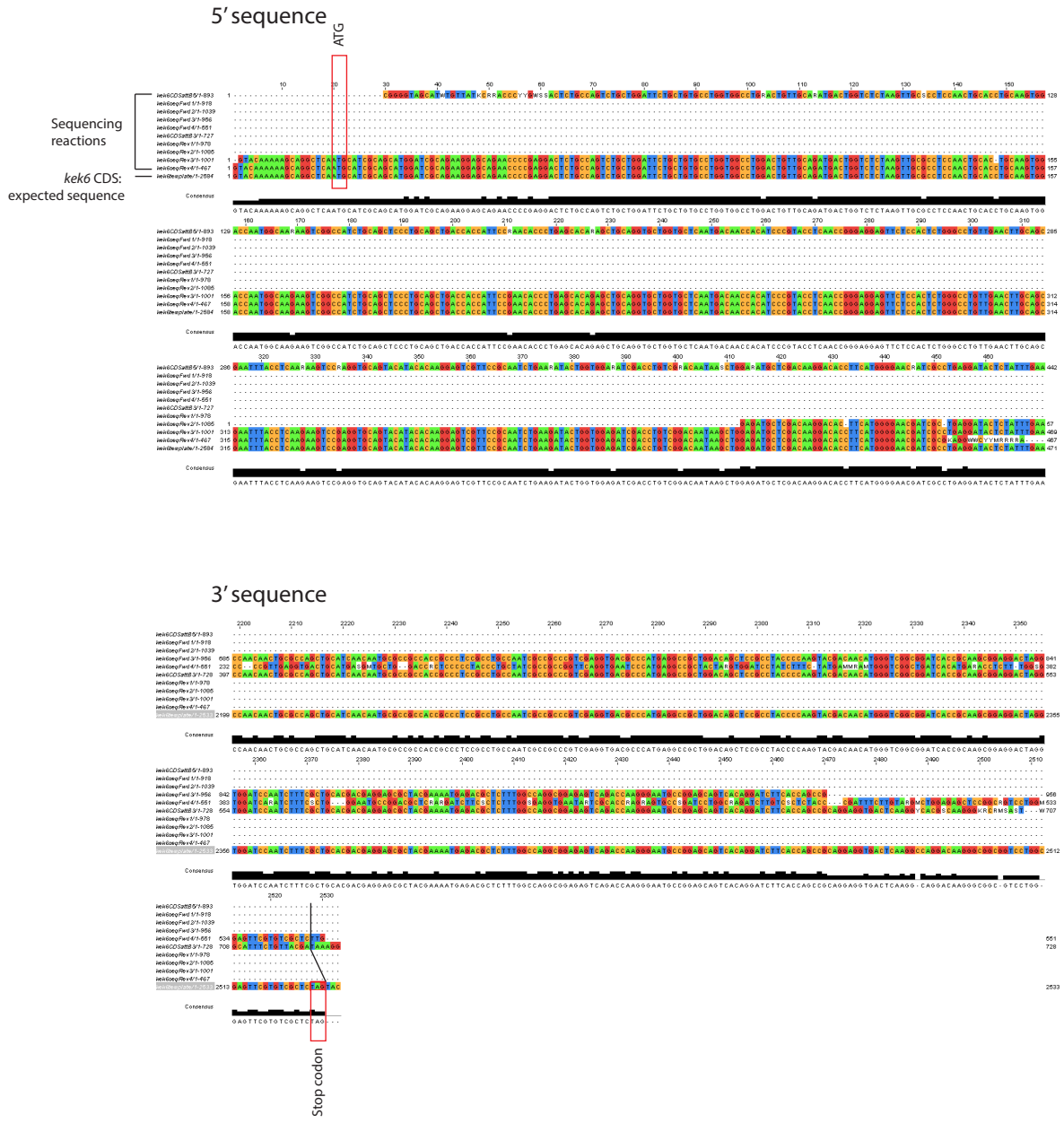

Maxiprepped *pAct-kek6-mCFP* (*kek6+pAWC*) DNA was verified by sequencing. 5′ and 3′ fragment ends are shown only. No point mutations or substitutions were detected in the entire *kek6* CDS. The STOP codon was successfully removed to allow the use of C-terminal Gateway tags.

Cloning of *kek1* into *pAct-attR-FLAG*

a

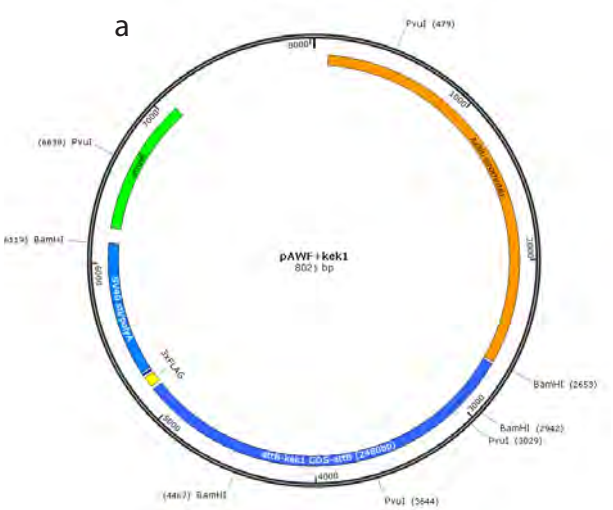

b

pAWF+kek1 Maxiprep digests

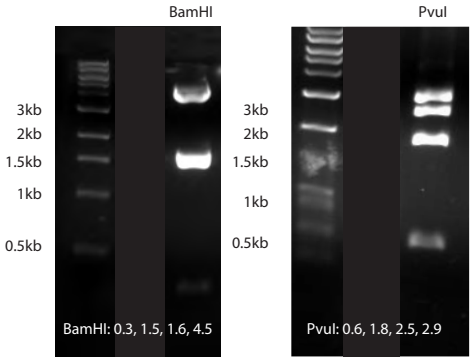

Cloning of *kek2* into *pAct-attR-FLAG*

a

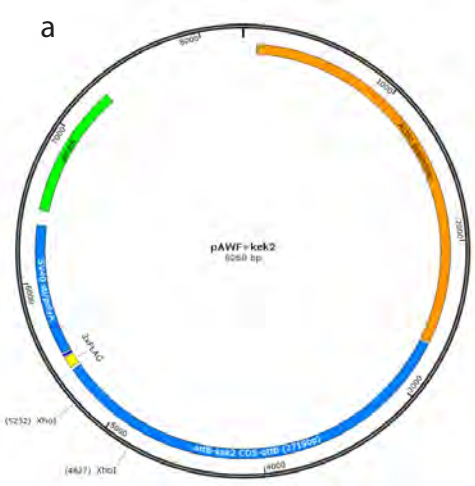

b

pAWF+kek2 Maxiprep digest

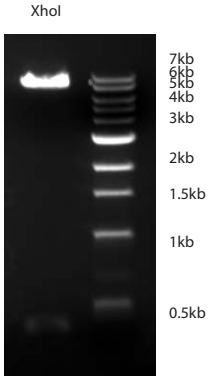

XhoI: 0.4, 7.9

Cloning of *kek3* into *pAct-attR-FLAG*

a

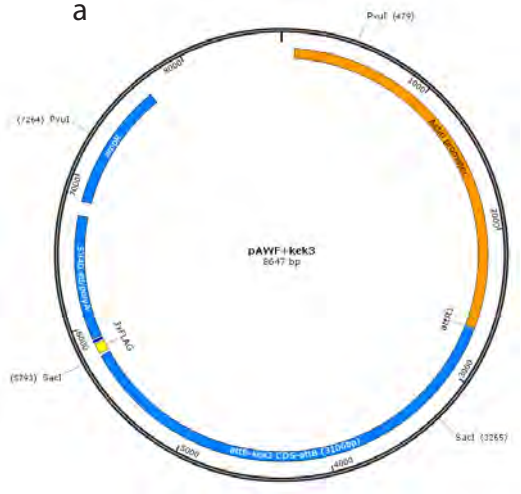

b

pAWF+kek3 Maxiprep digests

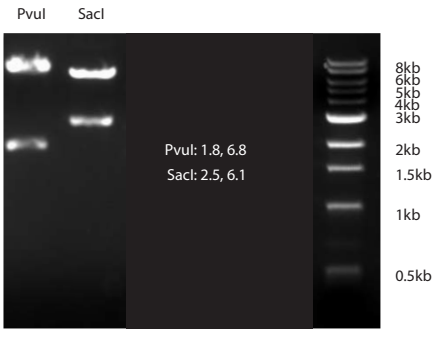

Cloning of *kek4* into *pAct-attR-FLAG*

a

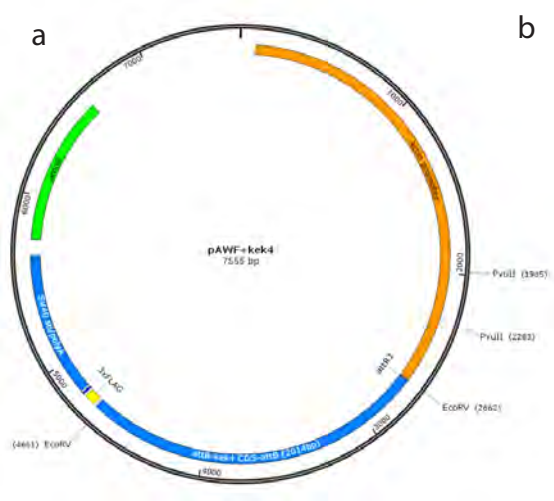

b

pAWF+kek4 Maxiprep digest

Cloning of *kek5* into *pAct-attR-FLAG*

a

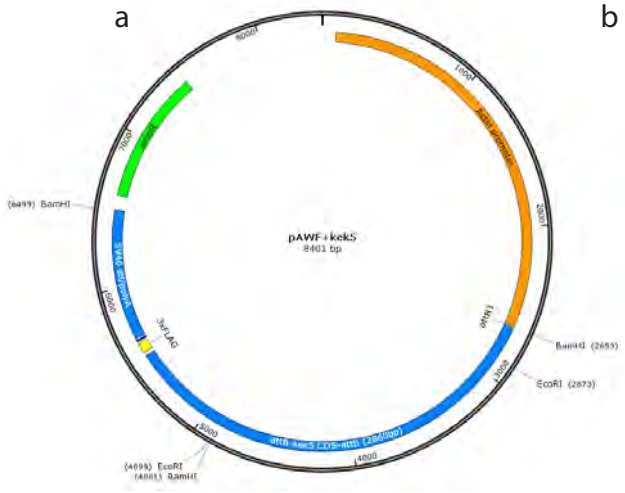

b

pAWF+kek5 Maxiprep digests

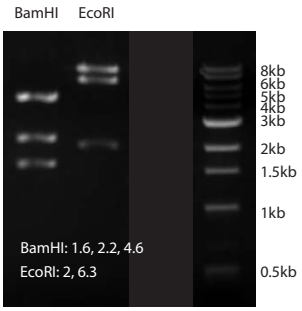

Cloning of *kek6* into *pAct-attR-FLAG*

a

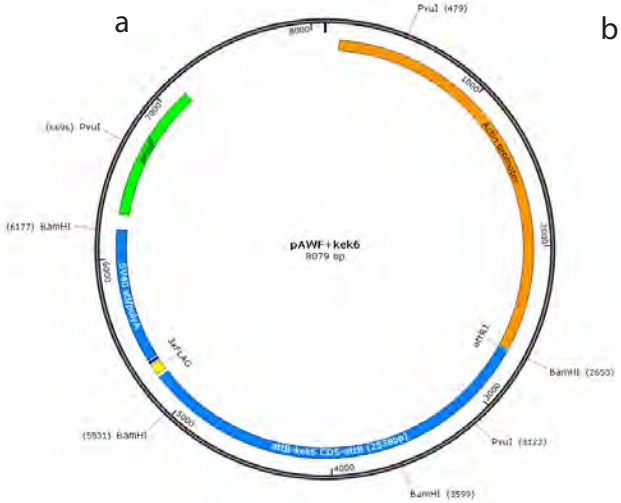

b

pAWF+kek6 Maxiprep digest

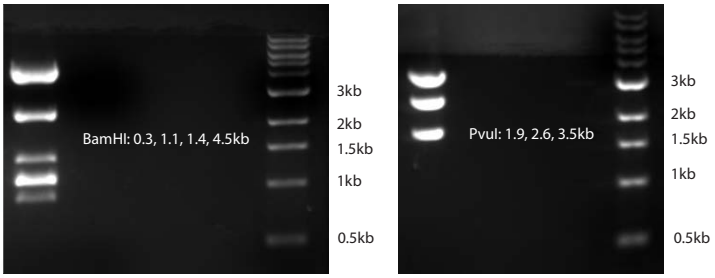

Cloning of *kek1* into *pUASt-attR-mRFP*

a

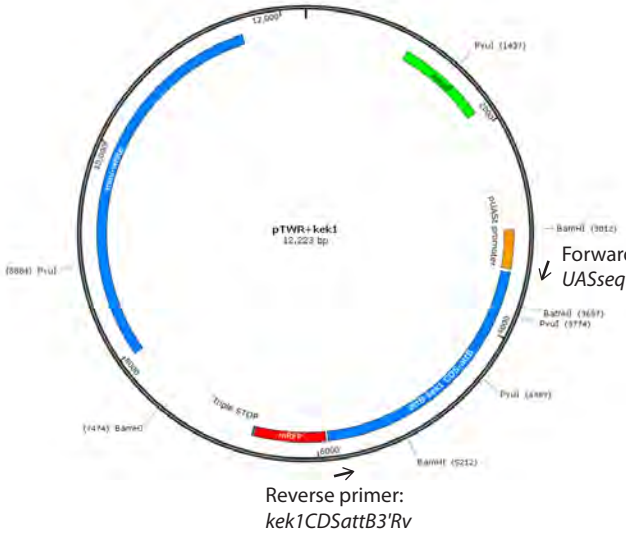

b *pTWR+kek1* Maxiprep digests

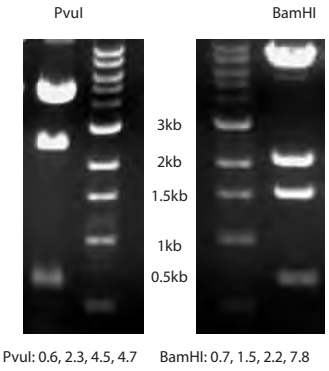

PvuI: 0.6, 2.3, 4.5, 4.7 BamHI: 0.7, 1.5, 2.2, 7.8

c *pTWR+kek1* PCR

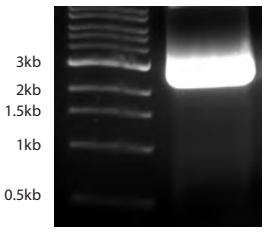

Expected fragment size: 2575nt

Cloning of *kek2* into *pUASt-attR-mRFP*

a

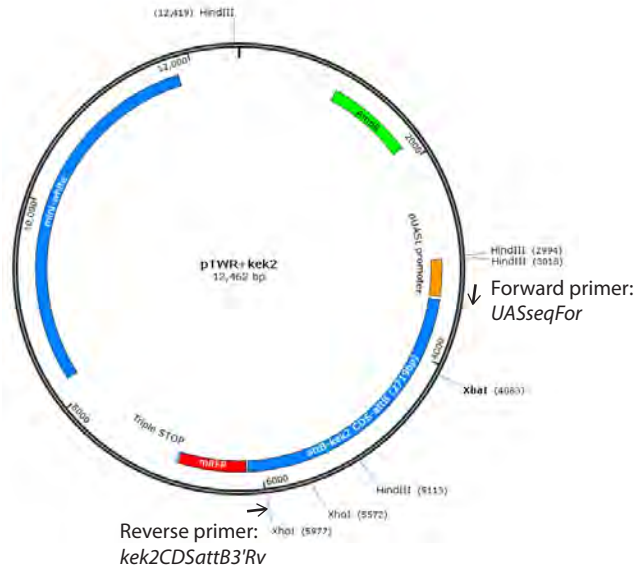

b *pTWR+kek2* Maxiprep digests

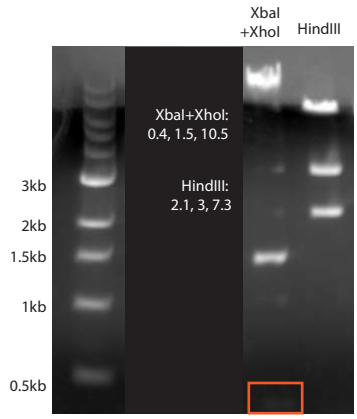

c *pTWR+kek2* PCR

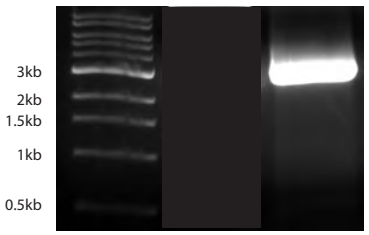

Expected fragment size: 2814nt

Cloning of *kek3* into *pUASt-attR-mRFP*

a

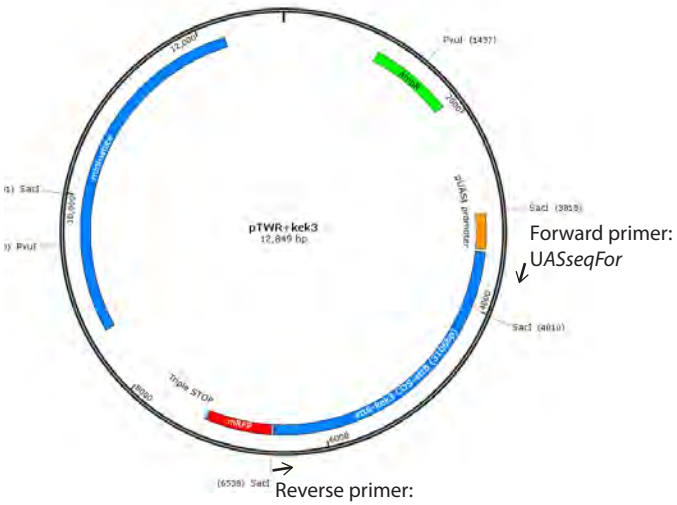

b *pTWR+kek3* Maxiprep digest

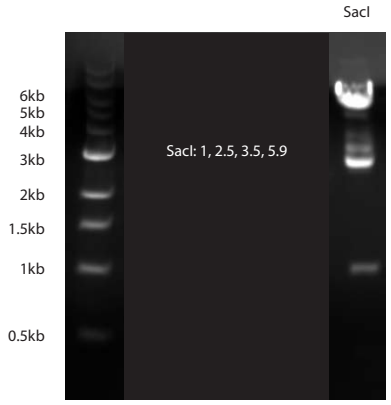

c *pTWR+kek3* PCR

Expected fragment size: 3300nt

Cloning of *kek4* into *pUASt-attR-mRFP*

a

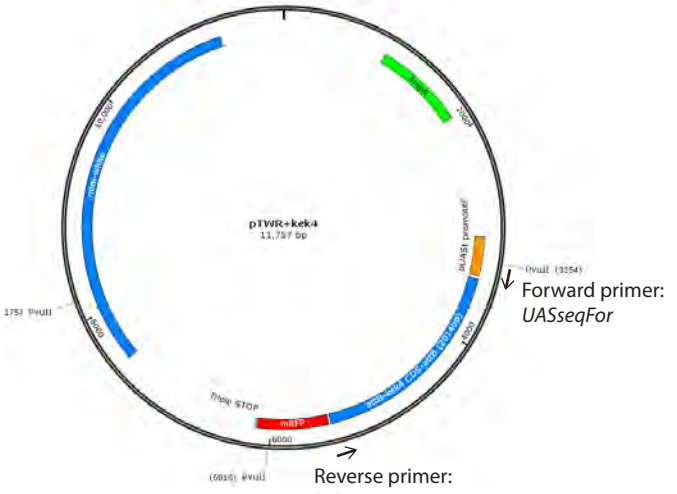

b *pTWR+kek4* Maxiprep digests

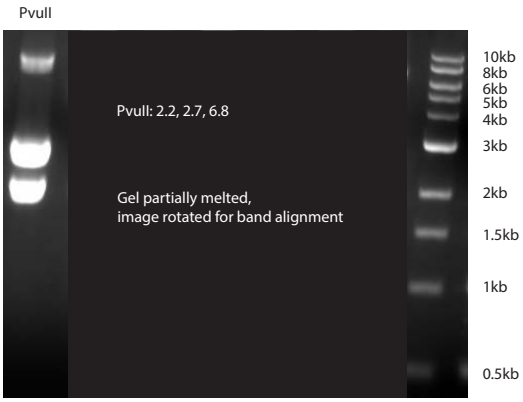

c *pTWR+kek4* PCR

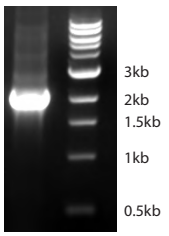

Expected fragment size: 2109nt

Cloning of *kek5* into *pUASt-attR-mRFP*

a

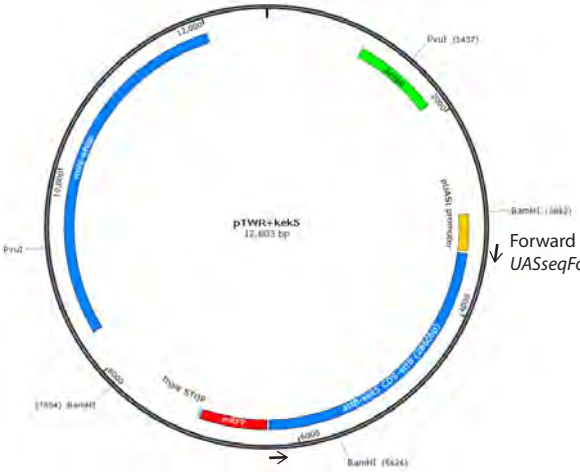

b *pTWR+kek5* Maxiprep digests

c *pTWR+kek5* PCR

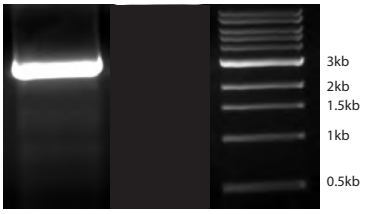

Expected fragment size: 2955nt

Cloning of *kek6* into *pUASt-attR-mRFP*

a

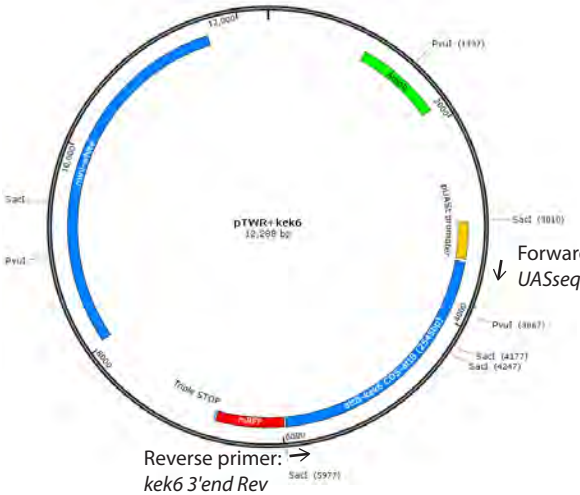

b *pTWR+kek6* Maxiprep digests

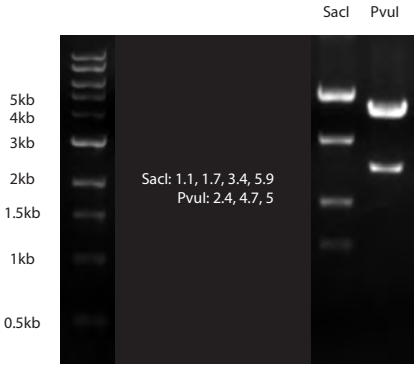

c *pTWR+kek6* PCR

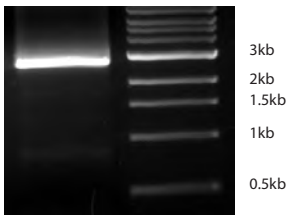

Expected fragment size: 2640nt

Chimaera cloning strategy

Regions of the *kek3-6* coding sequences that correspond to the extracellular and transmembrane regions were determined using protein prediction algorithms (Table 4.2). These regions were amplified by PCR from *pDONR*^{221} constructs, along with the intracellular domain-encoding sequence of *toll6*. **a** | Fragments were ligated at a unique introduced restriction site (EcoRI or BamHI). **b** | Ligated cloned into *pDONR*^{221} entry clones and subsequently into *pAct5c-attR-3xHA* (*pAWC*). **c** | PCR products prior to cloning.

Cloning of *kek3-kek6Ξtoll6* chimaeras into *pDONR*^{221}

For each construct: **a** | Plasmid maps of cloned constructs. Enzyme sites for restriction digest verification are shown. **b** | Restriction digest verification of cloned plasmids.

Cloning of *kek3-6Ξtoll6* chimaeras into *pAct5c-attR-3xHA*

For each construct: **a** | Plasmid maps of cloned constructs. Enzyme sites for restriction digest verification are shown. **b** | Restriction digest verification of cloned plasmids.

Sequencing of *kek3-6Ξtoll6+pAWH* chimaeras

Maxiprepped *pAct5c- kek3-6Ξtoll6-3xHA* (*kek3-6Ξtoll6 +pAWH*) DNA sequences were verified by sequencing. 5′ and 3′ fragment ends of the insert are shown only (*kek* ATG to end of *toll6* intracellular domain-coding sequence). No point mutations or substitutions were detected in the fragments.

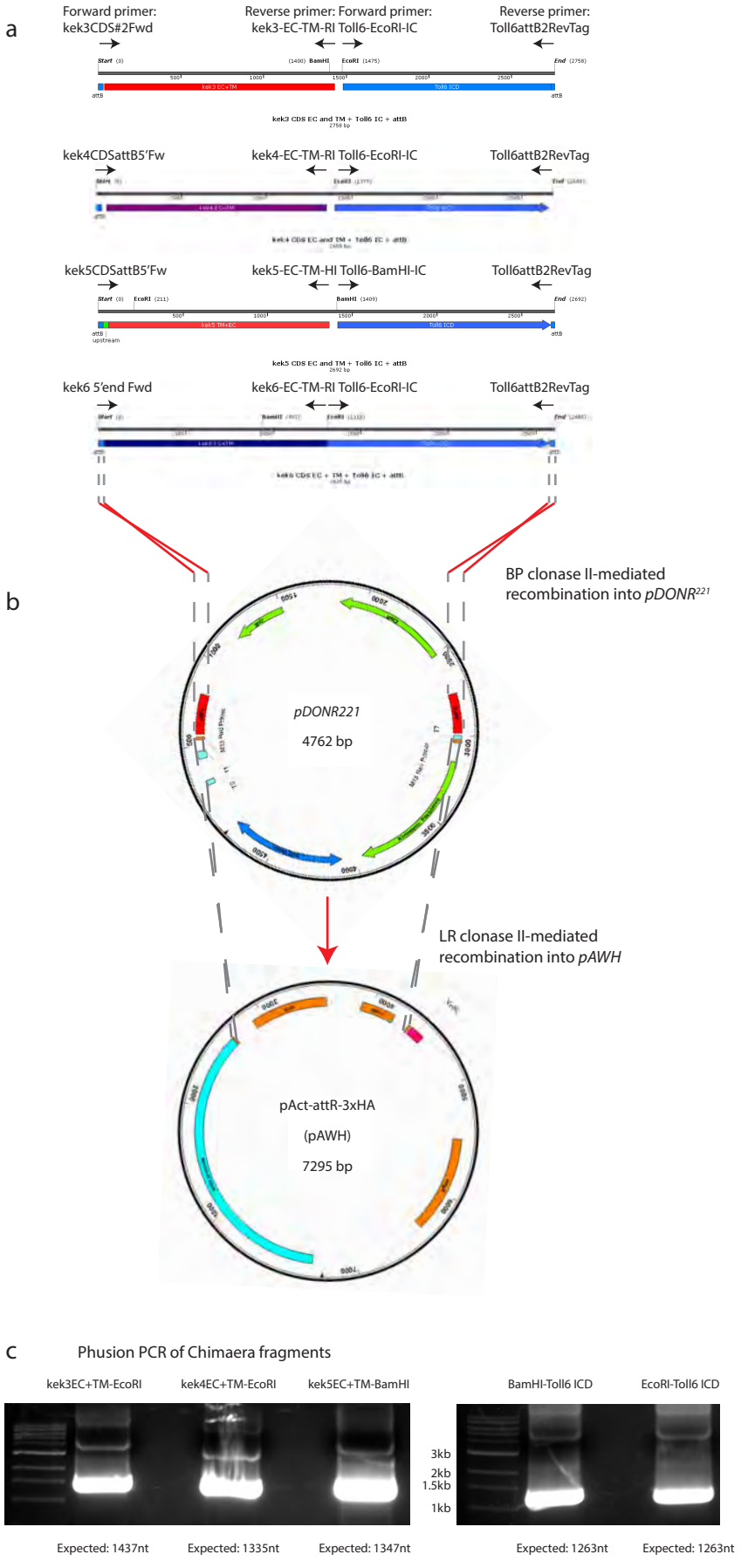
a
Forward primer:
kek3CDS#2Fwd
Reverse primer: Forward primer:
kek3-EC-TM-RI Toll6-EcoRI-IC
Reverse primer:
Toll6attB2RevTag
kek3 CDS EC and TM + Toll6 IC + attB
kek4CDSattB5'Fw
kek4-EC-TM-RI Toll6-EcoRI-IC
Toll6attB2RevTag
kek5CDSattB5'Fw
kek5-EC-TM-HI Toll6-BamHI-IC
Toll6attB2RevTag
kek5 CDS EC and TM + Toll6 IC + attB
kek6 5'end Fwd
kek6-EC-TM-RI Toll6-EcoRI-IC
Toll6attB2RevTag
b
BP clonase II-mediated
recombination into pDONR221
pDONR221
4762 bp
LR clonase II-mediated
recombination into pAWH
pAct-attR-3xHA
(pAWH)
7295 bp
c
Phusion PCR of Chimaera fragments
kek3EC+TM-EcoRI
kek4EC+TM-EcoRI
kek5EC+TM-BamHI
BamHI-Toll6 ICD
EcoRI-Toll6 ICD
3kb
2kb
1.5kb
1kb
Expected: 1437nt
Expected: 1335nt
Expected: 1347nt
Expected: 1263nt
Expected: 1263nt

Cloning of *kek3/4Ξtoll6* chimaeras into *pDONR*^{221}

a

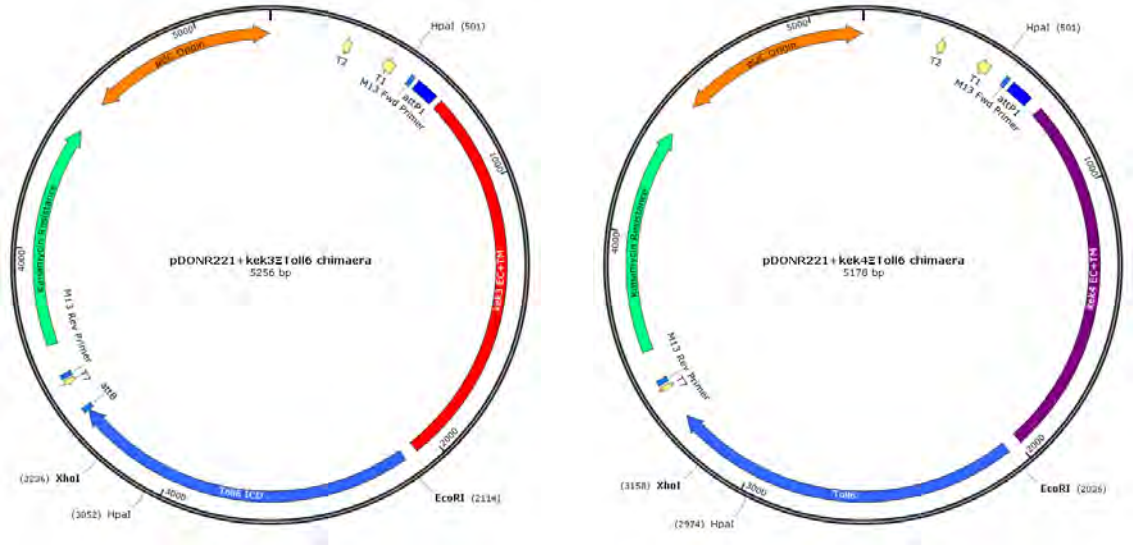

b

Kek3 and Kek4 chimaeras, in *pDONR*^{221}, Maxiprep digests

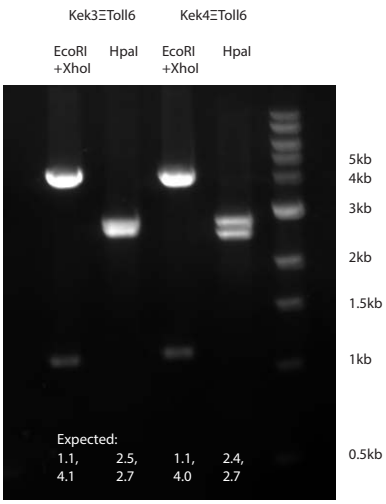

Cloning of *kek5Ξtoll6* chimaera into *pDONR*^{221}

a

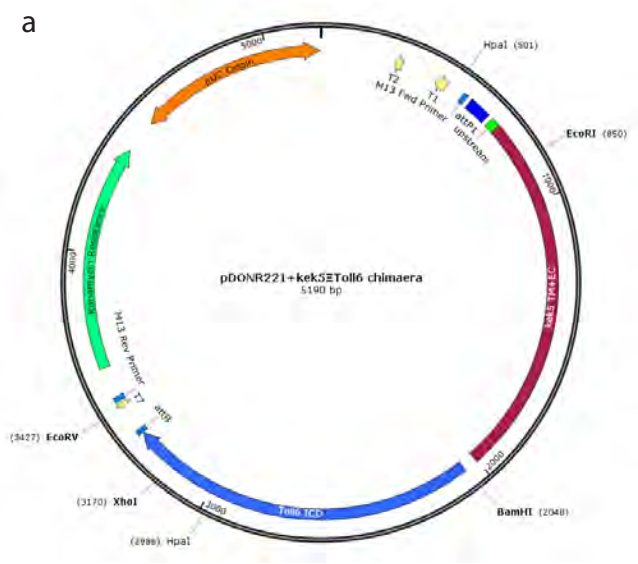

b

Kek5 chimaera, in *pDONR*^{221}, Maxiprep digests

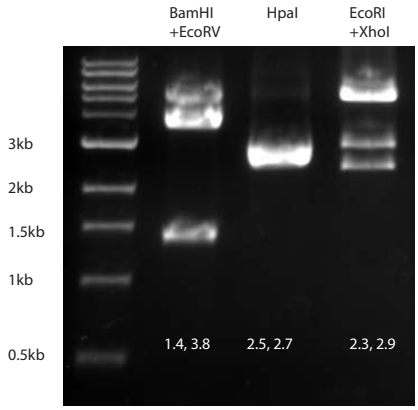

Cloning of *kek6Ξtoll6* chimaera into *pDONR*^{221}

a

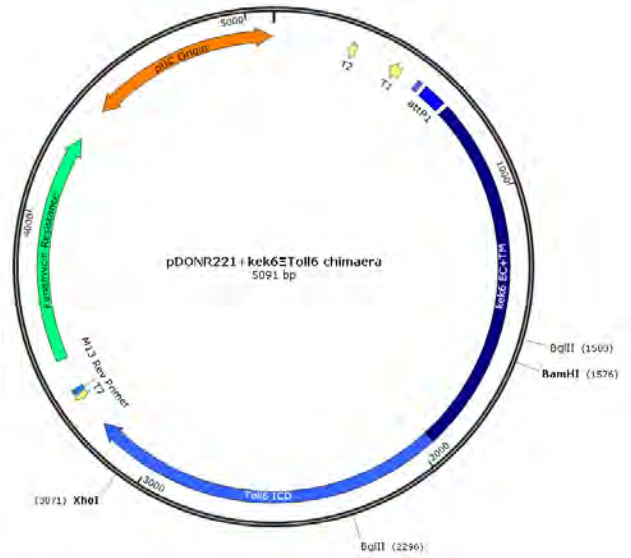

b

Kek6 chimaera, in *pDONR*^{221}, Maxiprep digests

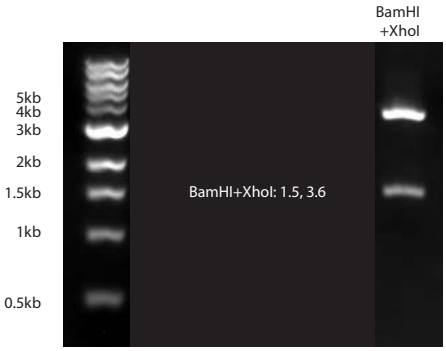

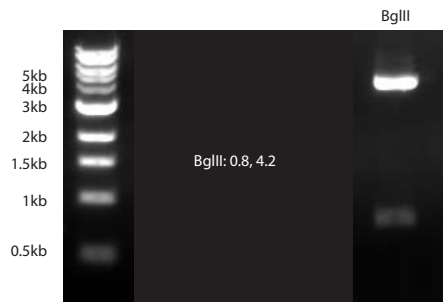

Cloning of *kek3Ξtoll6* chimaera into *pAct5c-attR-3xHA*

a

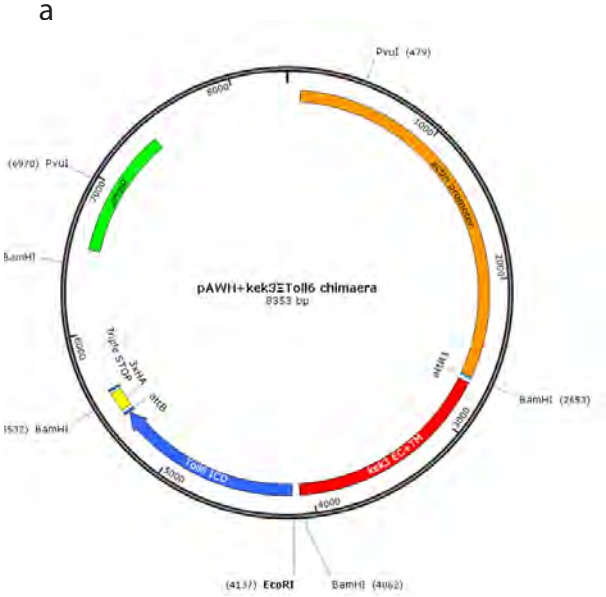

b

pAWH+kek3ΞToll6 chimaera
Maxiprep digests

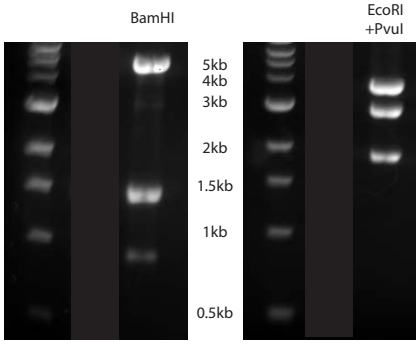

Cloning of *kek4Ξtoll6* chimaera into *pAct5c-attR-3xHA*

a

b

pAWH+kek4ΞToll6 chimaera
Maxiprep digests

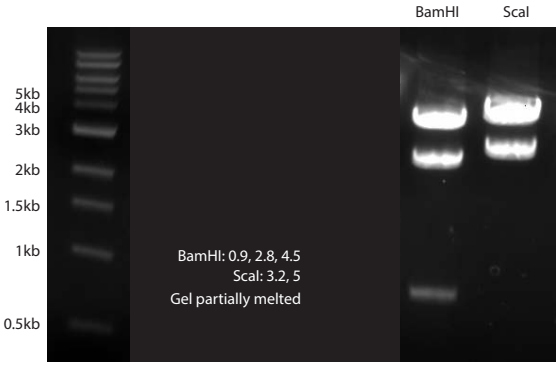

Cloning of *kek5Ξtoll6* chimaera into *pAct5c-attR-3xHA*

a

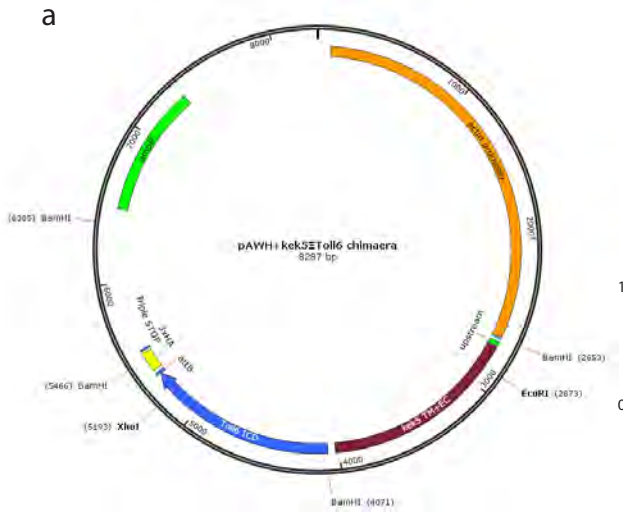

b

pAWH+kek5ΞToll6 chimaera
Maxiprep digests

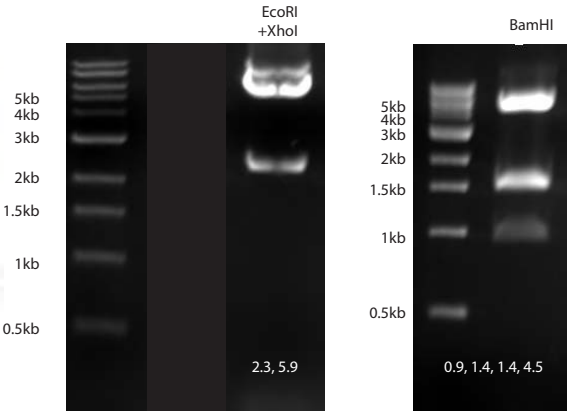

Cloning of *kek6Ξtoll6* chimaera into *pAct5c-attR-3xHA*

a

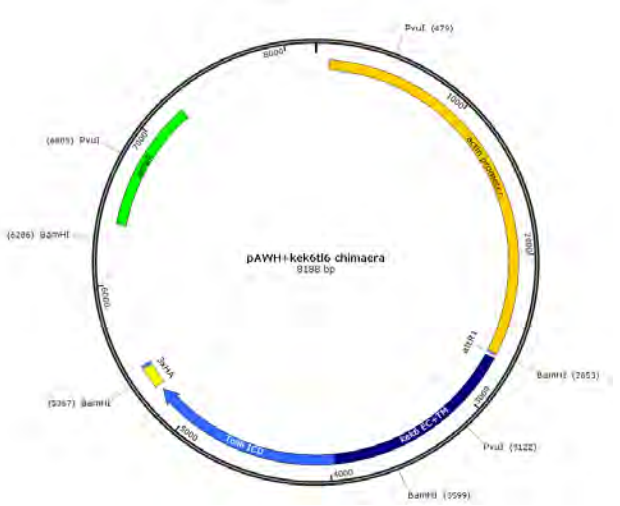

b

pAWH+kek6ΞToll6 chimaera
Maxiprep digests

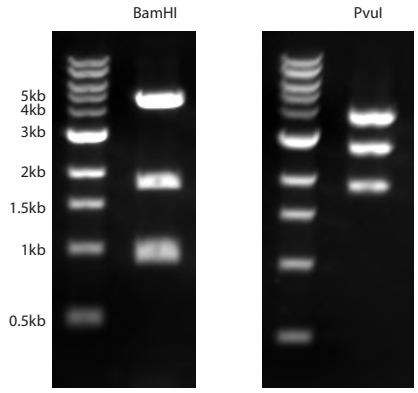

BamHI: 0.9, 0.9,1.7, 4.5

PvuI: 1.9, 2.6, 3.6

Sequencing of *kek3Ξtoll6+pAWH* chimaera

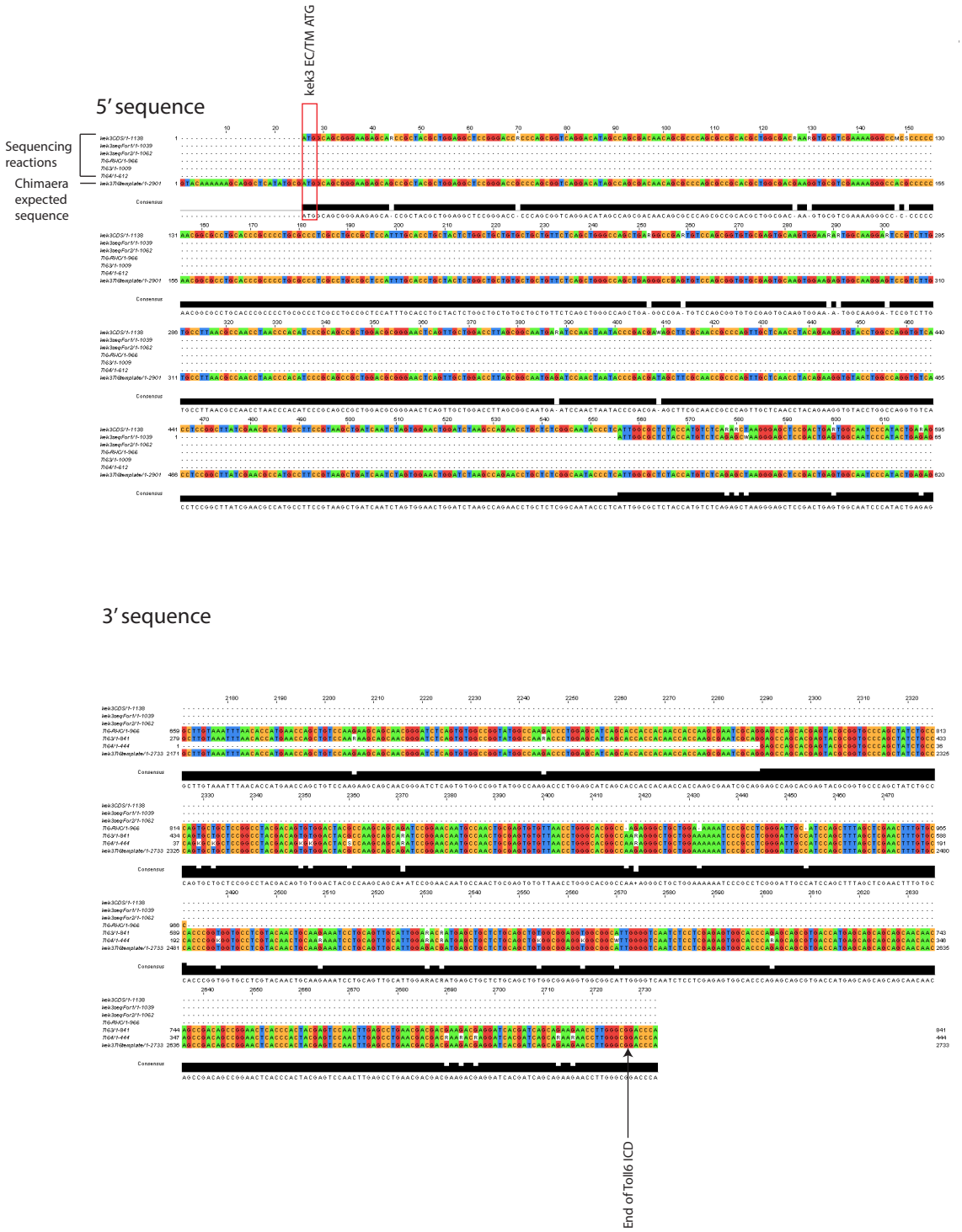

Sequencing of *kek4Ξtoll6+pAWH* chimaera

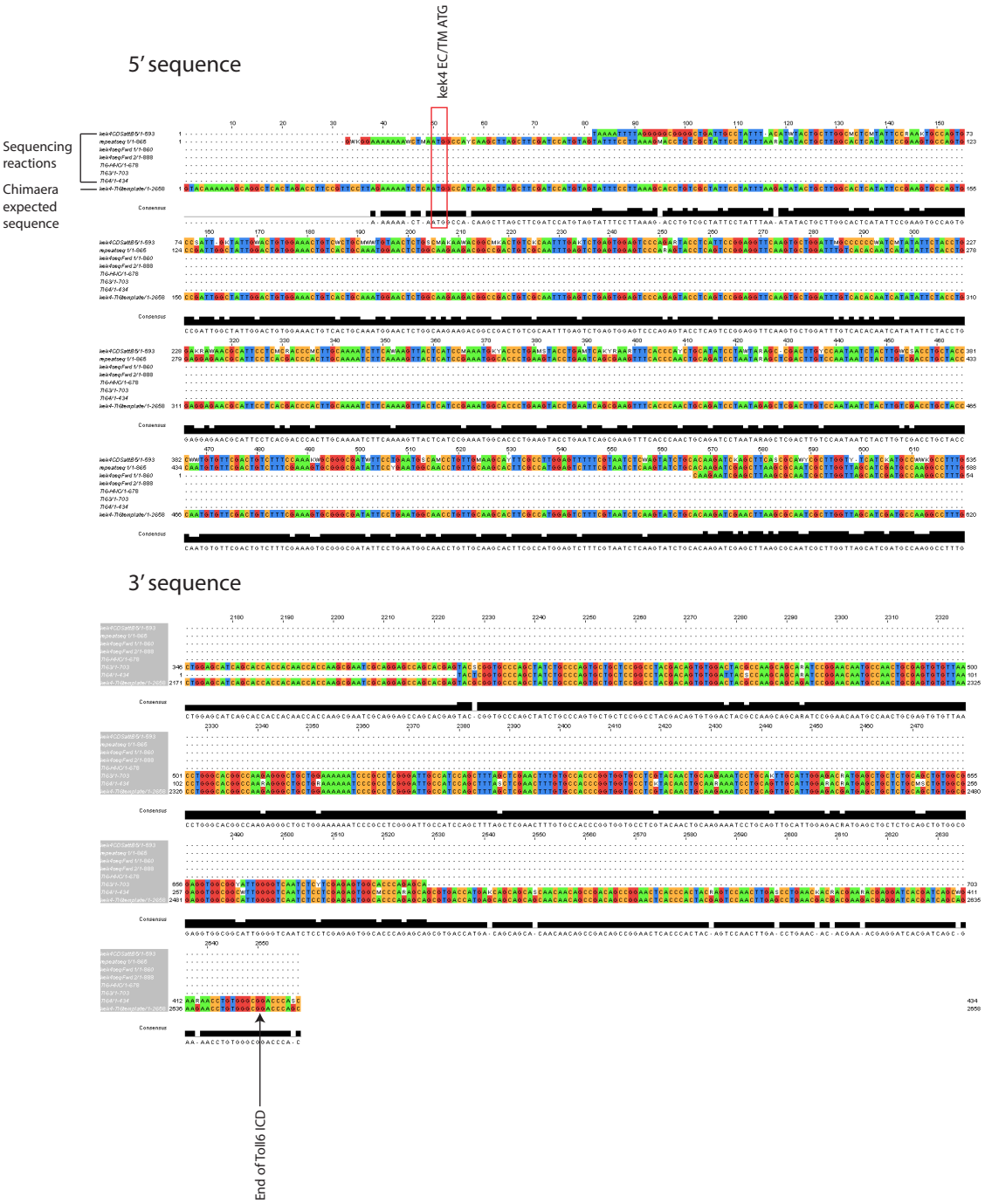

Sequencing of *kek5Ξtoll6+pAWH* chimaera

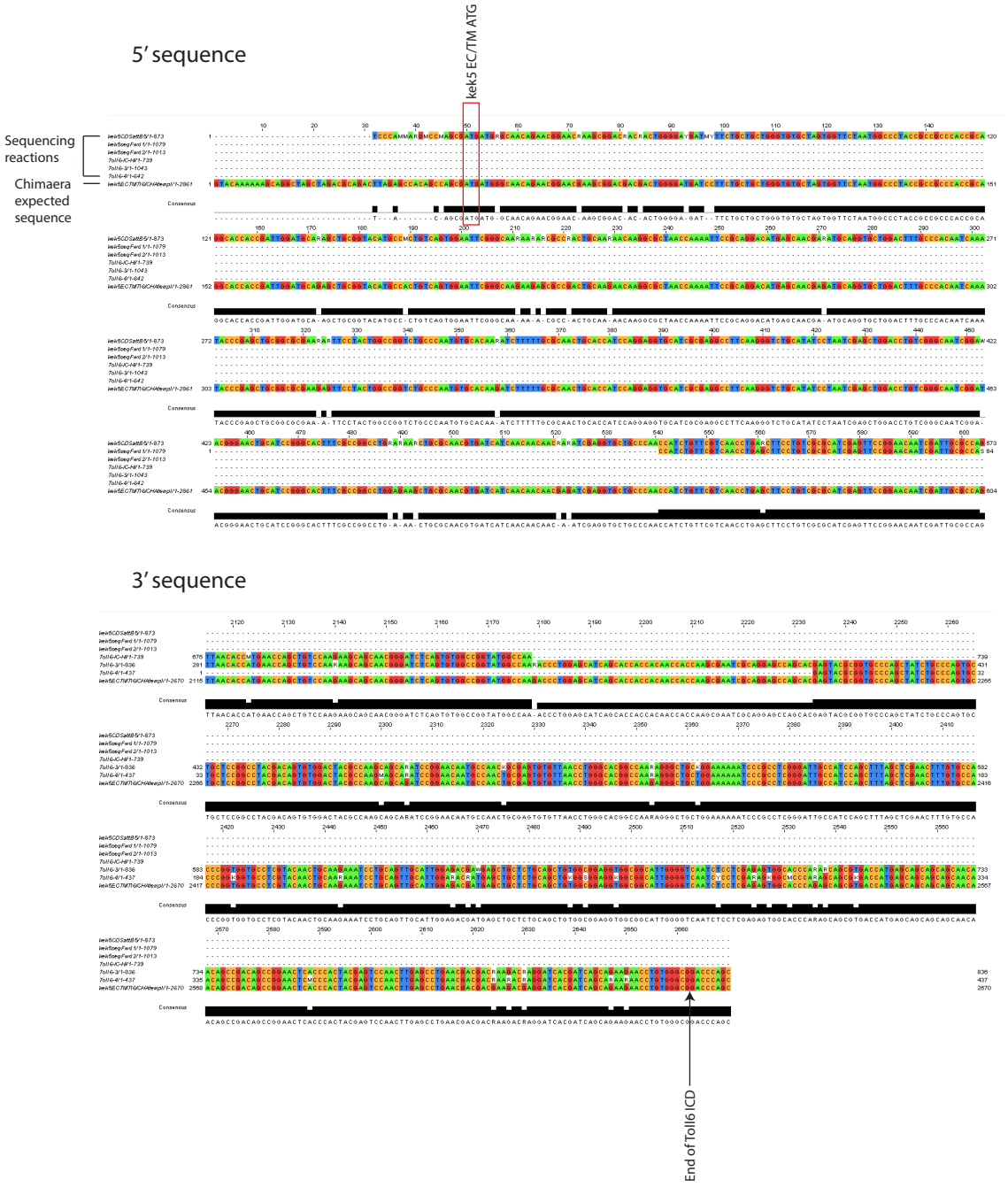

Sequencing of *kek6Ξtoll6+pAWH* chimaera

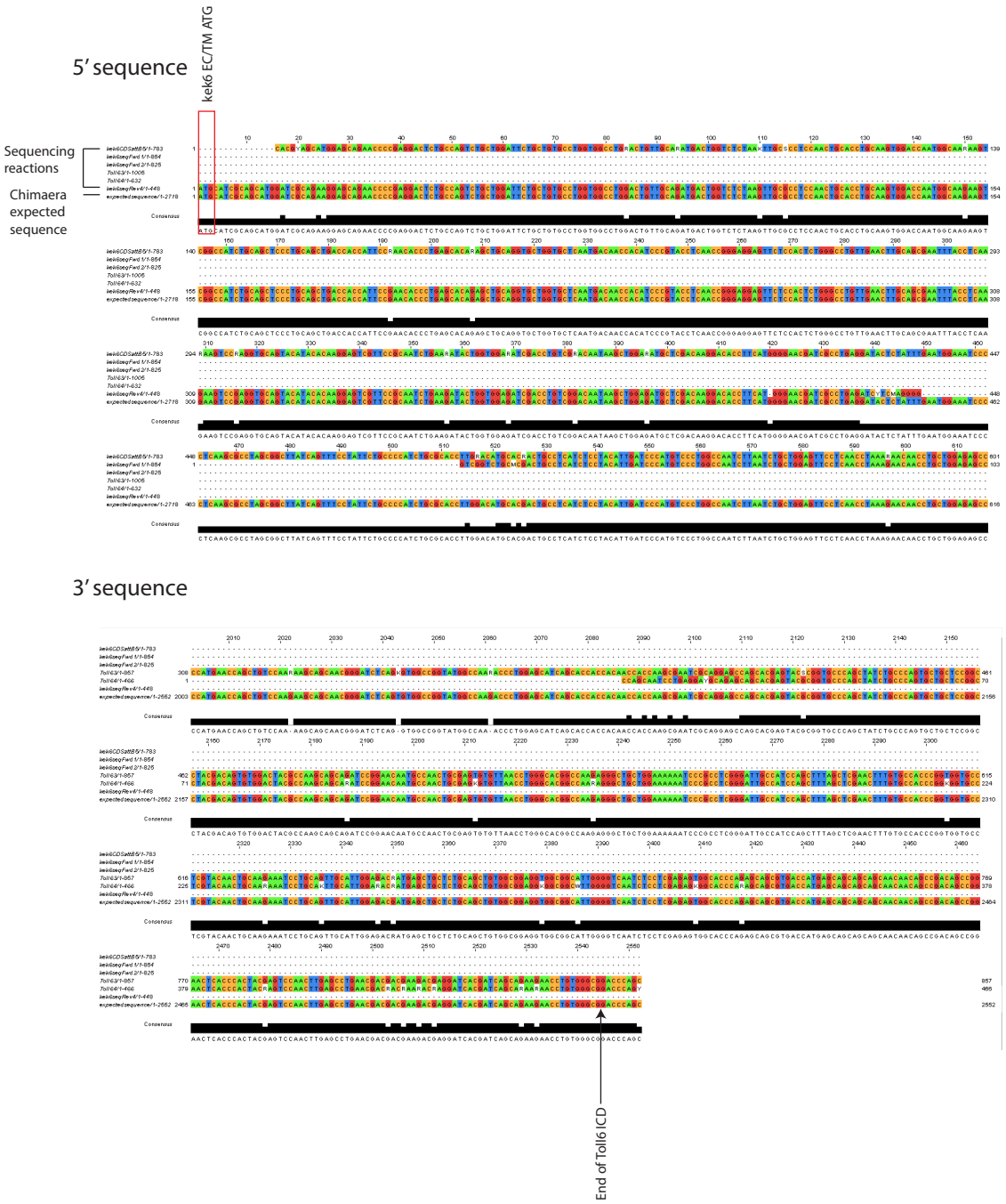

APPENDIX III

NULL MUTAGENESIS LINES SUMMARY

Null mutagenesis lines summary

Line	Internal genomic PCR (homozygous flies only)	Two-sided PCR		DNA quality test
		Left isolate	Right isolate	
kek3				
Primer	*kek3intgenF* & *kek3intgenR*	*kek3FRT GP Fwd* & *WH-WH- 2sid LI R*	*kek3FRT GP Rev* & *WH-WH- 2sid RI F*	
Expected				
Mutant	No band	~200nt	~200nt	
Not mutant	500nt	No band	No band	
Observed				
Parent: *f04709*	Not tested	No band	No band	*kek6* internal genomic 500nt band obtained
Parent: *f07027*	Not tested	No band	200nt	-
1	Deceased			-
2–15	500nt band			-
16	Heterozygous DNA only	No band	No band	*kek6* internal genomic 500nt band obtained
17	500nt band			-
18	Deceased			-
19–20	500nt band			-
21	Deceased			-
22–37	500nt band			-
38	No band	No band	No band	*kek6* internal genomic 500nt band obtained
39	500nt band			-
40	500nt band			-
41	No band	No band	No band	*kek6* internal genomic 500nt band obtained
42	Deceased			-
43–45	500nt band			-
46	Deceased			-
47–50	500nt band			-
Primer	*kek3intgenF* & *kek3intgenR*	*kek3FRT GP Fwd* & *WH-WH- 2sid RI F*	*kek3FRT GP Rev* & *WH-WH- 2sid LI R*	
Expected				
Mutant	No band	1.7kb	~250nt	
Not mutant	500nt	No band	No band	
Observed				
yw	500nt	No band	No band	
Parent: *f07029*	Not tested	1.7kb	No band	
Parent: *f07041*	Not tested	No band	250nt	
1–3		No band	No band	
4		No band	250nt	
5–11		No band	No band	
12	No band	1.7kb	250nt	*kek6* internal genomic 500nt band obtained
13		1.7kb	No band	
14		No band	No band	
15		1.7kb	No band	
16		1.7kb	No band	
17		No band	No band	
18		1.7kb	No band	
19		1.7kb	No band	
20		1.7kb	No band	

21		1.7kb	No band	
22–23		No band	No band	
24		1.7kb	No band	
25		1.7kb	No band	
26	No band	1.7kb	250nt	*kek6* internal genomic 500nt band obtained
27		No band	250nt	
28		No band	250nt	
29–50	Lines tested by 2-sided PCR, gels not run owing to verification of *kek3*^{12} and *kek3*^{26}			
51–104	Reserve lines, not tested			
105		1.7kb	No band	
106		No band	250nt	
107		No band	250nt	
108		1.7kb	No band	
kek4				
Mutant	No band	~200nt	~200nt	
Primer	*kek4intgenF* & *kek4intgenR*	*kek4FRT GP Fwd* & *WH-WH- 2sid RI F*	*kek4FRT GP Rev* & *WH-WH- 2sid RI F*	
Expected				
Mutant	No band	~200nt	~200nt	
Not mutant	500nt	No band	No band	
Observed				
Parent: *f05454*	Not tested	200nt	No band	
Parent: *e02457*	Not tested	No band	200nt	
1–4	500nt band			
5	Heterozygous DNA only	No band	No band	*kek6* internal genomic 500nt band obtained
6	500nt band			
7	No band			
8	No band	No band	200nt	
9–13	500nt band			
14	No band	200nt	No band	
15	No band	No band	No band	*kek6* internal genomic 500nt band obtained
16	No band			
17	500nt band			
18	No band			
19–21	500nt band			
22–23	Deceased			
24	500nt band			
25	Heterozygous DNA only	200nt	No band	
26	No band	No band	No band	*kek6* internal genomic 500nt band obtained
27	500nt band			
28	Heterozygous DNA only	200nt	No band	
29–37	500nt band			
38	Deceased			
39	500nt band			
40	Deceased			
41	500nt band			
42	Deceased			
43–44	500nt band			
45	Heterozygous DNA only	No band	No band	*kek6* internal genomic 500nt band obtained
46	500nt band			
47–50	Deceased			

	Repeat protocol			
yw	500nt	No band	No band	
1–8	Not tested			
9	Heterozygous DNA only	No band	200nt	
10	Heterozygous DNA only	200nt	No band	
11	Heterozygous DNA only	200nt	No band	
12	Deceased			
13	Heterozygous DNA only	200nt	No band	
14	Heterozygous DNA only	200nt	No band	
15	Heterozygous DNA only	200nt	No band	
16	Heterozygous DNA only	200nt	No band	
17	Heterozygous DNA only	200nt	No band	
18	Heterozygous DNA only	200nt	No band	
19	Heterozygous DNA only	200nt	No band	
20	No band	200nt	200nt	*kek6* internal genomic 500nt band obtained
21	Heterozygous DNA only	200nt	No band	
22	Heterozygous DNA only	200nt	No band	
23	No band	200nt	200nt	*kek6* internal genomic 500nt band obtained
24	Heterozygous DNA only	200nt	No band	
25	Heterozygous DNA only	200nt	No band	
26	Heterozygous DNA only	No band	No band	
27	Heterozygous DNA only	200nt	No band	
28	Heterozygous DNA only	No band	No band	
29	Heterozygous DNA only	200nt	No band	
30	Heterozygous DNA only	200nt	No band	
31	Deceased			
32	Heterozygous DNA only	200nt	No band	
33	Heterozygous DNA only	200nt	No band	
34	Heterozygous DNA only	200nt	No band	
35	Deceased			
36	Heterozygous DNA only	200nt	No band	
37–38	Deceased		200nt	
39	Heterozygous DNA only	No band	No band	
40	Heterozygous DNA only	200nt	No band	
41	Deceased			
42	Heterozygous DNA only	200nt	200nt	
43	Heterozygous DNA only	200nt	No band	
44	Heterozygous DNA only	No band	No band	
45	Heterozygous DNA only	200nt	No band	
46	Heterozygous DNA only	200nt	No band	
47	Heterozygous DNA only	No band	No band	
48	Heterozygous DNA only	200nt	No band	
49	Heterozygous DNA only	No band	No band	
50	Heterozygous DNA only	200nt	200nt	
51	Heterozygous DNA only	200nt	No band	
52	Heterozygous DNA only	No band	No band	
53	Deceased			
54	Heterozygous DNA only	No band	200nt	
55	Deceased			
56	Heterozygous DNA only	200nt	No band	
57	Heterozygous DNA only	200nt	No band	
58	Heterozygous DNA only	No band	No band	
59	Heterozygous DNA only	200nt	No band	
60	Heterozygous DNA only	200nt	No band	
61	Deceased			

62	Heterozygous DNA only	No band	No band	
63	Heterozygous DNA only	200nt	No band	
kek6				
Primer	*kek6intgenF* & *kek6intgenR*	*kek6FRT GP Fwd* & *WH-WH- 2sid LI R*	*kek6FRT GP Rev* & *WH-WH- 2sid LI R*	
Expected				
Mutant	No band	~200nt	~200nt	
Not mutant	500nt	No band	No band	
Observed				
yw	500nt	No band	No band	
Parent: *e00907*	Not tested	200nt	No band	
Parent: *f05733*	Not tested	No band	200nt	
1	Deceased			
2–3	Heterozygous DNA only	No band	No band	*kek3* internal genomic 500nt band obtained
4	Deceased			
5–6	Heterozygous DNA only	No band	No band	*kek3* internal genomic 500nt band obtained
7–10	Deceased			
11–12	Heterozygous DNA only	No band	No band	*kek3* internal genomic 500nt band obtained
13	500nt band			
14	Heterozygous DNA only	No band	No band	*kek3* internal genomic 500nt band obtained
15–16	Deceased			
17	Heterozygous DNA only	No band	No band	*kek3* internal genomic 500nt band obtained
18	Deceased			
19	500nt band			
20–25	Deceased			
26–27	500nt band			
28	Heterozygous DNA only	No band	200nt	
29	Deceased			
30	500nt band			
31–32	Deceased			
33	500nt band			
34	No band	200nt	200nt	*kek3* internal genomic 500nt band obtained
35	No band	200nt	200nt	*kek3* internal genomic 500nt band obtained
36				
37–38	Heterozygous DNA only	No band	No band	
39–40	Deceased			
41	Heterozygous DNA only	No band	200nt	
42	Deceased			
43	Heterozygous DNA only	No band	200nt	
44	Deceased			
45	500nt band			
46–50	Deceased			